GUIDEBOOK

for field trips accompanying 31st IAS Meeting of Sedimentology held in Kraków on 22nd–25th of June 2015

edited by Grzegorz Haczewski

31st IAS
Meeting of Sedimentology
Kraków, Poland • June 2015

GUIDEBOOK

for field trips accompanying 31st IAS Meeting of Sedimentology held in Kraków on 22nd–25th of June 2015

edited by Grzegorz Haczewski

Polish Geological Society

Kraków, June 2015

Photo on the cover by Paweł Krzan
Editorial assistance with illustrations Tomasz Rychliński
Main route maps for all guides drawn by Wojciech Wróblewski
Designed and typeset by Pracownia Kreatywna Bezliku
Printed by DELTA J.A. Jagła

ISBN 978-83-942304-0-1
Available online at http://www.ing.uj.edu.pl/ims2015

Contents

Sedimentation on the Serravalian forebulge shelf of the Polish Carpathian Foredeep

Stanisław Leszczyński[1], Wojciech Nemec[2]

[1]Jagiellonian University, Poland (stan.leszczynski@uj.edu.pl)
[2]University of Bergen, Norway (wojtek.nemec@uib.no)

Route (Fig. 1): From Kraków we drive NE by road 79 (direction Sandomierz) to Ostrowce (ca. 82 km from Kraków) and then northwards by local roads to Stopnica and by road 756 to Szydłów (**stops A1.1** and **A1.2**). From Szydłów we turn W by road 765 to Chmielnik (19 km), then turn S by road 73; after 4 km at Śladków Mały (near roadside inn 'Wilczyniec') we turn left to local dirt road leading (ca. 1 km) to the agrotourism farm Rafał Gawlik (**stop A1.3**, **lunch & accommodation**). After lunch, we drive back to Chmielnik and by road 78 and local roads reach **stop A1.4** between Sędziejowice and Chomentówek. We return to Chmielnik and Śladków Mały (road 73) and by local eastward road reach **stop A1.5** near Suskrajowice. From there we return to the agrotourism farm in Śladków Mały for the night. On the second day, we use local roads and road 73 to reach **stops A1.6–A1.13** (distance ca.12 km) between Chmielnik and Busko Zdrój. We drive further by road 73 to Busko Zdrój and continue to Kraków by road 776 (105 km).

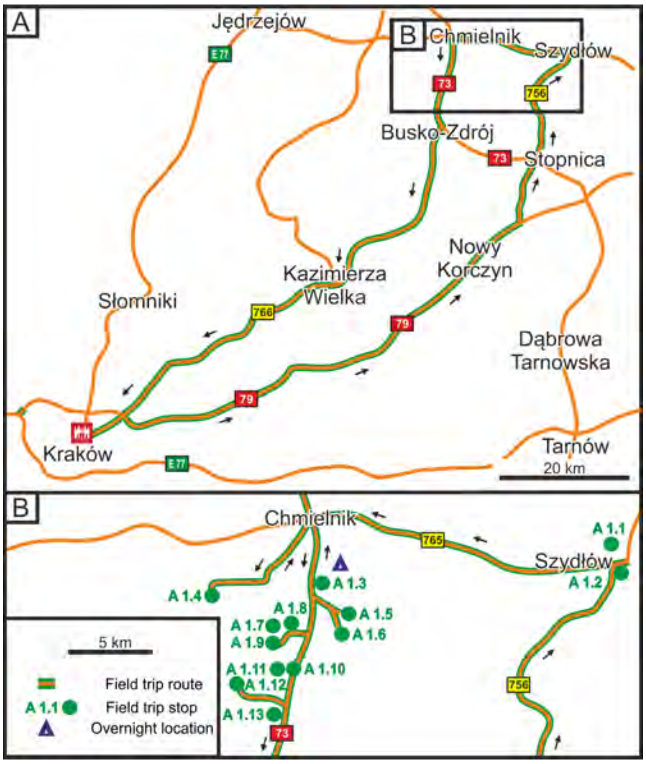

Fig. 1. Route map of field trip A1.

Introduction to the trip

Forebulge shelf depozone and peripheral unconformity

Peripheral bulge, or forebulge, is the outer marginal part of a foredeep basin formed by lithospheric flexure (Beaumont, 1981; Flemings & Jordan, 1989). Its width and bathymetric gradient depend upon the flexural rigidity of the underlying lithosphere and the orogen structural growth. The forebulge basinward flank is a flexural depozone that straddles the transition between the outer craton area of denudation and the deep-water realm of foredeep syncline. This shelf depozone receives sediment

Leszczyński, S. & Nemec, W., 2015. Sedimentation on the Serravalian forebulge shelf of the Polish Carpathian Foredeep. In: Haczewski, G. (ed.), *Guidebook for field trips accompanying IAS 31st Meeting of Sedimentology held in Kraków on 22nd–25th of June 2015*. Polish Geological Society, Kraków, pp. 5–23.
Guidebook is available online at www.ing.uj.edu.pl/ims2015

eroded off the adjacent craton, while its accommodation space is controlled by both tectonics and eustatic sea-level changes (Catuneanu *et al.,* 1998; Catuneanu and Sweet, 1999).

Forebulge depozones and foredeep peripheral unconformities have been little studied, as they are poorly exposed or virtually non-preserved. The simplified numerical models of a steady-state forebulge retreat, though most instructive, have inadvertently suggested that the resulting peripheral unconformity is a simple time-transgressive onlap feature (e.g., see Flemings and Jordan, 1989, figs 6–8, 11; Sinclair *et al.,* 1991, figs 8–13; Sinclair, 1997, fig. 2; Allen and Allen, 2005, fig. 4.33). This idealized model is by no means a universal stratigraphic guide, not least because the episodes of forebulge retreat alternate with episodes of its arching (Flemings and Jordan, 1990; Jordan and Flemings, 1991; Ettensohn, 1994; DeCelles and Currie, 1996; Currie, 1997). The sediment supply and eustatic sea-level changes come further into play, and their immediate impact is much stronger on the forebulge shelf than in the foredeep interior. The forebulge shelf is subject to frequent bathymetric changes and its shoreline is prone to rapid shifting, which renders the peripheral unconformity and onlap pattern far more intricate than portrayed by idealized 'steady-state' model.

These aspects of composite peripheral unconformity have been recently addressed by a sedimentological study of the Miocene forebulge shelf of the Polish Carpathian Foredeep (Leszczyński and Nemec, 2015). The topic of excursion A1 is to demonstrate some of the results of this study, which compares local sequence stratigraphy with the eustatic record and focuses on the deposits of a prominent mid-Serravalian clastic wedge known as the Chmielnik Formation. The forebulge shelf has a well-defined palaeogeographic gradient and its deposits have a negligible tectonic tilt, while showing several rapid shoreline shifts. High-resolution stratigraphy of regional palaeogeographic development remained difficult to reconstruct because of widely isolated outcrops. Biostratigraphic data are of little help, as the whole clastic wedge is within a single nannoplankton biozone. The excursion aims are: (1) to review the range of sedimentary systems in a classic forebulge depozone, as recognized from a typical mosaic of isolated outcrops; (2) to demonstrate how the local palaeoenvironmental changes can be regionally correlated on the logical basis of sequence stratigraphy; and (3) to show how this sedimentological approach can reveal the stratigraphic anatomy of a composite peripheral unconformity in a foredeep basin and shed light on the orogen-driven forebulge kinematics and basin tectonic history.

Geological setting of the excursion area

The excursion area is located in the outer central segment of the Polish Carpathian Foredeep (Fig. 2A), at the land-locked northwestern extremity of Miocene epicontinental Paratethys Sea (Fig. 2B). The flexural foredeep evolved by a northward thrusting of the Carpathian orogen against the margin of the European Platform,

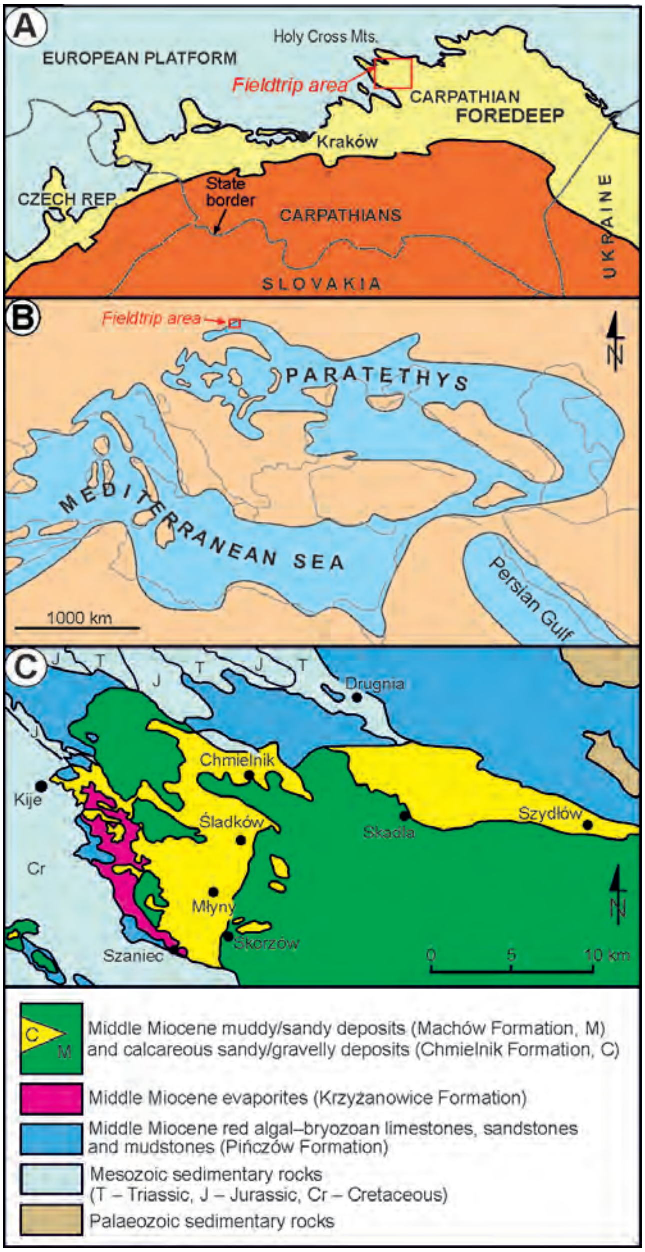

Fig. 2. (**A**) Location of the field trip area in the Polish Carpathian Foredeep. (**B**) The field trip area in a broader palaeogeographic framework of the Miocene Paratethys (map modified from Reuter *et al.*, 2012). (**C**) Geological map of the field-trip area without Quaternary cover (modified from Instytut Geologiczny, 1961).

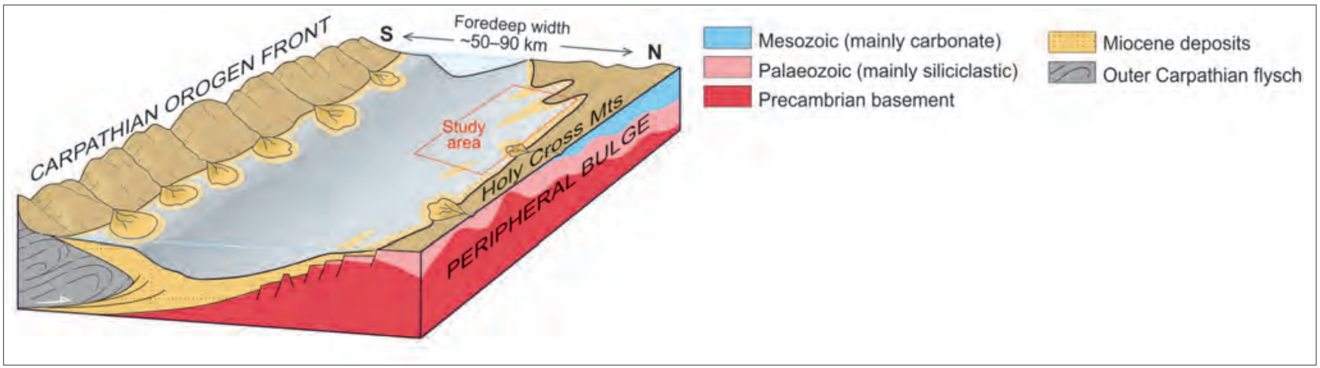

Fig. 3. Schematic model of the central segment of the Miocene Polish Carpathian Foredeep with an approximate location of the field trip area (studied by Leszczyński and Nemec, 2015). Note the peripheral bulge flank and its general N–S bathymetric gradient, with a roughly linear northern shoreline and a digitated western shoreline related to bedrock topographic ridges.

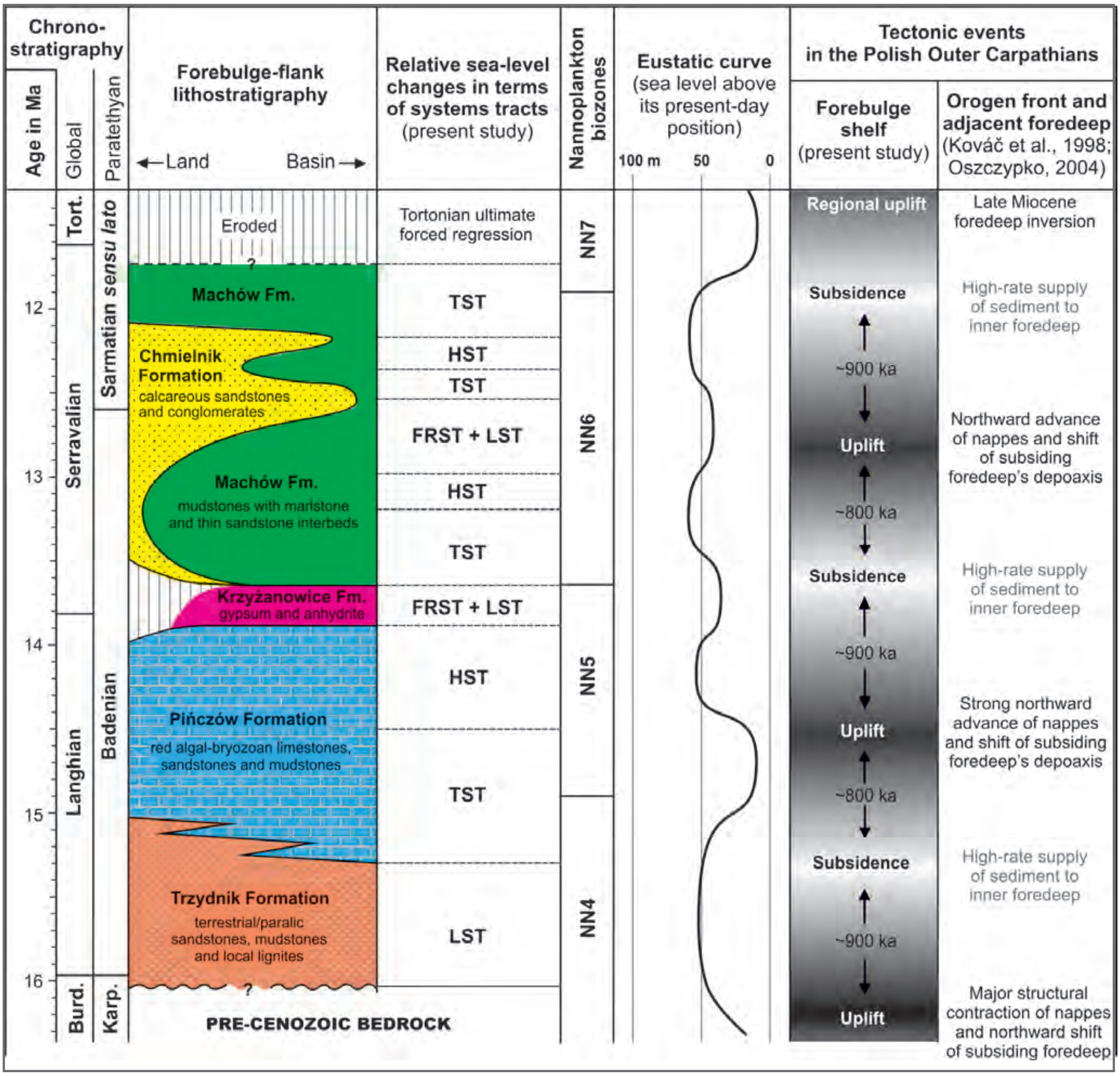

Fig. 4. Middle Miocene lithostratigraphy of the northern margin of Polish Carpathian Foredeep (based on Dudziak and Łaptaś, 1991; Jasionowski *et al.*, 2004; Stachacz, 2007; De Leeuw *et al.*, 2010) with a corresponding interpretation of relative sea-level changes in terms of systems tracts, the Tethyan calcareous nannoplankton zones (after Hilgen *et al.*, 2012) and eustatic sea-level curve (after Snedden & Liu, 2010; adjusted to the Neogene time scale of Hilgen *et al.*, 2012). The letter symbols of systems tracts (terminology after Helland-Hansen, 2009): FRST – forced-regressive systems tract; HST – normal-regressive highstand systems tract; LST – normal-regressive lowstand systems tract; TST – transgressive systems tract. The timing of orogen main thrusting events is after Kováč *et al.* (1998) and Oszczypko (2004).

where a peripheral bulge formed (Fig. 3). The forebulge crest is the bedrock ridge of the Holy Cross Mountains to the north of the excursion area. The forebulge shelf depozone has a pre-defined palaeogeographic gradient with land area to the north and deep-water realm to the south (Fig. 3). The foredeep in its inner part accumulated a thick (1–3 km) succession of early to middle Miocene deep-marine to deltaic siliciclastic deposits, which were partly overridden by the Carpathian thrust wedge (Fig. 3; Porębski et al., 2003; Oszczypko et al., 2006). In the outer part of the foredeep, a northwards-thinning succession of middle Miocene biogenic limestones, evaporites and clastic deposits (Fig. 4, left), up to a few hundred metres thick, onlapped the denudated Palaeozoic–Mesozoic bedrock of the peripheral bulge (Figs 2C, 3; Alexandrowicz et al., 1982).

The Chmielnik Formation

The Chmielnik Formation (Alexandrowicz *et al.,* 1982), originally referred to as the 'detrital Sarmatian' (Kowalewski, 1958; Rutkowski, 1976), consists of shallow-marine coarse clastic deposits that form the uppermost part of sedimentary succession in this central segment of the forebulge flank (Fig. 4). The formation occurs at the surface (Fig. 2C), beneath a thin cover of Quaternary deposits, and its isolated outcrops are mainly abandoned quarry pits. Sedimentation was controlled by both the orogen tectonism (Rutkowski, 1976, 1981; Czapowski and Studencka, 1990; Wysocka, 1999) and the Paratethys responses to eustatic sea-level changes (Rögl, 1998, 1999; Piller *et al.,* 2007). Marine sedimentation in this part of the foredeep commenced in the early Langhian (Alexandrowicz *et al.,* 1982; Jasionowski, 1997) with paralic deposits of the Trzydnik Formation and carbonates of the Pińczów Formation (Fig. 4). The evaporative drawdown recorded by the Krzyżanowice Formation (Fig. 4; Kwiatkowski, 1972; Peryt, 2006) was followed by another marine transgression, represented by the muddy Machów Formation (Fig. 4; Oszczypko *et al.,* 1992; Oszczypko, 1998). The Chmielnik Formation (Fig. 4) is a coarse-clastic nearshore equivalent of the Machów Formation that first extended basinwards and then was rapidly covered by the latter in the middle Serravalian (Jasionowski, 2006). The Tortonian witnessed a gradual withdrawal of the sea towards the southeast (Dziadzio, 2000; Dziadzio *et al.,* 2006).

The Chmielnik Formation forms a stratigraphic coarse-clastic wedge within the muddy Machów formation and pinches out basinwards. In cratonward direction, it covers unconformably the Pińczów Formation (Dudziak and Łaptaś, 1991; Garecka and Olszewska, 2011) or locally also the pre-Miocene bedrock (Rutkowski, 1976) (Fig. 2C). The Chmielnik Formation has been studied since the 19^{th} century (see review by Czapowski, 1984) and dated to the Paratethyan latest Badenian–early Sarmatian (Fig. 4) on the basis of foraminifers (Łuczkowska, 1964; Olszewska, 1999), macrofauna (Czapowski and Studencka, 1990) and calcareous nannonplankton (Peryt, 1987; Dudziak and Łaptaś, 1991; Garecka and Olszewska, 2011). The main part of the formation, up to 30 m thick (Czapowski, 2004), has an estimated time-span of ca. 1.1 Ma in the upper part of biozone NN6 (Fig. 4; Dudziak and Łaptaś, 1991; Peryt, 1997). The formation basal part (Fig. 4), with an estimated mean thickness of less than 10 m and a time-span of ca. 450 ka, has been recognized only locally (Dudziak and Łaptaś, 1991) and dated to the transition of biozones NN5–NN6 and lower NN6.

The deposits of the Chmielnik Formation range on a local scale from weakly cemented, nearly pure siliciclastic sandstones to well-cemented calcarenites and calcirudites with or without significant siliciclastic admixture, including interbeds of calcareous to non-calcareous mudstones and sporadic pelitic, microbial serpulid or coralline-algal limestones (Rutkowski, 1976; Czapowski, 1984; Czapowski and Studencka, 1990). Sarmatian marine fauna is locally mixed with transported plant leaves and terrestrial/freshwater gastropods (Zastawniak, 1974, 1980; Górka, 2008; Stworzewicz *et al.,* 2013). The deposits have generally been considered to be of nearshore origin, passing basinwards into offshore mudstones, with palaeocurrent directions in the azimuth range of 100–190° (Rutkowski, 1976; Czapowski, 1984; Czapowski and Studencka, 1990; Łaptaś, 1992), indicating a combination of seaward and alongshore sediment transport. However, sedimentological documentation was sparse and the exact pattern of relative sea-level changes, shoreline shifts and palaeogeographic development remained controversial and unclear.

According to the study by Leszczyński and Nemec (2015), the Chmielnik Formation consists of fluvio-deltaic, foreshore and shoreface deposits with a range of

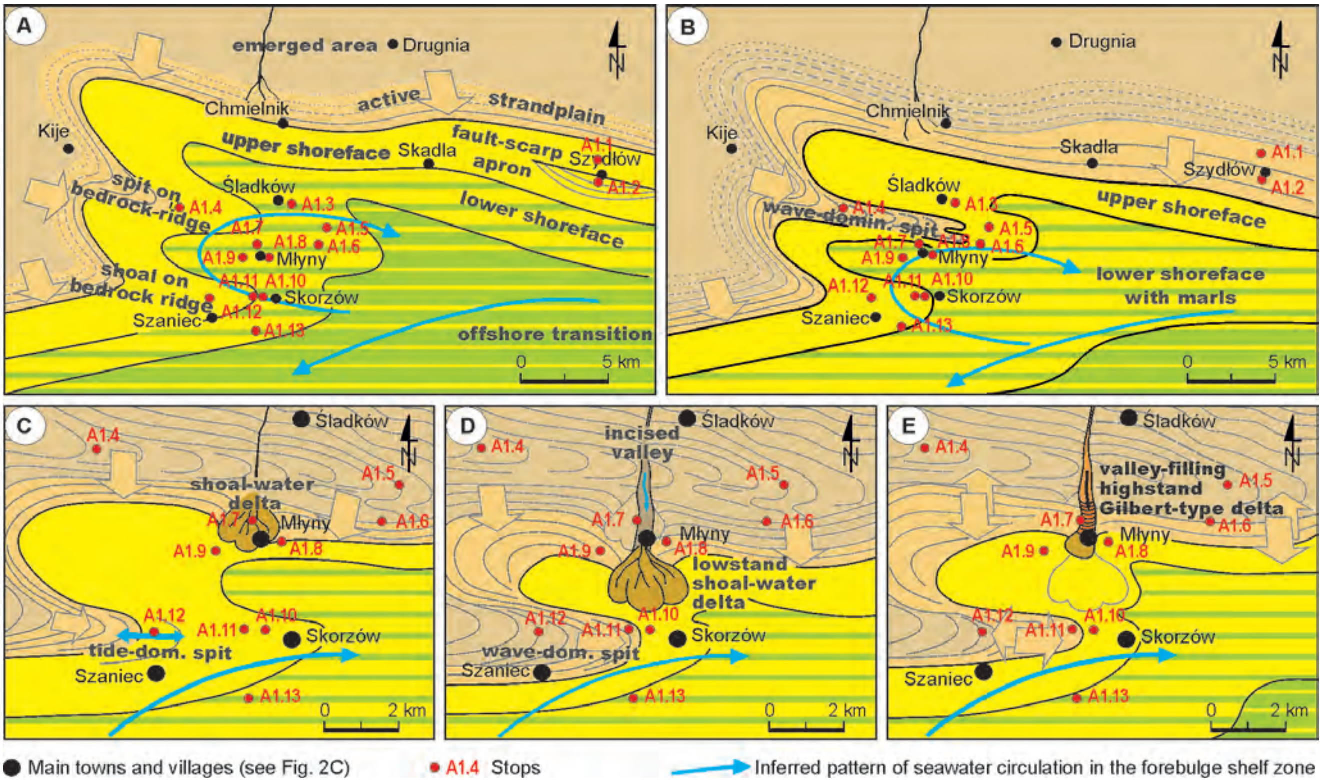

Fig. 5. Palaeogeographic reconstruction of the development of Chmielnik Fm. in the fieldtrip area (see regional setting in Fig. 2). Slightly modified from Leszczyński and Nemec (2015). (**A**) The mid-Serravalian regression begins with an encroachment of lower- to upper-shoreface sands onto the muddy offshore-transition deposits of the Machów Fm. (see Fig. 4). The northern shoreline passed Chmielnik and approaches locality A1.1, while the digitated western shoreline remains outside the study area. Western littoral sand shoals form on ESE-trending bedrock ridges, and fault scarp-attached sand bars form at localities A1.1 and A1.2. (**B**) The regressive northern shoreline approaches locality A1.3, while a wave-dominated spit bar extends to the ESE through localities A1.4–6 to become merged with the regressive shoreline. (**C**) A zoomed-in sketch showing the northern shoreline reaching localities A1.7–9, where beach deposits and sandy shoal-water delta form, while a tide-dominated new sandy spit begins to extend eastwards through locality A1.12. (**D**) The northern shoreline reaches locality A1.8 when forced regression forms an incised fluvial valley at locality A1.7 with a corresponding gravelly shoal-water lowstand delta developing to the south (Fig. 20) and a lowstand beach forming at locality A1.9. The east-advancing spit bar concurrently extends from locality A1.12 to localities A1.11 and A1.13, while becoming wave-dominated. (**E**) Minor marine transgression occurs, followed by a highstand normal regression, whereby the incised valley at locality A1.7 is drowned and filled by Gilbert-type bayhead delta, while the adjacent strandplain at locality A1.8 is concurrently inundated and covered with regressive upper-shoreface deposits. The subsequent major transgression forms a transgressive shoreface unit at all localities and brings back muddy offshore-transition deposits of Machów Fm. to the study area (see profile in Fig. 4, top).

large littoral sand bars, all enveloped in muddy offshore-transition deposits. The formation comprises a poorly exposed basal transgressive wedge and two subsequent regressive wedges (Fig. 4, left), which jointly reveal an active interplay of orogen-driven forebulge tectonism, sediment supply and 3rd-order eustatic cycles (Fig. 4, right). Facies analysis indicates rapid shoreline shifts and allows palaeogeographic reconstruction of environmental changes (Fig. 5). A similar interplay of the main controlling factors is recognizable in the whole mid-Miocene sedimentary succession that accumulated in the forebulge depozone, with the tectonic cycles of alternating forebulge uplift and subsidence spanning ca. 800–900 ka and the episodes of uplift correlating with the main pulses of Carpathian orogen thrusting (Fig. 4, right). The study by Leszczyński and Nemec (2015) has demonstrated that the forebulge depozone is an extreme case of an accommodation-controlled shelf, where the combination of tectonism, eustasy and sediment supply has a profound palaeogeographic, environmental and stratigraphic impact. Detailed facies analysis of forebulge deposits may allow recognition of the relative role of these factors.

The Miocene composite peripheral unconformity in the Polish Carpathian Foredeep (Fig. 6B) differs markedly from the idealized model of a 'steady-state' flexural onlap (Fig. 6A), as do also most other documented worldwide cases. It is therefore suggested that the forebulge sedimentary successions and peripheral unconformities, instead of being simplified in terms of the idealized model, should

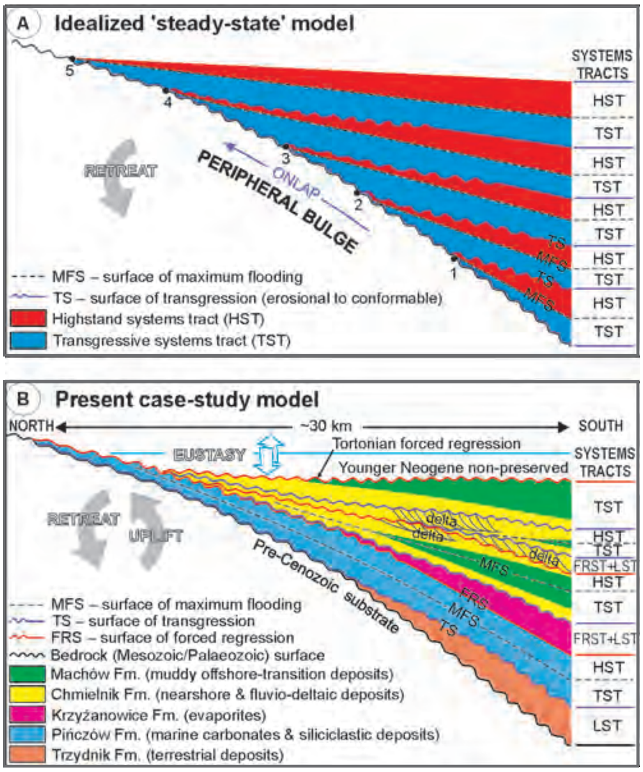

Fig. 6. Dynamic stratigraphy of foredeep peripheral unconformity. (**A**) An idealized 'steady-state' onlap portrayed by forebulge continuous-retreat models. (**B**) The present case model for the Miocene peripheral unconformity in the central segment of the Polish Carpathian Foredeep (see stratigraphy in Fig. 4). From Leszczyński and Nemec (2015).

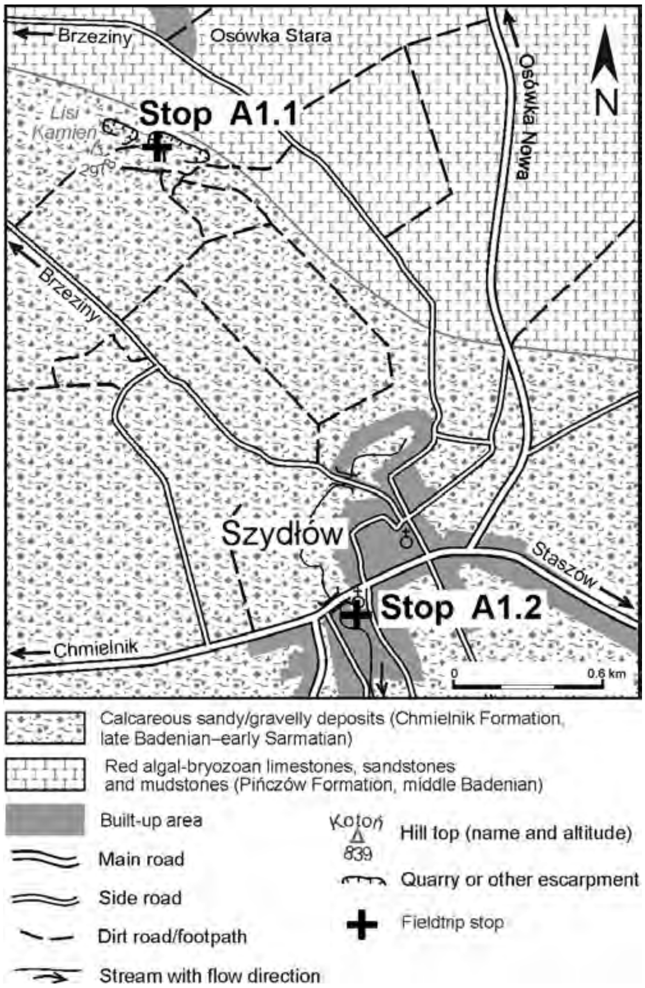

Fig. 7. Geological map showing detailed location of the fieldtrip stops A1.1 and A1.2.

rather be studied in detail as they bear a high-resolution record of regional events and give unique insights into the local role of tectonism, eustasy and sediment yield. Analysis of the stratigraphic anatomy of peripheral unconformity aids reconstruction of the forebulge kinematics and foredeep tectonic history (see Leszczyński and Nemec, 2015).

Stop descriptions

All outcrops in this field excursion are easily accessible from the car parking places, within a walking distance of 5–15 minutes. The excursion focuses on the isolated outcrops of the Chmielnik Formation in the Szydłów–Sędziejowice–Zwierzyniec area (Fig. 1B), and its aim is to demonstrate and discuss the spectrum of sedimentary systems on a classical forebulge shelf. It will be discussed further how the events recorded in the local outcrop sections can be correlated according to the basic principles of sequence stratigraphy to reveal the shelf depositional history (see also Leszczyński and Nemec, 2015). [The ensuing text refers also to Plates 1–3 given as attachments in the electronic version of the guide.]

Stop A1.1 Abandoned sandstone quarry on the Lisi Kamień hill near the village of Osówka Stara

(50°36′20″N, 20°59′29″ E; Fig. 7); access by local dirt road.

The deposits (coarse-grained to pebbly calcarenites) are upper-shoreface to foreshore facies representing the late Serravalian shoreline of the Chmielnik Fm. at its early-regressive northern location (north of locality A1.2). The shoreface deposits form giant foreset on the inferred hanging wall of an east-striking syndepositional normal growth-fault and appear to have been deformed by rotational sliding while burying the active fault escarpment (Fig. 8). They are covered with south-prograding gravelly foreshore deposits, which also seem to have been affected by a subsequent minor reactivation of the fault. The synsedimentary extensional faulting, better documented by Łaptaś (1992) in coeval deposits farther to the east, indicates forebulge doming (see e.g., Agarwal *et al.*, 2002).

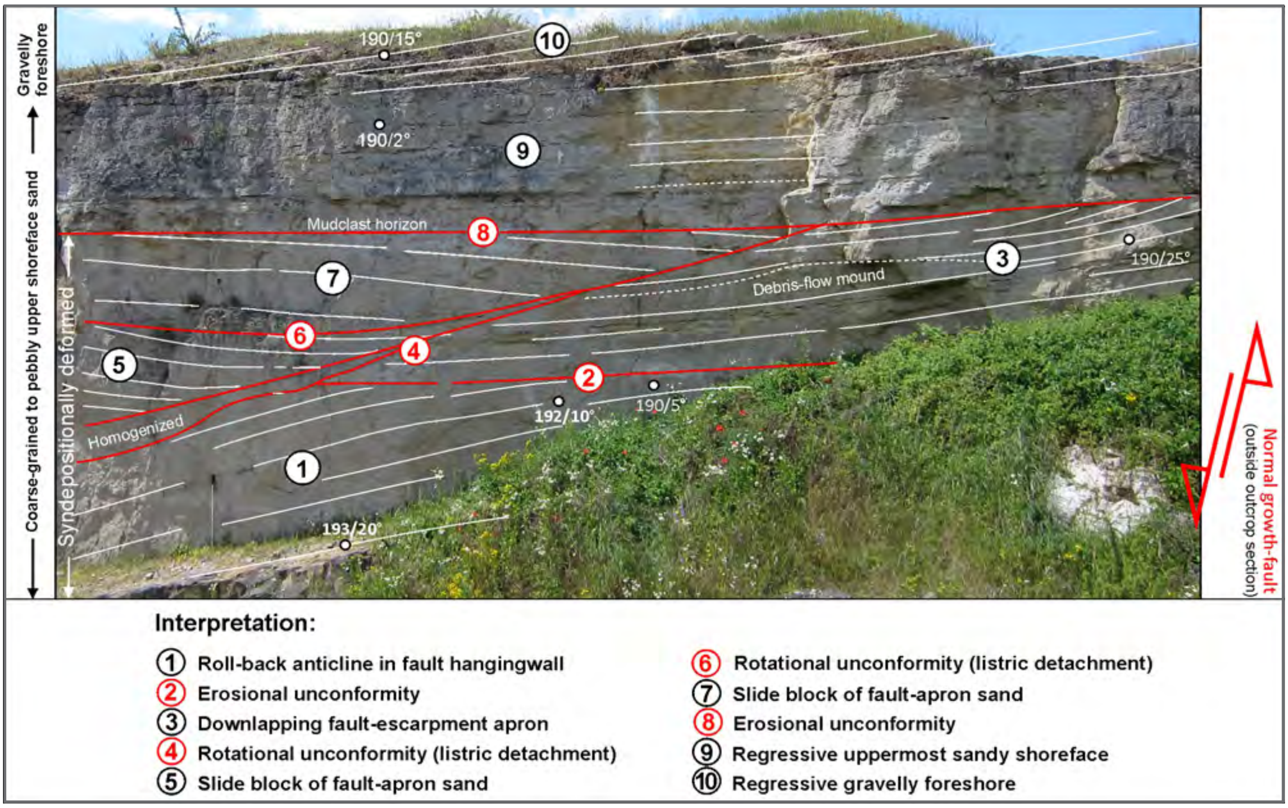

Fig. 8. Interpreted portion of the NW wall of outcrop at stop A1.1 (Figs 1B, 7). The main part of succession (units 1–7) consists of upper-shoreface deposits accumulated as a giant foreset on the hanging wall of an inferred normal fault, with evidence of syndepositional rotational sliding. The covering top part (units 9 and 10) comprises south-prograding uppermost shoreface and relic gravelly foreshore deposits. The walking stick (lower left) is 1 m.

Stop A1.2 Escarpment of the Ciekąca brooklet in Szydłów

(50°35′18″ N, 21°00′05″ E; Fig. 7) at the western foot of the church-hosting local hill.

Another fault scarp-attached, large littoral calcarenitic bar with giant-scale, south-dipping foreset stratification and listric rotational slide detachments (Fig. 9). This east-striking sandstone body is isolated and lenticular in plan-view shape, estimated to be a few kilometres long and less than 1 km wide (Łaptaś, 1992). Its foreset is at least 13 m thick (top unpreserved). The strata inclination of 25–35° decreases tangentially to 15–20° at the transition to a subhorizontal (<10°) bottomset of finer-grained sandstones (base unexposed). The bar foreset shows numerous reactivation surfaces and common

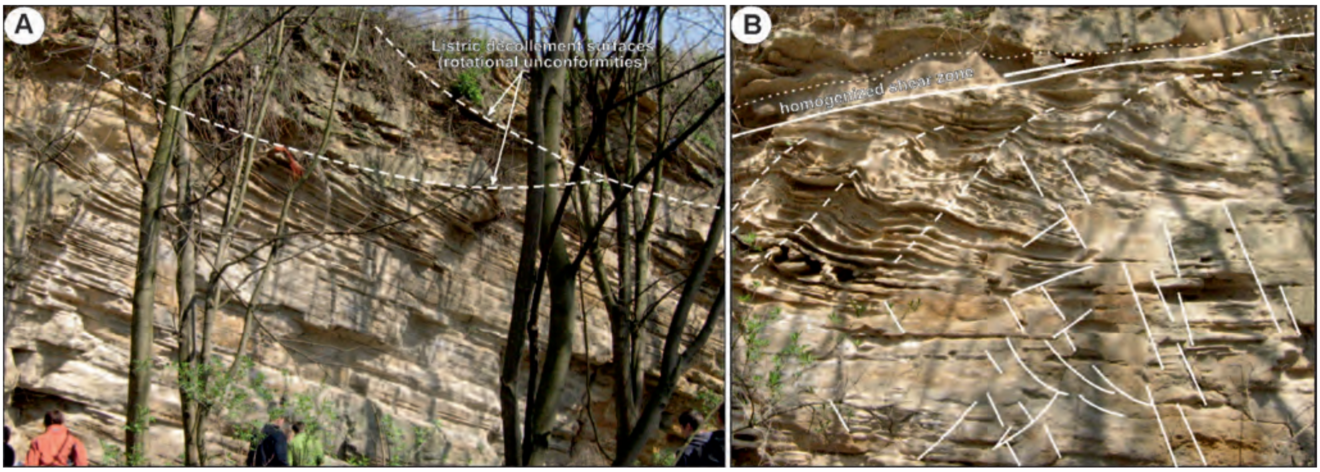

Fig. 9. (**A**) Giant foreset stratification with listric rotational slides in a fault scarp-attached littoral sand bar at stop A1.2 (Figs 1B, 7). (**B**) Close-up detail of the same bar, showing a listric detachment smeared with homogenized sand, shear-induced drag folds (dashed lines) and synsedimentary fractures; the outcrop portion is ~5 m high. (See also similar coeval cases in Plate 1.). From Leszczyński and Nemec (2015).

synsedimentary deformation in the form of slump folds, listric detachments (Fig. 9A), related drag folds and soft-sediment fracturing (Fig. 9B). The bottomset, recognized in wells, is underlain by a heterolithic succession of fine-grained sandstones intercalated with mudstone and marlstone layers (Łaptaś, 1992), considered to be lower-shoreface deposits. Similar other coeval large bars attached to syndepositional fault escarpments were recognized by Łaptaś (1992) over a distance of 30 km to the east (see Plate 1).

Stop A1.3 Rock escarpments around the Gawlik family agrotourism farm in Śladków Mały

(50°34′53″ N, 20°05′14″ E; Fig. 10)

The sandstones and conglomerates here represent the regressive upper shoreface and foreshore of the Chmielnik Fm. at the palaeoshoreline younger location to the south of stops A1.1 and A1.2. The well-sorted deposits have a variable proportion of calciclastic and siliciclastic components, reflected in their varied degree of cementation. The horizontally bedded arenites in the outcrop lower part (Fig. 11A) show mainly planar parallel stratification with numerous subhorizontal truncations, but also wave-ripple cross-lamina-

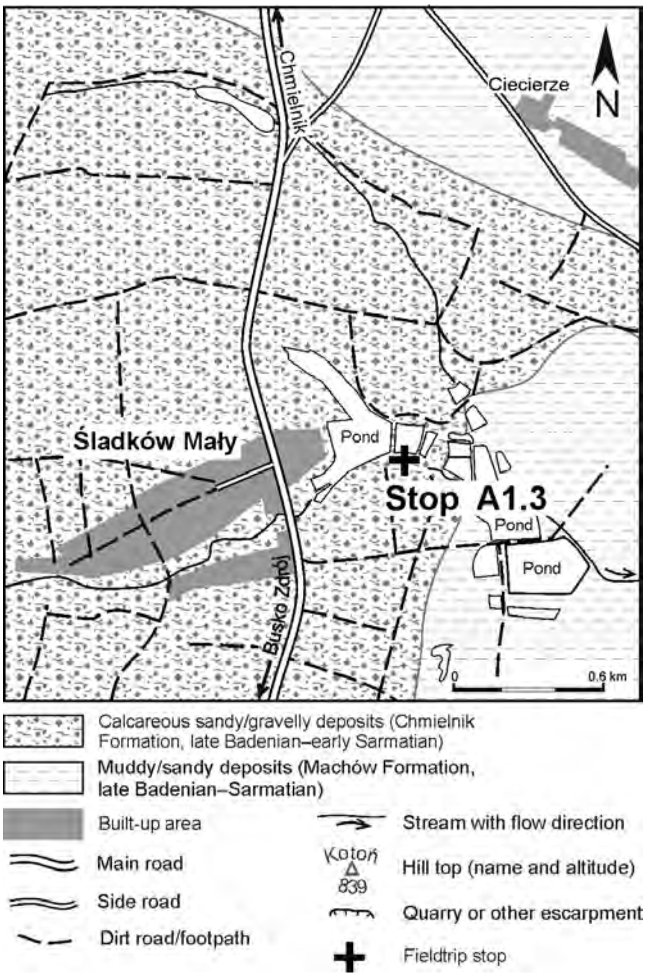

Fig. 10. Geological map showing detailed location of field-trip stop A1.3 (modified from Instytut Geologiczny, 1961).

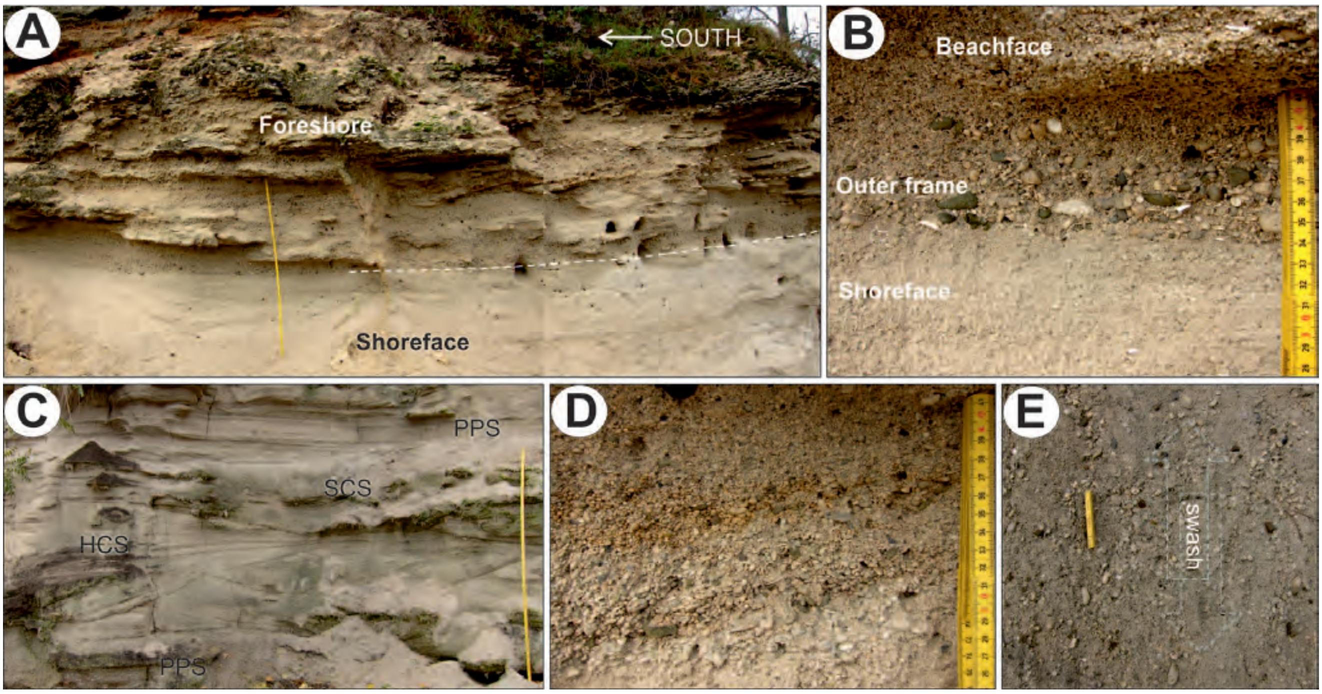

Fig. 11. (**A**) Interpreted portion of the outcrop at stop A1.3 (Figs 1B, 10); the measuring stick (scale) is 1 m. (**B**) Close-up view of the sharp contact between foreshore and underlying shoreface deposits; the visible part of measuring stick is 14 cm. (**C**) Close-up view of shoreface sandstones showing planar parallel (PPS), swaley (SCS) and hummocky stratification (HCS); the measuring stick is 1 m. (**D**) Close-up detail of inclined foreshore strata composed of well-sorted very coarse-grained sand rich in granules and small pebbles; the visible part of measuring stick is 16 cm. (**E**) Bedding surface of foreshore deposits with swash-aligned pebbles and diffuse sand ribbons; the measuring stick is 13 cm.

tion and both swaley and hummocky stratification in the lowest part (Fig. 11C). The range of stratification types and the lack of argillaceous interlayers indicate deposition in a perennially wave-worked upper shoreface environment (Clifton, 1981; Hampson, 2000). Planar parallel stratification alternating with subordinate wave-ripple cross-lamination indicates fair-weather wave action with generally high but fluctuating orbital velocities (Clifton et al., 1971; Komar and Miller, 1975). The associated trough cross-stratification represents linguoid or lunate dunes driven by wave-generated littoral currents (Clifton and Dingler, 1984). Swaley and hummocky stratifications indicate deposition by storm-generated combined flows (Dumas and Arnott, 2006).

The sandstones show slight upward coarsening and are overlain by a solitary foreset of granule to fine-pebble conglomerate, 120–140 cm thick, with strata inclined southwards at 15–25° (Fig. 11A). The basal part of tangential foreset shows coarse-grained sand rich in outsized subspherical pebbles and small cobbles (Fig. 11B). Sediment is polymictic, generally well rounded and well sorted (Fig. 11D), with the stratification surfaces showing dip-aligned pebbles and diffuse sand ribbons (Fig. 11E). These deposits are thought to represent a mixed sand-gravel foreshore system dominated by moderate- to high-energy waves (Massari and Parea, 1988). The sandy toeset rich in outsized gravel is the beach 'outer-frame' facies of Bluck (1999). The diffuse dip-parallel lineation on foreset surfaces is a signature of beach swash (Allen, 1982). These gravelly deposits are interpreted as a regressive strandplain that prograded rapidly to the south.

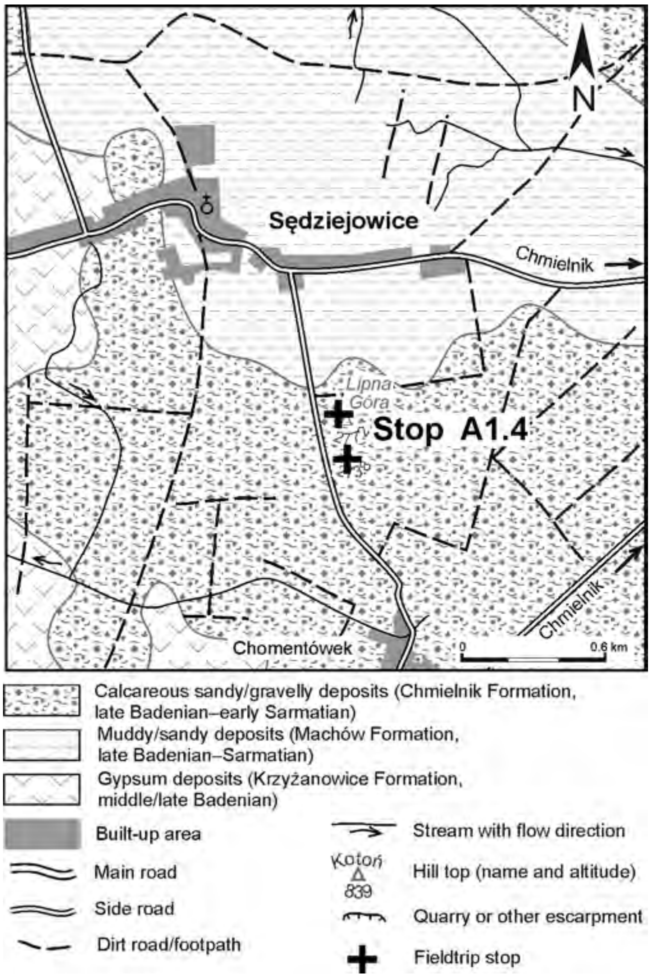

Fig. 12. Geological map showing detailed location of field-trip stop A1.4 (modified from Instytut Geologiczny, 1961).

Stop A1.4 Rock escarpments on the eastern side of the asphalt road between Sędziejowice and Chomentówek

(50°34′23″ N, 20°39′42″ E; Fig. 12)

The outcrops show foreset and bottomset deposits of an early-stage coarse-grained spit platform built towards the ESE in a relatively deep (≥10 m) shoreface water. The northern outcrop (Fig. 12) exposes the upper part of a thick foreset (>6 m; topset non-preserved) of steeply east-inclined cross-strata of well-sorted, granule-rich very coarse-grained sand. The lower part of the foreset and its transition to a less inclined bottomset are exposed in the southern outcrop (Fig. 12). The foreset abounds in internal truncation and reactivation surfaces (Fig. 13A). The bottomset consists of fine- to medium-grained sandstones with planar parallel stratification and both swaley and hummocky strata sets (Fig. 13B).

The deposits are thought to represent the subaqueous platform (*sensu* Meistrell, 1972) of a coarse-grained spit system similar to those described by Nielsen *et al.* (1988) and Nielsen and Johannessen (2008) (see Plate 2A). The wave-dominated spit prograded towards the ESE and is estimated to have been about 1.5 km wide and 11 km long, reaching the eastern stops A1.5 and A1.6 (Figs 1B, 12). The foreset truncation and reactivation surfaces are due to both storm erosion and gravitational collapses. The bottomset consists of upper-shoreface deposits, yet abnormally inclined (10–15°), as is generally characteristic of advancing spit systems (Nielsen and Johannessen, 2008).

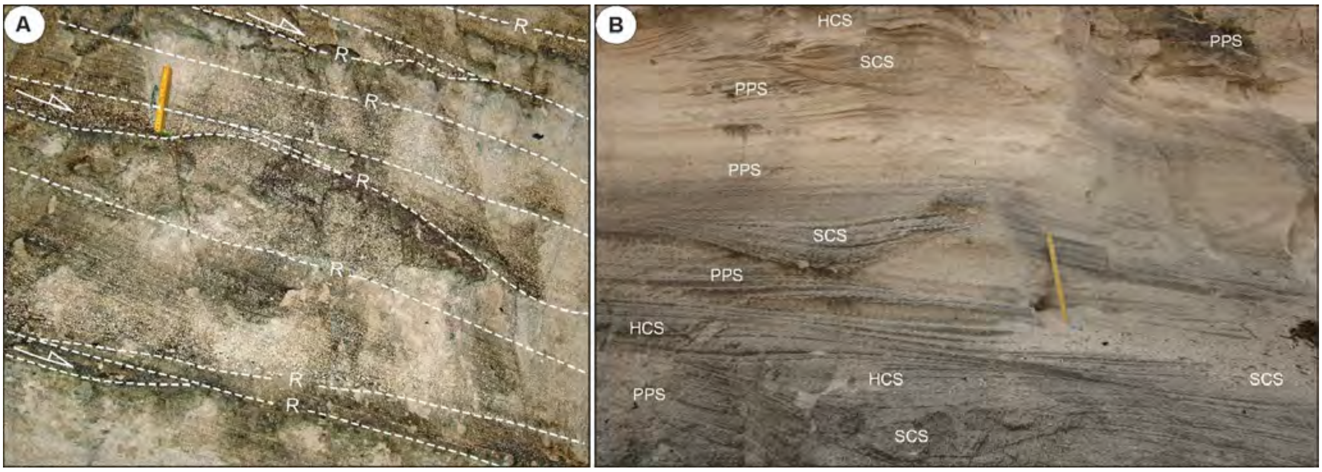

Fig. 13. (**A**) Foreset of granule sandstone with numerous reactivation surfaces (R) in a spit-bar platform at stop A1.4 (Figs 1B, 12; see Plate 2A); arrows indicate coarse-grained massive sediment avalanches; the measuring stick is 13 cm. (**B**) The upper-shoreface sandstones of spit platform bottomset at the same locality, with planar parallel (PPS), swaley (SCS) and hummocky (HCS) stratification; the direction of spit progradation is away from the viewer; the measuring stick is 21 cm.

Stop A1.5 Sand pit near Suskrajowice

(50°34′23″ N, 20°39′42″ E; Fig. 14)

The outcrop shows the most distal part of the same wave-dominated spit system (stop A1.4) that extended itself towards the ESE along the south-advancing and shoaling general shoreface (see Fig. 5B). The spit platform here, built in shallower water, is strikingly different. The inclined (15–18°) beds of upper-shoreface sandstones show planar parallel stratification and obliquely accreted dune cross-strata sets (Fig. 15) – similar as observed in the platforms of other shoal-water spits (Nielsen and Johannessen, 2008; see Plate 2B).

Stop A1.6 Sand pit in Borzykowa

(50°34′23″ N, 20°39′42″ E; Fig. 14).

The outcrop shows sandy deposits of the southern flank of the same distal shoal-water spit system (stop A1.5) with east-inclined (15–18°), parallel-stratified shoreface facies overlain by foreshore facies (Fig. 16A). The lower part of spit platform contains thin interbeds of calcareous mud (Fig. 16B), indicating deposition in a lower shoreface environment. The sparsely preserved coarse-sandy foreshore deposits at the top represent the spit-bar ridge.

Stop A1.7 Escarpment along a fish pond near the local shop in Młyny

(50°33′08″ N, 20°43′30″ E; Fig. 17).

The north–south outcrop section, 150 m long (Fig. 18), shows basal marl-interlayered mid-shoreface sandstones (poorly exposed) overlain by a sandy shoal-water delta and incised further by a fluvial valley that was flooded by

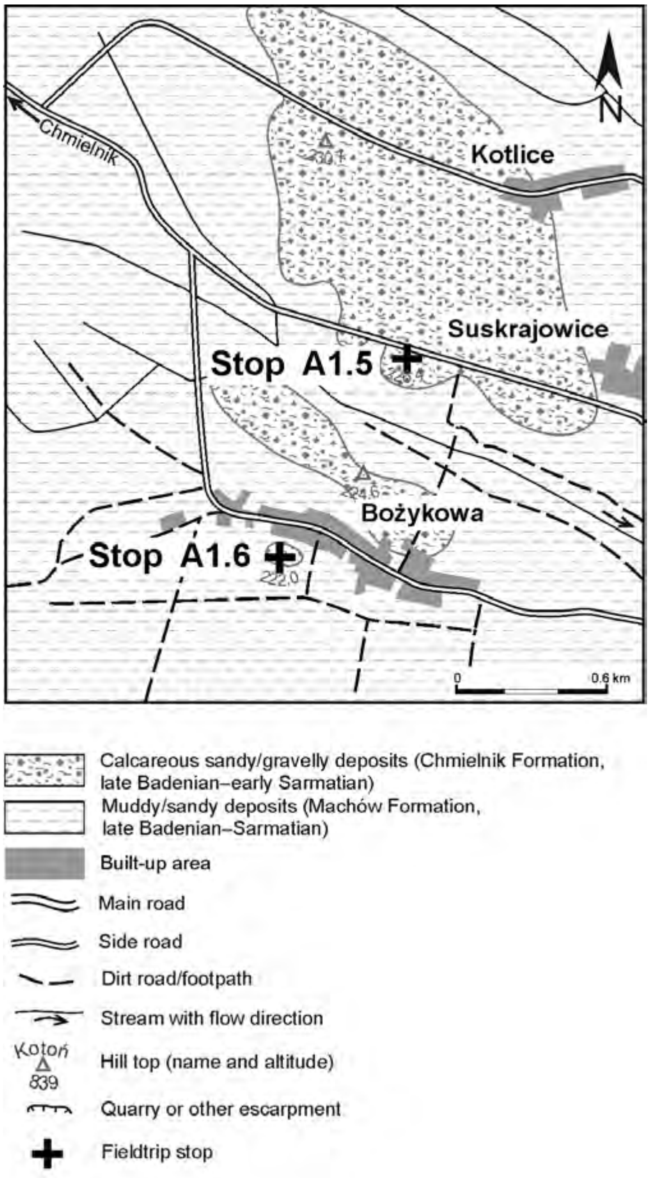

Fig. 14. Geological map showing detailed location of the field-trip stops A1.5 and A1.6 (modified from Instytut Geologiczny, 1961).

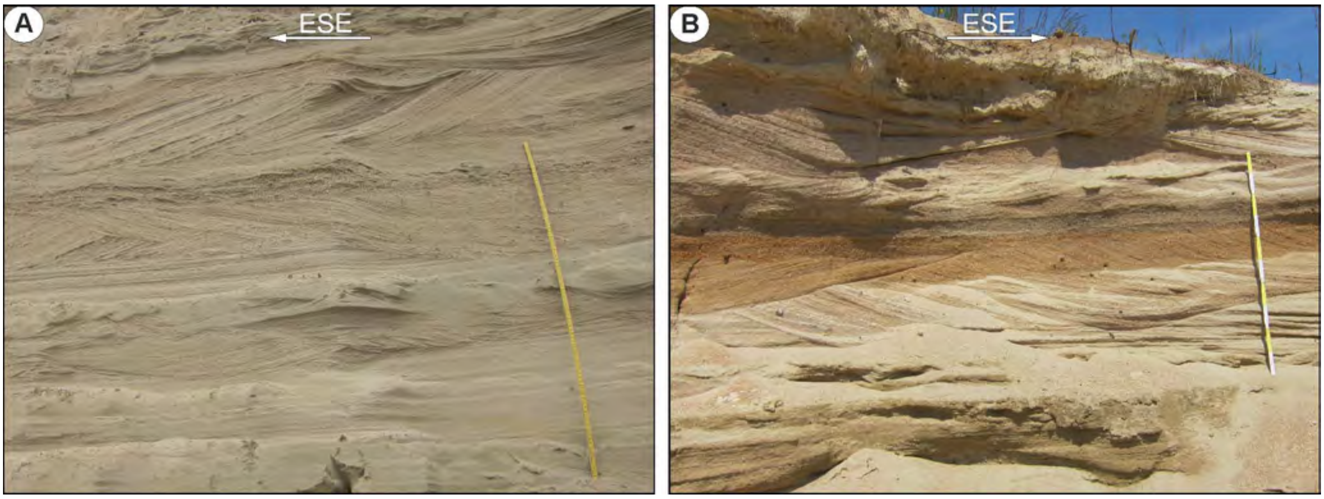

Fig. 15. (**A**, **B**) Close-up views of two opposite outcrop walls showing upper shoreface sandstones of spit-bar platform at stop A1.5 (Figs 1B, 14); note in **A** the alternation of trough cross-stratification and inclined (10–20°) planar parallel stratification. The spit bar prograded to the ESE and the dune cross-strata sets were accreted obliquely (see Plate 2B). The measuring stick is 1 m.

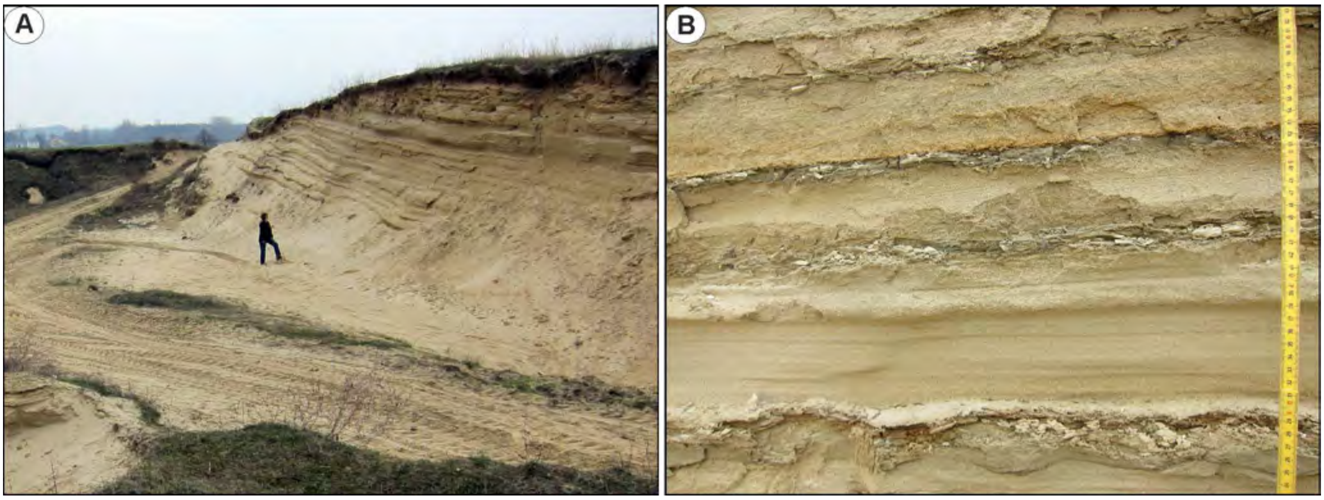

Fig. 16. Sandy deposits of spit-bar platform at stop A1.6 (Figs 1B, 14). (**A**) Lower- to upper-shoreface deposits, remarkably inclined towards the ENE, overlain by relic foreshore deposits in the sand-pit western wall. (**B**) Close-up detail of lower-shoreface deposits with mudstone interlayers. The visible part of measuring stick is 40 cm.

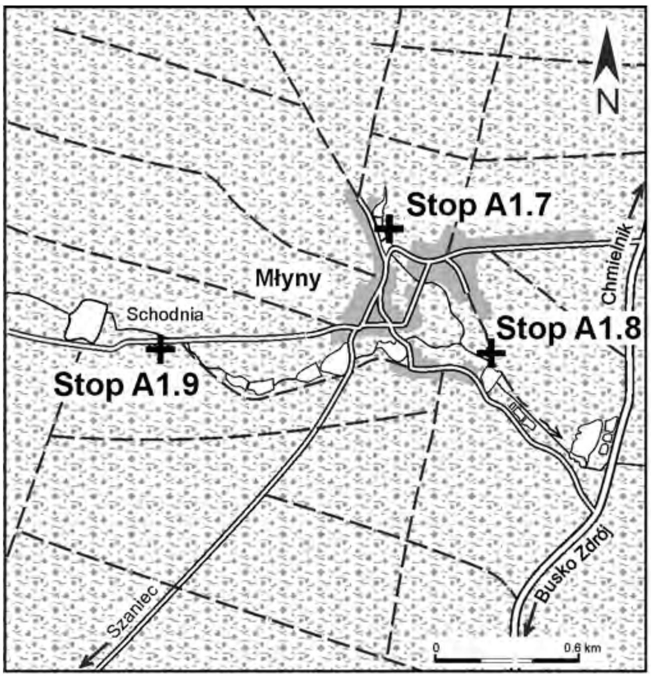

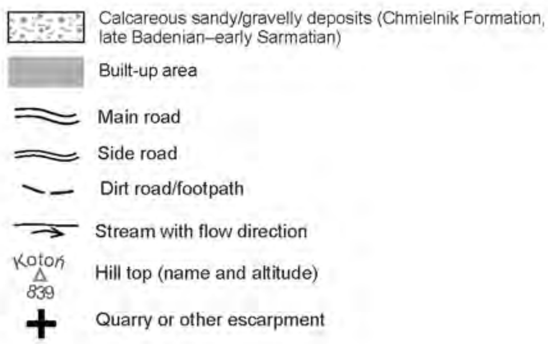

Fig. 17. Geological map showing detailed location of the field-trip stops A1.7–9 (modified from Instytut Geologiczny, 1961).

the sea and filled by a gravelly Gilbert-type bayhead delta (Fig. 19A) – all eventually drowned by a major marine transgression (see Fig. 5C–E). The lowstand shoal-water delta corresponding to the phase of valley incision is poorly exposed about 1.6 km to the south (Fig. 20; locality not included in this trip).

The incised valley-fill at stop A1.7 reaches 5 m in thickness and is estimated to be ca. 40 m wide. The south-

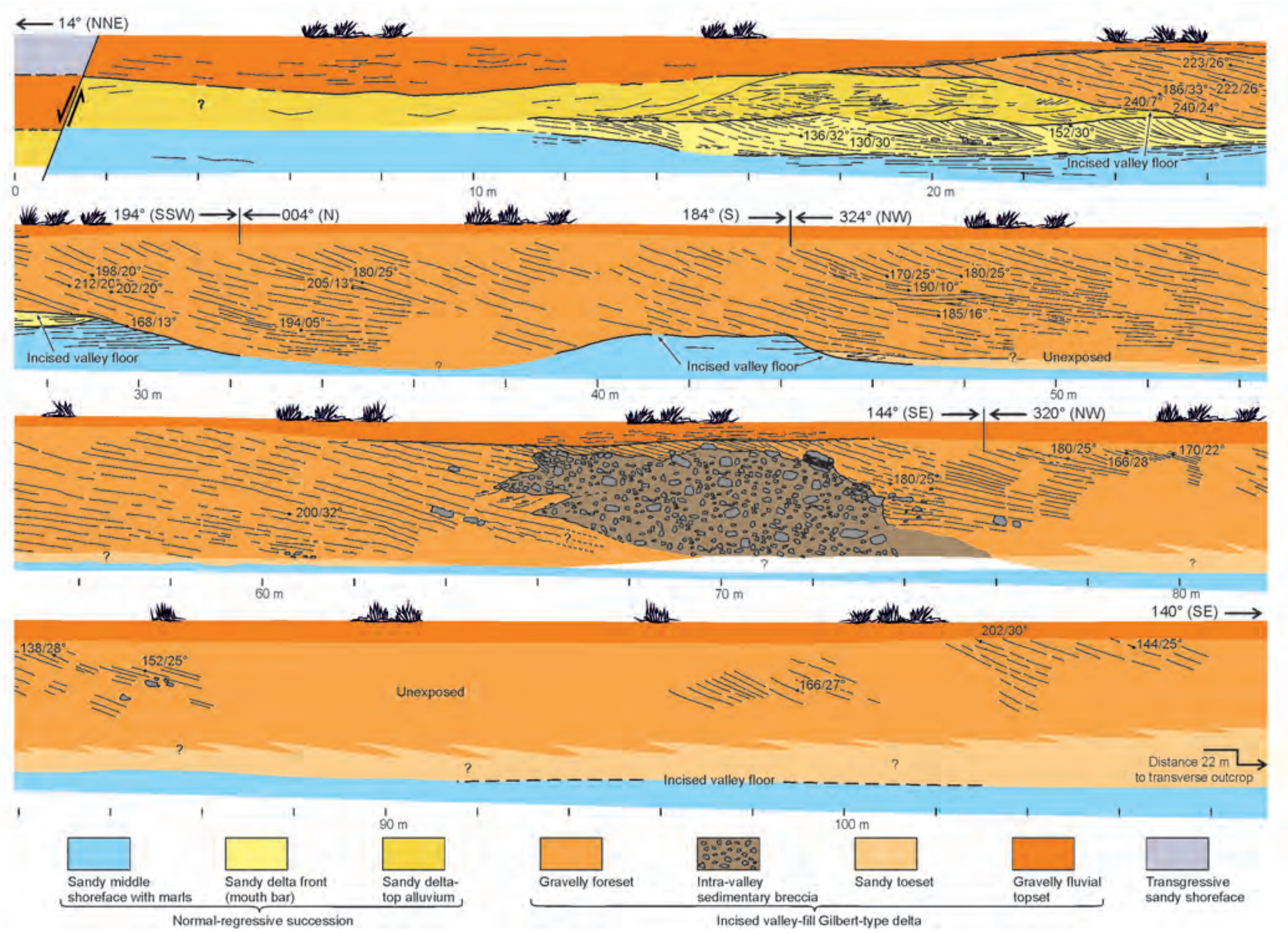

Fig. 18. A photomosaic overlay line-drawing of bedding architecture in the longitudinal outcrop section at stop A1.7 (Figs 1B, 17), approximately parallel to the incised palaeovalley. The numerical values on outcrop are the strata dip azimuth and angle. For facies interpretation, see legend. From Leszczyński and Nemec (2015).

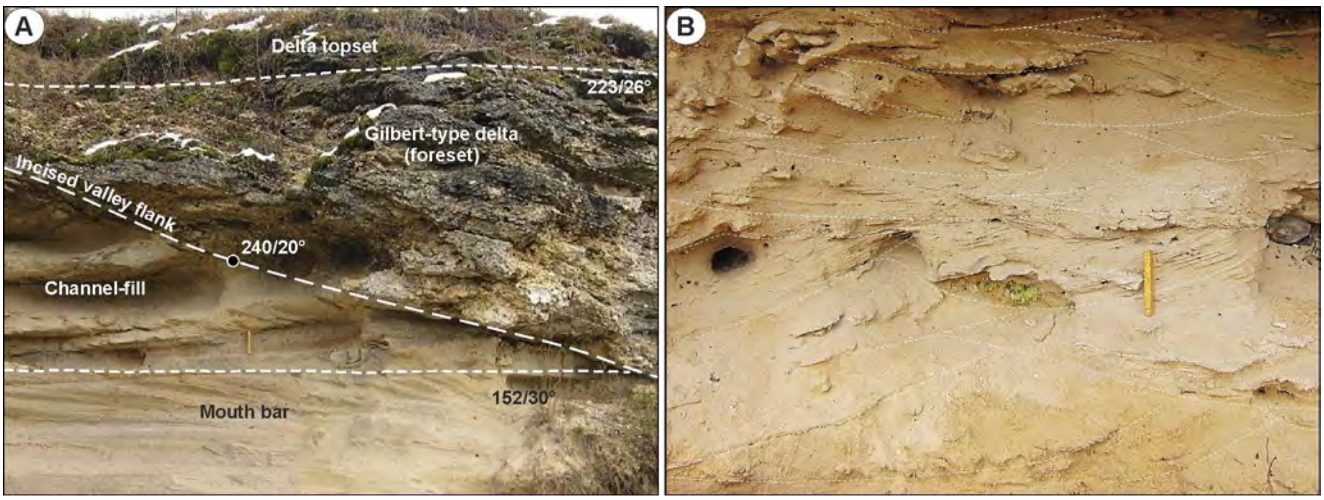

Fig. 19. (**A**) Deposits of a sandy shoal-water delta exposed beneath the incised palaeovalley floor at stop A1.7 (Figs 1B, 17 and 18, upper panel). Note also the nucleation point of the overlying valley-fill Gilbert-type delta. (**B**) Bedding architecture in the transverse outcrop section at stop A1.7 (Figs 1B, 17), approximately perpendicular to the incised palaeovalley, located 22 m to the south of the longitudinal section shown in Fig. 18. The delta foreset here is dipping towards the viewer. The photograph shows details of the delta-toe sandstones with spoon-shaped scour-and-fill strata sets cross-cutting one another; the yellow measuring stick (scale) is 12 cm.

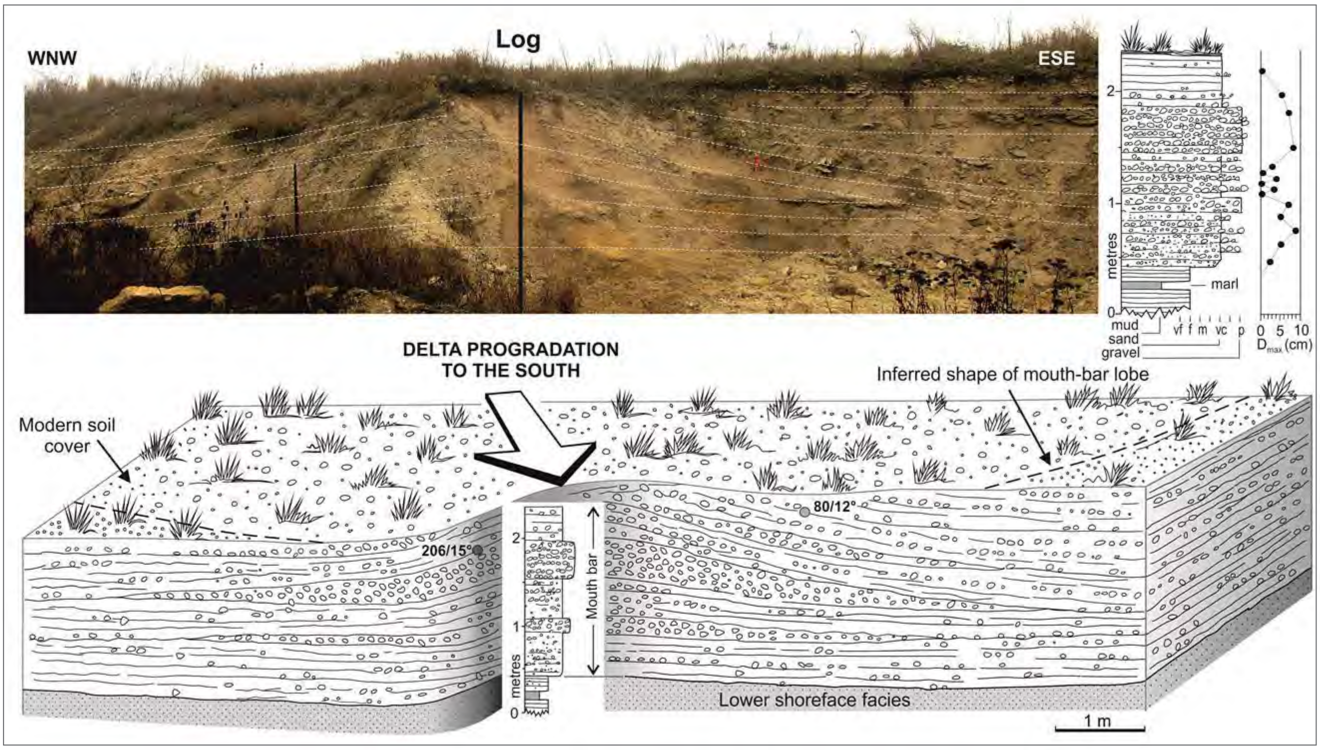

Fig. 20. Mouth bar of a gravelly shoal-water lowstand delta formed at the southern extension of the incised valley seen at stop A1.7. Outcrop at locality 12 in Fig. 5D, south of A1.7, not included in the excursion programme. From Leszczyński and Nemec (2015).

ward progradation of valley-filling delta was disturbed by a gravitational collapse of the valley's undercut western wall, recorded as a large mound of sedimentary breccia (Fig. 18, lower middle panel; see also Plate 3 and discussion in Leszczyński and Nemec, 2015). In a transverse outcrop section, the delta-toe pebbly sandstones show multiple scoop-shaped scour-and-fill features, 40–70 cm deep and a few metres wide, cross-cutting one another (Fig. 19B). Similar features, resembling trough cross-stratification and referred to as 'spoon-shaped depressions', were recognized at the toes of many modern and ancient Gilbert-type deltas (e.g., Breda *et al.*, 2007, 2009).

Stop A1.8 Escarpment along another fish pond in the south-eastern part of Młyny, less than 1km SE of previous stop

(50° 32′52″ N; 20° 43′50″ E; Fig. 17); access by footpath through private farm.

The small outcrops here – lateral to that at stop A1.7 – show a regressive shoreface to foreshore succession corresponding to the shoal-water delta and subsequent lowstand phase at the previous locality. The succession shows further the record of a brief marine transgression, coeval with the drowning of the incised valley at locality A1.7, followed by rapid shoreline progradation coeval with the advance of Gilbert-type bayhead delta at this adjacent locality (for outcrop details, see Leszczyński and Nemec, 2015, fig. 14).

Stop A1.9 An abandoned quarry in the hamlet of Schodnia, west of Młyny

(50°32′56″ N, 20°42′40″ E; Fig. 17); outcrop on the S side of local asphalt road

The quarry western wall, 4 m high (Fig. 21A), shows regressive foreshore deposits at the southern reaches of the mid-Serravalian regressive shoreline (see Fig. 5D) overlain by a gravelly transgressive lag and sandy transgressive shoreface deposits. The foreshore (strandplain) deposits form a foreset of steeply southwards-inclined granule to pebbly very coarse sand (Fig. 21B), underlain by coarse-sand upper-shoreface deposits (Fig. 21, log). The foreshore deposits are erosionally overlain by a transgressive lag of coarse-pebble gravel with small cobbles and numerous intraformational clasts (Fig. 21C). The overlying pebbly sandstones include an isolated set of planar cross-strata, ca. 70 cm thick, dipping towards the WSW (Fig. 21, log) and probably representing a longshore bar (see Allen, 1982). The overlying fining-upwards sandstones (Fig. 21, log) represent a transgressive shoreface succession (a relatively rare case, seldom reported from stratigraphic record, as most marine transgressions are erosive, rather than depositional).

Stop A1.10 Escarpment behind the roadside inn 'Leśna Chata' near Skorzów

(50°31′51″ N, 20°43′48″ E; Fig. 22)

The outcrop shows regressive shoreface deposits of a wave-worked, shoal-water spit platform at the distal eastern tip of a younger spit system formed farther to the south (Fig. 5D, E). The medium- to coarse-grained, parallel-stratified sandstones are inclined at 15–18° to the ESE and show at least one major surface of erosion and reactivation (Fig. 23A). Such an unusually high shoreface

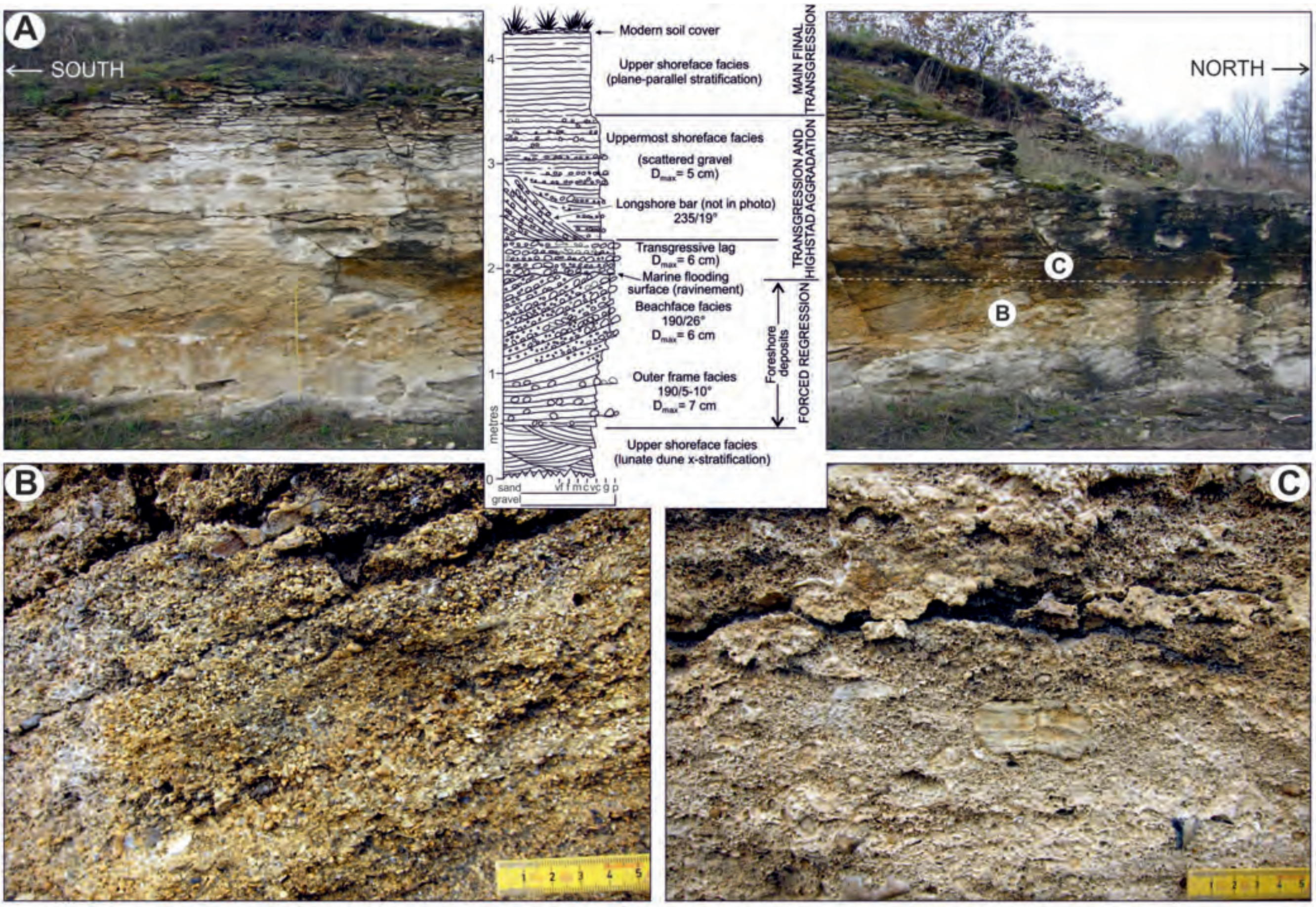

Fig. 21. (**A**) Outcrop photograph and a corresponding interpreted log of the deposits exposed at stop A1.9 (Figs 1B, 17). The yellow measuring stick is 1 m. The numerical values in the log are the strata dip azimuth and angle, and D_{max} is the maximum clast size. The close-up details show: (**B**) the cross-stratified well-sorted foreshore granule gravel and (**C**) the weakly planar-stratified transgressive gravel lag with scattered flat-lying marlstone clasts; the visible part of measuring stick is 5.5 cm.

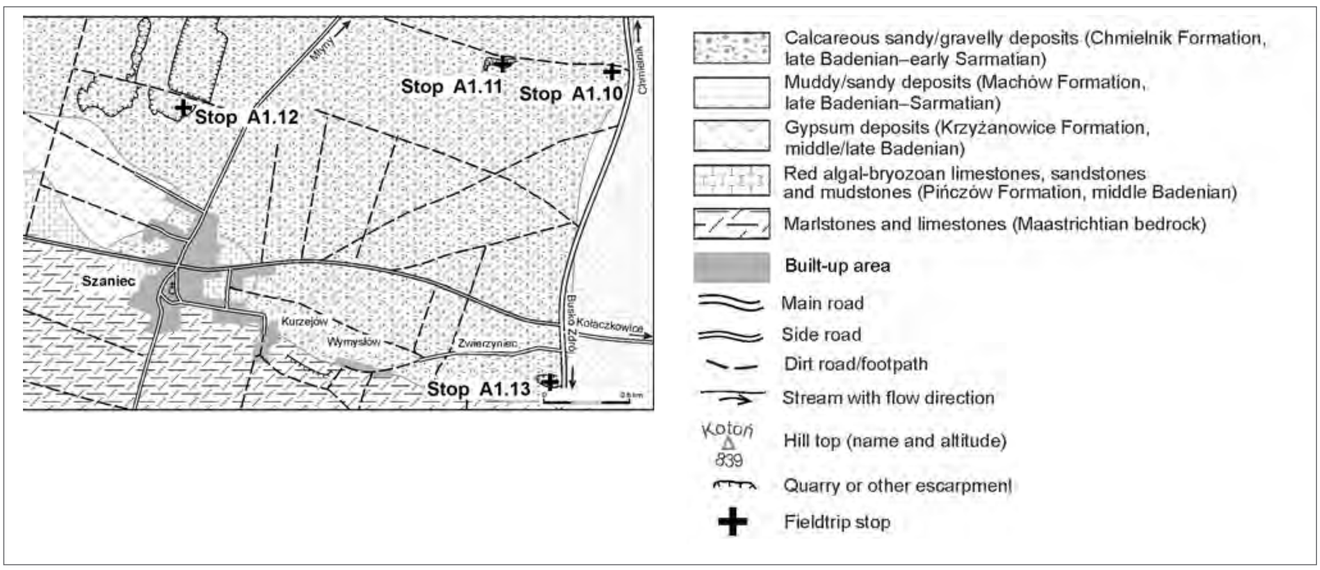

Fig. 22. Geological map showing detailed location of the field-trip stops A1.10–13 (modified from Instytut Geologiczny, 1961).

inclination is characteristic of spit platforms (see Plate 2B; Nielsen and Johannessen, 2008). The surface of erosion and reactivation is attributed to a rare violent storm event. The underlying fine-grained, parallel-stratified and wave-ripple cross-laminated sandstones show thin mudstone interlayers, indicating lower shoreface onto which the spit system advanced (see Fig. 23B).

Stop A1.11 Abandoned quarry 800 m to the west of stop A1.10

(50°31′52″ N, 20°43′12″ E; see Fig. 22); access by footpath from 'Leśna Chata' along a small valley.

The outcrop shows slightly more proximal deposits of the same late-stage spit system (Fig. 23B). Regressive upper-shoreface sandstones of the spit platform are

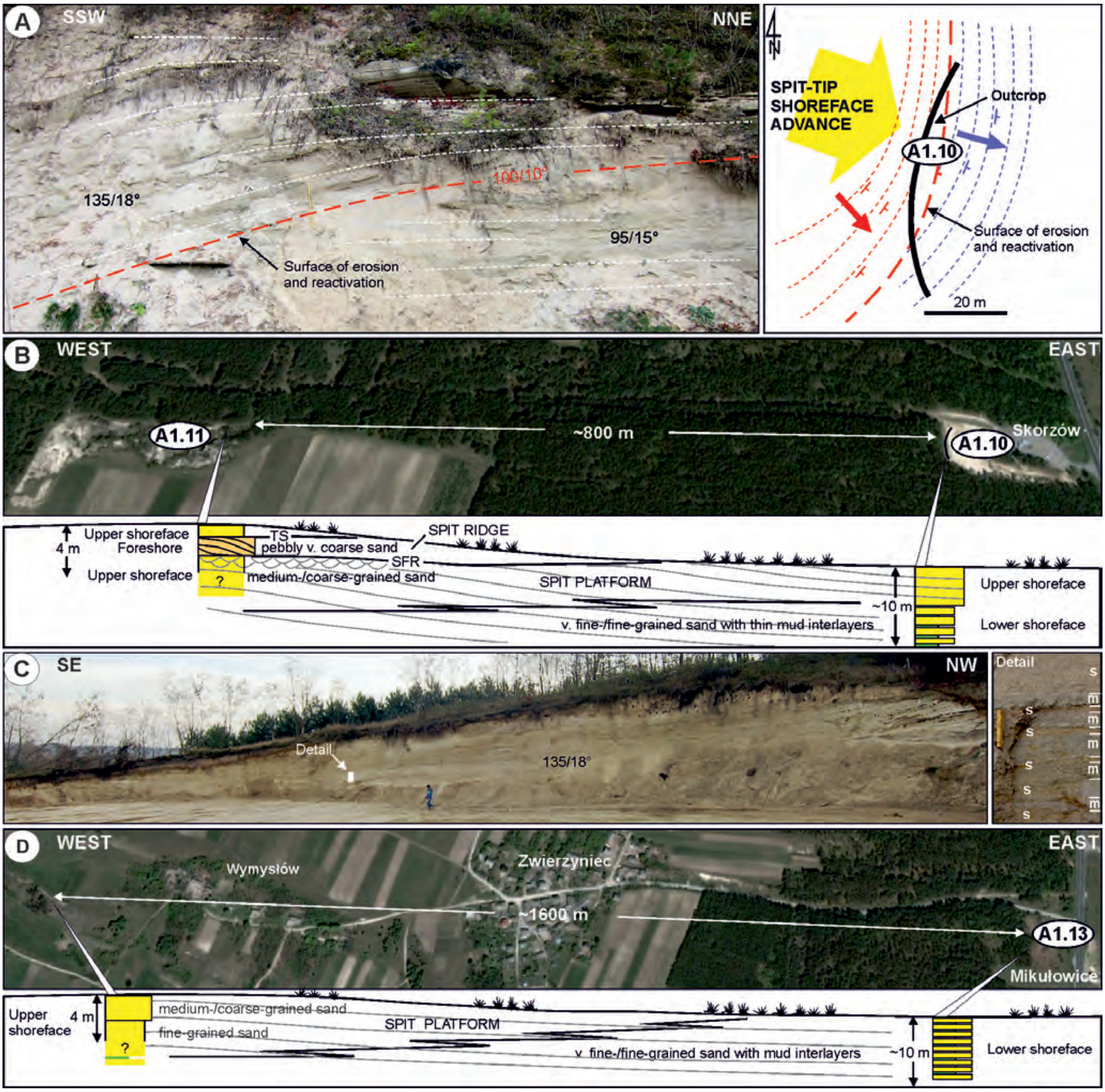

Fig. 23. (**A**) Wave-worked upper shoreface sandstones of the ESE-extended spit platform at stop A1.10 (Figs. 1B, 22); the relatively steep shoreface here was truncated by storm erosion and reactivated by spit re-advance (see the inset plan-view sketch of strata attitude). (**B**) Correlation of the spit-platform deposits at stop A1.10 with those at stop A1.11 (Figs 1B, 22), where the spit-ridge foreshore facies overlie spit-platform shoreface sandstones and are transgressively covered by similar shoreface facies. Letter symbols: SFR – surface of forced regression; TS – transgression surface. (**C**) Clinoform-bedded lower shoreface deposits at the southern flank of the same spit platform, exposed at stop A1.13 (Figs 1B, 22); the inset outcrop detail shows wave-worked fine-grained sandstones (s) intercalated with thin mudstone (m) and sporadic marlstone layers. (**D**) Correlation of the deposits at stop A1.13 with the upper-shoreface sandstones of spit platform exposed ca. 1.6 km to the west in the village of Wymysłów (Fig. 22). Land surface images from Google Earth. From Leszczyński and Nemec (2015).

overlain by spit-ridge pebbly foreshore sandstones (2 m thick) of the east-advancing spit bar. Foreshore strata are inclined at 15–20° to the ESE, with numerous flatter (5–10°) reactivation surfaces attributed to storm wave erosion. A gravel-paved ravinement surface and transgressive shoreface deposits at the top (Fig. 23B) are record of marine drowning – coeval with the ultimate transgression at stop A1.9.

Stop A1.12 Abandoned quarry on the hill Góra Kamnica north of Szaniec

(50°31′45″ N; 20°41′23″ E; Fig. 22); access by a short (400 m) dirt road to the W of the asphalt road Szaniec–Młyny

The deposits here represent an early development stage of the same southern spit system (stops A1.10 and A1.11), when it was initially dominated by tidal currents (Fig. 5C). The spit-ridge deposits are a succession of medium- to coarse-grained sandstones, ca. 3 m thick, with bidirectional (E–W) dune cross-stratification. They are underlain by poorly exposed spit-platform sandstones inclined eastwards at ca. 10° and showing plane-parallel stratification with subordinate wave-ripple cross-lamination and trough cross-stratification. The platform shoreface deposits, apparently uplifted by a local minor fault, are better exposed on the opposite side of the quarry.

Stop A1.13 Sand pit between the villages of Mikułowice and Zwierzyniec

(50°30′47″ N; 20°43′27″ E; Fig. 22), on the W side of main road 73.

The outcrop (Fig. 23C) shows regressive lower-shoreface deposits of distal spit platform (Fig. 23D) on the southern flank of the same spit system as seen at stops A1.10–12 (Fig. 22C, D). Characteristic is the unusual steep inclination (up to 18°) of the fine-grained, parallel-stratified and wave-ripple cross-laminated sandstones with thin mudstone interlayers. Microfauna is marine, but the deposits include horizons rich in terrestrial and freshwater gastropods. The malacofauna comprises aquatic and typical hygrophilous elements from coastal wetland habitats, some xerophilous species from dry open environments and gastropods from subtropical woodland (Stworzewicz *et al.,* 2013). The non-marine fauna was apparently derived from land by rain-wash and spread episodically by storms and tidal currents. The northern Paratethys in mid-Serravalian experienced the first spell of relatively warm and rainy climatic conditions heralding the Tortonian phases of 'washhouse' climate (Böhme *et al*., 2008).

References

Agarwal, K., Singh, I., Sharma, M., Sharma, S. & Rajagopalan, G., 2002. Extensional tectonic activity in the cratonward parts (peripheral bulge) of the Ganga Plain foreland basin, India. *International Journal of Earth Science,* 91: 897–905.

Alexandrowicz, S.W., Garlicki, A. & Rutkowski, J., 1982. Podstawowe jednostki litostratygraficzne miocenu zapadliska przedkarpackiego. *Kwartalnik Geologiczny*, 26: 470–471. [In Polish.]

Allen, J. R. L., 1982. *Sedimentary Structures: Their Character and Physical Basis, Volume 2. Developments in Sedimentology*, 30B. Elsevier, Amsterdam, 643 pp.

Allen, P. A. & Allen, J. R., 2005. *Basin Analysis: Principles and Applications*. 2nd Edn, Blackwell Publishing, Oxford, 549 pp.

Beaumont, C., 1981. Foreland basins. *Geophysical Journal of the Royal Astronomical Society*, 65: 291–329.

Bluck, B. J., 1999. Clast assembling, bed-forms and structure in gravel beaches. *Transactions of the Royal Society of Edinburgh, Earth Sciences*, 89: 291–323.

Böhme, M., Ilg, A. & Winklhofer, M., 2008. Late Miocene "washhouse" climate in Europe. *Earth and Planetary Science Letters*, 275: 393–401.

Breda, A., Mellere, D. & Massari, F., 2007. Facies and processes in a Gilbert-delta-filled incised valley (Pliocene of Ventimiglia, NW Italy). *Sedimentary Geology*, 200: 31–55.

Breda, A., Mellere, D., Massari, F. & Asioli, A., 2009. Vertically stacked Gilbert-type deltas of Ventimiglia (NW Italy): the Pliocene record of an overfilled Messinian incised valley. *Sedimentary Geology*, 219: 58–76.

Catuneanu, O., Hancox, P. J. & Rubidge, B. S., 1998. Reciprocal flexural behaviour and contrasting stratigraphies: a new basin development model for the Karoo retroarc foreland system, South Africa. *Basin Research*, 10: 417–439.

Catuneanu, O. & Sweet, A. R., 1999. Maastrichtian-Paleocene foreland-basin stratigraphies, western Canada: a reciprocal sequence architecture. *Canadian Journal of Earth Sciences*, 36: 685–703.

Clifton, H. E., 1981. Progradational sequences in Miocene shoreline deposits, southeastern Caliente Range, California. *Journal of Sedimentary Petrology*, 51: 165–184.

Clifton, H. E. & Dingler, J. R., 1984. Wave-formed structures and paleoenvironmental reconstruction. *Marine Geology*, 60: 165–198.

Clifton, H. E., Hunter, R. E. & Phillips, R. L., 1971, Depositional structures and processes in the non-barred high energy nearshore. *Journal of Sedimentary Petrology*, 41: 651–670.

Currie, B. S., 1997. Sequence stratigraphy of nonmarine Jurassic-Cretaceous rocks, central Cordilleran foreland-basin system. *Geological Society of America Bulletin*, 109: 1206–1222.

Czapowski, G., 1984. Osady barierowe w górnym miocenie południowego obrzeżenia Gór Świętokrzyskich. *Przegląd Geologiczny,* 32: 185–194. [In Polish, with English summary.]

Czapowski, G., 2004. Otoczenie Gór Świętokrzyskich. In: Peryt, T. M. & Piwocki, M. (eds), *Budowa Geologiczna Polski, Tom I. Stratygrafia, Część 3a: Kenozoik*. Państwowy Instytut Geologiczny, Warszawa, pp. 239–245. [In Polish.]

Czapowski, G. & Studencka, B., 1990. Studium sedymentologiczno-paleontologiczne osadów barierowych dolnego sarmatu w rejonie Chmielnika (południowe obrzeżenie Gór Świętokrzyskich). *Przegląd Geologiczny*, 38: 117–126. [In Polish, with English summary.]

DeCelles, G. P. & Currie, B. S., 1996. Long-term sediment accumulation in the Middle Jurassic-early Eocene Cordilleran retroarc foreland-basin system. *Geology*, 24: 591–594.

De Leeuw, A., Bukowski, K., Krijgsman, K. & Kuiper K. F., 2010. Age of the Badenian salinity crisis; impact of Miocene climate variability on the circum-Mediterranean region. *Geology*, 38: 715–718.

Dudziak, J. & Łaptaś, A., 1991. Stratigraphic position of Miocene carbonate-siliciclastic deposits near Chmielnik (Świętokrzyskie Mountains area, central Poland) based on calcareous nannofossils. *Bulletin of the Polish Academy of Sciences, Earth Sciences*, 39: 55–66.

Dumas, S. & Arnott, R. W. C., 2006. Origin of hummocky and swaley cross-stratification – the controlling influence of unidirectional current strength and aggradation rate. *Geology*, 34: 1073–1076.

Dziadzio, P., 2000. Sekwencje depozycyjne w utworach badenu i sarmatu w SE części zapadliska przedkarpackiego. *Przegląd Geologiczny*, 48: 1124–1138. [In Polish, with English abstract.]

Dziadzio, P., Maksym, A. & Olszewska, B., 2006. Sedymentacja utworów miocenu we wschodniej części zapadliska przedkarpackiego. *Przegląd Geologiczny*, 54: 413–420. [In Polish, with English abstract.]

Ettensohn, F. R., 1994. Tectonic control on formation and cyclicity of major Appalachian unconformities and associated stratigraphic sequences. In: Dennison, J. M. & Ettensohn, F. R. (eds), *Tectonic and Eustatic Controls on Sedimentary Cycles. SEPM Concepts in Sedimentology and Paleontology*, 4: 217–242.

Flemings, P. B. & Jordan, T. E., 1989. A synthetic stratigraphic model of foreland basin development. *Journal of Geophysical Research*, 94 (B4): 3853–3866.

Flemings, P. B. & Jordan, T. E., 1990. Stratigraphic modeling of foreland basins: interpreting thrust deformation and lithosphere rheology. *Geology*, 18: 430–434.

Garecka, M. & Olszewska, B., 2011. Correlation of the Middle Miocene deposits in SE Poland and western Ukraine based on foraminifera and calcareous nannoplankton. *Annales Societatis Geologorum Poloniae*, 81: 309–330.

Górka, M., 2008. „Sarmat detrytyczny" wschodniego Ponidzia: litofacje i środowiska sedymentacji. In: Wojewoda, J. (ed.), *Baseny śródgórskie: kontekst regionalny środowisk i procesów sedymentacji*. Materiały konferencyjne POKOS'3 (Kudowa Zdrój). WIND, Wrocław, pp. 5–6. [In Polish.]

Hampson, G. J., 2000. Discontinuity surfaces, clinoforms, and facies architecture in a wave-dominated, shoreface-shelf parasequence. *Journal of Sedimentary Research*, 70: 325–340.

Helland-Hansen, W., 2009. Towards the standardization of sequence stratigraphy: Discussion. *Earth-Science Reviews*, 94: 95–97.

Hilgen, F. J., Lourens, L. J., Van Dam, J. A., Beu, A. G., Boyes, A. F., Cooper, R. A., Krijgsman, W., Ogg, J. G., Piller, W. E. & Wilson, D. S., 2012. The Neogene Period.

In: Gradstein, F. M., Ogg, J. G., Schmitz, M. D. & Ogg, G. M. (eds), *The Geologic Time Scale 2012*. Elsevier, Amsterdam, pp. 923–978.

Instytut Geologiczny, 1961. *Mapa geologiczna regionu świętokrzyskiego bez utworów czwartorzędowych 1:200 000*. Wydawnictwa Geologiczne, Warszawa.

Jasionowski, M., 1997. Zarys litostratygrafii osadów mioceńskich wschodniej części zapadliska przedkarpackiego. *Biuletyn Państwowego Instytutu Geologicznego*, 375: 43–60. [In Polish, with English abstract.]

Jasionowski, M., 2006. Facies and geochemistry of Lower Sarmatian reefs along the northern margins of the Paratethys in Roztocze (Poland) and Medobory (Ukraine) regions: paleoenvironmental implications. *Przegląd Geologiczny*, 54: 445–454. [In Polish, with English abstract.]

Jasionowski, M., Peryt T. & Czapowski, G., 2004. Miocen. In: Peryt, T. M. & Piwocki, M. (eds), *Budowa Geologiczna Polski, Tom I. Stratygrafia, Część 3a: Kenozoik*. Państwowy Instytut Geologiczny, Warszawa, pp. 213–224. [In Polish.]

Jordan, T. E. & Flemings, P. B., 1991. Large-scale stratigraphic architecture, eustatic variation, and unsteady tectonism: a theoretical evaluation. *Journal of Geophysical Research*, 96: 6681–6699.

Komar, P. D. & Miller, M., 1975. The initiation of oscillatory ripple marks and the development of plane-bed at high shear stresses under waves. *Journal of Sedimentary Petrology*, 45: 697–703.

Kováč, M., Nagymarosy, A., Oszczypko, N., Csontos, L., Ślączka, A., Marunteanu, M., Matenco, L. & Marton, E., 1998. Palinspastic reconstruction of the Carpathian–Pannonian region during the Miocene. In: Rakus, M. (ed.), *Geodynamic Development of the Western Carpathians*. Geological Survey of Slovak Republic, Dionyz Stur Publisher, Bratislava, pp. 189–217.

Kowalewski, K., 1958. Miocene stratigraphy of southern Poland with special attention paid to the southern margin of the Święty Krzyż Mountains. *Kwartalnik Geologiczny*, 2: 3–27. [In Polish, with English abstract.]

Kwiatkowski, S., 1972. Sedymentacja gipsów mioceńskich południowej Polski. *Prace Muzeum Ziemi*, 19: 3–94. [In Polish.]

Leszczyński, S. & Nemec, W., 2015. Dynamic stratigraphy of composite peripheral unconformity in a foredeep basin. *Sedimentology*, 62: 645–680.

Łaptaś, A., 1992. Giant-scale cross-bedded Miocene biocalcarenites at the northern margin of the Carpathian foredeep. *Annales Societatis Geologorum Poloniae*, 62: 149–167.

Łuczkowska, E., 1964. The micropaleontological stratigraphy of the Miocene in the region Tarnobrzeg-Chmielnik. *Prace Geologiczne Polskiej Akademii Nauk, Komitet Nauk Geologicznych*, 20: 1–72. [In Polish, with English summary.]

Massari, F. & Parea, G. C., 1988. Progradational gravel beach sequences in a moderate- to high-energy, microtidal marine environment. *Sedimentology*, 35: 881–913.

Meistrell, F. J., 1972. The spit-platform concept: laboratory observation of spit development. In: Schwartz, M. L. (ed.), *Spits and Bars*. Dowden, Hutchinson & Ross, Stroudsburg (PA), pp. 225–283.

Nielsen, L. H. & Johannessen, P. N., 2008. Are some isolated shelf sandstone ridges in the Cretaceous Western Interior Seaway transgressed, detached spit systems? In: Hampson, G. J., Steel, R. J., Burgess, P. M. & Dalrymple, R. W. (eds), *Recent Advances in Models of Siliciclastic Shallow-Marine Stratigraphy. SEPM Special Publications*, 90: 349–370.

Nielsen, L. H., Johannessen, P. N. & Surlyk, F., 1988. A Late Pleistocene coarse-grained spit-platform sequence in northern Jylland, Denmark. *Sedimentology*, 35: 915–937.

Olszewska, B., 1999. Biostratigraphy of Neogene in the Carpathian Foredeep in the light of new micropalaeontological data. *Prace Państwowego Instytutu Geologicznego*, 168: 9–28. [In Polish, with English abstract.]

Oszczypko, N., 1998. The Western Carpathian Foredeep – Development of a foreland basin in front of the accretionary wedge and its burial history (Poland). *Geologica Carpathica*, 40: 1–18.

Oszczypko, N., 2004. The structural position and tectonosedimentary evolution of the Polish Outer Carpathians. *Przegląd Geologiczny*, 52: 780–791.

Oszczypko, N., Krzywiec, P., Popadyuk, I. & Peryt, T., 2006. Carpathian Foredeep Basin (Poland and Ukraine): its sedimentary, structural and geodynamic evolution. In: Golonka, J. & Picha, F. J. (eds), *The Carpathians and Their Foreland: Geology and Hydrocarbon Resources. AAPG Memoirs,* 84: 293–350.

Oszczypko, N., Olszewska, B., Ślęzak, J. & Strzępka, J., 1992. Miocene marine and brackish deposits of the Nowy Sącz Basin (Polish Western Carpathians) – new lithostratigraphic and biostratigraphic standards. *Bulletin of the Polish Academy of Sciences, Earth Sciences*, 40: 83–96.

Peryt, D., 1987. Middle Miocene calcareous nannoplankton stratigraphy of the Roztocze region (SE Poland). *Bulletin of the Polish Academy of Sciences, Earth Sciences*, 35: 391–401.

Peryt, D., 1997. Calcareous nannoplankton stratigraphy of the Middle Miocene in the Gliwice area (Upper Silesia, Poland). *Bulletin of the Polish Academy of Sciences, Earth Sciences*, 45: 119–131.

Peryt, T. M., 2006. The beginning, development and termination of the Middle Miocene Badenian salinity crisis in Central Paratethys. *Sedimentary Geology*, 188-189: 379–396.

Piller, W. E., Harzhauser, M. & Mandic, O., 2007. Miocene Central Paratethys stratigraphy – current status and future directions. *Stratigraphy*, 4: 151–168.

Porębski, S. J., Pietsch, K., Hodiak, R. & Steel, R. J., 2003. Origin and sequential development of Upper Badenian–Sarmatian clinoforms in the Carpathian Foredeep Basin, SE Poland. *Geologica Carpathica*, 54: 119–136

Reuter, M., Piller, W. E. & Richoz, S., 2012. The dispersal of *Halimeda* in northern hemisphere mid-latitudes: palaeobiogeographical insights. *Perspectives in Plant Ecology, Evolution and Systematics*, 14: 303–309.

Rögl, F., 1998. Palaeogeographic considerations for Mediterranean and Paratethys seaways (Oligocene to Miocene). *Annalen des Naturhistorischen Museums in Wien,* 99A: 279–310.

Rögl, F., 1999. Mediterranean and Paratethys: facts and hypotheses of an Oligocene to Miocene paleogeography (short overview). *Geologica Carpathica*, 50: 339–349.

Rutkowski, J., 1976. Detrital Sarmatian deposits on the southern margin of the Holy Cross Mountains (southern Poland). *Prace Geologiczne*, Polska Akademia Nauk – Oddział w Krakowie, Komisja Nauk Geologicznych, 100: 71p. [In Polish, with English abstract.]

Rutkowski, J., 1981. The tectonics of miocene sediments of the western part of the Połaniec graben (Carpathian foredeep, southern Poland). *Annales Societatis Geologorum Poloniae*, 5l: 117–131. [In Polish, with English abstract.]

Sinclair, H. D., 1997. Tectonostratigraphic model for underfilled peripheral foreland basins: an Alpine perspective. *Geological Society of America Bulletin*, 109: 324–346.

Sinclair, H. D., Coakley, B. J., Allen, P. A. & Watts, A. B., 1991. Simulation of foreland basin stratigraphy using a diffusion model of mountain belt uplift and erosion: an example from the Central Alps, Switzerland. *Tectonics*, 10: 599–620.

Snedden, J. W. & Liu, C., 2010. A compilation of Phanerozoic sea-level change, coastal onlaps and recommended sequence designations. *AAPG Search and Discovery, Article* 40594, 3 pp.

Stachacz, M., 2007. Remarks on age of the Middle Miocene deposits in the Szydłów area (southern margin of the Holy Cross Mountains). *Przegląd Geologiczny,* 55: 168–174. [In Polish, with English abstract.]

Stworzewicz, E., Prisyazhnyuk, V. A. & Górka, M., 2013. Systematic and palaeoecological study of Miocene terrestrial gastropods from Zwierzyniec (southern Poland). *Annales Societatis Geologorum Poloniae*, 83: 179-200.

Wysocka, A., 1999. Depositional and tectonic controls on Early Badenian clastic sedimentation in the Sandomierz–Tarnobrzeg area (Baranów Beds, northern Carpathian Foredeep). *Geological Quarterly*, 43: 383–394.

Zastawniak, E., 1974. Die Blätterflora der sarmatischen Sedimente des südlichen Rendgebietes des Heiligenkreuzgebirge (Góry Świętokrzyskie, Mittel-Polen). In: Seneš, J. (ed.), *Chronostratigraphie und Neostratotypen. Miozän der Zentralen Paratethys, IV. M5*. Veda, Briatislava, pp. 663–665.

Zastawniak, E., 1980. Sarmatian leaf flora from the southern margin of the Holy Cross Mts. (south Poland). *Prace Muzeum Ziemi,* 33: 39–107.

The Badenian evaporative stage of the Polish Carpathian Foredeep: sedimentary facies and depositional environment of the selenitic Nida Gypsum succession

Maciej Bąbel[1], Danuta Olszewska-Nejbert[1], Krzysztof Nejbert[1], Damian Ługowski[1]

[1]Faculty of Geology, University of Warsaw
(m.babel@uw.edu.pl, don@uw.edu.pl, knejbert@uw.edu.pl, lugowski.damian@gmail.com)

Route (Fig. 1): From Kraków we drive NE by road 776 to Skalbmierz, then by road 768 to Działoszyce, where we turn onto road 64T to Chroberz. Then by local roads we arrive to the hill near abandoned quarry at **Gacki (A2.1)**. From Gacki we follow east by local roads (ca. 2 km) to the **Leszcze quarry (A2.2)**. From Leszcze south by local roads (ca. 4 km) to **Zagość-Winiary road cut** in the escarpment of the Nida river valley **(A2.3)**. Then by local roads through Skorocice and Siesławice to Busko-Zdrój (ca. 12 km), to hotel "Gromada", Waryńskiego 10. From Busko-Zdrój by local roads to SW, to abandoned quarries at **Siesławice (A2.4)**. From Siesławice to SW by road 973 to the round-about crossing with 776, where we turn right. After ca. 9 km we turn east onto local roads to abandoned gypsum stone pits at Góry Wschodnie nature reserve at **Chotel Czerwony-Zagórze (A2.5)**. After returning to road 776 we continue south to the town of Wiślica (car parks) and walk to **Wiślica-Grodzisko (A2.6)** at the SE outskirts of the town. From Wiślica we drive to NW by local roads to Krzyżanowice Dolne (lunch at OSW Zacisze). From Krzyżanowice Dolne we drive N by local roads through Kowala to Pasturka, then NW by road 767 to Pińczów and by local roads through Włochy to the **Borków quarry (A2.7)**. From Borków eastward by local roads through Pińczów to road 7 (E77) and we follow it to Kraków.

Introduction to the trip

The Nida Gypsum deposits – the record of the Badenian salinity crisis in the northern margin of the Carpathian Foredeep Basin

Maciej Bąbel, Danuta Olszewska-Nejbert

Introduction

The Badenian salinity crisis, known also as the Wielician crisis, was a crucial event in the Miocene history of the Central Paratethys. The Middle Miocene (Badenian) seas occupying the area of the emerging Carpathian orogen lost their open connection with the Mediterranean Sea and were transformed into evaporite basins (Fig. 2A; Peryt, 2006). The widespread evaporite deposition has taken place at that time in the Carpathian Foredeep Basin developing in front of the advancing Carpathian thrust belt (Oszczypko *et al.*, 2006). In this basin gypsum deposits were formed mainly on the broad platformal marginal zone (Fig. 2B).

Bąbel, M., Olszewska-Nejbert, D., Nejbert, K. & Ługowski, D., 2015. The Badenian evaporative stage of the Polish Carpathian Foredeep: sedimentary facies and depositional environment of the selenitic Nida Gypsum succession. In: Haczewski, G. (ed.), *Guidebook for field trips accompanying IAS 31st Meeting of Sedimentology held in Kraków on 22nd–25th of June 2015.* Polish Geological Society, Kraków, pp. 25–50.
Guidebook is available online at www.ing.uj.edu.pl/ims2015

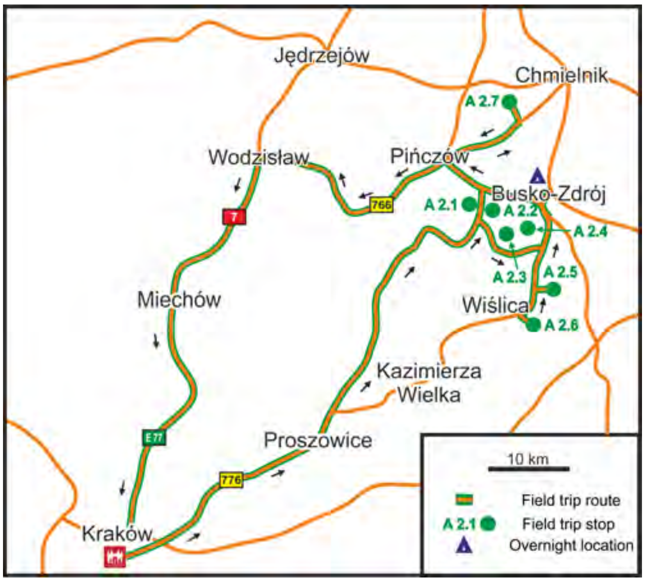

Fig. 1. Route map of field trip A2.

In Poland, the largest group of outcrops is situated in the Nida river valley in the area known as Ponidzie. These evaporites, named the Nida Gypsum deposits, and known also as the Krzyżanowice Formation, are represented by spectacular primary gypsum deposits which include selenite facies comparable to the famous Messinian selenites of the Mediterranean. The Nida Gypsum deposits are the best studied part of the Badenian sulphates in the Carpathian foredeep. Their outcrops offer an excellent insight into ancient sedimentary facies and environments of the giant-selenite dominated margin of the evaporite basin. The presentation of these unique facies is a primary aim of the field trip.

Regional geological background

The Nida Gypsum deposits are a part of the Cenozoic (Miocene) infill of the Carpathian foredeep, which at Ponidzie covers eroded Mesozoic substrate of the southern structural margin of the Holy Cross Mts. The Jurassic and Cretaceous carbonates forming this substrate were tectonically deformed and uplifted during the latest Cretaceous and Paleocene, and were subjected to intensive weathering and erosion in Paleogene and Miocene times (Fig. 3; Jarosiński *et al.*, 2009).

Then, in Badenian time (Middle Miocene, Paratethyan equivalent of late Burdigalian, Langhian and early Serravallian, Fig. 4), the Nida area was flooded with marine transgression coming from the side of the Carpathian foredeep. The biostratigraphic and sedimentologic studies suggest that the marine deposits covering the Mesozoic substrate can represent the second of the three major Badenian transgressive events in the Central Paratethys (i.e. the "major transgressive event within NN5"; Kováč *et al.*, 2007; or "the Mid-Badenian transgression"; Hohenegger *et al.*, 2014), characterized by dominant planktonic foraminiferal assemblages with

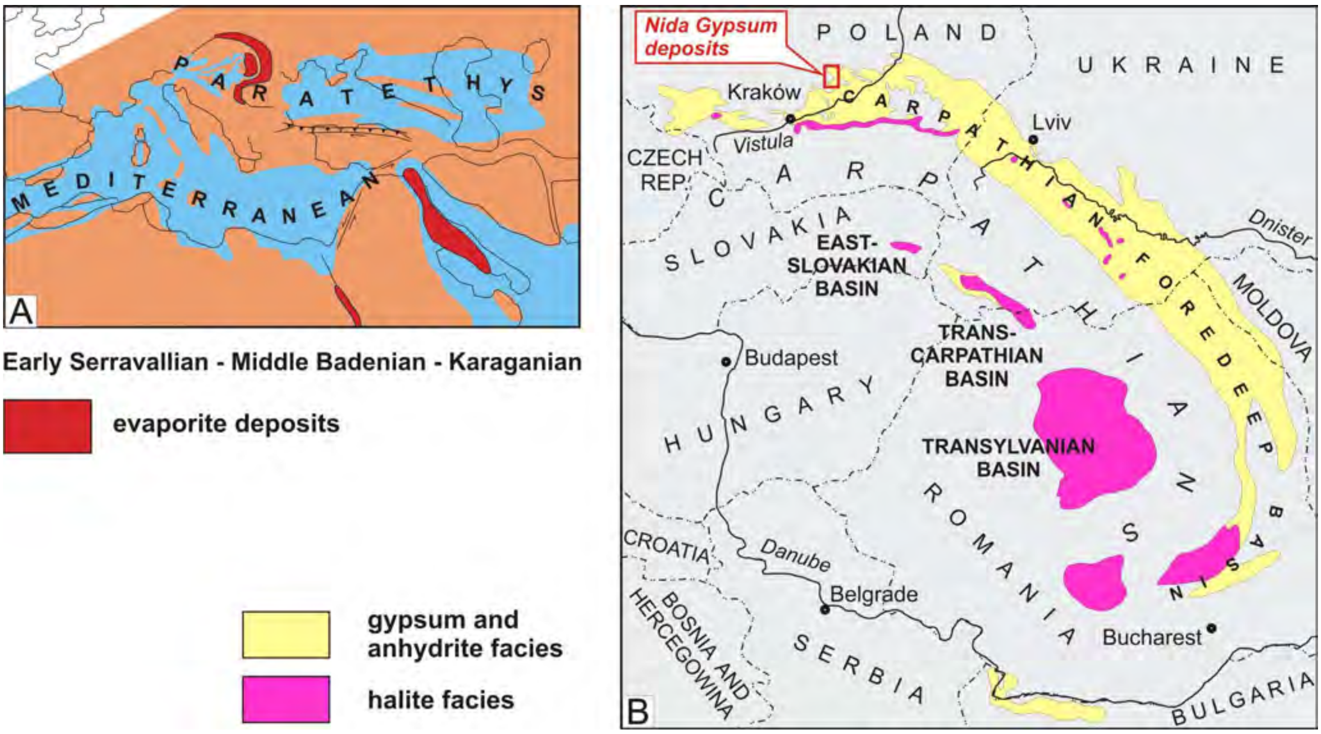

Fig. 2. Palaeogeography during the Badenian salinity crisis (**A** – after Rögl, 1999), and present-day distribution of the Badenian evaporites (**B** – after Khrushchov and Petrichenko, 1979, and other sources).

Fig. 3. Geological map of the Nida Gypsum area, without Pliocene and Quaternary cover, the carbonates enclosed within the Nida Gypsum deposits are shown in blue, after many sources cited in Bąbel (2002b), corrected after Remin (2004, Fig. 1C). Field trip stops A2.1–A2.7 shown with arrows. Broken line shows position of the cross section in Fig. 5B.

Praeorbulina glomerosa circularis (Blow) and *Orbulina suturalis* Brönnimann (Alexandrowicz, 1979; Osmólski, 1972; Dudziak and Łuczkowska, 1992; Kováč *et al.*, 2007; D. Peryt, 2013a; Paruch-Kulczycka, 2015). The deposition of the Badenian evaporites in the Ponidzie region started later and has been arrested by the next marine flooding, correlated with the last major transgressive event in the Central Paratethys, in late Badenian (Kováč *et al.*, 2007). In Ponidzie this last Badenian transgression has led to deposition of marine marls of the Pecten Beds overlying the gypsum deposits (Śliwiński *et al.*, 2012).

Miocene Central Paratethyan stratigraphy

The Neogene (Miocene) Central Paratethys was poorly connected with the ocean. Restricted faunal exchange and evolution of endemic species hamper biostratigraphic correlations between the Paratethyan and the Mediterranean deposits. The Neogene stratigraphy of the Central Parathetys is established according to the local stratigraphic scale and the deposits discussed during the field trip embrace two regional Paratethyan stages: the Badenian and the Sarmatian. The chronology of the Badenian, its subdivision into substages, and the age of the Badenian-Sarmatian boundary, are highly controversial and are a subject of the ongoing debate (Fig. 4; Kováč *et al.*, 2007; Śliwiński *et al.*, 2012; Hohenegger *et al.*, 2014; Wagreich *et al.*, 2014). In this paper we use the traditional subdivision of the Badenian in the Polish Carpathian Foredeep into the Lower, Middle and Upper Badenian, where the Middle Badenian is coeval with the time of evaporite deposition.

Chronology of the Badenian salinity crisis

Biostratigraphic and radiometric data indicate that in the Carpathian Foredeep Basin, the salinity crisis took place in the earliest part of the Neogene Nannoplankton Zone 6 (NN6: *Discoaster exilis* Zone), i.e. in the earliest Serravallian (Peryt, 1999; Garecka and Olszewska, 2011), and it lasted much less than 940 ky (Śliwiński *et al.*, 2012). Sedimentological data suggest that the crisis

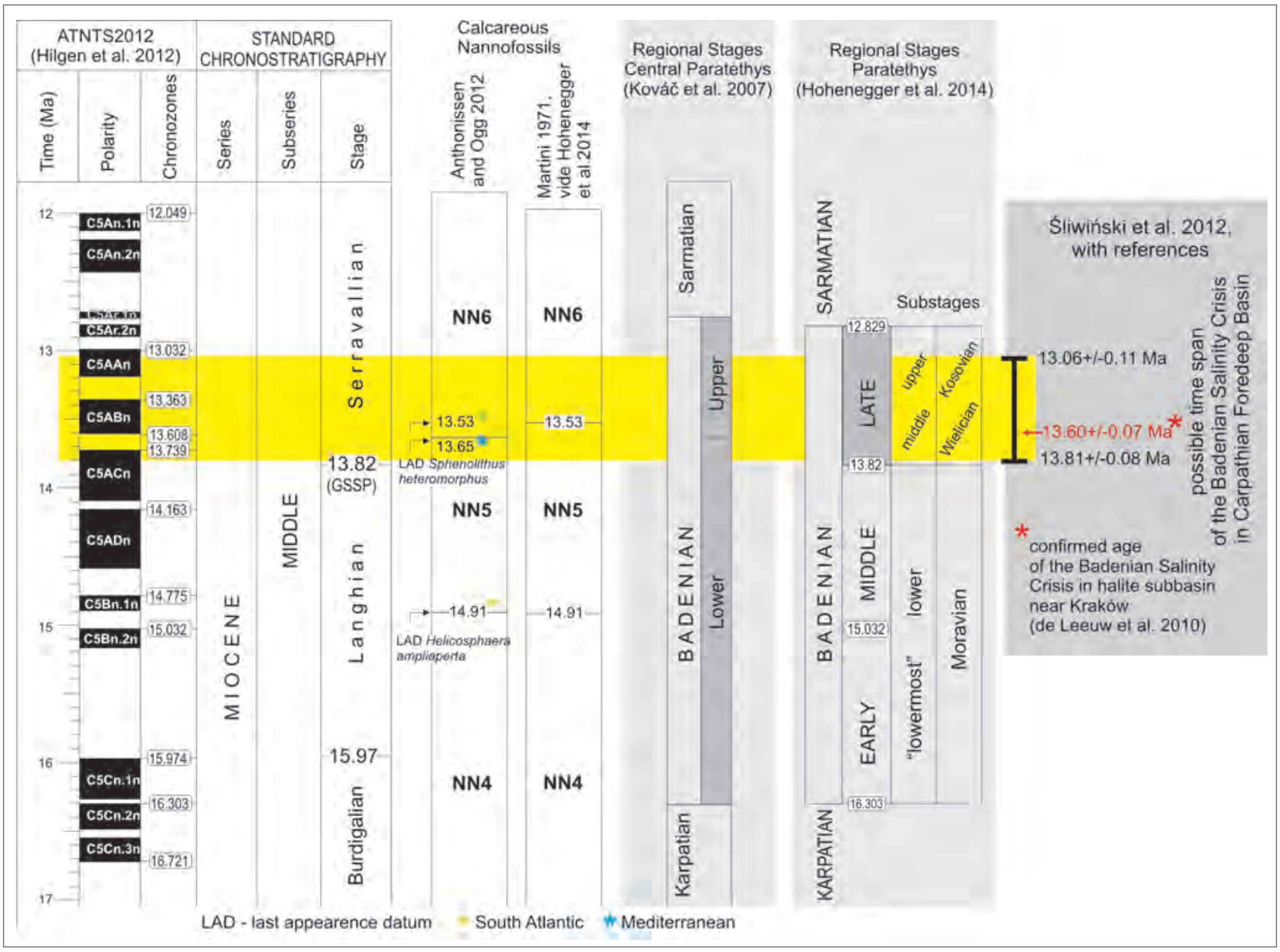

Fig. 4. Stratigraphy of the Middle Miocene regional Central Paratethys stages, according to selected current concepts, compared to the standard Mediterranean stages; chronology of the Badenian salinity crisis in the Carpathian foredeep shown in the last right column.

could be very short, only 20–40 ky in duration. According to radiometric dating of the pyroclastic deposits underlying, overlying and intercalating the evaporites in the Carpathian Foredeep, deposition of the Badenian evaporites started shortly after ca. 13.81±0.08 Ma, their deposition continued at ca. 13.60±0.07 Ma, and it ended before ca. 13.06±0.11 Ma (Fig. 4; de Leeuw *et al.*, 2010; Bukowski, 2011; Śliwiński *et al.*, 2012). The salinity crisis was apparently preceded by climate cooling correlated with the global oxygen isotope event Mi3b (de Leeuw *et al.*, 2010; Peryt and Gedl, 2010; D. Peryt 2013a).

Characteristics of the evaporites, paleogeography and model of the basin

The Carpathian Foredeep Basin is the largest Badenian evaporite basin in the Central Paratethys (Fig. 2B). The Badenian evaporites in this basin form one horizon of gypsum, anhydrite and halite deposits, up to a few tens of metres thick. The marginal gypsum deposits include extensive accumulations of selenites. The central axial areas of the basin were dominated by the laminated Ca-sulphate facies, clay and halite. This was presumably deeper zone of the basin (Fig. 5A; Kasprzyk and Ortí, 1998; Bąbel and Bogucki, 2007). The basin comprised several subbasins; halite subbasins along the axis of the foredeep and less pronounced gypsum subbasins in the northern margin of the basin, commonly considered to be a part of a giant sulphate platform or 'shelf' (Kasprzyk and Ortí, 1998). Presumed shoals and islands apparently lay in between and within the subbasins, and their position could change with time. The large area devoid of evaporite deposits, near Rzeszów, was interpreted as an island (Rzeszów Island; Figs 2B, 5A), and the area between this island and the Miechów Upland as a broad uplift or semi-emerged barrier separating sulphate and halite subbasins during deposition of the selenite facies (Becker, 2005; Bąbel and Becker, 2006; Bąbel and Bogucki, 2007). The Nida Gypsum deposits occupied the north side of this barrier, at least during the selenite deposition (Fig. 5A).

The gypsum basin was a depression without open-water connections with the seas and with the water level lowered below the global sea level due to evaporite drawdown a few tens of meters deep (Fig. 11D; Peryt, 2001, 2006; Bąbel, 2004, 2007b; D. Peryt, 2013b). Such an interpretation fits to the fact that the areal extent of the evaporites in the Carpathian Foredeep Basin is remarkably smaller than both, the under- and overlying marine Badenian deposits. This concept fits also geochemical data, and works very well for the event stratigraphic and facies analyses of the gypsum deposits (Bąbel, 2005a, b). The evaporite basin was similar to saline lakes, where water level changes independently on the global seawater level changes, and commonly more rapidly and irregularly than the sea level. Thanks to high accommodation available in such a basin, an extremely shallow water deposition could continue for a long time without any substantial erosion. The Badenian gypsum facies are indeed very similar to those recorded in modern coastal marine salinas (Kasprzyk, 1999).

The Nida Gypsum deposits

The Nida Gypsum deposits occupy the territory of three tectonic units: the Połaniec Trough, the Wójcza-Pińczów Horst, and the Solec Trough (Fig. 3). Formation of these structures is related mainly to the post-evaporitic late Badenian and to some degree to the Sarmatian and later faulting (Czarnocki, 1939; Rutkowski, 1981; Krysiak, 2000; Jarosiński *et al.*, 2009). Gypsum beds lay more or less horizontally and reach the thickness of nearly 52 m in boreholes, though this thickness was not corrected for dip. In Borków quarry, they are 37 m thick, and this is the largest thickness observed in outcrops. The sequence of the Nida Gypsum deposits is bipartite. The upper part is mostly clastic and represented by microcrystalline and fine-grained gypsum. This part of the sequence, called allochthonous, clastic or microcrystalline unit, is mostly eroded, mainly in the Quaternary. The lower part of the sequence is chiefly composed of coarse-crystalline gypsum (selenites) and is called autochthonous or selenite unit. This unit is better preserved and exposed. Anhydrite is absent and clay intercalations are quite common. In some places limestone occurs, and such limestone body at Czarkowy (6 km SSE of Wiślica) contained native sulphur exploited in the 18^{th} through 20^{th} centuries (Fig. 3; Osmólski, 1972).

Stratigraphy of the Badenian gypsum basin

Lithostratigraphy. The gypsum section comprises a set of thin layers showing the same characteristic features, and the same constant sequence in the northern margin of the Carpathian Foredeep Basin from the

Ponidzie region in Poland as far as environs of Horodenka in Ukraine, and also to the Czech Republic. These layers, representing the smallest-scale lithostratigraphic units, have been first recognized in the Nida area by Wala (1980, and earlier papers) who designated them by letters from a to r (Figs 5B, 7A, 8A, 9A, 12A, 17-18). The layers can be grouped into larger lithostratigraphic units recognized by Kubica (1992) in drill cores in the northern part of the Badenian basin, and designated by capital letters from A to G (Figs 5B, 17).

Event stratigraphy. Methodology of event stratigraphy applied to the Badenian gypsum deposits in the entire basin, permitted to recognize several marker beds and to connect them with isochronous basinal events (Peryt, 2001, 2006; Bąbel, 1996, 2005a). Two types of *isochronous surfaces* ("time lines" designated *A, C/D, Tb, Td, G/H, L1, F1*; Figs 5B, 17) were distinguished: *high-quality and low-quality isochronous surfaces*. The former represent short-term events not connected with dissolution and/or erosion. They are represented by dust or ash falls (*Tb, Td*) and growth zoning of selenite crystals (A). Low-quality *isochronous surfaces* are connected to basin-wide events of slowed deposition, non-deposition and/or erosion-dissolution (*C/D, G/H, L1, F1*).

Facies analysis

Facies analysis was performed using the facies definitions based on the original concept of mechanisms of deposition (Mutti and Ricci Lucchi, 1975). In the case of *in situ* grown selenites, the crucial depositional mechanism was syntaxial bottom-growth of crystals. Basing on the main mechanisms of deposition, several facies and subfacies can be distinguished in the Nida Gypsum deposits (which comprise gypsum, clay and carbonate sediments, Tab 1). Only the facies presented during the field trip are described below.

Giant gypsum intergrowths. *Description:* This facies is composed of large crystals (up to 3.5 m long), commonly arranged vertically and forming intergrowths similar to the $\bar{1}01$ twins. The facies does not exhibit layering except for rare dissolution surfaces. Two subfacies are distinguished according to crystal arrangement: the giant intergrowths with palisade and with non-palisade structure. Within the palisade intergrowths, two subordinate subfacies, showing different crystal structures are recognized: the skeletal and the massive intergrowths. The rare clay subfacies is built of isolated intergrowths and their aggregates (<0.5 m in size) placed in black laminated clay.

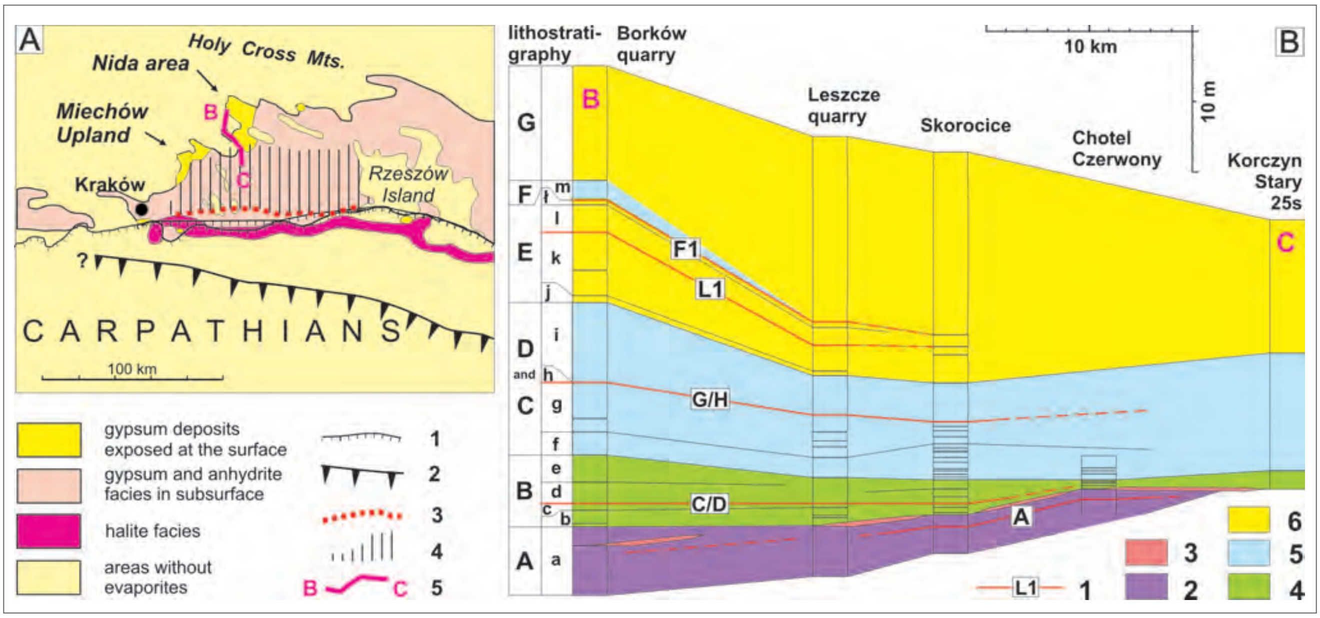

Fig. 5. Palaeogeography of the Badenian evaporite and gypsum basin. **A**) Distribution and palaeogeography of Badenian evaporites in Carpathian Foredeep Basin, 1 – main overthrusts – present-day outer boundary of the Carpathians, 2 – supposed position of the outer boundary of the Carpathians during evaporite deposition, after Ślączka and Kolasa (1997), 3–4 – paleogeographical units (Rzeszów Island is described on the map); 3 – barrier between sulphate and halite subbasins, after Połtowicz (1993), 4 – Miechów-Rzeszów barrier or shoal interpreted by Bąbel and Becker (2006), 5 – cross section shown in B; **B**) stratigraphic cross section of the Nida Gypsum deposits (see Fig. 3 for detailed location of the cross-section); 1 – isochronous surfaces, 2–6 – gypsum facies; 2 – giant intergrowths, 3 – selenite debris, 4 – grass-like facies, 5 – sabre facies, 6 – microcrystalline facies, distribution of facies after Bąbel and Olszewska-Nejbert (2012), simplified; section of the Korczyn Stary 25s borehole after Osmólski (1972).

Interpretation: This facies was created almost exclusively by upward bottom growth of gypsum crystals permanently covered with Ca-sulphate saturated brine (Bąbel, 2007b; see also Fig. 11E). The coarsest crystals, especially those lacking dissolution features, grew in the deepest zones of perennial saline pans, below an average pycnocline, at a depth not accessible to meteoric water. Because of low supersaturation, and/or organic compounds inhibiting the crystallization, gypsum nucleation was sparse and the crystal growth was mostly syntaxial. The protracted period of upward growth led to formation of extraordinarily large crystals. In the clay subfacies, this growth was accompanied by simultaneous clay deposition.

Selenite debris. *Description:* The debris is a mixture of clay and broken, abraded and dissolved crystals, up to 0.5 m long. The debris fills depressions between apices of intergrowths which are flattened by dissolution. The debris is overlain by the grass-like gypsum subfacies with clay intercalations. The deeper depressions contain small aggregates of lenticular crystals grown in situ within clay.

Interpretation: The debris is a kind of regolith and is a product of emersion and destruction of the original palisade selenite crusts by atmospheric agents and by weathering in a coastal "sabkha-like" flat, periodically flooded with meteoric waters loaded with clay. The debris accumulated in the coastal zones of the shrinking saline pans, with fluctuating water level.

Grass-like gypsum. *Description:* This facies is characterized by thin layering (<25 cm) and grass-like structures usually formed by a single generation of bottom-grown gypsum crystals. They create crusts 0.1–20 cm thick, intercalated with layers of fine-grained gypsum and/or clay. Larger grass-like crystals are similar in morphology to the giant intergrowths. The grass-like facies encloses four subfacies: (I) with crystal rows, (II) with stromatolitic domes, (III) with clay intercalations, and (IV) with alabaster beds.

Interpretation: This facies was deposited by two alternately acting main mechanisms: (I) syntaxial bottom-growth of large crystals, and (II) microbialite, clastic, or pedogenic gypsum deposition. The facies was formed in shallow periodically emerged saline pans or flats. The thickest selenite crusts intercalated with fine-grained gypsum were deposited at a depth that could be only occasionally reached by meteoric water and represent relatively deeper brines. The thinnest selenite crusts (<5 cm) intercalated fine-grained gypsum represent ephemeral saline pans passing into evaporite shoals.

Gypsum microbialites (gypsified microbial mats). *Description:* The facies is represented by layers of fine-crystalline gypsum showing wavy crenulated lamination and fenestral structures filled with coarse-crystalline gypsum cement transparent-to-honey in colour which is due to included organic matter. Such deposits commonly form thin intercalations within the grass-like facies and they appear in the layers *c* and *m1*. The lamination laterally disappears (commonly in layer c) and the facies passes into homogeneous or slightly nodular alabaster.

Interpretation: The layers represent gypsified microbial mats. They were deposited on a semi-emerged evaporite shoal at the margins of ephemeral to shallow perennial saline pans. The presence of such pans is recorded by thin grass-like selenite crusts, intercalated with gypsum microbialite deposits. Alabaster deposits associated with gypsified microbial mats are interpreted as pedogenic sediments formed during emersion of evaporite shoals, or as deposits of thin brine sheets.

Sabre gypsum. *Description:* This facies is characterized by curved ("sabre") crystals (10-95 cm long; Fig. 5B, C) and thick bedding (0.2-1.5 m). The crystals started to grow vertically and then curved laterally due to crystal lattice twisting. Minute *100* twins are commonly 'nuclei' of sabre crystals. A characteristic feature of this facies is concordant orientation of crystal apices traceable over long distances and presumably reflecting the direction of bottom brine currents. Locally, a few meters high and >10 m wide domal structures occur. The sabre gypsum encloses: flat bedded subfacies, entirely built of bottom-grown crystals, and wavy bedded subfacies, with bottom-grown crystals scattered within flat-to-wavy laminated fine-grained gypsum commonly showing microbialite domal structures. Selenite nucleation cones are common in this facies.

Interpretation: The flat bedded subfacies was created by syntaxial bottom growth of crystals associated with frequent formation of new individuals. The new crystals accreted on surfaces of older ones, especially on their upper faces. This subfacies was deposited in brine more than 1 m deep. Such a depth was necessary for existence of permanent density stratification maintaining bottom growth of large crystals and giant domes, which are primary forms. This growth was disturbed by refreshments, connected with the drop of the pycnocline in a perennial saline pan, recorded by dissolution surfaces, and microbial gypsum deposition which indicate a relatively shallow depth. The wavy bedded subfacies were deposited in a similar environment, but are associated with both, mechanical and microbialitic deposition of fine-grained gypsum. The fine-grained gypsum remained mostly uncemented and soft and it was subjected to deformations, which included both compactional deformations and gravity creep and slumps. Intercalations of debris flow deposits are noted in this facies.

Selenite debris flow. *Description:* This facies consists of broken, abraded and/or dissolved gypsum crystals scattered within a matrix of fine-grained gypsum. The clasts, mostly fragments of elongated sabre-like crystals, commonly show horizontal orientation. The facies appears in layers, up to >1 m thick, associated with microcrystalline and sabre gypsum facies.

Interpretation: The fabric of this facies and the occurrence of fine-grained matrix between the crystal clasts suggest a debris-flow transport mechanism, although local grain-flow cannot be excluded. Selenite clasts could derive from the wavy bedded sabre facies and originally could crystallize on basin slopes as loose aggregates, possibly within microbial mats or soft microbialite deposits. These selenites were then redeposited from there into deeper zones of saline pans as slumps and debris flows. Crystal fragmentation and abrasion took place during redeposition.

Microcrystalline gypsum. *Description:* This facies includes many lithologic varieties (subfacies) which are built of macroscopically invisible crystals. The most widespread subfacies are thin laminated gypsum (with laminae commonly less than 1 mm thick), alabasters or compact gypsum, and breccias. Traces of bottom-grown halite crystals (<1 cm in size) are present in some beds, as well as evidence of their synsedimentary dissolution both on the surface and within soft gypsum mud (Kwiatkowski, 1972). Slump and soft-sediment deformation structures are very common. This facies locally contains thick clay intercalations.

Interpretation: The microcrystalline facies represents a subaqueous environment of a brackish-to-saline pan (with fluctuating salinity), dominated by allochthonous clastic deposition. The laminated gypsum was deposited by fallout of gypsum grains from suspension clouds. Lamination and extremely small grain sizes suggest a calm environment, though the presence of rare wash-out surfaces and ripples indicates episodic action of strong bottom currents. Each lamina may represent one flood of run-off meteoric waters which swept out gypsum detritus from emerged coastal flats composed of earlier deposited gypsum sediments exposed to weathering (Kasprzyk, 1999). Lack of bottom-grown gypsum crystals and common soft-sediment deformations prove that gypsum crystallized neither within sediment nor at the sediment-water interface. Contrary to gypsum, halite crystallized directly at the bottom, indicating that the brine was saturated with NaCl at least temporarily.

Sedimentary environment

The distinguished facies, which correspond to the lithostratigraphic units, represent various environments (from subaqueous and more or less shallow-brine to subaerial) of a giant salina-type basin. The gypsum layers, particularly in the autochthonous unit, originated in a vast flat-bottom zone of the basin. This area was occupied by a system of variable perennial saline pans (<5–20 m deep, dominated by selenite deposition) and evaporite shoals (dominated by gypsum microbialite deposition). The various morphologies and fabric of the bottom-grown crystals in the giant intergrowths and sabre gypsum facies, reflect different compositions and properties of the brine in the separate saline pans evolving in time.

The layer-cake architecture of the gypsum facies visible in the autochthonous unit, suggests that the basin was infilled with evaporite deposits by vertical accretion (aggradation). Aggradational deposition was controlled by water or brine level fluctuations within the basin or subbasins (Bąbel, 2007b). Because the basin was separated from the sea by some emerged barriers (Fig. 11E), these fluctuations were only weakly dependent on sea level changes but were rather controlled by regional climate.

History of sedimentation

Integration of facies analysis and event stratigraphic studies allowed reconstruction of the sedimentary history of the gypsum basin. After initial evaporite drawdown, the northern margin of the basin evolved from a large perennial saline pan (with deposition of the giant gypsum intergrowths) into an evaporite shoal (with grass-like gypsum deposition) and then back again into a perennial pan (with sedimentation of the sabre gypsum). Later, deposition of clastic gypsum prevailed. It was due to a dramatic change in salinity and chemistry of the water. This deposition was interrupted by a short return to selenite deposition recorded in the northern part of the evaporite basin by a thin bed of grass-like and sabre gypsum (unit F in Figs 5B, 17). This event was preceded by an inflow of marine water to the basin, documented by foraminifers present in the underlying clays (D. Peryt, 2013b). Evaporite deposition was arrested by a flood of marine waters and rapid deepening.

Paleogeography

The distribution of the facies and the other data suggest that the relief of the Nida Gypsum basin raised slightly towards the south, towards the centre of the evaporite basin, especially during the deposition of the lower selenite unit. It was suggested that the broad morphological barrier elongated W-E separated the gypsum depositional area in the north from the halite-dominated zone and the halite subbasins in the south (Fig. 5; Bąbel, 2005b; Bąbel and Becker, 2006; Bąbel and Bogucki, 2007) and the Nida Gypsum deposits (particularly the selenite unit) formed on a broad northern margin of this barrier.

Badenian and Messinian selenite cycles

The vertical pattern of the Badenian selenite facies: giant intergrowths → grass-like gypsum → sabre gypsum, is similar to the Messinian selenitic cycle: massive selenites → bedded selenites → branching selenites, and both patterns were interpreted in nearly the same way, i.e. as large-scale fluctuations of the water level, namely highstand-lowstand-highstand cycle, in the basin with a drawdown water level (Kasprzyk, 1993a; Bąbel, 2005b, 2007b; Lugli *et al.*, 2010). The Badenian lowstand-highstand transition is associated with the rising trend in Sr content of the selenite crystals and therefore it was interpreted as having a character of deepening-upwards and also brining-upwards (Kasprzyk, 1994, 1999; Rosell *et al.*, 1998; Bąbel 2004, 2007b). This transition was also interpreted as the “autogenetic” or “autocyclic” transgression characteristic of the post-drawdown phase in evaporite basins (Rouchy and Caruso, 2006; Warren, 2006). The Messinian cycles were interpreted as driven by cyclic climatic changes (i.e. periodic transitions: wet climate – arid climate – wet climate) related to precessional changes in the position of Earth orbit, and according to this interpretation the selenite cycles record the time span of ca. 21 k.y. typical of the precessional cycles. Such time of deposition fits to the Badenian lower selenite unit as well.

Stop descriptions

A2.1 Gacki, pre-evaporite Badenian marls and basal part of the Nida Gypsum succession with the largest giant crystal

Leaders: Maciej Bąbel, Krzysztof Nejbert, Danuta Olszewska-Nejbert

A vast abandoned gypsum quarry at Gacki turned to undeveloped recreation area with some ponds (Fig. 6). The NE wall of the road cut at the entry is a protected exposure presenting pre-evaporite Badenian marls and basal selenite part of the Nida Gypsum succession, giant crystal intergrowths up to 3.5 m long, sabre gypsum facies, selenite nucleation cones, and evidence of post-evaporite tectonics. (50°27′15″ N, 20°35′18″ E)

The Badenian deposits are cut by a vertical fault, with a throw of ca. 13 m. Its east uplifted side is composed of the early Badenian marine marls underlying the giant intergrowths layer forming the top of the hill. The marls are >15 m thick, and lay on eroded surface of Cretaceous (Campanian) marls, once exposed 300-350 m SE, at the foot of the slope. The visible part of the Badenian marls contains glauconite, pyroclastic intercalations, mollusks – pectinids, the oyster *Neopycnodonte cochlear* (Poli) – and foraminifers characteristic of the regional biostratigraphic zone *Uvigerina costai*. Below these marls, which are ca. 10 m thick, the older *Orbulina suturalis* (=*Candorbulina universa*) zone was documented (Łuczkowska, 1974). The lower part of the marls represents the standard Neogene Nannoplankton Zone 5 (NN5, *Sphenolithus heteromorphus* Zone), and the marls above, directly underlying the gypsum may represent NN6 zone (Dudziak and Łuczkowska, 1992). The fossils indicate that marine sedimentation preceded the evaporite deposition.

The giant intergrowths attract attention by exceptionally large sizes of crystals which in this area are particu-

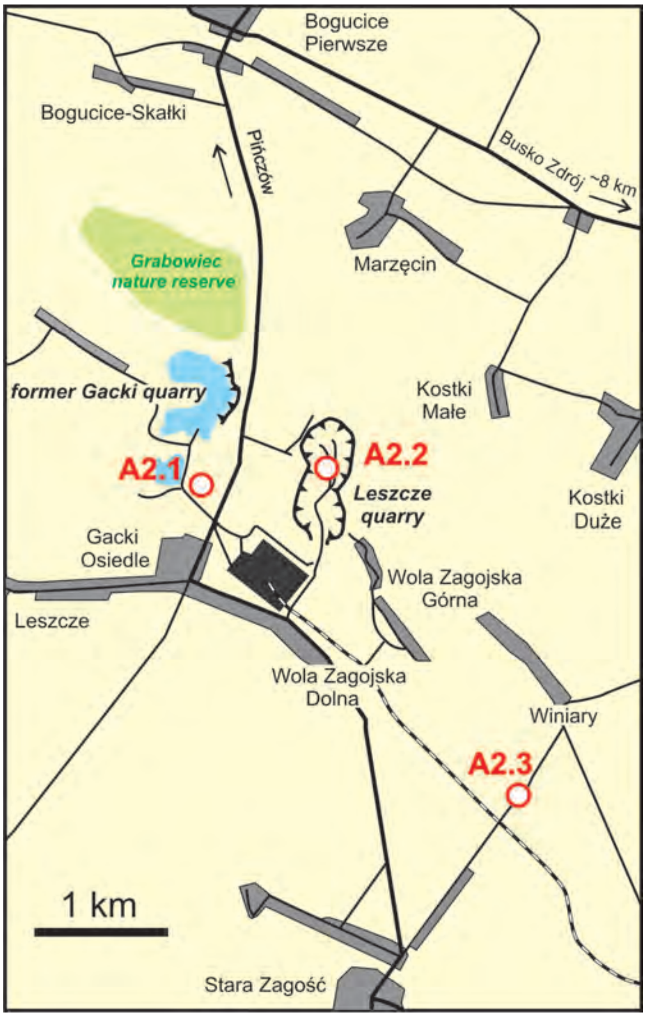

Fig. 6. Detailed location of the field trip stops Gacki (A2.1), Leszcze (A2.2) and Zagość-Winiary (A2.3).

Fig. 7. Outcrop at Gacki. **A)** View of the outcrop, the giant crystals are outlined, **B)** the largest gypsum crystal (after Bąbel *et al*., 2010, modified), **C)** selenite nucleation cones formed by sabre crystals.

larly large. The spectacular palisade of 1–2 m long crystals is seen high in the wall of the outcrop. One crystal attains the record size among the giant intergrowths and the minerals of Poland. The specimen is 3.2 m in length. It is partly destroyed and can be estimated as originally 3.5 long (Fig. 7A, B). This crystal is one of the two largest so far documented in Poland and still preserved natural crystals. The other crystal of the same estimated sizes is exposed in the outcrop of the giant intergrowths in nearby Bogucice-Skałki (Fig. 6; Bąbel, 2002a). The giant intergrowths are a crystallographic curiosity recognized so far only in the Carpathian Foredeep. Although similar to the contact *$\bar{1}$01* gypsum twins, the intergrowths differ from any twins in lacking crystallographic symmetry between component crystals (Fig. 8C, D). The other uncommon feature is the primarily skeletal structure of the giant crystals.

The sabre gypsum facies is exposed in the west downthrown side of the fault. The sabre crystals show apices turned in similar azimuths (to N and E), which is interpreted as a paleocurrent indicator (apices are oriented upstream, see Stop A2.4). The nucleation cone structures formed by synsedimentary load deformation generated by the crystals growing on the soft substrate are present in layer *h*, and also at the base of the giant intergrowths (Fig. 7A, B).

References to stop A2.1: Alexandrowicz (1967), Alexandrowicz and Parachoniak (1956), Bąbel (1986, 1987, 1991a), Bąbel *et al.* (2010, 2013, with references), Dudek and Bukowski (2004), Dudziak and Łuczkowska (1992), Łuczkowska (1974), Osmólski *et al.* (1978).

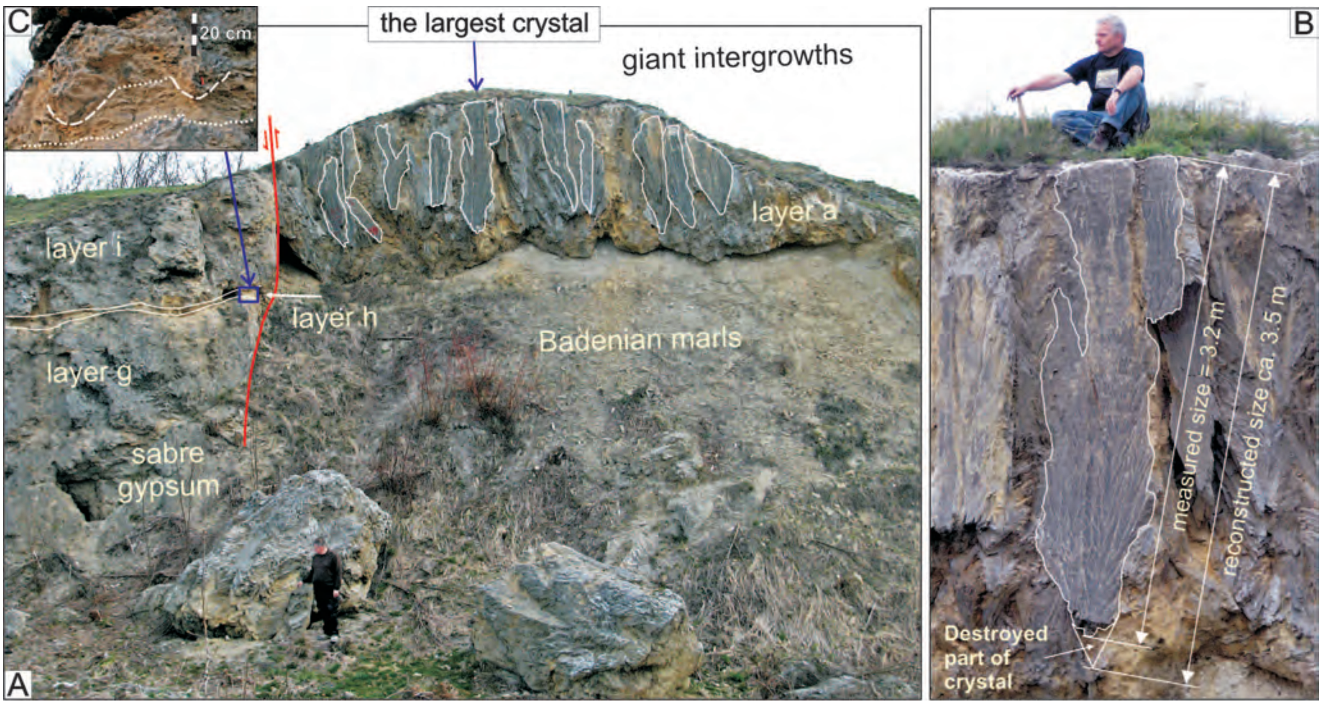

A2.2 The Nida Gypsum deposits in the Leszcze quarry

Leaders: Maciej Bąbel, Danuta Olszewska-Nejbert, Krzysztof Nejbert, Damian Ługowski, Teresa Lisek[1]

[1]ZG Kopalnia Gipsu "Leszcze" S.A
(teresa.lisek@dolina-nidy.com.pl)

This is a great active quarry (Fig. 6). Visits only by permission from the management. (Entrance to the quarry: 50°26′ 59″ N, 20°36′09″ E)

We observe here the typical facies range of the Nida Gypsum succession, with giant intergrowths showing skeletal structures, grass-like gypsum with clay intercalations, gypsum microbialitic structures, sabre gypsum, clastic microcrystalline and laminated gypsum, traces after halite-solution, and gypsum breccias and megabreccias related to halite-solution collapse and subsidence.

The pre-evaporite Badenian marls exposed in the quarry, underlying the giant intergrowths layer similarly as in stop A2.1, represent biostratigraphic zone *Uvigerina costai*, recognized here in the sampled 1.6 m interval below gypsum (D. Peryt, 2013a). The delphinid vertebra found in these deposits (Czyżewska and Radwański, 1991) confirm that marine deposition preceded the onset of evaporation.

The selenite unit is exposed in the lower exploitation level. The giant intergrowths represent palisade and skeletal forms, most probably typical of the deeper, less oxygenated brine (Fig. 8A, B). Higher up the section the microbialite structures are common in layer *e*, within the grass-like gypsum facies with clay intercalations. This subfacies represents a semi-emerged coastal evaporite shoal, covered with microbial mats and seasonally overflooded with clay-loaded meteoric waters transported by sheet floods. Further up the section the typical sabre facies is exposed, representing the same beds as in stop A2.1.

The 12–15 m thick clastic unit is exposed in the upper exploitation level. Laminated gypsum common in this interval contains traces of dissolved (<1 cm) halite cubes, which grew in situ at the bottom of the basin. In places, thin beds of residual gypsum ("alabaster") left after halite dissolution are present. Soft-sediment deformations, mostly folds and slump structures, as well as deformations related to synsedimentary and early diagenetic halite solution, commonly appear in some beds. There are also larger-scale deformations which involve the entire thickness of the clastic unit. Nearly the whole ca. 500 m long wall of the quarry is built of megabreccia with blocks up to 10 m and more in size, showing the features of in situ crushing (Fig. 8E, F). This megabreccia passes laterally into regularly bedded deposits seen currently in NW part of the quarry. Laminated gypsum forms the so-called "breccias without matrix" and is a component of the breccias with alabaster matrix. The former commonly forms vertically elongated bodies typical of the infillings of collapse chimneys (Fig. 8E, F). Various bodies of homogeneous alabaster are present and resemble clastic dykes. In many places such thin dykes run parallel to lamination. The structure of the wall is additionally complicated by veins or pockets of karst breccia in which rounded gypsum components are placed within gypsiferous dark clay. Various fault surfaces with slickensides are recorded but without druse-like gypsum mineralization, indicating that deformation took place in the soft unconsolidated or poorly consolidated rocks. The base of the brecciated zone is formed by a flat top surface of the selenite unit (top of layer *i*) and the breccia does not show any connections with the faults cutting the underlying layers *a-i*. The origin of these megabreccias, exposed in the quarry for a long time (Bąbel, 1991b, pl. 15, fig. 2; Bąbel, 1999b, pl. 4, fig. 1 and pl. 5), is related to large scale postdepositional solution of halite originally present in the lower part of the clastic unit. The breccias were formed by fracturing and gravitational collapse of sediments over the zones of dissolving halite.

At Leszcze, the gypsum deposits are covered with Miocene marls containing foraminifers, thin-walled mollusks, pteropods (planktonic gastropods, very common), and echinoids (M. Bąbel, unpubl. data). These fossils indicate a marine environment of normal salinity characteristic of the late Badenian transgression following the Badenian evaporite event. Coeval marls in nearby Winiary (Fig. 6; Urbaniak, 1985) contained abundant pteropods *Limacina* (="*Spiratella*") together with the endemic pectinid *Palliolum bittneri* (Toula, 1899), (=*Chlamys elini Zhizhchenko*, 1953), which both are typical of the Upper Badenian Pecten Beds (Śliwiński *et al.*, 2012).

References to stop A2.2: Bąbel (1987; 1991a, b), Czyżewska and Radwański (1991); Kwiatkowski (1972); D. Peryt (2013a).

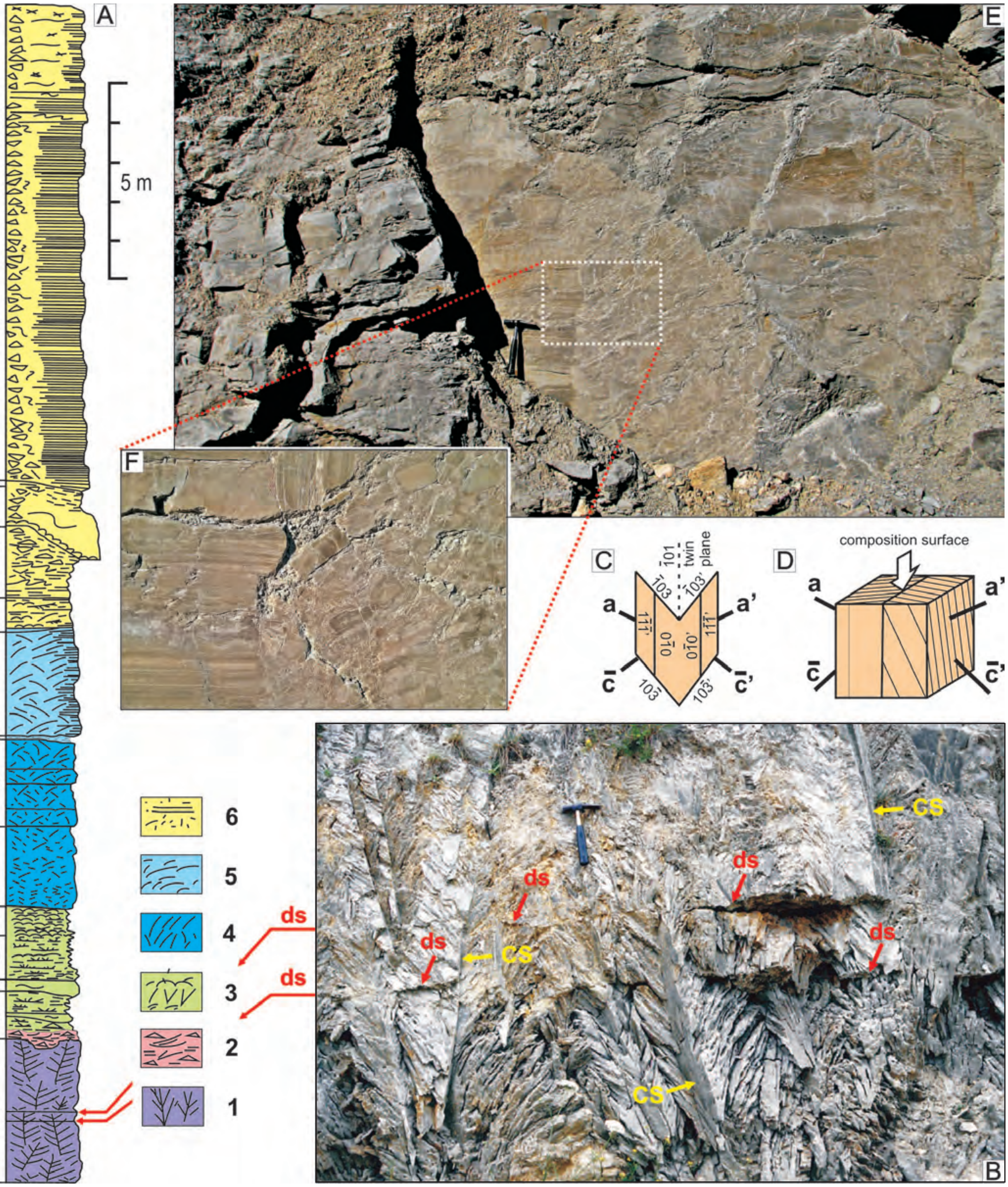

Fig. 8. Leszcze quarry. **A**) Section of the gypsum deposits, layers lettered after Wala (1980). Facies: 1 – giant gypsum intergrowths, 2 – selenite debris, 3 – grass-like gypsum, 4 – flat-bedded sabre gypsum, 5 – wavy-bedded sabre gypsum, 6 – microcrystalline gypsum. **B**) Giant gypsum intergrowths with palisade and skeletal structure, *ds* – dissolution surfaces, *cs* – composition surface of the intergrowth, **C**) orientation of gypsum crystals in the exemplary *$\bar{1}01$* twin, **D**) typical orientation of gypsum crystals in the intergrowths, hachure marks the position of *010* cleavage planes, **E**) megabreccia built of microcrystalline gypsum, **F**) detail of E with “breccias without matrix” on the right.

A2.3 Zagość-Winiary road-cut across the gypsum cuesta, gypsum sequence with reduced thickness on Cretaceous substrate

Leaders: Maciej Bąbel, Krzysztof Nejbert, Damian Ługowski, Danuta Olszewska-Nejbert

Artificial exposures on both sides of the road deeply entrenched into a steep erosional escarpment formed on the Nida Gypsum (Fig. 6). (50°25′58″ N, 20°37′29″ E)

We can see here Badenian evaporites overlying almost directly their Cretaceous substrate, a reduced section of the gypum succession, massive and non-palisade giant intergrowths subfacies, grass-like gypsum with clay intercalations, the sabre and the selenite debris-flow facies.

The gypsum deposits in this outcrop show dip of ca. 30°N and lie with the angular unconformity of ca. 40° almost directly on eroded Cretaceous substrate (Fig. 9). This substrate is built of Campanian marls and siliceous chalks (opokas) which contain remains of echinoids (*Echinocorys* sp.), inoceramids, ammonites (*Baculites* sp. and others) and belemnites. In the contact zone with the gypsum, the marls are brecciated and fractured and reveal shallow pockets filled with limonitic brecciated clay and numerous angular mud clasts (Fig. 9C). These deposits are covered with 1-3 cm thick discontinuous limestone layer, containing glauconite grains. The marls with brecciated clays are interpreted as remnants of pre-evaporite weathered zone developed on the surface of the Coniacian marls after their emersion. The limestone with glauconite probably represents Badenian marine deposits. Similar deposits are known from the described region (Alexandrowicz, 1967; Osmólski, 1972; Oszczypko and Tomaś, 1977; Krysiak, 2000).

The gypsum deposits directly overlying the Cretaceous substrate are commonly met at environs of Wiślica (Fig. 3; Czarnocki, 1939; Osmólski, 1972) and on the Miechów Upland (Becker, 2005, fig. 4). Close to stop A2.3, the early Badenian marine deposits underlying the evaporites are present and attain relatively large thickness, e.g. >15 m at Gacki (stop A2.1), 26 m at nearby Kobylniki (Fig. 13; Łyczewska, 1972), and up to 115 m at Młyny in the north (Fig. 3). The lack of such thick early Badenian marine deposits in the outcrop can be explained by non-deposition on the submarine uplift or emerged island, and existence of such paleouplifts and islands is known from the described area.

The giant intergrowths layer is ca. 1 m smaller in thickness than in neighboring outcrops (Stops A2.1 and A2.2), and the average crystal sizes in it are also smaller. Both palisade and non-palisade subfacies are present and they display rather massive structure characteristic of the shallow, well oxygenated brine (Fig. 9A, B). An unordered structure and smaller sizes of the crystals can be connected with a relatively shallower environment, closer to the coastline, and similar features were recorded in the Messinian San Miguel de Salinas basin in Spain (Rosell *et al.*, 1998).

The section above is reduced in thickness and is comparable to the section from the nearby Leszcze quarry (stop A2.2). The marker bed *c* is missing in the described section. Higher in the section the sabre facies with crystals predominantly oriented to N is present, and this orientation reflects the direction of the brine flow (see stop A2.4).

The sabre gypsum is covered with beds of selenite debris-flow ca. 2.3 m thick (Fig. 9D, E). The fragments of sabre crystals and their aggregates are common components of these beds and suggest that it was the wavy-bedded sabre gypsum facies which was destroyed in the shallower zones of the basin, and subjected to redeposition (Bąbel, 2005b). Similar redeposited selenite deposits were previously recorded in this area by Niemczyk (2005, and his earlier papers).

A2.4 Siesławice – sabre gypsum facies

Leader: Maciej Bąbel

Abandoned roadside gypsum quarries at Siesławice, slightly depressed beneath their surroundings (Fig. 10). Visible are: sabre gypsum facies with conformably oriented crystals, a selenite domal structure formed over a sunken drift tree. (50° 26′60″ N, 20° 41′31″ E)

Both the flat-bedded and the wavy-bedded sabre subfacies are seen in this outcrop, with common synsedimentary dissolution (and erosion) surfaces and compaction breaks of the crystals (Figs 11, 12). A rare sedimentary structure is seen in the lower part of layer *i*. The two empty cylinder-shaped holes are surrounded by radially grown gypsum crystals which create a kind of a domal structure over these holes (Fig. 12A, B). The holes

Fig. 9. Outcrop at Zagość-Winiary roadcut. **A)** Section of the gypsum cuest: a, e, f, g, i – layers after Wala (1980); 1 – marls and opokas (Cretaceous, Campanian); 2–9 – gypsum deposits (Miocene, Badenian); facies: 2 – palisade giant intergrowths, 3 – non-palisade giant intergrowths, 4 – selenite debris, 5 – grass-like gypsum with clay intercalations and stromatolitic structures, 6 – flat-bedded sabre gypsum, 7 – wavy-bedded sabre gypsum, 8 – selenite debris-flow, 9 – clastic and laminated gypsum; **B)** section of the gypsum cuesta in eastern scarp, **C)** details of the boundary between marls and gypsum, *lm* – limestone, *wd* – weathered clastic material (remnants of regolith?), *wm* – weathered marls, *lum* – less weathered and unweathered marls, **D)** hill west of the road, **E)** details of selenite debris-flow.

were formerly occupied by a tree trunk (the larger hole) and possibly its branch (the smaller hole). The tree was carried to this place from the land as a drift wood which sunk or was anchored there at the bottom, and became a substrate for the growth of gypsum crystals (Fig. 12C, D). The wood was later degraded during diagenesis. Moulds of tree trunks overgrown with gypsum crystals were found also in Borków quarry (Bąbel, 2007a, fig. 1).

The sabre gypsum facies in this outcrop shows apices of the curved crystals pointing in similar directions (to NE; Figs 11A-C, 12A), which is interpreted as a paleocurrent indicator (apices oriented upstream). The ordered

Fig. 10. Detailed location of the field trip stop A2.4, Siesławice.

orientation of the sabre crystals can be explained by competitive growth, influenced by unidirectional flow of Ca-sulphate saturated brine over the bottom (Fig. 11E). The crystals commonly started to grow from *100* twinned seeds attached to the substrate (Fig. 11F, G) and it was the earliest selection which eliminated the unfavorably oriented crystals (b in Fig. 11G) from the further growth. The sabre crystals developed from favorably oriented nuclei (*d-e* in Fig. 11G) and the specific feature of such crystals was that they grew by advance of the *120* prism faces in apical zone whereas the growth of side faces was extremely inhibited (Fig. 11F). Very regular growth zones of these faces seen on *010* cleavage surfaces suggest monomictic hydrography of the basin (Fig. 11D, E). During the further growth the sabre crystals with the apices (*120* prism faces) oriented favorably upstream grew at an accelerated rate and could survive the competition, and finally attained larger sizes then their less favorably oriented neighbours. Curved shape of the crystals is related to crystal lattice twisting which is a primary feature originating during crystal growth. The twisting of the crystal lattice finally eliminated the sabre crystal from further growth when its apex gradually became turned horizontally.

The conformable orientation of sabre crystals is a regional feature (see Stops A2.1, A2.2, A.2.3, A2.7) which indicates that the brine was flowing *en mass* generally along the coastline of the basin in the counterclockwise direction (Bąbel, 2002b). Presumably the oriented sabre crystals in the Nida area reflect only a fragment of the cyclonic longshore circulation of brine recorded in the entire basin (Bąbel and Becker, 2006; Bąbel and Bogucki, 2007). For more on this site see Bąbel (1996).

A2.5 Chotel Czerwony-Zagórze, giant intergrowths with selenite regolith covered with grass-like gypsum

Leader: Maciej Bąbel

Abandoned stone pits in Góry Wschodnie floristic nature reserve, and in its eastern margin, at Chotel Czerwony--Zagórze (Fig. 13). The main objects observed include: the giant intergrowths with massive and palisade structure, top surface of the intergrowths with morphology of crystal apices preserved under the clay cover, synsedimentary dissolution surfaces, selenite regolith and dome composed of giant intergrowths, grass-like facies. (Selenite dome: 50°22′24″ N, 20°43′47″ E)

The 200 m long western outcrop in its southernmost part presents giant gypsum intergrowths with massive and palisade structures, typical of shallow oxygenated brine, with dissolution surfaces, covered with the grass-like gypsum with thin alabaster beds (white fine-crystalline gypsum without clay components), (Fig. 14D). Small isolated intergrowths occur within the grass-like facies. In the north part of this outcrop surface of the giant intergrowths is covered with clay and selenite debris (Fig. 14C); the grass-like gypsum occurs above. Morphology of the crystal apices of the giant intergrowths is excellently preserved in many places under the clay cover. Aggregates of lenticular gypsum crystals resembling the gypsum “roses of desert” occur in clay in pocket-like depressions in the top surface of the giant-crystalline layer, among the selenite crystal clasts and blocks. The same type of contact is seen in the smaller eastern outcrop where a spectacular domal structure composed of giant gypsum intergrowths is seen elevated ca. 90 cm over the average level of the top surface of the giant-crystalline layer (Fig. 14A).

The transition from giant intergrowths to grass-like gypsum represents a shallowing-upwards sequence and emersion. Selenite debris was formed by weathering of the selenite substrate during emersion, when the aggregates of lenticular crystals could grow in clay soaked with Ca-sulphate saturated water. Clay was deposited from sheet floods of run-off meteoric waters and was carried from emerged land. Clay deposition was controlled by topography of the evaporite shoal. Sheet floods transported mud predominantly along broad depressions of the shoal and covered them with clay. However, on elevated areas (southern part of the western outcrop) fine-crystalline gypsum deposition took place, and the highest of the large gypsum crystals could grow syntaxially because they were free of the clay cover. Just in this way, by syntaxial growth, the selenite dome was formed (Fig. 14B). See more in: Bąbel (1987, 1991b, 1996, 1999a).

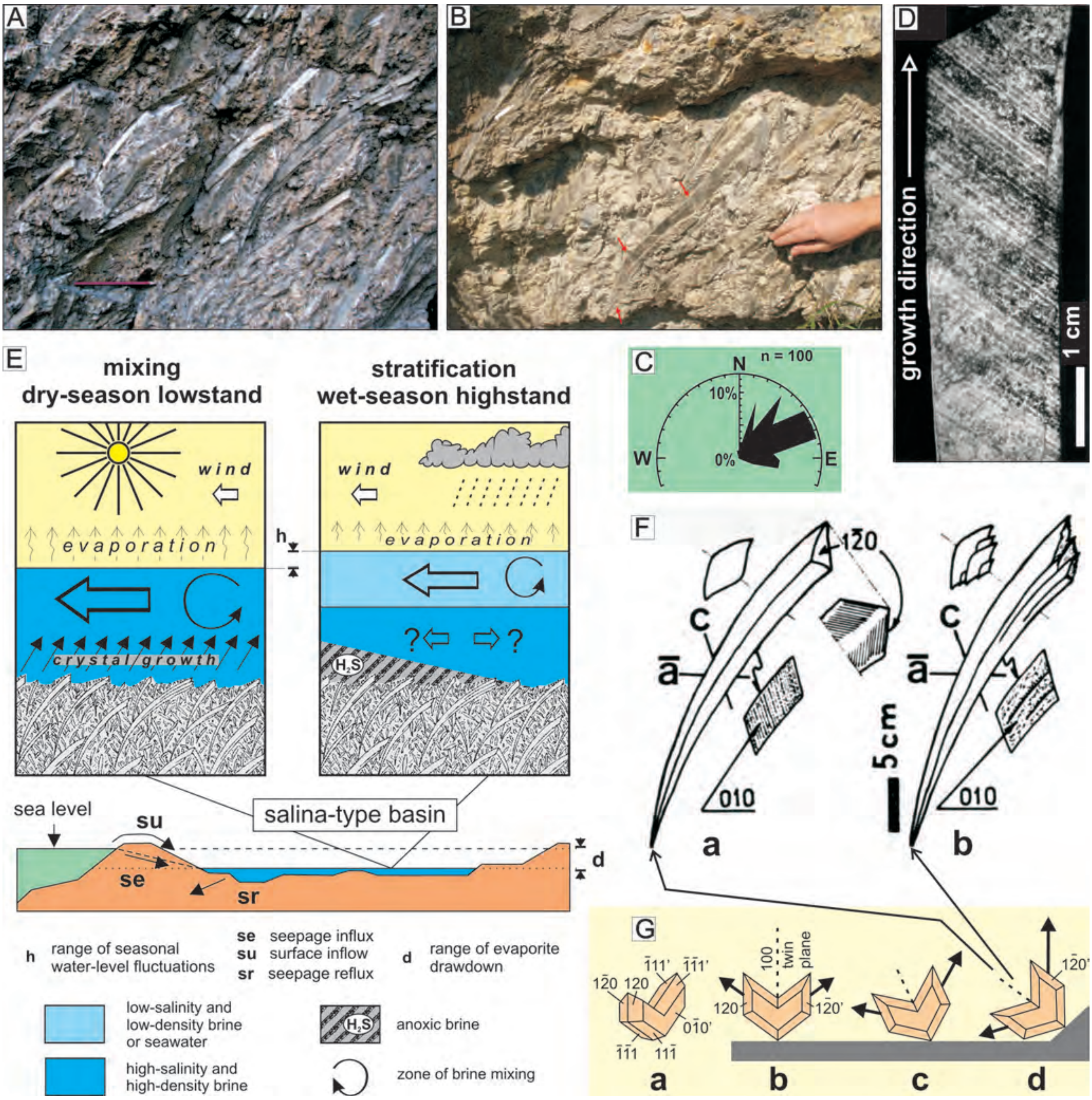

Fig. 11. Sabre facies in abandoned quarry at Siesławice. **A**) Sabre gypsum with conformably oriented crystals, layer *g*. **B**) Conformably oriented sabre crystals with compactional breaks (arrowed, photo by Stefano Lugli), layer *g*. **C**) Rose diagram showing orientation of apices of sabre crystals, layers *g* and *i*, Siesławice (see Fig. 12A), n – number of measurements. **D**) Growth zoning formed by advance of the apical *120* prism in the sabre crystal seen on the *010* cleavage surface in transmitted light. **E**) Interpreted depositional environment and structure of brine column during the growth of oriented sabre crystals (after Bąbel and Becker, 2006, modified). **F**) Sabre crystals growing by advance of the prism faces *120* (a) and lens-shaped subcrystals (b), note different growth structures visible on the *010* cleavage surface. **G**) *100* gypsum twin as a nucleus of the sabre crystals (a), b–d – twinned nuclei growing on the substrate with low chance (b), higher chance (c) and the highest chance (d) to survive the competitive growth.

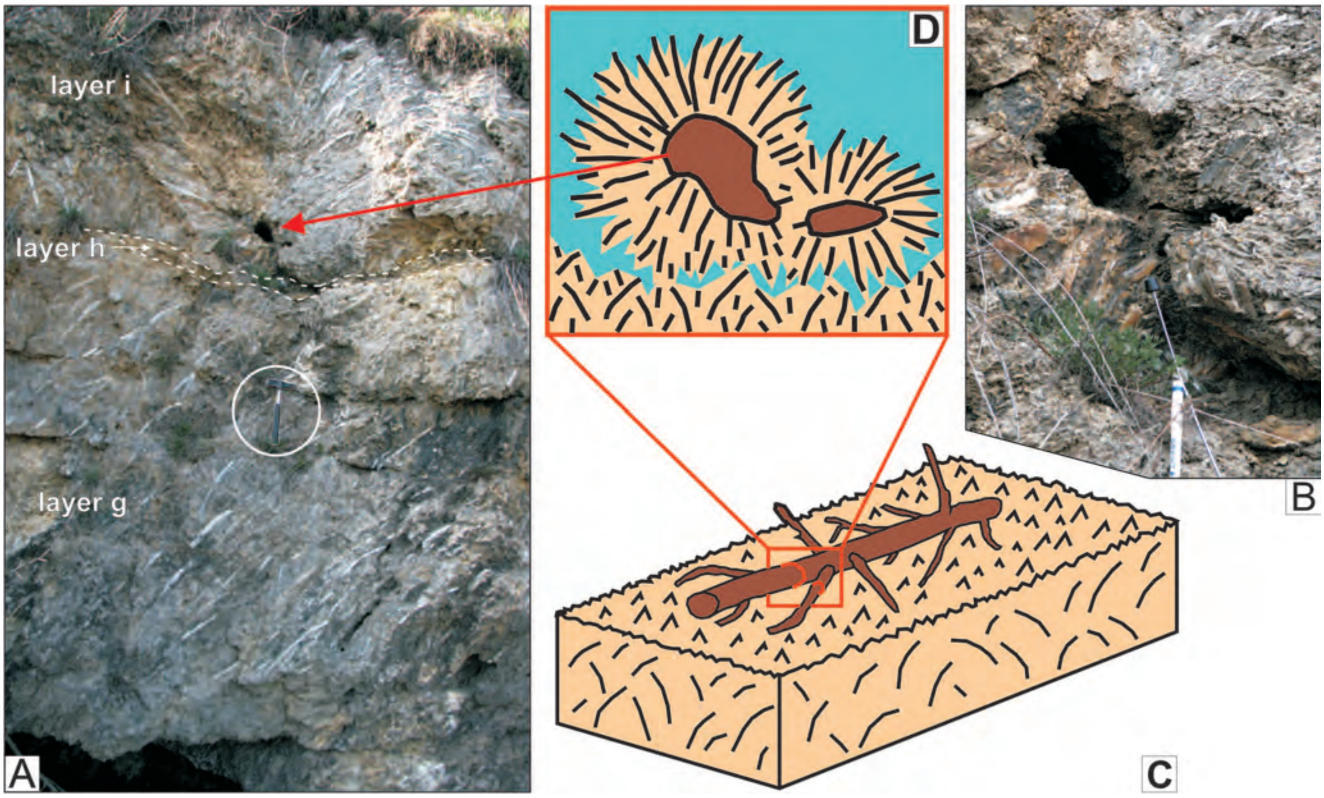

Fig. 12. Tree trunk trace in sabre gypsum, abandoned quarry at Siesławice. **A)** Mould of tree trunk overgrown by gypsum crystals. Sabre crystals show conformable orientation, layers are lettered after Wala (1980). **B)** Mould of tree trunk (and of its side branch?). Detail of A. **C)** Mode of deposition of the drifting tree on basin bottom. **D)** Way of incrustation of the tree by the growing gypsum crystals.

A2.6 Wiślica-Grodzisko, selenite dome composed of sabre gypsum

(50°20′40″ N, 20°40′43″ E)

Leader: Maciej Bąbel

A vertical section through a large selenite dome (one of the several known in this area), is exposed in the wall of an Early Mediaeval fortified settlement (Figs 13, 15A). The competitive growth structures of the sabre crystals seen on the slopes of the dome prove that the crystals grew horizontally in free space, i.e. in brine, on nearly vertical substrate (Fig. 15B, C) and that the dome is a primary form crystallized on the basin bottom. See also: Bąbel (1999a, 2007a), Kasprzyk *et al.* (1999).

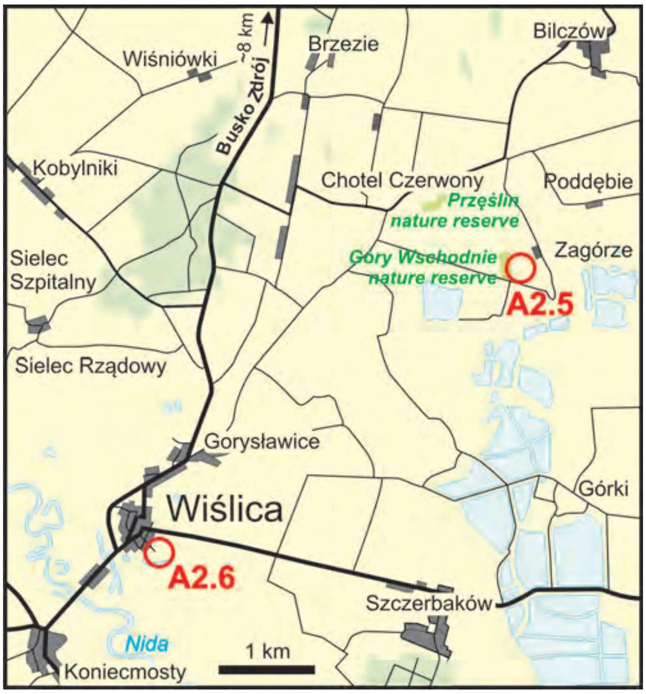

Fig. 13. Detailed location of the field trip stops A2.5 (Chotel Czerwony-Zagórze) and A2.6 (Wiślica-Grodzisko).

A2.7 Borków quarry, complete section of the Nida Gypsum

Leaders: Maciej Bąbel, Krzysztof Nejbert, Danuta Olszewska-Nejbert, Damian Ługowski, Sławomir Gębka[1]

[1]Saint-Gobain Construction Products, Poland (slawomir.gebka@saint-gobain.com)

We visit a working quarry (Fig. 16). Entrance to the quarry requires permission. We observe here: the most complete section of the Nida Gypsum deposits, with nearly all the characteristic Badenian gypsum facies and

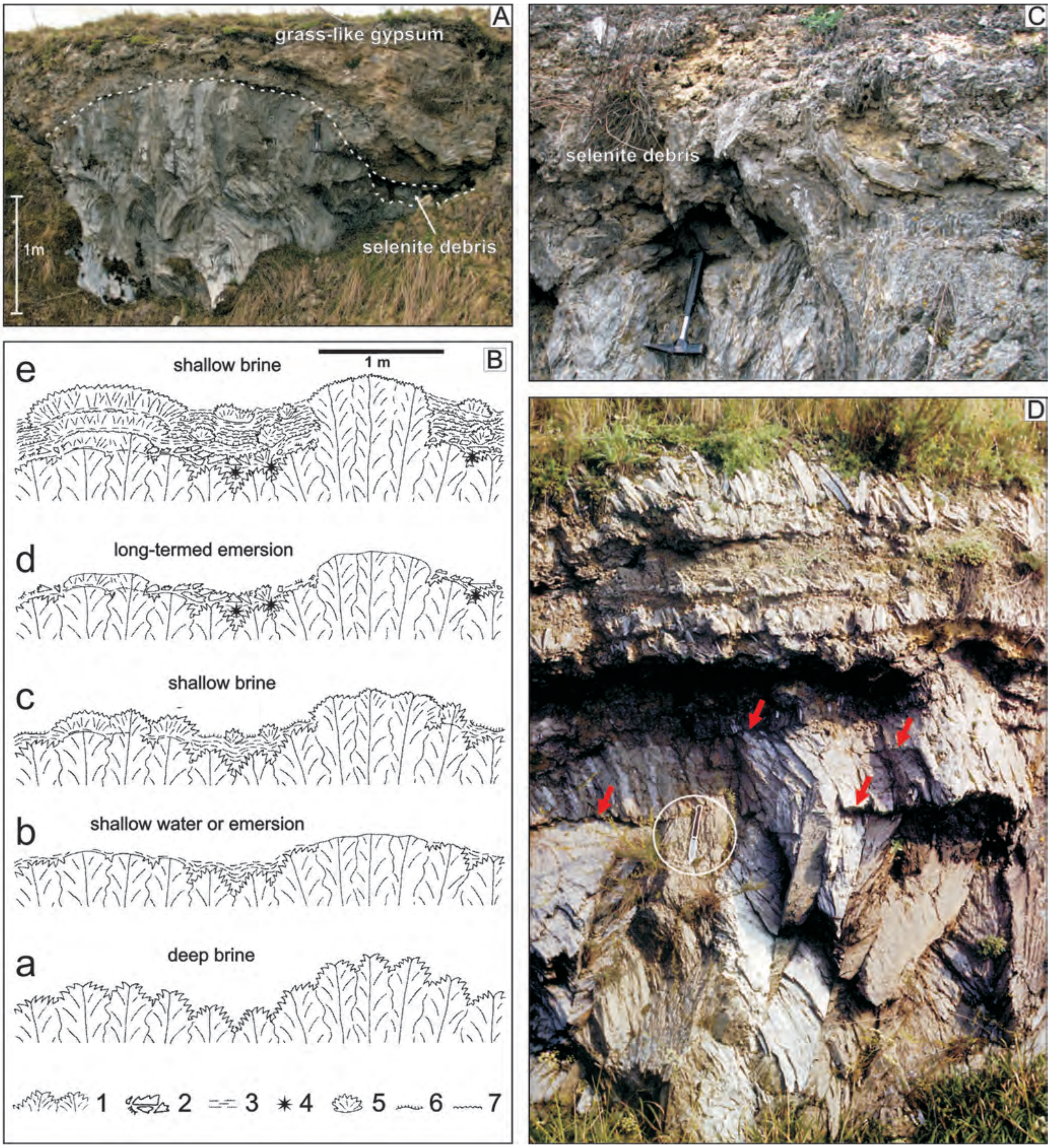

Fig. 14. Outcrops at Chotel Czerwony-Zagórze. **A)** Selenite dome composed of giant intergrowths, and grass-like gypsum, eastern outcrop. **B)** Deposition of selenite debris facies and grass-like gypsum subfacies with clay intercalations during shallowing and emersion of giant gypsum intergrowths (after Bąbel, 1999a): a – palisade growth of giant intergrowths in a deep brine, b – shallowing and influx of meteoric waters with clay; dissolution of highest crystal apices and clay deposition in depressions, c – deposition in shallow brine; growth of grass-like crystals, syntaxial growth of intergrowths, gypsification of microbial mats, d – long-lasting emersion: destruction and weathering of gypsum crystals; growth of lenticular gypsum aggregates in clay-filled depressions, e – deposition in shallow brine; accretion of domal selenitic structures built of grass-like crystals (left) and of giant intergrowths (right), and simultaneous deposition of clay and microbialite gypsum in depressions; 1 – giant gypsum intergrowths; 2 – broken, corroded and abraded gypsum crystals; 3 – clay; 4 – aggregates of lenticular gypsum crystals; 5 – separate aggregates of grass-like gypsum crystals; 6 – wavy-laminated microbial mats encrusted with small gypsum crystals; 7 – gypsified microbial mats with knobby morphology. **C)** Selenite debris covering the giant gypsum intergrowths, western outcrop. **D)** Transition from the massive giant intergrowths subfacies to the grass-like gypsum, synsedimentary dissolution surfaces are arrowed, western outcrop.

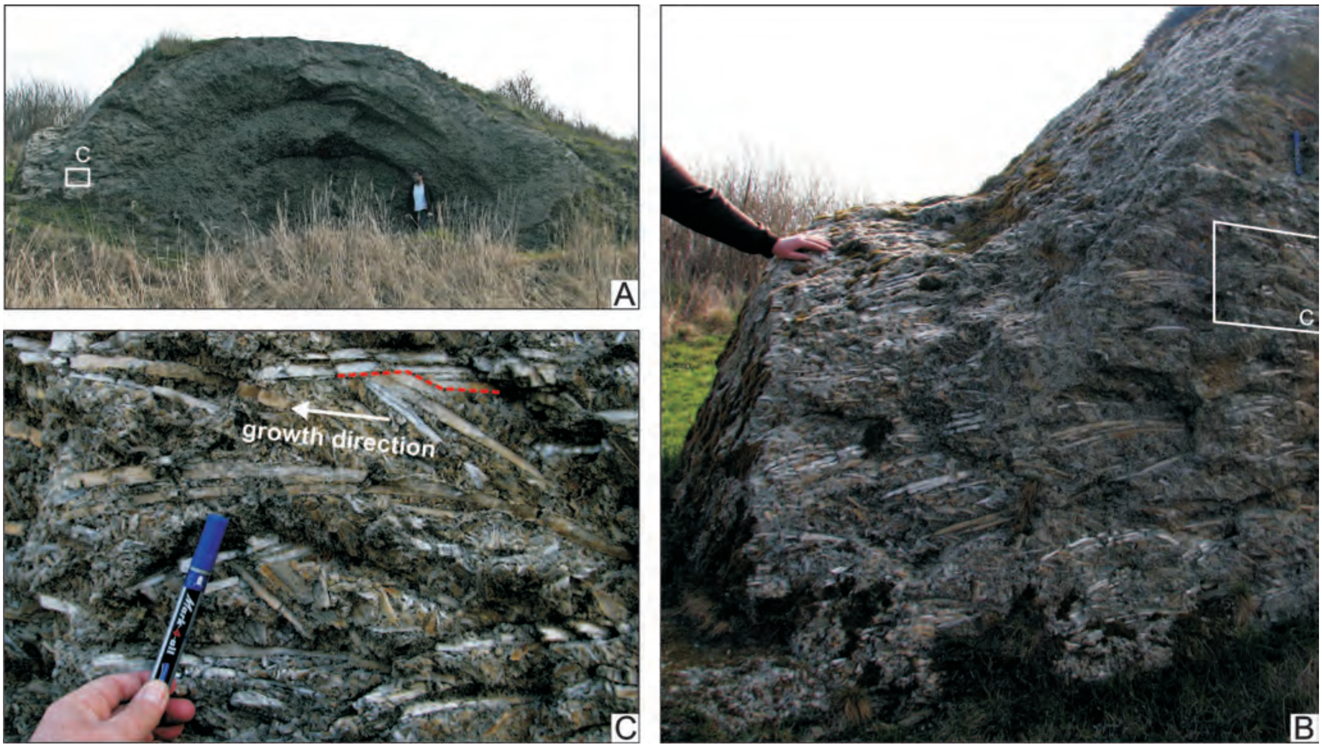

Fig. 15. The giant dome of sabre gypsum, Wiślica-Grodzisko: **A)** general view, **B)** slope of the dome, **C)** detail of A and B, the zig-zag competitive growth (compromise) boundary of the crystals is marked by red dotted line.

sedimentary structures, including selenite and selenite-dominated facies, gypsum microbialites and stromatolites, the clastic, microcrystalline and associated facies with traces of vanished halite. (Entrance to the quarry: 50°33′14″ N, 20°37′40″ E)

Fig. 16. Detailed location of the field trip stop at Borków quarry (A2.7).

This section is the best studied one in the Badenian gypsum basin with respect to geochemistry, sedimentology and palaeontology (Fig. 17; Peryt, 1999; 2013a, b; Peryt and Anczkiewicz, 2015, with references; Peryt and Gedl, 2010; Rosell *et al*., 1998).

The Badenian marine marls the underlying gypsum in the quarry represent a regional biostratigraphic foraminiferal *Uvigerina costai* zone (D. Peryt, 2013a).

The grass-like subfacies with stromatolitic domes contains flat-topped, up to 32 cm high gypsum domes which were first described from this area as stromatolites by Kwiatkowski as early as in 1970 and 1972 (Fig. 18). They are built of alternating crusts of bottom-grown crystals, gypsified knobby microbial mats and rather smooth laminae of "clastic" sugar-like gypsum. Fenestral pores occur near the bottom-grown crystals. These domes show complex (hybrid), organo-chemical origin. Small grass-like crystals and gypsified microbial mats were formed in a relatively calm environment possibly during salinity oscillations. The sugar-like gypsum was at least partly deposited mechanically during increased wave and current action. Mechanical deposition is suggested by features of the infilling and flattening of the substrate relief by some of these granular laminae. The grainy laminae run concordantly with dome shapes and also coat the steep slopes of the domes evidently "defying gravity" (Fig. 18C) which suggests that gypsum grains were trapped and bound on such slopes by cohe-

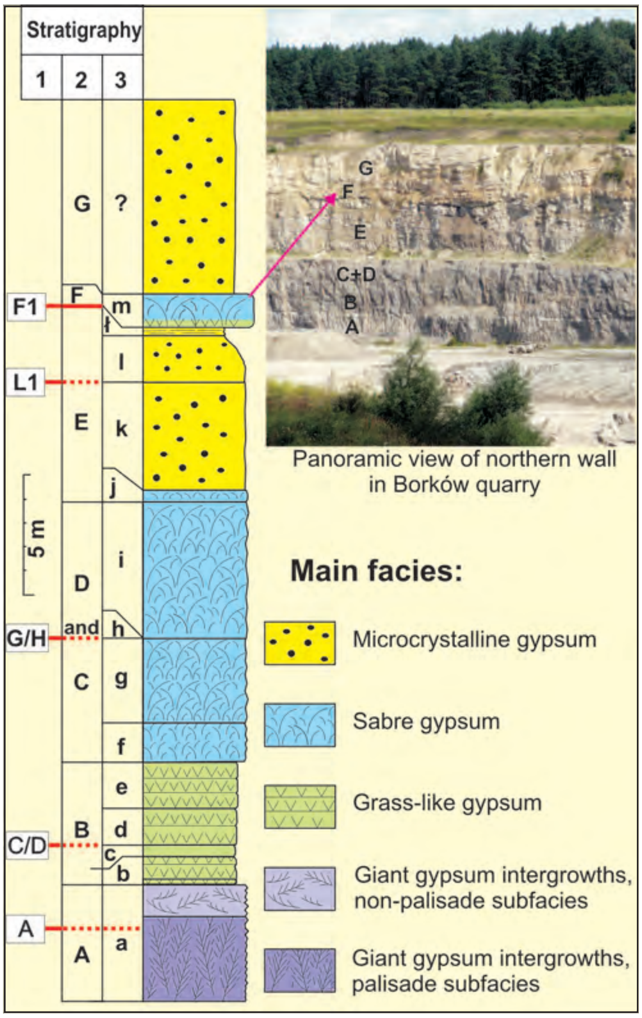

Fig. 17. Simplified geological column of the Badenian gypsum in the Borków quarry. Stratigraphy: 1 – isochronous surfaces after Bąbel (1999b, 2005a), 2 – lithostratigraphic units after Kubica (1992); 3 – layers after Wala (1980).

sive microbial mats (Demicco and Hardie, 1994). Trapping and binding is diagnostic for stromatolites and for microbialites, hence both names: stromatolite and microbialite fit to these laminated parts of the domes. This subfacies could be deposited on a broad windward side of a deeper saline pan, affected by waves and wave currents.

Higher in the section, the sabre facies is present, with crystals predominantly oriented to N and E, and this regionally conformable crystal orientation (see stops A2.1-A2.4 and A2.6) reflects the direction of the brine flow.

The upper clastic unit contains a thin intercalation of grass-like and sabre-like facies with a layer of gypsified microbial mats, a few cm thick, at the base (Figs 5B, 17). Below, there is a clay layer covering the uneven discontinuity surface and containing abundant foraminifers. This clay was interpreted as recording the influx of marine waters and invasion of foraminifers to the evaporite basin (D. Peryt, 2013b). The return to evaporite conditions was recorded by deposition of the selenite-dominated unit above and then the clastic laminated gypsum.

The laminated gypsum deposits covering the described selenite unit contain traces of halite cubes as well as thin layers of halite solution-and-collapse breccias and residual alabaster-like deposits, similar to those from the Leszcze quarry (stop A2.2). The presence of vanished halite proves that water in the basin was episodically saturated with NaCl during clastic gypsum deposition. See also: Bąbel (1991b), Bąbel and Olszewska-Nejbert (2012), Kasprzyk *et al.* (1999), Kowalski (1996), Peryt and Jasionowski (1994), Petryczenko *et al.* (1995).

Acknowledgements. Material presented in this guide is mainly based on the papers by Bąbel (1999a, 2005a) and companion papers (Bąbel, 1999b, 2007b; Bąbel and Becker, 2006; Bąbel and Bogucki, 2007, Bąbel *et al.*, 2010), and partly repeats fragments of the texts and illustrations already published.

References:

Alexandrowicz, S. W., 1967. Pozycja stratygraficzna warstw baranowskich w Woli Zagojskiej koło Pińczowa. *Sprawozdania z Posiedzeń Komisji, Polska Akademia Nauk, Oddział w Krakowie*, 10/1 [for 1966]: 199-202. [In Polish.]

Alexandrowicz, S. W., 1979. Middle Miocene (Badenian) sequence at Górki, southern part of the Korytnica Bay (Holy Cross Mountains, Central Poland). *Acta Geologica Polonica*, 29: 353-361.

Alexandrowicz, S. & Parachoniak, W., 1956. Miocene tuffites in the vicinity of Pińczów on the Nida-river. *Acta Geologica Polonica*, 6: 75-80, 301-325. [In Polish, English summary.]

Anthonissen, E. & Ogg, J. G., 2012. Appendix 3. Cenozoic and Cretaceous biochronology of planktonic foraminifera and calcareous nannofossils. In: Gradstein, F. M., Ogg, J. G., Schmitz, M. D. & Ogg, G. M. (eds), *The Geologic Time Scale 2012*. Elsevier, Amsterdam, pp. 1083-1127.

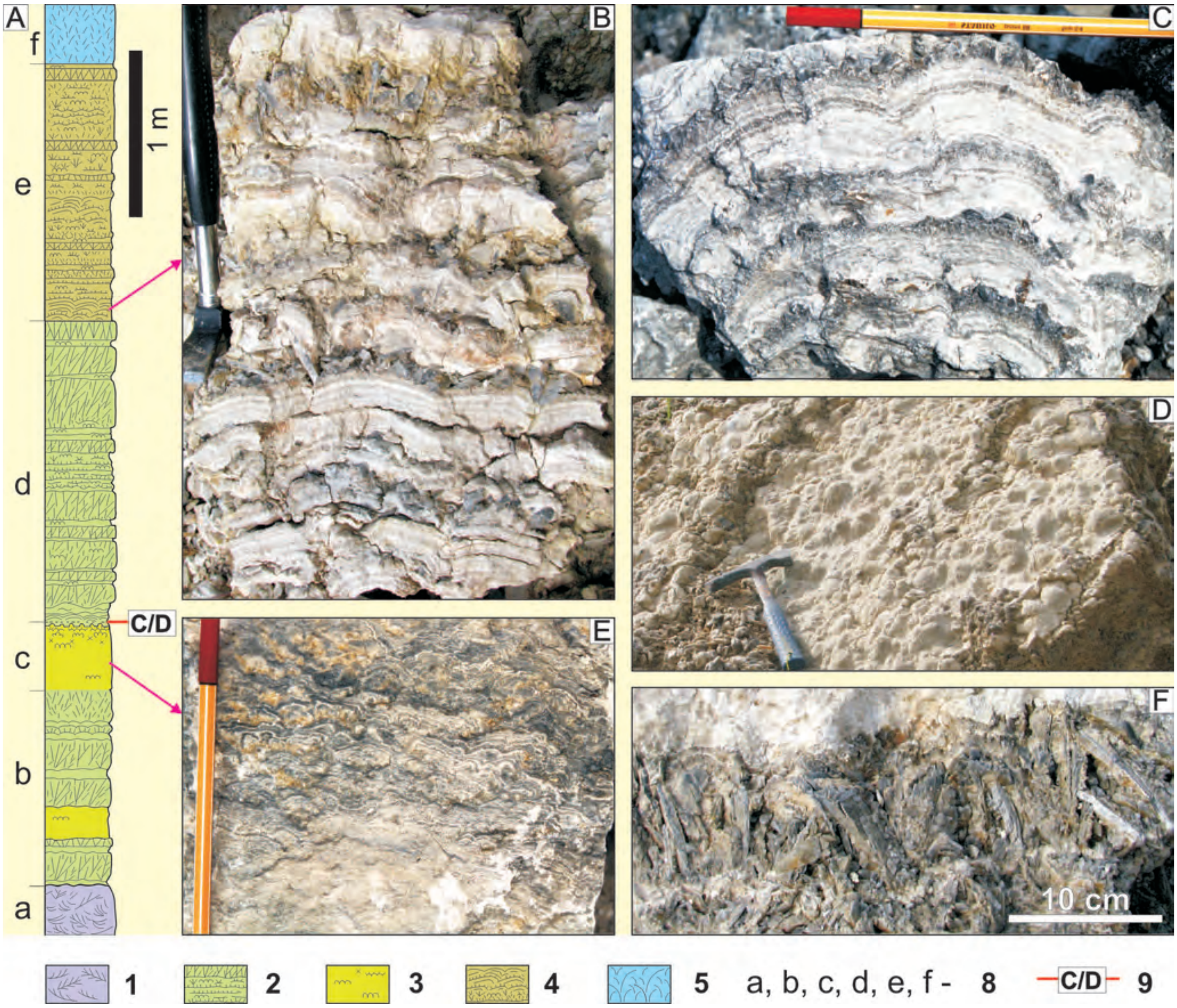

Fig. 18. Grass-like facies and gypsum microbialites in Borków quarry. **A**) Fragment of section containing grass-like facies with gypsum stromatolitic domes, hatchure reflects fabric of gypsum deposits and arrangement of crystals, layers lettered after Wala (1980) – left side, isochronous surface C/D after Bąbel (2005a) – marked on the right. Facies and subfacies: 1 – giant gypsum intergrowths, non-palisade subfacies, 2 – grass-like gypsum, subfacies with crystal rows, 3 – gypsified microbial mats facies, 4 – grass-like gypsum, subfacies with stromatolitic domes, 5 – sabre gypsum facies. **B**) Subfacies with gypsum stromatolitic domes. **C**) Gypsum stromatolitic dome with steep slopes, layer e. **D**) Gypsum microbialite domes over apices of grass-like crystals. **E**) Subfacies with gypsified microbial mats; gypsum cement crystals are honey in colour. **F**) Row of grass-like crystals with large intercrystalline pores.

Bąbel, M., 1986. Growth of crystals and sedimentary structures in the sabre-like gypsum (Miocene, southern Poland). *Przegląd Geologiczny*, 34: 204-208.

Bąbel, M., 1987. Giant gypsum intergrowths from the Middle Miocene evaporites of southern Poland. *Acta Geologica Polonica*, 37: 1-20.

Bąbel, M., 1991a. Crystallography and genesis of the giant intergrowths of gypsum from the Miocene evaporites of Poland. *Archiwum Mineralogiczne*, 44 [for 1990]: 103-135.

Bąbel, M., 1991b. Dissolution of halite within the Middle Miocene (Badenian) laminated gypsum of southern Poland. *Acta Geologica Polonica*, 41: 165-182.

Bąbel, M., 1996. Wykształcenie facjalne, stratygrafia oraz sedymentacja badeńskich gipsów Ponidzia. In: Karnkowski, P. (ed.), *Analiza basenów sedymentacyjnych a nowoczesna sedymentologia, Materiały Konferencyjne V Krajowego Spotkania Sedymentologów*, s. B1-B26. Warszawa. [In Polish.]

Bąbel, M., 1999a. Facies and depositional environments of the Nida Gypsum deposits (Middle Miocene, Carpathian Foredeep, southern Poland). *Geological Quarterly*, 43: 405-428.

Bąbel, M., 1999b. History of sedimentation of the Nida Gypsum deposits (Middle Miocene, Carpathian Foredeep, southern Poland). *Geological Quarterly*, 43: 429-447.

Bąbel, M., 2002a. The largest natural crystal in Poland. *Acta Geologica Polonica*, 52: 251-267.

Bąbel, M., 2002b. Brine palaeocurrent analysis based on oriented selenite crystals in the Nida Gypsum deposits (Badenian, southern Poland). *Geological Quarterly*, 46: 435-448.

Bąbel, M., 2004. Badenian evaporite basin of the northern Carpathian Foredeep as a drawdown salina basin. *Acta Geologica Polonica*, 54: 313-337.

Bąbel, M., 2005a. Event stratigraphy of the Badenian selenite evaporites (Middle Miocene) of the northern Carpathian Foredeep. *Acta Geologica Polonica*, 55: 9-29. [On-Line Appendix not attached to the new AGP Home Page is availabe from the author: m.babel@uw.edu.pl]

Bąbel, M., 2005b. Selenite-gypsum microbialite facies and sedimentary evolution of the Badenian evaporite basin of the northern Carpathian Foredeep. *Acta Geologica Polonica*, 55: 187-210.

Bąbel, M., 2007a. Gypsum domes in the karst relief of Ponidzie region, southern Poland. *Prace Instytutu Geografii Akademii Świętokrzyskiej w Kielcach*, 16: 71-89. [In Polish, English summary.]

Bąbel, M., 2007b. Depositional environments of a salina-type evaporite basin recorded in the Badenian gypsum facies in the northern Carpathian Foredeep. In: Schreiber, B. C., Lugli, S. & Bąbel, M. (eds), *Evaporites Through Space and Time. Geological Society, London, Special Publications*, 285: 107-142.

Bąbel, M. & Becker, A., 2006. Cyclonic brine-flow pattern recorded by oriented gypsum crystals in the Badenian evaporite basin of the northern Carpathian Foredeep. *Journal of Sedimentary Research*, 76: 996-1011.

Bąbel, M. & Bogucki, A., 2007. The Badenian evaporite basin of the northern Carpathian Foredeep as a model of a meromictic selenite basin. In: Schreiber, B. C., Lugli, S. & Bąbel, M. (eds), *Evaporites Through Space and Time. Geological Society, London, Special Publications*, 285: 219-246.

Bąbel, M. & Olszewska-Nejbert, D., 2012. Gipsy Borkowa – badeńska sedymentacja ewaporatowa na Ponidziu. In: Skompski, S. (ed.), *Góry Świętokrzyskie. 25 Najważniejszych Odsłonięć Geologicznych*, Wydział Geologii UW, Warszawa, pp. 138-144. [In Polish.]

Bąbel, M., Olszewska-Nejbert, D. & Bogucki, A., 2011. Gypsum microbialite domes shaped by brine currents from the Badenian evaporites of Western Ukraine. In: Reitner, J., Quéric, N.-V. & Arp, G. (eds), *Advances in Stromatolite Geobiology. Lecture Notes in Earth Sciences*, 131: 297-320. Springer, Berlin.

Bąbel, M., Olszewska-Nejbert, D. & Nejbert, K., 2010. The largest giant gypsum intergrowths from the Badenian (Middle Miocene) evaporites of the Carpathian Foredeep. *Geological Quarterly*, 54: 477-486.

Bąbel, M., Urban, J., Chwalik-Borowiec, A. & Łajczak, A., 2013. Stanowisko 6. Gacki: nieczynny kamieniołom gipsów – profil i tektonika serii ewaporatowej, zjawiska krasowe. In: Łajczak, A., Fijałkowska-Mader, A., Urban, J. & Zieliński, A. (eds), *Georóżnorodność Ponidzia*, Wyd. Instytut Geografii UJK w Kielcach, pp. 57-65. [In Polish.]

Becker, A., 2005. Facies development of the Badenian (Middle Miocene) gypsum deposits in the Racławice area (Miechów Upland, southern Poland). *Annales Societatis Geologorum Poloniae,* 75: 111–120.

Bukowski, K., 2011. Badenian saline sedimentation between Rybnik and Dębica based on geochemical, isotopic and radiometric research. *Rozprawy, Monografie*, 236: 1-184. Wyd. AGH, Kraków. [In Polish, English summary.]

Czarnocki, J., 1939. Poszukiwania ropy naftowej w okolicach Wójczy i na obszarach sąsiednich po obu stronach Wisły w r. 1929-31. *Biuletyn Państwowego Instytutu Geologicznego*, 18, Załącznik 1: 1-8. [In Polish.]

Czyżewska, T. & Radwański, A., 1991. Middle Miocene (Badenian) delphinid and phocoenid remains from the Fore-Carpathian Depression in southern Poland. *Acta Geologica Polonica*, 41: 183-191.

de Leeuw, A., Bukowski, K., Krijgsman, W. & Kuiper, K. F., 2010. Age of the Badenian salinity crisis; impact of Miocene climate variability on the circum-Mediterranean region. Geology, 38: 715–718.

Demicco, R. V. & Hardie, L. A., 1994. *Sedimentary Structures and Early Diagenetic Features of Shallow Marine Carbonate Deposits*. SEPM Atlas Series, No. 1: 265 pp. Tulsa, Oklahoma.

Dudek, K. & Bukowski, K., 2004. Badenian pyroclastic levels from Gacki in Nida Valley, Carpathian Foredeep, Poland. *Polskie Towarzystwo Mineralogiczne, Prace Specjalne,* 24: 141-144.

Dudziak, J. & Łuczkowska, E., 1992. Biostratigraphic correlation of foraminiferal and calcareous nannoplankton zones, Early-Middle Badenian (Miocene), Southern

Poland. *Bulletin of the Polish Academy of Sciences, Earth Sciences*, 39 [for 1991]: 199-214.

Garecka, M. & Olszewska, B., 2011. Correlation of the Middle Miocene deposits in SE Poland and western Ukraine based on foraminifera and calcareous nannoplankton. *Annales Societatis Geologorum Poloniae*, 81: 309–330.

Hilgen, F. J., Lourens, L. J., Van Dam, J. A., Beu, A. G., Boyes, A. F., Cooper, R. A., Krijgsman, W., Ogg, J. G., Piller, W. E. & Wilson, D. S., 2012. The Neogene Period. In: Gradstein, F. M., Ogg, J. G., Schmitz, M. & Ogg, G., *The Geologic Time Scale 2012*, Elsevier, Amsterdam, pp. 923-978.

Hohenegger J., Ćorić, S. & Wagreich, M., 2014. Timing of the Middle Miocene Badenian Stage of the Central Paratethys. *Geologica Carpathica*, 65: 55-66.

Jarosiński, M., Poprawa, P. & Ziegler, P. A., 2009. Cenozoic dynamic evolution of the Polish Platform. *Geological Quarterly*, 53: 3-26.

Kasprzyk, A., 1993a. Lithofacies and sedimentation of the Badenian (Middle Miocene) gypsum in the northern part of the Carpathian Foredeep, southern Poland. *Annales Societatis Geologorum Poloniae*, 63: 33-84.

Kasprzyk, A., 1993b. Gypsum facies in the Badenian (middle Miocene) of southern Poland. *Canadian Journal of Earth Sciences*, 30: 1799-1814.

Kasprzyk, A., 1993c. Stromatolitic facies in the Badenian (middle Miocene) gypsum deposits of southern Poland. *Neues Jahrbuch für Geologie und Paläontologie, Abhandlungen*, 187: 375-395.

Kasprzyk, A., 1994. Distribution of strontium in the Badenian (Middle Miocene) gypsum deposits of the Nida area, southern Poland. *Geological Quarterly,* 38: 497-512.

Kasprzyk, A., 1999. Sedimentary evolution of Badenian (Middle Miocene) gypsum deposits in the northern Carpathian Foredeep. *Geological Quarterly*, 43: 449-465.

Kasprzyk, A. & Ortí, F., 1998. Palaeogeographic and burial controls on anhydrite genesis: the Badenian basin in the Carpathian Foredeep (southern Poland, western Ukraine). *Sedimentology*, 45: 889-907.

Kasprzyk, A., Peryt, T. M., Turchinov, I. I. & Jasionowski, M., 1999. Badenian gypsum in the Ponidzie area, the northern Carpathian Foredeep, Poland. *International Conference "Carpathian Foredeep Basin – its evolution and mineral resources"*, Excursion 5, Kraków, 21 pp.

Khrushchov, D. P. & Petrichenko, O. I., 1979. Evaporite formations of Central Paratethys and conditions of their sedimentation. *Annales Géologiques des Pays Helléniques*, Tome hors série, No. 2: 595-612.

Kováč, M., Andreyeva-Grigorovich, A.S., Bajraktarević, Z., Brzobohatý, R., Filipescu, S., Fodor, L., Harzhauser, M., Nagymarosy, A., Oszczypko, N., Pavelić, D., Rögl, F., Saftić, B., Sliva, L. & Studencka, B., 2007. Badenian evolution of the Central Paratethys Sea: paleogeography, climate and eustatic sea-level changes. *Geologica Carpathica*, 58: 579–606.

Kowalski B. J. 1996. Young tectonic faulting in the Borków area, Nida Basin near Pińczów. *Prace Instytutu Geografii WSP w Kielcach*, 1: 129-146. [In Polish, English summary.]

Krysiak, Z., 2000. Tectonic evolution of the Carpathian Foredeep and its influence on Miocene sedimentation. *Geological Quarterly,* 44: 137-156.

Kubica, B., 1992. Lithofacial development of the Badenian chemical sediments in the northern part of the Carpathian Foredeep. *Prace Państwowego Instytutu Geologicznego*, 133: 1-64. [In Polish, English summary.]

Kwiatkowski, S., 1970. Origin of alabasters, intraformational breccias, folds and stromatolites in Miocene gypsum of Southern Poland. *Bulletin de l'Académie Polonaise des Sciences, Sér. Sciences Géologiques et Géographiques*, 18: 37-42.

Kwiatkowski, S., 1972. Sedimentation of gypsum in the Miocene of southern Poland. *Prace Muzeum Ziemi*, 19: 3-94. [In Polish, English summary.]

Łuczkowska, E., 1974. The Miocene profile in the exposure at Gacki near Pińczów. *Sprawozdania z Posiedzeń Komisji Naukowych, PAN, Oddział w Krakowie*, 17/1 [for 1973]: 192-194. [In Polish.]

Lugli, S., Manzi, V., Roveri, M. & Schreiber, B. C., 2010. The Primary Lower Gypsum in the Mediterranean: A new facies interpretation for the first stage of the Messinian salinity crisis. *Palaeogeography, Palaeoclimatology, Palaeoecology*, 297: 83–99.

Łyczewska, J., 1972. *Objaśnienia do Szczegółowej Mapy Geologicznej Polski, Arkusz Busko Zdrój, 1:50 000.* Wydawnictwa Geologiczne, Warszawa, 58 pp. [In Polish.]

Mutti, E. & Ricci Lucchi, F., 1975. Turbidite facies and facies associations. In: E. Mutti, E., Parea, G. C., Ricci Lucchi, F., Sagri, M., Zanzucchi, G., Ghibaudo, G. & Jaccarino, S. (eds), *Field trip guidebook A-11, Examples of turbidite facies and facies associations from selected formations of* *the Northern Apennines, 9th IAS Congress, Nice, France*, pp. 21-36.

Niemczyk, J., 2005. Outline of the gravitational tectonic in the Miocene gypsum formation of the Carpathian foreland in Poland. *Geologia, Kwartalnik AGH*, 31: 75–126. [In Polish, English summary.]

Osmólski, T., 1972. The influence of the geological structure of the marginal parts of the Działoszyce trough on the metasomatosis of gypsum. *Biuletyn Instytutu Geologicznego*, 260: 65-188. [In Polish, English summary.]

Osmólski, T., Krysiak, Z. & Wilczyński, M. S., 1978. New data on the Kurdwanów - Zawichost zone and the tectonics of the area between Busko and Nida and Vistula. *Kwartalnik Geologiczny*, 22: 833–850. [In Polish, English summary.]

Oszczypko, N., Krzywiec, P., Popadyuk, I. & Peryt, T., 2006. Carpathian Foredeep Basin (Poland and Ukraine): its sedimentary, structural, and geodynamic evolution. In: Golonka, J. & Picha, F. J. (eds), *The Carpathians and their foreland: Geology and hydrocarbon resources. AAPG Memoir*, 84: 293-350.

Oszczypko, N. & Tomaś, A., 1977. Fossil zones of weathering in Cretaceous and Jurassic sediments of the central part of Carpathian Foreland. *Sprawozdania z Posiedzeń Komisji Naukowych, Polska Akademia Nauk, Oddział w Krakowie*, 20/1 [for 1976]: 1940-1941. [In Polish.]

Paruch-Kulczycka, J., 2015. Foraminiferal biostratigraphy of the Miocene deposits from the Busko (Młyny) PIG-1 and Kazimierza Wielka (Donosy) PIG-1 boreholes (northern part of the Carpathian Foredeep). In: Czapowski, G. & Gąsiewicz, A. (eds), Paleogene and Neogene of Poland – new data. *Biuletyn Państwowego Instytutu Geologicznego*, 461: 115-131. [In Polish, English summary.]

Peryt, D., 1999. Calcareous nannoplankton assemblages of the Badenian evaporites in the Carpathian Foredeep. *Biuletyn Państwowego Instytutu Geologicznego*, 387: 158-161.

Peryt, D., 2013a. Foraminiferal record of the Middle Miocene climate transition prior to the Badenian salinity crisis in the Polish Carpathian Foredeep Basin (Central Paratethys). *Geological Quarterly*, 57: 141-164.

Peryt, D., 2013b. Foraminiferal record of marine transgression during deposition of the Middle Miocene Badenian evaporites in Central Paratethys (Borków section, Polish Carpathian Foredeep). *Terra Nova*, 25: 298-306.

Peryt, D. & Gedl, P., 2010. Palaeoenvironmental changes preceding the Middle Miocene Badenian salinity crisis in the northern Polish Carpathian Foredeep Basin (Borków quarry) inferred from foraminifers and dinoflagellate cysts. *Geological Quarterly*, 54: 487-508.

Peryt, T. M., 1996. Sedimentology of Badenian (middle Miocene) gypsum in eastern Galicia, Podolia and Bukovina (West Ukraine). *Sedimentology*, 43: 571-588.

Peryt, T. M., 2001. Gypsum facies transitions in basin-marginal evaporites: middle Miocene (Badenian) of west Ukraine. *Sedimentology*, 48: 1103-1119.

Peryt, T. M., 2006. The beginning, development and termination of the Middle Miocene Badenian salinity crisis in Central Paratethys. *Sedimentary Geology*, 188–189: 379–396.

Peryt, T. M., 2013. Palaeogeographical zonation of gypsum facies: Middle Miocene Badenian of Central Paratethys (Carpathian Foredeep in Europe). *Journal of Palaeogeography*, 2: 225-237.

Peryt, T. M. & Anczkiewicz, R., 2015. Strontium isotope composition of Middle Miocene primary gypsum (Badenian of the Polish Carpathian Foredeep Basin): evidence for continual non-marine inflow of radiogenic strontium into evaporite basin. *Terra Nova*, 27: 54–61.

Peryt, T. M. & Jasionowski, M., 1994. In situ formed and redeposited gypsum breccias in the Middle Miocene Badenian of southern Poland. *Sedimentary Geology*, 94: 153-163.

Peryt, T. M. & Kasprzyk, A., 1992. Earthquake-induced resedimentation in the Badenian (middle Miocene) gypsum of southern Poland. *Sedimentology*, 39: 235-249.

Petrichenko, O. I., Peryt, T. M. & Poberegsky, A. A., 1997. Pecularities of gypsum sedimentation in the Middle Miocene Badenian evaporite basin of Carpathian Foredeep. *Slovak Geological Magazine*, 3: 91-104.

Petryczenko, O. I., Peryt, T. M., Poberezski, A. W. & Kasprzyk, A., 1995. Inclusions of microorganisms in the Middle Miocene Badenian gypsum crystals of the Carpathian Foredeep. *Przegląd Geologiczny*, 43: 859-862. [In Polish, English summary.]

Połtowicz, S., 1993. Palinspastic palaeogeography reconstrution of Badenian saline sedimentary basin in Poland. *Geologia, Kwartalnik*, 19: 174–178, 203–233. [In Polish, English summary.]

Remin, Z., 2004. Biostratigraphy of the Santonian in the

SW margin of the Holy Cross Mountains near Lipnik, a potential reference section for extra-Carpathian Poland. *Acta Geologica Polonica*, 54: 587-596.

Rouchy, J. M. & Caruso, A., 2006. The Messinian saliniy crisis in the Mediterranean basin: a reassessment of the data and an integrated scenario. *Sedimentary Geology*, 188–189: 35–67.

Rosell, L., Ortí, F., Kasprzyk, A., Playa, E. & Peryt, T. M., 1998. Strontium geochemistry of Miocene primary gypsum: Messinian of southeastern Spain and Badenian of Poland. *Journal of Sedimentary Research*, 68: 63-79.

Rögl, F., 1999. Mediterranean and Paratethys. Facts and hypotheses of an Oligocene to Miocene paleogeography (short overview). *Geologica Carpathica*, 50: 339-349.

Rutkowski, J., 1981. The tectonics of the Miocene sediments of the western part of Połaniec Graben (Carpathian Foredeep. Southern Poland). *Annales Societatis Geologorum Poloniae*, 51: 117-131. [In Polish, English summary.]

Ślączka, A. & Kolasa, K., 1997. Resedimented salt in the Northern Carpathians Foredeep (Wieliczka, Poland). *Slovak Geological Magazine*, 3: 135-155.

Śliwiński, M., Bąbel, M., Nejbert, K., Olszewska-Nejbert, D., Gąsiewicz, A., Schreiber, B. C., Benowitz, J. A. & Layer, P., 2012. Badenian–Sarmatian chronostratigraphy in the Polish Carpathian Foredeep. *Palaeogeography, Palaeoclimatology, Palaeoecology*, 326-328: 12–29.

Urbaniak, J., 1985. New data for stratigraphy of Miocene alabaster gypsum deposit at Łopuszka Wielka near Kańczuga. *Przegląd Geologiczny*, 23: 121-126. [In Polish, English summary.]

Wala, A., 1980. Litostratygrafia gipsów nidziańskich (fm). In: *Symp. naukowe „Gipsy niecki nidziańskiej i ich znaczenie surowcowe"*. Printed manuscript, Kraków, 6pp.

Wagreich, M., Hohenegger, J. & Ćorić, S., 2014. Base and new definition of the Lower Badenian and the age of the Badenian stratotype (Middle Miocene, Central Paratethys). In: Rocha, R., Pais, J., Kullberg, J. C. & Finney, S. (eds), STRATI 2013, *First International Congress on Stratigraphy, At the Cutting Edge of Stratigraphy*, Springer, Cham, pp. 615-618.

Warren, J. K., 2006. *Evaporites: Sediments, Resources and Hydrocarbons. Springer*, Berlin, 1035 pp.

Appendix.

Facies of the Nida Gypsum deposits and their sedimentary environments; after Bąbel (1999a, 2005b), supplemented. The Badenian gypsum facies were also described and reviewed by Kasprzyk (1993a, b; 1999), Kubica (1992), T. Peryt (1996, 2001, 2013), Petrichenko *et al.* (1997).

Facies	Main depositional mechanism	Subfacies	Stops; illustrations	Inferred depositional environment	Selected references
Carbonate facies	Diagenetic processes	—		—	—
Porphyroblastic gypsum	Diagenetic processes	—		—	—
Microcrystalline gypsum	Mechanical deposition	Breccias	A2.2, A2.7; Figs 8E, F	Brackish-to-saline perennial pan with fluctuating salinity	Kwiatkowski, 1972, Peryt & Kasprzyk, 1992
	Gravity flows, halite-solution collapse,	Alabasters			
	Residual gypsum accumulation after halite solution, cohesive flows and slumps Periodic settling of redeposed and precipitating gypsum crystals from brine column, clay and gypsum mud suspension fallout	Laminated gypsum			
Selenite debris flow	Debris flow		A2.3; Fig. 9C	Slope of the saline gypsum pan	Bąbel, 2005b
Sabre gypsum	Syntaxial bottom growth of crystals with common creation of new crystals	Wavy bedded	A2.1, A2.2, A2.3, A2.4, A2.6, A2.7; Figs 14A, C; 18A, B	Density stratified monomictic saline pan with Ca-sulphate saturated brine of high salinity	Bąbel, 1986, Kasprzyk, 1993 a, b; Petryczenko et al., 1995; Bąbel & Becker, 2006, Bąbel & Bogucki, 2007
		Flat bedded			
Grass-like gypsum	Alternated syntaxial bottom growth of crystals and deposition of fine-crystalline gypsum	Subfacies with stromatolitic domes	A2.2, A2.3, A2.5, A2.7; Figs 14A, D; 18B, C, F	Semi-emerged evaporitic shoals passing into shallow saline pans (with Ca-sulphate saturated brine) and coastal clay-gypsum flats	Bąbel, 1999a
		Subfacies with crystal rows			
		Subfacies with alabaster beds			
		Subfacies with clay intercalations			
Gypsum microbialites	Microbialite deposition	Gypsified microbial mats	A2.2, A2.3, A2.7; Figs 14B, C	Semi-emerged evaporite shoal covered with microbial mats	Kwiatkowski, 1970, 1972; Kasprzyk, 1993c; Bąbel, 1999a, 2007; Bąbel et al., 2010
Selenite debris	Weathering		A2.2, A2.3, A2.5; Fig. 14C	Semi-emerged clay-gypsum (sabkha-like) flat	Bąbel, 1999a, 2005b
Giant intergrowths	Syntaxial bottom growth of crystals with rare creation of new crystals	Non-palisade intergrowths	A2.1, A2.2, A2.3, A2.5, A2.7; Figs 7A, B; 8B; 9B; 14A, C, D	Density stratified saline pan with Ca-sulphate saturated brine of low salinity	Bąbel, 1987, 1991a; Peryt, 1996
		Palisade intergrowths (skeletal and massive)			
		Clay subfacies			

Transgressive Callovian succession and Oxfordian microbial-sponge carbonate buildups in the Kraków Upland

Jacek Matyszkiewicz[1], Ireneusz Felisiak[1], Mariusz Hoffmann[2], Alicja Kochman[1], Bogusław Kołodziej[3], Marcin Krajewski[1], Piotr Olchowy[1]

[1]AGH University of Science and Technology, Kraków (jamat@geol.agh.edu.pl; felisiak@geol.agh.edu.pl; kochman@geol.agh.edu.pl; kramar@geolog.geol.agh.edu.pl; piotrolch@geol.agh.edu.pl)

[2]Soletanche Polska sp z o.o. (mariusz.hoffmann@soletanche.pl)

[3]Institute of Geological Sciences, Jagiellonian University, Kraków (boguslaw.kolodziej@uj.edu.pl)

Route (Fig. 1): From Kraków we take road 79 to Krzeszowice, then turn south onto a local road to Zalas. **Zalas quarry (stop A5.1)** is located in the eastern part of the village. From Zalas we take the local road to Krzeszowice, there turn right onto road 79 to Rudawa. At Rudawa, we turn left and follow local roads to NE to Bolechowice. We walk to the rock gate of **Bolechowice valley (stop A5.2)** visible NW of the village centre. From Bolechowice we drive south by local roads to road 79 at Zabierzów and turn right. After ca. 0.5 km a narrow road to the left enters **Zabierzów quarry (stop A5.3)** and a restaurant with a parking lot. The trips returns to Kraków along road 79 for overnight. On the second day, we drive NE by road 94 from Kraków to Modlnica and turn east onto a local road to Giebułtów, then north by road 794 to Skała. From Skała we follow road 773 east to Nowa Wieś, then we turn north onto a local road to Gołcza. At Gołcza we turn west to Wielkanoc village. **Wielkanoc quarry (stop A5.4)** is visible on the left after ca. 1 km. From Wielkanoc we drive SW by local roads to road 94, then passing Jerzmanowice we turn right Biały Kościół to Ujazd. Exposure at **Ujazd (stop A5.5)** is located by a small road along the main stream in the northern part of the village. From Ujazd we return to nearby Kraków.

Fig. 1. Route map of field trip A5.

Matyszkiewicz, J., Felisiak, I., Hoffman, M., Kochman, A., Kołodziej, B., Krajewski, M. & Olchowy, P., 2015. Transgressive Callovian succession and Oxfordian microbial-sponge carbonate buildups in the Kraków Upland. In: Haczewski, G. (ed.), *Guidebook for field trips accompanying 31st IAS Meeting of Sedimentology held in Kraków on 22nd–25th of June 2015*, Polish Geological Society, Kraków, pp. 51–73.
Guidebook is available online at www.ing.uj.edu.pl/ims2015

Introduction to the trip

Jacek Matyszkiewicz, Bogusław Kołodziej, Mariusz Hoffmann

The Kraków Upland is situated on the Silesian-Kraków Homocline built up of the Triassic, Jurassic and Cretaceous sedimentary rocks that dip gently to the NE and form a belt ca. 100 km long and 20 km wide on average (Figs 1, 2).

Middle Jurassic

Marine transgression began in the Kraków region in the latest Bathonian or earliest Callovian. The generalized section is characterized by small thickness (several dozen metres) and is clearly bipartite. The lower part consists of carbonate-free siliciclastic rocks passing upward into sandy limestone. Conversely, the upper part is strongly condensed (a dozen centimetres), with stratigraphic gaps in some sections, and it is composed of marls, limestones, ferruginous stromatolites, locally iron-ooidal limestones.

Sedimentary succession of the Callovian in the Kraków Upland documents progressive transgression on an island, or an archipelago of islands. The succession reflects a gradually deepening basin, decreasing supply of terrigenic components and increasing number of nektonic fossils. During the beginning of the transgression, facies distribution and strong variation in thickness resulted from topography of the basement. Conversely, lateral facies variation, variable thickness, presence of non-depositional surfaces, which characterizes the upper part of the succession dated to Middle and Upper Callovian, is interpreted as an effect of synsedimentary tectonic activity. Condensed deposits, with Fe-stromatolites, omission surfaces and traces of submarine erosion, were laid down on local horsts, whereas iron ooids, glaucony-rich marls and clays originated in intervening grabens which acted as submarine depressions. The non-deposition and condensation probably reflects a widespread crisis of the carbonate sedimentation at the turn of Callovian and Oxfordian. In this case, Jurassic of the Kraków region shows many similarities with the Middle Jurassic and Middle Jurassic–Late Jurassic transition successions known from the Peri-Tethys and northern margin of Tethys.

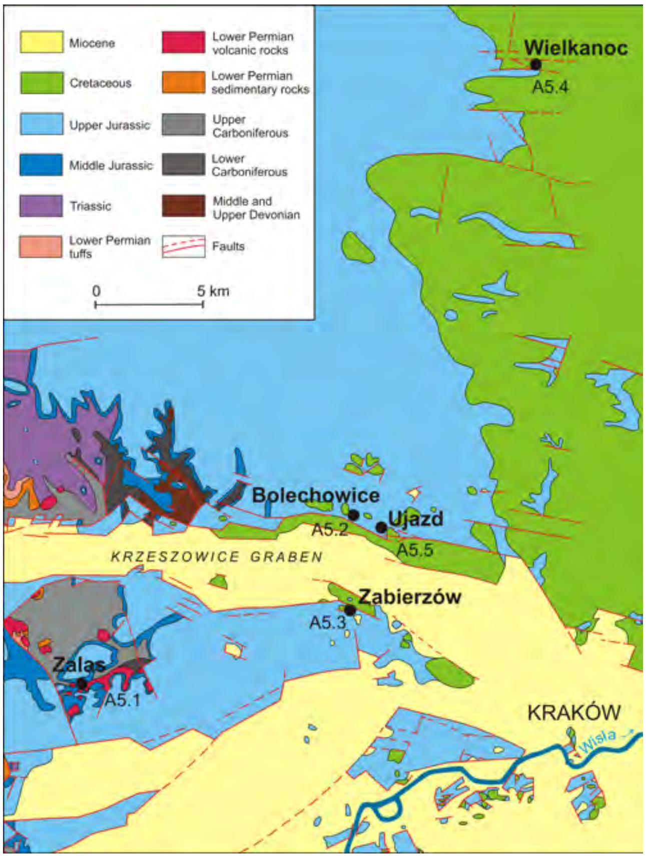

Fig. 2. Simplified geological map of Kraków region (after Gradziński, 2009; Kaziuk and Lewandowski, 1978) and field trip stop locations (A5.1-5)

Upper Jurassic

The Upper Jurassic rocks of the Kraków region are usually underlain by Callovian strata and, locally, by differentiated Palaeozoic substratum. The maximum thickness of the preserved Upper Jurassic strata is ca. 250 m (Fig. 3) in the eastern part of the region and it gradually diminishes to the west.

The Upper Jurassic carbonates of the Kraków Upland are Oxfordian and Kimmeridgian in age and they reveal high facies diversity. The main facies are: bedded facies, massive facies and sediments of lithologically variable gravity flows. The most spectacular landforms typical of the Kraków Upland landscape are built of the massive facies. There occur numerous sponge-microbial, microbial-sponge and microbial carbonate buildups and their complexes. The central parts of vast depressions between the carbonate buildups were presumably the sedimentary environment of a bedded facies. In the Late Jurassic, the area of present Kraków Upland was placed on a shelf of an epicontinental sea that bordered the Tethys Ocean on the north. The shelf contained elevations, the origin of which was related to local differentiation in subsidence between areas underlain and those not underlain by

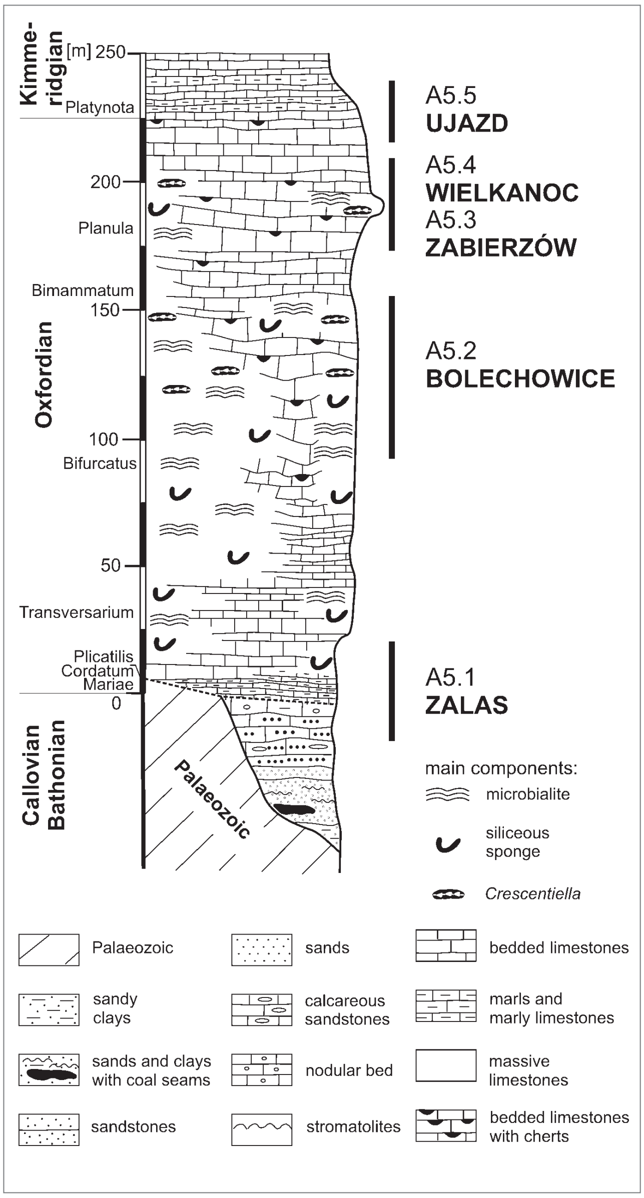

Fig. 3. Sequence of the Middle and Upper Jurassic strata in the Kraków region (after Krajewski *et al.*, 2011; modified)

Permian intrusions in the Palaeozoic basement. These elevations became colonised by microbialites and benthic fauna, mostly siliceous sponges, which initiated aggradational growth of the carbonate buildups, later merged into complexes by lateral growth.

The presence of neptunian dykes cutting through the Jurassic strata indicates activity of Late Jurassic synsedimentary tectonics in the Kraków region. Differentiated relief of the top of the Palaeozoic substratum, intensive Middle and Late Jurassic synsedimentary tectonics and local aggradational growth of carbonate buildups, all contributed to strong local vertical and lateral variability of the Upper Jurassic sediments in the Kraków region. Moreover, this picture became disturbed by differential compaction and subsequent Cretaceous and mostly Cenozoic faulting. As far as lithologic development is concerned, the Upper Jurassic sediments represent: bedded facies, massive facies, and lithologically variable sediment-gravity flows.

Bedded facies

The Upper Jurassic section begins with a series of thin-bedded marls and alternating calcareous-marly strata with abundant benthic fauna of Early and early Middle Oxfordian age (A5.1 Zalas). These strata pass upwards into a strongly differentiated limestone complex. Sediments of the bedded facies of the lower Middle Oxfordian represent thin- to medium-bedded platy-like limestones. Compared to the classical platy limestones of the Sohlnhofen-type, they are typified by a much higher share of detrital components and the lack of lithographic varieties. These strata are locally interbedded with marls and calciturbidites. The upper Middle Oxfordian and Upper Oxfordian section is dominated by thick-bedded limestones with flints, developed as microbial-sponge biostromes. Pelitic and chalky limestones occur locally. The topmost part of the Upper Jurassic section is composed of bedded limestone-marly strata, mostly known from borehole logs.

Massive facies

Deposits of the massive facies in the Kraków region are strongly diversified. These facies are represented by various types of carbonate buildups, as well as by olistoliths derived from the latter and present within gravity flow deposits. Carbonate buildups started to develop at the turn of the Early and Middle Oxfordian. The initial, small-size sponge-microbial low-relief carbonate buildups represent so-called loose bioherms (A5.1 Zalas). Following carbonate sedimentation, intensive aggraded carbonate buildups of laminar and reticulate rigid framework. Small, low-relief carbonate mud mounds turned with time into microbial-sponge segment reefs with laminar framework, filled frame reefs with initial reticulate rigid framework (A5.2 Bolechowice), which, in turn, became later replaced by open-frame reefs with well-developed reticulate rigid framework (A5.3 Zabierzów, A5.4 Wielkanoc). Development of carbonate buildups attained its climax at the turn of the Middle and Late Oxfordian, when intensive growth of such structures was accompanied by development of spectacular open-frame *Crescentiella*-reefs (A5.3

Zabierzów). Owing to lateral growth, carbonate buildups formed large complexes of distinct relief, underlined by locally differentiated subsidence and intensive synsedimentary tectonics. Carbonate buildups started to disappear at the turn of the Oxfordian and Early Kimmeridgian and the sea bottom relief became partly smoothed.

The Upper Jurassic sequence locally includes segment reefs (so called pseudonodular limestones), which reflect either initial stages of development of the rigid framework in carbonate buildups or periods when reticular framework vanished and became replaced by laminar framework. These deposits form nest-bodies within massive limestones and occur locally in marginal parts of carbonate buildups. The present-day features of segment reefs (A5.1 Zalas) are interpreted as a result of complex diagenetic processes, including first of all mechanical and chemical compaction, which proceeded in the inhomogeneous sediment of a delicate rigid skeleton of the laminar framework type (A5.1 Zalas). Stromatactis and stromatactis-like cavities are present in Upper Jurassic filled-frame and open-space reefs (A5.1 Zalas, A5.3 Zabierzów, and A5.4 Wielkanoc), whose origin and age are debatable.

Sediments of gravity flows

Sediments of gravity flows are common in the entire section of the Upper Jurassic, being particularly abundant at the turn of the Oxfordian and Kimmeridgian (A5.5 Ujazd). These are mostly grain-flow and nodular-mudflow sediments, as well as calciturbidites and tempestites. Their occurrence is associated with temporary worsening of the conditions favouring growth of carbonate buildups (initial drowning) and coeval active synsedimentary tectonics.

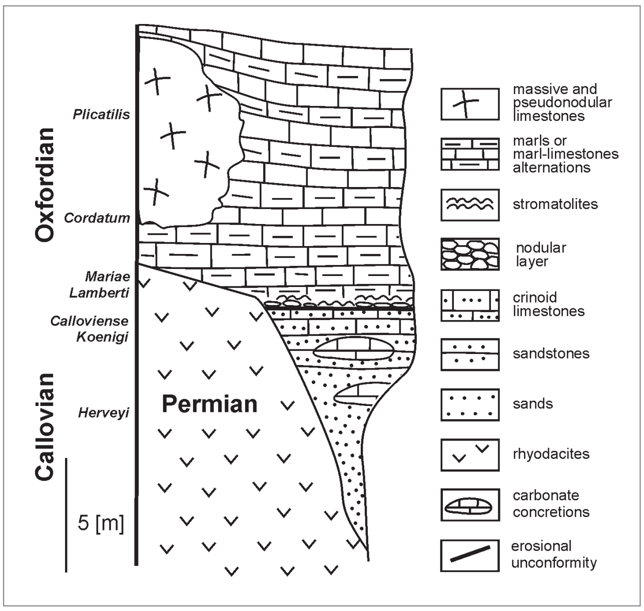

Fig. 4. Simplified section of the Callovian and Lower and Middle Oxfordian at Zalas (after Matyszkiewicz *et al.*, 2007a; modified).

Stop descriptions

A5.1 Zalas. Middle Jurassic transgressive deposits and Upper Jurassic microbial-sponge carbonate buildups in Zalas quarry

A busy active quarry; visits must be arranged with management. (50°05′ N, 19°38′40″ E)

Leaders: Mariusz Hoffmann, Alicja Kochman, Bogusław Kołodziej, Jacek Matyszkiewicz

Zalas quarry is located on the Tęczynek Horst, a complex elevation south of the Krzeszowice Graben (Figs 1, 2). Exploited in the quarry are Early Permian subvolcanic rhyodacitic porphyries intruded into Lower Carboniferous fine-grained siliciclastics. Sedimentary cover shows a succession of Callovian deposits discordantly overlying eroded and uneven Permian substrate. Above, there are Lower and Middle Oxfordian marls and limestones (Figs 3, 4). Stratigraphy of the Callovian and Oxfordian in Zalas is well established by ammonites, studied since the 19th century (Giżejewska and Wieczorek, 1976; Matyja and Tarkowski, 1981; Tarkowski, 1989; Matyja, 2006).

Callovian succession

Lower Callovian siliciclastics (Herveyi Zone). Sands, subordinately sandstones with patchy calcite cement and fine gravel quartz conglomerates (*a* and *b* in Fig. 5A) cover the substrate built of Permian ryodacites. These deposits are up to few meters thick and locally absent. Spheroidal blocks of ryodacites and silicified wood may be observed. Marine macrofauna, relatively common in some horizons, includes mostly bivalves, occasionally gastropods, brachiopods, colonial platy corals, ammonites and nautiloids. Large ammonites of the genus *Macrocephalites* prove the earliest Callovian age. Sands, sandstones, rarely conglomerates from the lower part of the Lower Callovian, were deposited in a near-shore environment. The presence of spheroidal blocks of ryodacites was interpreted earlier as an evidence of high energy at

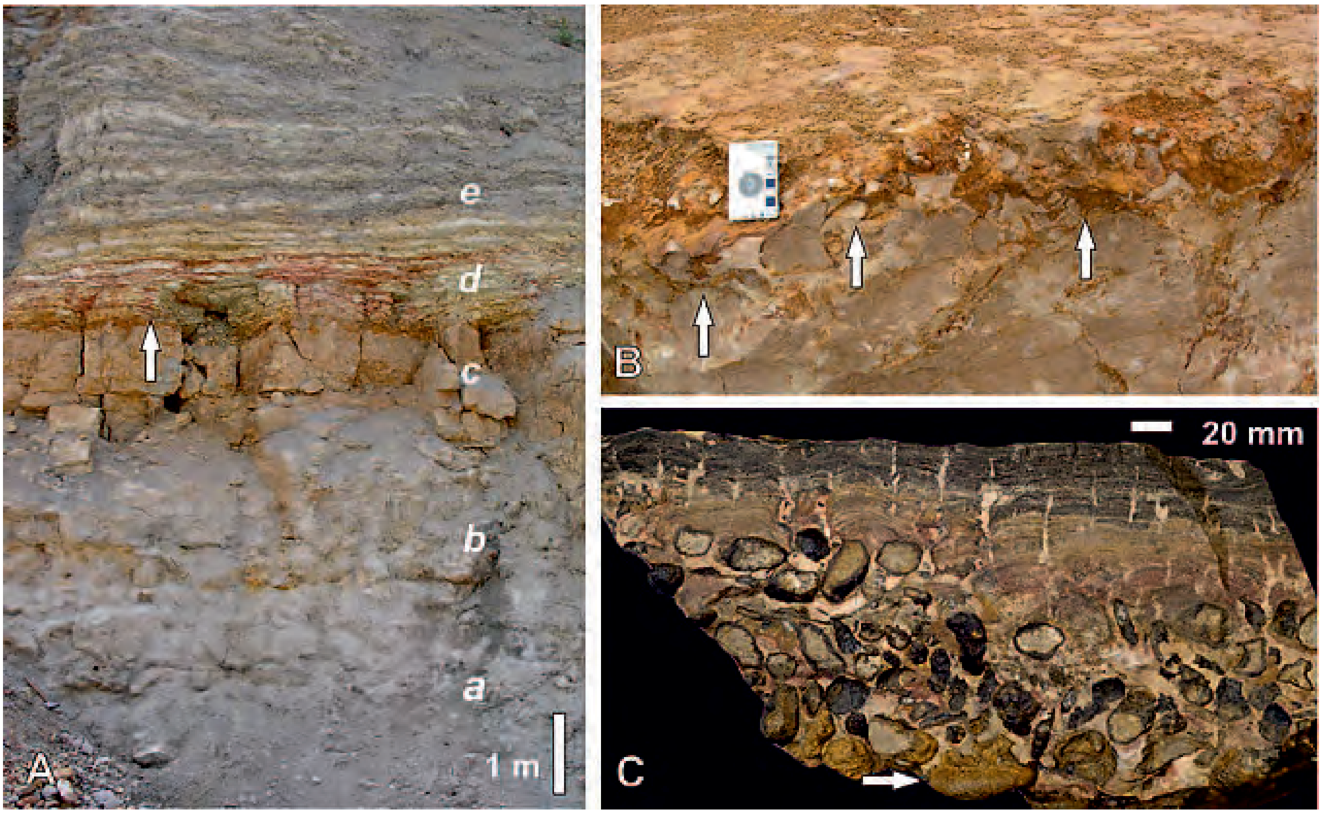

Fig. 5. Callovian and Lower Oxfordian at Zalas. **A.** *a* – Lower Callovian poorly lithified sands; *b* – sandstones; *c* – Lower Callovian sandy crinoid limestones; arrow indicates their truncated surface (a type of hardground); *d* – Upper Callovian condensed deposists (thin Fe-stromatolite, Fe-oncoids), and uppermost Callovian/lowermost Oxfordian pink limestones; *d* – Lower Oxfordian grey marls intercalated with limestones. **B.** Thin Fe-stromatolite covering truncated surface of sandy crinoidal limestones showing nodular structure (arrows). **C.** Fe-stromatolite and Fe-oncoids (clasts of crinoid limestones with thin, black Fe-crust); arrow indicates ammonite shell (coll. J. Wieczorek, Geological Museum, Institute of Geological Sciences, Jagiellonian University).

a near-shore cliff (Dżułyński, 1950), and recently as the result of corestone weathering of the Permian substrate (Matyja, 2006).

Lower Callovian sandy limestones (Koenigi Zone, in places Calloviense Zone). Subsequently, in the Lower Callovian succession, proportion of terrigenous components decreases and sandstones become more calcareous. The upper part of the Lower Callovian is developed as sandy crinoid limestones (the crinoid plates are hardly recognizable with a naked eye) – ca. 1.5 m in thickness – with horizons rich in bivalves, brachiopods, crinoid plates, less commonly echinoids, solitary corals and other benthic fauna (*c* in Fig. 5A, Fig. 5B). Ammonites, belemnites and nautiloids are less common. Sandy crinoid limestones were interpreted by Giżejewska and Wieczorek (1976) as deposited in a shallow, but sublitoral environment. The surprisingly high diversity of encrusters on the large bivalve *Ctenostreon*, higher than in Callovian tropical reefs, is interpreted by Zatoń *et al.* (2011) as the result of a deeper, less turbulent environment, the lack of salinity changes and lower sedimentation rate. The nodular structure at the top of crinoid limestones (Fig. 5B) is possibly related with activity of burrowing organisms, suggesting a low sedimentation rate which favoured early marine lithification (Giżejewska and Wieczorek, 1976; Wieczorek, 1982). The discontinuity surface at the topmost part of nodular limestones is a specific type of hardground (Fig. 4B), which resulted both from early lithification, submarine erosion and corrosion.

Uppermost Callovian condensed deposits. Ammonite studies revealed a stratigraphic gap embracing the Middle Callovian (Jason Zone and bulk of the Coronatum Zone; Giżejewska and Wieczorek, 1976; Matyja, 2006). This evidences prolonged non-deposition, erosion and reworking of underlying crinoid limestones. The truncated surface of crinoid limestones is usually covered by reddish or brownish Fe-stromatolites (but with significant participation of calcium carbonate), locally up to 40 cm thick (Fig. 5C; Giżejewska and Wieczorek, 1976). Inferred environmental factors favouring development

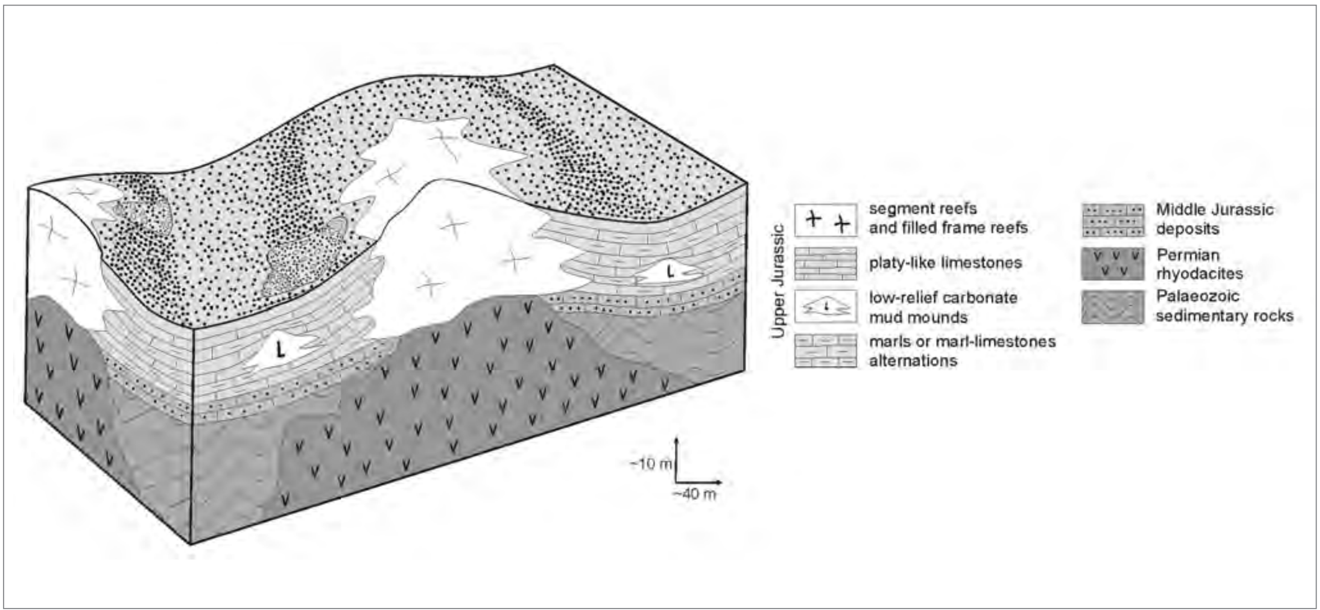

Fig. 6. Carbonate buildups at Zalas at the beginning of the Middle Oxfordian (after Matyszkiewicz *et al.*, 2012; modified).

of stromatolites include: hard substrate (hardground), a low sedimentation rate and the lack (or low activity) of burrowing organisms. Stromatolites from Zalas and other sites in the Kraków region formed on submarine swells created by synsedimentary tectonics (Giżejewska and Wieczorek, 1976; Wieczorek, 1982).

Specific oncoids occur below, within and above the stromatolite in pinkish marlstones (Fig. 5B). The oncoids consist of thin Fe, Mn lustrous cortex which coats pebbles of crinoid or pink marlstones and limestones present at the Callovian and the Oxfordian boundary (*d* in Fig. 5A). In the lowermost part of the Oxfordian (Mariae Zone), redeposited ammonites from the uppermost Callovian may be present (Giżejewska and Wieczorek, 1976). Locally, the Oxfordian marls lie directly on Permian ryodacites (Matyszkiewicz *et al.*, 2007a).

Oxfordian succession

On a rounded top of Permian rhyodacites, showing height differences of almost 10 metres, with overlapping unconformity lie Middle and Upper Jurassic deposits (Figs 2, 6). Above the stromatolite, which locally covers the rhyodacites top, lie marls and marl-limestone alternations rich in calcified siliceous sponges and other nektonic fauna. These deposits represent Lower Oxfordian and lower Middle Oxfordian (Tarkowski, 1989; Matyja, 2006). They include initial carbonate buildups (so called loose bioherms, cf. Trammer, 1982, 1985) – low-relief carbonate

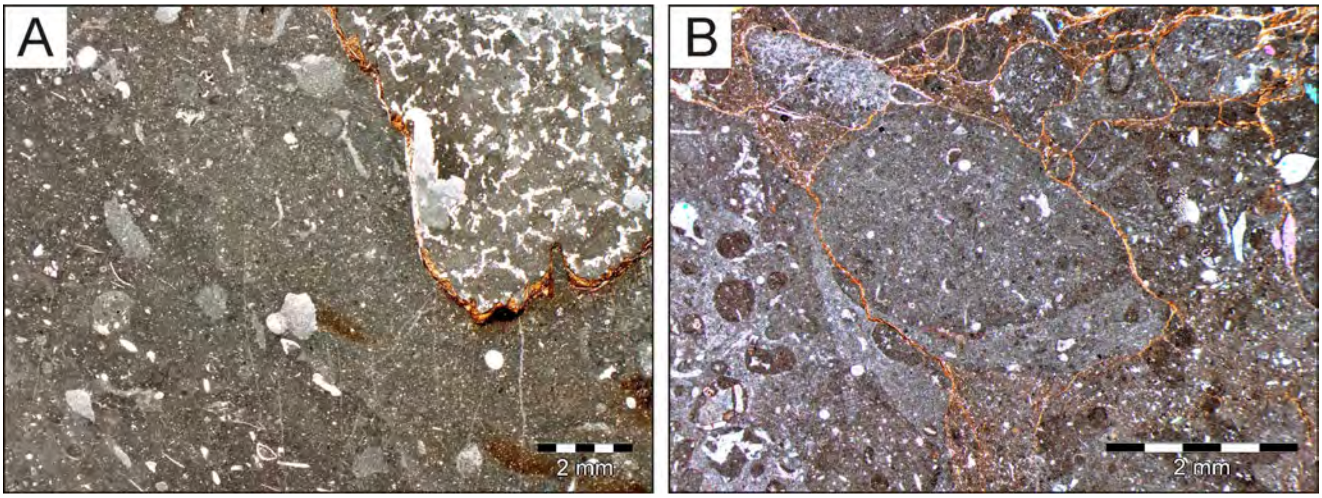

Fig. 7. Microfacies of the low-relief carbonate mud mound and segment reef from Zalas. **A.** Borings within pure leiolite. On the right, calcified siliceous sponge separated from pure leiolites by a stylolite lined by Fe-oxides. Low-relief carbonate mud mound. **B.** Nodules of clotted leiolites separated from fine-grained matrix by a stylolite filled with ferruginous substance. Segment reef.

mud mounds, several metres in diameter. The low-relief carbonate mud mounds are upsection replaced by carbonate buildups more than ten metres high, among which segment reefs and filled-frame reefs can be distinguished (Matyszkiewicz *et al.*, 2012; terminology after Riding, 2002). These types of carbonate buildups differ macroscopically and in development of microbialites, which are their main component.

Low-relief carbonate buildups are composed of limestone nodules, a dozen or so centimeters in diameter, residing in marly groundmass. The main macroscopic components of these buildups are dish-shaped calcified siliceous sponges Lithistida (cf. Trammer, 1982, 1985), which appear mainly in life positions. Ammonites, belemnites, brachiopods, bivalves and gastropods are also present. Microbialites observed in limestone nodules are formed as pure, clotted, and sometimes as layered leiolites (Matyszkiewicz *et al.*, 2012; terminology after Schmid, 1996). They show numerous penetrations filled with internal sediment (Fig. 7A). Low-relief carbonate buildups were formed in an environment with moderate water energy and low sedimentation rate, but with high nutrient availability (Matyszkiewicz *et al.*, 2012), which is confirmed by abundant calcareous nannoplankton dominated by *Watznaueria britanica* in the lowest Oxfordian marl deposits (Kędzierski, 2001).

Towards the top of the section, low-relief carbonate mud mounds turn into segment reefs (so-called pseudonodular limestones; cf. Dżułyński, 1952; Matyszkiewicz, 1994) and more than ten metres-high, complex filled-frame reefs (Matyszkiewicz *et al.*, 2012) with abundant fauna consisting of bryozoa, brachiopods, bivalves, echinoderms, ammonites, solitary corals and gastropods. Numerous discontinuities, enhanced by several centimetres thick layers of conglomerates, pink-red or grey-green, can be distinguished in these two types of carbonate buildups.

Segment reefs are composed of rounded nodules (Fig. 7B), which tend to disintegrate into grains with rounded edges (Dżułyński, 1952; Matyszkiewicz, 1994; Matyszkiewicz *et al.*, 2012). Their main components are microbialites, dish-shaped siliceous sponges Lithistida and Hexactinellida, but brachiopods, bryozoans, ostracods, polychaetes can also be found.

Filled-frame reefs are formed as tight massive limestones, with microbialites as the main component; secondarily occurs fauna similar to that in segment reefs (Matyszkiewicz *et al.*, 2012). In those parts of filled-frame reefs that are formed as very tight massive limestone, stromatactis, stromatactis cavities and stromatactis-like cavities (terminology after Matyszkiewicz, 1997a) are locally observed. Stromatactis form a characteristic sparitic network. Stromatactis cavities and stromatactis-like cavities are filled with internal sediment in their lower part, and in the upper – with several generations of calcite cements (Fig. 8A, B). Isolated stromatactis-like cavities have diameters exceeding 1 cm and uneven, digitate roofs. Internal sediment is formed as micropeloidal

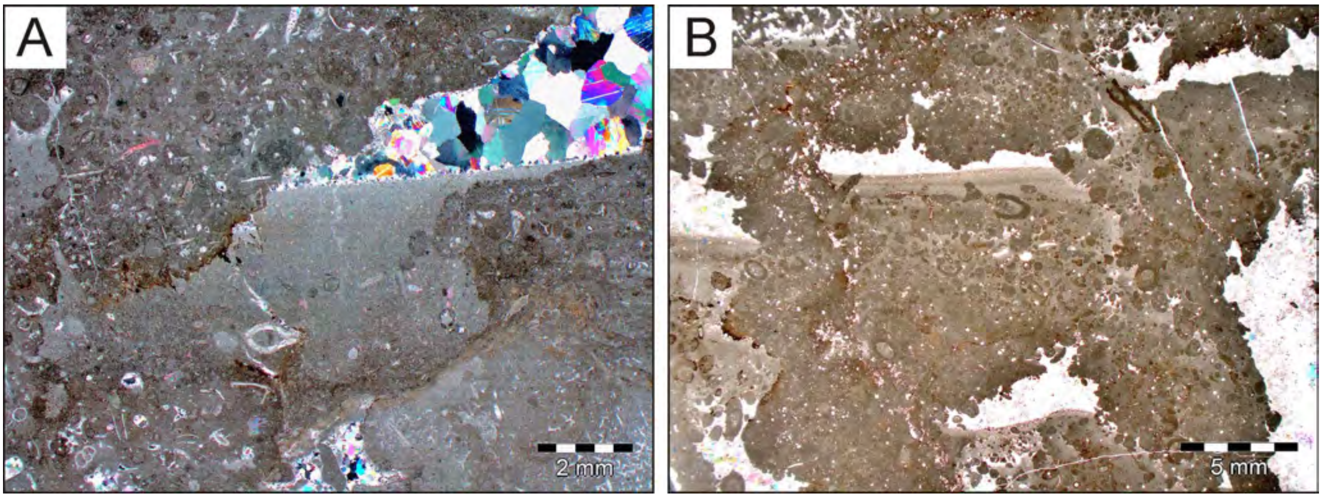

Fig. 8. Microfacies of the filled frame reef from Zalas. **A.** Stromatactis cavity. Internal sediment below the cement represents mudstone with single, rounded grains, and it is separated from the host rock by a stylolite locally lined by Fe-oxides. Layered thrombolite on the right. **B.** Stromatactis cavities filled with internal sediment in their lower part, and in the upper – with several generations of calcite cements. Internal sediment in the upper part, at the contact with cement, is represented by micropeloidal packstone and micropeloidal stromatolite. In the lower part internal sediment is developed as mudstone-wackestone with larger grains.

packstone, micropeloidal stromatolite or fine-grained mudstone-wackestone with fragments of undistinguishable bioclasts or small rounded grains in the upper part, which are in contact with cement. Sometimes the whole internal sediment is separated from host-rock by stylolites (Fig. 8A). Locally, isolated stromatactis-like cavities are filled with granular quartz. Segment reefs and filled-frame reefs were formed in an environment with slightly higher water energy, lower sedimentation rate and nutrient availability than the low-relief carbonate mud mounds (Matyszkiewicz *et al*., 2012).

Various traces of mechanical and chemical compaction of any severity grade are observed in all types of carbonate buildups from the Zalas quarry (Fig. 7A, B). Susceptibility to mechanical compaction of the deposits depends mostly on early-diagenetic cementation and appearance of rigid framework, which can show diverse formations, such as reticulate or laminar rigid framework (cf. Pratt, 1982). In turn, the development of pressure-dissolution connected with chemical compaction depends on clay content in the deposits. During burial diagenesis in limestones with low clay content, stylolites widely develop, whereas in rocks with bigger clay content, pressure-dissolution structures are practically absent. Low-relief carbonate mud mounds with high clay content, in which rigid framework developed only in separated nodules, were subject to significant mechanical compaction, but to a lesser extent than the fine-grained bedded marl-limestone alternations surrounding them. Given the substantial clay content, during burial diagenesis, pressure-dissolution phenomena did not develop in these deposits.

In segment reefs, in which initial laminar rigid framework developed (Matyszkiewicz, 1994, 1997b; Kochman and Matyszkiewicz, 2013), mechanical compaction processes occurred to a lesser extent than in low-relief carbonate mud mounds. Smaller clay content in the deposits allowed early-diagenetic cementation of laminar framework and intense pressure dissolution during burial diagenesis. In filled frame reefs with well-developed reticulate rigid framework, mechanical compaction was minimal due to intensive early-diagenetic cementation (Kochman and Matyszkiewicz, 2013), whereas chemical compaction occurred only occasionally.

In area around Zalas, and in the quarry, many faults are observed. A part of them were probably active during Middle and Late Jurassic, but the main faulting phase took place in Cenozoic. Some faults in the Zalas quarry are mineralised and contain chalcopiryte, piryte, iodargyrite, covelline, galena, native bismuth, malachite, cuprite, Fe- and Mn-oxides, Cu-sulfates and barite (Gołębiowska *et al*., 2010).

Installation of the first low-relief carbonate mud mounds was probably connected with appearance of sea

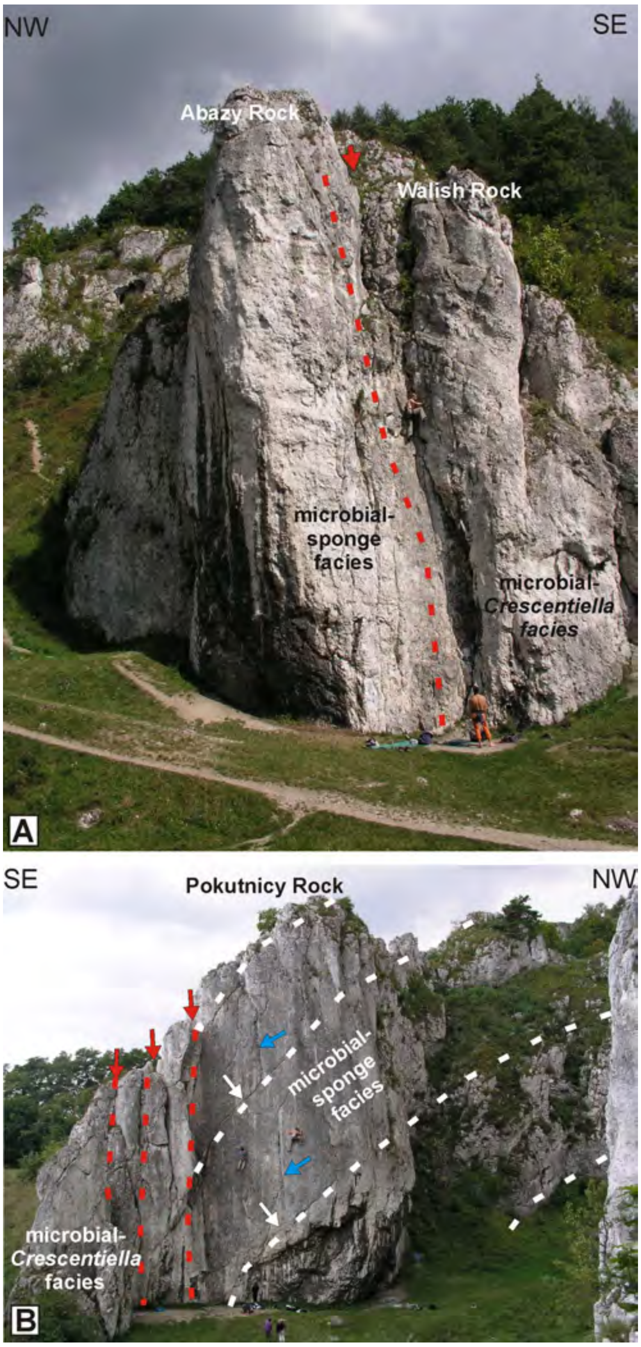

Fig. 9. Facies of Bolechowicka Valley. **A.** Southern part of Bolechowicka Valley, east slope. Abazy and Walish crags separated by a fault surface (red line). The fault surface separates microbial-sponge facies (boundstone) from the microbial-*Crescentiella* facies (grainstone-rudstone). **B.** Southern part of Bolechowicka Valley, west slope. Filar Pokutników located within the near-fault flexure (with line and arrows) that passes southwards into brittle deformation with faults (red lines and arrows). Vertical surfaces are joints (blue arrows).

bottom elevations related to Palaeozoic structures and of active synsedimentary tectonics, also generating submarine gravity flows (Trammer, 1985; Matyszkiewicz *et al*., 2006b; 2012). First initial low-relief carbonate mud mounds became transformed into segment and filled-frame reefs, in which microbialites formed a distinct rigid framework. Layers of conglomerates observed in the segment and filled-frame reefs mirror periods of growth inhibition of these carbonate buildups (so-called incipient drowning; cf. Bice and Stewart, 1990). Geochemical research results, mainly negative Ce anomalies, and distinct enrichment in HREE of microbialites in the Upper Jurassic carbonate buildups from the Kraków region (Matyszkiewicz *et al*., 2012), show that seawater on the whole Late Jurassic shelf in the Kraków region was generally well-oxygenated and corresponded with contemporary seawater in terms of alkalinity (cf. Olivier and Boyet, 2006; Olivier *et al*., 2007). Thus, the formation of microbialites that built the diverse carbonate buildups was affected mainly by local sedimentation environment not related to distinct changes in chemical composition of seawater. Therefore, the development of microbialites as the main component of carbonate buildups was controlled by contents of dissolved or fine-grained nutrients suspended in water, sedimentation rate and energy of sedimentation environment (Matyszkiewicz *et al*., 2012).

A5.2 Bolechowice. Upper Oxfordian facies and microfacies in Bolechowicka Valley and problems with facies relationships in a fault zone

Southern part of Bolechowicka Valley (50°09′09″ N, 19°47′06″ E)

Leader: Marcin Krajewski

Location and geological setting

Bolechowicka Valley is located at the northern margin of the Krzeszowice Graben (Fig. 2). In this area, the faults separate the Ojców Block, the main part of the Kraków Upland, from the Krzeszowice Graben. Numerous exposures of Jurassic rocks can be examined near Bolechowice (Fig. 9). The exposed rocks represent sedimentary sequence located from 100 to 150 m above the bottom surface of the Oxfordian succession (Fig. 3). Several outcrops in and near Bolechowicka Valley were studied in terms of detailed microfacies analysis (Matyszkiewicz and Krajewski, 1996). As a result, numerous microfacies were identified and classified in two groups of facies: microbial-sponge facies, and microbial-*Crescentiella* facies. From stratigraphic point of view, all these facies belong to the Upper Oxfordian (Fig. 3). Precisely, numerous ammonites found in the area indicate that the massive limestones represent the Upper Bifurcatus Zone

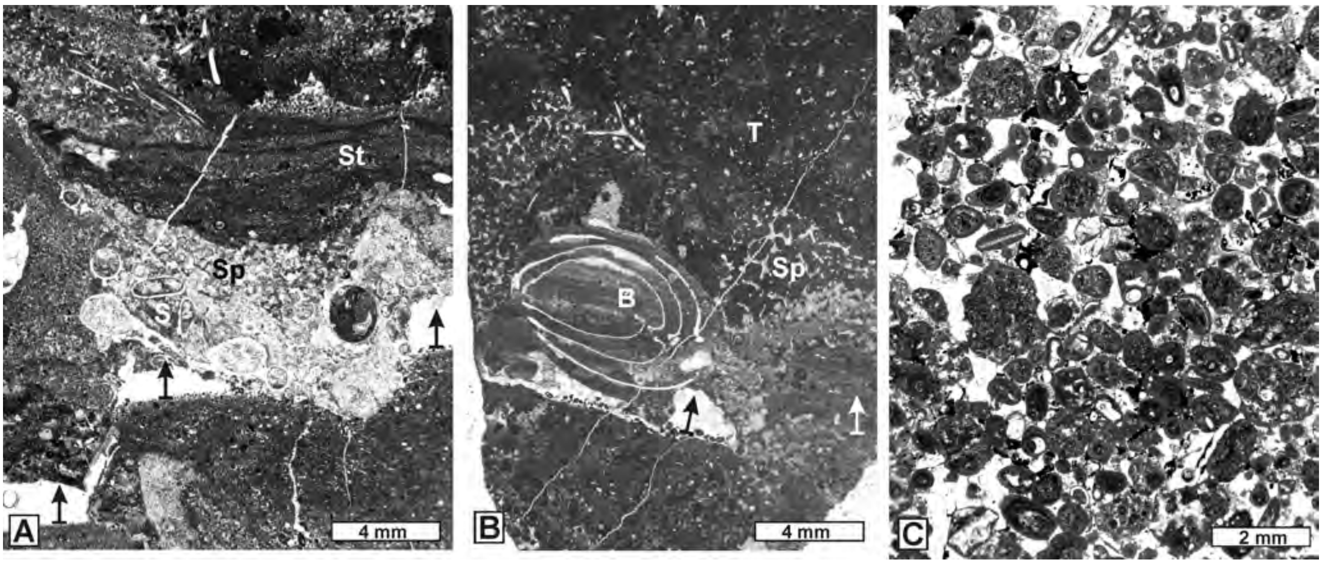

Fig. 10. Microfacies observed in massive limestones of Bolechowicka Valley. **A.** Microbial-sponge boundstone. Calcified seliceous sponge (Sp), stromatolite (St) and serpulids (S) visibele in the central part. The presence of rigid framework is documented by growth cavities with geopetal filling indicating orginal positionof the top. **B.** Microbial-sponge boundstone. Calcified siliceous sponge (Sp) displaying an extensive boring (B) with the shell of the boring organism. Thrombolites are growing on the sponge. Black arrow indicates original top. The present position of the bottom-top direction is indicate by white arrow. **C.** Grainstone with numerous *Crescentiella*, small ooids, oncoids, aggregate grains and bioclast.

(Stenocycloides-Grossouvrei subzones; Krajewski, 2000; Krajewski and Matyszkiewicz, 2004; Ziółkowski, 2007b).

The limestone rocks, particularly that observed in the southern part of the valley, at the margin of the Krzeszowice Graben includes numerous tectonic discontinuities (Fig. 9). Two types were distinguished: vertical joint systems and pene-horizontal surfaces dipping to the east, as evident on the valley western slope. Studies revealed their tectonic origin (Matyszkiewicz and Krajewski, 1996).

Facies description and interpretation

The microbial-sponge facies can be encountered in most rocks of Bolechowicka Valley (Fig. 9). Dominant are microbial-sponge boundstones and bioclastic wackestones, packstones and grainstones (Matyszkiewicz and Krajewski, 1996). In biolithites, numerous growth caverns and borings point out to the presence of a rigid framework typical of reefs (Fig. 10A, B). Many cavities are geopetally filled, which enables us to determine deviation of their roofs from original positions. The framework is formed mainly by siliceous sponges (*Lithistida* and *Hexactinellida*) overgrown by microbialites, dominated by fine crusts of dense micrite, clotted thrombolites and peloidal stromatolites (e.g. Matyszkiewicz, *et al*., 2012; Fig. 10A, B). Commonly observed are brachiopods, echinoids, peloids, tuberoids and abundant fine bioclasts. Frequent are microencrusting organisms, particularly bryozoans, benthic foraminifers (*Nubecularia*, *Bullopora*) and serpulids. In the microbial-sponge facies, distinct transition is observed (cf. Matyszkiewicz, 1997b; Krajewski, 2000): up the sequence, the number of sponges decreases in favour of microbialites (mostly agglutinuating) and peloidal stromatolites. In the upper parts of microbial-sponge facies, large amounts of problematic microencruster *Crescentiella* appear (Matyszkiewicz, 1997b; Krajewski, 2000) and at a short distance the sediment changes to microbial-*Crescentiella* facies.

This facies is representative of most of rock complexes in the Kraków Upland and it records the main stage of reef development in this area (e.g. Matyszkiewicz, 1997b; Krajewski, 2000). The microbial-sponge facies is typical of the Oxfordian in the Kraków Upland and is widely distributed in the northern shelf of the Tethys Ocean (e.g. Leinfelder *et al*., 1996; Matyszkiewicz, 1997b). Most of the results demonstrate that the microbial-sponge facies developed mostly in a low-energy, nutrient-rich environment. Commonly observed microencrusters, mostly benthic microbial communities, serpulids, bryozoans and foraminifers, all indicate low-energy environment, low deposition rates and low terrigenous influx. Environment conditions of this facies are usually interpreted as sea level high-stand mid-ramp, above the storm wave base.

The microbial-*Crescentiella* facies is observed mostly in exposures located in the southern part of the valley (Fig. 9). Two microfacies varieties are observed: microbial-*Crescentiella* boundstones and *Crescentiella*-bioclastic grainstones-rudstones (Fig. 10C). The microproblematica *Crescentiella* (*Tubiphytes* in older literature) build individual or colonial forms in which individual forms are often connected by cyanophycean crusts. Apart from *Crescentiella,* crushed bioclasts: bivalves shells, bryozoans, calcareous sponges, gastropods and echinoderms are common in the coarse grainstones-rudstones. They are accompanied by fine bioclasts, peloids, aggregate grains, intraclasts, oncoids and ooids (Fig. 10C).

The microbial-*Crescentiella* facies represents the mid-ramp setting. The presence of phototrophic *Crescentiella* and detrites indicates paleodephts between normal and storm wave bases (Leinfelder *et al*., 1996; Matyszkiewicz, 1997b; Krajewski, 2000). The limestones rich in microproblematica *Crescentiella,* which illustrate symbiosis between nubecularid foraminifera and cyanophyceans (Senowbari-Daryan *et al*., 2008), were included to the do *Tubiphytes-Terebella* association (e.g., Leinfelder *et al*., 1996). In this facies, common are coarse-grained sediments documenting an intensive reworking of material in the wave base zone (Krajewski, 2000). In grain-dominated sediments, one can observe coated grains pointing out to sedimentary conditions close to normal wave base. Transition from microbial-sponge to microbial-*Crescentiella* facies can be related to progressive shallowing of the basin in the Upper Oxfordian.

Problems with facies interpretation in the fault zone

The exposures examined in the Bolechowicka Valley are located in a tectonic zone, which hampers the observations and interpretation of primary facies architecture and, consequently, may lead to misinterpretations (cf. Koszarski, 1995; Matyszkiewicz and Krajewski, 1996). The primary sedimentary sequence is here disturbed by numerous hinge faults belonging to tectonic megabreccia at the margin of the Krzeszowice Graben (Fig. 11). Fortunately, analogous and contemporaneous sedimentary sequences can be observed in the vicinity, in undisturbed parts of the Ojców Block (Krajewski, 2000), which enables us to reconstruct the primary sedimentary sequences of the Bolechowice area.

In reconstruction of primary facies architecture, particular attention must be paid to numerous tectonic discontinuities (Krokowski, 1984; Matyszkiewicz and Krajewski, 1996; Fig. 9). Basing on the analysis of geopetal infillings found in the rock-tower named "Filar Pokutników" (Fig. 9B), it was concluded that rocks forming the southern part of Bolechowicka Valley were tilted by 30° from their primary position. The lack of substantial differences in lithology of rocks cut by discontinuities advocates the tectonic origin of these surfaces (Matyszkiewicz and Krajewski, 1996).

The vertical discontinuities cutting through the limestones are joints belonging to several joint systems (Fig. 9; Krokowski, 1984). In the southermost part of the valley, these discontinuities are presumably fault surfaces enlarged by karstic dissolution, genetically related to the broad tectonic zone that separates the Ojców Block from the Krzeszowice Graben. Some of these faults follow pre-existing joints. On the contrary, the discontinuities observed e.g., in Filar Pokutników, gently dip to the south and are genetically linked to shear surfaces in the fault-adjacent flexures developed at the northern margin of the Krzeszowice Graben (Fig. 11; Krokowski, 1984). Complicated facies relationships found in Bolechowicka Valley are, first of all, the effects of hinge faults and megabreccia zones developed in the tectonic zone separating the Ojców Block from the Krzeszowice Graben.

A5.3 Zabierzów Oxfordian microbial bioherm with exceptionally numerous microencruster *Crescentiella* (= "*Tubiphytes*") *morronensis* and common growth cavities and stromatactis-like cavities in Zabierzów

Zabierzów quarry, western part of the Zabierzów village, (50°06′49″ N, 19°47′12″ E)

Leaders: Ireneusz Felisiak, Jacek Matyszkiewicz

The abandoned limestone quarry is located in the western part of the Zabierzów village, 12 km west of Kraków center. Vast, east-west-trending depression north of the quarry is the Krzeszowice Graben (Fig. 12). The quarry was developed in the zone of fault megabreccia visible in the southern wall of the graben, along which it contacts the pre-Badenian horst of the Tenczynek Ridge (Felisiak, 1992). The quarry includes two major excavations: the lower, NE one with a pond and the upper, SW one; each corresponds to one of two small horsts built of the Oxfordian limestones. In the upper, SW part of the quarry, massive limestones predominate, belonging to a core of a buildup (see description below).

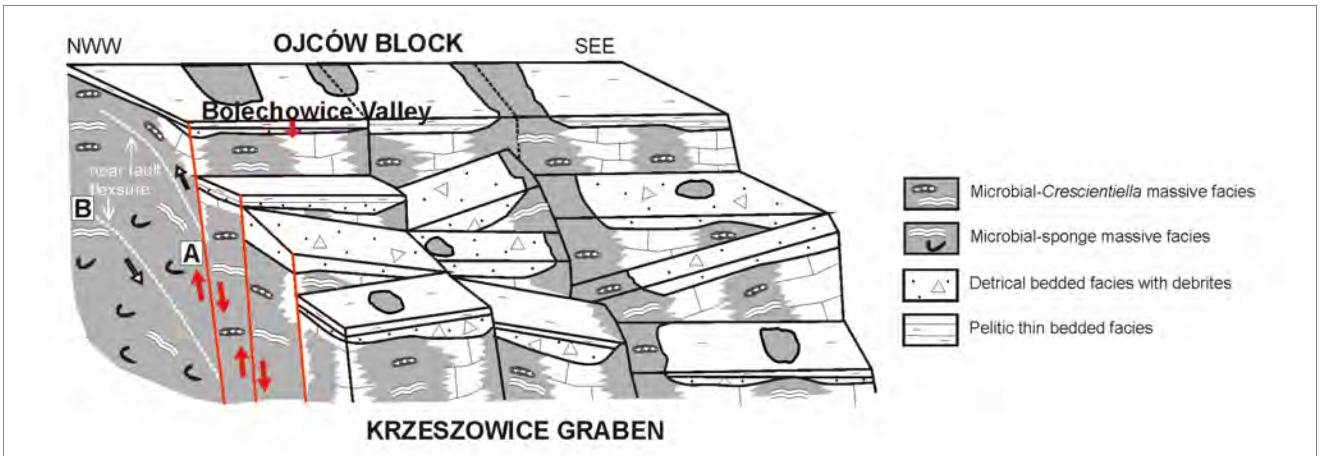

Fig. 11. Position of Bolechowicka Valley in the fault zone that separates the Ojców Block from the Krzeszowice Graben (after Matyszkiewicz and Krajewski, 1996; supplemented). Near-fault flexure passes southward into discontinuous deformations. The total vertical fault's displacement consists of numerous secondary faults, some of which are hinge faults. This caused dipping of sediments in various directions, accompanied by a fault-related megabreccia. A-B. Approximate location of outcrops presented in Fig. 9.

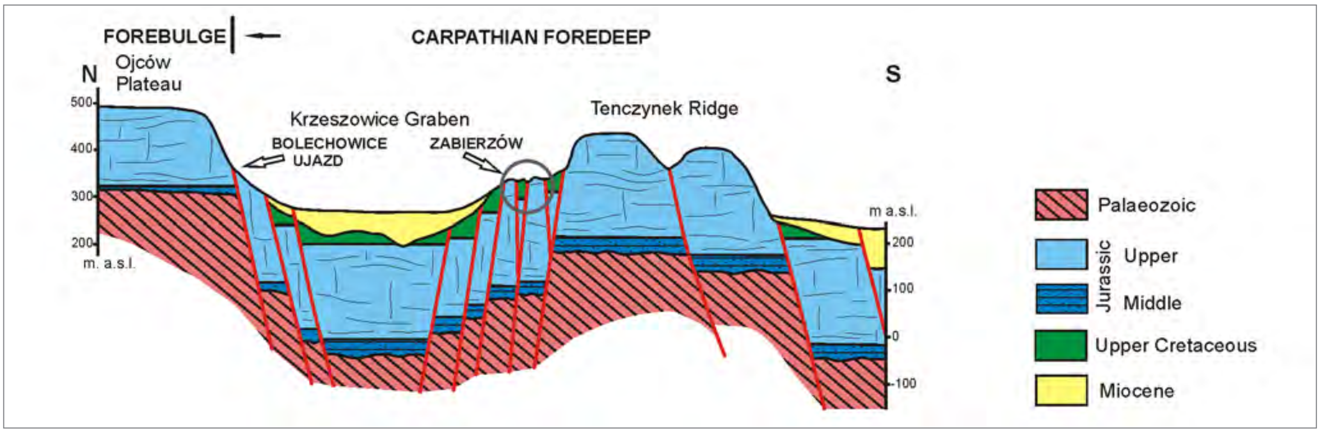

Fig. 12. Diagrammatic cross-section across the Krzeszowice Graben near Zabierzów.

The small graben which separates both horsts is filled with Cretaceous sediments. These rocks have not been quarried and recently form a morphological elevation seen as a NW-SE trending ridge. In the roadcut transversing the ridge we can observe the upper part of the Cretaceous succession – the Senonian marls. Their lowermost portion together with underlying Coniacian and Turonian limestones, as well as the contact surface with the Jurassic sediments are accessible in the upper parts of walls in both quarries.

The Oxfordian limestones are truncated by Cenomanian-Turonian abrasion platform with locally abundant borings (rock ground), which is covered by Upper Cretaceous sediments. Their succession starts with a thin layer of Turonian limestones (foraminifer-calcisphere wackestone/packstone with quartz pebbles, up to 65 cm thick; Jasionowski, 1995). Both layers are separated by a wavy surface of a soft-ground with scarce burrows. Flat, top surface of the Turonian sediments is a hard ground covered by the deep-water, phosphatic stromatolite, up to 4 cm thick (Golonka and Rajchel, 1972; Jasionowski, 1995), which represents the Late Turonian-Coniacian (after E. Machaniec, see Hoffmann *et al*., 2013). It is overlaid by marls grading up into white limestones and gaizes with interbeds of cherts and marls, 15 m thick.

The Upper Oxfordian *Crescentiella* reef with stromatactis-like cavities

The section of Upper Jurassic rocks (?*bimammatum*/*planula* zones; Fig. 3) in Zabierzów region (Fig. 13) is ca. 180 m thick, and the quarry exposes the uppermost part of this section (Matyszkiewicz, 1997a; Matyszkiewicz *et al*., 2012). The Upper Jurassic sediments are represented by massive limestones formed as microbial-

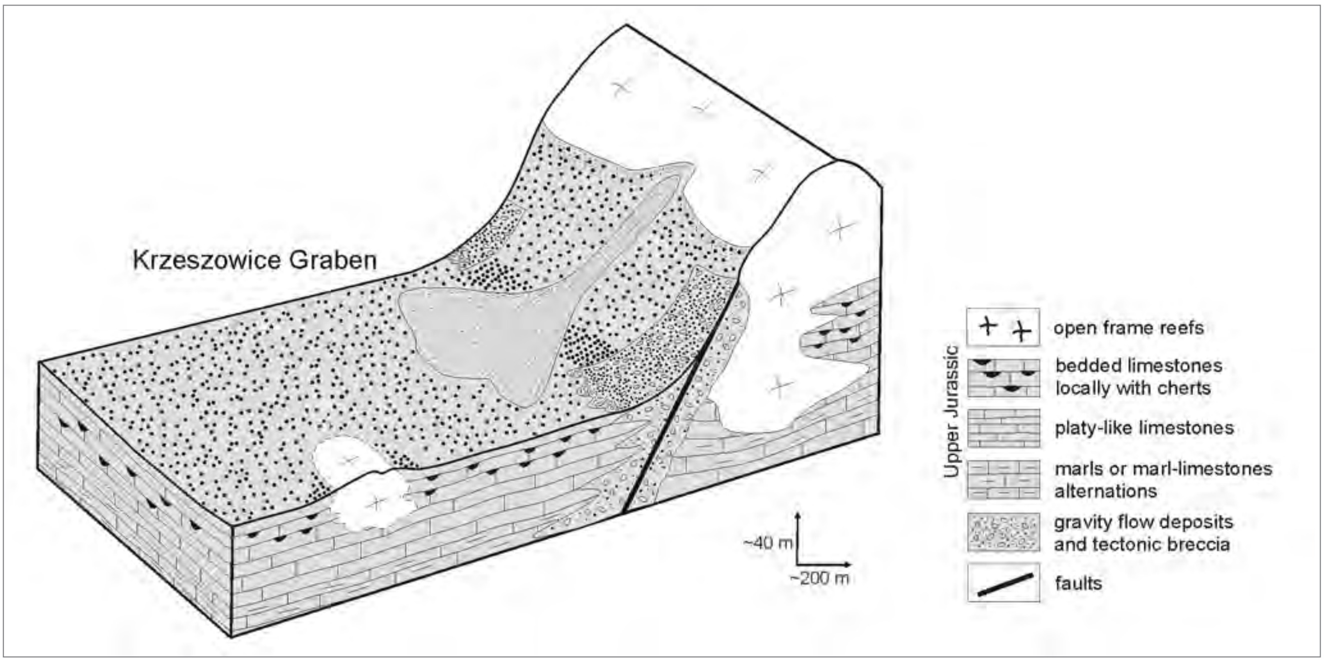

Fig. 13. Position of the open-frame reef at Zabierzów at the end of the Oxfordian (after Matyszkiewicz *et al*., 2012; modified).

sponge boundstone or locally as nest-filling grainstone. The massive limestones contain macroscopically visible abundant and diversified fauna of calcareous and siliceous sponges, serpulids, bivalves, brachiopods, gastropods, echinoids, crabs, and juvenile forms of ammonites. A carbonate buildup formed as an open-frame reef is exposed in the upper level of the quarry, on its SW wall. It represents the most advanced stage of development of the rigid framework (so-called reticulate rigid framework, cf. Pratt, 1982) among different types of microbial-sponge Upper Jurassic carbonate buildups in the Kraków region (Matyszkiewicz, 1997a; Matyszkiewicz *et al*., 2012).

The most important components of the rigid framework of the microbial-sponge open-frame reef are numerous *Crescentiella morronensis* (cf. Senowbari-Daryan *et al*., 2008). Microbialites are highly diversified. They are dominated by agglutinating stromatolites, micropeloidal stromatolites, pure leiolites and layered leiolites. Pure leiolites and layered leiolites compose massive, irregular envelopes that bind organisms building the framework of the open-frame reef and comprise abundant benthic fauna of bivalves, brachiopods, crabs, juvenile ammonites, serpulids, *Terebella* sp., bryozoans, siliceous and calcareous sponges and, first of all, *Crescentiella morronensis*.

The rocks bear frequent growth cavities, walls of which are encrusted with polychaetes. Moreover, in the central part of the open frame reef, numerous isolated stromatactis-like cavities about 2 cm high and several centimetres wide are observed (terminology after Matyszkiewicz, 1997a; Fig. 14A). The roofs of the stromatactis-like cavities are usually uneven and digitate, and the bottoms are smooth. In the upper part, stromatactis-like cavities are usually empty and their walls are covered by isopachous granular or dogtooth cement. Sometimes, the upper part contains blocky calcite or poikilotopic cements (Fig. 14B). In the lower part of the stromatactis-like cavities, internal sediment in the form of micropeloidal stromatolite with numerous thin laminae is observed. Some stromatactis-like cavities are filled with light green or yellow clay, which does not contain microfauna.

The open-frame reef from Zabierzów grew at a moderate energy of environment, low sedimentation rate, and moderate nutrient availability. Stromatactis-like cavities could have been formed as a result of: (i) almost synsedimentary internal erosion of weakly lithified parts of soft sediment, which fills spaces between fully lithified parts of rigid framework, caused by water turbulence connected with impact of gravity flows on the bedding (cf. Matyszkiewicz, 1993; Wallace, 1987), (ii) cavitation erosion of primary growth cavities during Late Jurassic regression or Late Cretaceous transgression (cf. Matyszkiewicz, 1997b), (iii) compressional and tensional stress of primary (e.g. growth cavities, shelter porosity) or secondary (e.g. dissolved aragonitic skeletons of corals) voids during early diagenesis, caused by multi-stage activity of faults (cf. Olchowy, 2011), or (iv) local dissolution and mineralization of limestones by hydrothermal solutions migrating along fault zones. The last two possibilities connect the formation of the stromatactis-like cavities with active fault tectonics that took place in the Zabierzów area during a period between at least Late Jurassic and Cenozoic time.

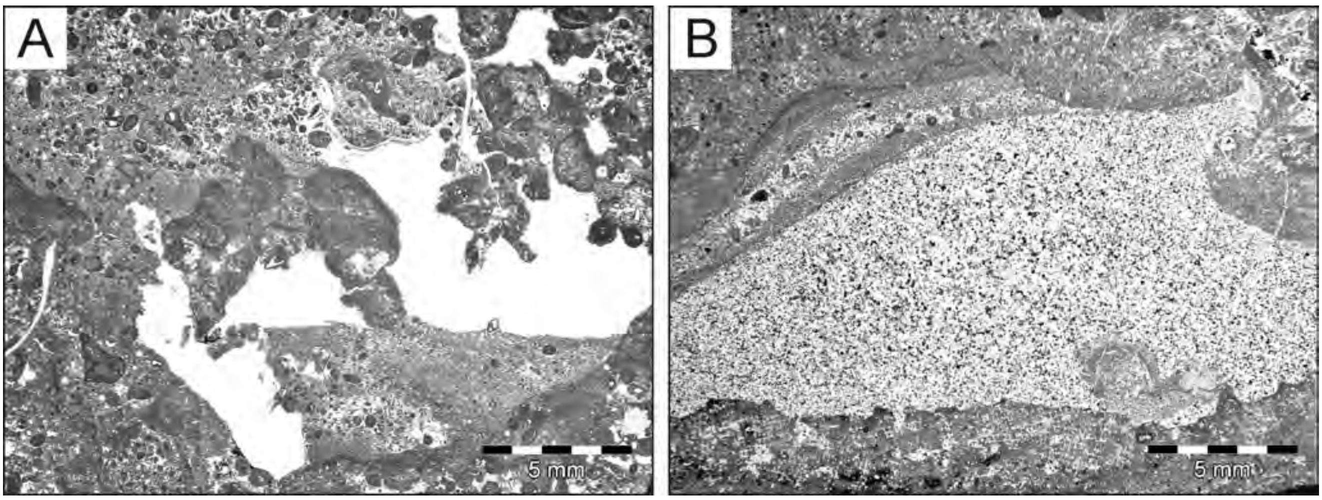

Fig. 14. Microfacies and stromatactis-like cavities in the open-frame reef at Zabierzów **A.** stromatactis-like cavity without internal sediment, partly filled in the uppermost part with greenish clay. **B.** stromatactis-like cavity completely filled with late diagenetic granular cement.

A5.4 Wielkanoc. The Uppermost Oxfordian massive limestones with stromatactis-like cavities; outcrop in Wielkanoc near Miechów

Western part of Wielkanoc village, right bank of the Gołczanka stream (50°20′17″ N, 19°54′31″ E)

Leader: Piotr Olchowy

The Wielkanoc Quarry is located in the eastern part of the Kraków-Częstochowa Upland, about 30 km north of Kraków (Fig. 2). The sub-Mesozoic basement of the Silesian-Kraków Homocline includes folded Paleozoic formations divided by the Kraków-Lubliniec Fault Zone into the Małopolska and the Upper Silesian blocks (Żaba, 1995, 1999; Buła *et al.*, 1997; Buła and Habryn 2008). The Wielkanoc Quarry is located in the western, marginal part of the Małopolska Block, about 7 km east of the Krzeszowice-Charsznica Fault.

The quarry is ca. 300 m long and 100 m wide. In its southeastern wall, we observe an about 15 m-thick succession of Upper Jurassic rocks (Oxfordian, *planula* Zone (Fig. 3), cf. Głazek and Wierzbowski, 1972) followed by an about 16 m-thick Upper Cretaceous sequence (Figs 15, 16). The top surface of the Upper Jurassic succession is an abrasion surface. The Upper Cretaceous sediments include Turonian sandy, sandy-organodetrital, organodetrital and pelitic limestones covered by Coniacian sandy-glauconitic limestones and Late Santonian marly-glauconitic limestones, and glauconitic marls (Olszewska-Nejbert, 2004; Olszewska-Nejbert and Świerczewska-Gładysz, 2009). The Upper Cretaceous strata are overlain by Quaternary loess, about 2 m thick.

Development of limestones in the Wielkanoc Quarry

The Upper Jurassic sediments from the Wielkanoc Quarry were described by Olchowy (2011). These are massive limestones with macroscopically visible, calcified, siliceous sponges up to 1.5 cm thick, serpules of diameters up to 0.5 cm, tuberoids up to 1 cm across, single ammonites and numerous stromatactis-like cavities (*sensu* Matyszkiewicz, 1997a). In the middle and lower parts of the massive limestones sequence, typical are numerous elongated pores, up to 2 cm long. Their transversal sections are commonly rounded and show diameters up to about 0.4 cm. Such pores occur as individuals or as clusters composed of several to a dozen of pores. In some pores, we observe partly dissolved cladophyllid corals. Locally, the massive limestones comprise lenses of granular bioclastic limestones built of irregular grains up to 3 mm across. The lenses of granular bioclastic limestones can be up to several tens of cm long and up to a dozen of cm thick but usually, their dimesions are much lower.

Under the microscope, the massive limestones are dominated by microbialites developed as laminated thrombolites and *Crescentiella*, up to 2 cm in diameter. Common are thrombolite-sponge associations and

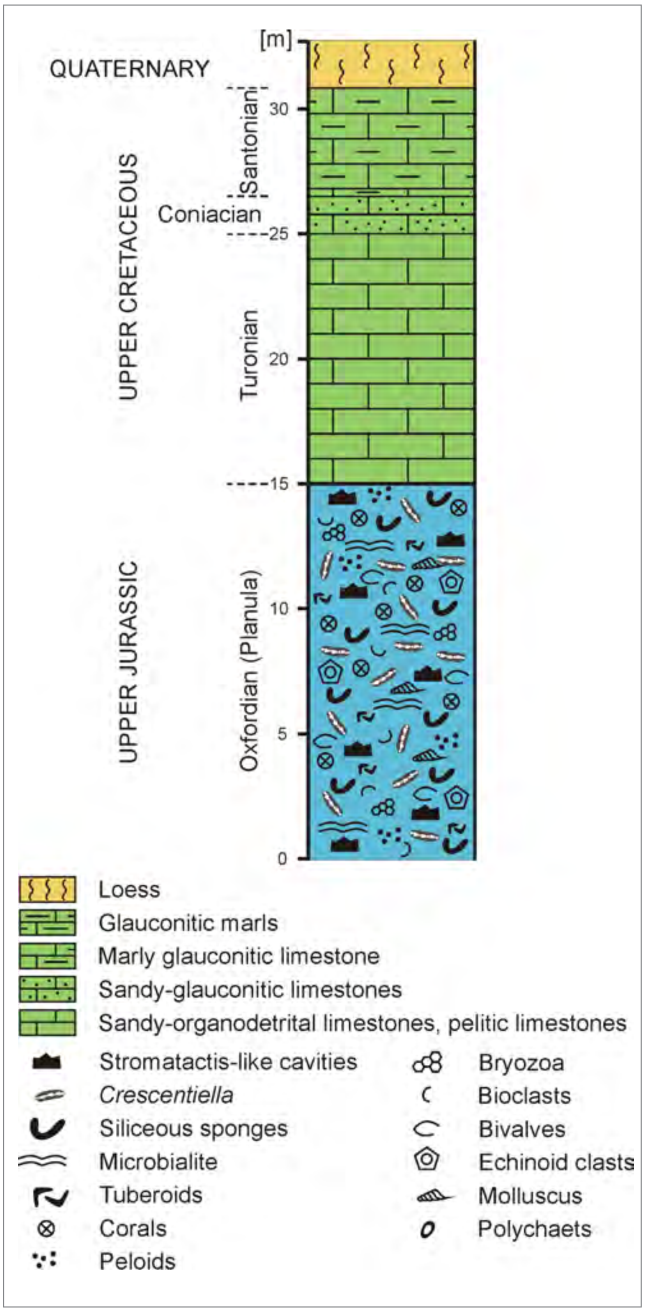

Fig. 15. Lithostratigraphic column of sediments in Wielkanoc Quarry. Upper Jurassic sediments with stromatactis-like cavities and main components.

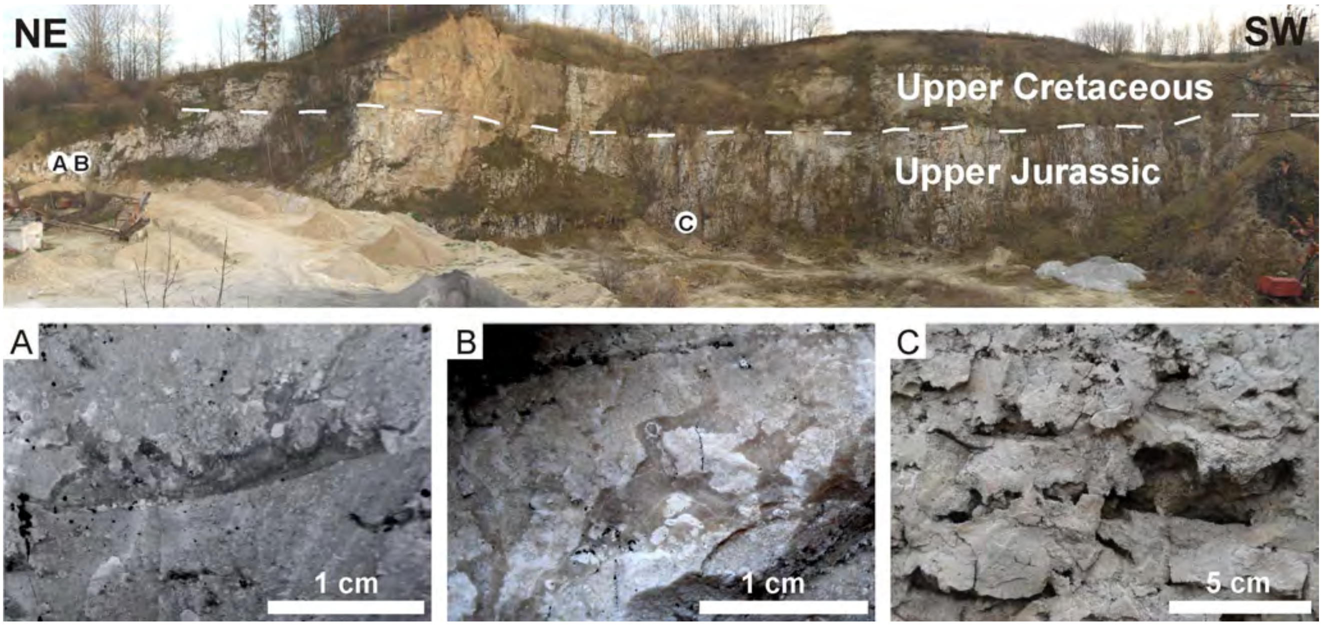

Fig. 16. General view of SE wall of Wielkanoc Quarry with a location of some stromatactis-like cavities. **A–C**. Stromatactis-like cavities at the weathered rock surface.

wackestones with fine peloids, numerous *Crescentiella*, tuberoids, serpules, calcified sponge spicules, echinoderms plates, echinoids spines, bryozoans with microbial rims, fragments of corals up to about 2 cm across, as well as single oncoids, up to 1 mm in diameter, and *Terebella lapilloides*. Abundant are *Stylosmilia* corals with distinct dissolution traces (Fig. 17A). Sometimes, corals have microbial rims, up to 0.6 mm thick. Close to corals, we often observe rounded pores filled with calcite. The lenses of bioclastic limestones consist of packstones/grainstones with *Crescentiella*, fragments of siliceous sponges with microbial crusts, up to 0.2 mm thick, serpules, bivalve shells and echinoderms plates. Most grains are rimmed with isopachous cement, up to 0.4 mm thick, whereas the remaining intergranular spaces are filled with blocky cement. Commonly, bioclastic packstones/grainstones are observed beneath the sponges. Locally, the spaces between the lower surfaces of sponges and bioclastic grainstones are filled with calcite cements.

Description of stromatactis-like cavities

The stromatactis-like cavities occur within the full thickness of the massive limestone succession. When observed on weathered rock surface, they can be up to about 4 cm wide and up to 2 cm high (Fig. 16A–C). These are cavities of rough or smooth, arcuate roofs whereas the

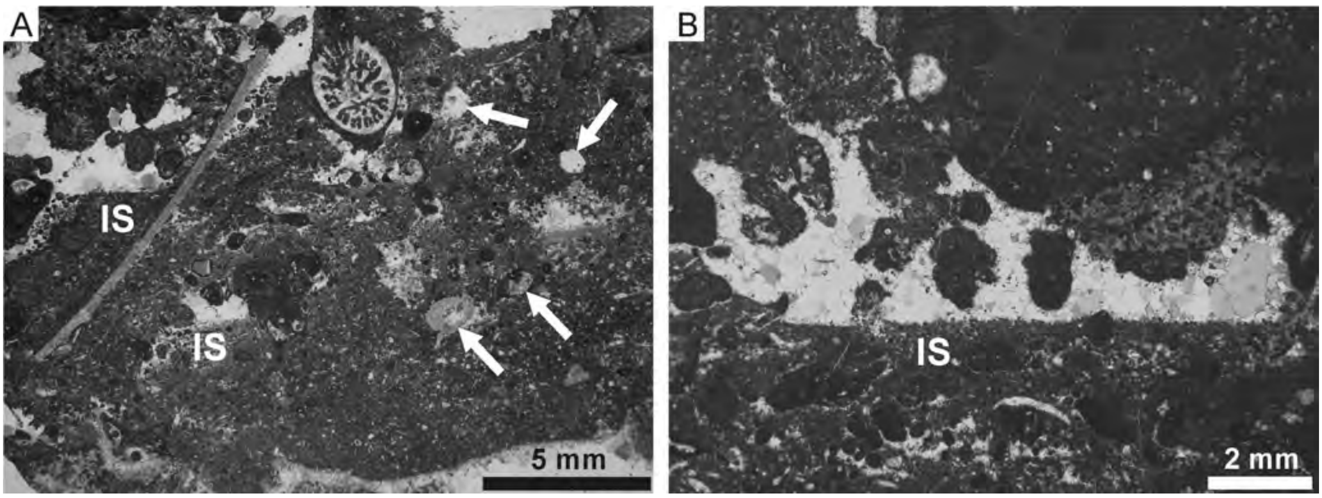

Fig. 17. Stromatactis-like cavities from the Wielkanoc Quarry. **A.** Partly dissolved Stylosmilia coral with microbial coating. Below the coral, stromatactis-like cavities with internal sediments (IS) and numerous voids after the dissolution of coral branches (white arrows). **B.** Stromatactis-like cavity with irregular roof in microbial wackestone. Numerous fragments of enclosing rock embedded within calcite cements. IS – internal sediment.

bottom parts are filled with internal sediments. The top surfaces of internal sediments are flat or slightly rough.

Under a microscope, the stromatactis-like cavities turn out to occur in thrombolite-sponge and *Crescentiella*-peloid wackestones. The roofs of the cavities are usually rough and locally they follow the shapes of large bioclasts or *Crescentiella*, but other cavities have smooth, arcuate roofs. The stromatactis-like cavities are filled with multi-generation calcite cements in their upper parts and with internal sediments in the lower parts. Single, irregular rock fragments composed of particles derived from the enclosing rocks are common in calcite cements (Fig. 17B). Such fragments are embedded within calcite cements or contact each other and/or contact upper surfaces of internal sediments (Figs 16B, 17B). The upper surfaces of the rock fragments embedded within calcite cements often fit well to the contours of the roofs of cavities.

In their lower parts, the stromatactis-like cavities are filled with internal sediments which contain the same components as the enclosing rocks. The internal sediments are wackestones with fine *Crescentiella*, peloids and sponge spicules. Some sediments are packstones with *Crescentiella* or, quite commonly, we observe packstones in the upper parts, then grading downwards into peloidal wackestones.

Proposed genesis of stromatactis-like cavities in the Wielkanoc Quarry

The carbonate buildup from the Wielkanoc Quarry was formed by successively overgrowing microbialites, siliceous sponges and hermatypic cladophyllid corals constituting the framework. The intra-framework spaces were filled with calcareous mudstones, wackestones and bioclastic packstones/grainstones (primary sediments, see Pratt, 1982). In these sediments, numerous rounded or elongated cavities were formed (Fig. 17A). It seems that these cavities have originated (at least partly) during the early diagenesis due to dissolution of corals when the sediment filling the intra-framework spaces has not been entirely lithified.

The formation of open spaces after dissolved corals have disturbed the primary stress field in the close neighbourhood of these spaces. The primary stress field have originated from the load of the overburden exerted on the components of the carbonate buildups (e.g., corals). This vertical load caused lateral compressive stress along the vertical surfaces developed within the corals.

The dissolution of corals led to the disappearance of lateral stress at the contact of sediment and walls of cavities. Simultaneously with the dissolution, the secondary stress field has developed, in which compressive stress has intensified in side walls of cavities acting as supports for their roofs loaded by the overburden. In the cavity roofs, the vertical tensional stress field has appeared due to the lack of support from the sediment. The cavities resulted from dissolution of phaceloidal clusters of coral colonies might have been several centimeters wide and high (see Morycowa and Roniewicz, 1990). Stability of the cavity shapes in time was controlled by the degree of lithification of the enclosing sediment. The shape of cavities developed within the highly lithified rock could not be remodeled later on but if the sediment was poorly lithified, the cavity roofs were susceptible to collapse.

Dissolution of corals was simultaneous with concentration of stress around the cavities. The presence of tensile stress field in the roofs of cavities, combined with low resistivity of sediments to pulling, facilitated separation of single grains from the roofs. Sometimes, compact aggregates of grains were separated, as well (Fig. 17B). Separated grains were then deposited at the bottoms of cavities forming the internal sediments. Hence, the falling of sediment from the cavity roofs and its deposition onto the cavity bottoms caused migration of cavities up the sequence. The presence of compressional stress in side walls of cavities and tensional stress in their roofs determined their stable geometry. If the stromatactis-like cavities formed in a well-sorted and homogenously lithified sediment, the cavities were ellipsoidal. If the sediment was random-grained and inhomogenously lithified, the cavities had irregular, ragged roofs (Figs 16A, B, 17B).

It is possible that the factor responsible for remodelling of the cavities was a dynamic load periodically present in the carbonate buildups with developed framework. The carbonate buildup observed in the Wielkanoc Quarry has grown in a marginal zone of the Małopolska Block, which was subjected to stronger tectonic deformations than the Upper Silesian Block (Żaba, 1999). The tectonic activity along the Kraków-Lubliniec Tectonic Zone and the Krzeszowice-Charsznica Fault documented in the Late Jurassic (Żaba, 1999; Krajewski and Matyszkiewicz, 2004; Matyszkiewicz *et al*. 2006a, b, 2012) might have stimulated the dynamic loads within the carbonate buildups, which affected the stability of sediment over the roofs of cavities and initiated their collapses.

A5.5 Ujazd. Upper Jurassic submarine gravity flows in Ujazd

Entrance part of Kluczwoda Valley, north of the Ujazd village (50°08′48″ N, 19°48′59″ E)

Leader: Jacek Matyszkiewicz

The exposure is situated near the northern edge of the Krzeszowice Graben (Fig. 2), and has been described in several papers (e.g., Matyszkiewicz, 1996, 1997b; Matyszkiewicz and Olszewska, 2007).

The exposure is ca. 50 m long and 10 m high (Fig. 18). Packstone is visible at the bottom of the exposure, in its northern part. It is mostly composed of very well sorted peloids (65%) and fragments of *Saccocoma* sp. (15%) with generally well developed syntaxial calcite cement. Among accessory components, calcified radiolaria, recrystallized planktonic foraminifera, isolated benthic foraminifera, and calcareous dinocysts are observed. The main characteristics of the established microfossil assemblage (Matyszkiewicz and Olszewska, 2007) is a significant amount of planktonic fauna. It consists of foraminifera, calcareous dinocysts, coralline algae, secundibranchia of pelagic crinoids *Saccocoma* sp. (Fig. 19) and radiolaria. The diameter of peloids and fragments of *Saccocoma* sp. gets gradually smaller towards the top of the exposure, and packstone smoothly turns into wackestone and then, closer to the top, into mudstone.

The packstone to mudstone complex is cut by subvertival joints and sometimes by steep listric surfaces. A few horizons of early-diagenetic cherts with diameters up to about 10 cm, decreasing towards the top of the exposure, are present in these deposits. A silicified limestone lens with flat top and bulges in the bottom, 0.4 m thick and several metres long, is present in the northern part of the exposure (Fig. 18). Concentric silica accretions surrounding early-diagenetic cherts are visible on fresh fractures. Crystallinity index values (CI; cf. Murata and Norman, 1976) of quartz from silicified lenses are CI=5.1 (Świerczewska, 1989). Nannoplankton S*chizosphaerella minutissima* and coccolites directly below the silicified limestone lens has been discovered using SEM (Matyszkiewicz, 1996; Matyszkiewicz and Olszewska, 2007; cf.

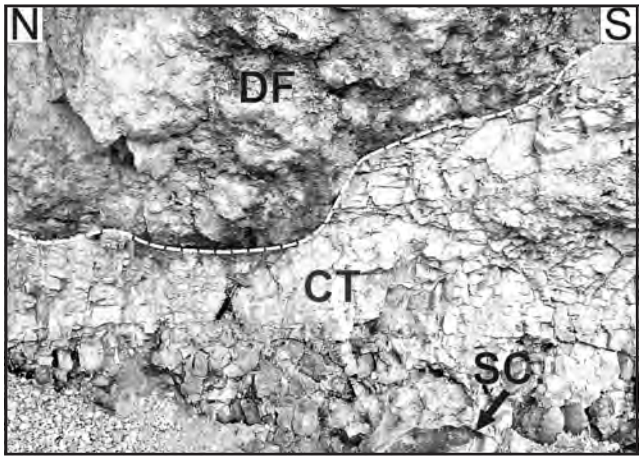

Fig. 18. Northern part of the exposure in Ujazd; DF – debris flow with olistolith of microbial-sponge massive limestone; CT – calciturbidite (packstone-wackestone-mudstone); SC – lens of silicified calciturbidite.

Kälin and Bernoulli, 1984; Bernoulli and Kälin, 1984). A fragment of another silicified limestone lens has been found in a trench situated about 0.1 m below the bottom of the exposure. Locally, oblong 10 cm-thick and several meters long fragmented early-diagenetic cherts are visible at the top of a mudstone layer. This intercalation continues into overlying debrite as a steep listric surface. Such sequnce of the lower part of the sediments can be observed between the northern edge of the exposure and a massive limestone block, which divides the exposure in two. Further to the south, near the bottom of the exposure, bedded limestone is present, represented by packstone-grainstone-boundstone with numerous fragments of benthic echinoderms. Some bedded limestone layers create biostromes formed as boundstone with thrombolites and *Crescentiella morronensis*, *Terebella* sp., echinoid spicules, bryozoans, hexactinellid sponge spicules, tuberoids, and brachiopods. Early-diagenetic cherts are locally present on the bedding planes and near them.

Above the described packstone to mudstone complex, the sediments are variable laterally. In the northernmost part of the exposure, a rounded block of massive limestone of microbial-sponge boundstone microfacies (Fig. 18) lies on the uneven top of limestone representing a packstone to mudstone complex. The massive limestone is locally separated from the underlying complex by a several centimetres-long intercalation of green marls containing breccia of early-diagenetic cherts. In these marls Dr. W. Barwicz discovered foraminifera, radiolaria (Spumellaria), skeletal elements of echinoderms and sclerosponges.

In the northern part of the exposure, limestone representing packstone to mudstone is separated by an intercalation of irregular clasts of massive limestone and early-diagenetic cherts embedded in fine-grained matrix. Clasts of massive limestone consist of microbial-sponge boundstone with thrombolites or of packstone with *Crescentiella morronensis*, fragments of echinoderms, bivalves, brachiopods and hexactinellid sponges, serpules, and benthic foraminifera. A little bit further to the south, on a packstone to mudstone complex with numerous penetrations on top, separated from it by a several centimetres-long layer of green marls, lies debrite containing fractured, irregular bodies of mudstone.

The Ujazd section represents the uppermost part of the Upper Jurassic section preserved in the vicinity of Kraków. It is situated about 200 m above the top of the Middle Jurassic. The presence of numerous fragments of *Saccocoma* sp. (Fig. 19), which appear in much lesser amounts in Upper Oxfordian facies, suggests that these deposits represent Kimmeridgian (cf. Matyszkiewicz, 1996, 1997b; Krajewski, 2001; Krajewski *et al.*, 2011). A discovery of ammonites in an exposure in Giebułtów, several kilometres east of Ujazd, confirms this (Ziółkowski, 2007a, b).

The packstones to mudstones complex at the bottom of the exposure represents at least one calciturbidite sequence. The *Saccocoma*-dominated sediments correspond with characteristics of typical calciturbidites, such as bimodality of grain composition, grading, and secondary silicification bringing out sedimentation structures (cf. Meischner, 1964; Eberli, 1987). In these deposits, T_{abc} and T_e members of Bouma sequence can be distinguished, though the boundaries between them are indistinct. It is possible that these deposits represent several amalgamated calciturbidites, as the bulges in the bottom of siliceous layer may be parallel in shape to erosive structures that may have formed at the base of a subsequent turbidity current. The highly laterally diversified deposits that cover the calciturbidite represent a debris flow. The presence of steep listric surfaces caused by discontinuity in underlying calciturbidites indicate rotational slides (cf. Hansen, 1984; Gawthorpe and Clemmey, 1985) that happened before total litification of the debris flow. It suggests that sedimentation of both types of submarine gravity flows probably took

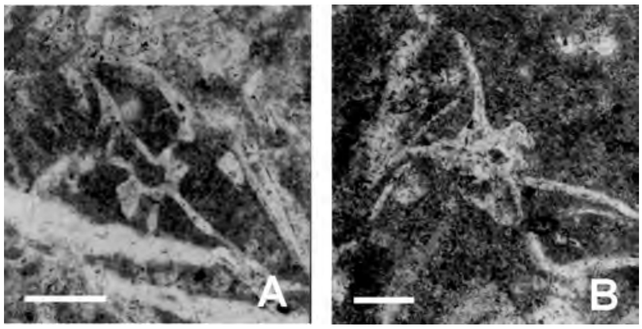

Fig. 19. A-B. Secundibranchia of *Saccocoma* sp. within packstone to mudstone complex. Bar scale 1 mm.

place on leaning fragments of the sea bottom, i.e. on slope and contraslope, where rotational slides usually form. For slightly leaned surfaces translational slides are more typical (cf. Prior and Coleman, 1984). Calciturbidites deposition ended with sedimentary pause documented by penetrations in the topmost part of the packstone to mudstone complex. It preceded another phase of sedimentation related with deposition of debris flows. The unevenness of the top of calciturbidites observed in the northern part of the exposure (Fig. 18), as well as the unevenness of the top of bedded limestone in the southernmost part of the exposure, is probably due to erosional channels, through which the debris flow deposits were transported.

A silicification model presented by Bustillo and Ruiz-Ortiz (1987) explains formation of extensive silicified limestone lenses in calciturbidites. It assumes that the siliceous banks are a result of early diagenetic silicification connected with enrichment of groundwater with silica caused by abrupt burial of sediments. According to Bustillo and Ruiz-Ortiz (1987), radiolarian skeletons and spicules of hexactinellid sponges were the source of silica, but concentric accretions in the silicified limestone lens in the calciturbidite from Ujazd suggest that the process of its formation had several phases, which was probably caused by a significant initial porosity of the silicified T_{ab} divisions of the calciturbidite and by small clay content inhibiting migration of silica (cf. Laschet, 1982). Clay was sieved out during spreading of the turbidity currents. It is indirectly proved by values of CI=5.1 of quartz found in the silicified lens. They are significantly higher than the values typical for Upper Jurassic early-diagenetic cherts (CI<1) and clearly smaller than in epigenetic siliceous deposits (CI>9; Matyszkiewicz, 1987; Matyszkiewicz *et al.*, 2015). Silicification in the calciturbidites was preceded by cementation with calcite, which reduced porosity and permeability of the sediment (cf. Hesse, 1987). The probable source of silica were opal radiolaria skeletons or an unknown external source.

The abundance of the fragments of planktonic *Saccocoma* sp., in calciturbidites, as compared with the predominance of benthic fauna in Oxfordian deposits in the Kraków region, suggests an abrupt change of conditions of sedimentation. The predominance of pelagic material indicates drowning of carbonate buildups complexes that were intensively developing in Middle and early Late Oxfordian times (Matyszkiewicz, 1996, 1997b; Krajewski, 2000, 2001; Matyszkiewicz *et al*., 2012). The predominant benthic fauna was replaced by planktonic fauna, as is shown by the abundance of planktonic crinoids *Saccocoma* sp., planktonic foraminifera, coccoliths, nannoplankton and radiolaria. When the development of microbialites that stabilized the carbonate buildups ceased (cf. Matyszkiewicz *et al*., 2012), loose pelagic sediments, which covered the sea bottom, could be easily moved by turbidity currents.

Local appearance of biostromes in the bedded limestone observed in southern part of the exposure indicates that after the deposition of calciturbidites related to the initial drowning (cf. Bice and Stewart, 1990) of the complexes of microbial-sponge carbonate buildups, again, for a short period, they could benefit from favourable conditions for development, and after that terminal drowning took place (cf. Bice and Stewart, 1990), which is expressed by sedimentation of debris flow deposits containing debris from destruction of upper parts of the microbial-sponge buildups. Debris-flow deposits document the main phase of destruction and smoothing of the sea bottom relief of the Late Jurassic basin in the Kraków region (Matyszkiewicz, 1997b; Krajewski, 2001), which had wide regional extent documented from the southern part of the Kraków Upland, Nida Basin and the foreland of the Carpathian Mountains (cf. Burzewski, 1969; Morycowa and Moryc, 1976).

The sedimentary and tectonic structures in the exposure in Ujazd indicate active Late Jurassic synsedimentary fault tectonics. Examples of material transport, in which synsedimentary faults are a linear source of material, are given - among others - by Schlager and Chermak (1979), Crevello and Schlager (1980) and Eberli (1987). The direction of erosional channels in the calciturbidite sequence (W-E) documents transport by debris-flows parallel to a nearby fault bounding the Krzeszowice Graben, which suggests that the fault was formed in the Late Jurassic (cf. Matyszkiewicz, 1996; Ziółkowski, 2007a, b).

Widely spread sediments of submarine gravity flows in the southern part of the Kraków Upland are probably an effect of Late Jurassic synsedimentary fault tectonics (cf. Koszarski, 1995), which is a reflection of supra-regional phenomena connected with the opening of the Northern Atlantic and the Tethys oceans (Faerseth, 1996; Helm and Schülke, 1998; Allenbach, 2001, 2002). In the Kraków region, these phenomena were accompanied by reactivation of old Palaeozoic structures, mainly the Kraków-Lubliniec and Krzeszowice-Charsznica fault zones (Żaba, 1999; Krajewski and Matyszkiewicz, 2004; Matyszkiewicz *et al.* 2006a, b, 2012, 2015). The presence of Upper Jurassic submarine gravity flows near the edges of the tectonic horsts in the Kraków region suggests a Late Jurassic origin of these structures (Matyszkiewicz, 1996, 1997b; Krajewski and Matyszkiewicz, 2004; Ziółkowski, 2007a, b; Matyszkiewicz *et al*., 2006b, 2007b, 2012), which applies also to the area of Ujazd.

References

Allenbach, R. P., 2001. Synsedimentary tectonics in an epicontinental sea: a new interpretation of the Oxfordian basin of northern Switzerland. *Eclogae Geologicae Helvetiae*, 94: 265–287.

Allenbach, R. P., 2002. The ups and downs of “Tectonic Quiescence” – recognizing differential subsidence in the epicontinental sea in the Oxfordian in the Swiss Jura Mountains. *Sedimentary Geology*, 150: 323–342.

Bernoulli, D. & Kälin, O., 1984. Jurassic sediments. Northwest African Margin: remarks on stratigraphy, facies, and diagenesis, and comparison with some Tethyan equivalents. In: Hinz, K., Winterer, E. L., et al. (eds), *Initial Reports of the Deep Sea Drilling Project,* 79: 437–448.

Bice, D. M. & Stewart, K. G., 1990. The formation and drowning of isolated carbonate seamounts: tectonic and ecological controls in the northern Apennines. In: Tucker, M., Wilson, J. L., Crevello, P. D., Sarg, J. R. & Read, J. F. (eds), *Carbonate Platforms; Facies, Sequences and Evolution. Special Publication of the International Association of Sedimentologists*, 9: 145–168.

Buła, Z. & Habryn, R., (eds.) 2008. Atlas geologiczno-strukturalny paleozoicznego podłoża Karpat zewnętrznych i zapadliska przedkarpackiego. Państwowy Instytut Geologiczny. [In Polish.]

Buła, Z., Jachowicz, M. & Żaba, J., 1997. Principal characteristics of the Upper Silesian Block and Małopolska Block border zone (southern Poland). *Geological Magazine*, 134: 669–677.

Burzewski, W., 1969. Strukturalne warunki Jury Olkusko-Wolbromskiej jako brzegowe dla hydrodynamiki złóż naftowych Niecki Nidziańskiej. *Prace Geologiczne*. Polska Akademia Nauk – Oddział w Krakowie, Komisja Nauk Geologicznych, 61: 3–91. [In Polish, French summary.]

Bustillo, M. A. & Ruiz-Ortiz, P. A., 1987. Chert occurrences in carbonate turbidites: examples from the Upper Jurassic of the Betic Mountains (southern Spain). *Sedimentology*, 34: 611–621.

Crevello, P. D. & Schlager, W., 1980. Carbonate debris sheets and turbidites, Exuma Sound, Bahamas. *Journal of Sedimentary Petrology*, 50: 1121–1148.

Dżułyński, S., 1950 (for 1949). Littoral deposits of the Middle Jurassic South of Krzeszowice. *Rocznik Polskiego Towarzystwa Geologicznego*, 21: 125–180. [In Polish, English summary.]

Dżułyński, S., 1952. The origin of the Upper Jurassic limestones in the Cracow area. *Rocznik Polskiego Towarzystwa Geologicznego*, 21: 125–180. [In Polish, English summary.]

Eberli, G. P., 1987. Carbonate turbidite sequences deposited in rift-basin of the Jurassic Tethys Ocean (eastern Alps, Switzerland). *Sedimentology*, 34: 363–388.

Faerseth, R. B., 1996. Interaction of Permo-Triassic and Jurassic extensional fault-blocks during the development of the northern North Sea. *Journal of the Geological Society*, 153: 931–944.

Felisiak, I., 1992. Oligocene-early Miocene karst deposits and their importance for recognition of the development of tectonics and relief in the Carpathian Foreland, Kraków region, Southern Poland. *Annales Societatis Geologorum Poloniae*, 62: 173–207. [In Polish, English Summary.]

Gawthorpe, R. & Clemmey, H., 1985. Geometry of submarine slides in the Bowland Basin (Dinantian) and their relation to debris flows. *Journal of the Geological Society*; 142: 555–565.

Giżejewska, M. & Wieczorek, J., 1976. Remarks on the Callovian and Lower Oxfordian of the Zalas area (Cracow Upland, Southern Poland). *Bulletin de l'Académie Polonaise des Sciences, Série Sciences des Sciences de la Terre,* 24: 167–175.

Głazek, J. & Wierzbowski, A., 1972. On the alleged Kimmeridgian transgression in the Cracow Upland. *Acta Geologica Polonica*, 22: 45–69. [In Polish, English summary.]

Golonka, J. & Rajchel, J., 1972. Stromatolity z górnej kredy okolic Krakowa. *Kwartalnik Geologiczny*, 16: 652–668. [In Polish.]

Gołębiowska, B., Pieczka, A., Rzepa, G., Matyszkiewicz, J. & Krajewski, M., 2010. Iodargyrite from Zalas (Cracow area, Poland) as an indicator of Oligocene-Miocene aridity in Central Europe. *Palaeogeography, Palaeoclimatology, Palaeoecology*, 296: 130–137.

Gradziński, R., 2009. Geological map of Krakow region without Quaternary and terrestrial Tertiary deposits. Wydawnictwo Instytutu Nauk Geologicznych PAN, KrakówHansen, H. J., 1984. Strategies for classification of landslides. In: Brunsden, D. & Prior, D. B. (eds), *Slope stability*, Wiley, New York, pp. 1–25.

Helm, C. & Schülke, I., 1998. A coral-microbialite patch reef from the Late Jurassic (*florigemma*-Bank, Oxfordian) of NW Germany (Suntel Mountains). *Facies*, 39: 75–104.

Hesse, R., 1987. Selective and reversible carbonate-silica replacements in Lower Cretaceous carbonate-bearing turbidites of the Eastern Alps. *Sedimentology*, 34: 1055–1077.

Hoffmann M., Kędzierski M., Kołodziej, B. & Machaniec, E., 2013. Punkt 3: Zabierzów. Punkt 3B. Górna kreda. In: Kędzierski, M. & Kołodziej, B. (eds), *XXII konferencja Naukowa Sekcji Paleontologicznej Polskiego Towarzystwa Geologicznego, „Aktualizm i antyaktualizm w paleontologii", Tyniec, 27-30.09.2013, Materiały Konferencyjne, Polskie Towarzystwo Geologiczne,* Kraków, pp. 97. [In Polish.]

Jasionowski, M., 1995. A Cretaceous non-depositional surface in the Kraków Upland (Mydlniki, Zabierzów):

burrows, borings, stromatolites. *Annales Societatis Geologorum Poloniae*, 65: 63–78. [In Polish, English Summary.]

Kaziuk, H. & Lewandowski J., 1978. Geological map of Poland, 1:200 000, sheet Kraków (A). Państwowy Instytut Geologiczy, Warszawa.

Kälin, O. & Bernoulli, D., 1984. *Schizosphaerella* Deflandre and Dangeard in Jurassic deeperwater carbonate sediments, Mazagran continental margin (Hole 547B) and Mesozoic Tethys. In: Hinz K., Winterer E. L., et al., (eds), *Initial Reports Deep Sea Drilling Project*, 79: 411–435, Washington.

Kędzierski, M., 2001. Nanoplankton wapienny z dolnego oksfordu okolic Krakowa. In: *II Spotkanie Polskiej Grupy Roboczej Systemu Jurajskiego JURASSICA, Polskie Towarzystwo Geologiczne, Państwowy Instytut Geologiczny,* Starachowice 27-29.09.2001, pp. 17. [In Polish.]

Kochman, A. & Matyszkiewicz, J., 2013. Experimental method for estimation of compaction in the Oxfordian bedded limestones of the southern Kraków-Częstochowa Upland, Southern Poland. *Acta Geologica Polonica*, 63: 681–696.

Koszarski, A., 1995. Tradycja a nowoczesność w interpretacji warunków powstania wapieni górnej jury krakowskiej. Szczególna rola procesów redepozycji. Studium terenowe. In: Doktor, M., Głuszek, A., Gmur, D. & Słomka, T. (eds), *Tradycja a nowoczesność w interpretacjach sedymentologicznych. Materiały Konferencyjne IV Krajowego Spotkania Sedymentologów*, Kraków, 9–22. [In Polish.]

Krajewski, M., 2000. Lithology and morphology of Upper Jurassic carbonate buildups in the Będkowska Valley, Kraków region, Southern Poland. *Annales Societatis Geologorum Poloniae*, 70: 51–163.

Krajewski, M., 2001. Upper Jurassic chalky limestones in the Zakrzówek Horst, Kraków, Kraków-Wieluń Upland (South Poland). *Annales Societatis Geologorum Poloniae*, 71: 43–51.

Krajewski, M. & Matyszkiewicz, J., 2004 Development and facial architecture of the Upper Jurassic complexes of buildups in the SW part of the Kraków Upland. In: Partyka, J. (ed.), *Zróżnicowanie i przemiany środowiska przyrodniczo-kulturowego Wyżyny Krakowsko-Częstochowskiej*, 1: 27–34. Ojcowski Park Narodowy. Ojców. [In Polish, English summary.]

Krajewski, M., Matyszkiewicz, J., Król, K. & Olszewska, B., 2011. Facies of the Upper Jurassic–Lower Cretaceous deposits from the southern part of the Carpathian Foredeep basement in the Kraków–Rzeszów area (southern Poland). *Annales Societatis Geologorum Poloniae*, 81: 269–290.

Krokowski, J., 1984. Mezoskopowe studia strukturalne wosadach permsko-mezozoicznych południowo-wschodniej części Wyżyny Śląsko-Krakowskiej. Rocznik Polskiego Towarzystwa Geologicznego, 54: 79–121. [In Polish.]

Laschet, C., 1982. On the origin of cherts. *Facies*, 10: 257–290.

Leinfelder, R. R., Werner, W., Nose, M., Schmid, D. U., Krautter, M., Laternser, R., Takacs, M. & Hartmann, D., 1996. Paleoecology, growth parameters and dynamics of coral, sponge and microbolite reefs from the Late Jurassic. In: Reitner, J., Neuweiler, F. & Gunkel, F. (eds), *Global and regional controls on biogenic sedimentation. I. Reef evolution. Research reports. Göttinger Arbeiten Geologische Paläontologische, Sb.,* 2: 227–248.

Matyja, B. A., 2006. Stop A17 – Zalas Quarry – Callovian transgressive to condensed pelagic deposits, Lower to lowermost Middle Oxfordian deposits of sponge megafacies. In: Wierzbowski, A., Aubrecht, R., Golonka, J., Gutowski, J., Krobicki, M., Matyja, B. A., Pieńkowski, G. & Uchman, A. (eds), *Jurassic of Poland and adjacent Slovakian Carpathians. Field trip guidebook of 7th International Congress on the Jurassic System Poland*, Kraków, September 6-18, 2006. pp. 70–72.

Matyja, B. A. & Tarkowski, R., 1981. Lower and Middle Oxfordian ammonite biostratigraphy at Zalas in the Cracow Upland. *Acta Geologica Polonica*, 31: 1–14.

Matyszkiewicz, J., 1987. Epigenetic silification of the Upper Oxfordian limetsones in the vicinity of Kraków. *Annales Societatis Geologorum Poloniae,* 57: 59–87. [In Polish, English summary.]

Matyszkiewicz, J., 1993. Genesis of stromatactis in an Upper Jurassic carbonate buildup (Młynka; Cracow Region, Southern Poland); Internal Reworking and Erosion of Organic Growth Cavities. *Facies*, 28: 87–96.

Matyszkiewicz, J., 1994. Remarks on the Deposition of Pseudonodular Limestones in the Cracow Area (Oxfordian, Southern Poland). *Berliner Geowissenschaftliche Abhandlungen*, E13: 419–439.

Matyszkiewicz, J., 1996. The significance of *Saccocoma*-calciturbidites for the analysis of the Polish Epicontinental Late Jurassic Basin: an example from the Southern Cracow-Wielun Upland (Poland). *Facies*, 34: 23–40.

Matyszkiewicz, J., 1997a. Stromatactis cavities and stromatactis–like cavities in the Upper Jurassic carbonate buildups at Młynka and Zabierzów (Oxfordian, southern Poland). *Annales Societatis Geologorum Poloniae*, 67: 45–55.

Matyszkiewicz, J., 1997b. Microfacies, sedimentation and some aspects of diagenesis of Upper Jurassic sediments from the elevated part of the Northern peri-Tethyan Shelf: a comparative study on the Lochen area (Schwäbische Alb) and the Cracow area (Cracow-Wieluń Upland, Poland). *Berliner geowissenschaftliche Abhandlungen*, E21: 1–111.

Matyszkiewicz J., Kochman, A. & Duś, A., 2012. Influence of local sedimentary conditions on development of microbialites in the Oxfordian carbonate buildups from the southern part of the Kraków-Częstochowa Upland (south Poland). Sedimentary Geology, 263–264: 109–132.

Matyszkiewicz, J., Kochman, A., Rzepa, G., Gołębiowska, B., Krajewski, M., Gaidzik, K. & Żaba, J., 2015. Epigenetic silicification of the Upper Oxfordian limestones in the Sokole Góry (Kraków-Częstochowa Upland); relation to facies development and tectonics. Acta Geologica Polonica, 65:181-203.

Matyszkiewicz, J. & Krajewski, M., 1996. Lithology and sedimentation of Upper Jurassic massive limestones near Bolechowice, Krakow-Wielun upland, South Poland. *Annales Societatis Geologorum Poloniae*, 66: 285–301.

Matyszkiewicz, J., Krajewski, M., Gołębiowska, B., Jędrys, J., Kochman, A. & Rzepa G., 2007a. Rozwój i ewolucja oksfordzkich budowli węglanowych w Zalasie. *Tomy Jurajskie*, 4: 77–86. [In Polish.]

Matyszkiewicz, J., Krajewski, M. & Kędzierski, J., 2006a. Origin and evolution of an Upper Jurassic complex of carbonate buildups from Zegarowe Rocks (Kraków--Wieluń Upland, Poland). *Facies*, 52: 249–263.

Matyszkiewicz, J., Krajewski, M. & Żaba, J., 2006b. Structural control on the distribution of Upper Jurassic carbonate buildups in the Kraków-Wieluń Upland (south Poland). *Neues Jahrbuch für Geologie und Paläontologie Monatshefte*, 3: 182–192.

Matyszkiewicz, J., Krajewski, M. & Żaba, J., 2007b. Przejawy późnojurajskiej tektoniki synsedymentacyjnej w rejonie Kamienia. *Tomy Jurajskie*, 4:63–70. [In Polish.]

Matyszkiewicz, J. & Olszewska, B., 2007. Osady podmorskich spływów grawitacyjnych pogranicza oksfordu i kimerydu w Ujeździe. *Tomy Jurajskie*, 4: 109–117. [In Polish.]

Meischner, K.-D., 1964. Allodapische Kalke. Turbidite in riffnahen Sedimentationsbecken. In: Bouma, A. H. & Brouwer, A. (eds), *Turbidites. Development in Sedimentology,* 3: 156–191.

Morycowa, E. & Moryc, W., 1976. The Upper Jurassic sediments in the Foreland of the Polish Carpathians (Sandomierz basin). *Rocznik Polskiego Towarzystwa Geologicznego*, 46: 231–288. [In Polish, English summary.]

Morycowa, E. & Roniewicz, E., 1990. Revision of the genus *Cladophyllia* and description of *Apocladophyllia* gen.n. (Cladophylliidae fam.n., Scleractinia). *Acta Palaeontologica Polonica*, 35: 165–190.

Murata, K. J. & Norman, M. B., 1976. An index of crystallinity of quartz. *American Journal of Science*, 276: 1120–1130.

Olchowy, P., 2011. Possible origin of stromatactis-like cavities in Upper Jurassic sediments from the Wielkanoc quarry near Gołcza (Kraków-Częstochowa Upland, southern Poland)–experimental studies. *Facies*, 57: 613–625.

Olivier, N. & Boyet, M., 2006. Rare earth and trace elements of microbialites in Upper Jurassic coral- and sponge-microbialite reefs. *Chemical Geology*, 230: 105–123.

Olivier, N., Pittet, M., Gaillard, C. & Hantzpergue, P., 2007. High-frequency palaeoenvironmental fluctuations recorded in Jurassic coral- and sponge-microbialite bioconstructions. *Comptes Rendus Palevolution*, 6: 21–36.

Olszewska-Nejbert, D., 2004. Development of the Turonian/Coniacian hardground boundary in the Cracow Swell area (Wielkanoc quarry, Southern Poland): *Geological Quarterly*, 48: 159–170.

Olszewska-Nejbert, D. & Świerczewska-Gładysz, E., 2009. The phosphatized sponges from the Santonian (Upper Cretaceous) of the Wielkanoc Quarry (southern Poland) as tool in stratigraphical and environmental studies. *Acta Geologica Polonica*, 59: 483–504.

Pratt, B. R., 1982. Stromatolitic framework of carbonate mud-mounds. *Journal of Sedimentary Petrology*, 52: 1203–1227.

Prior, D. B. & Coleman, J. M., 1984. Active slides and flows in underconsolidated marine sediments on the slopes of the Mississipi delta. In: Brunsden, D. & Prior, D. B. (eds), *Slope stability*, Wiley, New York, pp. 419–455.

Rais, P., Louis-Schimd, B., Bernasconi, S. M. & Weissert, H., 2007. Palaeoceanographic and palaeoclimatic reorganization around the Middle-Late Jurassic transition.

Palaeogeography, Palaeoclimatology, Palaeoecology, 251: 527–546.

Riding, R., 2002. Structure and composition of organic reefs and carbonate mud mounds: concepts and categories. *Earth-Science Reviews*, 58: 163–231.

Różycki, Z., 1953. Górny dogger i dolny malm Jury Krakowsko- Częstochowskiej. *Prace Instytutu Geologicznego*, 17: 1–412. [In Polish.]

Schlager, W. & Chermak, A., 1979. Sediment facies of platform-basin transition, Tongue of the Ocean, Bahamas. *Society of Economic Paleontologists and Mineralogists, Special Publication* 27: 193–208.

Schmid, D. U., 1996. Marine Mikrobolithe und Mikroinkrustierer aus dem Jura. *Profil*, 9: 101–251.

Senowbari-Daryan, B., Bucur, I. I., Schlagintweit, F., Săsăran, E. & Matyszkiewicz, J., 2008. *Crescentiella*, a new name for "*Tubiphytes*" *morronensis* Crescenti, 1969: an enigmatic Jurassic-Cretaceous microfossil. *Geologia Croatica*, 61: 185–214.

Świerczewska, A., 1989. Krzemienie z wapieni górnego oksfordu okolic Ujazdu. In: Rutkowski J. (ed), *Przewodnik LX Zjazdu Polskiego Towarzystwa Geologicznego*, 14-16 września, Polskie Towarzystwo Geologiczne, Kraków, pp. 88–90. [In Polish.]

Tarkowski, R., 1989. Stratygrafia utworów jury w Zalasie. In: Rutkowski, J. (ed.), *Przewodnik LX Zjazdu Polskiego Towarzystwa Geologicznego*, Kraków, 14-16 września, Polskie Towarzystwo Geologiczne, Kraków, pp. 74–78. [In Polish.]

Trammer, J., 1982. Lower to Middle Oxfordian sponges of the Polish Jura. *Acta Geologica Polonica*, 32: 1–39.

Trammer, J., 1985. Sponge bioherms in the Jasna Góra Beds (Oxfordian of the Polish Jura Chain). *Przegląd Geologiczny*, 33: 78–81. [In Polish, English summary.]

Wieczorek, J., 1982. Stromatolites versus burrowing organisms at the example of Jurassic deposits of the Cracow-Wieluń Upland. *Kwartalnik Geologiczny,* 26, 1: 117–136. [In Polish, English summary.]

Wallace, M. W., 1987. The role of internal erosion and sedimentation in the formation of stromatactis mudstones and associated lithologies. *Journal of Sedimentary Petrology*, 57: 695–700.

Wierzbowski, H., Dembicz, K., Praszkier, T., 2009. Oxygen and carbon isotope composition of Callovian-Lower Oxfordian (Middle-Upper Jurassic) belemnite rostra from central Poland: a record of a Late Callovian global sea-level rise? *Palaeogeography, Palaeoclimatology, Palaeoecology,* 283: 182–194.

Zatoń, M., Wilson, M. A. & Zavar, E., 2011. Diverse sclerozoan assemblages encrusting large bivalve shells from the Callovian (Middle Jurassic) of southern Poland. *Palaeogeography, Palaeoclimatology, Palaeoecology*, 307: 232–244.

Ziółkowski, P., 2007a. Stratygrafia i zróżnicowanie facjalne górnej jury wschodniej części Wyżyny Krakowskiej. *Tomy Jurajskie*, 4: 25–38. [In Polish.]

Ziółkowski, P., 2007b. Osady basenów międzybiohermalnych sąsiadujących z południową krawędzią zespołu biohermalnego Ojcowa. *Tomy Jurajskie*, 4: 119–122. [In Polish.]

Żaba, J., 1995. Strike-slip faults at the edge zone of Upper Silesia and Małopolska blocks (southern Poland). *Przegląd Geologiczny*, 43: 838–842. [In Polish, English summary.]

Żaba, J., 1999. The structural evolution of Lower Paleozoic succession in the Upper Silesia Block and Małopolska Block border zone, southern Poland. *Prace Państwowego Instytutu Geologicznego*, 166: 1–162. [In Polish, English summary.]

The inception, growth and demise of a pelagic carbonate platform: Jurassic and Lower Cretaceous of the Krížna Nappe in the Western Tatra Mountains

Renata Jach[1], Jacek Grabowski[2], Andrzej Gaździcki[3], Alfred Uchman[1]

[1]Institute of Geological Sciences, Jagiellonian University, Kraków (renata.jach@uj.edu.pl, alfred.uchman@uj.edu.pl)
[2]Polish Geological Institute, National Research Institute, Warsaw (jgra@pgi.gov.pl)
[3]Institute of Paleobiology, Polish Academy of Sciences, Warsaw (gazdzick@twarda.pan.pl)

Route (Figs. 1, 2): From Kraków we drive south by E77 to Rabka, then by road 958 to the village of Witów. In Chochołowska Valley (Dolina Chochołowska), to the exposures located near Huciska Glade (Polana Huciska). First-day hike starts from Huciska Glade, than leads through **Luciański Klin ridge** (**stops A6.1–A6.4**) and ends in **Lejowa Valley** (Dolina Lejowa; **stops A6.5, A6.6**). This all-day eastward traverse runs along unsigned trail through forest, with some fairly demanding hiking at altitudes 900–1300 m. The relatively short loop walk of the second day starts from Huciska Glade and leads up along **Długa Valley** (Dolina Długa) to the **Pośrednie ridge** (**stop A6.7**). The way back from the Pośrednie ridge is an easy downhill walk along **Kryta Valley** (Dolina Kryta; **stop A6.8.1–4**).

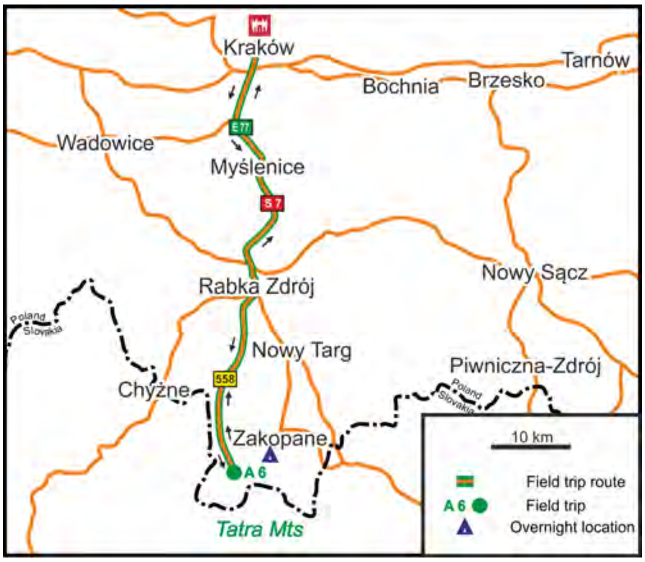

Fig. 1. Route map of field trip A6.

Introduction to the trip

The Tatra Mountains are the highest ridge of the Western Carpathians with the highest peak Gerlach (2655 m). The Tatra Mts were uplifted during Neogene and form a block which is asymmetrically tilted to the north and bounded from the south by a prominent fault (Fig. 3).

The block consists of a pre-Mesozoic crystalline core (granitoidic intrusions and older metamorphic rocks), ?Permian and Mesozoic autochthonous sedimentary cover, allochthonous Mesozoic sedimentary rocks, detached locally from their crystalline basement in form of nappes and smaller thrust sheets (Kotański, 1965,

Jach, R., Grabowski, J., Gaździcki, A. & Uchman, A., 2015. The inception, growth and demise of a pelagic carbonate platform: Jurassic and Lower Cretaceous of the Krížna Nappe in the Western Tatra Mountains. In: Haczewski, G. (ed.), *Guidebook for field trips accompanying 31st IAS Meeting of Sedimentology held in Kraków on 22nd–25th of June 2015*. Polish Geological Society, Kraków, pp. 75–101.
Guidebook is available online at www.ing.uj.edu.pl/ims2015

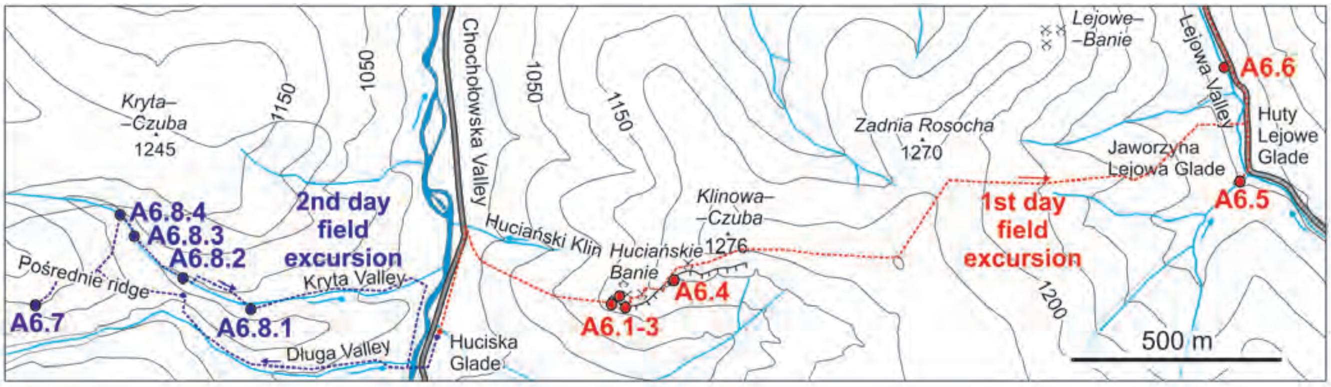

Fig. 2. Detailed itinerary of field trip A.6; A6.1–4 – Huciański Klin ridge; A6.5–6 – Huty Lejowe glade; stops:A6.7–8a–c – Długa Valley and Kryta Valley.

1971). The nappes were formed in Late Cretaceous. The Mesozoic sedimentary rocks are discordantly covered by rocks of the Central Carpathian Paleogene, which include Oligocene flysch, more than 2 000 m thick, in their upper part. The sedimentary rocks of the Tatra Mts dip generally to the north due to the Neogene uplift (Fig. 4; Bac-Moszaszwili *et al*., 1979). They are ascribed to three main tectonic-facies domains: Tatricum (High-Tatric autochthon and allochthon), Fatricum (Krížna Nappe = Lower Sub-Tatric Nappe) and Hronicum (Choč Nappe = Upper Sub-Tatric Nappe) on the basis of their characteristic facies successions and tectonic position.

The Krížna Nappe overlies the High-Tatric units and is covered by the Choč Nappe (Kotański, 1965). It comprises Lower Triassic to Lower Cretaceous deposits and is built of several thrust sheets and so called 'partial nappes'. The Krížna Nappe belongs to the Fatricum Domain of the Central Carpathian block (Plašienka, 2012). During most of the Jurassic time, it was one of the domains located between the Alpine Tethys to the north and the Meliata Ocean to the south (Fig. 5; Thierry and Barrier, 2000; Schmid *et al*., 2008). As a consequence of its location, the succession studied displays a strong similarity to the Jurassic of other Tethyan basins.

During the Jurassic, the Fatricum Domain was bordered by the uplifted Tatricum Domain to the north and the Veporicum and Hronicum domains to the south (Csontos and Vörös, 2004; Plašienka, 2012). The Fatricum Domain was regarded as being an extensional basin during the Jurassic, located on thinned continental crust (e.g., Plašienka, 2012). As a result, the Jurassic successions of the Fatricum Domain are characterized by an almost

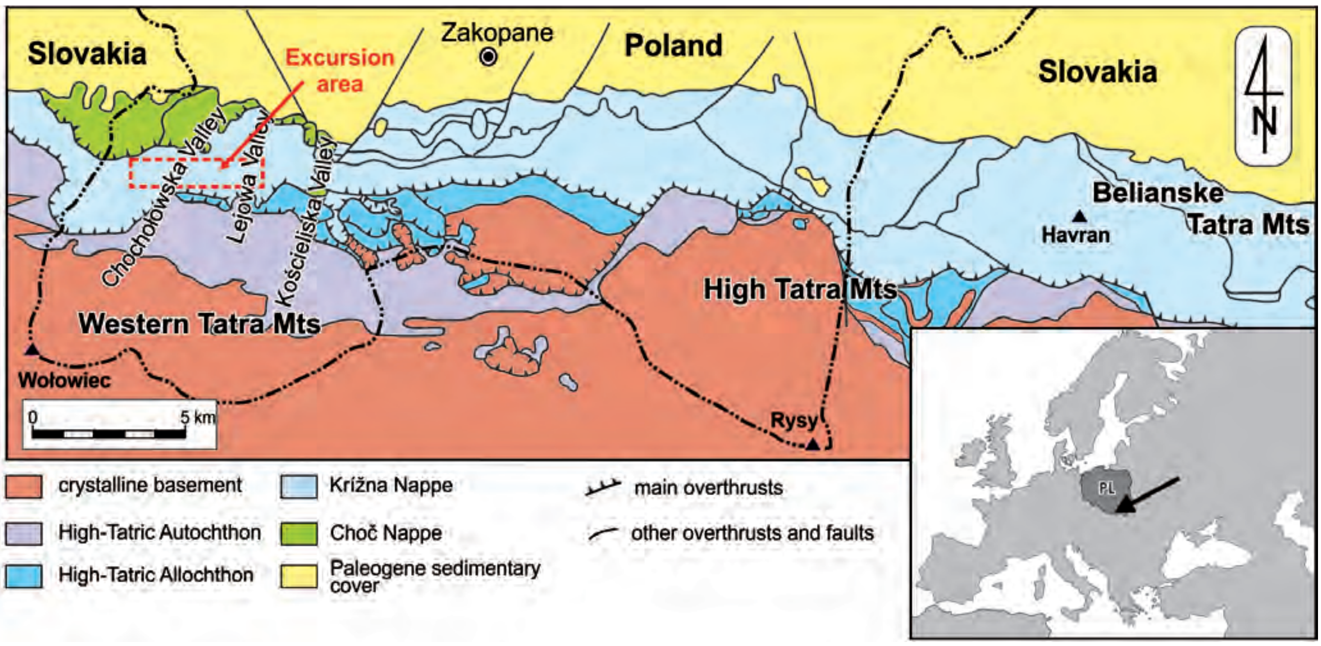

Fig. 3. Tectonic sketch map of the Tatra Mts showing location of the excursion area (after Bac-Moszaszwili *et al*,. 1979; modified)

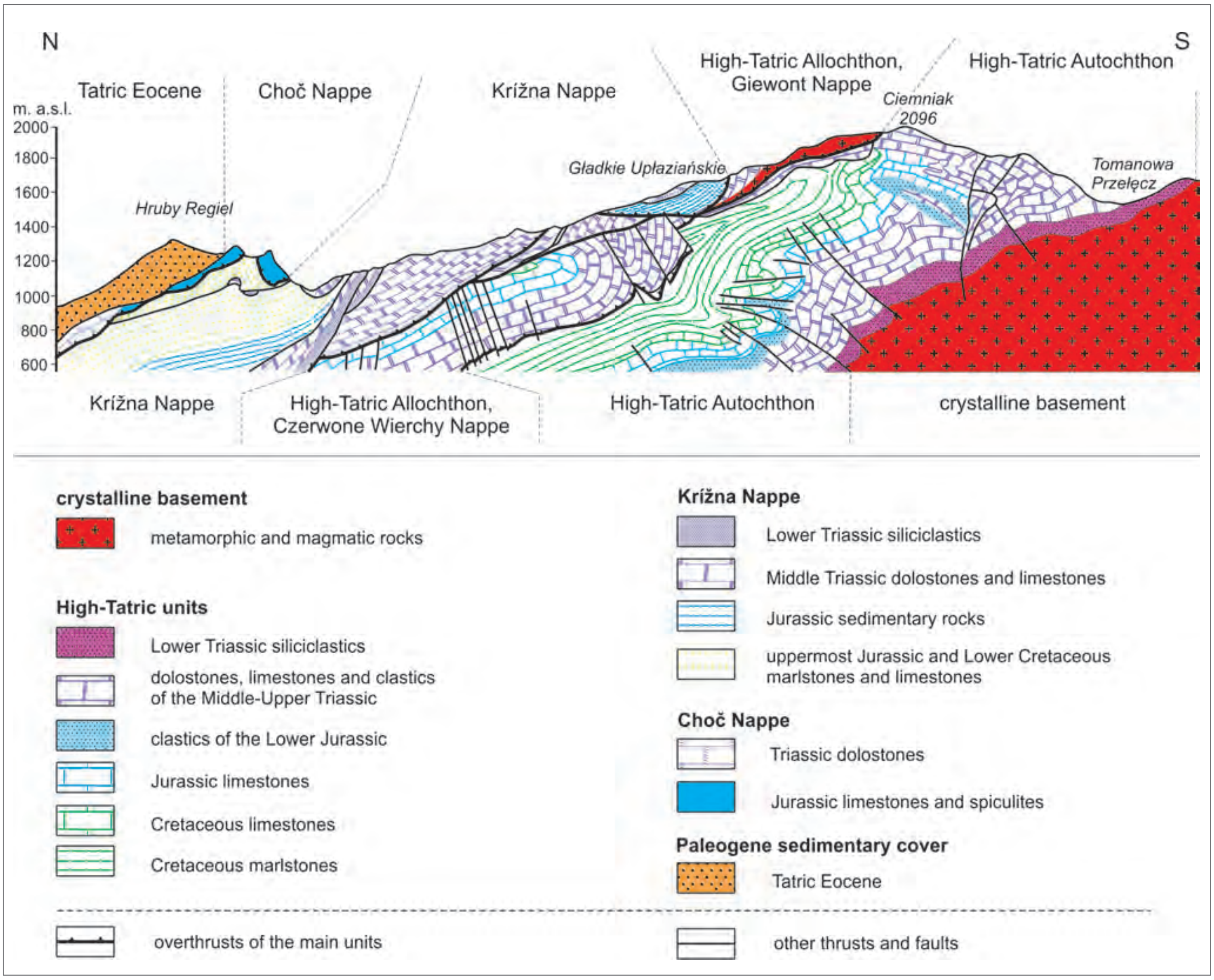

Fig. 4. Geological cross section through the Tatra Mts along the Dolina Kościeliska valley (after Kotański, 1965, changed)

continuous record of deepening, with a transition from littoral through hemipelagic to pelagic deep-sea sedimentation.

The Jurassic deposits of the Krížna Nappe in the Tatra Mts represent a generally deeper sea succession of the Zliechov type (Michalík, 2007; Plašienka, 2012; Jach *et al*., 2014). The oldest Jurassic deposits are represented by dark shelf carbonates and shales, which refer to sea transgression onto emerged lands (Figs 6–8; Gaździcki *et al*., 1979; Michalík, 2007). These Rhaetian–Hettangian deposits have diachronic lower and upper boundary. The Early Jurassic basin featured wide basins and narrow horsts, characteristic of the first phase of extension (Plašienka, 2012). The second phase of extension took place during the latest Early Jurassic and resulted in extensional tilting of blocks, which formed a horst-and-graben topography (Wieczorek, 1990; Gradziński *et al*., 2004; Jach, 2005; Plašienka, 2012). The formation of horsts (e.g., the excursion area) and grabens (in the High Tatra and the Belianske Tatry Mountains) led to distinct facies changes (Guzik, 1959; Jach, 2007). The subsiding basins were filled with *Fleckenmergel*-type sediments (bioturbated "spotted" limestones and marls, ranging from Sinemurian to Bajocian; Wieczorek, 1995; Iwańczuk *et al*., 2013). During the Late Pliensbachian–?Aalenian, the horsts acted as submarine highs with sedimentation of spiculites on their slopes (Jach, 2002a) and neritic crinoidal sedimentation (e.g., crinoidal tempestites; Jach, 2005), replaced by condensed pelagic carbonates (Gradziński *et al*., 2004) that were deposited on a pelagic carbonate platform (*sensu* Santantonio, 1993). During the Middle Jurassic, significant topographic relief was still present and controlled facies distribution. The deposition of carbonate sediments terminated with the onset of a uniform radiolarite sedimentation during the Middle Jurassic (Jach *et al*., 2012, 2014). Generally, the Lower–Upper Jurassic sediments of the Fatricum Domain record a gradual deepening and transition

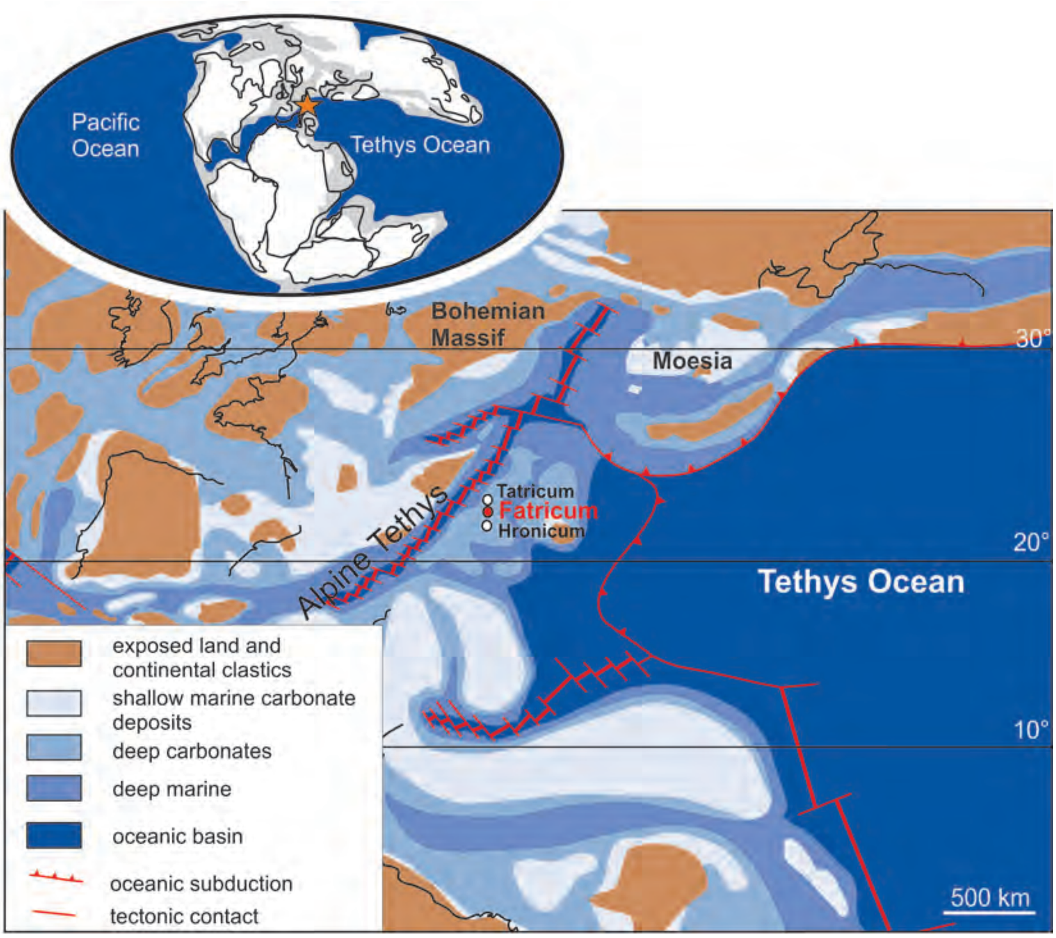

Fig. 5. General palaeogeographic position of the Fatricum Domain during the Callovian (after Thierry and Barrier, 2000; simplified)

from hemipelagic to pelagic deep sea environment. A major recovery of carbonate sedimentation started in the Late Tithonian and Early Berriasian, when the Maiolica-like deep sea limestones and marls were deposited (Pszczółkowski, 1996; Grabowski *et al*., 2013). Widespread marl and marly limestone sedimentation started in the Late Berriasian and continued to the Aptian, with intercalations of turbiditic sandstones and calcareous fluxoturbidites in the Valanginian and Hauterivian (Pszczółkowski, 2003a).

The main aim of this excursion is to present general depositional history of the studied part of the Krížna Unit and to discuss factors controlling their sedimentary environment.

Stop descriptions

Attention: All the localities are in the protected area of the Tatra National Park. Please do not hammer the rocks.

A6.1 Huciański Klin ridge – Late Pliensbachian spiculites

(49°15′37″ N, 19°49′17″ E)

Leader: Renata Jach

The section presented during the first part of the excursion is located on the forested southern slope of the Huciański Klin ridge. The oldest are 16–20 m thick spiculites which overlie basinal "spotted" limestones and marls of the Sinemurian–Lower Pliensbachian not exposed in the presented locality (about 150 m thick; see stop A6.6). Spiculites are well-exposed in crags a few metre high. Late Pliensbachian age is ascribed to the spiculites on the basis of their position in the section. They are dark, very hard and well-bedded, with bed thickness from a few to 30 cm. Siliceous sponge spicules, which belong to Hexactinellida and Demospongia (mainly Tetractinellida) with loose skeletons, are the major components of spiculites (Fig. 9A–C; Jach, 2002a). A gradual substitution of Hexactinellida by Demospongia is observed

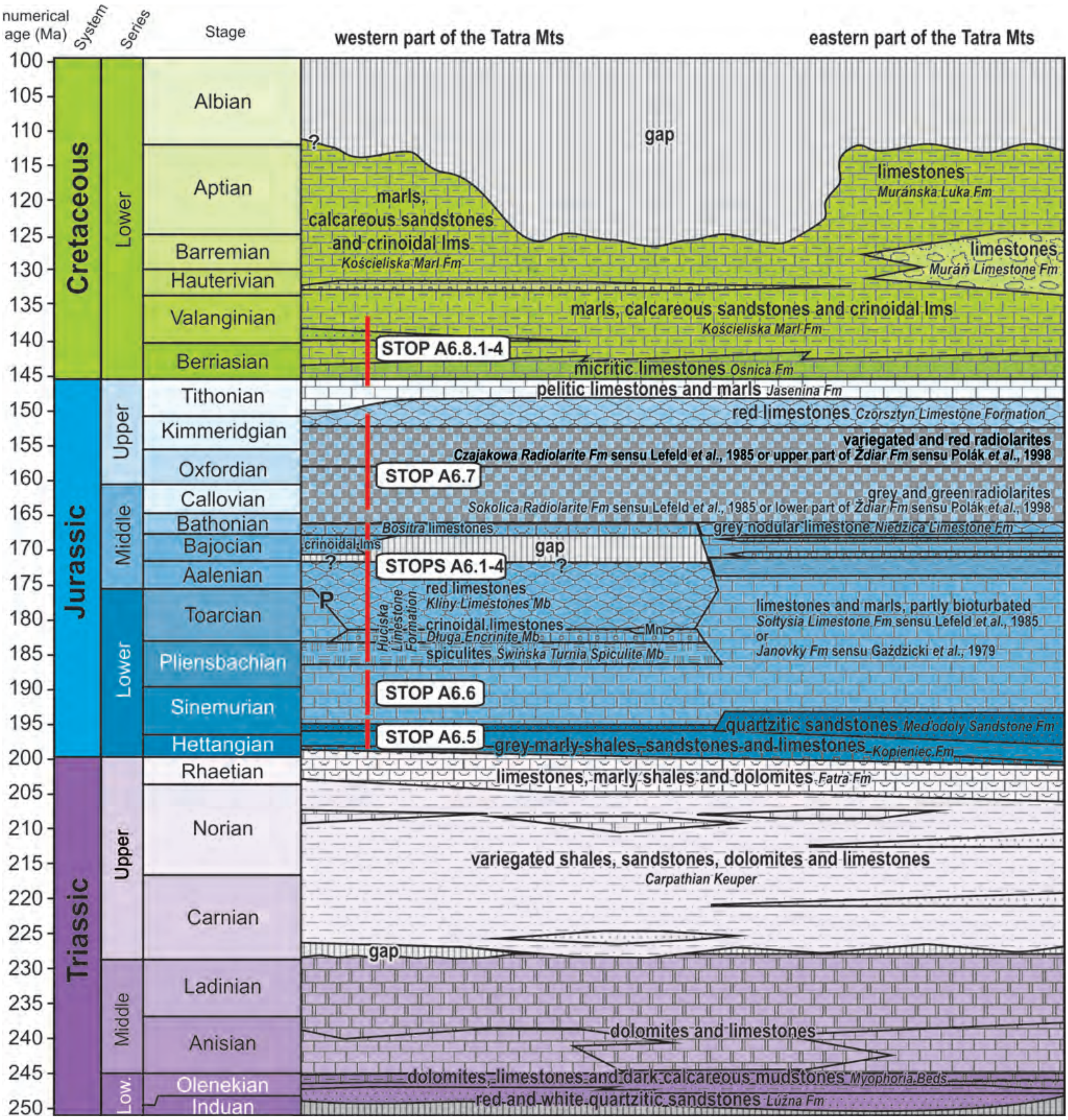

Fig. 6. Simplified litostratigraphic scheme of the Fatricum domain succession in the Tatra Mts (partly after Lefeld *et al.* (1985); modified)

upward the spiculite section. Crinoidal ossicles, benthic foraminifera and detrital quartz grains have also been found in very small quantities.

Spiculites are interbedded with some crinoidal wackestones, packstones and grainstones, which form beds up to 20 cm thick. Limestone beds thicken upwards and show a general trend of grain coarsening, accompanied by an increase in their textural maturity from wackestones to grainstones (Jach, 2005). Low-angle cross-bedding, normal grading and erosional bases observed in crinoidal interbeds indicate that they are laid down in higher energy conditions than the intervening spiculites. This is attributed to the currents generated by storms that were capable of sweeping crinoidal material from shallow, elevated parts of the basin to the area inhabited by siliceous sponges. As such, they represent event beds deposited below storm wave base on the slopes of an elevation. The gradual replacement of Hexactinellida by Demospongia and grain coarsening and thickening of crinoidal intercalations indicate a shallowing trend

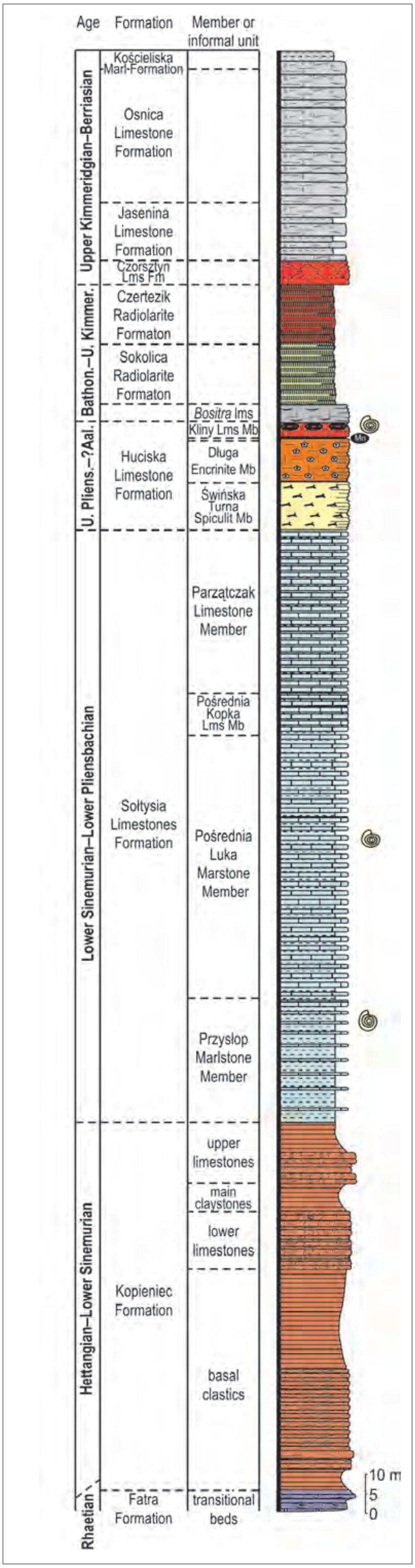

Fig. 7. Lithostratigraphic log of the Lower Jurassic–Early Cretaceous of the Krížna Nappe in the Western Tatra Mts (after Lefeld et al 1985; modified)

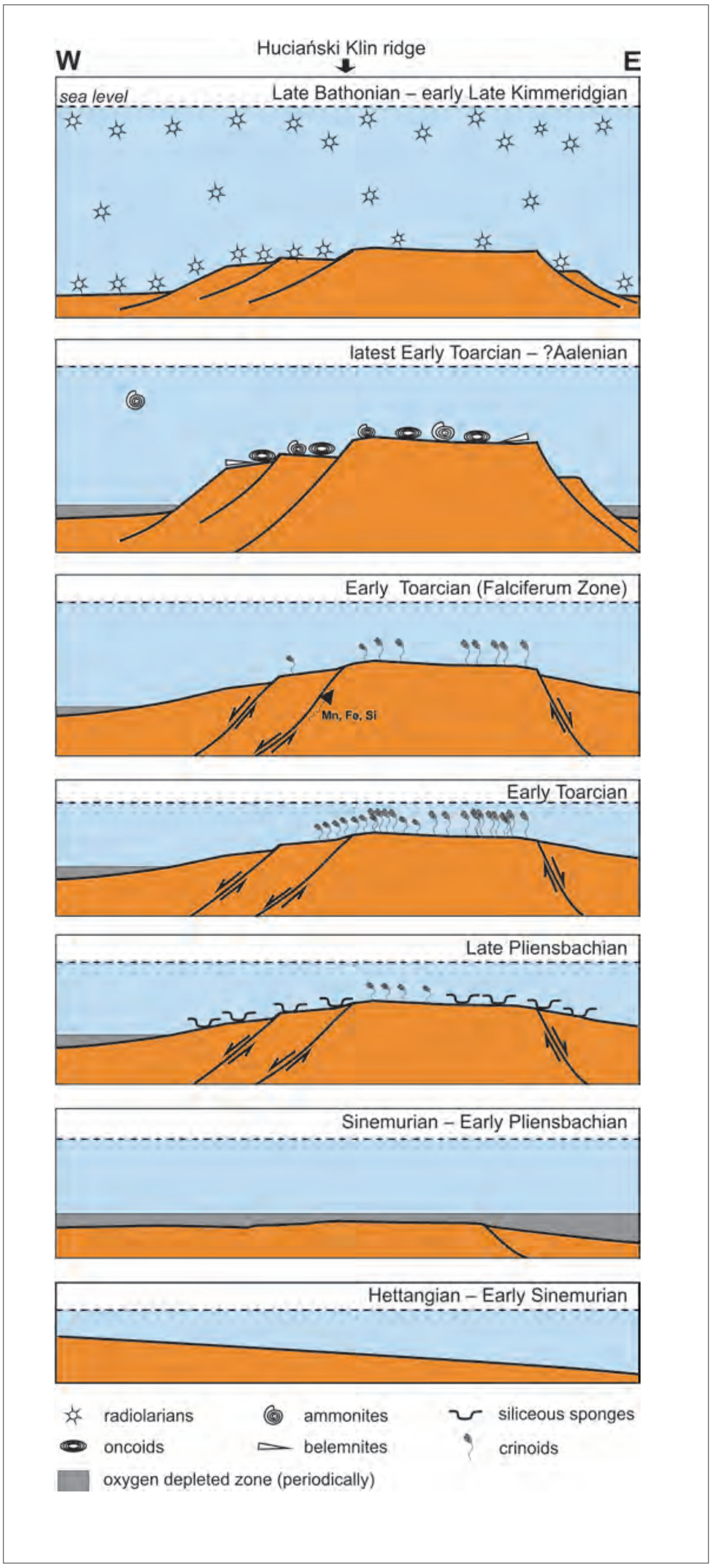

Fig. 8. Early–Middle Jurassic evolution of the studied part of the Fatricum Basin (after Jach, 2003; modified)

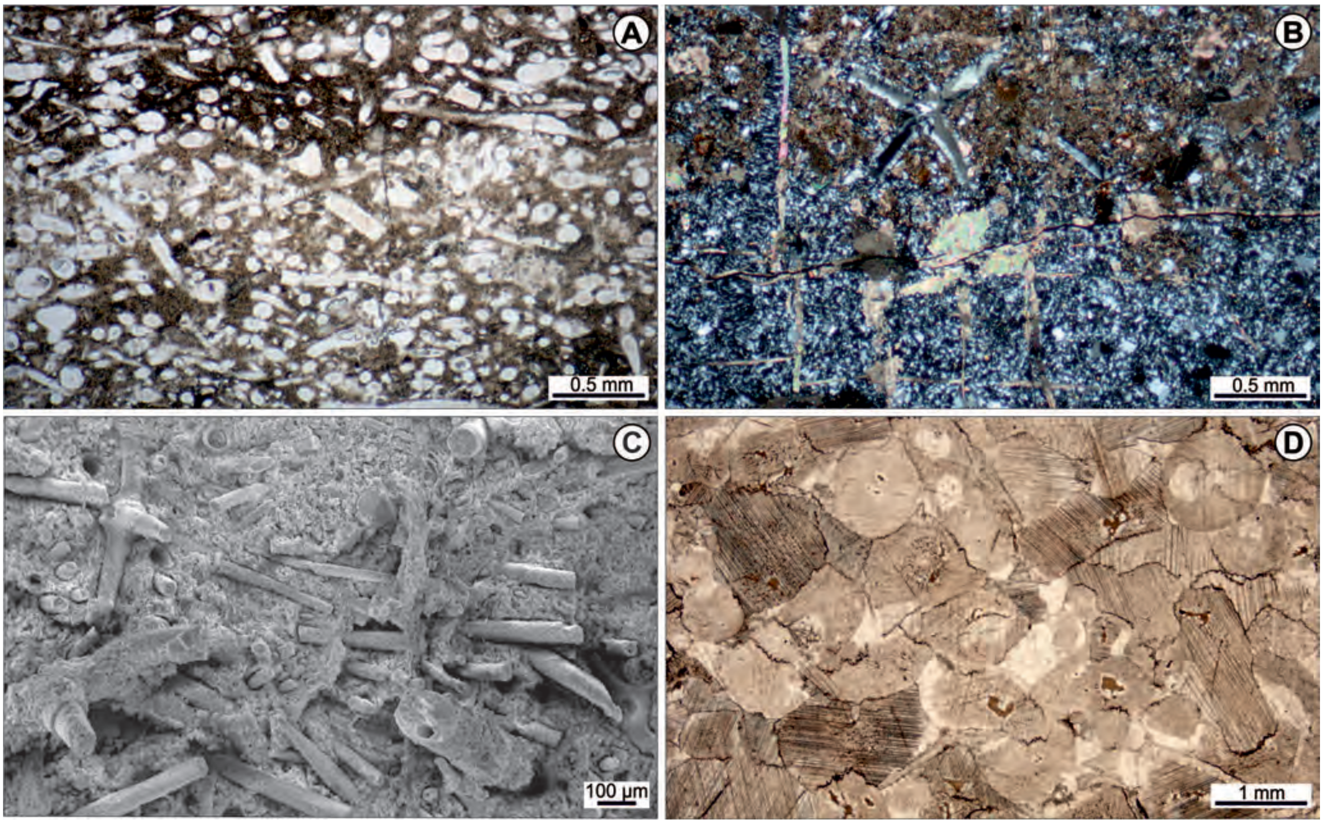

Fig. 9. Spiculites and crinoidal limestones. **A)** Spiculite in thin section. Plane-polarised light; **B)** Spiculite in thin section. Cross-polarised light; **C)** Densely packed siliceous sponge spicules. SEM image of HF-etched surface; **D)** Crinoidal grainstone with syntaxial cements. Thin section, plane-polarised light.

during spiculite deposition (Jach, 2002a). Most probably this trend was related to local changes of seafloor topography caused by synsedimentary faulting in the Fatricum Basin (Jach, 2005). This notion is supported by the occurrence of packages displaying chaotic bedding within the spiculites in the upper part of the spiculite succession. They are interpreted as submarine slumps.

A6.2 Huciański Klin ridge – Early Toarcian crinoidal limestones

(49°15′36″ N, 19°49′21″ E)

Leader: Renata Jach

White, grey and slightly pinkish crinoidal limestones (grainstones) overlie spiculites. They crop out directly over spiculites in rock crags. The crinoidal grainstones, about 12 m in thickness, display irregular bedding with subtle cross-bedding, graded bedding and erosional bed amalgamation. Crinoid stem plates (columnals) are predominant components whereas cirri and arm fragments are less common (Fig. 9D; Głuchowski, 1987). Crinoid assemblage is dominated by *Isocrinus* sp., *Balanocrinus* sp. while Cyrtocrinida occur less commonly (Świńska Turnia crag; Głuchowski, 1987). Fragments of echinoid spines, mollusc and brachiopod shells, ostracods, bryozoans, belemnite rostra, and benthic foraminifera occur subordinately (Jach, 2005). An indistinct trend in coarsening of the crinoidal grains from 0.5 mm to 1–1.2 mm is observed upward the sections.

A lack of stratigraphically diagnostic fossils hindered the precise age determination of the crinoidal limestones. They are ascribed to the Lower Toarcian since they are overlaid by red limestones of the latest Early–Late Toarcian (Lefeld *et al*., 1985; Myczyński and Lefeld, 2003; Myczyński and Jach, 2009; see stop A6.4). Chemostratigraphic data from crinoidal limestone indicate that in their uppermost part a significant $\delta^{13}C$ positive excursion occurs ($\delta^{13}C$ ~ 3.6‰; Krajewski *et al*., 2001). According to Jenkyns (2003), pronounced positive $\delta^{13}C$ excursion is associated with Early Toarcian Tenuicostatum and Falciferum zones; the excursion is interrupted with the negative shift in the early Exaratum subzone of the Falciferum Zone. As the isotope excursion occurs in the upper part of the crinoidal grainstones, it can be assumed that this part of the section refers most probably to the Tenuicostatum Zone of the Early Toarcian.

All the above described sedimentological characteristics point to a multiple reworking and winnowing of crinoidal material by storm-induced oscillatory currents from elevated parts of the basin. Thus, the sedimentation of the crinoidal grainstones took place between the storm and fair-weather wave bases. The succession of the crinoidal intercalations in the spiculites and the overlying crinoidal grainstones show a vertical transition from distal to proximal tempestites, which is a record of a progressive shallowing upward trend (Jach, 2005).

A6.3 Huciański Klin ridge – Early Toarcian manganese deposits

(49°15′37″ N, 19°49′20″ E)

Leader: Renata Jach

The Mn-bearing deposits of the Krížna Unit in the Western Tatra Mts occur locally between the crinoidal tempestites (Lower Toarcian) and the pelagic red limestones (Lower Toarcian–?Aalenian). They crop out exclusively between the Chochołowska and Lejowa valleys where they were mined as Mn ore in the 19th century (Jach, 2002b). The Mn-bearing deposits form a lens which is up to 2 m thick and stretches at the distance of a few hundred metres at the Huciański Klin ridge. The old shafts provide the only accessible outcrops of these rocks there. The longest of them is 41 m long (Jach, 2002b). The Falciferum Zone of the Early Toarcian may be estimated for the Mn-bearing deposits on the basis of their position in the section (Krajewski *et al*., 2001; Myczyński and Lefeld, 2003; Myczyński and Jach, 2009).

For the purpose of simplicity, the Mn-bearing deposits are subdivided in three parts: rocks underlying the Mn-rich bed (30–70 cm thick), the Mn-rich bed (up to 110 cm thick), and rocks overlying the Mn-rich bed (up to 40 cm thick; Jach and Dudek, 2005; Fig. 10).

Generally rocks underlying the Mn-rich bed consist of: (i) a Fe-rich layer, (ii) an X-ray amorphous Mn-oxide layer, (iii) shales, and (iv) a massive jasper bed. The 15 cm thick Fe-rich layer comprises up to ~30 wt% Fe (mainly hematite). The overlying 10 cm thick Mn-oxide layer is composed mainly of X-ray amorphous Mn oxide (up to 46 wt% Mn). Some 2–15 cm thick shales occur between the rocks described above and the main Mn-rich bed. Clay minerals comprise a complex suite dominated by mixed-layer clays with chlorite, smectite, and vermiculite layers (Dudek and Jach, 2006). The Fe-rich layer, and the Mn-oxide layer underwent locally silicification which resulted in the development of a massive jasper bed, which is 10 to 50 cm thick (Figs 10, 11A, B).

The Mn-rich bed, with sharp and well defined top and bottom, ranges in thickness from 35 cm to 1.1 m. It comprises clearly defined, lenticular zones composed either of Mn carbonates or of Mn silicates (Fig. 11C–E). The carbonate zones are purple-red, whereas the silicate zones are usually black.

The Mn-carbonate zones are built of calcite and Mn-calcite, with various Ca/Mn ratios whereas Mn sili-

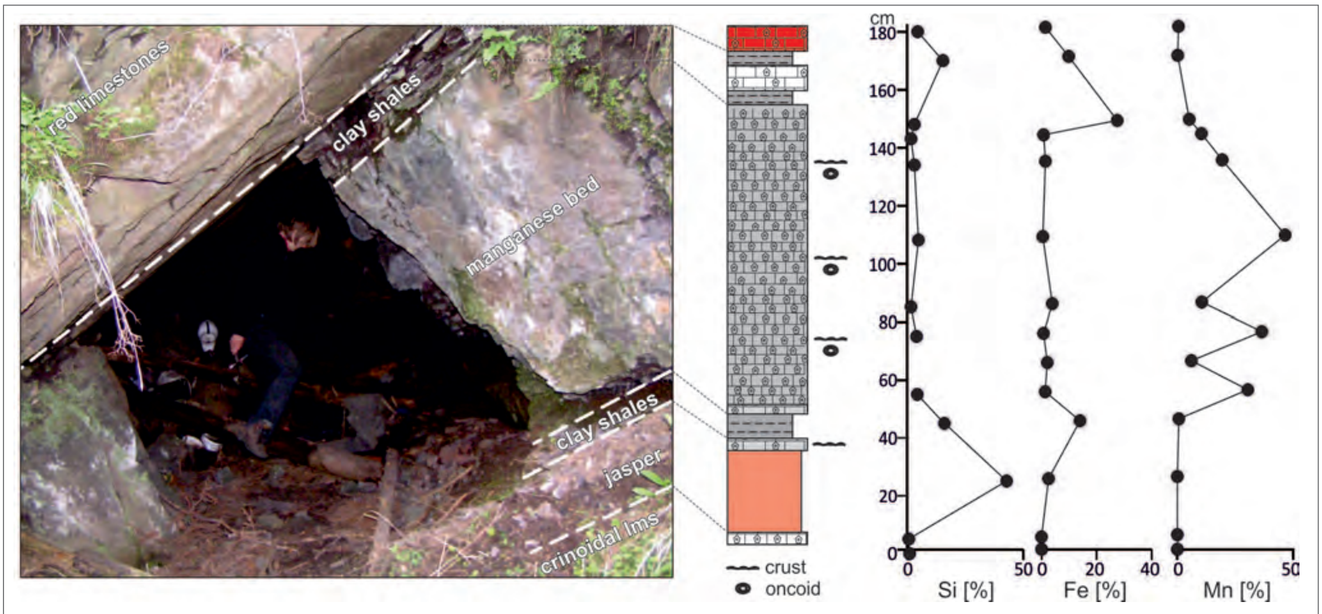

Fig. 10. Manganese-bearing deposits cropping out in a shaft entrance. Lithological section with general geochemical characteristic (Si, Fe and Mn).

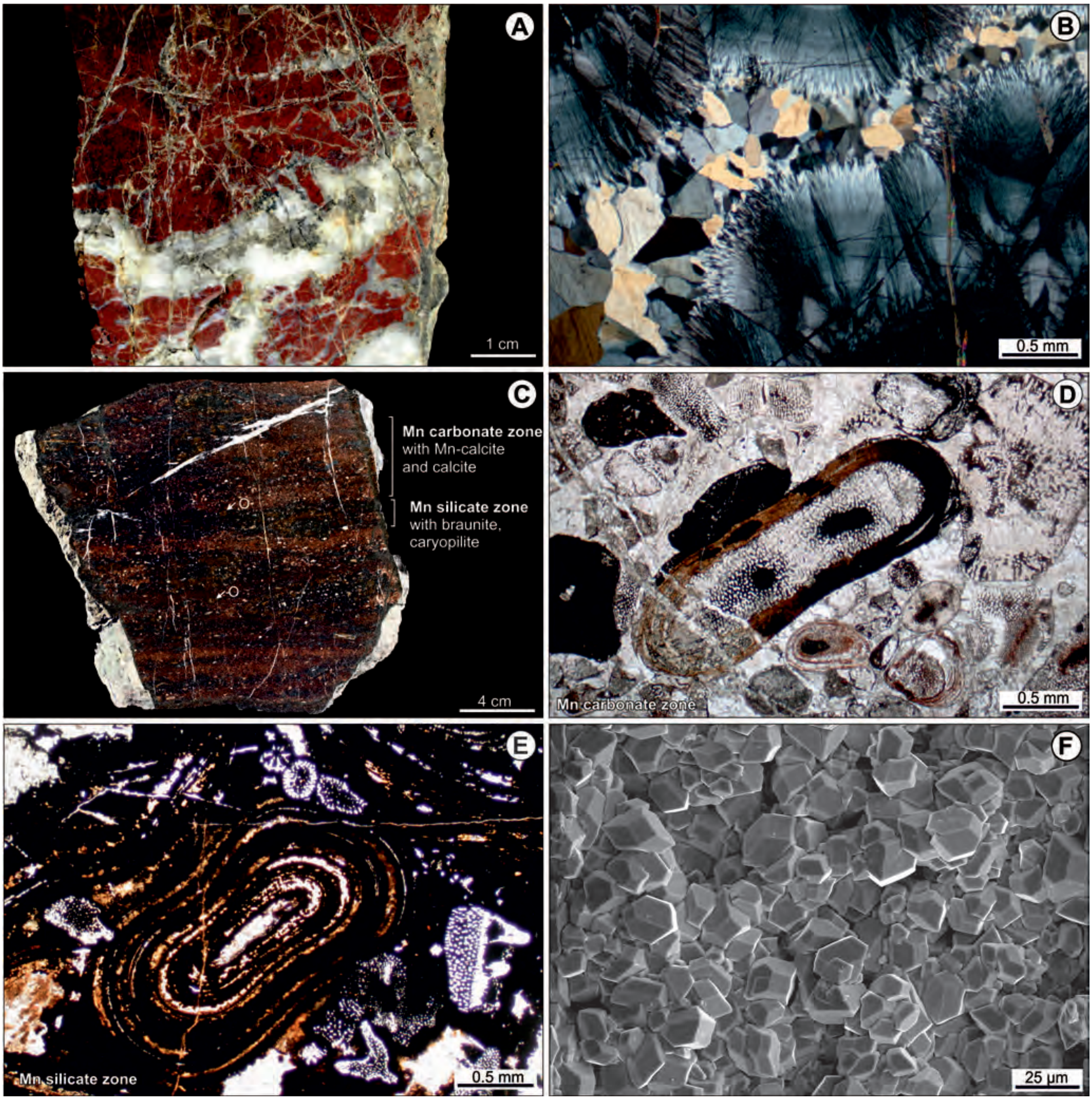

Fig. 11. Manganese-bearing deposits **A)** Jasper, polished slab; **B)** Internal structure of jasper bed, fibrous chalcedony and blocky quartz. Thin section, cross-polarised light; **C)** Mn-bearing bed shows subtle stratification underlined by occurrence of carbonate and silicate zones. Polished slab; **D)** Carbonate zone. Manganese oncoide within echinoderm grainstone, mainly echinoid-crinoidal, with syntaxial cements built of calcite and manganese calcite. Thin section, plane polarised light; **E)** Silicate zone with abundant microbial structures, mainly oncoids. Thin section, plane polarised light; **F)** Silicate zone. Authigenic idiomorphic crystals of braunite, SEM image of HCl-etched surface.

cates (braunite, caryopilite) occur in minor amounts (Korczyńska-Oszacka, 1978; Jach and Dudek, 2005). Pure rhodochrosite forms small lenses up to 6 cm long in the upper part of the bed (Korczyńska-Oszacka, 1979). Conversely, the silicate zones are dominated by braunite, forming frequently idiomorphic crystals (Fig. 11F), and caryopilite. Calcite and subordinate amounts of dolomite, apatite, and barite have been identified as non-manganese minerals. The chemistry of the carbonate and silicate zones differs mainly in the Mn content: ~5 wt% Mn in the former ones in contrast to more than ~50 wt% Mn in the latter ones (Jach and Dudek, 2005). The Mn-rich bed comprises low concentrations of transitional elements (Co + Ni + Cu < 0.01 wt%). On a ternary diagram of Co+Ni+Cu, versus Fe and Mn, our samples plot in the area of Mn deposits of hydrothermal and diagenetic origins. In contrast, it is enriched in Ba (up to 4500 ppm). Total REE (8 elements) contents range from 83 to 151 ppm which may indicate that the deposits studied may have formed by both hydrothermal and hydrogenetic processes.

The Mn-rich bed, especially the silicate zones, abounds in microbial structures: crusts and oncoids (Fig. 11C, E; Jach and Dudek, 2005). Crusts cover and bind bioclasts. Oncoids, 3–30 mm across, are usually elongated, rarely isometric. The nuclei of the oncoids are usually composed of bio- and lithoclasts, less frequently of barite crystals (cf. Krajewski and Myszka, 1958). Their cortex is composed of concentric laminae of Mn-silicates and Mn-calcite. Microbial structures are accompanied by bioclasts, namely fragments of echinoids and crinoids. Tests of benthic foraminifera, shells of molluscs, ostracods, holothurian sclerites, and bryozoan fragments are less common. This assemblage of fauna and microbial structures occurs exclusively within the Mn-rich sequence; it is not found in the overlying or underlying deposits or in deposits that are lateral equivalents of the Mn-rich sequence.

Rocks overlying the Mn-rich bed are composed of two layers of shale separated by a layer of bioclastic limestone. The agglutinating foraminifera, represented almost exclusively by *Recurvoides*, occur in the upper shale (Tyszka *et al*., 2010). The clay fraction of the shales is dominated by illite and illite-rich illite-smectite mixed-layer clays (Dudek and Jach, 2006).

The Mn-bearing deposits are interpreted as formed in several stages controlled by a pulse-like activity of a shallow submarine exhalative vent (Krajewski and Myszka, 1958; Jach and Dudek, 2005). It is proved by sedimentological, mineralogical and geochemical evidence, coupled with the occurrence of specific microbial structures and a peculiar fauna assemblage (Jach and Dudek, 2005). The limited lateral extent of the Mn-bearing sequence may be an effect of low efficiency of the vent and/or of the seafloor topography. The specific faunal assemblage dominated by deposit feeders was intimately associated with trophic conditions which persisted near the vent orifice. During cessation in the vent activity, the sediments would have been exposed to and would have interacted with sea-water. Other early diagenetic processes included silicification and reduction of Mn oxides during suboxic diagenesis (Krajewski *et al*., 2001). Hydrothermal activity was the most likely source of colloidal silica. Idiomorphic shapes of braunite crystals embedded in Mn-calcite indicate that silicification preceded crystallization of Mn carbonates. The process of silicification resulted in the formation of Mn silicates in the Mn-rich bed, the massive jasper bed in the lower part of the sequence, and possibly also numerous silica lenses in the underlying crinoidal grainstones. The following stage of diagenesis – precipitation of Mn carbonate cements in the Mn-rich bed, was controlled by abundance of organic matter in the sediments. The latter is interpreted as genetically related to the microbial productivity *in situ*.

The position of the Mn-bearing deposits over the crinoidal tempestites and below the red pelagic limestone indicates that they were laid down at neritic depths. Moreover, it implies that Mn-bearing deposits mark a substantial change from relatively shallow (tempestites) to deeper water (red pelagic limestones) sedimentation milieu. This change most probably resulted from synsedimentary tectonic activity. It is in line with expelling of fluids by the vent. It was associated with extensional faults which provided channelways for geofluid migration upward (Jach and Dudek, 2005). The internal facies variation of the Mn-bearing sequence may be explained by changes in bottom-water chemistry, geofluid temperature or by lateral migration of the vent orifices.

A6.4 Huciański Klin ridge – Lower Toarcian-?Aalenian red limestones and marlstones and Bathonian *Bositra* limestones

(49°15′37″ N, 19°49′24″ E)

Leaders: Alfred Uchman, Renata Jach

The Mn-bearing sequence is covered by red limestones and marlstones, about 4 m thick, which in turn, are overlain by thin-shelled bivalve-bearing limestones (hereafter called *Bositra* limestones). The latter are up to 3 m thick (Figs 12, 13A; Jach, 2007). The ammonites found in the red limestones indicate the upper part of Lower Toarcian–Upper Toarcian (Serpentinum–Pseudoradiosa zones; Myczyński and Jach, 2009). The outcrop of red limestones is located at the entrance to one of the Mn adits.

The red limestones and marlstones are characterized by concentrations of pelagic fauna remains (Fig. 13B), such as ammonites, belemnites and fish teeth, which are a common feature of the Jurassic pelagic limestones deposited on elevated settings (pelagic carbonate platforms *sensu* Sanantonio, 1993). Six microfacies have been distinguished within red nodular limestones: crinoidal-ostracod packstone, crinoidal packstone, crinoidal wackestone, marly mudstone, *Bositra* packstone and *Bositra*-crinoidal packstone (Gradziński *et al*., 2004). Finning-upward trend (from packstones to wackestones), is accompanied by increasing upward abundance of microborings.

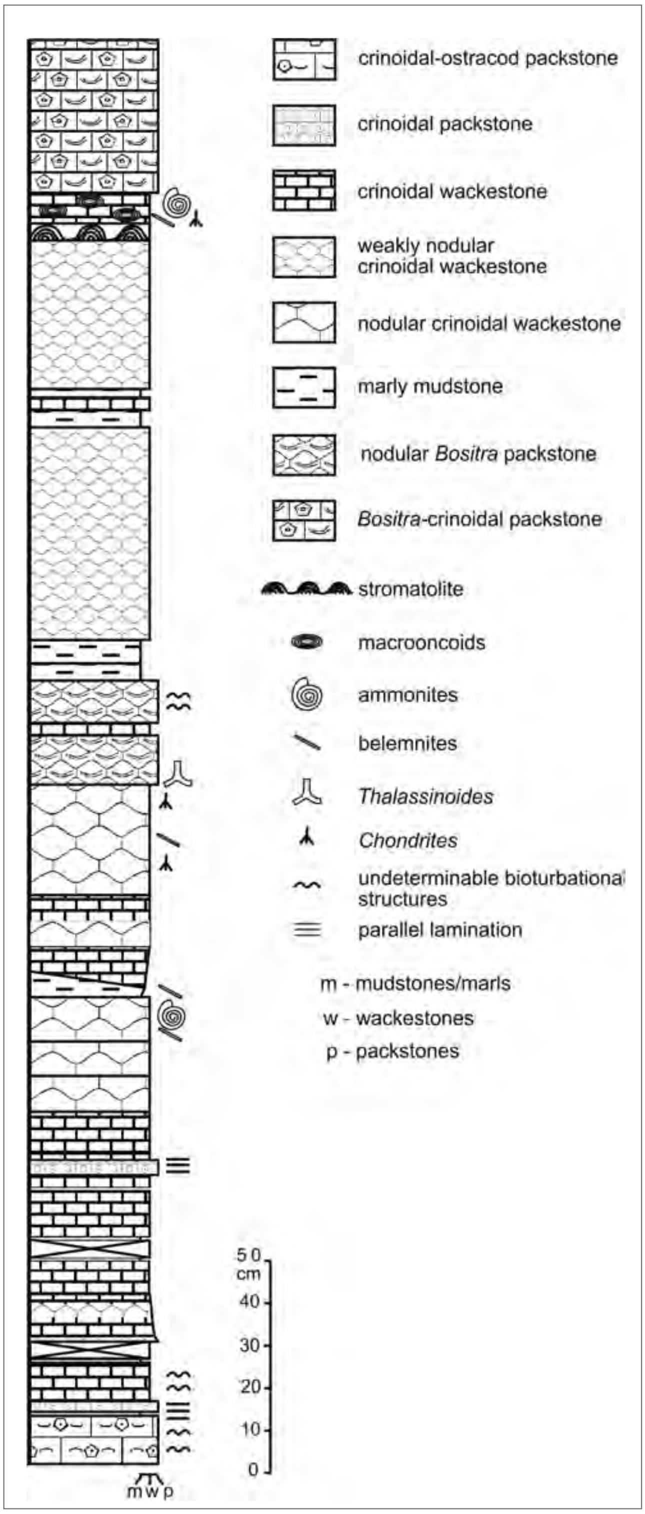

Fig. 12. Lithological section of the red limestones in the Huciański Klin site (Gradziński *et al*., 2004)

Crinoid and echinoid fragments are most abundant within microfossil assemblage. Fish teeth, benthic foraminifera, smooth-walled ostracods, juvenile ammonites are less common (Gradziński *et al*., 2004). Echinoid fragments dominate in the lower part of the red nodular limestone section and decrease upwards. Conversely, fish teeth are relatively rare in the lower part of the section and abundant in the upper part.

The upper part of red limestones and marlstones displays several features, such as concentration of nektonic fauna remains, occurrence of stromatolites and oncoids, and abundance of microborings typical of condensed section deposited on submarine elevations (Fig. 13A–D; Jenkyns, 1971; Bernoulli and Jenkyns, 1974). The features mentioned above collectively indicate a low depositional rate.

Microbial-foraminiferal oncoids, which have been recognized in the upper part of the red deposits, are the most peculiar feature of the studied section (Fig. 13C, D; Gradziński *et al*., 2004). The oncoids are up to 10 cm across and mostly display discoidal shape. Intraclasts or internal moulds of ammonites have acted as oncoid nuclei whereas oncoid cortices are composed of dark red laminae (mainly of iron hydrooxides/oxides), encrusting foraminifera (Fig. 13D; *Nubecularia* aff. *mazoviensis*, *Dolosella*, and agglutinated *Tolypammina*) and calcite cements. The dark red laminae dominate the oncoidal cortices and show a reticulate ultrastructure which is interpreted as mineralized biofilm, visible under SEM. Mineralized microbial bodies, globular and filamentous in shape, also built of iron hydrooxides/oxides, are abundant within the laminae. The association of foraminifera with microbes is supposed to be an adaptation of foraminifera to oligotrophic condition on the sea floor. It is very probable that biofilms served as food source for encrusting foraminifera. Formation of oncoids was possible under periodic water agitation (Gradziński *et al*., 2004).

The red limestones locally display nodular structure and contain a few discontinuity surfaces in the studied section (Gradziński *et al*., 2004). Some of such surfaces are burrowed with *Thalassinoides*, which indicates colonization of a firmground by crustaceans. Another discontinuity surface, which occurs in the uppermost part of the section, is manifested by concentration of internal moulds of ammonites and some fragments

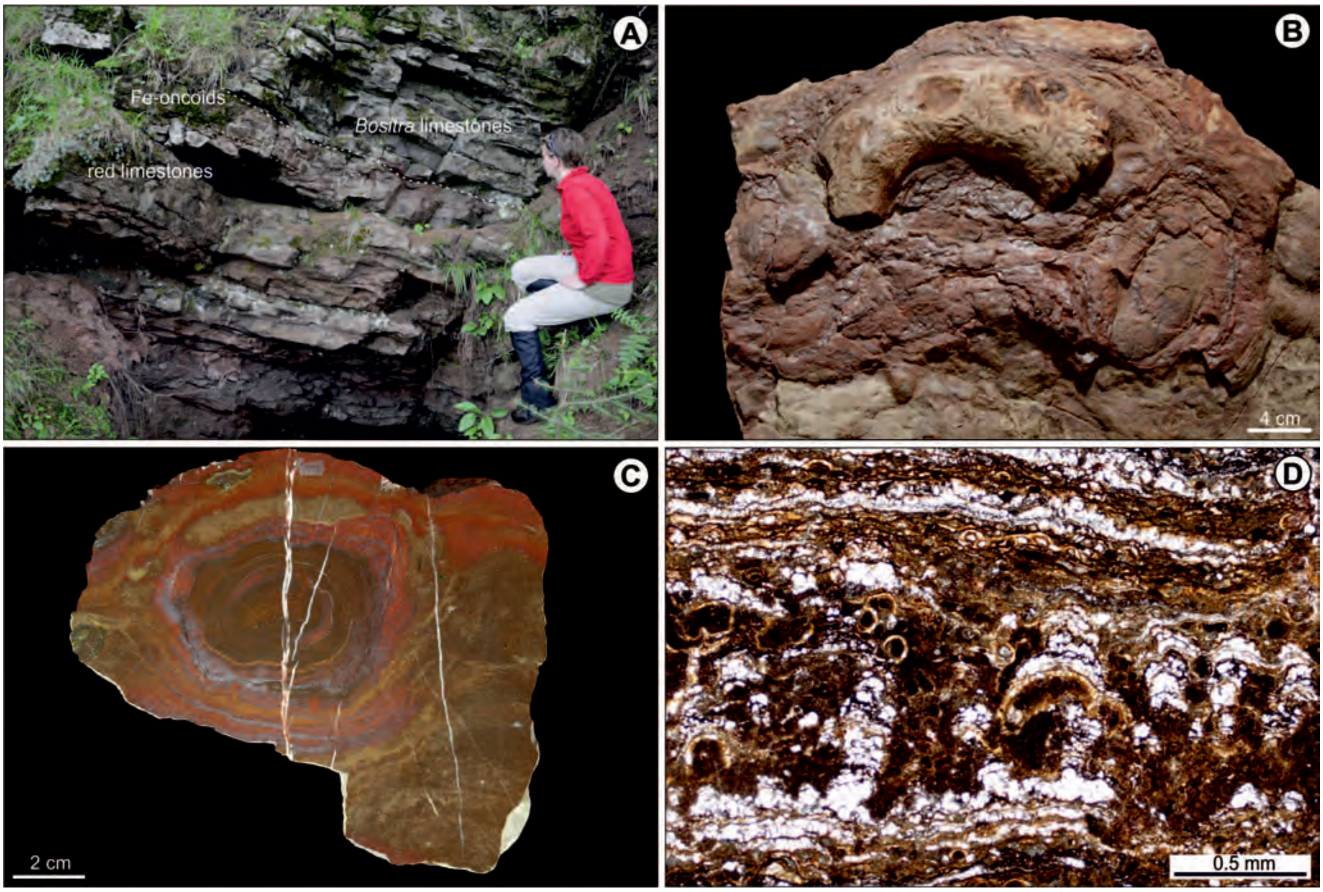

Fig. 13. Red limestones. **A)** Section of the red limestones and *Bositra* limestones at the entrance to one of the adits; **B)** Omission surface with ferruginous stromatolite encrusting ammonite mould and shell (*Lytoceras* sp.). Weathered surface; reprinted from Myczyński and Jach (2009); **C)** Cross-section through a microbial-foraminiferal ferrugineous macrooncoids. Polished slab; **D)** Cortex of oncoid built of encrusting foraminifers; thin section, plane-polarised light.

of ammonite shells covered with a stromatolite (Fig. 13B). There is a concentration of glaucony grains and crusts in the topmost part of the section, just at the contact of the red limestones and the *Bositra* limestones.

Overlying Bositra limestones are composed of Bositra-crinoidal packstones, and Bositra packstones/grainstones in this section (Jach, 2007). The latter dominate in the uppermost 3 m of the section. They were laid down in a relatively high-energy setting, which controlled the good sorting of these deposits. However, the domination of the Bositra bivalves seems to have resulted from some ecological factors, such as eutrophication of the water column. The dissolution of non-calcitic bioclasts is also suggested. Bositra-limestones lack of index fossils; their age is inferred as Lower Bathonian, based on superposition (Jach et al., 2014).

The red nodular limestones and the overlying *Bositra* limestones were formed during gradual deepening of the basin, which caused lowering of the depositional rate and, hence, condensation (Wieczorek, 2001). The deposition of *Bositra* limestones marks the first stage of unification of facies, which probably took place during Lower Bathonian. This process was later manifested by the deposition of radiolarites in the whole Fatricum Basin (Ožvoldová, 1997; Polák *et al*., 1998; Jach *et al*., 2012, 2014). Thus, the deposition of *Bositra* limestones reflected the intermediate stage in the basin evolution leading to formation of radiolarites (Lefeld, 1974; Jach, 2007).

A6.5 Lejowa Valley – Lower Jurassic mixed siliciclastic/carbonate deposits

(49°15′46″ N, 19°50′39″ E)

Leader: Andrzej Gaździcki

The uppermost Triassic and lowermost Jurassic strata of the Fatricum (Krížna Nappe) in the Tatra Mts are represented by marly shales and quartz sandstones with limestone intercalations (Uhlig, 1897; Goetel, 1917; Gaździcki, 1974, 1975, 1983, 2003, 2014; Uchman, 1991; Krobicki and Uchman, 1993; Hołda, 2002). They are assigned to the Fatra and Kopieniec formations (Gaździcki *et al.*, 1979; Lefeld *et al.*, 1985).

The Lower Liassic (= Grestener Schichten of Uhlig, 1897; Kopieniec Schichten of Goetel, 1917; Kopieniec Formation of Gaździcki *et al.*, 1979) strata crop out

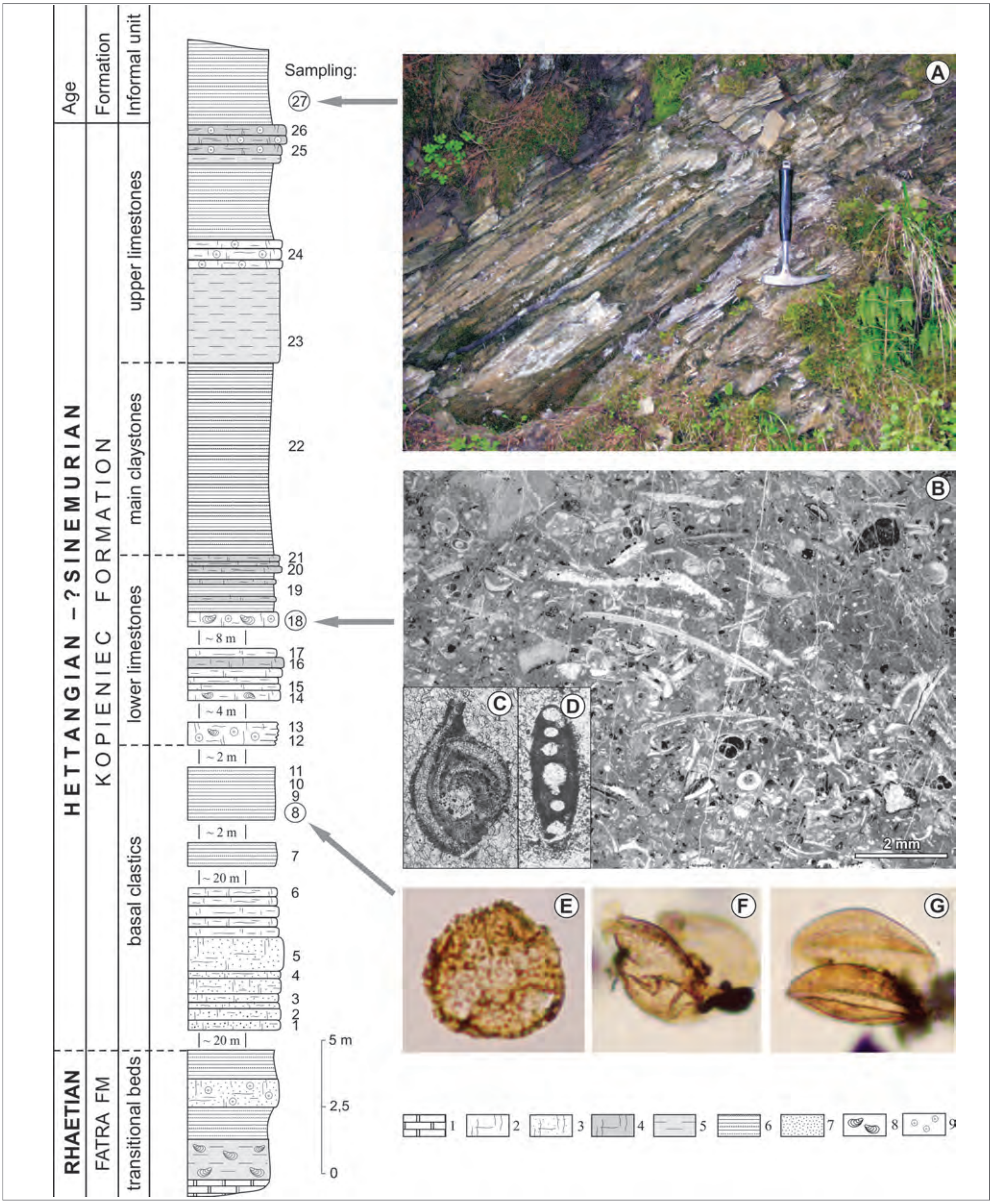

Fig. 14. Section of the uppermost Fatra and Kopieniec formations in Lejowa Valley. The section shows lithology and distribution of some important biota components. 1 – dolomites, 2 – limestones, 3 - sandy limestones, 4 – marly limestones, 5 – marls, 6 – shales, 7 – sandstones, 8 – bivalve shells, 9 – crinoids (trochites). **A)** Exposure of marly shales in the upper part of the formation (hammer for scale); **B)** Bivalve-crinoid-gastropod-foraminifer biopelmicrite microfacies; **C, D)** Benthic foraminifers *Ophthalmidium leischneri*; x 110; **E-G)** Palynomorphs: **E)** *Baculatisporites comaumensis*, x 500; **F)** *Schismatosporites ovalis*, x 300; **G)** *Quadreaqualina anellaeformis*, x 300.

over a large part of the Sub-Tatric (Krížna) Unit along the northern slopes of the Tatra Mts (Guzik *et al*., 1975, Bac-Moszaszwili *et al*., 1979; Gaździcki, 2014, figs 4.4.2, 5.1.1).

In the Lejowa Valley, the Kopieniec Formation is well exposed on the northeastern slopes of Wierch Spalenisko Mt. The presented section (Fig. 14) was traced along the ravine (creek) from Wierch Spalenisko Mt. to Huty Lejowe Glade at the altitude 1040–985 m a.s.l. and rests on the transitional beds of the Rhaetian Fatra Fm.

The Kopieniec Formation (up to 100 m thick) is subdivided into the following informal litostratigraphical units of the member rank: basal clastics, lower limestones, main claystones, and upper limestones (Fig. 14, see also Gaździcki *et al*., 1979). Quartz sandstones, slightly calcareous with clayey-limonitic matrix and represented in form of distinct layers in the basal part of the formation are the main lithological type here and belong to the "basal clastics" of the formation (Gaździcki, 2014, fig. 5.1.6). In the upper part of the unit, an assemblage of palynomorphs: *Baculatisporites comaumensis*, *Schismatosporites ovali*s, *Quadreaqualina anellaeformis* as well as *Concavisporites*, *Dictyophyllites* and *Leptolepidites* was found in the brown-gray laminated marly shales (Gaździcki *et al*., 2006, fig. 1) see also Fig. 14E–G). The next unit — "lower limestones" — contains of dark-grey sandy organodetrital limestones. These are bivalve-crinoid-gastropod-foraminifera biopelmicrites with *Pycnoporidium*? encrustacions and envelopes. The spores *Globochaete* and *Eotrix* are common. Among the foraminifera, *Ophthalmidium leischneri* (Fig. 14B–D), *Planiinvoluta, Nodosaria, Lenticulina* and post-Triassic involutinids predominate (Gaździcki 2014, figs 5.1.8). Brown-gray shales (claystones) with marly intercalations prevail in the "main claystones". The upper unit of the Kopieniec Formation — "upper limestones" — comprises a sequence of brown-gray marls, shales and dark-gray organodetrital limestones (mostly crinoid-ostracod-brachiopod biointrapelsparite). The limestone intercalations contain numerous benthonic foraminifera: *Ophthalmidium leischneri, O. walfordi, Involutina liassica, I. turgida, I. farinacciae* and nodosarids (Gaździcki, 2014, figs 5.1.10–11). The uppermost part of the Kopieniec Formation section is terminated by brown-gray marly shales with marly intercalations (Fig. 14A).

The clastic-carbonate shallow-marine Late Triassic/Early Jurassic successions of the Tatra Mts contain biostratigraphicaly important microfossils, mostly foraminifera, ostracodes, and conodonts, as well as palynomorphs and coprolites (Błaszyk and Gaździcki, 1982; Gaździcki, 1974, 1975, 1977, 1978, 1983, 2014; Fijałkowska and Uchman, 1993). They have been used to erect local zonations and they may also be of prime importance for regional biostratigraphic correlations and palaeogeographic reconstruction. The recognized evolutionary lineages and the rapid rates of evolutionary changes of representatives of the benthonic foraminifera families Involutinidae and Ammodiscidae and the subfamily Ophthalmidiinae permit an establishment of relatively high resolution zonation. A sequence of two foraminifera zones: *Glomospirella friedli* and *Triasina hantkeni* Zone (aassemblage zone, Rhaetian) and *Ophthalmidium leischneri* and *O. walfordi* (assemblage zone, Hettangian–?Sinemurian) is recognized (Gaździcki, 1983). The foraminifera biostratigraphical zonation of the late Triassic and Early Jurassic in the Tatra Mts shows that the boundaries of the litostratigraphical units, i.e. the Fatra- and Kopieniec formations in the Fatricum Domain are diachronous (Fig. 15, see also Gaździcki and Iwanow, 1976). It may coincide with the Rhaetian-Hettangian boundary, as was widely assumed, or pass through the Rhaetian.

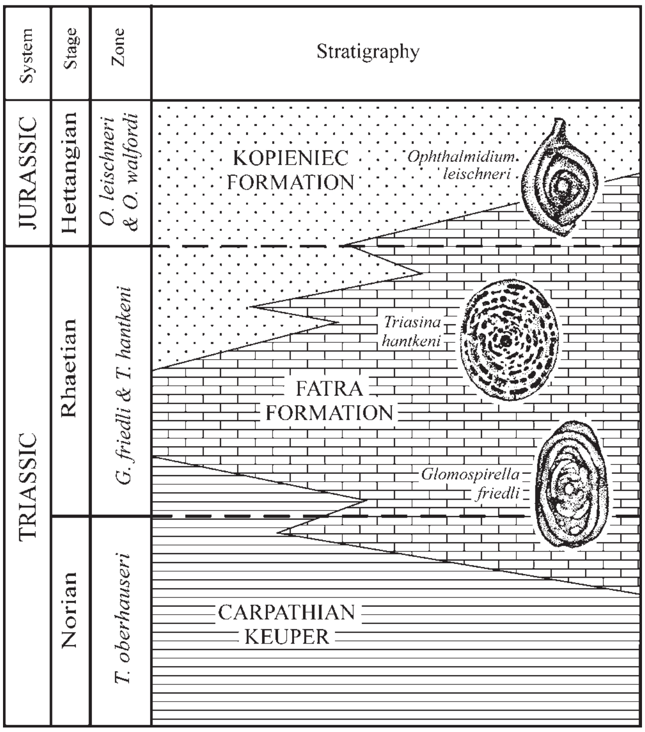

Fig. 15. Diachronism of the Fatra and Kopieniec formations in the Tatra Mts.

The Kopieniec Formation of the Tatra Mts comprises shallow-marine clastic (with trace fossils which indicate the *Cruziana* ichnofacies see Uchman, 1991) and mixed clastic-carbonate sediments (of tempestitic origin) deposited in the photic zone (Gaździcki, 2014). The character of these deposits reflects some general changes and especially epeiric movements at the turn of the Triassic and Jurassic. The sedimentary sequence and floral and faunal assemblages of the Kopieniec Formation are almost identical to those from contemporaneous strata of the Tethys realm. On the other hand, it is possible to note some similarity to contemporaneous deposits of the epicontinental basins in the north-western Europe. This was already noted by Goetel (1917), who emphasized a marked resemblance to the sandstones with *Cardinia* from the Tatra Mts and the Lower Liassic of Swabia in sedimentary environment and faunal community.

A6.6 Huty Lejowe Glade, Lejowa Valley – Late Sinemurian-Early Pliensbachian spotted limestones and marls

(49°15′55″ N, 19°50′37″ E)

Leaders: Alfred Uchman, Renata Jach

Bedded grey bioturbated limestones and marly limestones with marl intercalations are characteristic Early Jurassic, and locally Middle Jurassic, facies in the Krížna Unit. This hemipelagic facies is an equivalent of the Allgäu Formation (*Fleckenmergel/Fleckenkalk*) from the Northern Calcareous Alps (e.g., Gawlick *et al.*, 2009). It is called the spotted limestones and marls in the Carpathians.

An about 150 m-thick series of partly spotty calcilutites and calcisiltites (calcimudstone and wackestones) interbedded with darker marls is exposed along the Lejowy Potok stream near Huty Lejowe Glade (Polana Huty Lejowe) as well as in the lower part of a gully running from slopes of Pośrednia Kopka Kościeliska Mt. to Huty Lejowe Glade. According to Lefeld *et al.* (1985), the spotted limestones and marls, distinguished as the Sołtysia Marl Formation, are Early Sinemurian – Early Pliensbachian in age. Their Sinemurian age is based on the ammonites *Arnioceras falcaries* and *Arnioceras ceratitoides* of the Bucklandi Zone (Early Sinemurian) and *Echioceras raricostatum* and *Echioceras raricostatoides* of the Late Sinemurian Raricostatum Zone (e.g., Gaździcki and Wieczorek, 1984; Uchman and Myczyński, 2006). The same deposits are ascribed as the Janovky Formation in Slovakia (Gaździcki *et al.*, 1979).

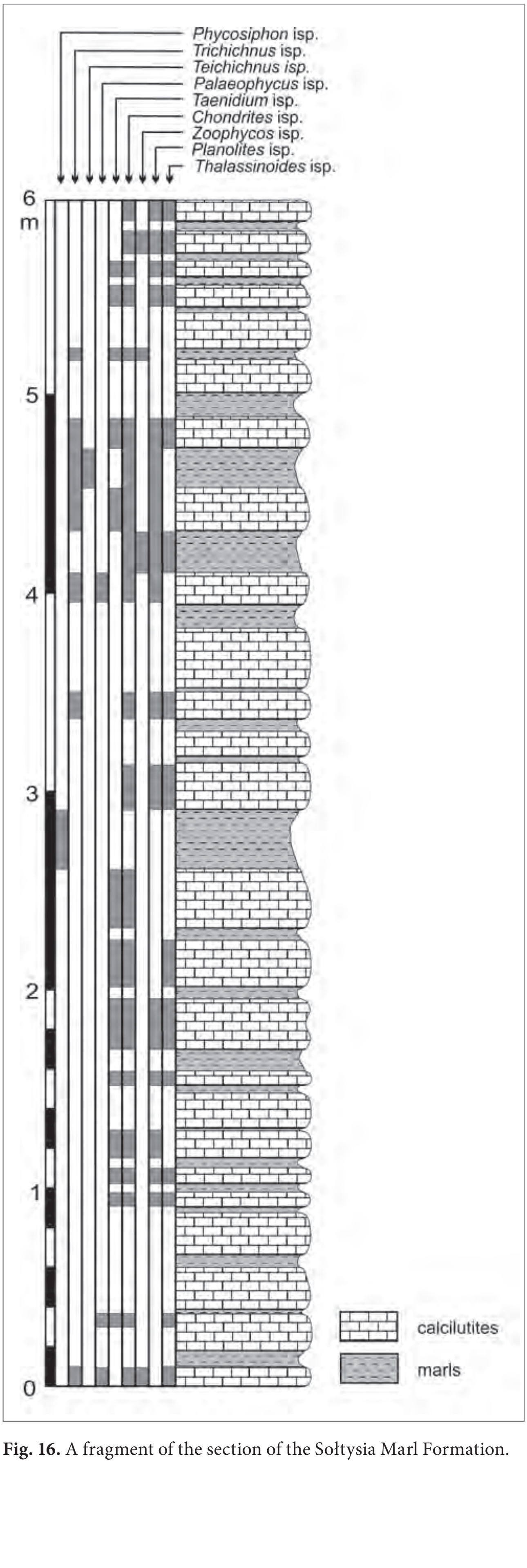

Fig. 16. A fragment of the section of the Sołtysia Marl Formation.

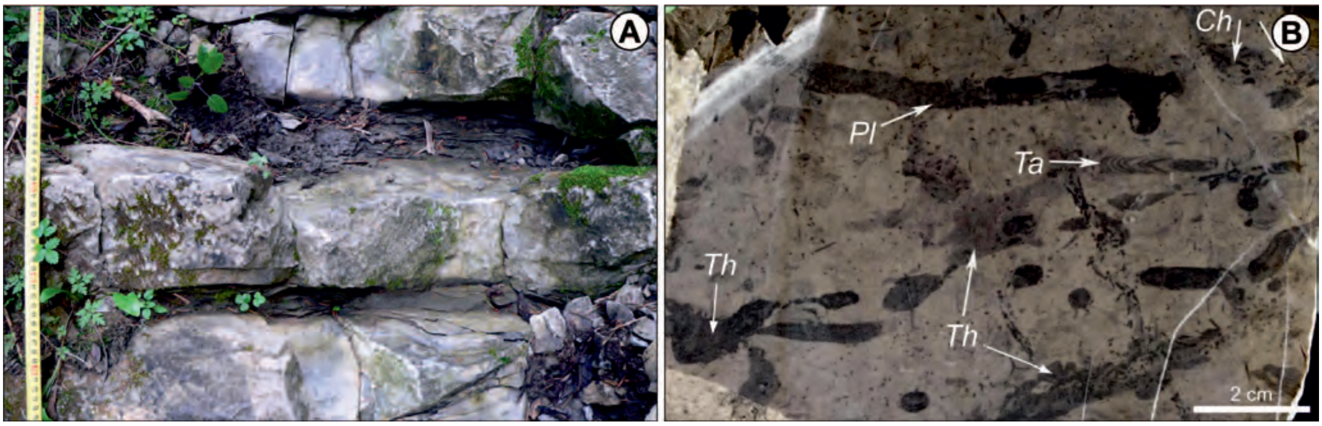

Fig. 17. Trace fossils from the Sołtysia Marl Formation, Lejowa Valley. **A.** Vertical cross section. *Th* – *Thalassinoides*; *Ch* – *Chondrites*; *Pl* – *Planolites*; *Ta* – *Taenidium*. **B.** Horizontal section. *Th* – *Thalassinoides*; *Pl* – *Planolites*; *Pa* – *Palaeophycus*; *Tr* – *Trichichnus*.

Proportions of the thickness of limestone beds to marl interbeds are variable (Figs 16, 17). For this reason spotted limestones and marls are subdivided into four subfacies:

- scarce in trace fossils, dark grey marls, interbedded with dark limestones, with average ratio of marl/limestone bed thickness 4:1 to 1:1. This subfacies occurs in the lower part of the section and refers to the Przysłop Marlstone Member (~ 30 m thick);
- bioturbated limestones, interbedded with dark marls, with marl/limestone bed thickness ratio 2:1 to 1:20. These deposits are ascribed to the Pośrednia Hala Marlstone Member;
- light grey limestones, subordinately interbeded with thin marls, with rare bioturbational structures. They are distinguished as the Pośrednia Kopka Limestone Member;
- dark grey limestones regularly interbeded with thin marls, which become strongly silicified toward the top. Trace fossils are scarce. This facies refers to the Parzątczak Limestone Member.

The deposits of the Sołtysia Marl Formation contain relatively common tests of benthic foraminifers, radiolarians, ostracods, sponge spicules, whereas macrofossils such as bivalve shells, ammonites, nautiloids and belemnite rostra are rare (e.g., Gaździcki *et al.*, 1979).

Trace fossils are observed in cross sections as variable dark spots visible against lighter, totally bioturbated background (Fig. 17B). *Planolites*, *Chondrites* and *Thalassinoides* are common. *Zoophycos*, *Teichichnus, Taenidium*, *Phycosiphon* (formerly *Anconichnus*) and *Palaeophycus* occur subordinately. The trace fossils were described by Wieczorek (1995), who supposed that their tracemakers were controlled by bathymetry, oxygenation and trophic changes. Wieczorek (1995) distinguished between two main phases of bioturbation related to oxygenation changes. During the first phase, the totally bioturbated background was produced in well-oxygenated sediment. The fodinichnia-dominated ichnoassemblage containing *Chondrites*, *Planolites* and *Zoophycos* is typical of the second phase, when oxygenation of the sea floor dropped.

All the trace fossils display typical cross-cutting relationships. *Planolites* and *Thalassinoides* are cross cut by *Zoophycos, Chondrites* and *Trichichnus*, and *Zoophycos* is cross cut by *Chondrites* and *Trichichnus*. This order can be related to vertical partitioning of burrows in sediment (tiering) and their gradual shift following sediment accumulation or to sequential colonization in time by changing burrowing communities.

Gaździcki *et al.* (1979) suggested a depths from deeper neritic to bathyal zones for the discussed deposits, and Wieczorek (1984) interpreted them as basinal but shallower sediments deposited at the beginning of basin deepening. The general vertical trend in trace fossils suggests changes in nutrient supply and oxygenation of sediments. Also geochemical data, such as the values of the V/(V+Ni) ratio, comprised between 0.55 and 0.65, additionally imply changes in oxygen content from oxic to strongly dysoxic conditions. It is not excluded that the changes of calcium carbonate content are related to some climatic oscillations. The limestone-marl alternations probably reflect periodic delivery of siliciclastic material from adjacent lands. Such a process seems to be climatically dependent probably due to Milankovitch cyclicity (see Mattioli, 1997).

A6.7 Długa Valley, Pośrednie ridge – Middle–Upper Jurassic radiolarites

(49°15′37″ N, 19°48′04″ E)

Leaders: Renata Jach, Alfred Uchman, Nevenka Djerić[1], Špela Goričan[2], Daniela Reháková[3]

[1] *Faculty of Mining and Geology, Belgrade University, Belgrade, Serbia*

[2] *Ivan Rakovec Institute of Palaeontology, ZRC SAZU, Ljubljana, Slovenia*

[3] *Department of Geology and Palaeontology, Faculty of Natural Sciences, Comenius University, Bratislava, Slovakia*

The Middle–Upper Jurassic radiolarites crop out in the rock cliff located in the Długa Valley along the southern slope of the Pośrednie ridge (Fig. 2). The radiolarite-bearing succession comprises the following facies: (1) grey spotted radiolarites, (2) green radiolarites, (3) variegated radiolarites, and (4) red radiolarites (Figs 18; 19A–C). They are overlain by red limestones. The radiolarian-bearing deposits are ~30 m thick.

The radiolarites, on the basis of $\delta^{13}C$, radiolarians and calcareous dinoflagellata are of the Late Bathonian–early Late Kimmeridgian age (Fig. 18; Unitary Association Zones 7–11; Moluccana Zone; Polák *et al.*, 1998; Jach *et al.*, 2012, 2014). The broad negative excursion recorded

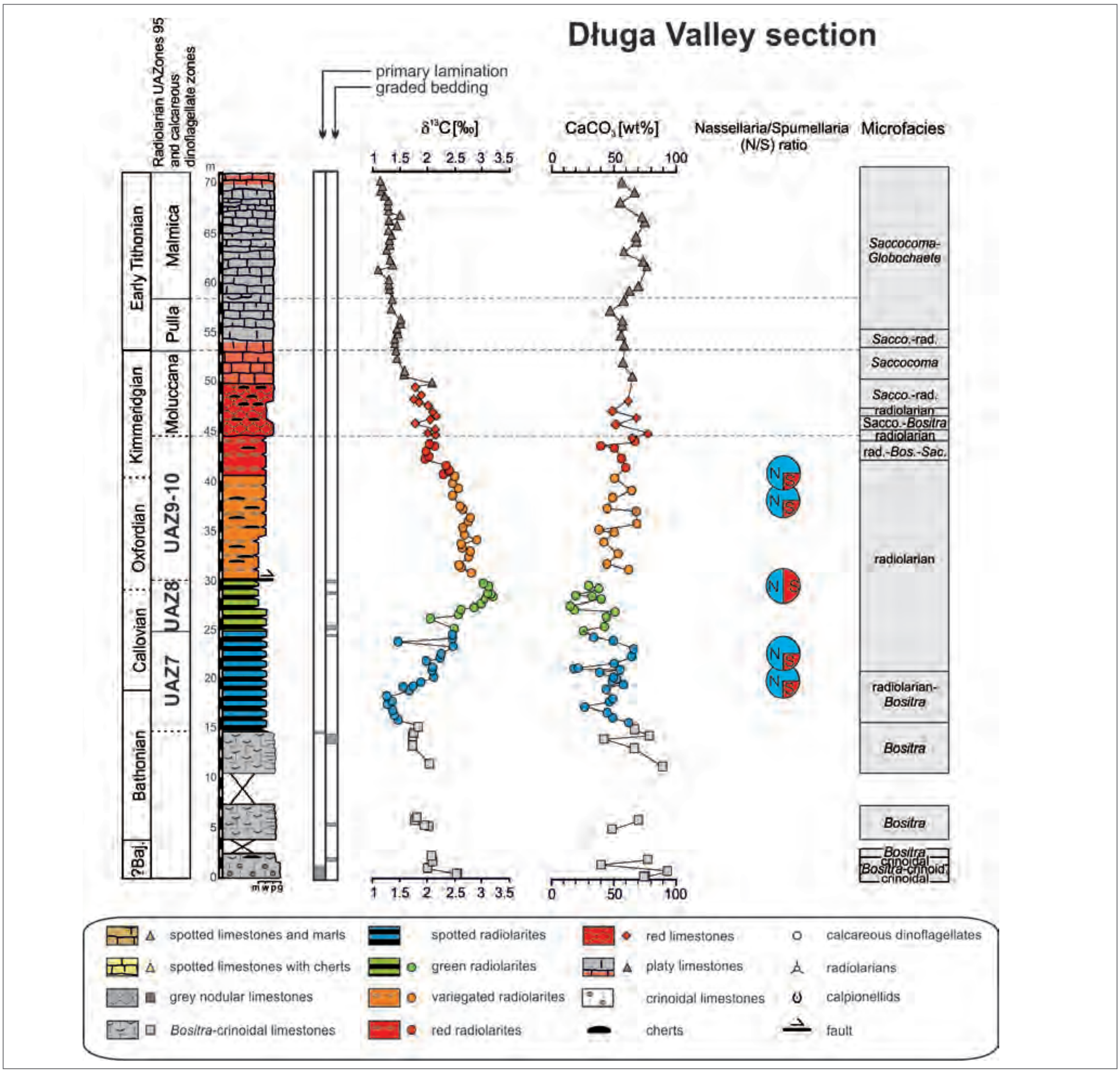

Fig. 18. Długa Valley section. Lithology, radiolarian and calcareous dinoflagellate biostratigraphy and results for carbon isotope measurements, $CaCO_3$ content and microfacies analysis (after Jach *et al.*, 2014; modified).

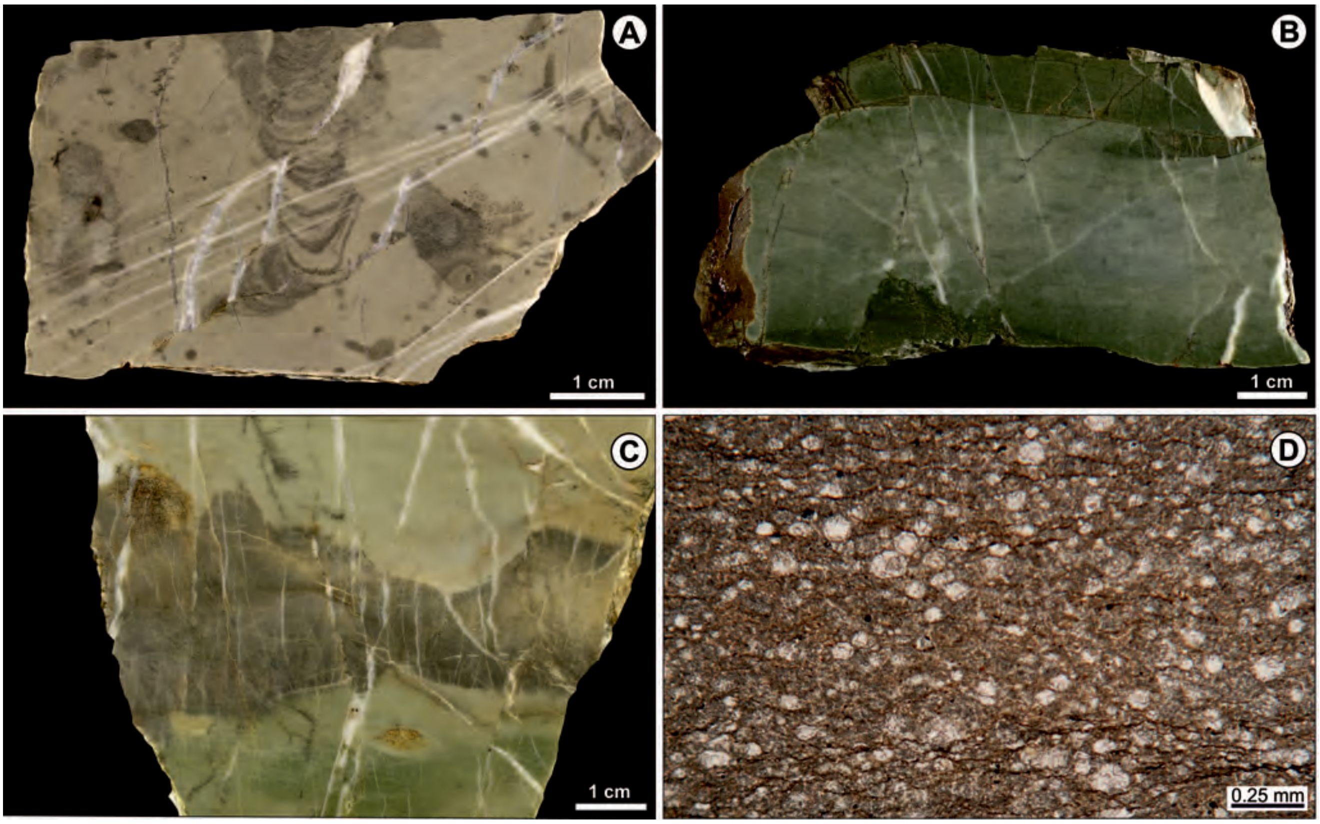

Fig. 19. Radiolarites. **A)** Bioturbated grey spotted radiolarites, polished slab; **B)** Green radiolarites. polished slab; **C)** Variagated radiolarites. polished slab; **D)** Green radiolarites, radiolarian wackestone-packstone. Thin section, plane polarised light.

in spotted radiolarites is Late Bathonian in age, whereas the pronounced positive $\delta^{13}C$ excursion detected in green radiolarites is referred to Late Callovian. It is worth mentioning that this excursion coincides with a distinct increase in radiolarian abundance and an extreme carbonate production crisis (Bartolini *et al*., 1999; Morettini *et al*., 2002). The variegated and red radiolarites and the overlying limestones display a pronounced decreasing $\delta^{13}C$ trend in the Oxfordian–Early Tithonian (Jach *et al*., 2014).

The oldest radiolarites are grey and green, highly siliceous, thin- to medium-bedded, alternated with 0.2–2 cm thick siliceous shales (Fig. 19A, B). These chert-shale couplets are the most characteristic feature of the grey and green radiolarites. Average $CaCO_3$ contents in grey radiolarites and in green radiolarites are 36 wt% and 25 wt% , respectively (Fig. 18). The grey and green radiolarites show transition from *Bositra*-radiolarian to radiolarian microfacies, with calcified and extensively dissolved radiolarian tests (Fig. 19D). Grey spotted radiolarites are intensively bioturbated whereas green radiolarites locally show subtle microscopic lamination. The primary lamination can be referred to incidental rapid sedimentation marked by a subtle increase in grain size, or a short episode of anoxia.

The variegated and red radiolarites are calcareous, distinctly bedded, with bed thicknesses of about 10–15 cm (Fig. 19C). They have a higher content of $CaCO_3$, 50 wt% on average (Fig. 18). The common occurrence of massive chert nodules of various colours, mainly reddish or greyish, is typical of this facies. The very rare occurrence of thin shale intercalations is characteristic of the variegated radiolarites. The red radiolarites are calcareous, red and greyish red, and thin- to medium-bedded, with beds from 5 to 30 cm. The variegated and red radiolarite facies show upward transition from radiolarian to the *Bositra* and *Saccocoma* microfacies. They contain calcified or partially silicified radiolarians, sponge spicules, crinoids, planktonic foraminifera *Globuligerina* and cysts of calcareous dinoflagellates.

Almost all radiolarite and the associated deposits are bioturbated (Jach *et al*., 2012). They contain the trace fossils *Chondrites*, *Planolites*, *Zoophycos*, *Teichichnus*, *Phycodes, Trichichnus, Phycosiphon* and *Thalassinoides* (Uchman and Jach, 2014). They belong to the *Zoophycos* ichnofacies, which characterizes deeper shelf – basin plain settings with pelagic and hemipelagic sedimentation. Generally, the abundance and diversity of trace fossils decrease up the succession. In the Upper Bathonian–Lower Callovian, the grey spotted radiolarites display typical spotty structures, that is relatively dense and diverse cross sections of trace fossils *Chondrites*, *Planolites*, *Thalassinoides*, and *Zoophycos* are common. Up the succession, in the green, variegated and red facies, the spots decrease in density, contrast and diversity, up to disappearance. The changes are not ideally linear, but fluctuations in these features do not discard the general trend. They are not related to grain size or lithology.

The changes of ichnological features in the studied interval are caused mainly by decrease in food content in the sediments (Jach *et al.*, 2012; Uchman and Jach, 2014). With deepening of the basin and decreasing sedimentation rate associated with generally advancing flooding of epicontinental areas, less and less food was supplied to the basin from shallower areas and less and less of it was buried in sediment. In more eutrophic conditions (lower part of the interval), organisms penetrated deeply in the sediment, where distinct trace fossils were produced. A thicker layer of nutritional sediment gave an ecospace for a higher diversity of burrowing organisms. In more oligotrophic conditions (higher part of the succession), the organic matter was concentrated in the soupy sediment near the sediment-water interface, where preservation of distinct trace fossils was limited or impossible.

In the Długa Valley section, the Nassellaria/Spumellaria (N/S) ratio among radiolarians fluctuates, most probably in accordance with bioturbation intensity (Jach *et al.*, 2015). It seems that the greater abundance of trace fossils coincides with the Nassellaria-dominated assemblage. It is thus possible that the observed pattern results from ecological requirements of these two groups of radiolarians. Spumellaria, which tend to be predominantly symbiont bearing, develop in more oligotrophic near-surface waters, whereas Nassellaria are non-symbiotic forms, which live in more eutrophic, deeper water column. Such a correlation may be explained by fluctuating input of nutrients from the neighboring lands, caused most probably by climate changes, for instance by enhanced continental weathering and runoff (cf. Baumgartner, 2013). An increased input of nutrients during humid climate leads to sea-water eutrophication, whereas decreased input leads to its oligotrophication.

The Late Bathonian–Kimmeridgian radiolarites are an evidence of deepening, with sedimentation taking place between the ACD and CCD or below the CCD. The middle Oxfordian–upper Kimmeridgian, variegated and red radiolarian-bearing facies, and finally red nodular and platy micritic limestones, record the recovery of carbonate sedimentation. It is evidenced by the middle Callovian – lower Oxfordian intervals characterised by drastically reduced $CaCO_3$ content, whereas an increase of carbonate content occurs in the middle Oxfordian–upper Kimmeridgian part of the section.

A6.8 Kryta Valley – Tithonian – Lower Valanginian limestones and marlstones: biostratigraphy, magnetostratigraphy, carbon isotope stratigraphy and paleoenvironmental changes

(49°15′41″ N, 19°48′ 20″ E)

Leaders: Jacek Grabowski, Andrzej Pszczółkowski

The Uppermost Jurassic (Tithonian) and Lower Cretaceous limestones and marlstones of the Krížna Nappe crop out in the Kryta Valley and in neighbouring ridges between the Kryta and Długa valleys. Lithostratigraphically, this interval is divided into three units (Fig. 20). Shaly marls and olive grey, thinly-bedded micritic limestones occur in the upper part of the Jasenina Formation (Upper Tithonian to lowermost Berriasian). The light grey, calpionellid-bearing limestones of the Osnica Formation (Berriasian) overlie the Jasenina Formation deposits. The limestones are 25–37 m thick in various sections (Pszczółkowski, 1996) and pass gradually into the overlying strata of the Kościeliska Marl Formation (Lefeld *et al.*, 1985). This formation, of Late Berriasian-Aptian age, comprises marls and limestones about 260 m thick (Lefeld *et al.*, 1985; Pszczółkowski, 2003a; Kędzierski and Uchman, 1997).

Magneto- and biostratigraphic data were obtained from the Tithonian and Berriasian strata (Fig. 20; Grabowski, 2005; Grabowski and Pszczółkowski, 2006a), which enabled correlation of these sections with GPTS (Geomagnetic Polarity Time Scale), estimation of sedimentation rates and of palaeolatitudinal position of the area in the Berriasian (28°N, ± 4.5°). Detailed magnetic susceptibility (MS) and field gamma ray spectrometry (GRS), supported by geochemical analyses were used for reconstruction of palaeoenvironmental changes (Grabowski *et al.*, 2013, see Fig. 21).

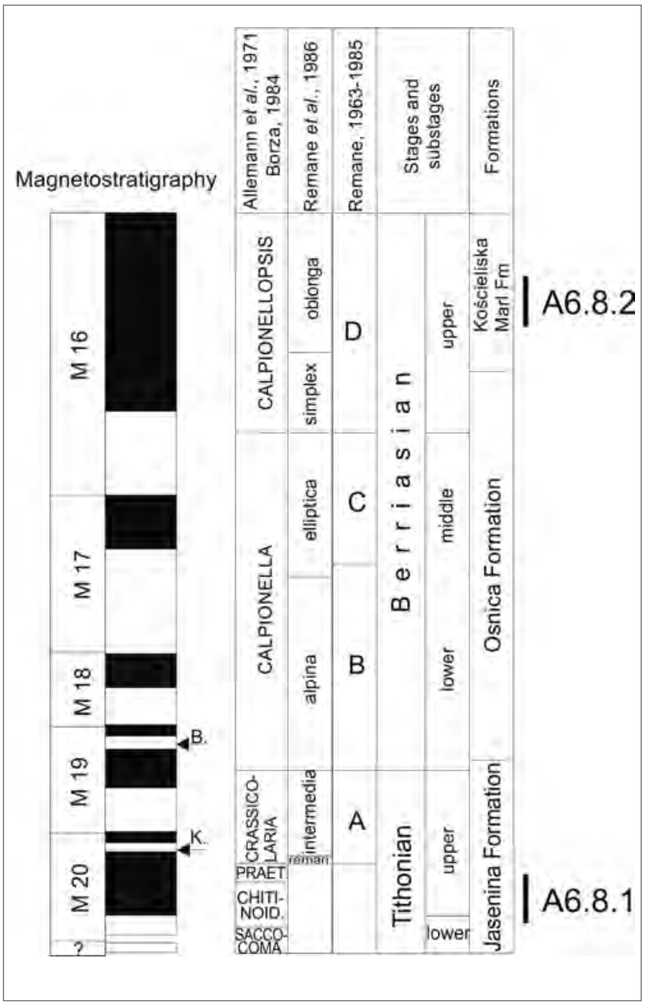

Stop A6.8.1

Platy, green to grey, micritic limestones of the Jasenina Formation, dipping to the north, are exposed along the road (Fig. 22).

The thickness of the section amounts to 6 m. In the lower part limestones prevail, while the upper part is dominated by marlstones. Limestones contain numerous remnants of crinoids (Saccocomidae) and chitinoidellids. The latter microfossils indicate the Boneti Subzone of the Chitinoidella Zone. The uppermost part of the section belongs to the Praetintinopsella Zone (Upper Tithonian). Bed K-1 is reversely magnetized while the bulk of the section, between beds K-2 and K-17, belongs to a normal magnetozone (interpreted as M20n). The sedimentation rate for the Boneti Subzone is estimated as 5.8–7 m/My (minimum value, without influence of compaction). In the neighbouring Pośrednie III section, the sedimentation rate calculated for entire magnetozone M20n is

Fig. 20. Litho-, bio- and magnetostratigraphic scheme of the Upper Tithonian and Berriasian of the Lower Sub-Tatric (Krížna Nappe) succession in the Western Tatra Mts (not to scale), after Grabowski and Pszczółkowski 2006b. B – Brodno magnetosubzone (M19n1r); K - Kysuca magnetosubzone (M20n1r).

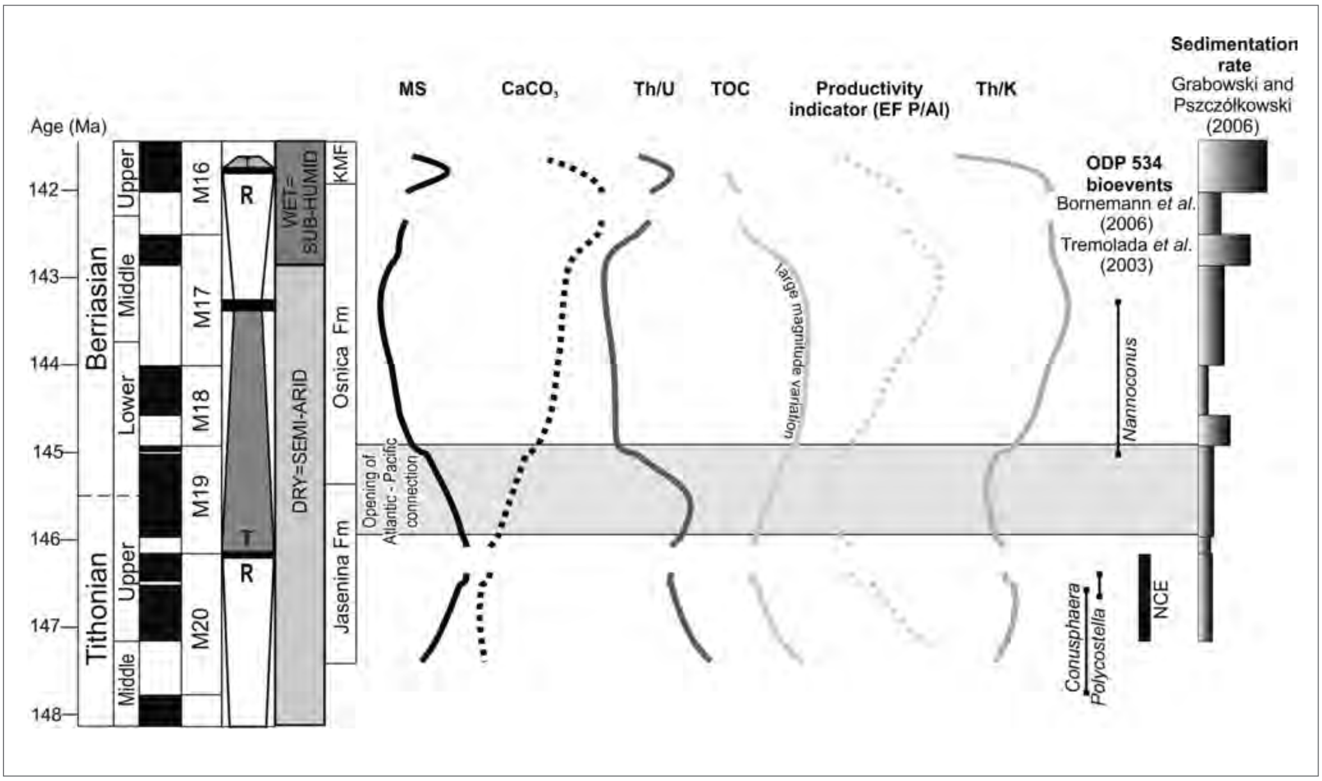

Fig. 21. Summary of magnetic and geochemical palaeoenvironmental trends at the Jurassic/Cretaceous boundary interval in the Pośrednie III section, Western Tatra Mts (after Grabowski *et al.*, 2013, slightly modified). The transgressive/regressive (T-R) cycles in the Tethyan domain, after Hardenbol *et al.*, (1998); paleoclimatic trends in ODP 534 after Bornemann *et al.*, 2003 and Tremolada *et al.*, 2006; general paleohumidity trends after Abbink *et al.* (2001) and Schnyder *et al.* (2006). NCE – Nannofossil calcification event.

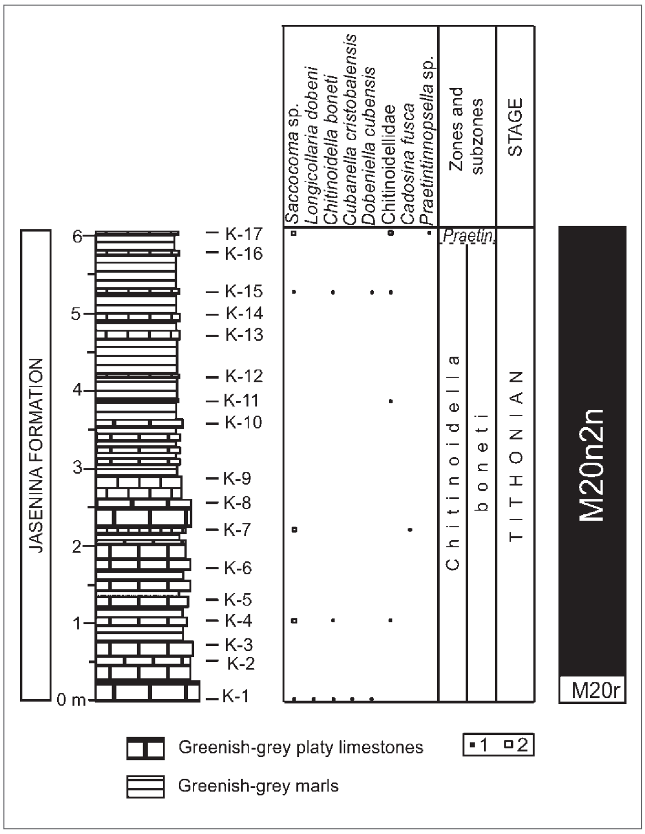

Fig. 22. Kryta section of the Jasenina Formation (Kryta Valley). *Praetin.* – *Praetintinopsella*. After Grabowski and Pszczółkowski (2006a). Taxon frequency: 1 – rare; 2 – common.

even lower (4.83 m/My). The distinct rhythm manifested by marlstone/limestone couplets might be related to Milankovich cyclicity (precession cycles of ca. 20 ky). The interval observed represents a local maximum of clastic input towards the basin. It is characterized by relatively high MS, high contents of Th, K and other lithogenic elements (Al, Ti, Zr, Rb etc.). High values of the Th/U ratio, abundant hematite horizons and rather low values of EF (enrichments factors) Cd/Al, Ni/Al and Mo/Al are evidences of well oxidized bottom waters. Decreasing values of productivity indicators (EF P/Al and Mn/Al) negatively correlate with terrigenous input (Fig. 21). The interval might be correlated to middle to a late Tithonian cooling phase evidenced by changes in calcareous phytoplankton (Tremolada *et al.*, 2006).

Stop A6.8.2.

We observe micritic limestones with *Calpionellopsis oblonga* (Cadisch) indicating the Oblonga Subzone (*sensu* Remane *et al.*, 1986) of the Upper Berriasian (Figs 20, 23).

They belong to the lowermost part of the Kościeliska Marl Formation. The gradual passage between the limestone-dominated Osnica and the marl-dominated

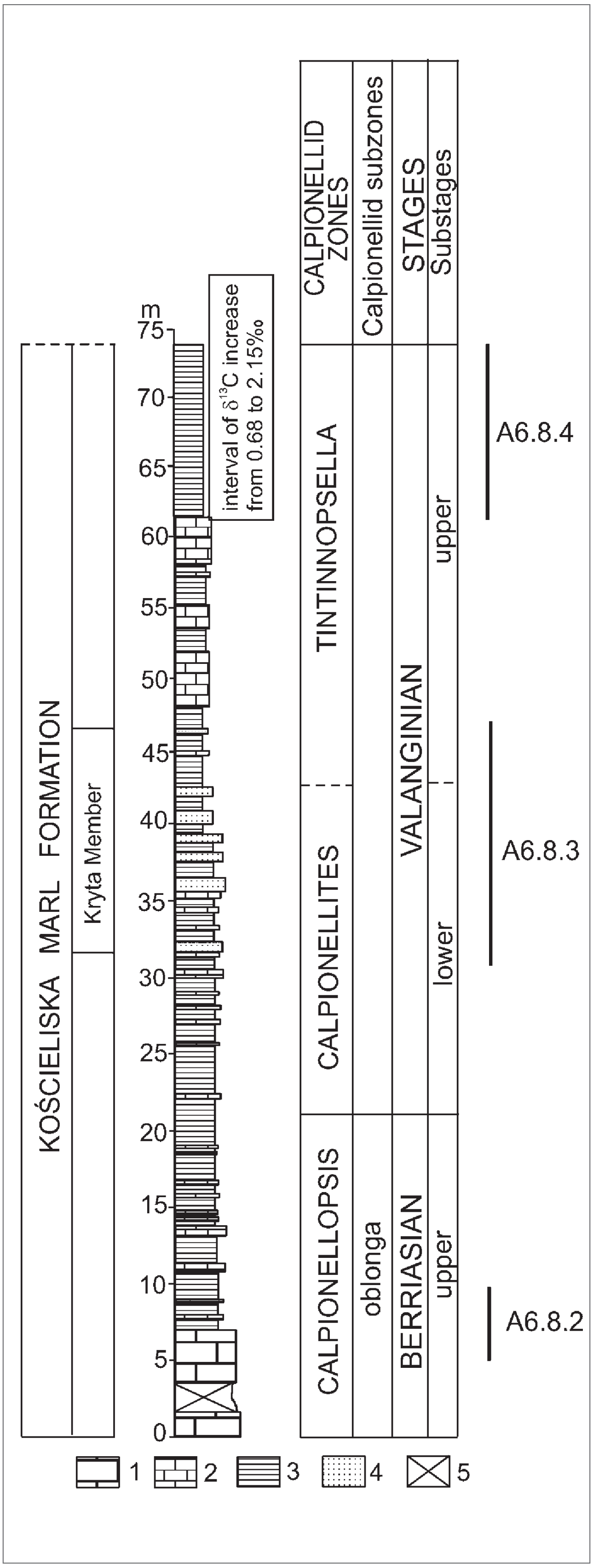

Fig. 23. Generalized stratigraphical section of the Kościeliska Marl Formation (lowermost part) in the Kryta Valley. After Grabowski and Pszczółkowski, 2006b, slightly modified. Calpionellid zones after Allemann *et al.* (1971) and Remane *et al.* (1986). Position of $\delta^{13}C$ event after Pszczółkowski (2003b) and Pszczółkowski *et al.* (2010). 1 – pelagic limestones; 2 –micritic and marly limestones; 3 –marlstones; 4 – sandstones (turbidites); 5 – covered intervals.

Kościeliska formations is covered in the Kryta creek. In the section localized in the adjacent Pośrednie ridge and section Rówienka (in the Lejowa Valley), the boundary between the two formations is situated in the lower part of the M16n magnetozone (close to the boundary between the Simplex and Oblonga subzones; see Fig. 20). The sedimentation rate of the Osnica Formation brackets between 10 and 17 m/My, and increases upward to 18–23 m/My in the lower part of the Kościeliska Marl Formation. In this section, the boundary between the Calpionellopsis and Calpionellites zones (i.e., the Berriasian-Valanginian boundary) falls in the magnetozone M14r. The Osnica Formation represents interval of carbonate sedimentation with limited influx of detrital material (Grabowski *et al.*, 2013). It is characterized by relatively low MS values, low contents of Th and K and other lithogenic elements (Fig. 21). The interval bears evidence of slightly oxygen-depleted conditions (low Th/U ratio, elevated values of EF Cd/Al, Ni/Al and Mo/Al) and enhanced productivity (higher EF P/Al and Mn/Al). The phenomena seem to be coeval with the warming period documented in the DSDP 534A core in the central Atlantic between magnetozones M18r and M17n (Tremolada *et al.*, 2006).

The transition between the Osnica and Kościeliska formations is manifested again by an increase in sedimentation rate, higher terrigenous influx, lower productivity and higher redox indices. The latter feature is independently supported by ichnofossil assemblages (Kędzierski and Uchman, 1997). The onset of terrigenous fraction delivery in the Late Berriasian might be regarded as a regional event within the Krížna (Fatric Domain) succession in the Slovak part of the Central Western Carpathians (e.g., Grabowski *et al.*, 2010). It can be followed as well, in similar stratigraphic position, in many sections of the Western Tethys: Northern Calcareous Alps, Western Balkan and Western Cuba (Grabowski and Sobień, 2015).

Stop A6.8.3

The Kryta Member of the Kościeliska Marl Formation is well exposed in the Kryta creek. This is the stratotype section of the member, containing marls interbedded with sandstones and marlstones, 15 m thick (Fig. 23).

The sandstones are mainly medium-grained lithic and arkosic arenites. However, hybridic arenites also occur (Świerczewska and Pszczółkowski, 1997). Magnetic separation revealed that Cr-spinels are an important component of the sandstones. The sandstones occur in similar stratigraphic position in the Oravice area, Slovakia, just 6–7 km west of our locality. After this locality, the Oravice event has been distinguished (Reháková, 2000; Pszczółkowski, 2003b). According to Reháková (2000), the Oravice event took place in the uppermost part of the Calpionellites Zone which was correlated with the ammonite Pertransiens Zone. Pszczółkowski (2003a) dated the sandstones as the upper part of the Calpionellites Zone

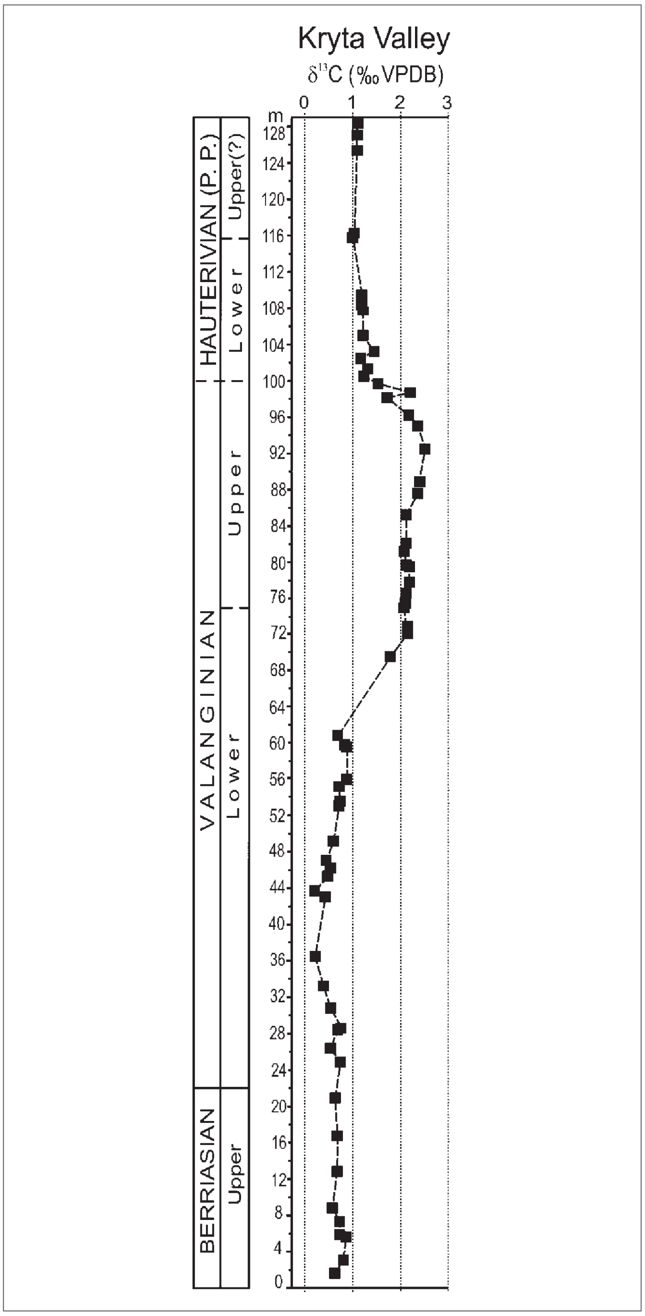

Fig. 24. δ13C isotope curve within the uppermost Berriasian – Hauterivian interval of the Kryta section (after Pszczółkowski *et al.*, 2010).

and the lowermost Tintinopsella Zone (higher part of the Lower Valanginian).

Rocks of the Meliata suture zone situated to the (present day) east and/or south east of the Zliechov Basin (Slovakia) were probably the source of the clastic sediment (comp. Vašiček *et al*., 1994). The sedimentation rate within the Calpionellites Zone is estimated at 28–20m/My.

Stop A6.8.4

Within the upper Valanginian marls of the Kościeliska Marl Formation, a complete record of the $\delta^{13}C$ event was documented (see Fig. 24; Pszczółkowski, 2001; Pszczółkowski *et al*., 2010; see also Kuhn *et al*., 2005). The $\delta^{13}C$ values increase quickly from the values below 1‰ up to 2.15‰ close to the lower-upper Valanginian boundary. The event occurs in the interval of marly sedimentation and is not marked by any black shale deposition. This is similar to other Tethyan sections where anoxic sediments do not occur within the anomaly interval (e.g., Westermann *et al*., 2010). The integrated palaeoenvironmental study of the Kryta section is in progress, comprising detailed magnetic susceptibility logging and geochemical investigations.

Acknowledgments

The field-trip guide is partly based on the guidebook prepared on the occasion of 7th International Congress on the Jurassic System, Jurassic of Poland and adjacent Slovakian Carpathians (Wierzbowski *et al*., 2006). This field trip is supported by the Tatra National Park (TPN, Zakopane).

References

Abbink, J., Targona, J., Brinkhuis, H. & Visscher, H., 2001. Late Jurassic to earliest Cretaceous palaeoclimatic evolution of the southern North Sea. *Global and Planetary Change*, 30: 231–256. The field trip is supported by the Tatra National Park (TPN, Zakopane).

Allemann, F., Catalano, R., Farès, F. &, Remane, J., 1971. Standard calpionellid zonation (Upper Tithonian–Valanginian) of the western Mediterranean Province. In: Farinacci, A. (ed.), *Proceedings II Planktonic Conference*, 1970, Roma, Tecnoscienza, 2: 1337–1340.

Bac-Moszaszwili, M., Burchart, J., Głazek, J., Iwanow, A., Jaroszewski, W., Kotański, Z., Lefeld, J., Mastella, L., Ozimkowski, W., Roniewicz, P., Skupiński, A. & Westwalewicz-Mogilska, E., 1979. *Geological Map of the Polish Tatra Mountains 1:30 000*. Wydawnictwa Geologiczne, Warszawa.

Bernoulli, D. & Jenkyns, H. C., 1974. Alpine, Mediterranean and Central Atlantic Mesozoic facies in relation to the early evolution of the Tethys. In: Dott, R. H. & Sharer, R. H. (eds), *Modern and Ancient Geosynclinal Sedimentation. Society of Economic Paleontologists and Mineralogists, Special Publication*, 19: 129–160.

Bartolini, A., Baumgartner, P. O. & Guex, J., 1999. Middle and Late Jurassic radiolarian palaeoecology versus carbon-isotope stratigraphy. *Palaeogeography, Palaeoclimatology, Palaeoecology*, 145: 43–60.

Baumgartner, P. O., 2013. Mesozoic radiolarites – Accumulation as a function of sea surface fertility on Tethyan margins and in ocean basins. *Sedimentology*, 60: 292–318.

Błaszyk, J. & Gaździcki, A., 1982. Lower Lias ostracodes of the Tatra Mts (West Carpathians). *Acta Palaeontologica Polonica*, 27: 129–136.

Bornemann, A., Aschwer, U. & Mutterlose, J., 2003. The impact of calcareous nannofossils on the pelagic carbonate accumulation across the Jurassic – Cretaceous boundary. *Palaeogeography, Palaeoclimatology, Palaeoecology,* 199: 187–228.

Csontos, L. & Vörös, A., 2004. Mesozoic plate tectonic reconstruction of the Carpathian region. *Palaeogeography, Palaeoclimatology, Palaeoecology*, 210: 1–56.

Dudek, T. & Jach, R., 2006. Minerały ilaste jako wskaźnik środowiska sedymentacji jurajskich utworów manganowych w Zachodnich Tatrach. In: *II Polska Konferencja Sedymentologiczna POKOS2*, Zwierzyniec, 20-23.06.2006 r., p. 115. [In Polish.]

Fijałkowska, A. & Uchman, A., 1993. Contribution to Triassic palynology in Polish part of the Tatra Mts. *Przegląd Geologiczny*, 41: 373–375. [In Polish, English summary.]

Gawlick, H.-J., Missoni, S., Schagintweit, F., Suzuki, H., Frisch, W., Krystyn, L., Blau, J. & Lein, R., 2009. Jurassic tectonostratigraphy of Austroalpine domain. *Journal of Alpine Geology*, 50: 1–152.

Gaździcki, A., 1974. Rhaetian microfacies, stratigraphy and facies development in the Tatra Mts. *Acta Palaeontologica Polonica*, 24: 17–96.

Gaździcki, A., 1975. Lower Liassic („Gresten Beds") microfacies and foraminifers from the Tatra Mts. *Acta Geologica Polonica*, 25: 385–398.

Gaździcki, A., 1977. Rhaetian-Lower Hettangian foraminifer zonation and the problem of Triassic-Jurassic boundary in the Tatra Mts, West Carpathians. *Actes du VIe Colloque Africain de Micropaléontologie. Annales des Mines et de la Géologie, Tunis*, 28: 89–101.

Gaździcki, A., 1978. Conodonts of the genus *Misikella* Kozur and Mock, 1974 from the Rhaetian of the Tatra Mts (West Carpathians). *Acta Palaeontologica Polonica*, 23: 341–350.

Gaździcki, A., 1983. Foraminifers and biostratigraphy of Upper Triassic and Lower Jurassic of the Slovakian and Polish Carpathians. *Palaeontologia Polonica*, 44: 109–169.

Gaździcki, A., 2003. Triassic/Jurassic Boundary of the Tatra Mountains in light of micropaleontological data. In: Michalík, J., (ed.), IGCP 458: Triassic/Jurassic Boundary Events. *Third Field Workshop, Stará Lesná, Slovakia, Tatra Mts, October 11–15th 2003.* Bratislava, 72 p.

Gaździcki, a., 2014. Skały klastyczne i węglanowe jury dolnej (formacja z Kopieńca). In: Jach, R., Rychliński, T. & Uchman, A. (eds), *Skały osadowe Tatr (Sedimentary Rocks of the Tatra Mountains).* Tatrzański Park Narodowy, pp. 154–159.

Gaździcki, A. & Iwanow, A., 1976. The diachronism of the Rhaetic and „Gresten Beds" in the Tatra Mts (West Carpathians). *Bulletin de l'Académie Polonaise des Sciences. Série des Sciences de la Terre*, 24: 117–122.

Gaździcki, A., Michalík, J., Plenderová, E. & Sýkora, M., 1979. An Upper Triassic-Lower Jurassic sequence in the Križna nappe (West Tatra mountains, West Carpathians, Czechoslovakia). *Západne Karpaty, Séria Geológia*, 5: 119–148.

Gaździcki, A., Waksmundzka, M. & Hołda-Michalska, A., 2006. Rhaetian/Hettangian palynomorphs of the Tatra Mountains (West Carpathians). *Volumina Jurassica*, 4: 280–281.

Gaździcki, A. & Wieczorek, J., 1984. Trasa B2. Dolina Lejowa. In: *Paleontologia Mezozoiku Tatr. Materiały VIII Konferencji Paleontologów, Zakopane, 8-10 czerwca 1984.* Wydawnictwo AGH, Kraków, pp. 50–52. [In Polish.]

Głuchowski, E., 1987. Jurassic and Early Cretaceous Articulate Crinoidea from the Pieniny Klippen Belt, and the Tatra Mts., Poland. *Studia Geologica Polonica*, 94: 1–102.

Goetel, W., 1917. Die rhätische Stufe und der unterste Lias der subtatrischen Zone in der Tatra. *Bulletin International de l'Académie des Sciences Mathématiques et Naturelles. Sciences Mathématiques", série A* [for 1916]: 1–232.

Grabowski, J., 2005. New Berriasian palaeopole from the Central West Carpathians (Tatra Mountains, southern Poland): does it look Apulian? *Geophysical Journal International,* 161: 65–80.

Grabowski, J. & Pszczółkowski, A., 2006a. Magneto- and biostratigraphy of the Tithonian – Berriasian pelagic sediments in the Tatra Mountains (central Western Carpathians, Poland): sedimentary and rock magnetic changes at the Jurassic/Cretaceous boundary. *Cretaceous Research*, 27: 398–417.

Grabowski, J. & Pszczółkowski, A., 2006b. Field trip B3. Inside Tethys. Jurassic of the Krížna unit in the Tatra Mts. Stop B3.9. Kryta Valley – sedimentation rate of the Tithonian – Lower Valanginian limestones and marlstones: biostratigraphic and magnetostratigraphic approach. In: Wierzbowski, A., Aubrecht, R., Golonka, J., Gutowski, J., Krobicki, M., Matyja. B., Pieńkowski, G. & Uchman, A. (ed.), *Jurassic of Poland and adjacent Slovakian Carpathians. Field trip guidebook of 7th International Congress on the Jurassic System. September 6–18, 2006, Kraków, Poland*. Polish Geological Institute, Warszawa, pp. 104–106.

Grabowski, J., Michalík, J., Pszczółkowski, A. & Lintnerová, O., 2010. Magneto- and isotope stratigraphy around the Jurassic/Cretaceous boundary in the Vysoka unit (Male Karpaty Mountains): correlations and tectonic implications. *Geologica Carpathica*, 61: 309–326

Grabowski, J., Schnyder, J., Sobień, K., Koptiková, L., Krzemiński, L., Pszczółkowski, A., Hejnar, J. & Schnabl, P., 2013. Magnetic susceptibility and spectra gamma logs in the Tithonian – Berriasian pelagic carbonates in the Tatra Mts (Western Carpathians, Poland): palaeoenvironmental changes at the Jurassic/Cretaceous boundary. *Cretaceous Research*, 43: 1–17.

Grabowski, J. & Sobień, K., 2015. Variation of clastic input in the Berriasian of the Lower Sub-Tatric (Križna) succession in the Tatra Mts (Central Western Carpathians, Poland) – data from magnetic susceptibility and inorganic geochemistry. *Annales Societatis Geologorum Poloniae* (in press).

Gradziński, M., Tyszka, J., Uchman, A. & Jach R., 2004. Large microbial–foraminiferal oncoids from condensed Lower–Middle Jurassic deposits: A case study from the Tatra Mountains, Poland. *Palaeogeography, Palaeoclimatology, Palaeoecology,* 213: 133–151.

Guzik, K., 1959. Notes on some stratigraphic problems of the Lias-Dogger rocks in the Lower Sub-Tatric Nappe of the Tatra Mountains. *Biuletyn Instytutu Geologicznego*, 149: 183–188. [In Polish, English summary.]

Guzik, K., Guzik, S. & Sokołowski, S., 1975. Mapa Geologiczna Tatr Polskich 1: 10 000. A2 – Hruby Regiel. Instytut Geologiczny. Warszawa.

Hardenbol, J., Thierry, J., Harley, M. B., Jacquin, Th., de Graciansky, P.-C. & Vail, P. R., 1998. Mesozoic and Cenozoic Sequence Chronostratigraphic Framework of European basins. Appendix. *SEPM Special Publication*, 160: 763–786.

Hołda, A., 2002. Mikroskamieniałości późnego triasu i wczesnej jury jednostki križniańskiej Tatr Polskich. In: *Przemiany środowiska przyrodniczego Tatr, Kraków – Zakopane 2002*, Instytut Botaniki PAN, Kraków. Nakładem Tatrzańskiego Parku Narodowego oraz Polskiego Towarzystwa Przyjaciół Nauk o Ziemi, Oddział Kraków, pp. 29–34. [In Polish.]

Iwańczuk, J., Iwanow, A. & Wierzbowski, A., 2013. Lower Jurassic to lower Middle Jurassic succession at Kopy Sołtysie and Płaczliwa Skała in the eastern Tatra Mts (Western Carpathians) of Poland and Slovakia: stratigraphy, facies and ammonites. *Volumina Jurassica*, 11: 19–58.

Jach, R., 2002a. Lower Jurassic spiculite series from the Križna Unit in the Western Tatra Mts, Western Carpathians, Poland. *Annales Societatis Geologorum Poloniae,* 72, 131–144.

Jach, R., 2002b. Traces of historical exploitation of manganiferous ores in the Western Tatra Mountains. *Przegląd Geologiczny*, 50: 1159–1164. [In Polish, English summary.]

Jach, R., 2005. Storm-dominated deposition of the Lower Jurassic crinoidal limestone in the Krížna Unit, Western Tatra Mountains, Poland. *Facies*, 50: 561–572.

Jach, R., 2007. *Bositra* limestones – a step towards radiolarites: case study from the Tatra Mountains. *Annales Societatis Geologorum Poloniae*, 77: 161–170.

Jach, R., Djerić, N. & Goričan, Š., 2015. Nassellaria/Spumellaria ratio vs. palaeoproductivity proxies in the Middle–Upper Jurassic radiolarian-bearing deposits of the western Tethys Fatricum Domain (Poland and Slovakia). *International conference on Fossil and Recent Radiolarians – INTERRAD 14, 22-26. 03. 2015, Antalya, Turkey, Radiolaria Newsletter*, 35: 174–175.

Jach, R., Djerić, N., Goričan, Š. & Reháková, D., 2014. Integrated stratigraphy of the Middle Upper Jurassic of the Krížna Nappe, Tatra Mountains. Annales Societatis Geologorum Poloniae, 84: 1–33. Jach, R. & Dudek, T., 2005. Origin of a Toarcian manganese carbonate/silicate deposit from the Krížna unit, Tatra Mountains, Poland. *Chemical Geology*, 224: 136–152.

Jach, R., Reháková, D. & Uchman, A., 2012. Biostratigraphy and palaeoenvironment of the Kimmeridgian–Lower Tithonian pelagic sediments of the Krížna Nappe, Lejowa Valley, Tatra Mts., southern Poland. *Geological Quarterly*, 56: 773–788.

Jenkyns, H., 1971. The genesis of condensed sequences in the Tethyan Jurassic. *Lethaia*, 4: 327–352.

Jenkyns, H. C., 2003. Evidence for rapid climate change in the Mesozoic-Palaeogene greenhouse world. *Philosophical Transactions of the Royal Society, Series A*, 361: 1885–1916.

Kędzierski, M. & Uchman, A., 1997. Age and palaeoenvironment of the Kościeliska Marl Formation (Lower Cretaceous) in the Tatra Mountains, Poland: preliminary results. *Annales Societatis Geologorum Poloniae.*, 67: 237–247.

Korczyńska-Oszacka, B., 1978. Minerały manganu wapieni jurajskich Doliny Chochołowskiej (Tatry, Polska). *Prace Mineralogiczne*, 58: 7–62. [In Polish, English summary.]

Korczyńska-Oszacka, B., 1979. Minerały węglanowe skał manganowych Doliny Chochołowskiej (Tatry). *Prace Mineralogiczne*, 54: 67–82. [In Polish, English summary.]

Kotański, Z., 1965. La coupe géologique du versant est de la vallée Kościeliska dans les Tatras Occidentales dans son development historique. *Acta Geologica Polonica*, 15, 3: 239–256. [In Polish, French summary.]

Kotański, Z., 1971. Przewodnik geologiczny po Tatrach. Wydawnictwa Geologiczne, Warszawa, pp. 280. [In Polish.]

Krajewski, K. P., Lefeld, J. & Łącka, B., 2001. Early diagenetic processes in the formation of carbonate-hosted Mn ore deposit (Lower Jurassic, Tatra Mountains) as indicated from its carbon isotopic record. *Bulletin of the Polish Academy of Sciences. Earth Sciences*, 49: 13–29.

Krajewski, R. & Myszka, J., 1958. Manganiferous limestones in the Tatra between the Chochołowska and Lejowa Valleys. *Biuletyn Instytutu Geologicznego*, 126: 209–300. [In Polish, English summary.]

Krobicki, M. & Uchman, A., 1993. Uwagi o paleoekologii i sedymentologii wapieni z formacji kopienieckiej (fm) (retyk górny – synemur dolny) w Tatrach. *Sprawozdania z Posiedzeń Komisji Naukowych PAN Kraków*, 35: 285–286. [In Polish.]

Kuhn, O., Weissert, H., Föllmi, K. B. & Hennig, S., 2005. Altered carbon cycling and trace metal enrichment during the Late Valanginian and Early Hauterivian. *Eclogae Geologicae Helveticae*, 98: 333–344.

Lefeld, J., 1974. Middle-Upper Jurassic and Lower Cretaceous biostratigraphy and sedimentology of the Sub-Tatric Succession in the Tatra Mts. (Western Carpathians). *Acta Geologica Polonica*, 24: 277–364.

Lefeld, J., Gaździcki, A., Iwanow, A., Krajewski, K. & Wójcik, J., 1985. Jurassic and Cretaceous litho- stratigraphic units of the Tatra Mountains. *Studia Geologica Polonica*, 84: 1–93.

Mattioli, E., 1997. Nannoplankton productivity and diagenesis in the rhytmically bedded Toarcian-Aalenian Fiuminata section (Umbria-Marche Apennine, central Italy). *Palaeogeography, Palaeoclimatology, Palaeoecology*, 130: 113–133.

Michalík, J., 2007. Sedimentary rock record and microfacies indicators of the latest Triassic to mid-Cretaceous tensional development of the Zliechov Basin (Central Western Carpathians). *Geologica Carpathica*, 58: 443–453.

Morettini, E., Santantonio, M., Bartolini, A., Cecca, F., Baumgartner, P. O. & Hunziker, J. C., 2002. Carbon isotope stratigraphy and carbonate production during the Early-Middle Jurassic: example from the Umbria-Marche-Sabina Apennines (central Italy). *Palaeogeography, Palaeoclimatology, Palaeoecology,* 184: 251–273.

Myczyński, R. & Jach, R., 2009. Cephalopod fauna and stratigraphy of the Adnet type red deposits of the Krížna unit in the Western Tatra Mountains, Poland. *Annales Societatis Geologorum Poloniae*, 79: 27–39.

Myczyński, R. & Lefeld, J., 2003. Toarcian ammonites (Adneth facies) from the Subtatric Succession of the Tatra Mts (Western Carpathians). *Studia Geologica Polonica*, 121: 51–79.

Ožvoldová, L., 1997. The radiolarian research into Jurassic radiolarite sequences in the Western Carpathians. *Sborník védeckšch praci Vysoké školy báňské – Technické university v Ostravì*, 18–31.

Plašienka, D., 2012. Jurassic syn-rift and Cretaceous syn-orogenic, coarse-grained deposits related to opening and closure of the Vahic (South Penninic) Ocean in the Western Carpathians – an overview. *Geological Quarterly*, 56: 601–628.

Polák, M., Ondrejíčková, A. & Wieczorek, J., 1998. Lithostratigraphy of the Ždiar Formation of the Krížna nappe. *Slovak Geological Magazine*, 4: 35–52.

Pszczółkowski, A., 1996. Calpionellid stratigraphy of the Tithonian – Berriasian pelagic limestones in the Tatra Mts (Western Carpathians). *Studia Geologica Polonica*, 109: 103–130.

Pszczółkowski, A,. 2001. Stratygrafia kalpionellidowa i podział litostratygraficzny dolnej części formacji margli z Kościeliskiej w Tatrach Zachodnich. In: Bąk, K. (ed.), *Trzecie Ogólnopolskie Warsztaty Mikropaleontologiczne (MIKRO-2001), Zakopane 31.05-02.06.2001.* Akademia Pedagogiczna w Krakowie, Kraków, pp. 54–57. [In Polish.]

Pszczółkowski, A., 2003a. Kościeliska Marl Formation (Lower Cretaceous) in the Polish Western Tatra Mountains: lithostratigraphy and microfossil zones. *Studia Geologica Polonica*, 121: 7–50.

Pszczółkowski, A., 2003b. Tithonian – Hauterivian events from the lower Subtatric succession of the Tatra Mts (Western Carpathians) in the framework of calpionellid stratigraphy (southern Poland). *Przegląd Geologiczny*, 51: 987–994. [In Polish, English summary.]

Pszczółkowski, A., Grabowski, J., Michalík, J. & Sobień, K., 2010. Latest Berriasian – Hauterivian carbon isotope stratigraphy and magnetic susceptibility: new data from three West Carpathian sections of Poland and Slovakia. In: Granier, B. (ed.), STRATI 2010 *Abstracts. 4th French Congress on Stratigraphy*, Paris, pp. 194–195.

Reháková, D., 2000. Calcareous dinoflagellate and calpionellid bioevents versus sea-level fluctuations recorded in the West Carpathian (Late Jurassic/Early Cretaceous) pelagic environments. *Geologica Carpathica*, 51: 229–243.

Remane, J., Borza, K., Nagy, I., Bakalova-Ivanova, D., Knauer, J., Pop, G. & Tardi-Filacz, E., 1986. Agreement on the subdivision of the standard calpionellid zones defined at the IInd Planktonic Conference, Roma 1970. *Acta Geolog-*

ica Hungarica, 29: 5–14.

Santantonio, M., 1993. Facies associations and evolution of pelagic carbonate platform/basin systems: examples from the Italian Jurassic. *Sedimentology*, 40: 1039–1067.

Schmid, S. M., Bernoulli, D., Fügenschuh, B., Matenco, L., Scheffer, S., Schuster, R., Tischler, M. & Ustaszewski, K., 2008. The Alpine-Carpathian-Dinaridic orogenic system: correlation and evolution of tectonic units. *Swiss Journal of Geosciences*, 101: 139–183.

Schnyder, J., Ruffell, A., Deconinck, J.-F. & Baudin, F., 2006. Conjunctive use of spectral gamma-ray logs and clay mineralogy in defining late Jurassic–early Cretaceous palaeoclimate change (Dorset, U.K.). *Palaeogeography, Palaeoclimatology, Palaeoecology*, 229: 303–320.

Świerczewska, A. & Pszczółkowski, A., 1997. Skład i pochodzenie materiału detrytycznego piaskowców ogniwa z Krytej (Kreda dolna, Tatry). In: Wojewoda, J. (ed.), *Obszary Źródłowe: Zapis w Osadach*, *VI Krajowe Spotkanie Sedymentologów, Lewin Kłodzki, 26-28 września 1997 r. Materiały Konferencyjne*. Wrocław, Wind, pp. 55–56. [In Polish.]

Thierry, J. & Barrier, E., 2000. Middle Callovian. In: Dercourt, J., Gaetani, M., Vrielynck, B., Barrier, E., Biju-Duval, B., Brunet, M. F., Cadet, J. P., Crasquin, S. & Sandulescu, M. (eds), Atlas Peri-Tethys, Paleogeographical Maps. CCGMCGMW, Paris, Map 9.

Tremolada, F., Bornemann, A., Bralower, T. J., Koeberl, C. & van de Schootbrugge, B., 2006. Paleocenographic changes across the Jurassic/Cretaceous boundary: the phytoplankton response. *Earth and Planetary Science Letters*, 241: 361–371.

Tyszka, J., Jach, R. & Bubik, M., 2010. A new vent–related foraminifer from the lower Toarcian black claystone of the Tatra Mountains, Poland. *Acta Palaeontologica Polonica,* 55: 333–342.

Uchman, A., 1991. *Isopodichnus* and other trace fossils from marine Kopieniec Formation (Rhaetian-Sinemurian) in the Tatra Mts., Poland. *Geologica Carpathica*, 42: 117–121.

Uchman, A. & Jach, R., 2014. Ichnological record of food content change in Middle–Upper Jurassic pelagic sediments of the Fatricum domain in the Tatra Mountains, southern Poland. In: Beqiraj, A., Ionescu, C., Christofides, G., Uta, A., Beqiraj Goga, E. & Marku, S. (eds), *Proceedings*, *XX Congress of the Carpathian-Balkan Association, September 24–26, 2014, Tirana, Albania. Buletini i Shencave Gjeologjike, Special Issue*, 2: 100.

Uchman, A. & Myczyński, R., 2006. Stop B3.14 – Lejowa Valley: eastern of the Polana Huty Lejowe Alp – Upper Sinemurian-Lower Pliensbachian Spotted Limestones. In: Wierzbowski, A., Aubrecht, R., Golonka, J., Gutowski, J., Krobicki, M., Matyja., Pieńkowski, G. & Uchman, A. (eds), *Jurassic of Poland and adjacent Slovakian Carpathians. Field trip guidebook of 7th International Congress on the Jurassic System. September 6–18, 2006*, *Kraków, Poland*. Polish Geological Institute, Warszawa, pp. 114–116.

Uhlig, V., 1897. Die Geologie des Tatragebirges. I: Einleitung und stratigraphischer Teil. *Denkschrifte der Akademie derf Wissenschaften in Wien, Mathematisch-Naturwissenschaftliche Klasse*, 64: 643–684.

Vašíček, Z., Michalík, J. & Reháková, D., 1994. Early Cretaceous stratigraphy, paleogeography and life in Western Carpathians. *Beringeria*, 10: 3-168.

Westermann, S., Föllmi, K. B., Adatte, T., Matera, V., Schnyder, J., Fleitmann, D., Fiet, N., Ploch, I. & Duchamp-Alphonse, S., 2010. The Valanginian $\delta^{13}C$ excursion may not be an expression of a global anoxic event. *Earth and Planetary Science Letters*, 290: 118–131.

Wieczorek, J., 1984. Skamieniałości śladowe z wapieni plamistych jury Tatr. In: *Materiały VIII Konferencji Paleontologów, Zakopane, 8–10 czerwca 1984*, Wydawnictwo AGH, Kraków, pp. 15–16.

Wieczorek, J., 1990. Main phases of the geological evolution of the western Tethys - an outline. *Kwartalnik Geologiczny*, 33: 401–412.

Wieczorek, J., 1995. Trace fossils from Fleckenmergel facies (Jurassic) of the Tatra Mts. *Geobios. Mémoir Spécial*, 18: 425–431.

Wieczorek, J., 2001. Condensed horizons as turning events in passive margin evolution: the Tatra Mts. examples. *Zentralblatt für Geologie und Paläontologie*, Teil 1, 1/2: 199–209.

Wierzbowski, A., Aubrecht, R., Golonka, J., Gutowski, J., Krobicki, M., Matyja. B, Pieńkowski, G. & Uchman, A., 2006. *Jurassic of Poland and adjacent Slovakian Carpathians. Field trip guidebook of 7th International Congress on the Jurassic System*. *September 6–18, 2006*, *Kraków, Poland*. Polish Geological Institute, Warszawa, 235 p.

Geology and wines of the Kraków area – regional rebirth of vineyards as a result of climate change

Joachim Szulc[1]

[1]Institute of Geological Sciences, Jagiellonian University, Kraków, Poland (joachim.szulc@uj.edu.pl)

Route (Fig. 1): From Kraków we drive NW by road 94 to Jerzmanowice, then we turm right onto a local road to Ojców. From Ojców north along the Prądnik Valley to **Hercules' Club (stop A7.1)** near Royal Castle at Pieskowa Skała, and back along the valley to **Maszyce Cave (stop A7.2)**. Then to **Krokoszówka Górska Vineyard (stop A7.3)** at Smardzowice (the part of the road south from Ojców is closed for public traffic; we will drive with a permission). After wine testing and lunch in the vineyard we follow road 794 south to a roadside cliff at **Januszowice (stop A7. 4)**. Then west by a local road through Giebułtów to Modlnica and then south by road 94 to motorway 7 leaving it at Węzeł Mirowski following signs "Kraków – centrum". At the end of the slip road we turn right to **Piekary (stop A7.4)**. From Piekary by Mirowska Street to **Srebrna Góra Vineyard in Bielany (stop A7.5)**. After wine testing we return to Kraków centre.

Fig. 1. Route map of field trip A7.

Introduction to the trip

Joachim Szulc

Geology of the Kraków area

The Kraków region is situated within the boundary zone between two collided microplates: the Małopolska Terrain (called also Małopolska Massif) and the Brunovistulian Terrain (called also Moravo-Silesian Block). The first one docked from the west to the major Baltic continental land mass (Fig. 2) in middle Cambrian times. In turn, the Brunovistulian microplate accreted to Małopolska Massif in early Devonian (Nawrocki & Poprawa, 2006). The resulted, SE-NW trending, collision line makes one of the most important master fault in Central Europe, stretching from Kraków to Hamburg in Germany (Fig. 3).

Szulc, J., 2015. Geology and wines of the Kraków area – regional rebirth of vineyards as a result of climate change. In: Haczewski, G. (ed.), *Guidebook for field trips accompanying 31st IAS Meeting of Sedimentology held in Kraków on 22nd–25th of June 2015*. Polish Geological Society, Kraków, pp. 103–114.
Guidebook is available online at www.ing.uj.edu.pl/ims2015
Polskie Towarzystwo Geologiczne 2015, ISBN 978-83-942304-0-1

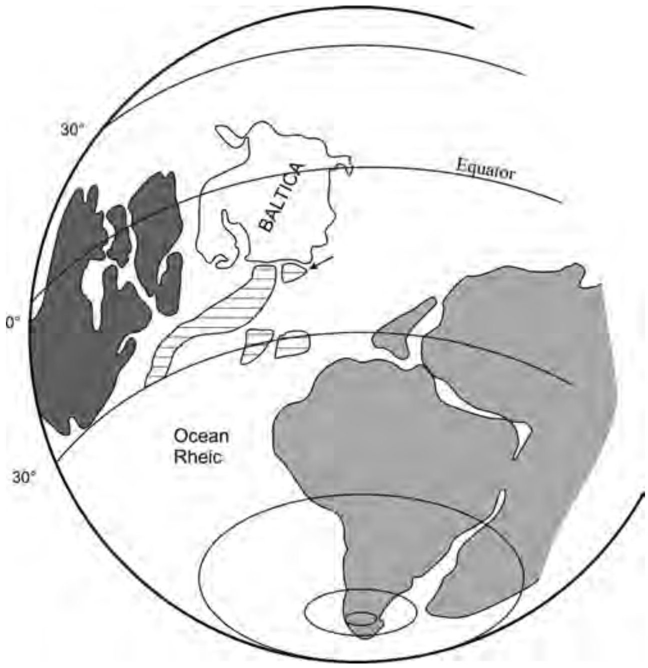

Fig. 2. Paleozoic position of the Małopolska and Brunovistulian microplates (arrow).

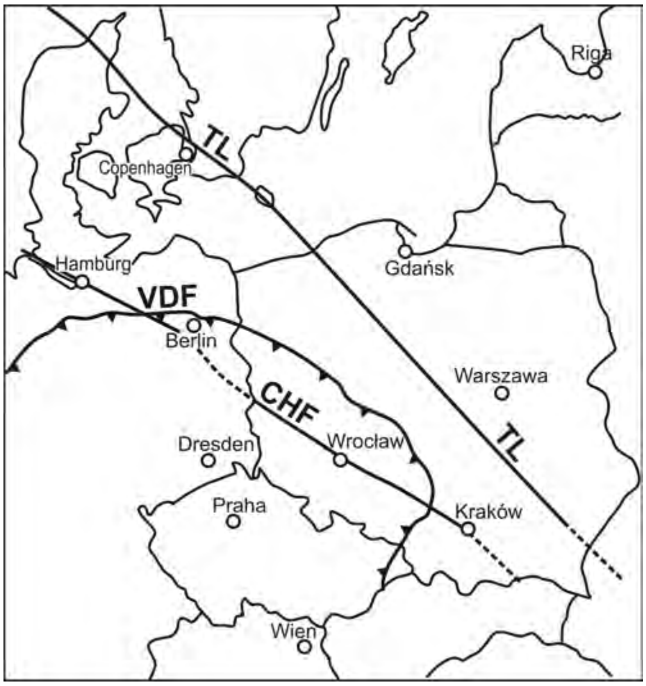

Fig. 3. Main tectonic lineaments of Central Europe. TL – Teiseyere –Tornquist Line, CHF – Cracow-Hamburg Fault, VDF – Variscan front (from Szulc, 2000).

The basic structural framework of Southern Poland was established during Hercynian orogeny, when the Kraków area became far eastern foreland of the Hercynian mountain range.

Paleozoic

The oldest rocks cropping out in the Kraków vicinity are Middle Devonian-Lower Carboniferous, shallow water, platform carbonates (Fig.4A), rich in benthic fauna: stromatoporoids, corals, brachiopods and bryozoans. Hercynian orogeny, that began at the Early/Late Carboniferous break, resulted in eventual closing of the marine basins and in replacement of carbonate sediments by brackish and continental, coal-bearing, Upper Carboniferous clastics.

The intensive Hercynian tectonism involved also magmatic activity in the region manifested chiefly by intrusive rocks. Most of the igneous rocks are acid and display chemical composition typical for intracontinental magmatic provenance.

The tectonic and magmatic activity continued also in early Permian times. The tectonic regime changed however from orthogonal W–E oriented compression into transtensional rotation. The strike-slip movement at the NE margin of the Upper Silesian Basin resulted in development of narrow (<15 km) trough structure (Sławków Graben). The faults bounding the graben, reached deep enough to enable magma to migrate and form intrusive and volcanic rocks (Fig. 4 A)

The graben was filled with continental molasse deposits composed of fanglomerates (Fig. 4B) volcaniclastics, playa redbeds with evaporites (Fig. 4C) and travertines.

Mesozoic

After the Hercynian orogeny, the discussed region was subjected to denudation that continued throughout the early Triassic. Thin (up to several meters) Buntsandstein continental clastics represent this period.

By the end of the early Triassic, the Silesian-Kraków region was inundated by Röt transgression, which gave way to the subsequent, very pronounced Muschelkalk transgression in the middle Triassic (Fig. 6A). The Silesian-Kraków area formed a treshold block, that divided the Tethys Ocean from the epicontinental Germanic Basin (Fig.5). According to dominating open marine fauna (including coral-sponge reefs), the visited region should be recognized as an integral part of the Tethys Ocean.

During late Triassic times, the Silesian-Kraków region was affected by eo-Cimmerian tectonic movements that caused its emersion. The Keuper and Rhaetian are developed mostly in continental clastic (fluvial) and carbonate (palustrine) facies.

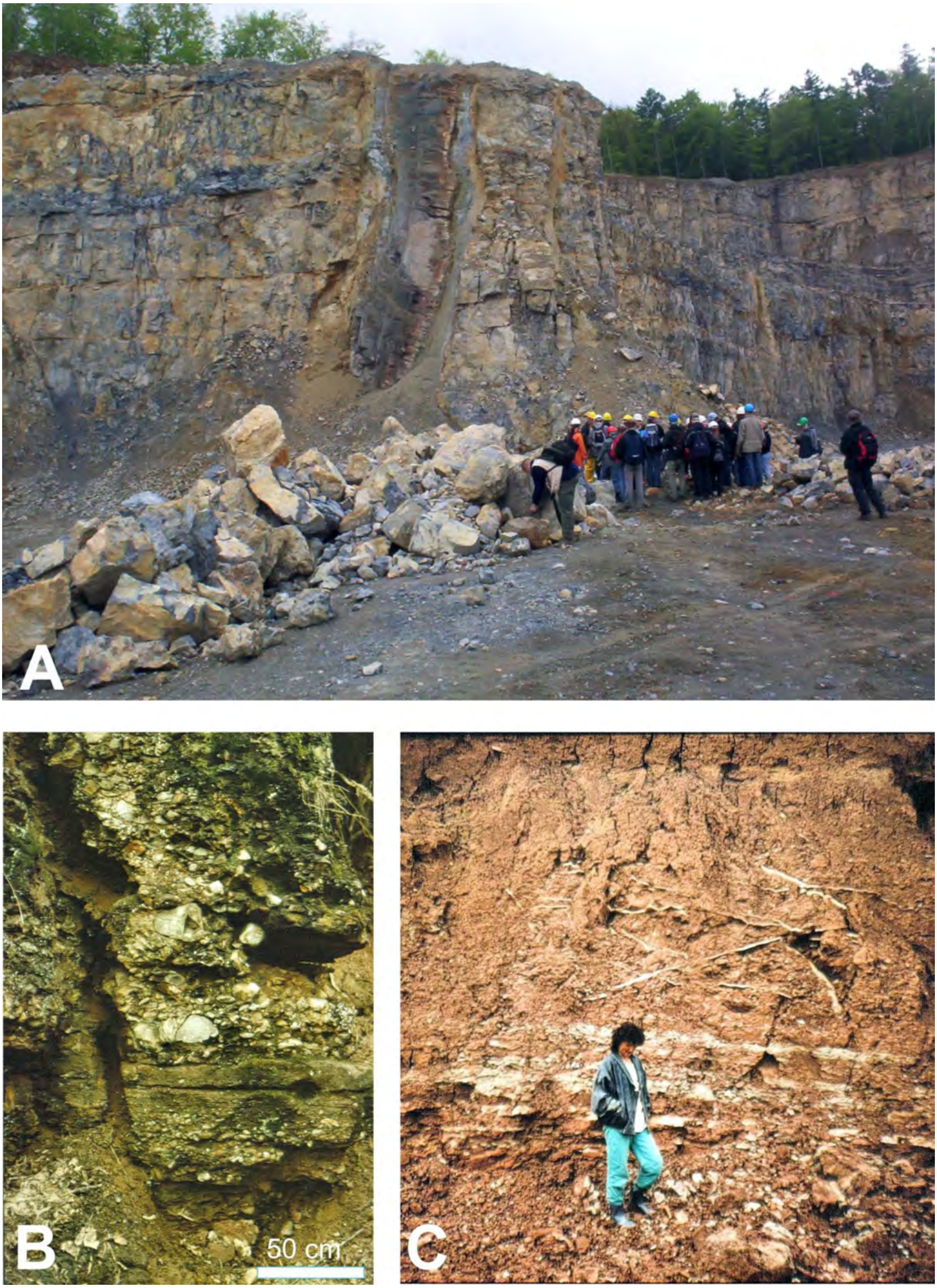

Fig. 4. Chosen Paleozoic rocks of the Cracow Upland: **A.** Givetian dolomites dissected by a Lower Permian intrusive dyke. Dubie quarry. **B.** Lower Permian fanglomerates. Karniowice. **C.** Lower Permian playa redbeds with gypsum veins. Sławków claypit.

The eo-Cimmerian tectonics discharged Pb-Zn – bearing hydrothermal fluids and provided tectono-karstic conduits for their migration. The resulted Mississippi Valley-type ores have been exploited here since Mediaeval times.

Continental environments persisted until the early Jurassic and the next transgression came only in middle Jurassic.

The transgression reached its maximum in Callovian-Oxfordian interval, when entire central Europe was flooded by shallow sea. In this time, carbonate sedimentation dominated in Kraków region (Fig. 6 B),. The carbonate facies of the Oxfordian are very similar to those from the Jura Mountains and southern Germany and comprise sponge-microbial bioherms, and detrital cherty limestones, and marls deposited between the bioherms (Stop A 7.5) (Fig. 6 C-D, Fig. 7).

Tectonic movements that took place in early Cretaceous caused upwarping of the Kraków region and resulted in its emersion. Nonetheless the global late Cretaceous transgression (Cenomanian-Senonian) overlapped also the southern Poland platform. During maximum phase of the transgression glauconitic marls and limestones deposited.

Because of the tectonic movements related to closing of the nearby Carpathian basins, and because of eustatic

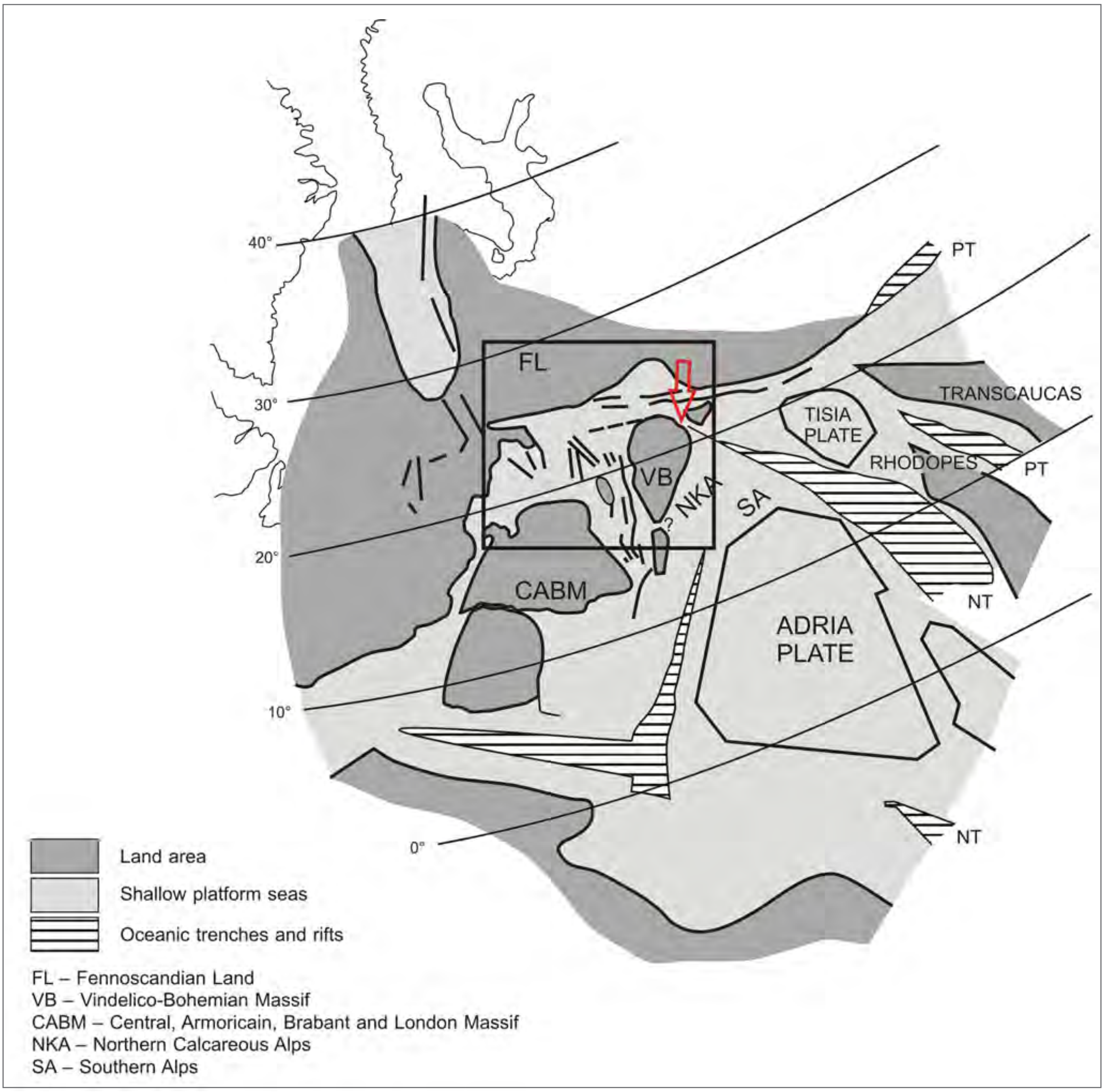

Fig. 5. Paleogeography of the Western Tethys and Peritethys in middle Triassisc. Arrow indicates position of the Kraków-Silesian region (from Szulc, 2000).

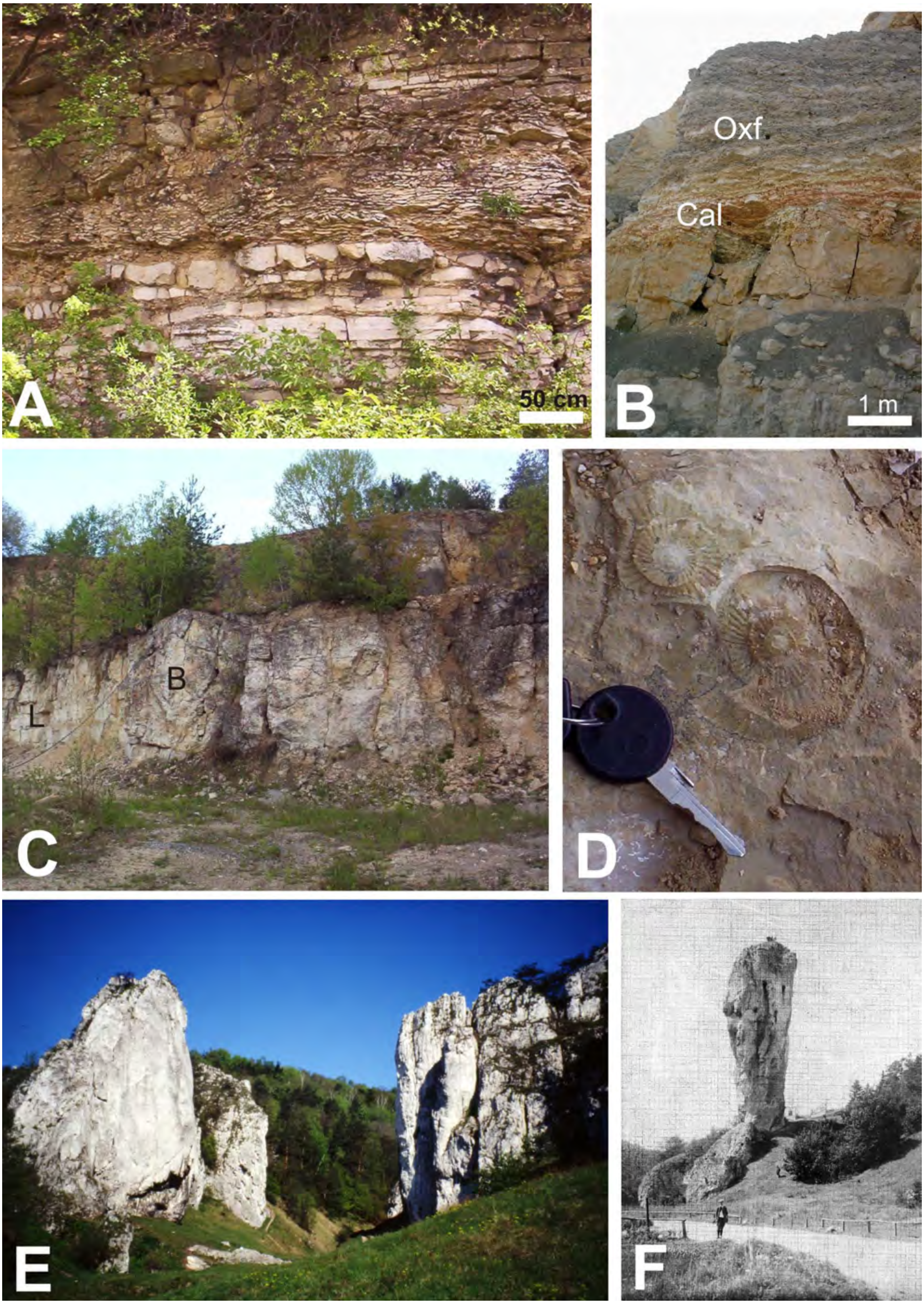

Fig. 6. Chosen Mesozoic rocks of the Cracow Upland. **A** – Middle Triassic Muschelkalk limestones. Libiąż quarry; **B** – Callovian-Oxfordian transgressive succession in Zalas quarry; **C** – Oxfordian biohermal (B) and bedded limestone facies. Młynka quarry; **D** – Oxfordian platy limestones with ammonites. **E** – Cliffs built of Upper Jurassic massive limestones. Bolechowicka Valley (photograph by Michał Gradziński). **G** – Hercules' Club in Ojców National Park. Postcard from the 19th century.

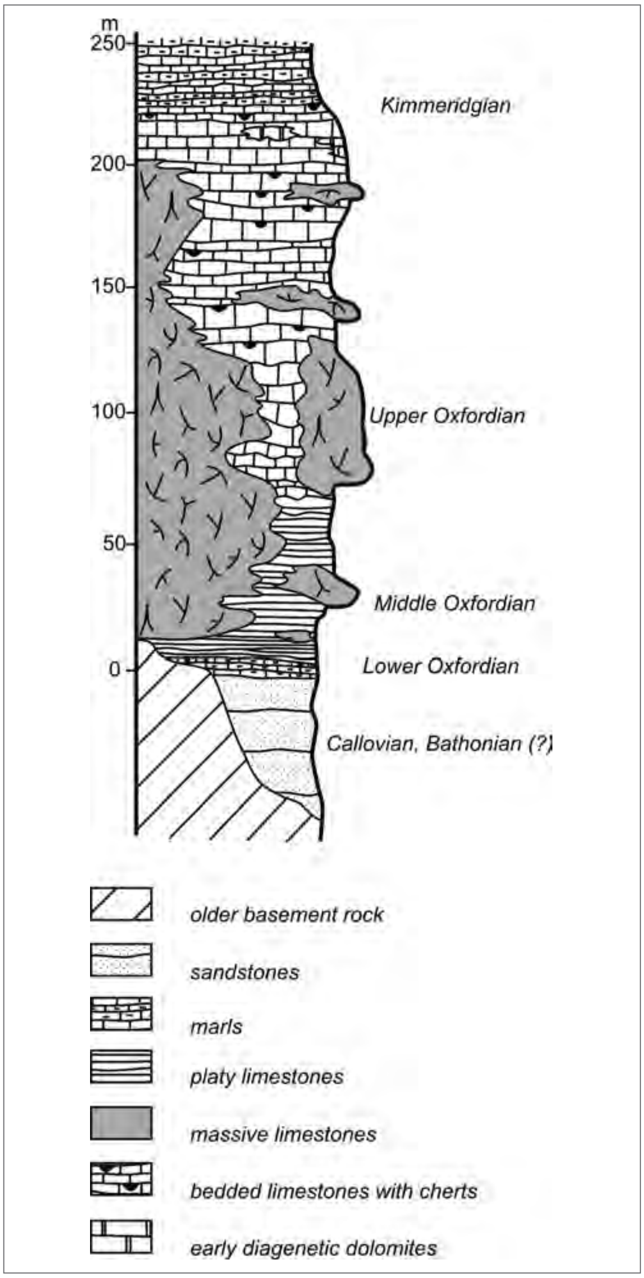

Fig. 7. Geological section of the Jurassic of the Kraków region. After Matyszkiewicz and Krajewski, 2007 (simplified).

fluctuations, the Upper Cretaceous succession of the Silesian-Kraków area displays several stratigraphic gaps and disconformities (Stop A 7.4).

Cenozoic

The Alpine orogeny and closing of the Carpathian basins caused uplift of the Kraków-Silesian region probably already in latest Cretaceous. After emersion the carbonate rocks, that dominate in the region underwent vigorous karstification. Extensive underground and surficial karst forms developed (Stop A 7.1 and 2). The Kraków Upland abounds in caves and sinkholes. These forms are believed to be founded in Paleogene though their exact age is not established because of the lack of stratigraphical indicators and because of polyphase history of chemical denudation.

After Paleogene emersion, the Miocene transgression of the remnant Carpathian basin (Paratethys Sea) (Fig. 8) encompassed the Kraków region. In the shallow perilittoral zone marls with bivalves (oysters) deposited. In the basin centre, saline brine concentrated and halite precipitated. It has been exploited in the famous Wieliczka Salt Mine near Kraków. The coastal limestone cliffs were encrusted by caliche coatings.

The present tectonic and topographic pattern of the Kraków environs was shaped in Miocene time. The Kraków area was dissected into several horsts and grabens that strike more or less parallely to the Carpathian front (Figs. 9-10). The faults resulted from breaking of the rigid Kraków platform when the Carpathian nappes were emplaced from the south.

Pleistocene ice lobes invaded the Kraków Upland once. The melted glaciers left tills, glaciofluvial sands and glaciolacustrine muds and clays. The last glaciation (Vistulian) did not reach the visited area, however it provided loess material, that accumulated on slopes creating a several metres-thick cover on the older rocks.

The Pleistocene deposits were partly eroded in Holocene so the older topography has been exhumed. In spring zones and river valleys, peats and travertines accumulated.

The past and present of vine in Kraków region

First historical annotations about winery of Kraków come from a 12th century travel chronicle, by Al-Idrisi – a Sicilian-Arab geographer, who mentioned several vineyards from the Kraków area (Lewicki, 1945). According to archeological studies, the royal Wawel hill was overgrown by *Vitis* plants on its SW site as early as the 10th century. This vine cultivation was certainly introduced to Kraków by Czech monarchs ruling in this period the Malopolska region.

The other important center of wine production was the Benedictine Abbey of Tyniec (some 10 km SW from Kraków downtown), founded in the 11th century by monks coming here from Lower Lotharingia. Vine cultivation and wine production persisted until the 18th century in the entire Kraków region. Gradual decline of vine cultivation is observed since the 17th century as a

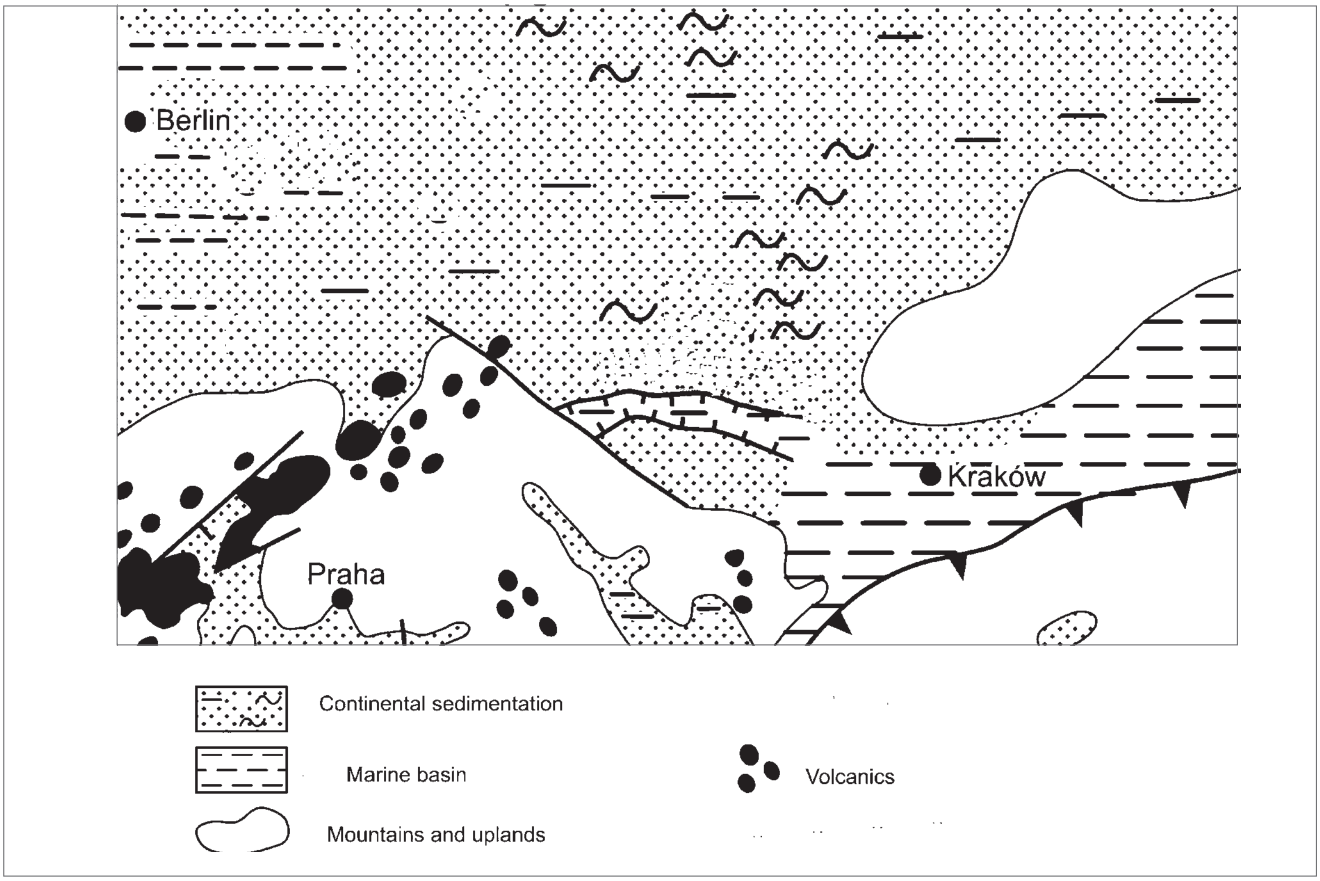

Fig. 8. Paleogeography of southern Poland in Miocene time.

combined effect of climate cooling and political changes in central Europe. Poland lost its power position and was divided in the 18th century between three neighbors – Prussia, Russia and Austria. Kraków became a part of Austrian monarchy, which beside Austria, included Czech and Hungary territories, i.e. countries much more predisposed for vine cultivation. This led to collapse of wine production in Kraków area. Nonetheless some small vine refuges persisted in Kraków - among others on the Wawel hill and in Camaldolese Hermitage on the Bielany hill (Stop. A 7.)

Vine revival in Kraków region, and in entire southern Poland, began around 2000, as some wineries originated in Kraków vicinity. Wineries have been also supported with professional consulting aid by Polish Institute of Vine and Wine, founded in Kraków in 2003. Concurrent climatic amelioration (in particular milder winters) favoured development of this branch of economical activity in the region.

Average annual temperature reaches some 8.5°C while the average winter temperature is around 0 °C in Kraków Town, and even cooler in higher situated vineyards. Therefore the winemakers cultivate mostly frost-

Fig. 9. Geological map of the Kraków region (after Gradziński, 1985) and location of the visited vineyards: KG - Krokoszówka Górska, SG – Srebrna Góra).

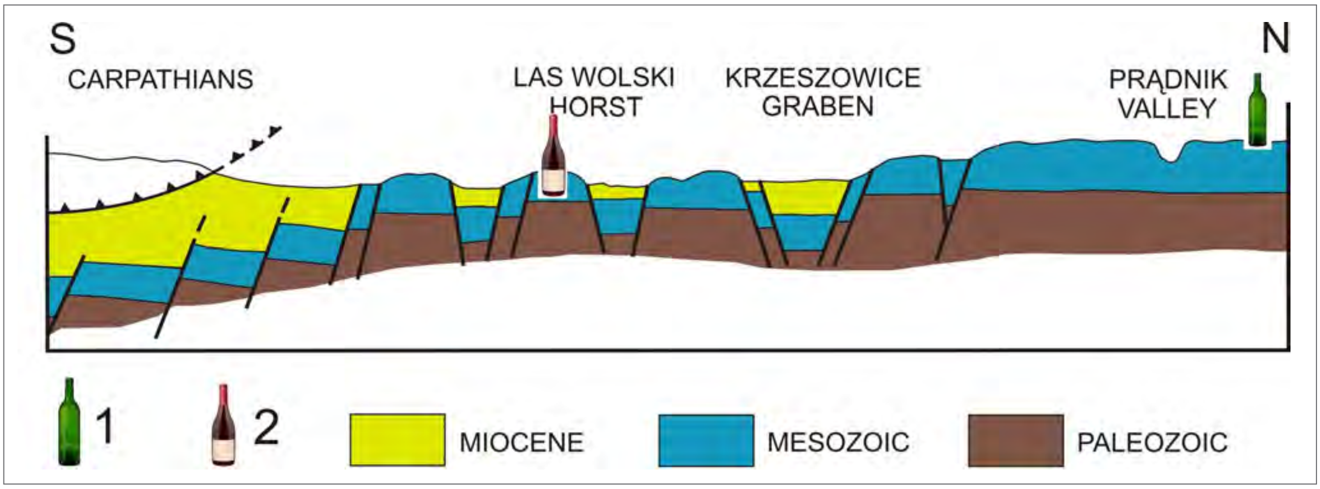

Fig. 10. N-S geological section of the Kraków region (after Gradziński, 1985, simplified) with marked positions (bottles) of the visited vineyards – 1. Krokoszówka Górska, 2 – Srebrna Góra.

resistant (able to withstand temperatures as low as minus 30 °C !) hybrids of the Vitis vinifera species. This implies shorter vine-growing period and earlier ripening and maturation. of grapes. Cooler climate forces the grapes to ripen earlier, which produces a fresher and more acidic harvest. Another handicap for viticulture in southern Poland is the rainfall regime with a maximum in July, what promotes fungal diseases and berry splitting. Sunshine amount ranges between 1200 and 1800 hrs/year (see: http://www.klimat.geo.uj.edu.pl/tematyczne/klimatkrakowa/index2.htm).

The cultivated vine hybrids (Polish spelling is used herein for names of vine varieties) come mostly from German oenological institutes and comprise, among others, solaris, johanniter, hibernal, seyval blanc, sibera, bianca, phoenix, muscaris – for white wines, and regent, rondo, leon millot, marechal foch, cabernet cortis, cabernet carol, rössler, rathay and bolero – for red wines. Subordinate role play "noble species – chardonnay, pinot gris, traminer, riesling, zweigelt, pinot noir or dornfelder.

Stop descriptions

A7.1 Hercules Club (Maczuga Herkulesa) in Ojców National Park

(50°24′28″ N; 19°73′00″ E)

Leader: Joachim Szulc

The scenic Prądnik valley is incised in Upper Jurassic carbonate rocks, developed in three facies. The first one, massive biolithic limestones, is built of sponges and microbial bioherms that pass laterally through thick-bedded limestones into platy marls. Such a facies pattern resulted in present-day topography: the massive, erosion-resistant biohermal and thick-bedded limestones are exposed in high cliffs (Fig. 6E) and isolated towers – like the Hercules Club (Fig. 6F) – a topographical trade mark of the region, while the adjoining soft marls underwent substantial erosion, giving way to depressions. Chemical denudation has been enabled by post-sedimentary tectonic disturbances.

A7.2 Maszycka Cave

(50°17′84″ N; 19°84′49″ E)

Leader: Joachim Szulc

Maszycka Cave is situated on the left slope of the Prądnik Valley, close to Maszyce village. The relatively small (6 m wide and 3 m high)and inconspicuous cave is one of the most important archeological sites in Poland. During its long exploration that started already in 1883 with excavation by Godfryd Ossowski (Fig. 11), numerous Palaeolithic and Neolithic artefacts have been found here (Ossowski, 1885; Kozłowski et al., 2012). The most interesting are bone tools (including points, navettes and decorated antler (Fig. 12) and other items from late Palaeolithic i.e. from the Late Glacial, as evidenced by their radiometric age of ca. 15 ky BP. The tools represent the Magdalenian culture showing close connections to the French Middle Magdalenian. Other intriguing Palaeolithic finding are human bones of 16 people, displaying traces of cannibalistic practices.

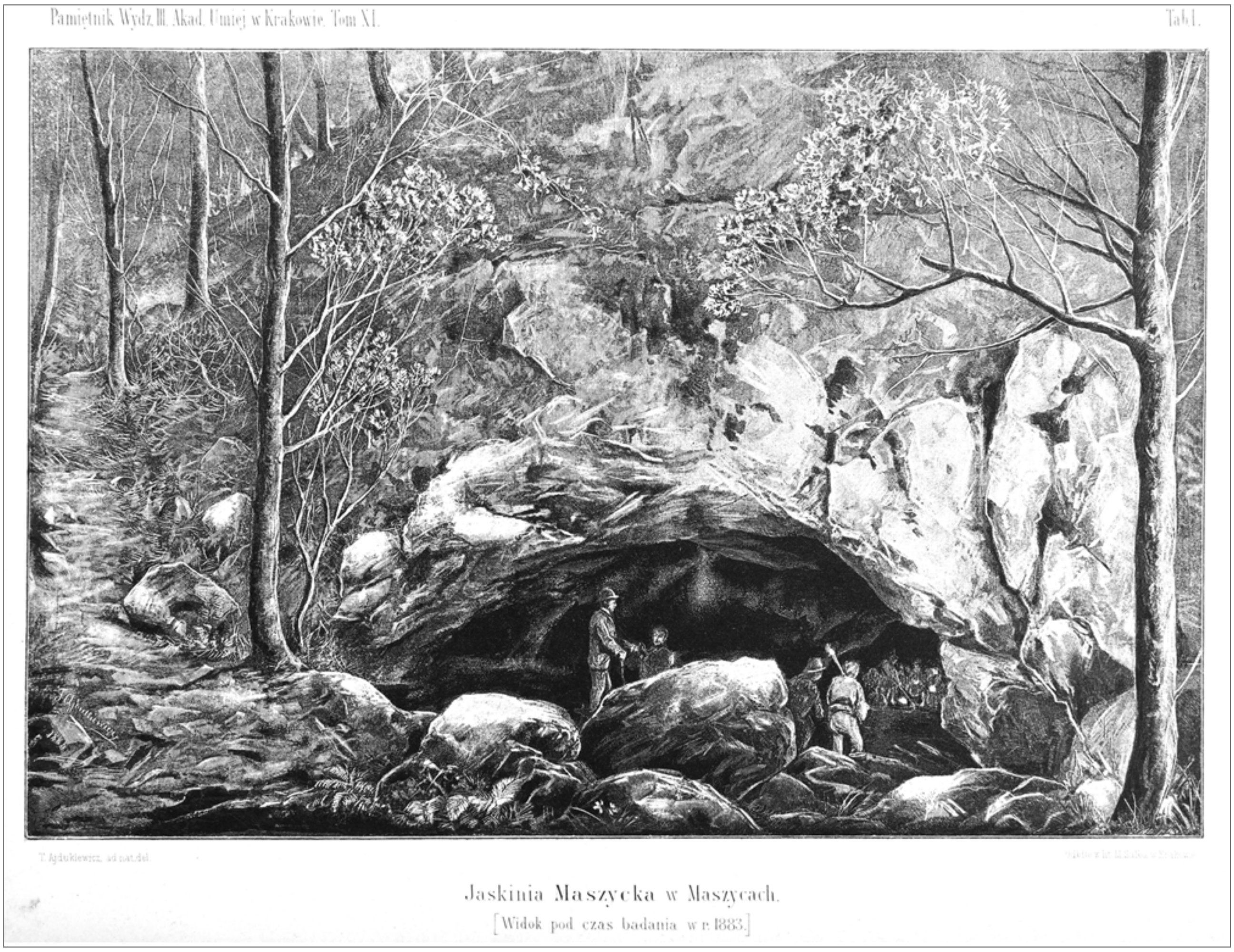

Fig. 11. Exploration of Maszycka Cave in 1883. From Ossowski, 1885.

Fig. 12. Paleolithic bone tools from Maszycka Cave. From Ossowski, 1885.

A7.3 Krokoszówka Górska vineyard

(50°19′20″ N, 19°86′57″ E)

Leaders: Marek Górski[1], Joachim Szulc

[1]Vineyard Krokoszówka Górska
(poczta@krokoszowka-gorska.pl)

The small (ca. 1 hectare) vineyard (Fig. 13) lies at altitude of some 400 m a.s.l. and is founded on clayey soils developed on Quaternary loess and Upper Jurassic limestones. The soil is rich in P, Mg and K elements. Average annual temperature reaches some 6°C, i.e. 2°C less than in Kraków (altitude effect). Harvest time falls on late September – early October. Temperatures in winter average around 0°C. The cultivated grapes are hybrids – leon millot, marechal foch, swenson red, kristaly, jutrzenka (local hybrid), seyval blanc, solaris, regent and chardonnay.

The wines are well structured. Layers of lilac, blackberry, blueberry and cherry fruits with slight tobacco hints are distinguishing features. Detailed information on the winery at: /www.krokoszowka-gorska.pl/kontakt.html

A7.4 Januszowice roadcut

(50°14′35″ N, 19°89′65″ E)

Leader: Joachim Szulc

Upper Jurassic-Upper Cretacous disconformity. Abrasion surface cutting Upper Jurassic limestones and overlain by Turonian limestones.

A7.5 Piekary village

(50°01′72″ N, 19°79′50″ E)

Leader: Joachim Szulc

Exposure of Upper Oxfordian limestones in an abandoned quarry set in a small horst on the left bank of the Vistula river. The outcrop presents lateral transition between massive, biohermal limestones (in the southern part of the outcrop) and the bedded, chert-bearing limestones (in the northern part of the outcrop). On the opposite bank of the Vistula river stays the Benedictine Abbey at Tyniec – the 12th century centre of viniculture. The Abbey is built on another horst. The Vistula valley follows here a graben structure between the two horsts.

A7.6 Srebrna Góra vineyard

(50°02′44″ N, 19°50′28″E)

Leaders: Mirosław Jaxa Kwiatkowski[1], Joachim Szulc

[1]Vineyard Srebrna Góra, Kraków
(mjk@winnicasrebrnagora.pl)

The vineyard on the Bielany horst is the biggest one in southern Poland and occupies a territory of 12 hectares (Fig. 14 A). The hill is owned by Camaldolese monks who have cultivated vines (on a much smaller scale) from the 17th century up to recent times. From the hill, the tectonic framework of the Kraków region is clearly visible (Fig. 14 B).

Fig. 13. Krokoszówka Górska vineyard in Smardzowice and white wine label produced in the vineyard.

The horst is built of Oxfordian limestones giving way to calc-magnesian rendzina soils with varied humic components. Only the northern part of the vineyard is founded on glacial clays and sands.

Average annual temperature is around 8°C. The grapes are harvested from August (siegerrebe, solaris, acolon and rondo) to late October (riesling).

The cultivated grapes are hybrids – solaris, johanniter, hibernal, seyval blanc – for white wines, and regent, rondo, cabernet cortis – for red wines (Fig. 14 C-D). In contrast to other vineyards, the Srebrna Góra vineyard is experimenting with species of *Vitis vinifera* – chardonnay, riesling, pinot gris, traminer, auxerrois, siegerrebe and zweigelt, pinot noir and acolon.

Fig. 14. Srebrna Góra vinery and wines and other local wines. **A** – Bielany horst in Kraków with Camaldolese hermitage and Srebrna Góra vineyard (photograph by Łukasz Sakiewicz). **B** – View from the Bielany hill on the Vistula valley in Kraków and the front of Carpathians (in the background). **C–D** – Wines from the Srebrna Góra vineyard. **E–G** – Labels of wines from other vineyards in the Kraków region.

The white wines are fresh and display good concentration of fruit with refreshing acidity and aromas of flowers, white fruits and lemon. The red wines, first of all Pinot noir, are light bodied, subtle, earthy, with right acidity and aromas of dark fruits such as red currant and cherries.

Detailed information on the winery one may find at: www.winnicasrebrnagora.pl.

References

Gradziński, R., 1985. First Day. Introduction. In: Birkenmajer, K. (ed.), *Main Geotraverse of the Polish Carpathians (Cracow-Zakopane). Guide to excursion 2. Carpatho-Balcan Geological Association XIII Congress, Cracow, Poland*. Geological Institute, Poland, pp. 14-17.

Lewicki, T. 1945. Polska i kraje sąsiednie w świetle Księgi Rogera geografa arabskiego z XII w. al-Idrīsīego. Cz. 1, (Uwagi ogólne, tekst arabski, tłumaczenie). *Prace Komisji Orientalistycznej Polska Akademia Umiejętności*, nr 34: 144 pp. [in Polish.]

Kozłowski, S. K., Połtowicz-Bobak, M., Bobak, D. & Terberger, T., 2012. New information from Maszycka Cave and the Late Glacial recolonisation of Central Europe. *Quaternary International*, 272-273: 288-296.

Matyszkiewicz, J. & Krajewski, M., 2007. Litologia i zróżnicowanie facjalne wapieni górnojurajskich okolic dolin Szklarki i Będkowskiej. *Tomy Jurajskie*, 4: 87–101 [in Polish.]

Nawrocki, J. & Poprawa, P., 2006. Development of Trans-European Suture Zone in Poland: from Ediacaran rifting to Early Palaeozoic accretion. *Geological Quarterly*, 50: 59–76.

Ossowski, G., 1885. Jaskinie okolic Ojcowa pod względem paleontologicznym. *Pamiętnik Akademii Umiejętności w Krakowie. Wydział Matematyczno-Przyrodniczy*. T. 11: 1-50 [in Polish.]

Szulc, J., 2000. Middle Triassic evolution of the northern Peri-Tethys area as influenced by early opening of the Tethys Ocean. *Annales Societatis Geologorum Poloniae*, 70: 1–70.

(www.klimat.geo.uj.edu.pl/tematyczne/klimatkrakowa/index2.htm).

Sedimentary evolution and trace fossils of Carboniferous turbidite systems in the Variscan foreland, Czech Republic

Ondřej Bábek[1], Radek Mikuláš[2], Daniel Šimíček[1]

[1]Department of Geology, Palacký University of Olomouc, Czech Republic (babek@prfnw.upol.cz; daniel.simicek@upol.cz)
[2]Institute of Geology AS CR, v. v. i., Praha, Czech Republic (mikulas@gli.cas.cz)

Route (Fig. 1): From Brno we drive NE to Vyškov (**Mokrá and Luleč quarries, stops A8.1 and A8.2**) using local roads and then continue to Olomouc using R46 motorway. In Olomouc we turn N taking road 46 to Šternberk and then taking various local roads we drive to **Bělkovice Quarry (stop A8.3)**, then to **Malý Rabštejn and "Railway section" near Domašov nad Bystřicí (stop A8.4)** (about 15 – 20 km NE of Olomouc) and finally to Hotel Akademie in Hrubá Voda village (**accommodation**). On the second day we use mainly local roads E and NE of Olomouc, in the area between Lipník nad Bečvou, Hranice, Moravský Beroun and Šternberk visiting **Skoky (stop A8.5)**, **Hrabůvka quarry (stop. A8.6), Olšovec (stop. A8.7), Budišov nad Budišovkou (stop A8.8**) and return back to Hotel Akademie (**accommodation**). On the third day, we drive first S to Olomouc and then N and NE using road 46, direction Šternberk and Opava to **Slezská Harta (Stop A8.9**). From Stop 9 we turn to

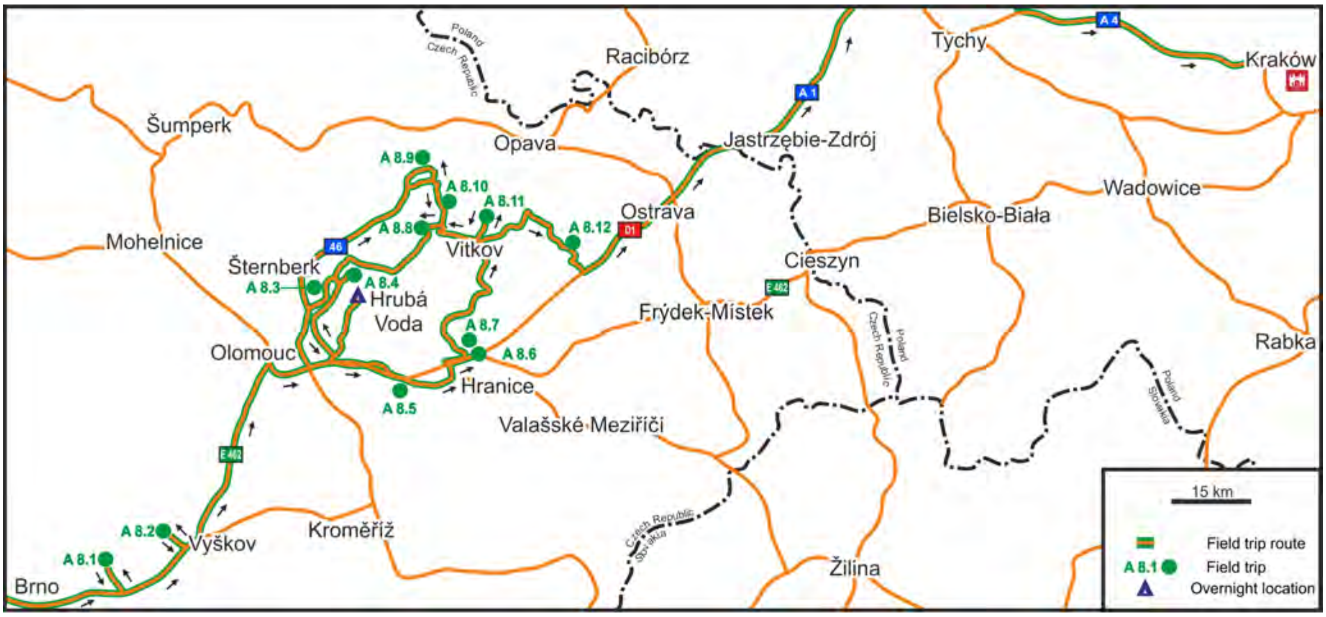

Fig. 1. Route map of field trip A8

Bábek, O., Mikuláš, R. & Šimíček, D., 2015. Sedimentary evolution and trace fossils of Carboniferous turbidite systems in the Variscan foreland, Czech Republic. In: Haczewski, G. (ed.), *Guidebook for field trips accompanying 31st IAS Meeting of Sedimentology held in Kraków on 22nd–25th of June 2015*. Polish Geological Society, Kraków, pp. 115–143.
Guidebook is available online at www.ing.uj.edu.pl/ims2015

S and SE to **Kružberk (stop A8.10), Vítkov – Annina dolina (stop A8.11)** and **Stará Ves (stop A8.12)** using local roads. From Stop 12, we take the shortest way to motorway D1, direction Ostrava, Polish border and then using Polish motorways A1 and A4 to **Kraków**.

Introduction to the trip

Variscan flysch of the Moravo-Silesian Culm Basin

Ondřej Bábek, Jiří Kalvoda[1] Radek Mikuláš, Daniel Šimíček

[1]Department of Geological Sciences, Masaryk University of Brno, Czech Republic (dino@sci.muni.cz)

The term "Culm" ("kulm" in Czech) was first introduced into the geology of the Bohemian Massif in the second half of the 19th century to denote fossiliferous successions of dark shales, siliceous shales, sandstones and rare limestones with *Posidonia* bivalves, goniatites and fossil plants (Roemer, 1860; Wolf, 1863; Zapletal, 2000). At present, it is recommended to use the term "Culm" as an informal term to describe sediments with unique lithology (see above) related to the Variscan plate convergence (Zapletal, 2000).

The Bohemian Massif represents the easternmost outcrop of the Variscan orogene in Europe. Pre-Permian successions of the Bohemian Massif can be subdivided into the Moldanubian, Central Bohemian, Saxothuringian, Lugian and Moravo-Silesian Zones (Chlupáč and Vrána, 1994, Franke and Żelaźniewicz, 2002). The former four zones represent the Armorican Terrane Assemblage with affinity to Gondwana, whereas the Moravo-Silesian Zone belongs to the Brunovistulian Terrane located at the southern passive continental margin of Laurussia. During the Variscan orogeny, the Brunovistulian Terrane acted as a lower plate that was subducted beneath the Armorican Terrane Assemblage (Kalvoda, 1995; Finger and Steyrer, 1995, Kalvoda *et al.*, 2002). For the most part, deposition of the Culm facies was to a certain extent related to the collision events in various geotectonic settings.

There are numerous outcrops of the Culm facies all over the Bohemian Massif including the Ještěd Ridge at the SW edge of the Karkonosze-Izera Massif in the West Sudetes, occurrences in the Nepasice borehole in the basement of the Bohemian Cretaceous Basin, the so-called Mírov Culm Unit in the eastern part of the Bohemian Terrane and Givetian "Culm-like" deposits of the Barrandian area (Central Bohemian Zone (Chlupáč, 1994; Chlupáč *et al.*, 2002; Zapletal, 2003). However, the most extensive occurrence of the Culm facies, traditionally referred to as the Moravo-Silesian Culm Basin, is located in the Variscan foreland of the Moravo-Silesian Zone (Fig. 2).

Moravo-Silesian Culm Basin: geological setting and structure

The Moravo-Silesian Culm Basin (MSCB) is an elongated, SW-NE to SSW-NNE trending structure, bordered by the Moravo-Silesian Fault Zone in the W (Schulmann *et al.*, 1991) and covered by Tertiary to Quaternary deposits of the Carpathian Foredeep to the E. Deposits of the MSCB are preserved in two major outcrops, the Drahany Basin and the Nízký Jeseník Basin (NJB) (Fig. 2). Minor relics of the MSCB are known from the Maleník Horst, Miroslav Horst (Hostěradice), Boskovice Graben and the centre of the city of Olomouc. A great deal of the MSCB is now covered by upper Carboniferous to Neogene deposits of the Upper Silesia Coal Basin, Jurassic platform cover of the Bohemian Massif, the nappes of the Outer Western Carpathians and the Carpathian Foredeep. Relics of the MSCB are also known from the Cracow-Upper Silesia region of Poland and the Polish Sudetes region (Kumpera *et al.*, 1995; Narkiewicz, 2005) and from many boreholes in Moravia.

The MSCB belongs to the system of lower Carboniferous deep-marine basins of the Rhenohercynian Zone of Western and Central Europe (Franke and Engel, 1988; Ricken *et al.*, 2000; Hartley and Otava, 2001). The basin evolved in the Tournaisian to Early Namurian times, in response to the Variscan plate convergence between the Brunovistulian Terrane and the overriding Lugodanubian Terranes encompassing the Moldanubian, Central Bohemian and Lugian Zones (Fritz and Neubauer, 1995; Franke *et al.*, 1995; Grygar and Vavro, 1996; Kalvoda *et al.*, 2003, Bábek *et al.*, 2006). The filling of the MSCB is interpreted as a multiphase geotectonic event, which can be subdivided into an initial, remnant basin phase (Lower to Middle Viséan) and a subsequent peripheral foreland basin phase (Upper Viséan to lowermost Namurian) (Kumpera and Martinec, 1995).

Structure of the MSCB is interpreted as an E-directed, thin-skinned stack of tectonic slices overlying the Proterozoic Brunovistulian crystalline basement and its pre-flysch, Devonian to lower Carboniferous sedimentary cover (Bábek *et al.*, 2006; Čížek and Tomek, 1991). Two major tectonic units were revealed in the southern part of the MSCB (Hladil *et al.*, 1999; Bábek *et al.*, 2006). The western (Protivanov) unit, which is allochthonous, is comparable in tectonic style to the Giessen nappe of the Rhenish Massif in Germany (Kalvoda *et al.*, 2008). Three strongly sliced units, the Němčice Vratíkov, the Northern and Southern Moravian Karst units, constitute the eastern parautochthon (Hladil *et al.*, 1999; Bábek *et al.*, 2006). Structure of the northern part of the MSCB is similar, comprising the western allochthonous unit (Andělská Hora and Horní Benešov formations) and the eastern parautochthonous (Moravice and Hradec-Kyjovice Fm.) unit (Grygar and Vavro, 1996; Hladil *et al.*, 1999). The MSCB shows a distinct W-E to NW-SE polarity in deformation and thermal metamorphism. The intensity of deformation and metamorphic alteration generally decreases to the the E to SE (Franců *et al.*, 2002; Rajlich, 1990). This trend continues further to the E to essentially undeformed Culm strata, which are known only from subsurface of the Outer Western Carpathians.

The Drahany Basin and the Nízký Jeseník Basin are separated by the NW-SE trending Haná Fault Zone, a post-Variscan structure, which accommodates late Cenozoic graben-like basins of the Upper Morava Valley (Fig. 2). During their deposition, the Drahany and Nízký Jeseník basins were connected, as suggested by their similar paleocurrent and clastic provenance patterns showing proximal (Drahany) to distal (Nízký Jeseník) sediment dispersal patterns (Kumpera and Martinec, 1995; Hartley and Otava, 2001).

Drahany Basin

The Drahany Basin consists of three formal lithostratigraphic units (Fig. 3): Protivanov Formation, Rozstání Fm. and Myslejovice Fm. (Dvořák, 1965; Hladil and Dvořák, 1994).

The Protivanov Fm. is the oldest unit of the Drahany Basin, which comprises greywackes with subordinate siltstones, mudstones and conglomerates. The Protivanov Fm. is subdivided into basal Velenov Shale Member and the overlying Brodek Greywacke Mbr. Total thickness of the formation is thought to reach almost 3000 m (Hladil and Dvořák, 1994). The formation is free of body fossils and it is dated only indirectly. The dating is based on limestone pebbles present in the (so-called) Kořenec conglomerate, which contains foraminifers of Lower to Middle Viséan age (V1b-V2a of traditional Belgian division, Kalvoda *et al.*, 1995; Špaček and Kalvoda, 2000). The $^{40}Ar/^{39}Ar$ dating of detrital white micas yielded youngest cooling ages of 350 Ma (Early Carboniferous) in the source area (Schneider *et al.*, 2000). Hartley and

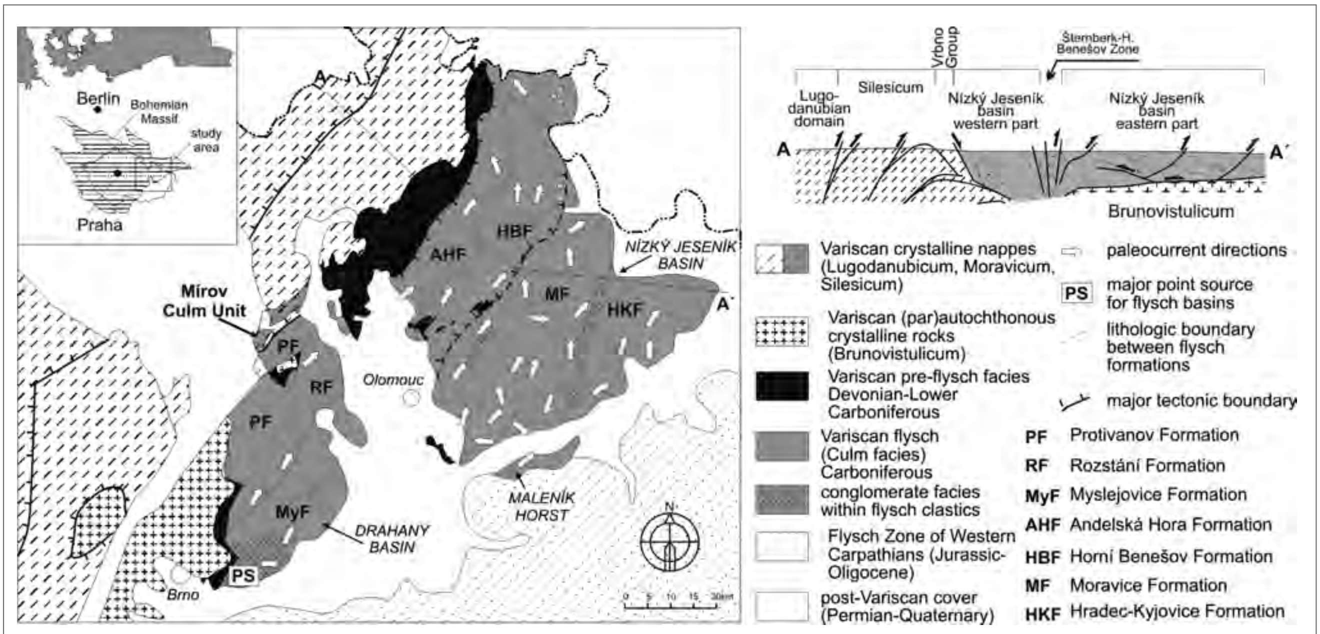

Fig. 2. Moravo-Silesian Culm Basin: major outcrops, lithology, lithostratigraphy and structure (adopted from Bábek *et al.*, 2004).

Otava (2001) defined three Heavy Mineral Zones (HMZ) in the MSCB; each one is confined to a distinct stratigraphic interval. The changes in heavy mineral spectra up-section reflect increasing proportion of high-grade metamorphics at the expense of low-grade metamorphics in the source area, as a result of upper Viséan unroofing of the Moldanubian source area (Hartley and Otava, 2001). In the Lower HMZ (Peγ goniatite Zone to base of Goα goniatite Zone), the heavy mineral assemblages obtained from greywackes and conglomerates are composed mainly of epidote, tourmaline, garnet, sphene and zircon. Spessartine, grossular and almandine predominate in the Middle HMZ (base of Goα Zone to Goβ/Goγ Zone boundary) whereas pyrope and almandine are the predominant constituents of heavy mineral assemblages in the Upper MHZ (Goβ/Goγ Zone boundary to E1 Zone). The whole Protivanov Fm. correlates with the Lower HMZ.

The Rozstání Fm. is about 250 m-thick and it is composed of fine-grained sandstones, siltstones and mudstones with subordinate sandstone and conglomerate layers. Sandy limestone layers and limestone pebbles in conglomerates contain foraminifers of late Early Viséan / early Middle Viséan (V1b-V2a) to Late Viséan (V3a) age (Kalvoda and Bábek, 1995; Špaček and Kalvoda, 2000). Conil (in Holub *et al.*, 1973) described limestone clasts containing Upper Viséan foraminifers (V3a) from conglomerates located near Křtiny. From superposition relationships with the underlying Březina Formation (Tn3c-V1b, ?V2a) in the southern part of the Drahany Upland, the age of the Rozstání Formation can be considered to be post Early- to Middle Viséan. Youngest cooling ages of detrital white micas are 328 Ma (Tournaisian – Early Viséan) (Schneider *et al.* 2000). The whole Rozstání Fm. correlates with the Lower HMZ (Hartley and Otava, 2001). The two basal formations are in tectonic contact with the underlying pre-flysch sediments.

The overlying Myslejovice Fm. is composed of sandstones and conglomerates with subordinate siltstones and mudstones. Maximum thickness of the formation is about 2000 m. The formation is further subdivided into the Studnice Shale Member and two prominent conglomerate bodies, the Račice and Luleč Conglomerate Mbrs (Dvořák, 1965). The siltstones and mudstones yielded relatively rich late Viséan goniatites, bivalves, nautiloids, trilobites as well as trace fossils (Kumpera, 1973; Kumpera and Lang, 1975, Lang and Chlupáč, 1975; Lang *et al.*, 1979). The goniatites indicate Goα to Goγ1 goniatite zones (Upper Viséan). Foraminifers in limestone pebbles of the Račice Mbr indicate late Viséan ages

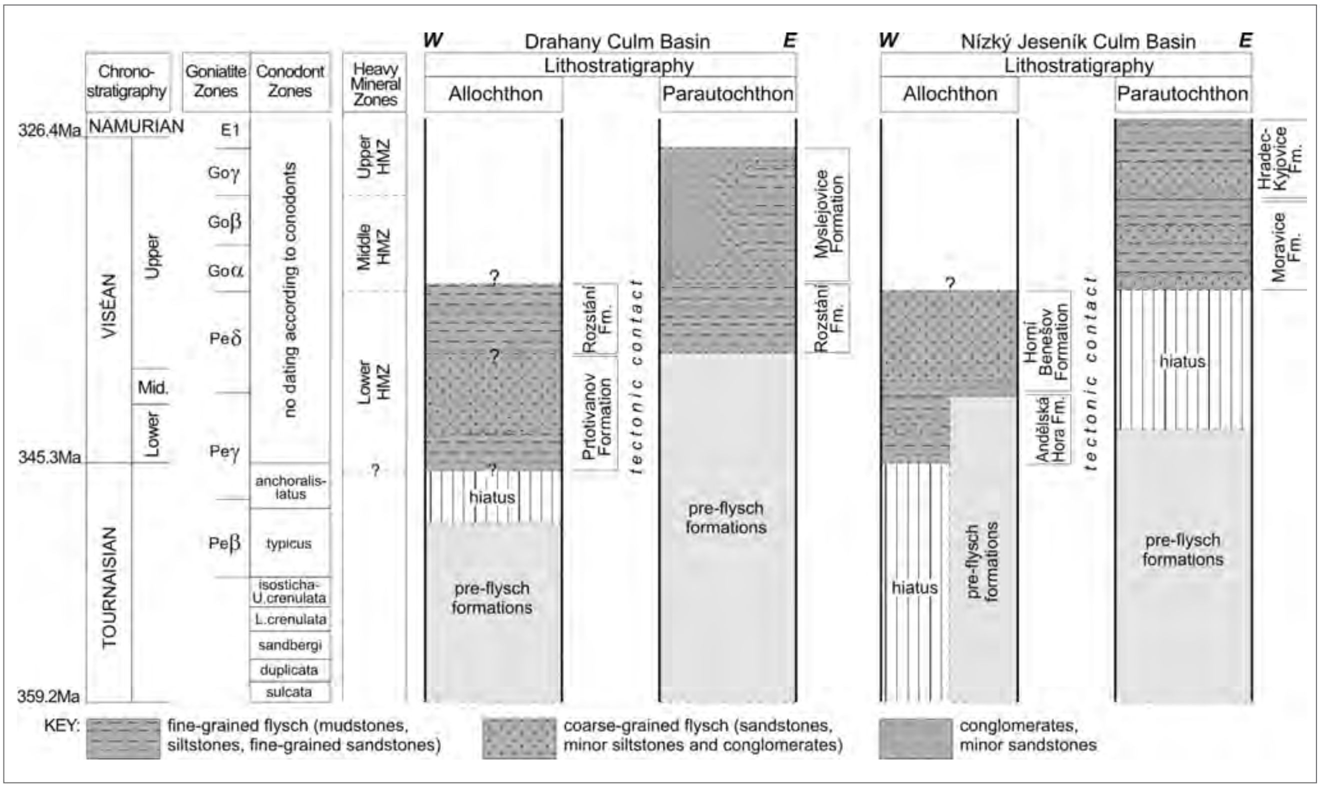

Fig. 3. Lithostratigraphy and chronostratigraphy of the Drahany and Nízký Jeseník Culm Basins (adopted from Kalvoda and Bábek, unpublished).

(V2a-V3b) (Špaček and Kalvoda, 2000). Rich floristic remains include 50 species (Purkyňová and Lang, 1985). Youngest detrital white micas yielded 332 Ma cooling ages (Late Viséan) $^{40}Ar/^{39}Ar$ cooling ages (Schneider *et al.*, 2000). Lower part of the Myslejovice Fm (Račice Mbr) correlates with the Middle HMZ, whereas its upper part (Luleč Mbr.) correlates with the Upper HMZ (Hartley and Otava, 2001. Lateral equivalents of the Myslejovice Formation are known from subsurface below the Western Carpathians, but they wedge out rapidly to the E.

Nízký Jeseník Basin

The Nízký Jeseník Basin is subdivided into four lithostratigraphic units, Andělská Hora, Horní Benešov, Moravice and Hradec – Kyjovice Formation (Patteisky, 1929; Kumpera, 1966; Zapletal *et al.*, 1989).

The Andělská Hora Fm is about 1000 to 2000 m-thick succession of thin, fine-grained sandstones, siltstones and mudstones with thicker, 1m to several hundred m-thick bodies of sandstones, fine-grained conglomerates and pebbly mudstones. The formation is free of body fossils, but Famennian and Tournaisian conodonts were found in limestone interlayers within the basal parts of the formation (Dvořák *et al.*, 1959; Koverdynský and Zikmundová, 1966; Zikmundová and Koverdynský, 1981). However, the same limestone layers have been interpreted as conformable sedimentary layers, tectonic slices and limestone pebbles in sheared pebbly mudstone beds by different authors. In the light of this controversy, the Andělská Hora Fm. can be younger than is indicated by conodonts. More recently, lower Carboniferous (Viséan) ages of the formation are preferred, based on the findings of the tree ferns *Asterocalamites* (Purkyňová, 1977) and rugose corals *Lithostrotion* and *Tetraporinus* ex gr. *T. virgatus* in conglomerate pebbles (Otava *et al.*, 1994). The $^{40}Ar/^{39}Ar$ dating of detrital white micas indicate 350 Ma cooling ages (Tournaisian) (Schneider *et al.*, 2000). The Andělská Hora Fm correlates with the Lower Heavy Mineral Zone of Hartley and Otava (2001). Owing to the lack of body fossils, its correlation with the Drahany Basin is uncertain.

The overlying Horní Benešov Fm is about 1500 to 2000 m-thick succession of thick, massive sandstones with subordinate lenses of fine-grained conglomerates and rhythmic successions of siltstones, mudstones and fine-grained sandstones. The formation is subdivided into three members: the Laryšov, Brantice and Dalov members (Kumpera, 1966). The formation is free of fauna and contains only rare fossil plants (*Archaeocalamites*). Based on superposition, its age is inferred to be Early- to Middle Viséan (Zapletal *et al.*, 1989). The only indirect biostratigraphic evidence comes from the boreholes near Moravský Beroun where foraminifers from sandy limestones and breccias underlying the Horní Benešov Fm suggest late Early Viséan to early Middle Viséan (V1b-V2a) age (Dvořák, 1994). The 40Ar/39Ar dating of detrital white micas indicates the youngest ages of 350 Ma (Tournaisian) (Schneider *et al.*, 2000). The whole Horní Benešov Fm correlates with the Lower HMZ (Hartley and Otava, 2001). No lateral equivalents of the Andělská Hora and Horní Benešov Fms are known from subsurface outside their outcrop area.

The Moravice Fm. is an ca. 1800 to 2500 m-thick succession of fine-grained sandstones, siltstones and mudstones with minor proportion of thicker sandstone and conglomerate bodies. The Moravice Fm. is subdivided into four lithostratigraphic units: the Bělá, Bohdanovice, Cvilín, Brumovice and Vikštejn members. Frequent findings of goniatites allowed dating of the Moravice Fm to Late Viséan (Goα2-3 to Goβmu Subzone, Kumpera, 1966, 1983; Zapletal *et al.*, 1989). The most common fossils include *Posidonia becheri*, *Streblochondria*, *Goniatites crenistria crenistria*, *Goniatites crenistria intermedius*, *Goniatites striatus falcatus*, frequent trace fossils and fossil plants including horsetails and seed ferns (Kumpera, 1972a, 1983; Zapletal and Pek, 1999; Mikuláš *et al.*, 2002). The youngest cooling ages of detrital white micas correspond to 330 Ma (Late Viséan) (Schneider *et al.*, 2000). The bulk of the Moravice Fm. correlates with the Middle HMZ of Hartley and Otava (2001) save its lowermost (Bělá Mbr) and uppermost (Vikštějn Mbr) parts, which correspond to the Lower and Upper HMZ, respectively (Hartley and Otava, 2001).

Conformably underlain by the Moravice Fm., the Hradec-Kyjovice Fm. constitutes a ca. 1800 m-thick succession of siliciclastics. The formation is subdivided into two members, the basal Hradec Member composed of thick layers of coarse-grained sandstones with subordinate fine-grained conglomerates, and the overlying Kyjovice Mbr composed of thin layers of fine-grained sandstones alternating with siltstones and mudstones. The Hradec-Kyjovice Fm. contains abundant goniatites, nautiloids, bivalves, brachiopods, trace fossils and fossil plants including lycopods, horsetails and ferns (Kumpera, 1983; Purkyňová, 1981). Based on abundant goniatites, the formation has been dated to Late Viséan to earliest Namurian (Goβspi to E1 Zones, Kumpera, 1983). Findings of fossil ferns and horsetails suggest Namurian age (Purkyňová, 1981). The $^{40}Ar/^{39}Ar$ dating of detrital white micas indicates the youngest cooling ages of 330 Ma (Late Viséan) (Schneider *et al*., 2000). The whole Hradec-Kyjovice Fm correlates with the Upper HMZ (Hartley and Otava, 2001). The Hradec-Kyjovice Fm is overlain by coal-bearing paralic siliciclastics of the Upper Silesia Coal Basin.

Minor outcrops and subsurface of the MSCB

Deposits of the Culm facies are exposed in the Maleník Horst in central Moravia, comprising a ca. 900 m thick succession of thick- and thin-bedded sandstones with minor fine-grained conglomerates, siltstones and mudstones. Based on goniatite fauna, they are dated to the Goγ zone and correlated with the Moravice Fm. and Hradec-Kyjovice Fm. of the Nízký Jeseník Basin, located to the N. Outcrops of the Culm facies are also known from the historical centre of Olomouc and its vicinity. They comprise a several hundred-m-thick succession of massive or thick-bedded sandstones with minor conglomerates, siltstones and mudstones. They are correlated with the basal parts of the Moravice Formation (Bohdanovice and Cvilín Beds) based on general lithology, modal composition of sandstones, and $^{40}Ar/^{39}Ar$ dating of detrital micas (Kumpera, 1983; Schneider *et al*., 2000).

Lower Carboniferous Culm facies has been described from several deep boreholes in SE and NE Moravia and in the subsurface of the Upper Silesia Coal Basin. The deposits belong to the parauthochthonous units and correlate with the Myslejovice, Moravice and Hradec-Kyjovice formations. Thickness of the subsurface Culm deposits vary from ~40 m (Němčičky-1 borehole) to ~290 m (Uhřice-2 borehole), but occasionally may exceed 1000 m (Těšany-1 borehole) (Zukalová *et al*., 1981). Generally, the Culm deposits rapidly wedge out towards E. The Culm deposits in SE and NE Moravia are conformably overlain by Upper Carboniferous (Namurian A) siliciclastic molasse sediments of the Upper Silesia Coal Basin (Dvořák, 1982; Zukalová *et al*., 1981).

Facies, processes and depositional environment

Lithology and facies

The MSCB is essentially composed of rhythmic alternation of siltstones and sandstones, with minor proportion of mudstones and conglomerates. Most of the sediments are considered deep-water in origin, although some previous authors suggested shallow-marine, tidal-flat, deltaic, or even fluvial depositional setting for at least a part of the MSCB (Kukal, 1980; Dvořák, 1994). More recently, detailed facies analysis works have indicated that the MSCB consists essentially of gravity-flow deposits (Tab. 1) including: clast-supported conglomerates (facies *F1*); pebbly/granule sandstones (*F2*); normally graded or massive, coarse-grained sandstones (*F3*); coarse- to fine-grained sheet sandstones and sandstone-mudstone couplets; fine-grained sandstone – silstone – mudstone couplets *(F5*) and mudstones with rare siltstone laminae (*F6*). These sediments are thought to be deposited from high-density turbidity currents, sandy debris flows, low-density turbidity currents (sometimes "quasi-steady") and hemipelagic fall-out (Nehyba and Mastalerz, 1995; Zapletal, 1991; Hartley and Otava, 2001; Bábek *et al*., 2004).

High-density turbidity current deposits

Clast-supported conglomerates with sandy matrix (facies *F1*) and pebbly sandstones of facies *F2a* are normally or sometimes inversely graded (Tab. 1). Both facies are thought to be deposited from high-density turbidity currents (Lowe, 1982) as their normal grading indicates suspension settling and high flow concentration is required for transport and deposition of sediment particles larger than coarse sand (Middleton and Hampton, 1973; Lowe, 1982; Mulder and Alexander, 2001). In contrast to the typical features of cohesive debris-flows, the beds of facies *F1* have sometimes basal erosive scours, flat upper bed contacts (cf. Plink-Björklund *et al*., 2001) and low to zero content of clay matrix (cf. Mulder and Alexander, 2001). Most beds of facies *F1* correspond to *R3* beds of Lowe (1982). In several beds of facies *F1*a there is a basal massive layer sometimes showing clast imbrication, which is followed by a normally graded conglomerate layer. This sequence suggests flow transformation from a basal layer deposited by friction freezing from non-turbulent hyperconcentrated flow (cf. Sohn, 2001) to an upper layer deposited by suspension settling from concentrated (high-density) turbidity flow (division *R3*). High-density flows that deposited the pebbly sandstones of facies *F2a* were highly erosive as suggested by abundant basal scours and mud intraclasts distributed near bed bases (Tab. 1). The beds show abrupt grain size jumps from basal pebbly/granule sandstone layer (division *R3*) to upper, usually parallel-stratified sandstone layer (*S1* of Lowe, 1982).

Sandstone beds of facies *F3a* have a thick (up to 4m), often normally graded and/or parallel stratified, interval of coarse-grained sandstone, which is usually overlain by a relatively very thin $T_{b,c,d}$ Bouma sequence (up to 30cm). The normal grading, basal and internal scours, and coarse sand lithology in the basal interval, all indicate deposition from turbulent density flows and this facies can be interpreted as deposited from sand-dominated high-density turbidity currents (the *S1* and *S3* divisions of Lowe, 1982; concentrated flows of Mulder and Alexander, 2001). High erosive efficiency of these flows is indicated by abundant mud intraclasts distributed near the bed bases and by frequent basal scours. Beds of facies *F3b* share similar succession of sedimentary structures with facies *F3a* and can thus be interpreted as sediments of high-density sandy turbidity flows. However, individual beds are very thick (usually about 8 to 10m, occasionally up to 15m, Table 1) and show frequent traces of amalgamation such as internal scours and rip-up clasts (cf. Mattern, 2002; Plink-Björklund *et al.*, 2001) distributed in discontinuous layers at variable heights above the bed bases. Facies *F3b* is therefore assumed to represent amalgamated layers consisting of several high-density turbidite beds.

Sandy debris flows

Beds of pebbly sandstones of facies *F2b* are ungraded, have non-erosive bases and contain abundant outsized clasts (Tab;le 1). The outsized clasts include both, rounded extraclasts and plastically deformed intraclasts of thin-bedded turbiditic siltstones, mudstones and fine-grained sandstones. They are usually several dm to about 1m in α-axis diameter but outsized clasts as long as 5m were also found. The outsized clasts show random vertical distribution in the bed and they are not aligned in any discrete levels. Absence of bedforms, non-erosive nature and abundance of outsized clasts indicate that these beds were deposited by friction freezing from non-turbulent, high-concentration density flows (Shanmugam, 1996; Mulder and Alexander, 2001). Most likely, these beds were not deposited from cohesive debris flows, as their clay content is very low to zero (macroscopic observation) and no clast projection typical of cohesive debris flows is visible in them (cf. Hiscott and James, 1985; Carter, 2001). The overall bed characteristics of this facies type suggest deposition from cohesionless, sandy debris flows (Shanmugam, 1996; Falk and Dorsey, 1998).

Quasi-steady turbidity current deposits (?)

Up to 17 m thick layers of medium grained sandstone of facies *F3c* are non-erosive and structureless, except for occasional low-angle cross stratification and occasional faint normal grading and convolute lamination in the topmost parts of most beds (Table 1). The layers are unusually thick but they do not show any traces of amalgamation and, therefore, each one probably represents a single depositional event. Great bed thickness is a feature typical of contained (ponded) turbidites, but thick mudstone intervals and upper-flow regime bedforms usually associated with contained deposits (cf. Pickering and Hiscott, 1985; Haughton, 2001) are not present in the beds of facies *F3c*. Lateral pinch-out bed geometry can be observed in some of the beds of facies *F3c*. Absence of grading and great bed thickness may indicate deposition from quasi-steady hyperpycnal flows that may owe their origin to fluvial discharge (Kneller and Branney, 1995), while surges and surge-like turbidity flows, unless ponded, do not produce thick sediment layers (Rothwell *et al.*, 1992). The presence of cross stratification is in contradiction to sandy debris flow interpretation, as such stratification forms solely beneath turbulent traction flows (Hickson and Lowe, 2002, p. 349). Many examples of hyperpycnal flows are known from modern submarine fans (e.g. Kneller and Branney, 1995; Mulder *et al.*, 2001) and the occurrence of such deposits is probably underestimated in the fossil record, partly due to the difficulties with recognition of such flows from the bed characteristics (Kneller and Buckee, 2000). Convex-upward shape and lateral pinch-out geometry of the beds of facies *F3c* can be attributed to deceleration of a hyperpycnal current, loss of momentum and rapid deposition associated with a decrease in slope gradient (hydraulic jump).

Low-density turbidity current deposits

Heterolithic sandstone-siltstone-mudstone beds of facies *F4a* and *F4b* have usually sheet-like geometry and they are organised into well-developed, complete or incomplete Bouma sequences. Frequent basal erosion marks and $T_{a,b,c,d}$ Bouma sequences present in facies *F4a* suggest deposition from low-density turbidity currents (Middleton and Hampton, 1973). The well-developed succession of bedforms expressed in the Bouma sequence indicates a progressive decrease in flow regime and an

Table 1. Facies classification of the Moravo-Silesian Culm Basin (adopted from Bábek *et al.*, 2004).

Facies code / Lithology	Sedimentary structures	Bed thickness	Bed contacts, bed geometry	Intraclasts, outsized extraclasts	Depositional process
F1 Clast-supported conglomerate	Normally graded, occassionally inversely graded, sometimes massive in lower parts of beds, ocassional clast imbrication near bed bases	2 to 13 m	Sometimes basal scours, flat upper contacts, bed geometry unknown	Very rare intraclasts, max. size 10 cm	High-density turbidity currents
F2 Pebbly sandstone to granulestone	*F2a* Normally graded, sometimes parallel-stratified, grain-size jumps from basal pebbly sandstone division to upper sandstone division, internal scours	2 to 4 m	Frequent basal scours, flat upper contacts, bed geometry unknown	Abundant mud intraclasts distributed near bed bases, max. size 40 cm	
	F2b Massive	8 to 12 m	Non-erosive basal contacts, flat upper contacts, bed geometry unknown	Abundant intraclasts and outsized extraclasts distributed throughout the bed thickness, max. size 500 cm	Sandy debris flows
F3 Sandstone	*F3a* Normally graded or massive, parallel-stratified, internal scours, $T_{b,c,d}$ Bouma sequences near bed tops	1 to 4 m	Erosive basal contacts, flat upper contacts, bed geometry unknown	Sometimes mud intraclasts distributed near bed bases, max. size 15 cm	High-density turbidity currents
	F3b Massive, normally graded , sometimes coarse-tail graded, rarely inversely graded near bed bases, sometimes parallel-stratified, internal scours, $T_{b,c,d}$ Bouma sequences near bed tops	3 to 15 m	Erosive basal contacts, flat upper contacts, bed geometry unknown	Abundant mud intraclasts distributed in bed-parallel or irregular zones in variable height above bed base, max. size 50 cm	Amalgamation of high-density turbidity current deposits
	F3c Massive, near bed tops faintly normally graded, convolute-laminated, parallel laminated or low-angle cross-laminated	1.5 to 17 m	Flat, non-erosive basal contacts, sometimes lateral pinch-out geometry, concave-up upper contacts	N/A	Quasi-steady turbidity currents
F4 Sandstone to mudstone	*F4a* $T_{a,b,c,d}$ Bouma sequences, sometimes massive	several cm to 1 m	Abundant tool marks and flute casts, sheet-like bed geometry	N/A	Low-density turbidity currents
	F4b $T_{b,c,d}$ (base-cut-out) Bouma sequences, frequently convolute-laminated	several cm to ca. 50 cm	Non-erosive, flat bed bases, wavy tops	N/A	
F5 Siltstone to mudstone, rarely fine-grained sandstone	Normally graded, parallel laminated, ripple-cross laminated, low-angle cross-laminated	several mm to 20 cm	Basal scours, load casts (load balls), flame structures, wavy tops, lateral pinch-outs of basal siltstone layers	N/A	
F6 Mudstone, rare siltstone	Faintly parallel laminated, sometimes bioturbated	Several cm to several dm	N/A	N/A	Hemipelagic fall-out, low-density turbidity currents

increase in traction during flow passage (Walker, 1965), that is features typical of surges or surge-like flows (Normark and Piper, 1991; Kneller and Buckee, 2000). Base-cut-out $T_{b,c,d}$ Bouma sequences and predominant fine- to medium-grained sandstone lithology represent typical features of facies *F4b*. Prevalence of upper flow regime traction structures and relatively great thickness of individual beds (several dm to 1m) suggest deposition from thick, low velocity turbidity flows, possibly in channel overbank settings (cf. Leverenz, 2000).

Heterolithic siltstone-mudstone beds of facies *F5* typically have an erosive base, a thin (0.5 to 3cm), parallel laminated, ripple-cross laminated and/or normally graded siltstone layer showing frequent lateral pinch-outs, and a thick, sometimes bioturbated, upper mudstone layer (Tab. 1). Bed bases are sharp, commonly highly irregular due to scouring and loading of basal siltstone layers into underlying mudstones. The extreme loading sometimes results in formation of detached load balls. The vertical succession of bedforms, low silt-clay ratio and loading features indicate that these sediments may be classified as fine-grained or silt turbidites with Bouma *A-E* divisions (Shanmugam, 1980; Piper and Stow, 1991), deposited from low-density turbidity currents. Thick successions of more-or-less regular zebra-type repetition of the beds of facies *F5* were previously referred to as the "laminite" in the literature (Lombard, 1963; Kumpera, 1983) and they occur ubiquitously all over the MSCB. For the major part, these successions cannot be interpreted as bottom current deposits (contourites) due to the frequent erosive bases, normal grading and load casts present in individual beds (Stow, 1979).

Deep-water mudstones

Massive black mudstones of facies *F6*, sometimes with thin silt laminae or bioturbated, are very rare in the Moravice Formation. These deposits are difficult to interpret. Due to their common occurrence with silt turbidites (*F5a*) it is possible to interpret these deposits as base-cut-out silt turbidites or mud turbidites (Piper and Stow, 1991). Alternatively, the mudstones may represent hemipelagic deposits of hypopycnal plumes associated with river discharge.

Trace fossil assemblages

The deep-water depositional setting is also supported by relatively abundant trace fossil assemblages. Fine-grained facies are usually associated with low-diversity assemblages including *Dictyodora liebeana*, *Nereites*, and *Planolites* indicating bathyal, aphotic, low-energy dysoxic environments. Upper Viséan sandstone facies are usually associated with higher-diversity assemblages comprising *Dictyodora liebeana*, *Nereites*, *Cosmorhaphe*, *Diplocraterion*, and *Rhizocorallium* indicating relatively higher levels of nutrients and bottom oxygenation (Mikuláš *et al.*, 2004; Bábek *et al.* 2004).

Three types of ichnocoenoses were observed in the Moravice Formation, each reflecting a distinct environmental control: (i) diversified *Dictyodora-Planolites*; (ii) simple *Dictyodora-Planolites*; and (iii) *Diplocraterion-Nereites*.

The diversified *Dictyodora-Planolites* ichnocoenosis consists mostly of fodinichnia (feeding traces) accompanied by agrichnia, pascichnia (grazing traces) and traces showing complex feeding strategies. The most common ichnogenera are *Chondrites, Dictyodora*, *Phycosiphon*, *Zoophycos* and *Planolites*. In the classical Seilacher's (1967) concept, this ichnocoenosis can be considered as a transitional *Zoophycos-Nereites* ichnofacies indicating typically bathyal, aphotic, low-energy, oxygen-depleted environments, which are unfavourable for the benthic communities to live and evolve (Frey and Pemberton, 1984).

The simple *Dictyodora-Planolites* ichnocoenosis shows extremely low diversity, comprising only two nominal ichnogenera. This ichnocoenosis can be assigned to the *Nereites* ichnofacies indicating deep-marine environment with extremely low energy levels (Frey and Pemberton, 1984; Stepanek and Geyer, 1989; Orr, 2001). The relatively highly diverse *Diplocraterion-Nereites* ichnoceonosis comprises abundant domichnia (dwelling traces), fodinichnia, agrichnia-pascichnia type traces and abundant traces of suspension feeders or possible surface-scraping detritus feeders (*Diplocraterion*). The most common trace fossils are *Rhizocorallium*, *Diplocraterion*, *Dictyodora liebeana*, *Cosmorhaphe*, *Protopaleodictyon*, *Furculosus*, etc. The ichnogeneric composition of this ichnocoenosis corresponds to the *Cruziana* ichnofacies mixed with traces of the *Nereites* ichnofacies sensu Seilacher (1967) and Frey and Pemberton (1984) and suggests deposition in environments more favourable to colonisation, compared to the previous ichnocoenoses. Map distribution of the ichnocoenoses in the Moravice Formation is shown in Fig. 4.

Paleocurrent data

Both, unidirectional and bi-directional paleocurrent data were obtained from the orientation of flute casts and tool marks, mostly from low-density turbidity current deposits (F4a, F5). The absolute majority of both published and our own paleocurrent data indicate S-N to SW-NE directions of flow with SSW-NNE frequency maximum (Fig. 4). This direction has been assumed to be parallel to the basin depocentre axis (Kumpera, 1983; Hartley and Otava, 2001). Such paleocurrent patterns are typical of the whole MSCB successions, indicating axial-trough topography at the time of deposition. A much smaller amount of the paleocurrent indicators show alternate W-E and NW-SE directions, which are oblique to perpendicular to the basin axis. Especially in the basal parts of the Moravice Formation the paleoflow patterns are relatively more complex, showing a relatively higher proportion of the oblique to perpendicular W-E to NW-SE directions. In the upper parts of the Moravice Formation,the paleoflow patterns are more uniform and tend to the SSW-NNE frequency maximum.

Depositional model

Five facies associations have been recognised (Hartley and Otava, 2001; Bábek *et al.*, 2004; Nehyba and Mastalerz, 1995). Proximal gravity-flow (fan-delta) deposits are composed of thick accumulations of clast-supported conglomerates (*F1*) locally interbed-

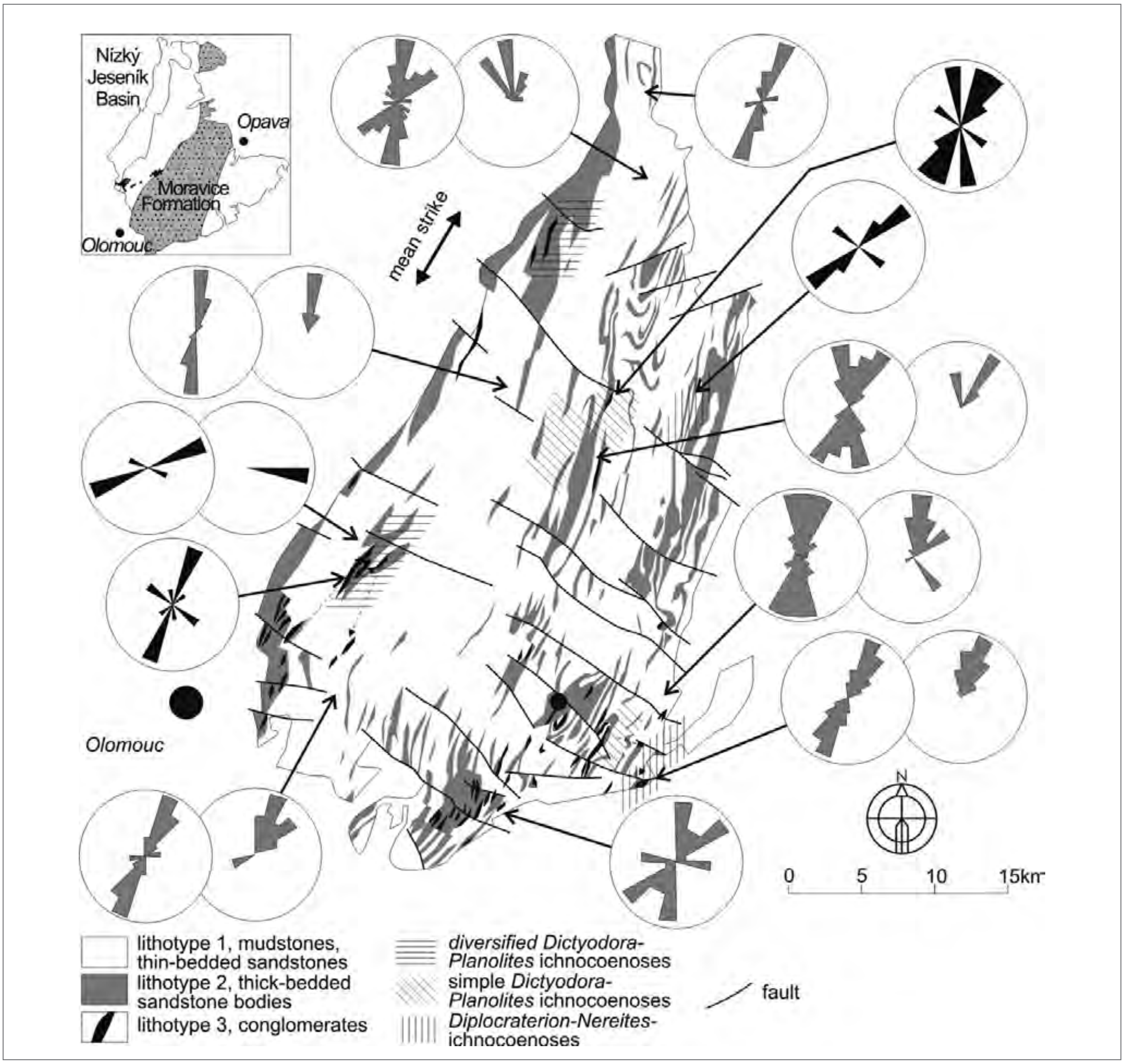

Fig. 4. Basic lithotypes, palaocurrent data and distribution of trace fossils in the Moravice Formation, Nízký Jeseník Culm Basin (adopted from Bábek *et al.*, 2004).

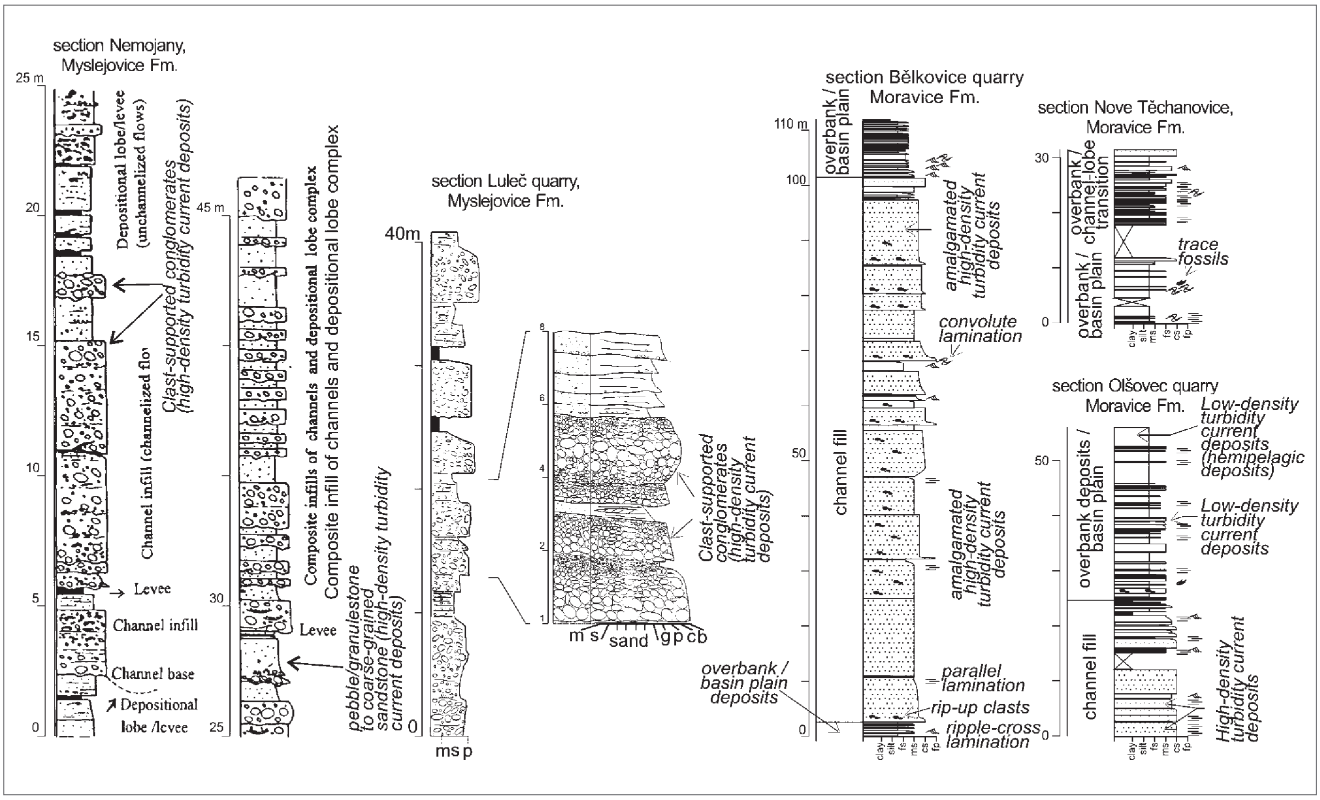

Fig. 5. Selected lihofacies columns across the MSCB in SW – to NE direction representing proximal (left) – to – distal (right) direction (adopted from Nehyba and Mastalerz, 1995; Hartley and Otava, 2001; Bábek *et al*., 2004).

ded with high-density turbidite sandstones (*F2a*, *F3a*, *F3b*). Channel-fill and channel-lobe transition deposits comprise high-density turbidites (*F1*, *F2a*, *F3a*, *F3b*) interbedded with minor low-density turbidites (*F4a*, *F4b*, *F5*) and occasional sandy debris-flows (*F2b*). Slope apron deposits are composed of quasi-steady turbidity current deposits (*F3c*) interbedded with low-density turbidity currents (*F4a*, *F4b*, *F5*) and occasional sandy debris flows (*F2b*). Lenticular sandstone bodies (depositional lobes) comprise high-density turbidite sandstones (F3a, F3b) interbedded with quasi-steady flow turbidites (*F3c*) and low-density turbidites (*F4a*, *F4b*, *F5*). Basin plain deposits comprise low-density turbidity current deposits (*F4a*, *F4b*, *F5*) and deep-water mudstones (*F6*). The proximal fan-delta deposits are developed almost uniquely in the southern part of the Drahany Basin, whereas the majority of the basin-plain deposits are developed in the Nízký Jeseník Basin, interbedded with the channel and sheet sandstone deposits (Fig. 5). This general grain-size trend, together with the NNE paleocurrent directions and sandstone composition data, indicate a predominant NNE sediment dispersal from point sources located in the Drahany Basin (Hartley and Otava, 2001), with minor sediment supply from the hinterland located in the present-day western direction (Zapletal, 1989; Bábek *et al*., 2004).

An overall cyclic alteration of the channel and sheet sandstone deposits, and the basin plain deposits, with megacycle thickness reaching several hundred metres, has been interpreted as a result of pulsating tectonic activity associated with switching of major point sources (Bábek *et al*., 2004).

The Moravice Formation (Nízký Jeseník Basin) comprises two asymmetric megacycles, each about 500 to 900 m thick. In their lower parts, the megacycles are composed of erosive low-efficiency, relatively coarse-grained turbidite systems indicating relative sea-level lowstand. The basal lowstand systems pass up-section into about twice as thick distal, low-efficiency turbidite systems. A combined tectonic-sediment supply model is suggested that explains the cyclic stratigraphy. Periods of increased tectonic activity resulted in slope oversteepening, probably combined with increased rate of lateral, W-E sediment supply into the basin, producing the basal sequence boundary and the subsequent lowstand turbidite systems. During subsequent periods of tectonic quiescence the system was filled mainly from a distant southern point source, producing the thick, low-efficiency turbidite systems (Fig. 6).

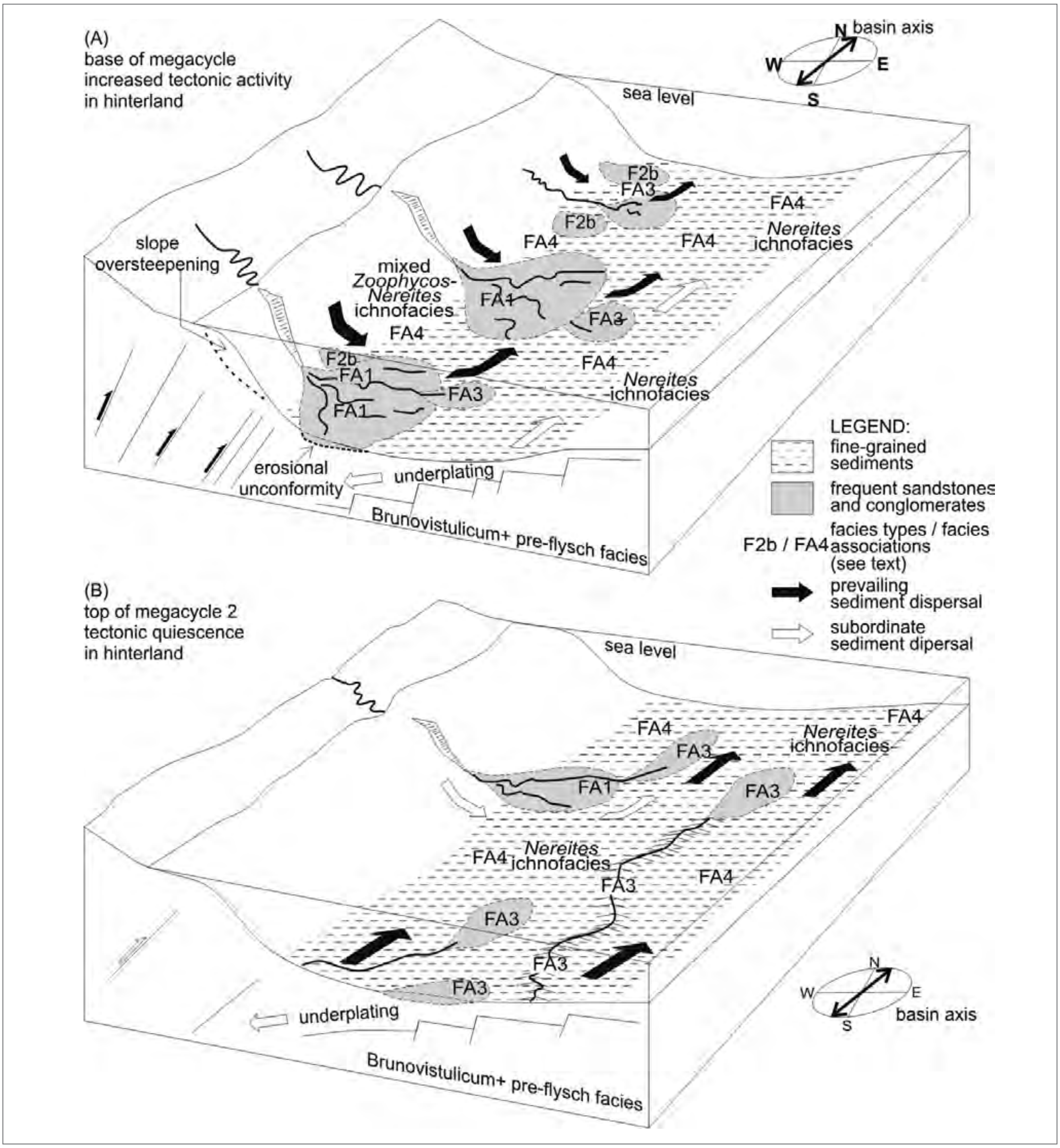

Fig. 6. Depositional model of the Moravice Formation, Nízký Jeseník Culm Basin.Basic lithotypes, palaocurrent data and distribution of trace fossils in the Moravice Formation, Nízký Jeseník Culm Basin (adopted from Bábek *et al.*, 2004).

Sediment composition and provenance

There is a wealth of sediment composition and provenance data in the literature, including modal composition of sandstones, clast analyses of conglomerate facies, heavy-mineral spectra, geochemistry and gamma-ray spectrometry (Hartley and Otava, 2001; Čopjaková *et al.*, 2003; Bábek *et al.*, 2004; Šimíček *et al.*, 2012). The data suggest that the lower part of the MSCB was derived mostly from mixed sedimentary- low-grade metamorphic-plutonic sources with minor proportion of volcanic sources (indicated mainly by potassium feldspars and polycrystalline quartz in the sandstones and volcanic and sedimentary lithic clasts in the conglomerates). The overall trend in this lower part is the up-section increase in concentrations of magmatic lithic clasts and quartz clasts due to increasing proportion of sediment derived from high-grade metamorphic rocks and magmatic rocks and decreasing supply from volcanic/low-grade metamorphic sources.

There is a distinct change towards higher concentrations of potassium feldspars in sandstones, accompanied by higher concentrations of U, Th and U/Th ratios in gamma-ray spectra and high sandstone radioactivity as compared to the mudstones in the Brumovice Beds (Goβ zone, Upper Viséan, Moravice Formation, Nízký Jeseník Basin). This indicates increased supply from plutonic sources, in particular the ultrapotassic plutonites of the Moldanubian nappe pile (durbachites).

Another provenance shift is associated with the onset of deposition of the Luleč Member (Myslejovice Formation, Drahany Basin) and Hradec-Kyjovice Formation (Nízký Jeseník Basin) approximately in the Goβto Goγ interval (boundary between the Middle and Upper Heavy Mineral Zone). The sudden shift towards quartz-rich conglomerate compositions at this boundary is thought to reflect even more significant supply from high-grade metamorphic terrains. This is supported by the published heavy mineral spectra (Hartley and Otava, 2001), in which high concentrations of pyrope and almandine suggest low sediment maturity and derivation from metamorphic sources. The same authors considered this compositional change to reflect a basin-wide progradation associated with sediment oversupply from the source areas. These compositional and GRS changes reflect extremely rapid exhumation of mid- and deep-crustal rocks of the Moldanubian Zone of the Bohemian Massif, which represented the major source area of the Nízký Jeseník Basin foreland basin.

Stop descriptions

A8.1 Mokrá active quarry, eastern part

Active quarry (Českomoravský cement, Heidelberg Cement Group) located 7 km NW of Exit 210 Holubice, D1 motorway between Vyškov and Brno. The Mokrá quarries are situated NE of Mokrá Horákov village. Access to the quarries requires permission from the quarry authorities. Safety hard hats and safety reflective vests are required. (S42: 49°13′39″ N, 16°46′30″ E)

Stratigraphy of the eastern part: Rozstání Formation, Drahany Culm Basin, upper Viséan Račice Member, Myslejovice Formation, Drahany Culm Basin, upper Viséan (Goα to Goβ Zone).

This quarry exposes basal parts of the MSCB at their contact with their pre-flysch formations. Across the MSCB, this contact is considered as diachronous and often modified by basal MSCB thrusts. However, in Mokrá quarry, this transition is syndepositional and relatively well dated by goniatite faunas.

The pre-flysch formations, represented by Devonian and Lower Carboniferous, mostly carbonate sequences of the Macocha Formation (carbonate platform) and Líšeň Formation (calciturbidites), are exposed in the Central and Western Mokrá quarries. Nevertheless, our interest is focused on the Culm Facies developed only in the Eastern Quarry, known also as „Břidla“ (the Shale). The oldest part of the Culm facies in this part of the MSCB belongs to the Rozstání Formation (heterolithics – rhytmic alternation of shales, siltstones and fine-grained sandstones) which is underlain by „transitional facies“ (Buriánek – Gilíková – Otava, 2013). We place the transitional type of sedimentation in time and space between calciturbidites of the Líšeň Formation and the typical Drahany Culm. The most distinct here is the facies of variegated, mostly red-brown shale, rich in trilobites of lower to middle Viséan age. The shale belongs to the Březina Formation, which has variable mineral and chemical composition, in particular the contents of calcium carbonate (CaO = 0.53 to 0.98 wt.%). Compared with the typical Culm facies shales, the clastic component of Březina shale exhibits a higher degree of chemical weathering. The ratio of Al to Na oxides mostly varies between 20 and 30 in the Březina shales, while the values in Culm shales are below 10 (Buriánek –Gilíková – Otava, 2013).

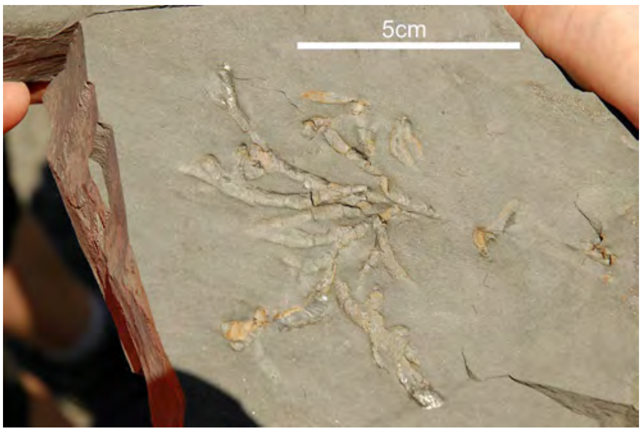

Fig. 7. *Chondrites* trace fossil in siltstones of the basal parts of Rozstání Formation, Mokrá Quarry.

The overlying Culm facies (Rozstání Formation) consists of grey siltstones and distal, thin-bedded turbidite sandstones with occasional trace fossils (*Chondrites*) (Fig. 7). The thickness of sediments of the typical Culm facies exposed in the eastern part of the Mokrá quarry does not exceed 50 m. It is often tectonically sliced and interbedded with carbonates of the Líšeň Formation, especially in its lower part.

Heterolithics of the Rozstání Formation are generally dipping eastwards, composed of interbedded siltstones (with normal grading) and shales mostly 2–5 cm thick, considered generally as distal turbidites.

Upper part of the eastern quarry face exposes fine- to coarse-grained, polymict conglomerates (Račice Member of the Myslejovice Formation), which alternate with the heterolithics. They are dated to Goα goniatite subzone of the upper Viséan, based on goniatite findings in the intercalated shales. The pebble assemblage of the conglomerates includes wide range of metamorphics (mostly gneiss), granitoids, volcanites and sediments (mainly limestones and greywackes) and less frequent quartz grains.

A8.2 Luleč active quarry

Active quarry (Českomoravský štěrk, a.s.) located 2.9 km WNW of Exit 226, D1 motorway between Brno and Vyškov, Czech Republic. The quarry is a property of Českomoravský štěrk, a.s. and it can be accessed only with a permission from the quarry owner. Hard hats and safety vests are necessary. (S42: 49°15′43″ N, 16°56′12″ E)

Stratigraphy and structure: Luleč Member, Myslejovice Formation, Drahany Culm Basin, upper Viséan (Goβto Goγ Zone) Structurally the area of the most important faunistic localities represents two large brachystructures – the Olšany Brachysyncline and the Luleč Brachysyncline.

About 400 m of quarry faces at five storeys expose >60 m thick body of proximal fan-delta deposits (Nehyba and Mastalerz, 1995). They are composed predominantly of coarse-grained, often inversely graded clast-supported conglomerates with sandy matrix. The conglomerate beds are about 2 to 3 m thick, lens like, rapidly pinching-out and containing outsized clasts (rafts) up to 2 m across (!). Conglomerate lenses alternate with several dm thick layers of coarse-grained sandstones in mega cross-bedding fashion. The basal bed contacts are sometimes erosive and associated with flute casts and load casts. Paleocurrent measurements indicate generally N- to NNE transport directions, which is in line with the proximal-distal facies relationships in the Upper Viséan MSCB.

Up-section the conglomerate facies grade into thick-bedded sandstones and finally into thin-bedded and fine-grained heterolithic facies, making up together an approx-

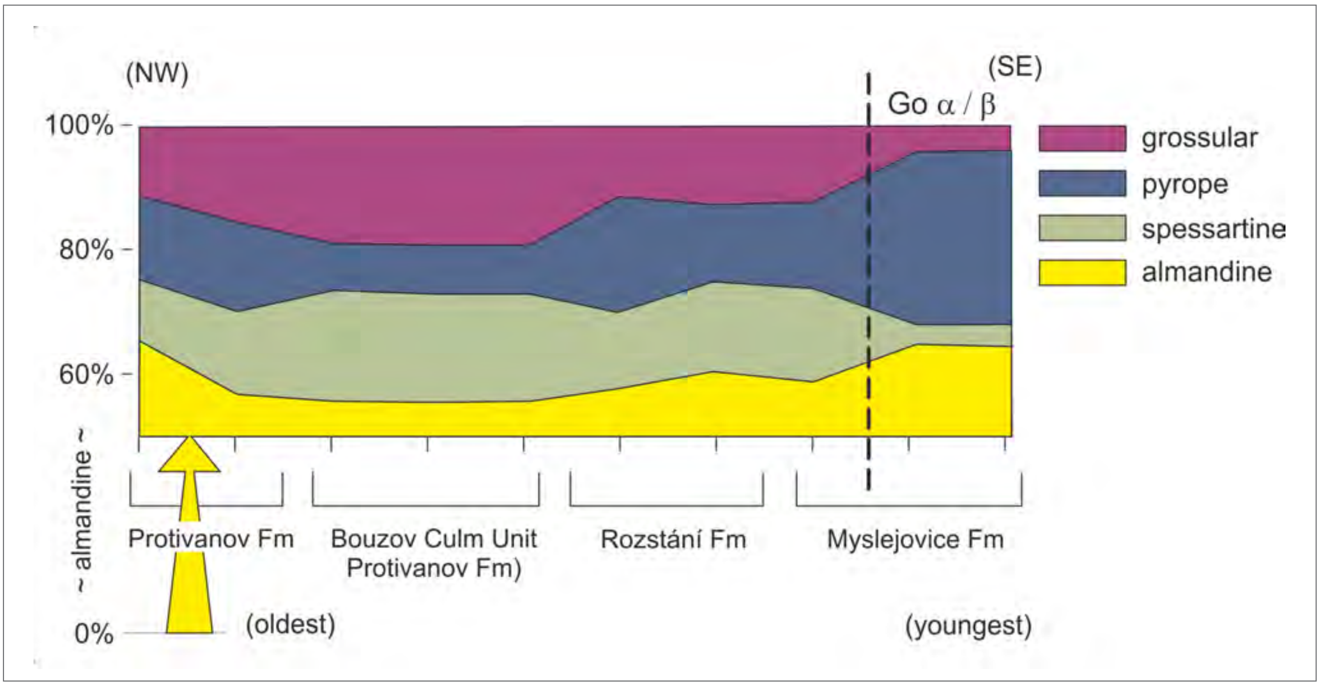

Fig. 8. Change in detrital garnet composition in the upper Luleč Member of the Myslejovice Formation reflects rapid increase in the contents of HT-HP granulites and garnet-bearing gneisses in the source area (Otava, unpublished).

imately 150 m thick succession. The conglomerate facies are interpreted as channel-fill, channel-levee and channel-lobe transition deposits of proximal, coarse-grained fan delta. The sandstone facies are thought to represent depositional lobes (Nehyba and Mastalerz, 1995).

The conglomerates are composed predominantly of igneous and high-grade metamorphic rocks typical of the Moldanubian unit of the Bohemian Massif, including ultrametamorphics (granulites). Heavy mineral spectra from siliciclastics of the Luleč Member in general are dominated by pyrope-almandine garnets poor in LREE, showing enrichment in HREE. Their chondrite-normalized patterns are almost flat from Dy to Lu showing a significant negative Eu anomaly, typical for granulite-grade garnets. Major element compositions of detrital low-grossular pyrope-almandines can only be matched with some granulites and garnet-bearing felsic gneisses of the Bohemian Massif. Garnets from granulites cropping out at the present-day erosion level of the Bohemian Massif usually have higher Ca and/or lower Mg contents (Čopjaková *et al.*, 2005). The Luleč Member therefore sensitively picks up the change in drainage area related to the late Viséan unroofing of the Moldanubian and Moravian nappe pile.

The Luleč conglomerate, which is the youngest member of the Drahany Culm subbasin, is underlain by polymict Račice conglomerates of Upper Viséan Goα age. The gradual change in pebble composition up-section, i.e. from the Račice to the Luleč conglomerate, reflects the following general changes in composition of the source area: (i) decrease in sedimentary rocks; (ii) decrease in effusives and intrusives; (iii) decrease in quartz, and (iv) increase in metamorphics, especially of HP-HT varieties, e.g. granulites. The changes in pebble composition were accompanied by changes in detrital garnet assemblages, form the predominance of spessartine-almandines, grossular-almandines and pyrope-almandines in the Račice Member, to pyrope-almandine in the Luleč Member (Fig. 8)

A8.3 Bělkovice Quarry

Active quarry (Českomoravský štěrk, a.s.) located 5.6 km ESE of the Šternberk railway station, Czech Republic. This is an active quarry, which is normally closed for visitors without permission from the quarry owner. Safety vests and hard hats are necessary. (S42: 49°42′09″ N, 17° 01′30″ E)

Stratigraphy: Bohdanovice Member, Moravice Formation, Nízký Jeseník Culm Basin, upper Viséan (Goα Zone).

The active, six-storey quarry (dimensions ~400 x ~300 m) is open in the Bohdanovice Bed, a basal member of the Moravice Formation. It exposes extremely thick beds of coarse-grained sandstones of facies *F3b* (Fig. 5). Individual beds are massive and usually normally graded at the tops, sometimes coarse-tail graded at the bottom. Thickness of sandstone units may reach up to 15 m, but they often represent multiple amalgamated turbidite events as indicated by occasional erosive basal contacts and abundant mud intraclasts (rip-up clasts) in multiple levels above the unit bases. Nearly one hundred m thick succession of *F3b* beds is exposed in a prominent anticlinal structure at the fourth floor of the quarry. The basal contact of the sandstones with the underlying succession of heterolithics, mostly low-density turbidites and thin mudstone layers, is sharp and emphasized by a layer of rip-up clasts. Upwards, the sandstone succession passes into heterolithics again but this passage is gradual, fining upward. Although the geometry of the sandstone succession is largely unknown due to limited exposure, it is interpreted as a channel-fill succession, owing to the numerous signs of sediment erosion, FU trend in its upper part, abundant internal scours, rip-up clasts and amalgamation implying high erosive competence of the sediment flows.

The Moravice Formation is composed of two megacycles, each about 500 to 900 m thick. The megacycles start with 50- to 250-m-thick, basal segments of erosive channels: overbank successions and slope apron deposits interpreted as lowstand turbidite systems. Up-section they pass into hundred metre-thick, fine-grained, low-efficiency turbidite systems. The Bělkovice quarry exposes basal parts of the lower megacycle, which was supplied from point sources located laterally to the basin axis, in the present-day west.

A8.4 Malý Rabštejn and "Railway section" near Domašov nad Bystřicí

About 60 m high natural cliff in the bend of the Bystřice River located 1.9 km SSE of the Domašov nad Bystřicí railway station. The cliff is situated in the deeply incised valley of the Bystřice River. It forms a natural landmark and a training site for rock climbers. From the cliff we will take a short hike (about 3 km) along the river to observe various turbidite facies in a series of several smaller outcrops and in a big inactive quarry ("railway section" near Domašov nad Bystřicí). (S42: 49°43′21″ N, 17°27′04″ E)

Stratigraphy: Bohdanovice Member, Moravice Formation, Nízký Jeseník Culm Basin, upper Viséan (Goα Zone).

The Malý Rabštejn cliff exposes a succession of massive, coarse-grained sandstones with occasional rip-up clasts and parallel lamination (facies *F3a* and *F3b*), which alternate with normally graded, fine- to medium grained conglomerates and pebbly sandstones (facies *F1* and *F2a*). The conglomerate beds typically have basal layers rich in rip-up mudstone intraclasts

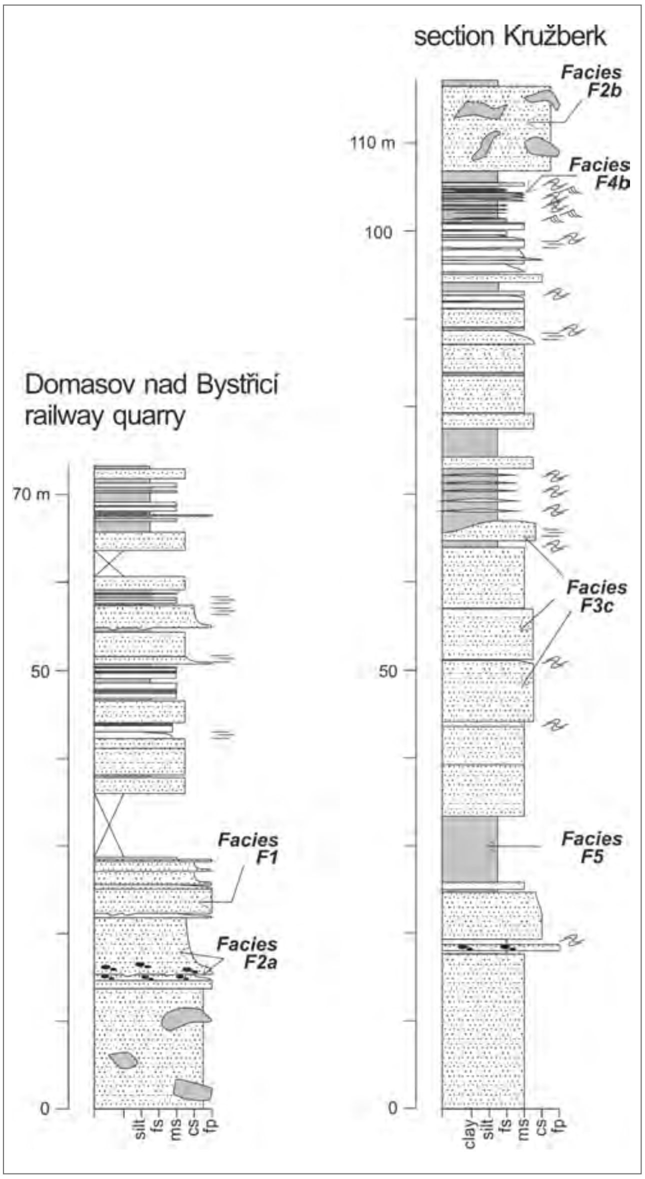

Fig. 9. Representative lithological logs of the "railway section" near Domašov nad Bystřicí (left) and Kružberk dam (right) (adopted from Bábek *et al.*, 2004).

and some of them show erosive bases with large-scale flutes. The abundant evidence for erosion suggests that this is a channel-fill body, composed predominantly of high-density turbidity current deposits. The uppermost part of the cliff shows a fining-upward succession into heterolithics and very thinly laminated siltstones, which are rich in trace fossils of the Zoophycos- and mixed Zoophycos – Nereites ichnofacies. Most abundant are the following ichnotaxa: *Chondrites* isp., *Phycosiphon incertum*, *Planolites beverleyensis*, *Planolites* isp. and more rarely *Cosmorhaphe timida*, *Chondrites* cf. *intricatus*, *Falcichnites lophoctenoides*, *Pilichnus* isp., *Protopaleodictyon* isp, *Spinorhaphe rubra* and *Zoophycos* isp. (Zapletal and Pek, 1998).

The Malý Rabštejn section is a part of large-scale, multi-storey submarine channel body, in which coarse-grained facies alternate with fossiliferous heterolithics and even black shales. A similar succession is exposed in the nearby "railway section" in Domašov nad Bystřicí (Fig. 9). The intercalated fossiliferous heterolithic layers are exposed in the uppermost parts of the Malý Rabštejn section see above) and in section "Bělský mlýn" located about 300 m E of Malý Rabštejn. The channel-fill succession belongs to the same basal segment of the first megacycle of the Moravice Formation, which is exposed in the Bělkovice quarry (stop 3).

A8.5 Skoky

About 260 m long road cut located 3.8 km ESE of Exit 290, D1 motorway between Olomouc and Hranice. This section is situated along a local road with infrequent traffic. Reflective vests will be provided for safety. (S42: 49°32′56″ N, 17°32′03″ E)

Stratigraphy: Brumovice – Vikštejn members, Moravice Formation, Nízký Jeseník Culm Basin, upper Viséan (Goβ Zone).

This outcrop exposes nearly 200 m thick succession at the passage from coarse-grained facies to very thick succession of fine-grained heterolithics and shales. The basal parts of the section consist of several-m thick layers of massive and/or normally graded, coarse-grained sandstones (facies *F3a*). They may represent outer reaches of distributary channels or sandstone lobe deposits. In this particular case, closer interpretation is extremely difficult. This succession passes upward into dm-thick layers of medium-grained sandstones, often parallel-laminated, wavy-laminated and convolute-laminated (*F4b*), alternating with thin siltstone interlayers. The sandstone beds often exhibit base-cut-out Bouma sequences ($T_{b,c,d}$). Frequent convolute lamination present in facies *F4b* suggests rapid suspension settling and water escape, which may be associated with deposition in proximal, high-energy channel-overbank environments. Upwards, this succession passes into monotonous unit composed almost solely of siltstones and shales, which is crosscut by several faults. The whole section is a good example of fining- and thinning-upward trends, which occur ubiquitously throughout the Moravo-Silesian Culm Basin. Of special interest is the variety of wavy and convolute lamination in facies *F4b* and the overlying thick shale succession.

Modal composition of sandstones reveals their relative low mineral and textural maturity, which is characteristic for synorogenic siliciclastics. Average contents of framework components (quartz, feldspars and lithic clasts), recalculated to sum 100%, show dominancy of quartz grains (59%) over feldspar grains (33%) and lithic clasts (8%). Ratio of polycrystalline/monocrystalline quartz is up to 2:1. Potassium feldspars strongly dominate. Plagioclase grains, mainly albite, are rare and usually altered. Lithic clasts group contains mainly fragments of plutonic and high-grade metamorphic rocks, such as gneisses, granitoids and durbachites. Clasts of acid volcanic rocks and sediments (mainly siltstones and shales from older Culm strata) are rare. In addition, micas are abundant non-framework minerals (more or less chloritized biotite flakes prevail over muscovite). Silty-to-clayey sandstone matrix is fine-grained derivative of framework grains (quartz, feldspars), supplemented with chlorite, sericite, clay minerals and heavy minerals. In QFL ternary diagrams of Dickinson *et al.* (1983) most of samples plot near the boundary between transition continental and recycled orogeny provenance field. Relative low mineral maturity and preservation of less stable components in sandstones indicate rapid deposition and short transport of clastic material due to high topographic gradient, which eliminated effects of chemical weathering and selective hydrodynamic sorting (Šimíček *et al.*, 2012).

Relatively high contents of less stable components of sandstones, which can carry radioactive K (K-feldspars, micas, components of sandstone matrix) and U and Th (especially heavy minerals such as zircon, thorite, monazite, xenotime and secondary REE-minerals contained in durbachite clasts and within the sandstone matrix) are responsible for "inverse" nature of spectral gamma-ray signal in siliciclastic sediments. Gamma-ray spectrometry was originally utilized as indicator of fine-grained lithology with high contents of clay minerals, which usually reveal higher values of radioactivity compared to sandstone facies. However, greywackes of the Brumovice member are more radioactive than mudstones from the same stratigraphic levels. The average concentrations of radioactive elements in sandstones at Skoky are 19.8 ppm of Th, 6.7 ppm of U and 2.9% of K. Average values in mudstones are 16.2 ppm of Th, 4.9 ppm of U and 4% of K (Šimíček *et al.*, 2012).

Fossils are rare and usually not well preserved in Skoky. Lehotský (2002) described bivalve *Posidonia becheri* and horsetail *Archaeocalamites scrobitulatus*. More frequent are trace fossils, which belong to the simple Dictyodora–Planolites ichnocoenosis (*Dictyodora liebeana*, *Planolites* isp. and *Planolites beverleyensis*). This ichnocoenosis is characteristic for deep marine environment with extremely low energy and low content of nutrients (Bábek *et al.*, 2004).

A8.6 Hrabůvka quarry

Active quarry (Českomoravský štěrk, Heidelberg Cement Group) located 2.5 km E of Exit 308 Hranice, D1 motorway between Hranice and Lipník nad Bečvou. This is an active quarry – permission from quarry owner is required. Hard hats and reflective vests are necessary. (S42: 49°34′38″ N, 17°41′51″ E)

Stratigraphy: Vikštejn Member, Moravice Formation – or perhaps basal parts of Hradec–Kyjovice Formation, Nízký Jeseník Culm Basin, upper Viséan (Goβel to Goβmu or even Goγ).

The active, six-storey quarry (dimensions ~800 x ~ 350 m), which exposes the uppermost part of the Moravice Formation, is situated near the fault line separating outcrop area of the Nízký Jeseník Culm and Moravian Gate trough.

Several species of goniatites have been described at this locality (*Nomismoceras vittiger*, *Goniatites* sp., *Arnsbergites falcatus* and *Paraglyphioceras elegans*) and they mostly indicate goniatite sub-zones Goβel to

Goβmu, which correspond with the Vikštejn Member of the Moravice Formation. However, the presence of *Neoglyphioceras spirale* indicates, that part of the section may belong to the goniatite sub-zone Goγ and so to the Hradec Member of the Hradec-Kyjovice Formation (Lehotský, 2008). However, goniatites are rare and usually not well preserved. More frequent are trace fossils at the surfaces of greywacke lenses. Similarly to the Olšovec quarry, species of relatively shallow water, Cruziana (*Diplocraterion* isp. and *Rhizocorralium* isp.) and deep water, Nereites (*Dictyodora liebeana* and *Planolites* isp.) ichnofacies are present (Bábek *et al.*, 2004).

The dominant part of the section is formed by ~10 m thick lenticular coarse-grained sandstone bodies (facies *F3a–b*) interbedded with fine-grained sandstones and mudstones (facies *F4a–b* and *F5*). The lack of amalgamation surfaces, lower average bed thickness, small size of mudstone rip-up clasts, absence of internal compensation cycles and dominance of sandy-rich facies over mud-rich facies allow to interpret this facies stacking pattern as channel-lobe transition deposits (Mutti and Ricci Lucchi, 1972) or infills of shallow channels parallel with basin axis (Bábek *et al.*, 2004). Near the base of the section is present a sedimentary succession predominantly formed by low-density turbidites (facies *F4a–b* and *F5*) and deposits of hemipelagic suspension (facies *F6*). They represent outer submarine fan settings (lobe fringe) or channel levee environment. In the upper part of the section we can observe ~10 m thick facies stacking patterns formed by facies *F1*, *F2* and *F3a–b*. Facies *F4a–b* and *F5* are in minority. Blocky-to-fining upward cycles, overall coarse-grained lithology, frequent basal scours, amalgamation surfaces and large mudstone rip-up clasts indicate deposition within proximal, erosional or mixed erosional-depositional channels during their progressive migration (Mutti and Ricci Lucchi, 1972; Reading and Richards, 1994; Shanmugam, 2006).

Analyses of pebble assemblages in fine-grained conglomerates reveal high contents of metamorphic rocks (47%), supplemented with magmatic (29%) and sedimentary (24%) rocks (Gilíková *et al.*, 2003). The most abundant metamorphic rocks are orthogneiss, phyllite and quartzite. Pebbles of granites predominate among the magmatic rocks. However, clasts of acid-to-intermediate volcanic rocks are also abundant. Pebbles of sedimentary rocks are usually represented by rocks from older Culm strata (basin cannibalism). The arenites can be characterized as lithic and litho-feldspathic greywackes. Composition of lithic fragments in greywackes corresponds with the above mentioned composition of pebble assemblages. Matrix of the greywackes is a mixture of detrital quartz, feldspars, sericite and clay minerals. Arenites from Hrabůvka quarry are characteristic by variable textural and low mineral maturity which is typical for sediments of the Brumovice and Vikštejn members of the Moravice Formation. From the geotectonic point of view, the main sources of clastic material were identified in the recycled orogene (Maštera, 1997; Gilíková *et al.*, 2003).

Paleocurrent data correspond with direction from SW to NE, which is consistent with elongation of the MSCB and the confirm the axial-trough topography of the basin (Hartley and Otava, 2001; Bábek *et al.* 2004).

Hydrothermal polymetallic mineralization (galena, sphalerite, chalkopyrite, tetraedrite and Ag-minerals) was previously described in the quartz-dolomite veins (Slobodník and Dolníček, 2001).

A8.7 Olšovec

Abandoned quarry located about 600 m NW from the chapel in Olšovec, about 2.9 km NNW of Exit 308, D1 motorway between Olomouc and Ostrava. This section is located in an abandoned quarry, which is partly filled with water, providing a favourite bathing and fishing place for local people. (S42: 49°35′56″ N, 17°42′39″ E)

Stratigraphy: Vikštejn Member, Moravice Formation – or perhaps basal parts of Hradec – Kyjovice Formation, Nízký Jeseník Culm Basin, upper Viséan (Goβel to Goβmu or even Goγ).

The lowermost 12 m of the section is submerged. Above the water level, an about 15 m thick succession of several m thick beds of coarse-grained, massive sandstones (*F3a* facies) is exposed, which is assumed to represent high-density turbidity current deposits. They are intercalated by thin layers of medium- to fine-grained, cross and convolute stratified sandstones deposited from low-density turbidity currents. These facies are characterized by a relatively lower proportion of amalgamation surfaces and a lack of mudstone intraclasts. The facies architecture and lithological marks probably document deposition at the mouths of distributary channels or as axial channel fills. From the middle to the upper part of the section, a fining-upward trend can be observed in the vertical facies succession. The predominant heterolithic sediments are intercalated with thin layers of massive and normally graded fine- to medium-grained greywackes, sometimes with cross- or wavy lamination. Flute marks, groove marks and load casts are frequent at the bases of the greywacke beds. Heterolithic sediments represent deposition from low-density turbidity currents and bottom currents at distal parts of continental slopes. Greywacke beds can be interpreted as sandstone lobes of an outer submarine fan (Bábek *et al*., 2001).

Gamma-ray logging of the Olšovec section (Fig. 10) revealed that the facies dependence of the gamma-ray signal (in particular Th and K) is weak. This is a typical pattern for the lower parts of the Moravice Formation, which is caused by low compositional contrast between framework grains and matrix in greywackes and, in general, low chemical maturity of the siliciclastic material.

The fine-grained upper parts of the section are rich in paleontological material. In spite of their generally low preservation, several species of goniatites (*Neoglyphioceras spirale, Hibernicoceras kajlovencense, Sudeticeras crenistriatum*), bivalves (*Posidonia becheri*) and crinoids (*Cyclocaudiculus edwardi*) were described from the locality. Fossil flora predominantly includes fragments of horsetail *Archaeocalamites scrobitulatus* (Zimák *et al*., 1995). Trace fossils are frequently preserved on the contacts of greywacke beds and include the ichnospecies: *Cosmoraphe kettneri*, *Rhizocorallium* sp., *Diplocraterion parallelum* (U-shaped burrows), *Dictyodora liebeana* (meandering), *Nereites missouriensis*, *Chondrites indricatus* and *Planolites* sp. (Lehotský, 2008). The presence of specimens typical for both relative shallow-water, Cruziana ichnofacies (*Rhizocorallium*, *Diplocraterion*) and deep-water, Nereites ichnofacies (*Dictyodora, Cosmoraphe, Nereites*) can be explained by either characteristics of the environment, which allowed existence of both groups or by periodic oxygenation of bottom, coupled with supply of nutrients and coarse-grained clastic material.

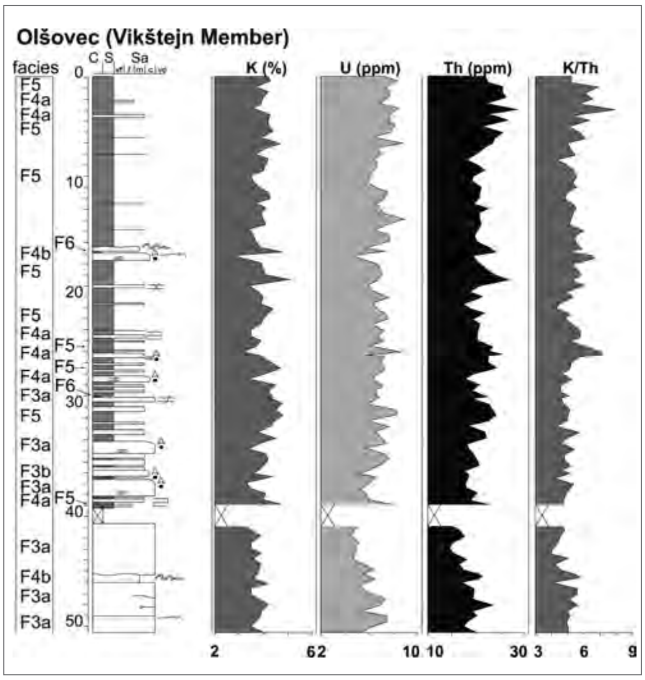

Fig. 10. Lithological and gamma-ray spectrometry logs of the Olšovec quarry (Šimíček *et al*., 2012). Note relatively poor gamma-ray representation of the prominent fining-upward trend.

Hydrothermal mineralization occurs in cracks and contains mainly calcite and quartz. Chlorite (clinochlore-chamosite) and pyrite were also described, but their occurrence is rare.

A8.8 Budišov nad Budišovkou

Abandoned quarry on the right side of a local road from Budišov nad Budišovkou to Stará Libavá, about 26 km SW of the centre of Opava. The quarry is used as a shooting range and it is closed for public. Permission for access is required. (S42: 49°48′03″ N, 17°36′10″ E)

Stratigraphy: Cvilín Member, Moravice Formation, Nízký Jeseník Culm Basin, upper Viséan (lower part of Goβ subzone).

A succession of thin-bedded, sheet-like turbidite beds is exposed in this abandoned quarry. The predominating facies type is fine-grained, normally graded sandstone with $T_{a,b,c}$ Bouma sequences or incomplete (base-cut-out) Bouma sequences, which are interpreted as sediments

Fig. 11. Example of tool marks from basin-plain deposits at the Budišov nad Budišovkou section.

of distal low-density turbidity currents, deposited in a basin plain environment. Bed bases are exposed in several instances, showing well-developed tool marks, flute casts and bounce casts (Fig. 11). The paleocurrent data show predominant SSW to NNE flow directions, often combined with S to N directions. These patterns can be observed throughout the MSCB, indicating axial-trough topography of this deep marine foreland basin.

A8.9 Slezská Harta

A road-cut ca. 260 m long along road 452 between Leskovec nad Moravicí and Bílčice. This section is situated just next to the dam of the Slezská Harta reservoir – one of the biggest reservoirs in North Moravia. The section itself is situated along one of the main roads and caution is needed when moving along the section. Reflection vests will be provided. Coordinates (S42: 49°53′29″ N, 17°35′06″ E)

Stratigraphy: Bohdanovice Member, Moravice Formation, Nízký Jeseník Culm Basin, upper Viséan (Goα Zone).

This section exposes a fine-grained succession of the Bohdanovice Member, comprising dark grey siltstones and mudstones alternating with thin laminae of fine-grained turbiditic sandstones, facies F5 and F6. The fine-grained sediment is very well preserved including mm-thick lamination. The turbiditic laminae are typically 0.5 to 2.5 cm thick, normally graded, parallel- or ripple-cross laminated. The bed bases are sharp and often associated with very prominent load casts. The extreme sediment loading results in numerous cases in bed contortion, thinning of laminae and development of load balls. This is a good example of synsedimentary and early post-sedimentary deformation due to loading in distal fine-grained turbidites. This facies is devoid of body- and trace fossils, presumably due to high sediment accumulation rates.

Situated several kms from the locality there are young, Plio-Pleistocene volcanic rocks, which include lava flows of alkali basanite and related rocks, thick layers of pyroclastic material (scoria) and lacustrine volcaniclastic sediment (including relics of maars). They are related to the deep-seated faults of the upper Elbe fault system and represent one of the youngest volcanic rocks in the Bohemian Massif. A big quarry in Bílčice, about 2 km away from the locality, exposes an instructive lava flow with thick columnar jointing.

A8.10 Kružberk

Natural outcrop in the Moravice River valley, about 400 m ENE of the Kružberk reservoir dam. The section is located in a scenic valley. Cliffs at the section are frequently used by rock climbers. Coordinates (S42: 49°49′28″ N, 17°40′3″ E)

Stratigraphy: Basal part of the Brumovice Member, Moravice Formation. Nízký Jeseník Culm Basin, upper Viséan (lower part of Goα subzone).

This section exposes a somewhat unusual sedimentary succession in the MSCB, comprising up to several m thick, massive, granulometrically uniform sandstones with occasional convolute- and parallel lamination in the upper parts of beds (facies *F3c*) (Fig. 9). The beds have flat, non-erosive contacts and sometimes lateral pinch-out geometry with concave-up tops. The absence of grading and unusual bed thickness may indicate deposition from quasi-steady hyperpycnal flows that may owe their origin to fluvial discharge (Kneller and Branney, 1995), in contrast to surges and surge-like turbidity flows, which, unless ponded, do not produce thick sediment layers (Rothwell *et al.*, 1992). Convex-upward shape and lateral pinch-out geometry of the beds of facies *F3c* can be attributed to deceleration of hyperpycnal currents, loss of momentum and rapid deposition associated with a decrease in slope gradient (hydraulic jump). Any alternative hydrodynamic interpretation of these beds is open to discussion at the locality and will be highly welcome.

These beds occur in association with conglomerates rich in outsized clasts (*F2b*), interpreted as sandy debris flows and heterolithic facies including sediments of low-density turbidity flows (*F4b*). This facies association is present in laterally continuous sand-rich units. Thicker mudstone-dominated successions, the presence of sandy debris flows and their distribution in form of laterally incoherent bodies, have been reported as indicative of slope or base-of-slope deposition (*cf.* Shanmugam and Moiola, 1995). Similarly, deposits of quasi-steady turbidity currents have been reported from slope apron settings (Plink-Björklund *et al.*, 2001) or indicating a close link to shelf-edge river systems (Sinclair, 2000; Mulder *et al.*, 2001). The blocky cycle and fining-upwards cycle organisation of these deposits reflect filling of smaller-scale channels probably connected to a shelf-edge river system. Unusually high bed thickness and pinch-out geometry of the quasi-steady turbidity current deposits of *F3c* (see above) may reflect deposition in settings with significant decrease in bathymetric gradient, where the turbidity currents underwent hydraulic jumps (*cf.* Mutti and Normark, 1987; Weimer *et al.*, 1998). Deposition in lower reaches of a slope apron setting or in a topographically complex slope setting (slope basins) is inferred for the Kružberk section.

The basal parts of the Brumovice Member in Kružberk are characterized by extremely high concentrations of radioactive elements, U, Th, K, especially in the sandstone facies. The major carriers of the GRS signal, observed in optical microscopy, CL microscopy and WDX SEM include K-feldspars, muscovite, sericite, biotite and albite for K; zircon, apatite, monazite and xenotime for U and monazite, thorite, REE secondary minerals, xenotime, apatite and zircon for Th.

This particular stratigraphic level reflects a sudden, early Late Viséan (330 – 335 Ma; Fig.12) shift from low-grade metamorphic, volcano-sedimentary provenance to predominantly magmatic sources with ultrapotassic plutonites (= durbachites) showing Moldanubian (Lugo-Danubian) affinity (Šimíček *et al.*, 2012). This change is associated with facies shift to coarse-grained turbidite systems at the base of the second megacycle of the Moravice Formation (Bábek *et al.*, 2004).

A8.11 Vítkov – Annina dolina

Abandoned quarry + several outcrops along the quarry access road, located about 4 km NE from the crossroads of 442 and 462. (S42: 49°48′24″N, 17°46′43″ E)

Stratigraphy: Hradec Member, Hradec–Kyjovice Formation, Nízký Jeseník Culm Basin, upper Viséan to lower Namurian (Goγ to E1).

Abandoned shelf quarry (dimensions ~ 170 x ~ 50 m) is located in the central part of the Moravice river Natural Park. It is lectostratotype locality of the coarse-grained facies stacking patterns in the basal part of the Hradec–Kyjovice Formation, which is known as "Nýtek conglomerate horizon" (Kumpera, 1976). In the quarry, and on numerous outcrops along its access road, binominal conglomerate-greywacke rhythmic interbedding can be seen. The thickness of conglomerate beds varies from several dm up to 5 m. We can observe medium- to fine-grained clast-supported conglomerates (facies *F1*) and fine-grained matrix-supported conglomerates to pebbly sandstones (facies *F2a–b*). All conglomerate facies have unsorted coarse-grained greywacke matrix. The average size of clasts varies between 3 and 5 cm in α clast-axis. However, you can find floating outsized clasts up to 20 cm in the longest clast-axis, especially in facies *F1*. Also large mudstone rip-up clasts (up to 80 cm) are present

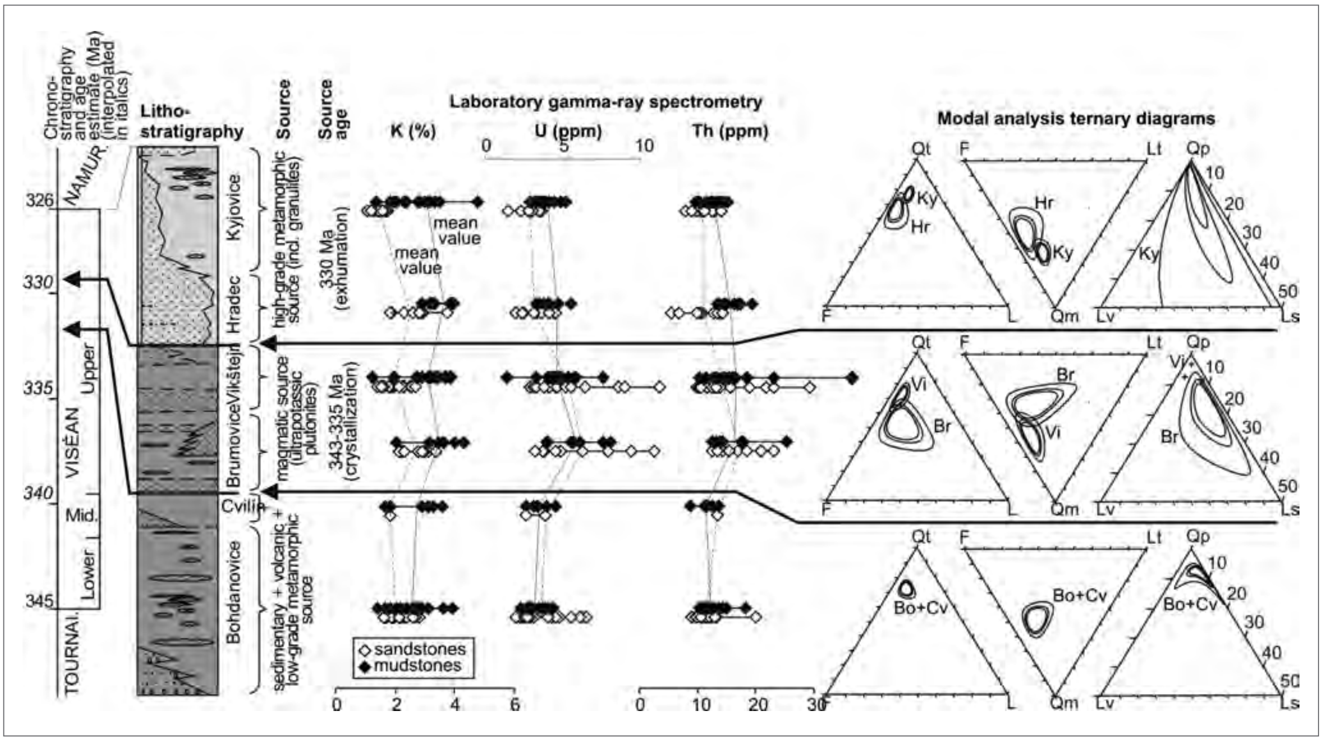

Fig.12. Stratigraphic distribution of gamma-ray spectrometric concentrations in sandstones (white diamonds) and mudstones (black dots) of the MSCB. (Šimíček *et al.*, 2012).

in facies *F2a–b*. Roundness of clasts can be described as subangular to subrounded. The beds are usually massive or normally graded. Occasionally, inverse grading can be observed above the base and planar stratification near the top of some beds. The load casts (up to 20 cm deep) are often developed at the base of conglomerate beds. The thickness of arenitic beds ranges from several dm to 10 m. They are mostly coarse- to medium-grained, massive (facies *F3a*) or normally graded with planar, cross or convolute stratification near the top of beds (facies *F3b*). Mudstone rip-up clasts can be observed above the base of some beds. Traction carpets are developed at the base of some greywacke beds. The presence of internal erosional surfaces and mudstone rip-up clasts within some beds indicates amalgamation. Packets of sandstone-conglomerate beds are separated by thin fine-grained sedimentary successions formed by mudstones (facies *F6*), heterolithic facies (facies *F5*) and thin bedded fine-grained sandstones corresponding to the Tcd division of Bouma sequence (facies *F4b*) (Šimíček *et al.*, 2012).

This sedimentary succession is an example of channel-fill sedimentation, which is characterized by presence of coarse-grained sedimentary facies, several m thick, sometimes amalgamated beds and deep load casts at the base of beds. Higher portion of normally graded sandstone facies indicates deposition in the proximal part of a distributary channel, close to the boundary between the inner and central parts of a submarine fan system (Mutti and Ricci Lucci, 1972; Reading and Richards, 1994; Shanmugam, 2006). Paleocurrent data indicate dominant directions from NNW to SSE, which roughly correspond with the N–S elongation of the MSCB, but some paleocurrent indicators in conglomerate facies show almost perpendicular, W to E direction (Dvořák, 1994). Composition of rock pebbles is strongly polymict. Most pebbles belong to quartz, garnet and muscovite-biotite gneisses, biotite granodiorites and acid-to-intermediate volcanic rocks, supplemented with quartzites, mica-schists and greywackes (Maštera, 1975). Arenites can be generally described as sublitharenite, but sandstones with subarcose composition are also abundant. The average content of quartz is 60%, feldspars 29% (K-feldspars prevail over plagioclases) and lithic clasts 11%. Among the lithic group, clasts of gneiss, granite and acid volcanic rocks predominate, which is consistent with the above-mentioned composition of pebble assemblages from conglomerates (Maštera, 1975; Šimíček *et al.*, 2012). Cathodoluminescence microscopy revealed abundant contents of volcanic quartz in sandstones of the Hradec Member (red-to-pink CL-colour; Fig. 13). The QFL data plot mainly within the recycled orogene provenance field in ternary diagrams of Dickinson *et al.* (1983).

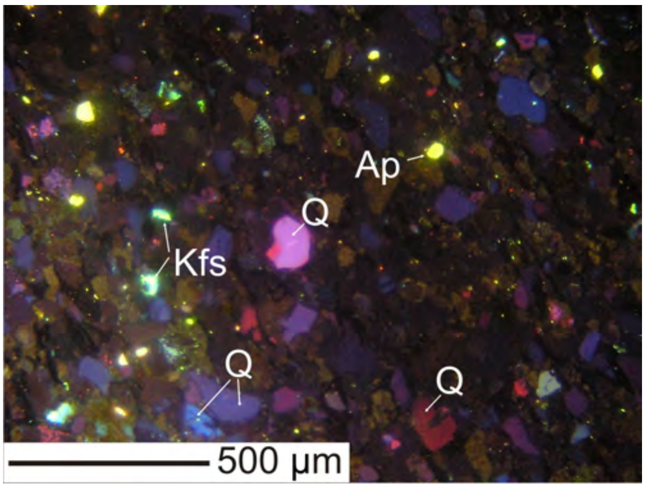

Fig. 13. Photomicrograph from cathodoluminescence microscope which shows relative abundance of quartz grains with red-to-pink CL-colour indicating their volcanic source.

Minerals of garnet group form the dominant portion in the heavy mineral assemblages. In several samples, garnets form up to 80% of all grains (cf. Maštera, 1975; Hartley and Otava, 2001). Apatite, tourmaline, zircon and sphene are also relatively abundant heavy minerals. Whole-rock chemical analyses of mudstones revealed high contents of Al_2O_3 (20–25%), MgO (4.5%) and MnO (up to 1%). The ratio of Al_2O_3/Na_2O indicates deposition of mainly fresh, chemically unweathered material (Maštera, 1975). The spectral gamma-ray logging shows only a weak effect of facies changes on variations in K, U and Th concentrations. It is most probably due to low compositional contrast between different facies related to the low mineral, chemical and textural maturity of sediments. High contents of feldspars, lithic fragments, silty-to-clayey matrix and low contents of non-radioactive quartz grains are responsible for relatively high radioactivity of sandstones, which is very close to values obtained from the mudstones (Fig. 12). Hence, usefulness of gamma-ray spectrometry as indicator of lithological changes is very limited at the base of the Hradec–Kyjovice Formation. Overall coarse-grained nature of sediments, low maturity of sandstones and mudstones in combination with low spectral gamma-ray contrast between different facies indicate short transport and rapid deposition of clastic material due to extreme uplift and erosion of the source area (cf. Hartley and Otava, 2001; Šimíček, *et al.*, 2012).

The frequent hydrothermal veins, which penetrate greywacke beds are composed of quartz, calcite and chlorite, sometimes even minerals of clinochlore–chamosite series occur. The thickness of veins is up to 10 cm. An interesting technical relic – a wooden discharge hopper – is preserved in the quarry .

Stop 12 Stará Ves

Abandoned quarry located about 520 m E of the chapel in Stará Ves near Bílovec, about 5.4 km NNW of Exit 336, Dl motorway between Olomouc and Ostrava. This is an easily accessible abandoned quarry. (S42: 49°46′14″ N, 17°58′56″ E)

Stratigraphy: Kyjovice Member, Hradec Kyjovice Formation, Nízký Jeseník Culm Basin, upper Viséan (Goγ subzone) to Namurian A (Goy subzone).

This abandoned quarry, 200 x 150 m in size, is an excellent exposure of the Kyjovice Member of the Hradec-Kyjovice Formation. The locality is important from sedimentological, mineralogical and tectonical points of view.

Sedimentary succession is characterized by a rhytmic alternation of fine-grained turbiditic sandstones (low-density turbidites, facies *F4a* and *F4b*) with siltstones and silty shales (*F5* and *F6*). Thickness of greywacke beds ranges from 10 to 60 cm. They are massive or parallel stratified, normal grading is less common. Flute marks and other sole marks are frequently present at the lower contacts of the beds, and their orientation documents dominant axial (S to N) filling of the Variscan foreland basin. The average modal composition of the greywackes comprises: 50% of quartz, 20% of plagioclases, 10% of volcanic lithic clasts and 20% of sedimentary and meta-sedimentary lithic clasts, mostly silty shales, phyllites and gneisses (Dvořák, 1999). Black-greyish micaceous siltstones and silty shales with parallel lamination form cm to dm thick layers. Locally abundant plant debris includes typical Lower Carboniferous genera *Lepidophloios* sp., *Archaeocalamites* sp. and *Calamites* sp. A thin horizon of acid volcaniclastics was described by Dvořák (1999) in the face of the northern quarry.

Gamma-ray spectrometric (GRS) logs show generally lower K, U and Th concentrations and total gamma-ray counts than the underlying Moravice Formation. In addition, there is a marked contrast between low-radioactivity sandstones and high-radioactivity mudstones/heterolithics (Fig. 14). This reflects a compositional shift towards highly mature, quartz-rich sandstones derived from high-grade metamorphic sources with granulites in the late Viséan (approximately at 330 Ma level, Fig. 12). These compositional and GRS changes reflect extremely rapid exhumation of mid- and deep-crustal rocks of the Moldanubian Zone of the Bohemian

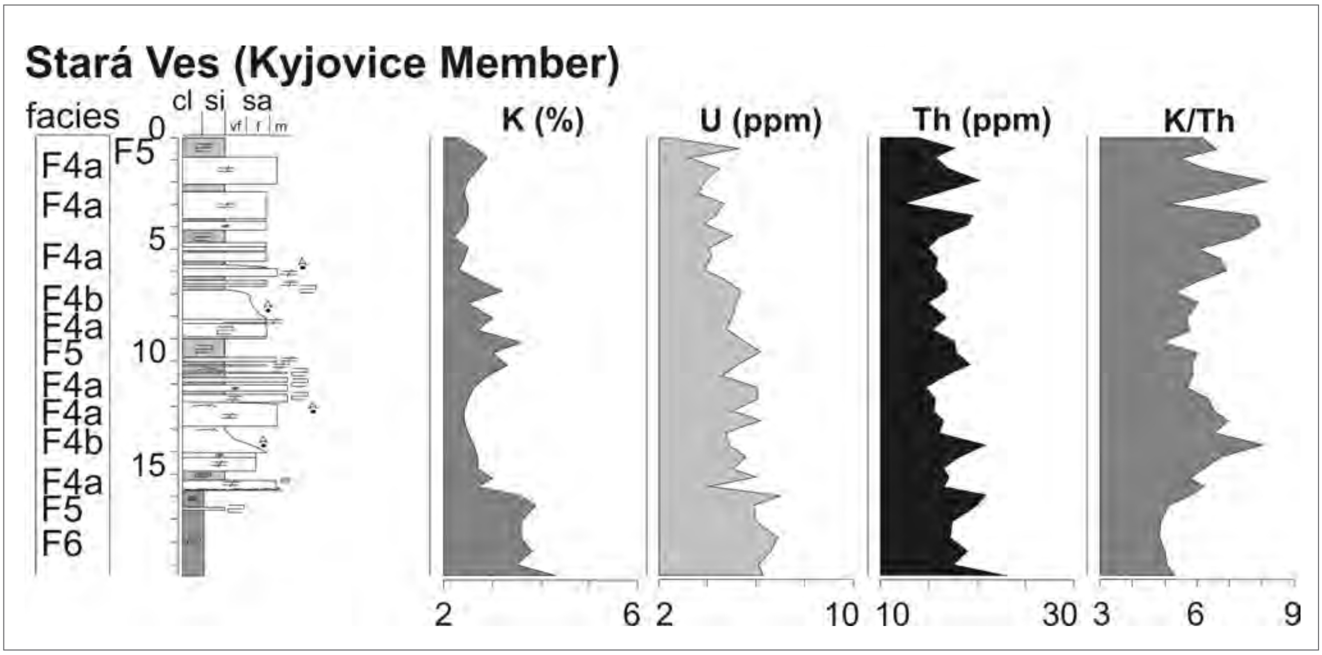

Fig. 14. Facies and gamma-ray spectrometry logs at the Stará Ves section. Note good correspondence between K log and facies stacking patterns, which indicate well-developed grain size dependence of gamma-ray data (Šimíček *et al.*, 2012)

Massif, which represented the major source area of the Nízký Jeseník Basin foreland basin. In this respect, the base of the Hradec – Kyjovice Formation is well correlatable with the base of the Luleč conglomerate indicating a sudden influx of granulite-rich Moldanubian-type material.

The sandstone beds are frequently cut by small hydrothermal veins containing quartz (so called Bristol diamond) and carbonate minerals (calcite and dolomite-ankerite). In addition, sage-green aggregates of chlorite (clinochlore-chamosite) and rare barite, pyrite, chalcopyrite and sphalerite were described. Secondary minerals include relative abundant limonite and rare malachite (Zimák *et al*., 2002).

The north face of the quarry presents one of the best exposures of fold-and-thrust tectonics in the Moravo-Silesian Culm Basin (Grygar, 1997). The architecture of the quarry is characterized by presence of inverted to recumbent east-vergent folds, which are cut by faults dipping towards WNW. Asymmetric flexures (kink folds) are accompanied by intra-stratal dislocations, subparallel with flat flexure limbs.

References

Bábek, O., Mikuláš, R., Zapletal, J. & Lehotský, T., 2004. Combined tectonic-sediment supply driven cycles in a lower Carboniferous deep-marine forehand basin, Moravice Formation, Czech Republic. *International Journal of Earth Sciences*, 93: 241–261.

Bábek, O., Mikuláš, R., Zapletal, J. Lehotský, T., & Pluskalová, J., 2001. Litofacie a fosilní stopy jemnozrnného turbiditního systému v jižní části moravického souvrství jesenického kulmu: Český masív. *Geologické výzkumy na Moravě a ve Slezsku v roce 2000*, 8: 38–41. [In Czech.]

Bábek, O., Tomek, C., Melichar, R., Kalvoda. J., Otava. J., 2006. Structure of unmetamorphosed Variscan tectonic units of the southern Moravo-Silesian Massif: a review. *Neues Jahrbuch für Geologie und Paläontologie, Abhandlungen*, 239: 37–75.

Chlupáč, I., Brzobohatý, R., Kovanda, J. & Stráník, Z., 2002. *Geologická minulost České republiky*. Academia, Praha, 436 pp. [In Czech.]

Chlupáč I. & Vrána S. (eds.), 1994. Regional geological subdivision of the Bohemian Massif on the territory of the Czech Republic. *Journal of Czech Geological Society*, 39: 127–144.

Čížek, P. & Tomek, C., 1991. Large-Scale Thin-Skinned Tectonics in the Eastern Boundary of the Bohemian Massif. *Tectonics*, 10: 273–286.

Čopjaková, R., Sulovský, P. & Paterson, B. A., 2005. Major and trace elements in pyrope-almandine garnets a sediment provenance indicators of the Lower Carboniferous Culm sediments, Drahany Uplands, Bohemian Massif. *Lithos*, 82: 51–70.

Dickinson, W. R., Beard, S., Brakenridge, G. R., Erjavec, J. L., Ferguson, R. C., Inman, K. F., Knepp, R. A., Lindberg, F. A. & Ryberg, P. T., 1983. Provenance of North American Phanerozoic sandstones in relation to tectonic setting. *Geological Society of America Bulletin*, 94 (2): 222–235.

Dvořák, J., 1965. Zpráva o spodnokarbonské stratigrafii kulmu na drahanské vrchovině. (Report of Lower Carboniferous stratigraphy of the Culm facies in the Drahany Upland). *Zprávy o geologických výzkumech v roce 1964*: 182–185. [In Czech.]

Dvořák, J., 1982. The Devonian and Lower Carboniferous in the basement of the Carpathians south and southeast of Ostrava (Upper Silesia Coal Basin, Moravia, Czechoslovakia). *Zeitschrift der Deutschen Gesellschaft für Geowissenschaften*, 133: 551–570.

Dvořák, J., 1994. *Variský flyšový vývoj v Nízkém Jeseníku, na Moravě a ve Slezsku*. Práce ČGS, 3, Praha, 77 pp. [In Czech.]

Dvořák, J., l995. Moravo-Silesian Zone; Autochthon; Stratigraphy. In: Dallmeyer, R. D., Franke, W. & Weber, K. (eds), *Pre-Permian geology of Central and Eastern Europe*. Springer, Berlin, pp. 477–489.

Dvořák, J., Freyer, G. & Slezák, I., 1959. Další paleontologický důkaz devonského stáří andělskohorských vrstev. *Vestník Ústředního Ústavu geologického*, 34: 457–458.

Falk, P. D. & Dorsey, R. J., 1998. Rapid development of gravelly high-density turbidity currents in marine Gilbert type fan deltas, Lorento Basin, Baja California Sur, Mexico. *Sedimentology*, 45: 331–349.

Finger, F. & Steyrer, H.-P., 1995. A tectonic model for the eastern Variscides: indications from a chemical study of amphibolites in the south-eastern Bohemian Massif. *Geologica Carpathica*, 46: 137–150.

Franců, E., Franců, J., Kalvoda, J., Polcheau, H. S. & Otava, J., 2002. Burial and uplift history of the Palaeozoic Flysch in the Variscan foreland basin (SE Bohemian Massif, Czech Republic). *Special Publications of EGS Stephen Mueller Series* l: 259–278.

Franke, W., 2002. The mid-European segment of the Variscides: tectonostratigraphic units. tenane boundaries and plate tectonic evolution. In: Winchester, J. A., Pharaoh, T. C. & Verniers, J. (eds), *Palaeozoic amalgamation of Central Europe. Geological Society Special Publications*, 201: 35–61.

Franke, W., Dallmeyer, R. D. & Weber, K., 1995. Geodynamic evolution. In: Dallmeyer, R. D., Franke, W. & Weber, K. (eds), *Pre-Permian Geology of Central and Eastern Europe*. Springer, Berlin, pp. 579–593.

Franke, W. & Engel, W., 1988. Tectonic settings of synorogenic sedimentation in the Variscan Belt of Europe. In: Besly, B. M. & Kelling, G. (eds), *Sedimentation in a synorogenic basin complex; the Upper Carboniferous of Northwest Europe*. Blackie and Son, London, pp. 8–17.

Franke, W. & Żelaźniewicz, A., 2002. Structure and evolution of the Bohemian Arc. In: Winchester, J. A., Pharaoh, T. C. & Verniers, J. (eds), *Palaeozoic amalgamation of Central Europe. Geological Society Special Publications*, 201: 279–293.

Frey, R. W. & Pemberton, S. G. 1984. Trace fossils facies models. In: Walker, R. G. (ed), *Facies models, 2nd ed*. Geoscience Canada, Ainsworth Press, Ontario, pp. 189–201.

Fritz, H. & Neubauer, F., 1995. Moravo-Silesian Zone; Autochthon; Structure. In: Dallmeyer, R. D., Franke, W. & Weber, K. (eds.), *Pre-Permian geology of Central and Eastern Europe*. Springer, Berlin, Heidelberg, New York, pp. 490–494.

Gilíková, H., Maštera, L. & Otava, J., 2003. Charakteristika spodnokarbonských flyšových sedimentů na listu 25-123 Hranice. *Geologické výzkumy na Moravě a ve Slezsku v roce. 2002*, 44–47. [In Czech.]

Grygar, R. & Vavro, M., 1996. Evolution of Lugosilesian Orocline, north-eastern periphery of the Bohemian Massif: kinematics of Variscan deformation. *Journal of Czech Geological Society*, 40: 65–90.

Hartley, A. & Otava, J., 2001. Sediment provenance and dispersal in a deep marine foreland basin: the Lower Carboniferous Culm Basin, Czech Republic. *Journal of Geological Society*, 158 (1): 137–150.

Haughton, P. D. W., 2001. Evolving turbidite systems on a deforming basin floor. Tabernas. SE Spain. *Sedimentology*, 47: 491–518.

Hickson, T. A. & Lowe, D. R., 2002. Facies architecture of a submarine fan channel-levee complex; the Juniper Ridge Conglomerate, Coalinga. California. *Sedimentology*, 49: 335–362.

Hiscott, R. N. & James, N. P., 1985. Carbonate debris flows, Cow Head Group, western New Foundland. *Journal of Sedimentary Petrology*, 55: 735–745.

Hladil, J. & Dvořák, J., 1994. Carboniferous. In: Klomínský, J. (ed), *Geological Atlas of the Czech Republic - Stratigraphy*. Czech Geological Survey, pp. 1–17.

Hladil, J., Melichar, R., Otava, J., Galle, A., Krs, M., Man, O., Pruner, P., Cejchan, P. & Orel, P., 1999. The Devonian in the Easternmost Variscides, Moravia; a Holistic Analysis Directed Towards Comprehension of the Original Context. *Abhandlungen der Geologischen Bundesanstalt*, 54: 27–47.

Kalvoda., J., 1995. Devonské pánve při okraji východní Avalonie na Moravě (Devonian basins at the margin of Eastern Avalonia in Moravia). *Geologické výzkumy na Moravě a ve Slezsku v roce 1994*, 2: 48–50. [In Czech.]

Kalvoda, J., Bábek, O., Fatka, O., Leichmann, J., Melichar, R., Nehyba, S. & Špaček, P., 2008. Brunovistulian Terrane (Bohemian Massif, Central Europe) from Late Proterozoic to Late Palaeozoic: a review. *International Journal of Earth Sciences*, 97 (3): 497–518.

Kalvoda, J., Leichmann, J., Bábek, O. & Melichar, R., 2003. Brunovistulian Terrane (Central Europe) and Istanbul Zone (NW Turkey): Late Proterozoic and Paleozoic tectonostratigraphic development and paleogeography. *Geologica Carpathica*, 54: 139–152.

Kalvoda, J., Melichar, R., Bábek, O. & Leichmann, J., 2002. Late Proterozoic - Paleozoic Tectonostratigraphic Development and Paleogeography of Brunovistulian Terrane and Comparison with Other Terranes at the SE Margin of Baltica-Laurussia. *Journal of Czech Geological Society*, 41: 81–102.

Kalvoda, J., Otava, J., Hladil, J. & Bábek, O., 1995. Nové stratigrafické údaje z bouzovského a západodrahanského kulmu (New stratigraphic data from the Bouzov and West Drahany Upland Culm). *Geologické výzkumy na Moravě a ve Slezsku v roce 1994*, 2: 51–52. [In Czech.]

Kneeler, B. C. & Branney, M. J., 1995. Sustained high-density turbidity currents and the deposition of thick massive beds. *Sedimentology*, 42: 607–616.

Kneller, B. & Buckee, C., 2000. The structure and fluid mechanics of turbidity currents; a review of some recent studies and their geological implications. *Millenium reviews, Sedimentology*, 47: 62–94.

Koverdynský, B. & Zikmundová., J., 1966. K stratigrafické příslušnosti vrbenské série a andělskohorských vrstev v oblasti Jeseníků. *Vestník Ústředního Ústavu geologického*, 41: 367–373. [In Czech.]

Kukal, Z., 1980. The sedimentology of Devonian and Lower Carboniferous deposits in the western part of the Nízký Jeseník Mountains, Czechoslovakia. *Sborník geologických Věd, Geologie*, 34: 131–208.

Kumpera, O., 1966. Stratigraphische, lithologische und tektonische Probleme des Devons und Kulms am Nordrande der Šternberk-Horní Benešov-Zone. *Freiberger Forschungshefte*, C 204: 1–106.

Kumpera, O., 1973. A contribution to the study of the Upper Visean fauna in Culm of Drahany Plateau and to its stratigraphic testimony. *Sborník věd. prací VŠB řada hornicko-geologická*, 219: 143–114.

Kumpera, O., 1983. *Lower Carboniferous geology of Jeseníky Block*. Knihovna Ústředního Ústavu geologického, 59: 1–172. [In Czech.]

Kumpera, O. & Lang., V., 1975. Goniatitová fauna v kulmu Drahanské vysočiny (moravskoslezská oblast Českého masivu). (Goniatite fauna in the Culm facies of the Drahany Upland (Moravo-Silesian Zone, Bohemian Massif). *Časopis Slezského Muzea*, A24 (1): 11–32. [In Czech.]

Kumpera, O. & Martinec, P., 1995. The development of the Carboniferous accretionary wedge in the Moravian-Silesian Paleozoic Basin. *Journal of Czech Geological Society*, 40: 47–60.

Kumpera, O., Paszkowski, M., Wajsprych, B., Foldyna, J., Malec, J. & Zakowa, H., 1995. Transition of the early Carboniferous pelagic sedimentation into synorogenic flysch. *XIII International. Congress on Carboniferous-Permian, Kraków, Poland, guide to Excursion*. Polish Geological Institute, Warszawa, 58 pp.

Lang, V. & Chlupáč, I., 1975. New finds of trilobites in the Culm of the Drahanska vrchovina Upland (Moravia, Czechoslovakia). *Vestník Ústředního Ústavu geologického*, 50: 337–344.

Lang, V., Pek, I. & Zapletal, J., 1979. Ichnofosilie kulmu jihovýchodní části Drahanské vrchoviny. *Acta Universitatis Palackiana Olomucensis Facultas Rerum Naturalium Geographica-Geologica*, 62: 57–96.

Lehotský, T., 2002. Nové lokality výskytu ichnofauny v moravickém souvrství kulmu Nízkého Jeseníku a Oderských vrchů (sp. karbon, Český masiv). *Přírodovědné Studie Muzea Prostějovska*, 5: 7–11. Prostějov. [In Czech.]

Lehotský, T., 2008. *Taxonomie goniatitové fauny, biostratigrafie a paleoekologie drahanského a jesenického kulmu*. Unpublished Ph.D. Thesis, Masaryk University, Brno. [In Czech.]

Leverenz, A., 2000. Trench sedimentation versus accreted submarine fan - an approach to regional-scale facies analysis in a Mesozoic accretionary complex: ‘’Torlesse” terrane, northeastern North Island, New Zealand. *Sedimentary Geology*, 132: 125–160.

Lombard, A., 1963. Laminites: a structure of flysch type sediments. *Journal of Sedimentary Petrology*, 33: 14–22.

Lowe, D. R., 1982. Sediment gravity flows: II. Depositional models with special reference to the deposits of high-density turbidity currents. *Journal of Sedimentary Petrology*, 52: 219–297.

Maštera, L., 1997. Petrofaciální zhodnocení drob hornobenešovského, moravického a hradecko-kyjovického souvrství v Nízkém Jeseníku (severní Morava). *Zprávy o geologických výzkumech v roce 1996*, 125–127. [In Czech.]

Matte, P., Maluski, H., Rajlich, P. & Franke, W., 1990. Terrane boundaries in the Bohemian Massif: results of large-scale Variscan shearing. *Tectonophysics*, 177: 151–170.

Mattern, F., 2002. Amalgamation surfaces, bed thicknesses, and dish structures in sand-rich submarine fans; numeric differences in channelized and unchanellized deposits and their diagnostic value. *Sedimentary Geology*, 150: 203–228.

Middleton, G. V. & Hampton, M. A., 1973. Sediment gravity flows: mechanics of flow and deposition. In: Middleton, G. V. & Bouma, A. H. (eds), *Turbidites and deep water sedimentation. Soc. Econ. Paleont. Mineral. Short course notes*, 1–38.

Mikuláš, R., Lehotský, T. & Bábek, O., 2002. Ichnofabric of the Culm facies: A case study of the Moravice Formation (Lower Carboniferous; Moravia and Silesia, Czech Republic). *Geologica Carpathica*, 53: 141–148.

Mikuláš, R., Lehotský, T. & Bábek, O., 2004. Trace fossils of the Moravice Formation in the southern part of the Nízký Jeseník Mts. (Lower Carboniferous, Culm facies; Moravia, Czech Republic). *Bulletin of Geosciences*, 79: 81–98.

Mulder, T. & Alexander, J., 2001. The physical character of subaqueous sedimentary density flows and their deposits. *Sedimentology*, 48: 269–299.

Mulder, T., Migeon, S., Savoye, B. & Faugěres, J.-C., 2001. Inversely graded turbidite Sequences in the deep Mediterranean: a record of deposits from flood-generated turbidity currents? *Geo-Marine Letters*, 21: 86–93.

Mutti, E. & Normark, W. R., 1987. Comparing examples of modern and ancient turbidite systems: problems and concepts. In: Leggett, J. K. & Zuffa, G. G. (eds), *Marine Clastic Sedimentology; Concepts and Case Studies*. Graham and Trotman, London, pp. 1–38.

Mutti, E., & Ricci Lucchi, F., 1972. Turbidites of the northern Apennines: Introduction to facies analysis (English translation by Nilson, T. H., 1978). *International Geology Review*, 20: 125–166.

Narkiewicz, M., 2005. Devonian and Carboniferous carbonate complex in the southern part of the Upper Silesian Block. *Prace Państwowego Instytutu Geologicznego*, 112: 1–46 [In Polish.]

Nehyba, S. & Mastalerz, K., 1995. Sedimentologický příspěvek ke studiu račických a lulečských slepenců (Sedimentological remarks to the Račice and Luleč conglomerates). *Geologické výzkumy na Moravě a ve Slezsku v roce 1994*, 2: 66–68. [In Czech.]

Normark, W. R. & Piper, D. J. W., 1991. Initiation processes and flow evolution of turbidity currents; implications for the depositional record. In: Osborne, R. H. (ed), *From shoreline to abyss; contributions in marine geology in honor of Francis Parker Shepard. Society of Economic Paleontologists and Mineralogists Special Publications*, 46: pp. 201–230.

Orr, P. J., 2001. Colonization of the deep-marine environment during the early Phanerozoic: the ichnofaunal record. *Geological Journal*, 36: 265–278.

Otava, J., Hladil, J. & Galle, A., 1994. The age of the Andělská Hora Formation: new facts and their possible interpretation. *Geologické výzkumy na Moravě a ve Slezsku v roce 1993*, 1: 52–56.

Patteisky, K., 1929. *Die Geologie und Fossilführung der mährisch-schlesischen Dachschiefer und Grauwackenformation*. Naturwiss, Opava, 354 pp.

Pickering, K. T. & Hiscott, R. N., 1985. Contained (reflected) turbidity currents from the Middle Ordovician Cloridorme Formation, Quebec. Canada; an alternative to the antidune hypothesis. *Sedimentology*, 32: 313–394.

Piper, D. J. W. & Stow, D. A. V., 1991. Fine-Grained Turbidites. In: Einsele, G., Ricken, W. & Seilacher, A. (eds), *Cycles and Events in Stratigraphy*. Springer, Berlin, pp. 360–316.

Plink-Björklund, P., Mellere, D. & Steel, R. J., 2001. Turbidite variability and architecture oť sand-prone, deepwater slopes; Eocene clinoforms in the Central Basin, Spitsbergen. *Journal of Sedimentary Research*, 71: 895–912.

Purkyňová, E., 1971. Karbonská flóra z Dětřichovic u Andělské Hory (kulm Nízkého Jeseníku). *Časopis Slezského Muzea. Opava, Vědy přírodní*, 26: 131–138. [In Czech.]

Purkyňová, E., 1981. Makroflóra hradeckého souvrství kulmu Nízkého Jeseníku (dinant, svrchní visé). *Časopis Slezského Muzea. Opava, Vědy přírodní*, 30: 269–214. [In Czech.]

Purkyňová, E. & Lang, V., 1985. Fosilní flóra z kulmu Drahanské vrchoviny. *Časopis Slezského Muzea. Opava, Vědy přírodní*, 35: 43–64. [In Czech.]

Rajlich, P., 1990. Strain and tectonic styles related to Variscan transpression and transtension in the Moravo-Silesian Culmian basin, Bohemian Massif, Czechoslovakia. *Tectonophysics*, 174: 351–361.

Reading, H. G., Richards, M., 1994. Turbidite systems in deep-water basin margins classified by grain size and feeder system. *Bulletin of American Association of Petroleum Geologists*, 78: 792–822.

Ricken, W., Schrader, S., Oncken, O. & Pletsch, A., 2000. Turbidite basin and mass dynamics related to orogenic wedge growth; the Rheno-Hercynian case. In: Franke, W., Haak, V., Oncken, O. & Tanner, D. (eds), *Orogenic Processes: Quantification and Modelling in the Variscan Belt. Geological Society Special Publications*, 179: 257–280.

Roemer, F., 1860. Notiz Über die Auffindung Von Posidonomya Becheri im Graurvackengebirge der Sudeten. *Zeitschrift der Deutschen Geologischen Gesellschaft*, 12: 350–352.

Rothwell, R. G., Pearce, T. J. & Weaver, P. P. E., 1992. Late Quaternary evolution of the Madeira abyssal plain, Canary Basin. NE Atlantic. *Basin Research*, 4: 103–131.

Schneider, D., Handler, R., Tomek, Č., Kalvoda, J. &

Neubauer, F., 2000. 40Ar/39Ar dating of detrital white mica from pre-, syn- and postorogenic sandstones in the Moravo-Silesian Basin. Czech Republic. In: Ristedt, H., Janoschek, W., Hofmann, T., Scharbert, S. & Freiler, M. (eds), *Geology 2000, Terra Nostra 2000-1,* 102 pp.

Schulmann, K., Ledru, P., Autran, A., Melka, R., Lardeaux, J.-M., Urban, M. & Lobkowicz, M., 1991. Evolution of nappes in the eastern margin of the Bohemian Massif: a kinematic interpretation. *Geologische Rundschau*, 80: 73–92.

Seilacher, A., 1967. Bathymetry of trace fossils. *Marine Geology*, 5: 413–428.

Shanmugam, G., 1980. Rhythms in deep sea, fine-grained turbidite and debris flow sequences, Middle Ordovician, eastern Tennessee. *Sedimentology*, 27: 419–432.

Shanmugam, G., 1996. High-density turbidity currents: are they sandy debris flows? *Journal of Sedimentary Research*, 66: 2–10.

Shanmugam, G., 2006. *Deep-Water Processes and Facies Models: Implications for Sandstone Petroleum Reservoirs. Handbook of Petroleum Exploration and Production, vol. 5*. Elsevier, Amsterdam, 496 pp.

Shanmugam, G. & Moiola, R. J., 1995. Reinterpretation of depositional processes in a classic flysch sequence (Pennsylvanian Jackfork Group), Quachita Mountains, Arkansas and Oklahoma. *Bulletin of American Association of Petroleum Geologists*, 79: 612–695.

Sinclair, H. D., 2000. Delta-fed turbidites infilling topographically complex basins: A new depositional model for the Annot Sandstones, SE France. *Journal of Sedimentary Research*, 70: 504–519.

Slobodník, M. & Dolníček, Z., 2001. Základní charakteristika fluid z hydrotermální mineralizace u Hrabůvky, Nízký Jeseník. *Geologické výzkumy na Moravě a ve Slezsku v roce 2000*, 8: 52–54.

Sohn, Y. K., 2001. Depositional processes of submarine debris flows in the Miocene fan deltas, Pohang Basin, SE Korea with special reference to flow transformation. *Journal of Sedimentary Research*, 70: 491–503.

Šimíček, D., Bábek, O. & Leichmann, J., 2012. Outcrop gamma-ray logging of siliciclastic turbidites: Separating the detrital provenance signal from facies in the foreland-basins turbidites of the Moravo-Silesian basin, Czech republic. Sedimentary Geology, 261–262: 50–64.

Špaček, P. & Kalvoda, J., 2000. Reconstruction of syn- and postsedimentary tectonic events in flysch basin from limestone pebbles variation: Drahany Culm of the Moravian Rhenohercynian Zone. *Geologica Carpathica*, 51: 31–41.

Stepanek, J. & Geyer, G., 1989. Spurenfossilien aus dem Kulm (Unterkarbon) des Frankenwaldes. *Beringeria*, l: 1–55.

Stow, D. A. V., 1979. Distinguishing between fine-grained turbidites and contourites on the Nova Scotian deep water margin. *Sedimentology*, 26: 371–384.

Walker, R. G., 1965. The origin and significance of the internal sedimentary structures of turbidites. *Proceedings of the Yorkshire Geological Society*, 35: 1–32.

Weimer, P., Varnai, P., Budhijanto, F. M., Acosta, Z. M., Martinez, R. E., Navarro, A. F., Rowan, M. G., McBride, B. C., Villamil, T., Arango, C., Crews, J. R. & Pulham, A. J. 1998. Sequence stratigraphy of Pliocene and Pleistocene turbidite systems, northern Green Canyon and Ewing Bank (offshore Louisiana), northern Gulf of Mexico. *Bulletin of American Association of Petroleum Geologists*, 82: 918–960.

Wolf, H., 1863. Über die geologische Verhältnisse bei Weiskirchen, Eckersdorf, Hotzenplotz und Engelsberg. *Verhandlungen der Kaiserlich-Königlichen geologischen Reichanstallt Wien*, 13: 19–20.

Zapletal, J., 1986. Paraconglomerates of Moravice Formation from Bílčice (Nízký Jeseník Mts.). Časopis Slezského Muzea, A35: 111–182. [In Czech.]

Zapletal, J., 1989. Viséská gravelitová sedimentace v kulmu Nízkého Jeseníku (Viséan gravelite sedimentation in the Culm beds of Nízký Jeseník Mts, Moravia, Czechoslovakia). *Acta Universitatis Palackiana Olomucensis Facultas Rerum Naturalium Geographica-Geologica*, 28: 15–29. [In Czech.]

Zapletal, J., 1991. Slide paraconglomerates in Lower Carboniferous of Nízký Jeseník Mts. (Culm of Moravian-Silesian Belt, Bohemian Massif). *Acta Universitatis Palackiana Olomucensis Facultas Rerum Naturalium Geographica-Geologica*, 30: 105–112. [In Czech.]

Zaptetal, J., 2000. Termín kulm v geologii Českého masívu (The term ‚'Culm" in the geology of the Bohemian Massif). *Facultatis Scientiarum Naturalium Universitatis Masarykiana Brunensis, Geology*, 27: 41–44.

Zapletal, J., 2003. Remarks of the Geology and Stratigraphy of the Mírov Unit, Bohemicum (Saxothuringian Zone, Bohemian Massif). *Acta Universitatis Palackiana Olomucensis Facultas Rerum Naturalium Geologica*, 38: 33–37.

Zapletal, J., Dvořák, J. & Kumpera, O., 1989. Stratigrafická klasifikace kulmu Nízkého Jeseníku (Stratigraphic classification of the Nízký Jeseník Culm). *Vestník Ústředního Ústavu geologického*, 64: 243–250. [In Czech.]

Zapletal, J. & Pek, I., l999. Ichnofacies of the Lower Carboniferous in the Jeseník Culm (Moravo-Silesian region, Bohemian Massif, Czech Republic). *Bulletin of Czech Geological Survey*, 74: 343–346.

Zikmundová, J. & Koverdynský, B., 1981. Výskyty konodontních faun ve spodní části andělskohorského souvrství v oblasti Jeseníků. *Práce přírodovědné Krajského Vlastivědného Muzea Olomouc*, 33: 17–28. [In Czech.]

Zukalová, V., Kalvoda, J., Galle, A. & Hladil, J., 1981. Biostratigrafie paleozoika v hlubokých vrtech jihovýchodně od Brna (The Biostratigraphy of the Paleozoic rocks in the deep boreholes southeast of Brno). *Knihovnička Zemního plynu a nafty*, 2: 7–30.

Bedded chalk marls in the Opole Trough: epicratonic deposits of the Late Cretaceous super-greenhouse episode

Mariusz Kędzierski[1], Alfred Uchman[1]

[1]Institute of Geological Sciences, Jagiellonian University, Kraków
(mariusz.kedzierski@uj.edu.pl; alfred.uchman@uj.edu.pl)

Route (Fig. 1): From Kraków, we drive west by motorway A4 (direction of Wrocław). Leave motorway on the first slip road after crossing the Odra River (about 160 km from Kraków) towards the city of Opole (route 45). After nine kilometres turn left to the road leading to the active **Folwark Quarry (stop B1.1)**, which is our main destination. Visitors need a permission from Górażdże Heidelberg Cement Group office. Leaving the quarry we return to motorway via route 45 and turn toward Kraków again. After 7 km we leave the motor highway toward Gogolin and drive along route 409 toward Strzelce Opolskie. After next 12 km we turn right to Ligota Górna, then by next

Fig. 1. Route map of field trip B1.

Kędzierski, M. & Uchman, A., 2015. Bedded chalk marls in the Opole Trough: epicratonic deposits of the Late Cretaceous super-greenhouse episode. In: Haczewski, G. (ed.), *Guidebook for field trips accompanying 31st IAS Meeting of Sedimentology held in Kraków on 22nd–25th of June 2015*. Polish Geological Society, Kraków, pp. 145–158.
Guidebook is available online at www.ing.uj.edu.pl/ims2015

4 km, we turn right to Wysoka and Góra Św. Anny. Driving up and down the hill along the Góra Św. Anny village we get to the Zdzieszowice-Leśnica crossroads and car park. The second (optional in the case of bad weather) stop of the field trip is located in an abandoned quarry in the **Góra Św. Anny Geopark (stop B1.2)** easily recognizable on the right side, a hundred metres north from the car park (Fig. 1).

Introduction to the trip

Geological background along the route

Driving west from Kraków we leave the Carpathian Foredeep Basin filled up with the Miocene fine-grained molasse sediments and we start to cross the Kraków-Silesian Monocline (Fig. 2) embracing the Permian through Upper Cretaceous sedimentary cover of the Variscan, partly folded, non-metamorphosed basement of the Brunovistulicum Domain. Locally, the cover is cut by Permian intrusions. The monocline is gently dipping to the west, hence, the route runs from the youngest, poorly exposed Upper Cretaceous marls and the underlying Middle/Upper Jurassic, mostly Oxfordian limestones, which are easily noticeable in the City of Kraków and its north vicinity as the white monadnocks or rock gates closing the narrow valleys deeply incised in the Ojców Plateau. The Oxfordian limestones are exposed also along the motorway, several kilometres west of Kraków. A large quarry at Zalas, visible on the left (southern) side of the motorway, 15 km from the entrance, reveals the Lower Callovian –Middle Oxfordian sandstone, marlstone to limestone sediments which cover Permian subvolcanic ryodacites (Matyja, 2006).

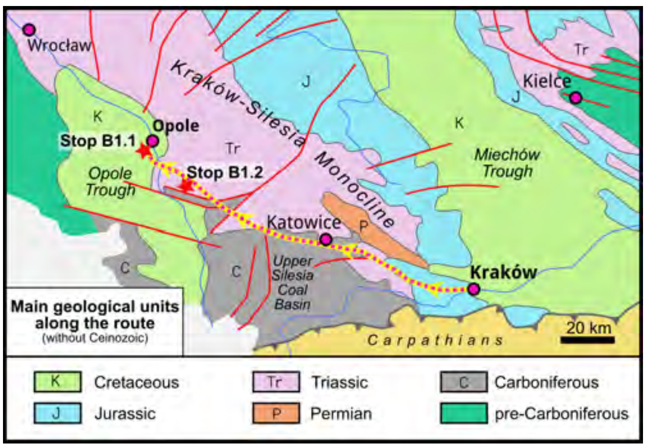

Fig. 2. The main geological units along the route.

Then, the route crosses an area built of the Triassic of the Germanic type, including a carbonate ramp of the Muschelkalk, which covers continental, variegated, fine-grained sandstones and clays with evaporates of the Buntsandstein. Further to the west, we enter an area of the Upper Permian continental playa-like basin facies intercalated with lavas and tuffs, which attain a considerable thickness in the Sławków Trough (50 km west from Kraków, vicinity of Jaworzno along our route). Passing by the Jaworzno power plant we enter the Upper Silesia Coal Basin, filled up with the Upper Carboniferous Paralic (Namurian A), Upper Silesia Sandstone (Namurian B–C), Mudstone (Westphalian A–B) and the Kraków Sandstone (Westphalian C–D) Series (Kotas, 1995). This is the largest industrial area in Poland, exploating one of the largest steam (hard) coal deposits in the world, rendering Poland as the largest coal producer in Europe, with resources estimated as high as 57 gigatons (to 2000 m of depth in beds over 0.6 m thick; Białecka, 2008). An exposure of the Upper Silesia Sandstone Series is visible on the right-side motorway escarpment between Katowice and Zabrze. Leaving the Upper Silesia Coal Basin in Gliwice we enter again the Kraków-Silesia Monocline at its Muschelkalk part. The Muschelkalk limestones are extensively explored in numerous quarries feeding the nearby cement industry. The Góra Św. Anny hill, the highest elevation along our route, reveals some Muschelkalk exposures, visible on the left side when crossing the hill pass. Then, going down from the pass, we enter the main venue of the trip – the Late Cretaceous filling of the Opole Trough, covering discordantly the Palaeozoic and Triassic basement.

The mid-Cretaceous world

The Cretaceous is known as a time of the Earth's climate and, at once, oceanic and atmospheric circulation, significantly different than nowadays (Hay, 2011). Moreover, it is also considered as a period of pronounced high global average temperature (both, on land and in the ocean), especially at high latitudes, of the lack of polar ice-caps and globally high sea-level, and it is thus called a 'greenhouse' period in the Earth history (Frakes, 1979; Gale, 2011). Furthermore, the middle of the Cretaceous period is even described as a 'super-greenhouse' making this time of particular interest for sedimentological and palaeoenvrionmental studies. For instance, the estimation of the Cenomanian–Turonian sea-surface temperature (SST) based on the $\delta^{18}O$ and Mg/Ca ratio of planktonic foraminifera revealed temperatures exceeding 35 °C in tropics (Huber *et al.*, 2002; Wilson *et al.*, 2002; Forster *et al.*, 2007; Friedrich *et al.*, 2012) and possibly reaching even 42 °C (Bice *et al.*, 2006). Generally, the Turonian is considered a time of the highest global average temperature throughout the whole Cretaceous (Hay and Floegel, 2012). Such temperatures remained up to the Turonian-Coniacian transition. This extremely high SST was unarguably connected to elevated atmospheric pCO_2 (Barron and Washington, 1985) which should have attained at least 3500 ppm required in the models to achieve the assumed maximum SST (Bice *et al.*, 2006). A submarine volcanic activity of the Ontong Java and Caribbean plateaus is regarded as the main source enhancing the mid-Cretaceous pCO_2 (Leckie *et al.*, 2002; Jarvis *et al.*, 2011).

The idea of the 'greenhouse' and 'icehouse' period in Earth's history was originally introduced by Fischer (1982), however, has been recently developed by Kidder and Worsley (2010, 2012) who recognized three basic modes for Earth's climate: icehouse, greenhouse and hothouse (= super-greenhouse). Moreover, the greenhouse can be further subdivided into cool- and warm-greenhouse.

The Albian through Coniacian climate is accepted as generally warm-greenhouse, however, three shifts into hothouse are pointed out at the Albian-Cenomanian, Cenomanian-Turonian and Turonian-Coniacian boundaries (Holz, 2015). The warm greenhouse is then characterized by global average temperature between 24 °C and 30 °C, no polar ice-caps and pCO_2 about 1200–4800 ppm. The oceans may become less oxygenated or anoxic under such conditions. In turn, the hothouse is assumed as a relatively short period of time (less than 3 my) which occurred during anomalously high atmospheric pCO_2 reaching up to 4800 ppm as a result of formation of the Large Igneous Provinces (LIPs). Vanishing of LIP usually ends hothouse due to rapid sequestration of CO_2 via enhanced weathering (Jarvis *et al.*, 2011; Flögel *et al.*, 2011).

However, some short-term coolings, when the surface waters were of about 2–4 °C cooler, are postulated for the mid-Cretaceous warm-greenhouse time (Forster *et al.*, 2007; Jarvis *et al.*, 2011). These periods were interpreted as cooling phases induced by formation of polar ice-caps which triggered glacio-eustatic changes of the sea-level in the Early Turonian and the late Early Coniacian (Uličny *et al.*, 2009). The cooling phases are still problematic due to unknown mechanisms that may have caused them during warm-greenhouse or even hothouse in contrast to cool-greenhouse, where some 'cold-snaps' are more obvious, e.g., the Campanian-Maastrichtian Boundary Event (Holz, 2015).

Such warm-greenhouse or hothouse during the middle of Cretaceous may be inflated because none of the assumed odd heat stress for land plants caused by warm ocean temperatures has been reported so far (Hay and Floegel, 2012). Furthermore, Hasegawa *et al.* (2012) suggested also, that pCO_2 above the 1000 ppm triggered a drastic equatorial-ward shrinking of Hadley circulation to latitudes about 25–30° in the mid-Cretaceous. Accordingly, the hothouse would be characterized by a narrow zone of arid climate, similarly to the icehouse mode, but it would lack the polar ice-caps. Besides these internal mechanisms regulating the Earth's climate, there is a report of globally widespread enhanced helium (^3He) concentrations in the Turonian sediments, which are about 4-fold higher than in the Cenomanian or Coniacian, suggesting an extraterrestrial cause (a comet or an asteroid shower) of the cooling effect during the mid-Cretaceous warm-greenhouse time (Farley *et al.*, 2012).

Moreover, the Cretaceous has had a specific oceanic condition which allowed accumulation of waste amount of organic-rich sediments during 'oceanic anoxic events – OAE' (Schlanger and Jenkyns, 1976; Arthur *et al.*, 1990). Especially, the Cenomanian–Turonian boundary event (OAE-2) is considered a major disturbance of global carbon cycle in the last 100 Myr (Jarvis *et al.*, 2011). Changes of the ocean's circulation were associated with formation of the Atlantic Ocean extending between the subarctic and subantarctic regions and its gateways connecting the northern with the southern parts, and the North Atlantic with the Pacific and the Tethys (e.g., Friedrich *et al.*, 2012). During the mid-Cretaceous, the North Atlantic may be regarded as a nutrient trap with respect to the Pacific, in consequence of estuarine type of circulation. Intense upwellings along the North Atlantic coasts brought series of organic-rich sediments in response to the influx of intermediate or thermocline nutrient-rich and warm (>20 °C) Pacific seawater, connected with submarine igneous events (Trabucho-Alexandre *et al.*, 2010; Friedrich *et al.*, 2012). Such accumulation of the organic-carbon-rich sediments also prevailed in the equatorial and mid-latitudinal Atlantic as well as in the neighbouring basins during the OAE-3 (Coniacian–Santonian). Meanwhile, the Tethys and North Atlantic sedimentation of that interval was dominated by occurrence of the oceanic red beds (see Wagreich, 2012).

Chalk and bedded-chalk facies

The chalk facies is unequivocally one of the most conspicuous facies of the Cretaceous, giving the period's name (see Hay, 2011). The chalk composition shows a predominant contribution of nannofossils, which seems to be a result of the Late Cretaceous seawater ionic specificity favourings precipitation of low Mg calcite (Stanley *et al.*, 2005). On the other hand, the chalk was deposited in the vast epicontinental basins that became flooded during the mid-Cretaceous high sea-level stage. This caused vanishing of the shelf-break front that separated the oceanic and shelf seawaters and allowed invasion of oceanic organisms such as calcareous nannoplankton into the epeiric seas (Hay, 2008). The bedded-chalk facies differs from the massive chalk in having distinctive bedding caused by varying siliciclastic contribution usually seen as marlstone-limestone alternation. Especially, the several cm thick clay-rich beds in the Turonian deposits are a noticeable feature of the chalk in northwestern Europe. According to Wray (1995), most of these beds are composed of detrital clays, and bentonites occur only exceptionally. This may indicate changes in terrigenous input resulting from sea-level fluctuations. As reported from the nearby Opole Trough Bohemian Cretaceous Basin, such short-term fluctuations involved sea-level falls of about 10–20 m during the Turonian through Lower Coniacian and they show frequency interval of 100 kyr, interpreted as glacio-eustatic changes (Uličny *et al.*, 2014).

The Opole Trough

The Opole Trough is an erosional remnant of the much more widespread Late Cretaceous cover filled up by epicontinental marls, marlstones, marly mudstones, marly limestones and limestones (Fig. 3). In general, this marly sedimentation in the Opole Trough coincides with the global maximum of the chalk accumulation and its products can be described as bedded-chalk marls (Walaszczyk, 1992). The total thickness of the Upper Cretaceous deposits in the Opole Trough is estimated at about 300 m, and most of them belong to the Upper Coniacian–?Santonian (Kotański and Radwański, 1977). They rest discordantly upon the Palaeozoic and Triassic basement, and are covered discordantly by Cenozoic, mainly Miocene and Quaternary deposits. The Opole Trough deposits dip gently to the west, therefore the oldest (Upper Cenomanian) layers are known from its eastern part (near Opole), whereas the youngest (Upper Coniacian–?Santonian) are known from the western part (Kotański and Radwański, 1977; Tarkowski, 1991; Walaszczyk, 1992). The main exposures are available in large quarries near Opole, important suppliers of cement industry.

The Opole Trough attracts the attention of geologists since the early 19th century (Oeynhausen, 1822). Important works to be mentioned include those by Roemer (1870), Biernat (1960) and Kotański and Radwański (1977). Stratigraphy of the Opole Trough was the subject of Tarkowski's (1991), Walaszczyk's (1992) and Kędzierski's (2008) studies, which determined the age of deposits exposed in the Folwark quarry as the Middle Turonian–Middle Coniacian. Alexandrowicz

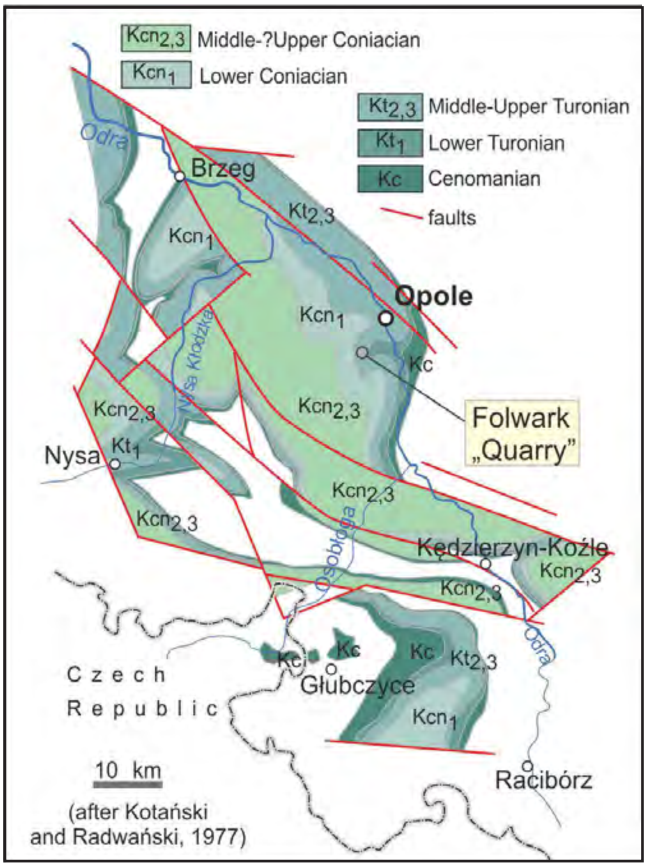

Fig. 3. The geological map of the Opole Trough Cretaceous deposits.

and Radwan (1973) subdivided the section of the Opole Trough on the grounds of the CaO content. According to this subdivision, the presented Folwark Quarry section embraces the Lower Clayey Marl, Lower Marl, Marly Limestone, Upper Marl and Upper Clayey Marl. All these lithologic units are easily recognizable in the field, since they differ in colour, related to the carbonate content which varies from 25 % to 88 % of $CaCO_3$ (Kędzierski, 2002). It is noteworthy that all of these units are sporadically intercalated with layers, up to 30 cm thick, of dark clayey marls and marly clays with considerably lower contents of carbonates (Fig. 4).

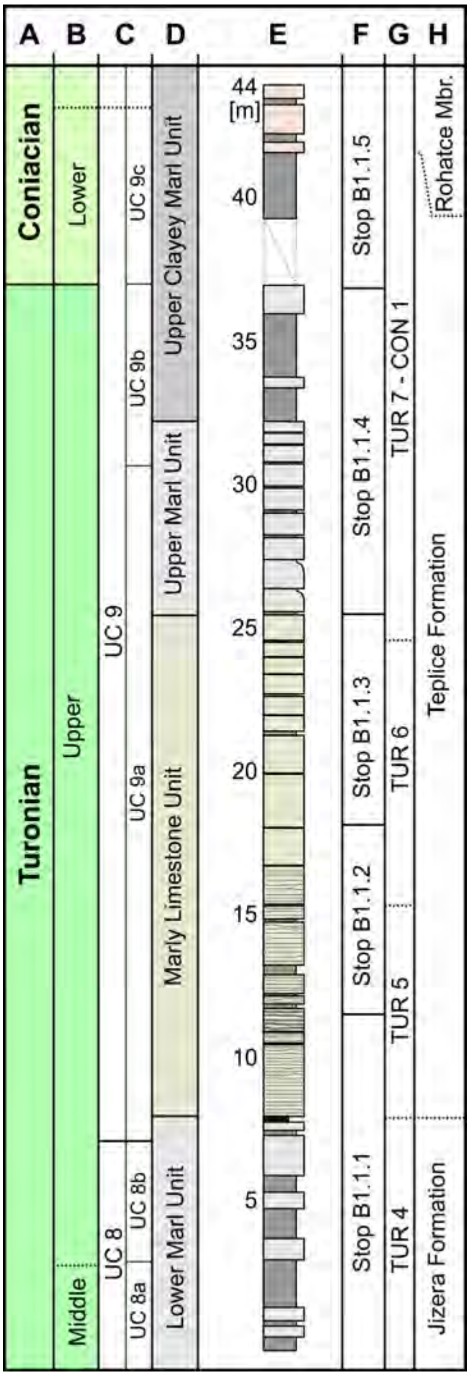

Fig. 4. Stratigraphy, lithology of the Folwark Quarry section compared with genetic sequences and litostratigraphical units of the Bohemian Cretaceous Basin. Meaning of the columns:
A – stages; B – substages; C – nannofossil biozones (Kędzierski, 2008); D – lithological units (Alexandrowicz and Radwan, 1973); E – composite Folwark Quarry section; F – part of the section visible at stops; G – genetic units sensu Uličny *et al.* (2009); H – formations of the Bohemian Czech Basin applied to the Opole Trough.

Other general palaeoecological and palaeoenvironmental studies were based on the following evidence: ichnofabrics (Kędzierski and Uchman, 2001), sharks (Niedźwiedzki and Kalina, 2004), echinoids (Olszewska-Nejbert, 2007) and sponges (Świerczewska-Gładysz, 2012). All of these studies were carried out on the best accessible Middle Turonian–Middle Coniacian sediments, since the other are only fragmentarily exposed or known from cores, now destroyed. Taking into account all data from these studies, one may obtain a general picture of the Middle Turonian throughout Middle Coniacian sea floor of the Opole Trough with a rather soft substrate and placed below the storm-wave base in a calm-water environment with a low to moderate rate of sedimentation. Sediments of the Middle Turonian *Inoceramus lamarcki* Zone represent the deepest environments (Kędzierski and Uchman, 2001; Niedźwiedzki and Kalina, 2004).

The Opole Trough lies in the transitional zone between the Tethyan and Boreal realms. Its nearest basins, which span the same time of sedimentation and show similar facies development, are the Bohemian Cretaceous and the Intra-Sudetic (Nysa Trough) basins. These basins were supplied by clastics mainly from the nearby Sudetic Islands (Western and Eastern) during the Cenomanian–Coniacian, therefore, the Opole Trough is regarded as a part of the so-called Circum-Sudetic Trap Basin (Walaszczyk, 1992; Fig. 5).

Stop descriptions

B1.1 Folwark quarry

The Folwark quarry is located a few km south of Opole, between Folwark, Chrzowice and Chrząszczyce. (50°36′43″ N, 17°54′38″ E; Fig. 5)

The quarry is the largest one supplying the Górażdże cement factory via a conveyor belt. Middle Turonian through Middle Coniacian strata are exposed at the three excavation levels in the quarry. The part of the quarry section available to study between the lowermost and the

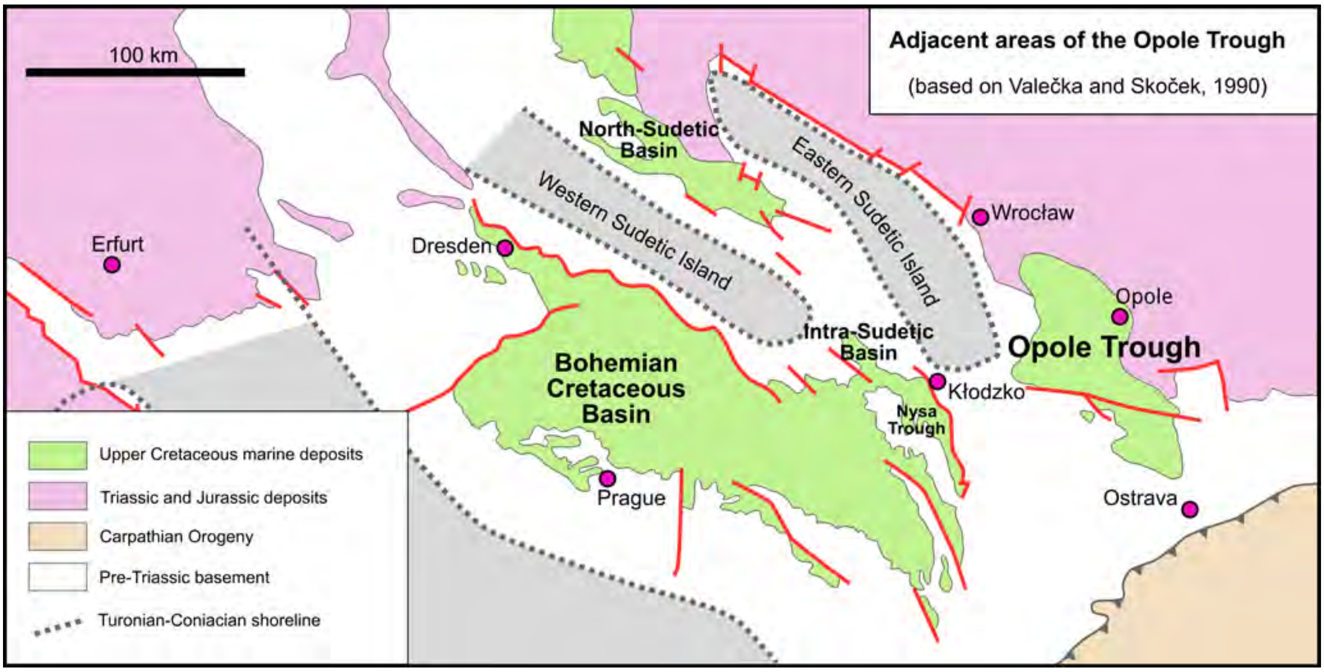

Fig. 5. Geological units adjacent to the Opole Trough.

middle levels represents the Lower Marl and the Marly Limestone units, embracing the Middle and Upper Turonian (Stops B1.1.1 and B1.1.2). The next higher part of the section, between the middle and uppermost levels, shows the Upper Turonian Marly Limestone and the Upper Marl units (Stop B1.1.3). The Upper Turonian through Middle Coniacian strata are exposed above the uppermost excavation level (Stops B1.1.4 and B1.1.5; Fig. 6).

The lithologic units best depict the general trends in carbonate contents, reaching the highest values in the Marly Limestone Unit, that can be partly described also as nodular limestones. The under- and overlying beds consist of sediments with lower carbonate contents, according to a scheme – the farther away from the nodular limestone, the lower is carbonate content, except for a siliceous marls package, a few meters thick, in the uppermost part of the quarry section (Stop B1.1.5; Fig. 7).

Fig. 6. Aerial view of the Folwark quarry and location of the stops and route (based on Google Maps).

This facies order is very similar to that known from the Bohemian Cretaceous Basin, where the Middle Turonian deposits with high carbonate content compose the Jizera Formation, which is under- and overlain by less carbonatic units: the Bílá Hora Formation and the Teplice Formation, respectively. Moreover, the package of siliceous marls can be compared to the Bohemian Rohatce Member (Teplice Fm.) (Čech *et al.*, 1980). Also, a general trend in long-term accommodation and supply rates, exponentially growing since the Early Turonian until Middle Coniacian, is similar to that observed in the Bohemian Cretaceous Basin (Uličny *et al.*, 2009). Generally, we suggest that the genetic sequences TUR 1–CON 1 sensu Uličny *et al.* (2009), distinguished in the Bohemian Cretaceous Basin, can be also recognized in the Opole Trough.

B1.1.1 The Lower Marl Unit, Middle Turonian, *inoceramid I. lamarcki* Zone

(50°36′43″N, 17°54′38″ E)

The lowest level in the quarry reveals thick-bedded, gray, massive marls altered with thick-bedded, a bit softer, dark gray clayey marls (Fig. 8).

The sediments are totally bioturbated with predominance of *Thalassinoides* isp. and *Planolites* isp. (*Thalassinoides* ichnofabric; Kędzierski and Uchman, 2001). *Chon-*

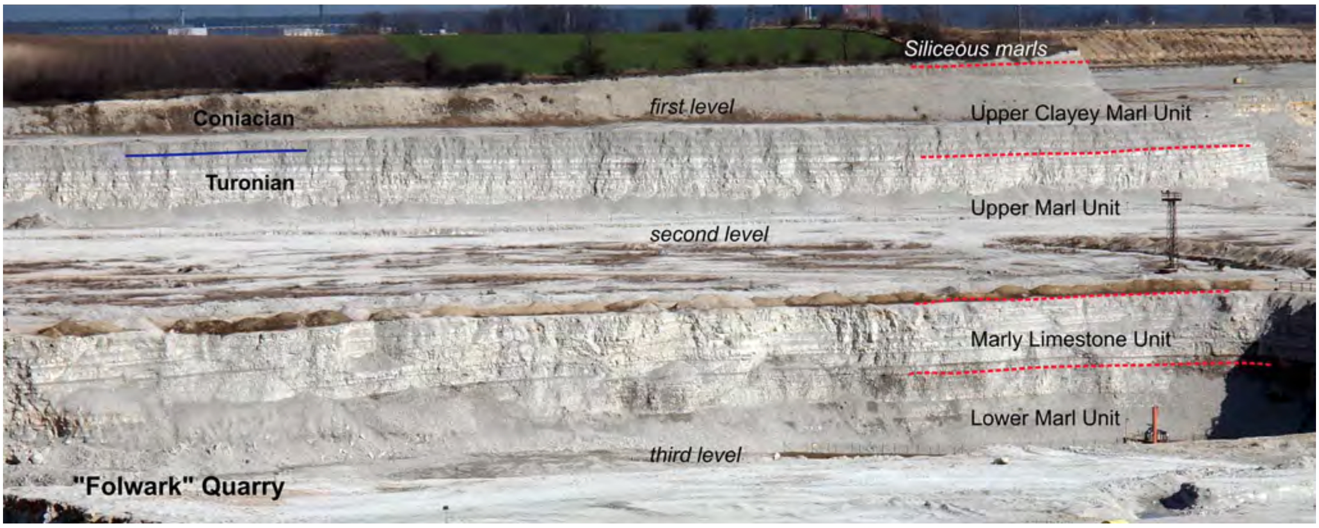

Fig. 7. General view of the Folwark quarry with stratigraphy and lithological units marked.

drites isp. is abundant in the lowest part. *Trichichnus* isp. is common and *Zavitokichnus* isp. is very rare (Fig. 9). Among body fossils, inoceramids and pyritized sponges are common. Some large inoceramid shells (possibly *I. cuvieri*) are commonly covered by worm incrustations.

The lowermost part of the section available here, used to be better exposed in the nearby Odra Quarry, where the *Chondrites* ichnofabric was recognized (Kędzierski and Uchman, 2001). This ichnofabric may indicate less oxygenated pore waters in the sediment, in coincidence with the deepest phase of the basin development, as recognized on the basis of shark teeth (Niedźwiedzki and Kalina, 2004).

Going up the section available at this stop, ~10 metres above the excavation level (13 m in Fig. 8) , there are prominent dark clay intercalations which visible the best from a distance. Below one of these intercalations, *Chondrites* and *Thalassinoides* are well visible thanks to their black filling. These intercalations gradually pass into the surrounding sediments and we did not find any evidence of the accompanying them bottom erosion. However, one of downfallen blocks shows that the clayey layer is underlain by eroded clasts. This can be interpreted as an omission surface marking the maximum of regression followed by lowstand system tract (LST) deposits with enhanced input of terrigenous material visible as the clayey intercalation (Fig. 10). We assume that the other prominent clay-rich intercalations visible in the quarry, also record sea-level falls and LST. These can be interpreted as boundaries of genetic sequences. Therefore, the Lower Marl Unit may correspond to the TUR 4 genetic sequence sensu Uličny *et al.* (2009) (Fig. 4).

B1.1.2 The Marly Limestone Unit, Upper Turonian, inoceramid *I. costellatus* + *M. incertus* zones

(50°36′48″ N, 17°54′30″ E)

The Marly Limestone Unit is exposed in the upper part of the section visible from the lowermost part of the excavation, and along the road going to the middle part of the quarry. A characteristic feature of this marly limestones is their nodular character that makes them appear as thick-bedded strata stripped irregularly with thin layers of clays (Fig. 8). Due to their highest carbonate content in the whole section of the Opole Trough, they can be easily distinguished as the brightest sediments. The nodular limestones are totally bioturbated with predominance of *Thalassinoides* isp., *Planolites* isp. and subordinately *Chondrites* isp. Noteworthy, *Thalassinoides* reaches its maximum size here (Fig. 9). Apart from frequent inoceramids and sponges, the marly limestones bear also the common echinod *Micraster* ex. gr. *leskei* (see Olszewska-Nejbert, 2007).

On the basis of studies of ichnofabric (Kędzierski and Uchman, 2001) and shark teeth (Niedźwiedzki and Kalina, 2004), the depositional environment of this unit is interpreted as shallower than that of the underlying Lower Marl Unit. The Marly Limestone Unit coincides with the Late Turonian cooling phase that triggered a sea-level fall and changes in weathering and water fertility (Voigt and Wiese, 2000; Wiese and Voigt, 2002). Accordingly, this unit corresponds to TUR 5 through TUR 6 genetic sequence sensu Uličny *et al.* (2009; Fig. 4).

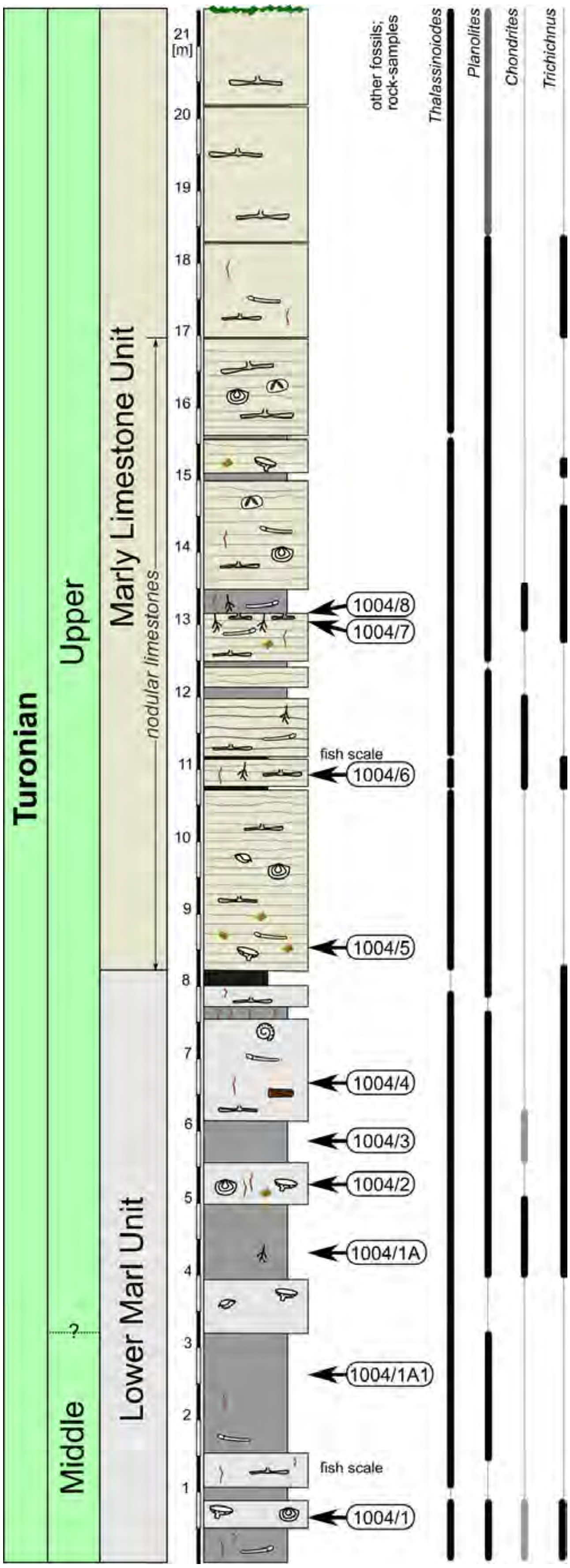

Fig. 8. The lower part of the Folwark Quarry section.

B1.1.3 The Marly Limestone and Upper Marl units, Upper Turonian, *M. incertus* inoceramid Zone

(50°36′44″ N, 17°54′28″ E)

The Upper Marl Unit is available at the base of the second exploitation level. It is similar to the Lower Marl Unit and shows alternation of softer and darker marls with brighter and harder marls, medium to thick- bedded in both types. A distinct dark, clay-rich intercalation, several cm thick, present ca. 4 m above the exploitation level (Fig. 11), may represent the maximum of regression at the base of the layer and the following LST clayey deposits. It can be interpreted as the boundary between the TUR 6 and TUR 7 genetic sequences sensu Uličny *et al.* (2009) (Fig. 4).

The sediments of this unit are strongly bioturbated, and the ichnofossil assemblage is similar to the previous units with the predominance of *Thalassinoides* and *Planolites*, and, subordinately *Chondrites* (*Thalassinoides* ichnofabric in Kędzierski and Uchman, 2001; Fig. 12). Body fauna is common, with inoceramids and sponges (partly pyritized).

B1.1.4 The Upper Clayey Marl Unit, Upper Turonian – Lower Coniacian, inoceramid *C. waltersdorfensis*+*C. brongniarti*+*C. deformis* zones

(50°36′54″ N, 17°54′37″ E)

The next Upper Clayey Marl Unit is available from the uppermost exploitation level and it is represented mainly by thick bedded soft, dark clayey marls gradually passing into brighter marls, also soft (Fig. 11). The *Thalassinoides* ichnofabric (Kędzierski and Uchman, 2001) and ichnofossil assemblage does not differ from the underlying unit, and body fossils alike (Fig. 12). However, predominance in thickness of clayey marls over marly clays and marls record increasing input of terrigeneous material in this unit. This coincides with the same trend recognized in the Bohemian Cretaceous Basin (Uličny *et al.*, 2009), and is the result of the uplift of the East Sudetic Island in its Śnieżnik Massif part (~70 km south-west from the City of Opole; Kędzierski, 2002). This part of the Folwark Quarry section can be compared to the TUR 7 and CON 1 genetic sequences sensu Uličny *et al.* (2009).

B1.1.5 The Upper Clayey Marls Unit with intercalations of the siliceous marls, Lower Coniacian – Middle Coniacian, inoceramid *C. crassus*+*I. kleini* zones

(50°36′54″ N, 17°54′24″ E)

The uppermost part of the section available in the Folwark quarry is represented by hard, bright, thick- to medium-bedded (0.3 to 1 m thick) siliceous marls intercalated with thin (several cm) layers of dark clayey marls. These siliceous marls differ from the underlying sediments in the *Chondrites* ichnofabric (Kędzierski and Uchman, 2001). This may indicate deposition on a sea-floor depleted in oxygen (dysoxic) as a result of a sea-level rise. Therefore, this part of the section represents deeper sedimentary environment than the underlying units, but similar to that suggested for the Lower Clayey Marl Unit (see Stop B1.1.1). The supposed Early Coniacian relative sea-level rise was triggered by tectonic rearrangement of the East Sudetic Island and it is connected to the high rate of subsidence in the adjacent areas such as the Bohemian Cretaceous Basin and the Opole Trough (see Uličny *et al.*, 2009).

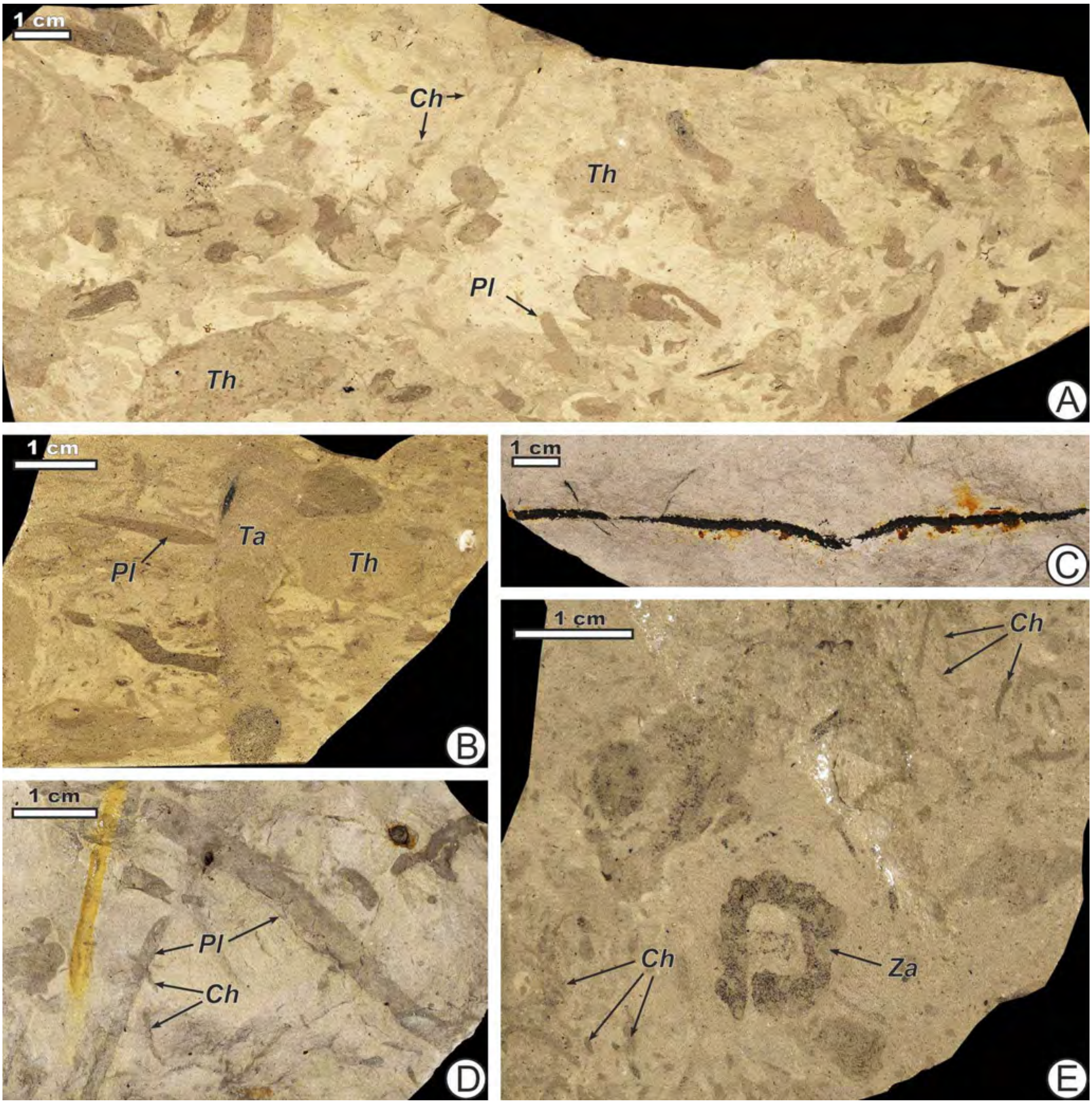

Fig. 9. Ichnofabrics and trace fossils in horizontal sections (wet surfaces, contrast improved by means of a software). Lower part of the quarry. Trace fossils: *Chondrites* (*Ch*), *Thalassinoides* (*Th*), *Planolites* (*Pl*), *Zavitokichnus* (*Za*). **A.** Sample 1004/7A1. **B.** Sample 1004/1A. **C.** *Trichichnus*, sample 1004/2. **D.** Sample 7. **E.** Sample 1004/1.

Fig. 10. Genetic sequence boundary – an example from Lower Marl Unit.

The siliceous marls are also characterized by the occurrence of exceptionally large *Trichichnus* isp. (Fig. 12). The recent studies (Kędzierski *et al.*, 2015) show that this trace fossil can be interpreted as a pyritized remnant of a bacterial mat produced by sulphide-reducing large bacteria related to *Thioploca* spp. Moreover, since the *Thioploca* is operating across the redox boundary in sediments, *Trichichnus* is thus considered as a fossilized wire enabling electron transfer between the reduced and oxide zones (Kędzierski *et al.*, 2015). Applying the ecology of modern Thioploca and similar bacteria to the Lower–Middle Coniacian siliceous marls of the Opole Trough, we suggest that the occurrence of large *Trichichnus* reflects powerful bioelectrical processes developed in dysoxic sediments across the redox boundary. This implies that siliceous marls are a facies which recorded specific conditions in the water column (radiolaria bloom?) and on the sea-floor, related somehow to the increasing rate of terrigenous supply.

Moreover, the siliceous marls are similar to the so-called 'clinking marls', known from the Nysa Trough (Intra-Sudetic Basin), in their high content of silica. Micropalaeontological studies have shown that the high silica content reflects enhanced contribution of radiolaria in the microfauna assemblages (Kozdra, 1993). Altogether, the enrichment in radiolaria and stratigraphic position allow us to describe these siliceous marls as an equivalent of the Rohatce Member (Teplice Fm.) in the Bohemian Cretaceous Basin (Čech *et al.*, 1980).

B1.2 Góra Św. Anny Geopark

(50°27′10″ N, 17°09′56″ E)

This optional stop presents a part of the St. Anna Hill (Góra Św. Anny) Geopark, a former quarry of nepheli-

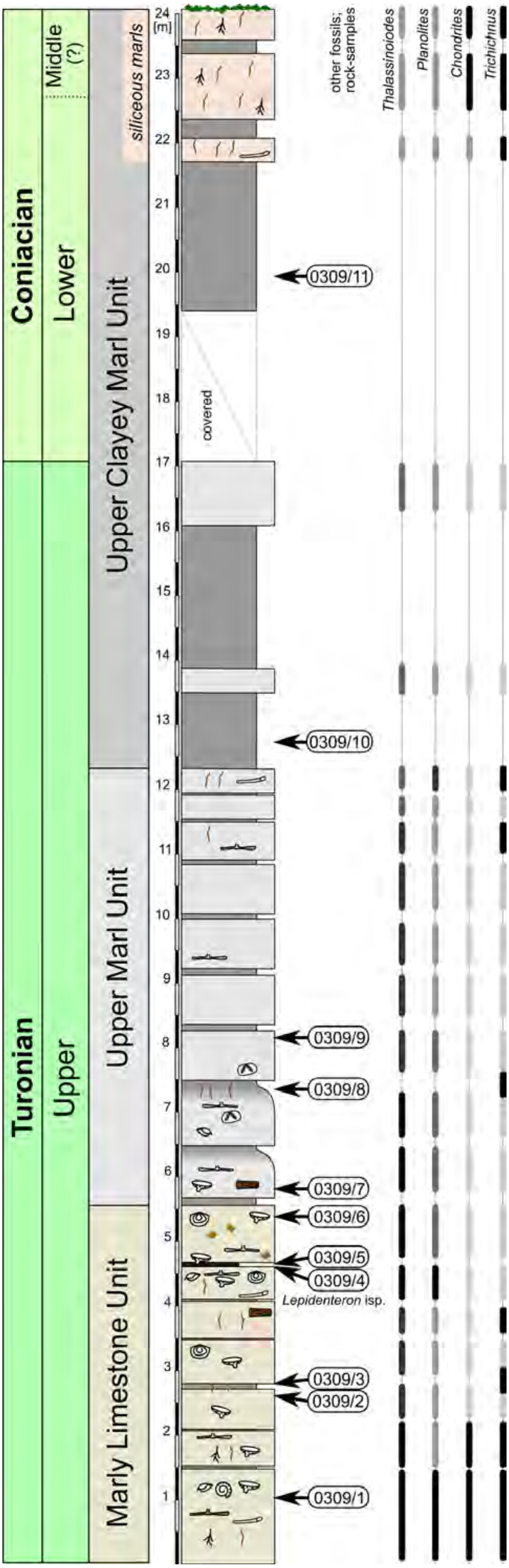

Fig. 11. The upper part of the Folwark Quarry section.

nite in an eroded Late Oligocene volcanic caldera (Fig. 14). The caldera has a sedimentary cover which contains Triassic (Muschelkalk) and Upper Cretaceous, recognized in xenoliths. The latter are represented by Cenomanian coarse-grained sandstones and Upper Turonian marly limestones (Niedźwiedzki, 1994).

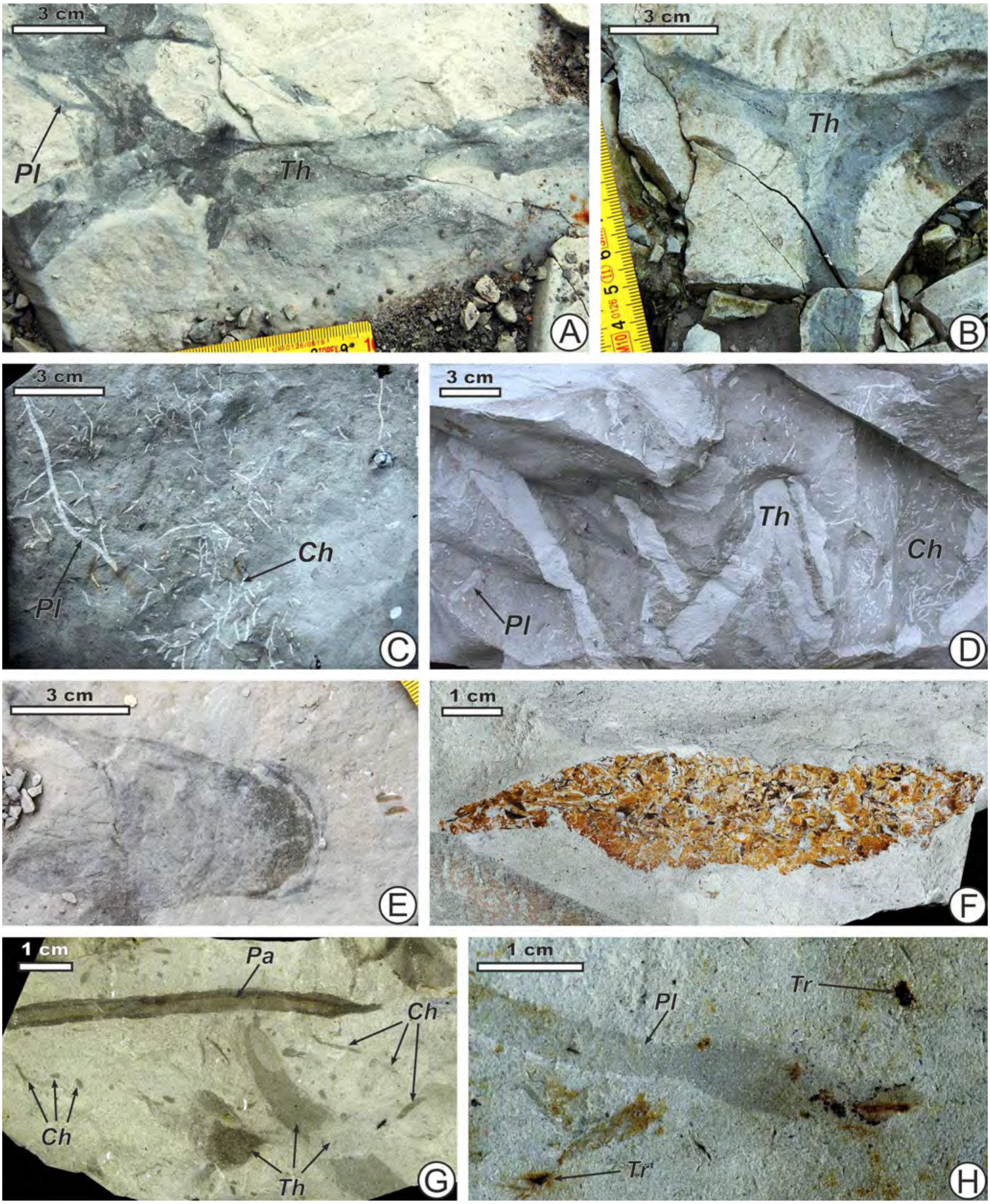

Fig. 12. Ichnofabrics and trace fossils in horizontal sections (wet surfaces, contrast improved by means of a software). Upper part of the quarry. Trace fossils: *Chondrites* (*Ch*), *Thalassinoides* (*Th*), *Planolites* (*Pl*), *Palaeophycus* (*Pa*), *Trichichnus* (*Tr*). **A–E** – field photographs. **A–B.** *Thalassinoides* suevicus and other trace fossils filled with darker sediments on the floor of the upper level. **C–D.** Trace fossils filled with lighter sediments. **E.** *Rhizocorallium* isp. **F.** *Lepidenteron lewesiensis*, sample 0309/4. **G.** Sample 0309/8. **H.** Sample 0309/10.

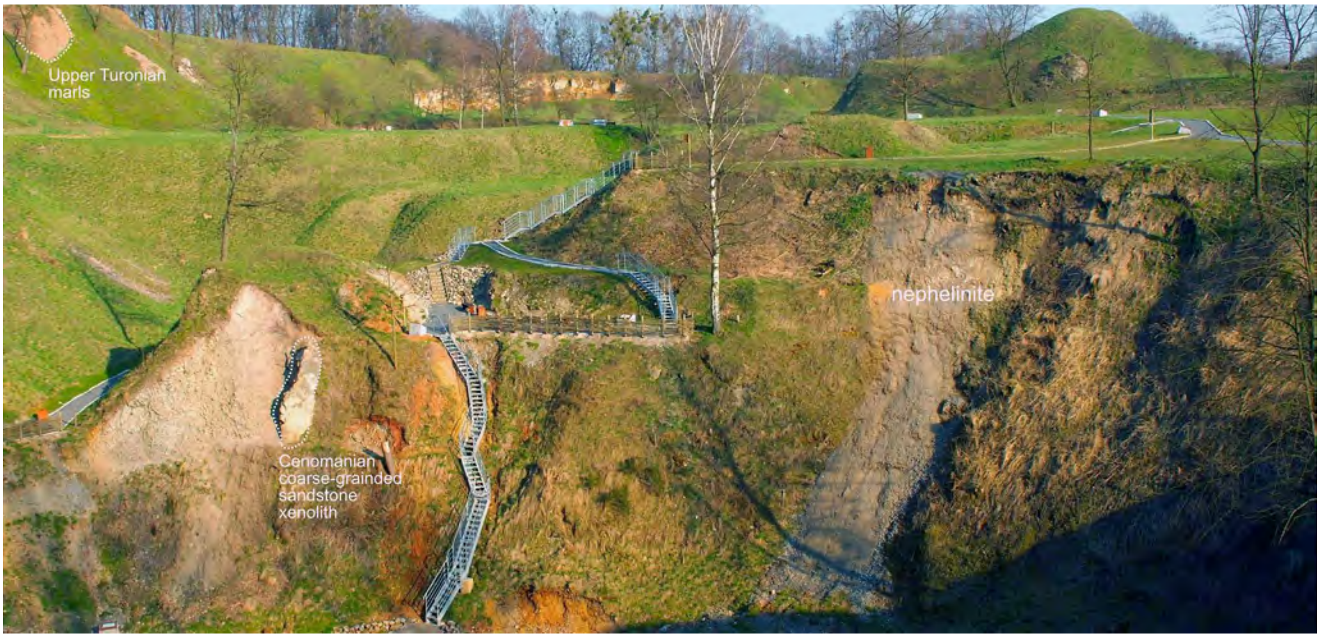

Fig. 13. General view of the abandoned nephelinite quarry in the Góra Św. Anny geopark.

References:

Alexandrowicz, S. W. & Radwan, D., 1973, Kreda opolska – problematyka stratygraficzna i złożowa, *Przegląd Geologiczny*, 240: 183–188. [In Polish.]

Arthur, M. A., Jenkyns, H. C., Brumsack, H. J. & Schlanger, S. O., 1990. Stratigraphy, geochemistry, and paleoceanography of organic-carbon-rich Cretaceous sequences. In: Ginsburg, R. N. & Beaudopin, B. (eds), *Cretaceous Resources, Events and Rhythms*. Kluwer Academic Publishers, Dordrecht, The Netherlands, pp. 75–119.

Barron, E. J. & Washington, W. M., 1985. Warm Cretaceous climates: high atmospheric CO_2 as a plausible mechanism. In: Sundquist, E. T. & Broecker, W. S. (eds), *The Carbon Cycle and Atmospheric CO2: Natural Variations Archaean to Present*. American Geophysical Union Geophysical Monograph, vol. 32, pp. 546–553.

Białecka, B., 2008. Estimation of Coal Reserves for UCG in the Upper Silesian Coal Basin, Poland. *Natural Resources Research*, 17: 21–28.

Bice, K. L., Birgel, D., Meyers, P. A., Dahl, K. A., Hinrichs, K.-U. & Norris, R. D., 2006. A multiple proxy and model study of Cretaceous upper ocean temperatures and atmospheric CO_2 concentrations. *Paleoceanography*, 21: PA2002. doi:10.1029/2005PA001203

Biernat, S., 1960, Budowa geologiczna kredy opolskiej, *Biuletyn Instytutu Geologicznego*, 152, 173-241. [in Polish.]

Čech, S., Klein, V., Kříž, J. & Valečka, J., 1980. Revision of the Upper Cretaceous stratigraphy of the Bohemian Cretaceous Basin. *Věstník Ústředního ústavu geologického*, 55: 277–296.

Farley, K. A., Montanari, A. & Coccioni, R., 2012. A record of the extraterrestrial 3He flux through the Late Cretaceous. *Geochimica et Cosmochimica Acta*, 84: 314–328.

Fischer, A. G., 1982. Long-term climatic oscillations recorded in stratigraphy. In: Berger, W. H. & Crowell, J. C. (eds), *Climate in Earth History*. National Academy Press, Washington D.C., pp. 97–104.

Flögel, S., Wallmann, K. & Kuhnt, W., 2011. Cool episodes in the Cretaceous — exploring the effects of physical forcing on Antarctic snow accumulation. *Earth and Planetary Science Letters*, 307: 279–288.

Forster, A., Schouten, S., Baas, M. & Sinninghe Damsté, J. S., 2007. Mid-Cretaceous (Albian-Santonian) sea surface temperature record of the tropical Atlantic Ocean. *Geology*, 35: 919–922. doi:10.1130/G23874A.1

Frakes, L. A., 1979. *Climates throughout Geologic Time*. Elsevier Scientific Publishing Company, Amsterdam, The Netherlands. 310 pp.

Friedrich, O., Norris, R. D. & Erbacher, J., 2012. Evolution of middle to Late Cretaceous oceans – A 55 m.y. Record of Earth's temperature and carbon cycle. *Geology*, 40: 107–110. doi:10.1130/G32701.1

Gale, A. S., 2011. The Cretaceous world. In: Culver, S. J. & Rawson, P. F. (eds), *Biotic Response to Global Change. The Last 145 Million Years*. Cambridge University Press, Cambridge, pp. 4–19.

Hasegawa, H., Tada, R., Jiang, X., Suganuma, Y., Imsamut, S., Charusiri, P., Ichinnorov, N. & Khand, Y., 2012. Drastic shrinking of the Hadley circulation during the mid-Cretaceous Supergreenhouse. *Climate of the Past*, 8: 1323–1337.

Hay, W. W., 2008. Evolving ideas about the Cretaceous climate and ocean circulation. *Cretaceous Research,* 29: 725–753.

Hay, W. W., 2011. Can humans force a return to a 'Cretaceous' climate? *Sedimentary Geology*, 235: 5–26.

Hay, W. W. & Floegel, S., 2012. New thoughts about the Cretaceous climate and oceans. *Earth-Science Reviews*, 115: 262–272.

Holz, M., 2015. Mesozoic paleogeography and paleoclimates – A discussion of the diverse greenhouse and hothouse conditions of an alien world. J*ournal of South American Earth Sciences,* doi: 10.1016/j.jsames.2015.01.001

Huber, B.T ., Norris, R. D. & MacLeod, K. G., 2002. Deep-sea paleotemperature record of extreme warmth during the Cretaceous. *Geology*, 30: 123–126.

Jarvis, I., Lignum, J. S., Grcke, D. R., Jenkyns, H. C. & Pearce, M. A., 2011. Black shale deposition, atmospheric CO_2 drawdown, and cooling during the Cenomanian-Turonian Anoxic Event. *Paleoceanography*, 26: PA3201. doi:10.1029/2010PA002081

Kędzierski, M., 2002. *Biostratigrafia i paleobiogeografia osadów niecki opolskiej i wartsw idzikowskich górnych z rowu górnej Nysy.* Unpublished PhD Thesis, Jagiellonian University, Kraków, 152 ms. pp. [In Polish.]

Kędzierski, M., 2008. Calcareous nannofossil and inoceramid biostratigraphies of a Middle Turonian to Middle Coniacian section from the Opole Trough of SW Poland. *Cretaceous Research*, 29: 451–467.

Kędzierski, M. & Uchman, A. 2001. Ichnofabrics of the Upper Cretaceous marlstones in the Opole region, southern Poland. *Acta Geologica Polonica*, 51: 81–91.

Kędzierski, M., Uchman, A., Sawlowicz, Z. & Briguglio, A., 2015. Fossilized bioelectric wire – the trace fossil *Trichichnus*. *Biogeosciences,* 12: 2301–2309. doi:10.5194/bg-12-2301-2015

Kidder, D. L. & Worsley, T. R., 2010. Phanerozoic large igneous provinces (LIPs), HEATT (Haline Euxinic Acidic Thermal Transgression) episodes and mass extinctions. *Palaeogeography, Palaeoclimatology, Palaeoecology,* 295: 162–191.

Kidder, D. L. & Worsley, T. R., 2012. Human-induced hothouse climate? *GSA Today*, 22: 4–11.

Kotański, Z., Radwański, S., 1977, Geologia wgłębna opolszczyzny. *Biuletyn Instytutu Geologicznego*, 303: 91-163. [in Polish.]

Kotas, A., 1995. Litostratigraphy and sedimentologic-paleogeographic development, Moravian-Silesian-Cracovian region, Upper Silesian Coal Basin. In: Zdanowski, A. & Żakowa, H. (eds), *The Carboniferous System in Poland.* Prace Państwowego Instytutu Geologicznego, 148: 124–134.

Kozdra, T., 1993. *Mikrofauna otwornicowa kredy opolskiej i interpretacja paleoekologiczna*. Unpublished MSc thesis, Jagiellonian University, Kraków, 50 ms. pp. [In Polish.]

Leckie, R. M., Bralower, T. J. & Cashman, R., 2002. Oceanic anoxic events and plankton evolution: Biotic response to tectonic during the mid-Cretaceous. *Paleoceanography*, 17. doi: 10.1029/2001PA000623

Matyja, B. A., 2006. Stop A17 – Zalas Quarry – Callovian transgressive to condensed pelagic deposits, Lower to lowermost Middle Oxfordian deposits of sponge megafacies. In: Wierzbowski, A., Aubrecht, R., Golonka, J., Gutowski, J., Krobicki, M., Matyja, B. A., Pieńkowski, G. & Uchman, A. (eds), *Jurassic of Poland and adjacent Slovakian Carpathians. Field Trip Guidebook of 7th International Congress on the Jurassic System, Kraków, September, 6–18 2006.* Polskie Towarzystwo Geologiczne, Kraków, pp. 70–72.

Niedźwiedzki, R., 1994. A caldera from the Góra Św. Anny, Upper Silesia: new data in the geologic structure. *Annales Societatis Geologorum Poloniae*, 63: 333–351. [In Polish, English summary.]

Niedźwiedzki, R. & Kalina, M., 2004. Late Cretaceous sharks in the Opole Silesia region (SW Poland). *Geologia Sudetica*, 35: 13–24.

Oeynhausen, C. von, 1822. *Bersuch einer geognostischen Beschreibung von Oberschlesien und den nächt angrenzenden Gegenden von Polen, Galizien und Östreichisch Schlesien*. pp. 471, Essen.

Olszewska-Nejbert, D., 2007. Late Cretaceous (Turonian–Coniacian) irregular echinoids of western Kazakhstan (Mangyshlak) and southern Poland. *Acta Geologica Polonica*, 57: 1–87.

Roemer, F., 1870. *Geologie von Oberschlesien*. Nischkowski Verlag, Breslau, pp. 587.

Schlanger, S. O. & Jenkyns, H. C., 1976. Cretaceous oceanic anoxic events: causes and consequences. *Geologie en Mijnbouw*, 55: 179–184.

Stanley, S. M., Ries, J. B. & Hardie, L. A., 2005. Seawater chemistry, coccolithophore population growth, and the origin of Cretaceous chalk. *Geology*, 33: 593–596.

Świerczewska-Gładysz, E., 2012, Late Turonian and Early Coniacian ventriculitid sponges (Lychniscosida) from Opole Trough (southern Poland) and their palaeoecological significance. *Annales Societatis Geologorum Poloniae*, 82: 201–224.

Tarkowski, R., 1991, Stratygrafia, makroskamieniałości i paleogeografia utworów górnej kredy niecki opolskiej, *Geologia, Zeszyty Naukowe AGH*, 51, pp. 156, Kraków

Trabucho-Alexandre, J., Tuenter, E., Henstra, G. A., van der Zwan, K. J., van de Wal, R. S. W., Dijkstra, H. A. & de Boer, P. L., 2010. The mid-Cretaceous North Atlantic nutrient trap: Black shales and OAEs. *Paleoceanography*, 25: PA4201. doi:10.1029/2010PA001925

Uličny, D., Laurin, J. & Čech, S., 2009. Controls on clastic sequence geometries in a shallow-marine transtensional basin: the Bohemian Cretaceous Basin, Czech Republic. *Sedimentology*, 56: 1077–1114.

Uličny, D., Jarvis, I., Gröcke, D. R., Čech, S., Laurin, J., Olde, K., Trabucho-Alexandre, J., Švabenická, L. & Pedentchouk, N. 2014. A High-Resolution Carbon-Isotope Record of the Turonian Stage Correlated to a Siliciclastic Basin Fill: Implications for Mid-Cretaceous sea-Level Change. *Palaeogeography, Palaeoclimatology, Palaeoecology*, 405: 42-58.

Voigt, S. & Wiese, F., 2000. Evidence for Late Cretaceous (Late Turonian) climate cooling from oxygen-isotope variations and paleobiogeographic changes in Western and Central Europe. *Journal of Geological Society, London*, 157: 737–743.

Wagreich, M., 2012. “OAE 3” – regional Atlantic organic carbon burial during the Coniacian–Santonian. *Climate of the Past*, 8: 1447–1455.

Walaszczyk, I., 1992. Turonian through Santonian deposits of the Central Polish Uplands; their facies development, inoceramid paleontology and stratigraphy. *Acta Geologica Polonica*, 42: 1–122.

Wiese, F. & Voigt, S., 2002. Late Turonian (Cretaceous) climate cooling in Europe: faunal re- sponse and possible causes. *Geobios*, 35: 65–77.

Wilson, P. A., Norris, R. D. & Cooper, M. J., 2002. Testing the Cretaceous greenhouse hypothesis using glassy foraminiferal calcite from the core of the Turonian tropics on Demerara Rise. *Geology*, 30: 607–610.

Wray, D. S., 1995. Origin of clay-rich beds in Turonian chalks from Lower Saxony, Germany – a rare-earth element study. *Chemical Geology*, 119: 161–173.

Paleokarst, neptunian dykes, collapse breccias, mud-mounds and sedimentary unconformities in Slovakian Western Carpathians

Roman Aubrecht[1, 2]

[1]Department of Geology and Paleontology, Faculty of Natural Sciences, Comenius University, Mlynská dolina – G, SK-842 15 Bratislava, Slovakia (aubrecht@fns.uniba.sk)

[2]Geophysical Institute, Slovak Academy of Sciences, Dúbravská cesta 9, SK-845 28 Bratislava, Slovakia

Route (Fig. 1): The trip starts from Kraków centre to the south by E77 to Dolný Kubín in Slovakia, then by road 709 km southwest to Párnica village, where we take road 583 northwards to Zázrivá and by local roads to its northern part **Zázrivá**-Havrania. To get to the first locality (stop **B4.1**), it is necessary to use a local forest road, for which a permission from the forest owners is necessary. Then the route goes back to Zázrivá and by road 583 to Žilina where by a slip road we enter motorway E75 (E50) to Beluša where we take a local to SE to **Mojtín** village. We walk ca. 15 minutes north to locality **B4.2**. We return to Beluša and take road 61 to SW to Ilava, turn NW, and through Pruské village follow to Vršatské Podhradie, to the parking place at the mountain pass above the village. The **Vršatec** sites (**B4.3**) are distributed around the pass. After returning to Pruské village we take road 507 to the neighbouring Bohunice where we turn to a local road towards the **Krivoklát** village and visit an abandoned quarry (**B4.4**) below the Babin**á hill** on the half-way. The next locality is in the second valley after Bohunice by road 507, near **Slavnické Podhorie**. It is an abandoned quarry (**B4.5**) at the northern margin of the village. Then by road 507 to Dubnica nad Váhom and by road 61 we reach **Trenčín**, for overnight.

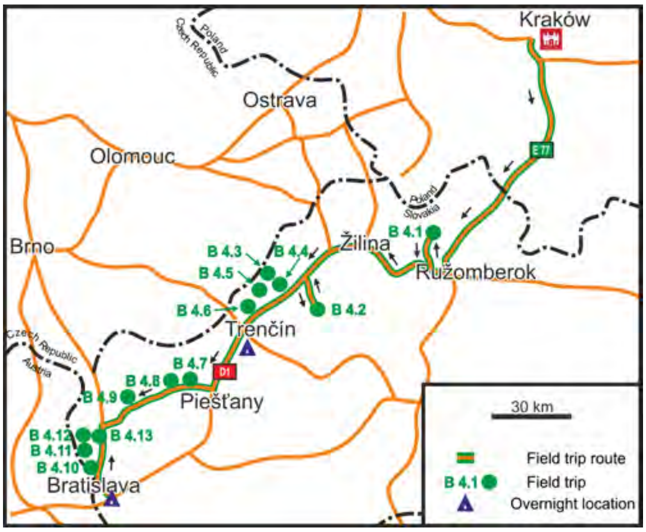

Fig. 1. Route map of field trip B4.

On the second day the trip leads by a local road to **Dolná Súča** village, to an abandoned quarry NW from the village (**B4.6**). Then back to Trenčín and by motorway E75(D1) to Piešťany, where. we turn to 499 through Vrbové to Prašník and by a local road to a dam nead the **Pustá Ves** village. Stop **B4.7** is on the mountain ridge, about 1 km SE from the dam. Then the route again follows road 499 to Brezová pod Bradlom, where it connects to road 501. Stop **B4.8** is by the road, about 2 km

Aubrecht, R., 2015. Paleokarst, neptunian dykes, collapse breccias, mud-mounds and sedimentary unconformities in Slovakian Western Carpathians. In: Haczewski, G. (ed.), *Guidebook for field trips accompanying 31st IAS Meeting of Sedimentology held in Kraków on 22nd–25th of June 2015*. Polish Geological Society, Kraków, pp. 159–193.
Guidebook is available online at www.ing.uj.edu.pl/ims2015

from the **Brezová pod Bradlom**. Then we continue along road 501 at the NW toe of the Malé Karpaty Mts. to **Sološnica** village. Stop **B4.9** is in an abandoned quarry at the SE end of the village. The trip continues along road 501 to Rohožník and by a local road to Malacky, and by motorway E65(D2) to Bratislava for overnight.

The third day route leads by the local roads to **Devín** and **Devínska Nová Ves** within the limits of Bratislava (stops **B4.10, B4.11, B4.12**). By local roads we follow to road 2 northwards to **Záhorská Bystrica** (now a part of Bratislava). Stop **B4.13** is in an abandoned quarry at the western margin of the village. After the end of the field-trip, the participants have several possibilities, either to go back to Kraków, or to spend some more days in Bratislava, or to leave for Vienna airport using very frequent bus and train connections.

Introduction

The aim of the field trip is to see examples of sedimentary unconformities, mainly those related to emersion. Erosional and karstification phenomena can be studied at several sites.

An older period of emersion was related to the Mid-Cretaceous crustal shortening and nappe stacking in the Central Western Carpathians. The nappe stacking resulted in emersion and karstification of the highest nappe surfaces, forming paleokarst surface depressions filled with bauxites and breccias with fossil terra rosa and fresh-water cyanophyte limestones resting on the unconformity surfaces.

In the Pieniny Klippen Belt there was an Early Cretaceous emersion of so-called Czorsztyn Swell which resulted in nice paleokarst karren surface. The emersion period ended in Albian with sudden flooding (ingression) and deposition of red pelagic marls. Therefore, until recognition of the paleokarst features, this break in sedimentation was considered to be caused by submarine non-deposition and erosion.

The oldest features which can be observed during the field trip are related to the Middle Jurassic rifting and rising of the Czorsztyn Swell. This was again accompanied by breakage (neptunian dykes), emersion and erosion of new lithified sediments and formation of toe-of-slope megabreccias. There is an interesting cave-dwelling fauna of ostracods *Pokornyopsis feifeli* Triebel, descendants of which still inhabit submarine caves in tropical seas. Further drowning of the Czorsztyn swell led to deposition of the Rosso Ammonitico facies, with local occurrences of stromatactis mud-mounds. Stromatactis structures were enigmatic for over a century but at one of the sites the participants will have a chance to see that stromatactis are just cavities after collapsed siliceous sponges.

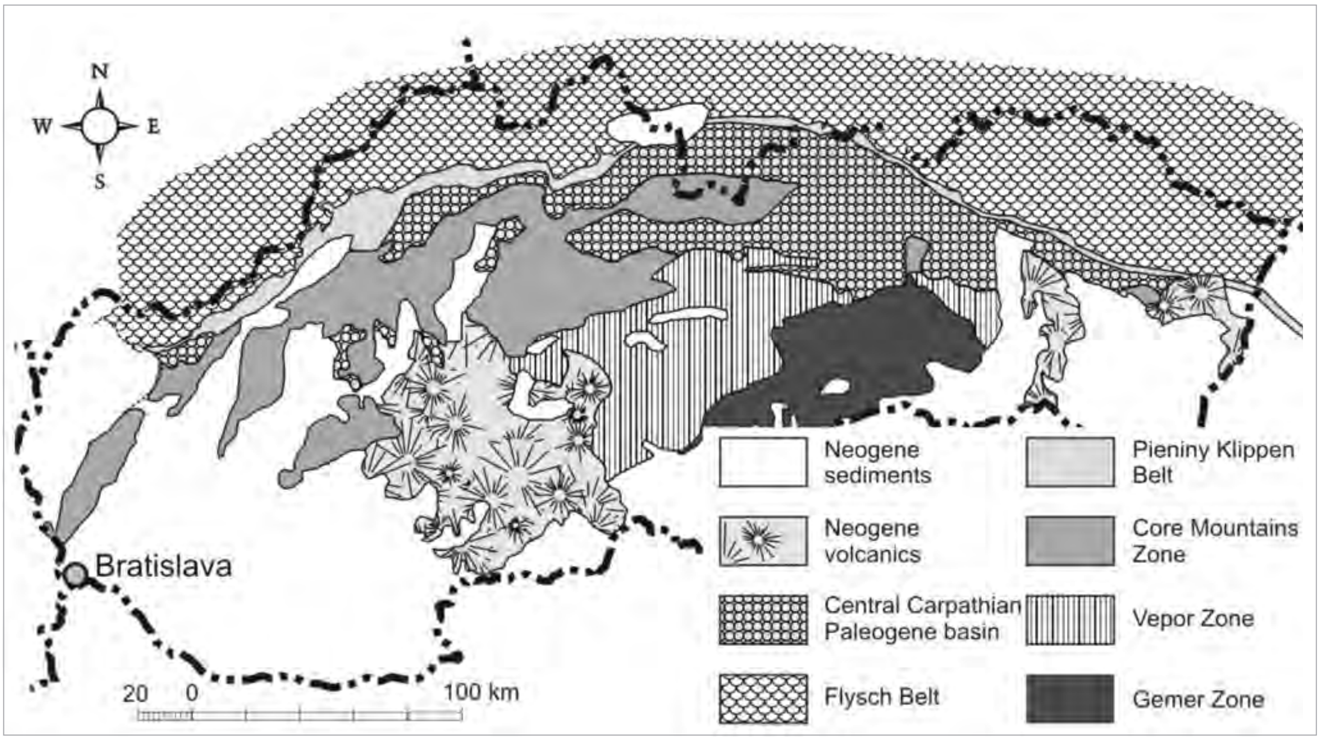

Fig. 2. Simplified geological map of Slovakia, showing the main tectonic zones.

The first two days of the field-trip are dedicated to the manifestations of Jurassic synrift deposition in the Pieniny Klippen Belt, including hardgrounds, cliff- and cave collapse-breccias, neptunian dykes, stromatactis mud mounds, Mid-Cretaceous paleokarst in the Pieniny Klippen Belt, Upper Cretaceous unconformity surfaces, continental deposits and paleokarst which originated after main tectonic phases in the Central Western Carpathians.

Younger erosional and karstification phenomena are best manifested along the former, Miocene eastern shoreline of the Vienna Basin. This pull-apart basin was formed and completely flooded in Badenian (Langhian). The field trip participants will have a chance to observe the pre-transgressional surfaces and manifestation of the latest marine transgression in the West Carpathian-Pannonian realm.

Middle Jurassic synrift sedimentation on the Czorsztyn Swell of the Pieniny Klippen Belt – breccias, neptunian dykes and stromatactis-mud-mounds

The Pieniny Klippen Belt is a melange zone situated between the Central and Outer Western Carpathians (Fig. 2). The melange consists of several units compressed and strongly deformed between the Central Western Carpathians and the Carpathian foreland (e.g., Bohemian Massif, Polish Platform). The individual successions now form tectonic blocks in this melange. The Czorsztyn Succession is the most shallow-marine unit of this belt and it was deposited on the Czorsztyn pelagic carbonate platform (Fig. 3). This swell was strongly influenced by the Middle Jurassic rifting, as evidenced by numerous neptunian dykes and syntectonic breccias (Aubrecht *et al.*, 1997). The initial Bajocian deposition of shallow-water crinoidal limestones was later replaced by more condensed neritic deposition of Ammonitico Rosso facies (Fig. 4). Within this basin with relatively low deposition rate, some uncondensed sections can be found. As they bear traces of microbial cementation and presence of the so-called stromatactis structures, they were interpreted as stromatactis mud-mounds.

Lower Cretaceous emersion and paleokarst on the Czorsztyn Swell

The Czorsztyn Swell (see introduction to the previous topic) all through its history was a submarine pelagic swell with only one exception. There was a break in sedimentation during Early Cretaceous (Valanginian to Aptian). Earlier theories considered this break as caused by submarine non-deposition and erosion. The main reason for this opinion was that this break was followed by deep-marine pelagic deposition of Albian red marls (Chmielowa Formation – see Fig. 4). Some other authors proposed an emersion and subsequent flooding of the Czorsztyn Swell. Only latest data showed that the pre-Albian surfaces bear many features characteristic for paleokarst surfaces. It was an evidence that the non-

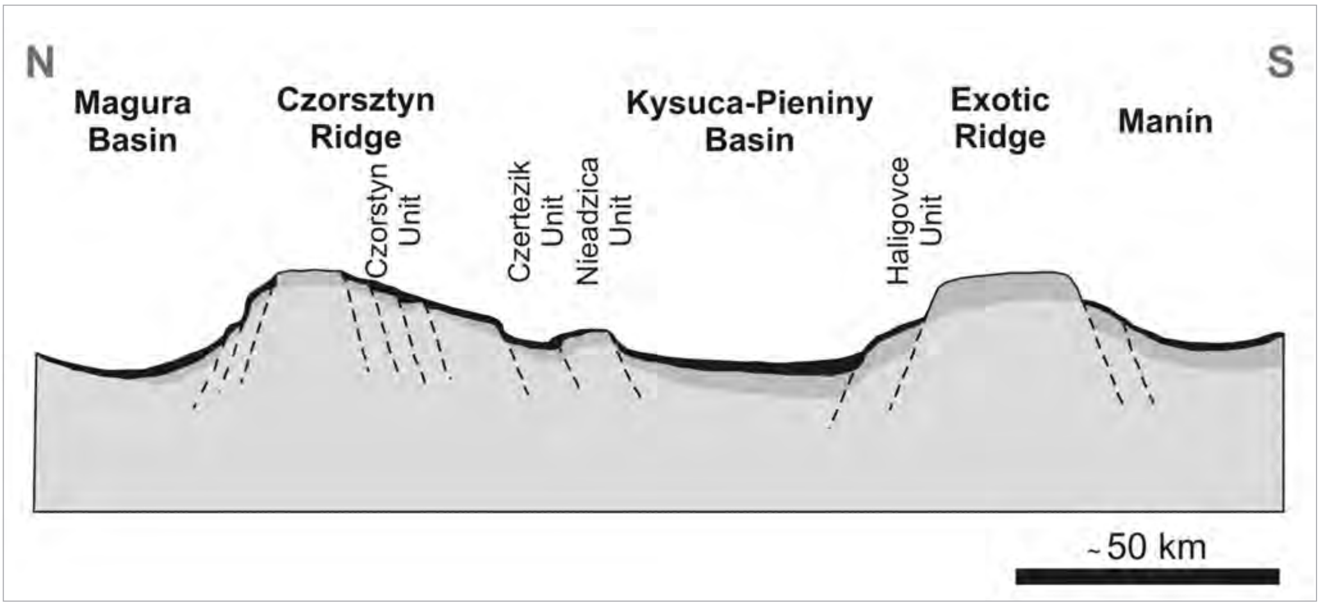

Fig. 3. Paleogeographic reconstruction of the units presently constituting the Pieniny Klippen Belt (slightly modified after Birkenmajer, 1977).

deposition was caused by emersion of the Czorsztyn Swell, accompanied by karstification and erosion. The period of emergence ended by sudden flooding (ingression) in the latest Aptian-Early Albian.

Cretaceous–Paleocene unconformity after the main nappe stacking in the Central Western Carpathians

The main tectonic phase that affected the Central Western Carpathians was the Mediterranean phase in the Middle Turonian. It resulted in nappe stacking over the Tatric crystalline basement and its Mesozoic cover units (Fig. 5). The nappes are known as so called Subtatric nappes – the Fatric and Hronic nappes. After this period, most of the Central Western Carpathians area was emerged and affected by erosion. On the most exposed carbonate complexes of the Subtatric (mainly Hronic) nappes, karstification started at that time. Paleokarst depressions formed on the surface were filled either by red karstic soils (terra rossa) or by bauxites. The latter originated by severe lateritic weathering of nearby crystalline complexes, products of which were transported through the paleokarst area and trapped in sinkholes.

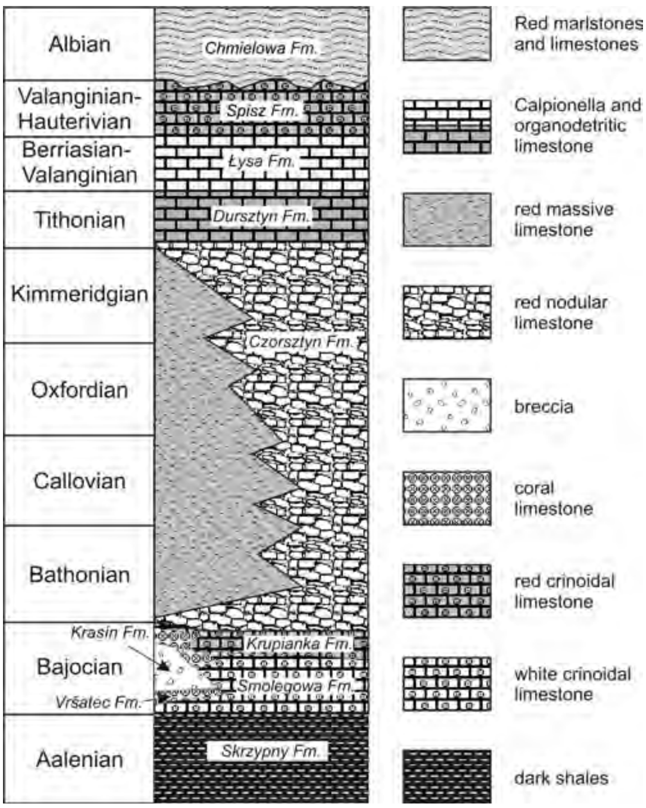

Fig. 4. Lithostratigraphic scheme of the Czorsztyn Succession.

Lower and Middle Miocene transgression on the shores of Vienna Basin and the pre-transgression paleokarst

The next topic of the field trip is to study Middle/Upper Badenian and earlier, Eggenburgian transgressive surfaces along the eastern shore of the Vienna Basin (Fig. 6). In the early Miocene, the Vienna Basin was only a small piggy-back basin on the Carpathian Flysch Zone. This basin underwent large re-building during Karpatian-Badenian time (uppermost Burdigalian to Serravalian – for correlation between the Central Para-

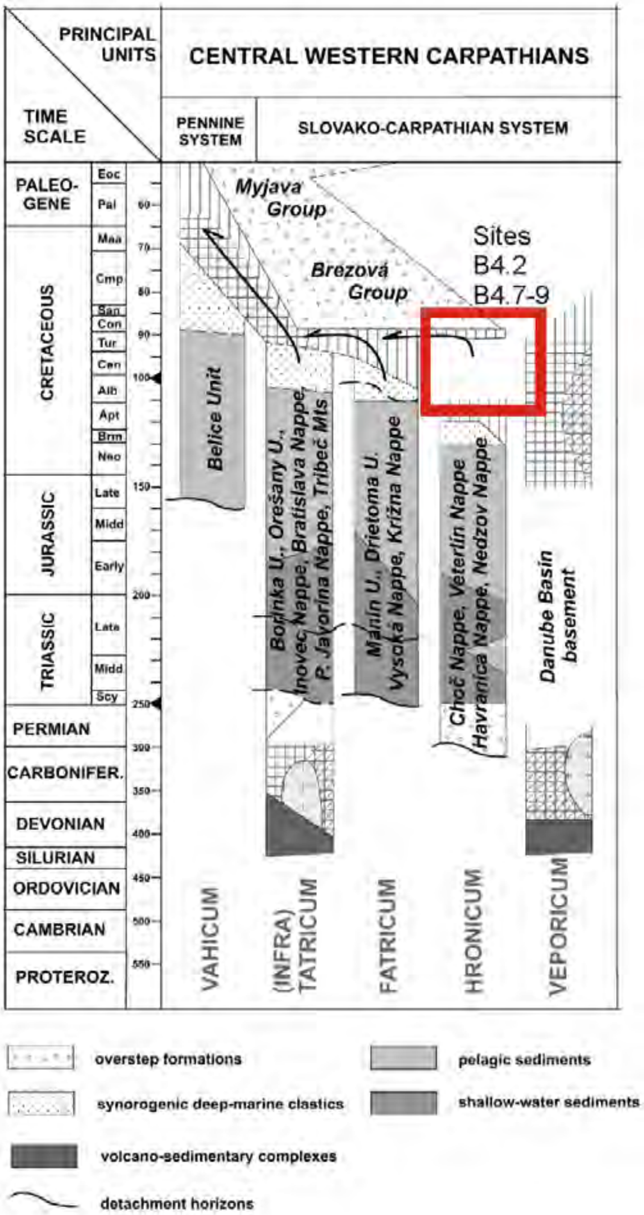

Fig. 5. Correlation table of the pre-Tertiary tectonic units of the Central Western Carpathians, with marked tectonostratigraphic position of the sites Pustá Ves, Brezová pod Bradlom, Sološnica and Mojtín.

tethys and Mediterranean stratigraphic scale, see Fig. 7) when the basin opens to its present form in a pull-apart regime (Kováč *et al.*, 2004). In this time, the horst of the Male Karpaty Mts. (Small Carpathians) originated and limited the basin from the east. The new horst underwent immediate erosion and its limestone series were karstified. Paleokarst phenomena, such as clefts and caves were initially filled with sinters, as well as by terrestrial sediments locally with rich fauna. These phenomena can be traced from the Hainburg Hills in Austria (geologically part of the Male Karpaty Mts.), across the Danube River to the Devín Castle Hill and to the neighbouring hill Devínska Kobyla. The erosion and karstification phase was followed by the Middle/Late Badenian marine transgression. It was the last true marine incursion to this area, leaving littoral to neritic sediments rich in stenohaline fauna. Various abrasion phenomena, animal borings and other features typical for intertidal zone can be observed on the transgressive surface.

Stop descriptions

B4.1 Zázrivá

(49°17′51″N, 19°13′14″E)

The Early Cretaceous emersion episode of the Czorsztyn Swell, which was accompanied with erosion and karstification, has been documented at several localities. The best locality near Horné Sŕnie was almost destroyed by quarying. Recently, a similar locality with well preserved paleokarst surface was discovered north of the Zázrivá Village in the Orava sector of the Pieniny Klippen Belt (Jamrichová *et al.*, 2012). The klippe of the Czorsztyn Succession is in overturned position (Fig. 8). Its stratigraphy starts with red nodular Czorsztyn Limestone Formation (Ammonitico Rosso facies) of Kimmeridgian to Middle Tithonian age, followed by Dursztyn Limestone Formation (Fig. 9). The latter consists of red bedded micritic limestones of Korowa Limestone Member and white micritic limestones of

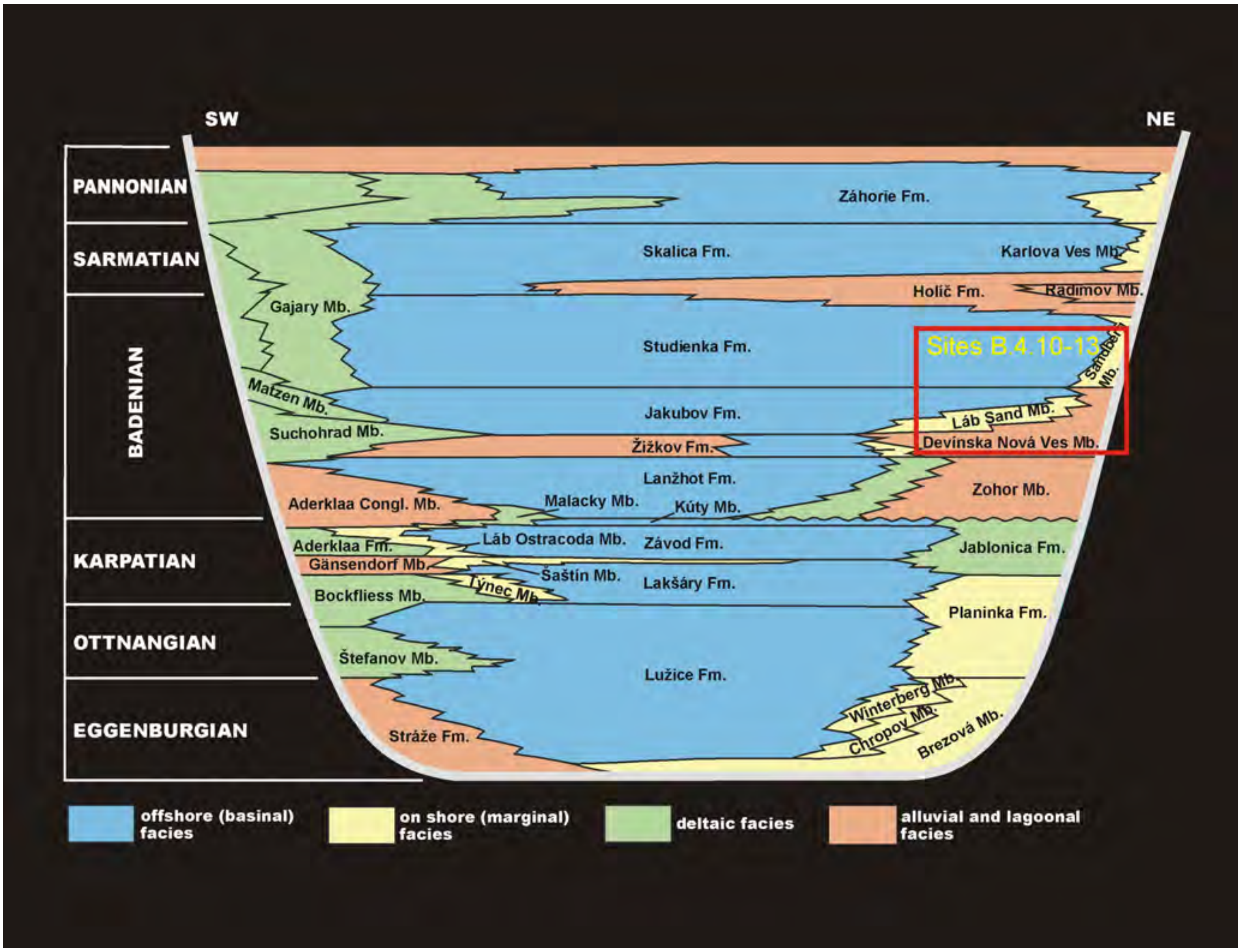

Fig. 6. Lithostratigraphy of the Neogene filling of the Vienna Basin (after Kováč et al., 2004). Rectangle marks the lithostratigraphic position of the visited sites.

the Sobótka Limestone Member. The Korowa Lst. Mb. displays unusual succession of calpionellids, starting with predominance of *Calpionella alpina* which would indicate Early Berriasian, but higher up it is dominated by *Crassicollaria brevis* which indicates Late Tithonian. Then *Calpionella alpina* becomes dominant again in the entire Sobótka Lst. Mb. This repetition of the microfacies dominated by *Calpionella alpina* was reported also from Puerto Escaño section in Southern Spain (province of Córdoba).

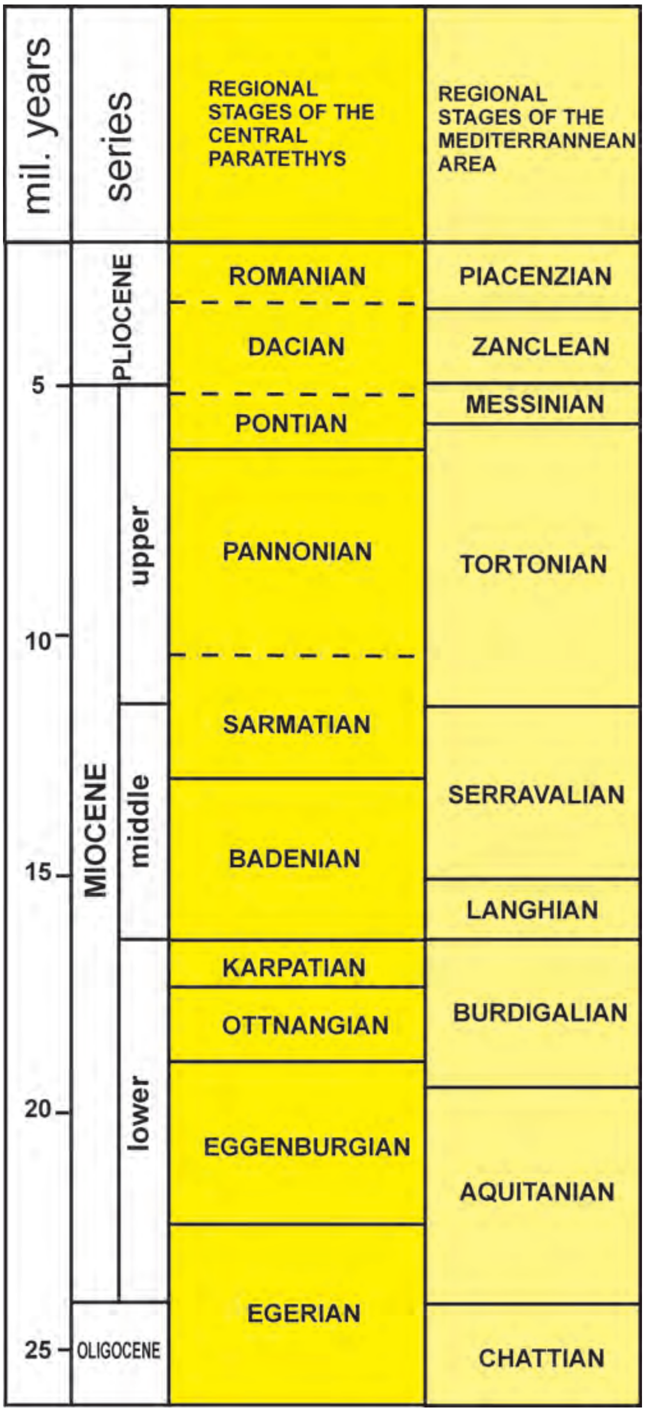

Fig. 7. Correlation between the Central Paratethys and Mediterranean stratigraphic scales.

On the stratigraphic top of the Sobótka Lst. Mb., shallow karren surface (Fig. 8 B-E) was developed (maximum 30-40 cm deep). It is visible not only at the base of the klippe but even better on a large fallen block some tens of meters below the klippe (Fig. 8 C). The surface is similar to that described from the Horné Sŕnie locality (Aubrecht *et al.*, 2006), *i.e.* a relatively flat surface is covered by loafs and hummocks with rounded tops (Fig. 8 D-E). On some hummocks, rainwater grooves perpendicular to the paleokarst surface were observed (Fig. 8E). In the eastern part of the klippe, the paleokarst surface penetrated deeper to the underlying limestone, forming a smooth depression. Shallow bivalve borings (*Gastrochaenolites*) are common on the paleokarst surface (Fig. 10A). Rich fauna of belemnites and some ammonites can be found at the very base of the condensed Albian sequence. The underlying Sobótka Lst. Mb. is dissected by some blocky-calcite veinlets which do not continue to the Albian sediments and are bored by bivalves (Fig. 10B), i.e. they are pre-Albian. Similar cases were also described from Lednica and Horné Sŕnie localities (Aubrecht *et al.*, 2006).

The upper surface of the underlying Sobótka Limestone Member is irregular also in microscale; it is bored (microboring filled with opaque Fe-Mn minerals, Fig. 10 C-D), covered with Fe-Mn-encrustations and phosphatic stromatolites with frequent sessile foraminifers. The karstic surface is covered by condensed succession of red pelagic marly limestones and marlstones (Chmielowa Formation) starting with Late Albian *Rotalipora appennica* Interval Zone. The stratigraphic gap at the studied locality then encompasses the time from Berriasian to Late Albian, with Upper Berriassian to Valanginian rocks presumably removed by erosion. The lowermost part of the Chmielowa Formation locally contains pebble-size detritic admixture, composed mostly of clasts of the underlying limestones with calpionellids (Fig. 10E). Single clast of garnet gneiss was also found (Fig. 10F).

B4.2 Mojtín

(48°59′32″ N, 18° 24′55″ E)

Near Mojtín village in the Strážovské vrchy Mts., one of the few Slovak occurrences of bauxites is situated. In these mountains, other occurrences are near Domaniža and Ďurďová. The occurrences are concentrated in paleokarst depressions and clefts in limestones (Fig. 11) of the

Fig. 8. A – Overall view on the klippe north of the Zázrivá village with preserved pre-Albian paleokarst surface (indicated by arrows). **B** – View on the paleokarst surface preserved at the bottom of the klippe. **C** – View on the paleokarst surface in vertical position on the fallen block below the klippe. **D** – Detailed view on a hummock paleokarst body protruding from the stratigraphically older underlying limestones (h). The paleokarst surface is covered by Late Albian to Cenomanian marls (m). **E** – Another hummock on which rainwater grooves are visible (arrow), being perpendicular to the paleokarst surface.

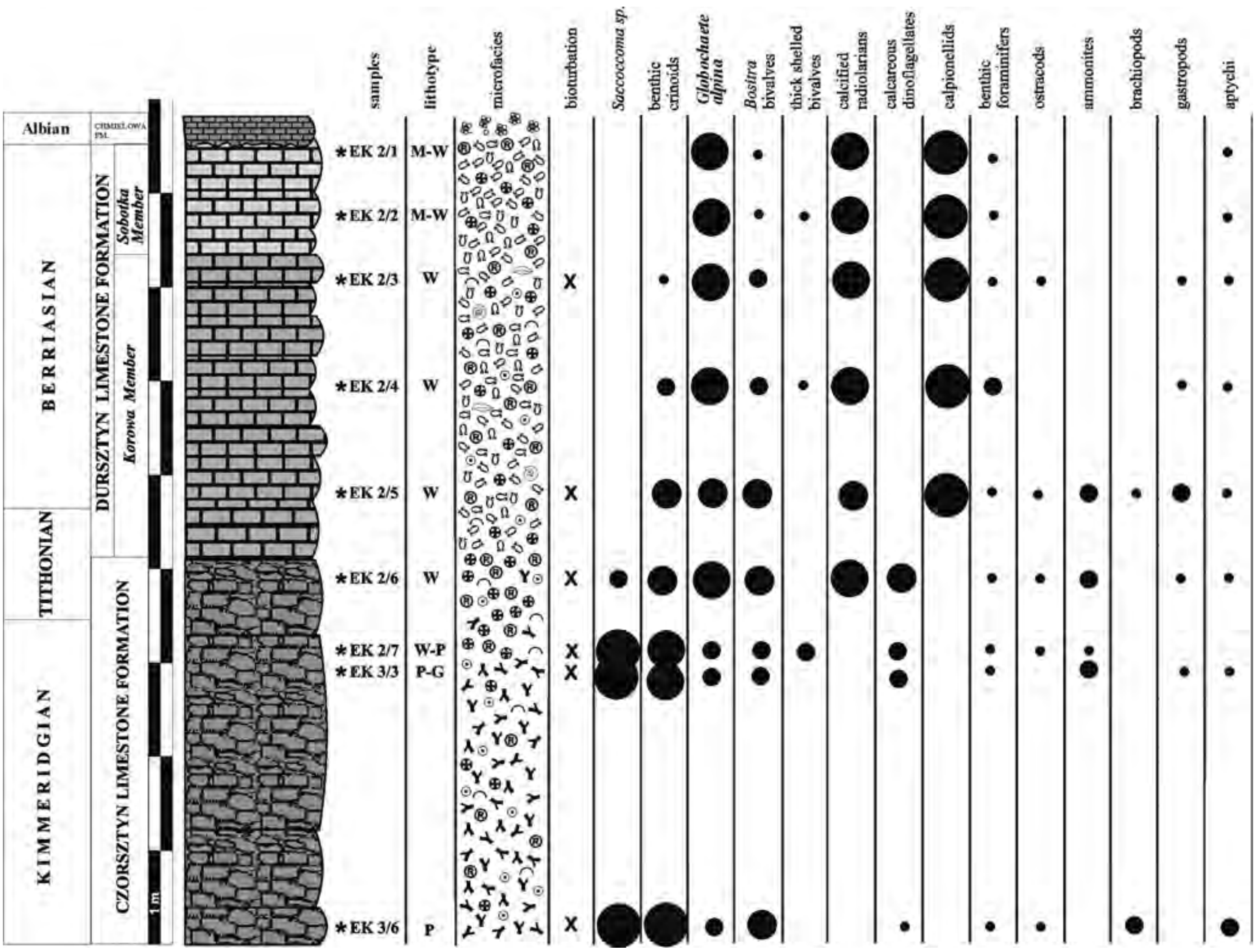

Fig. 9. Lithological section of the examined locality, showing facies and distribution of the allochems.

Strážov Nappe and in dolomites of the Choč Nappe. Outside the Strážovské vrchy Mts., bauxites were found near Markušovce in Spiš (eastern Slovakia). The largest occurrence near Mojtín is situated above Lopušná. The Mojtín bauxites had to originate after thrust of the Subtatric nappes and before Eocene (Lutetian), as the bauxite layers are covered by nummulitic limestones and breccias with bauxitic cement. Presumed age of the bauxites is Upper Cretaceous (Senonian). Part of the bauxites was likely eroded still before Eocene. Presence of the spores of lycopodian plants (*Reticulatiporites* sp.), spores and pollen grains of *Stereisporites stereoides* (Potonić & Venkatachala) Pflug, *Taxodium* sp., pollen grains of the genera *Ginkgo*, *Tilia* (lime-tree), *Nymphea*, etc. indicate that the bauxite originated in very humid and warm environment of lakes or swamps.

The bauxite occurrences are small and without industrial importance. At the locality, a bauxite waste-dump originated by experimental mining can be seen, together with uncovered Senonian paleokarst sinkholes. Technically the bauxites represent hydrargilite-boehmite type of red, yellowish, brown to greyish-white colour. Their mineralogical composition is as follows: 35% hydrargilite, 20-30% kaolinite, 15-20% boehmite, 18% hydrogoethite, 2-3% haematite (mostly in sphaerical forms – pisoids – Fig. 12). Haematite is missing in pale types. Chemical composition of the bauxites is: Al_2O_3 – 43%, Fe_2O_3 – 19%, SiO_2 – 16%, TiO_2 – 4% (Číčel 1958).

The bauxites originated most likely by pervasive lateritic weathering of acidic (indicated by: B, Zr, Sn, Li) or basic (indicated by: V, Ni, Cr, Co) eruptive rocks, which were situated outside the karstic area. The weathering products were transported in form of fine mud and colloidal solutions and trapped in paleokarst depressions and clefts.

B4.3 Vršatec

(top of the Javornik hill: 49°04′17″ N, 18°09′36″ E)

The group of main Vršatec Klippen is the largest in Slovak territory and in the entire Pieniny Klippen Belt. They are situated above the Vršatské Podhradie village,

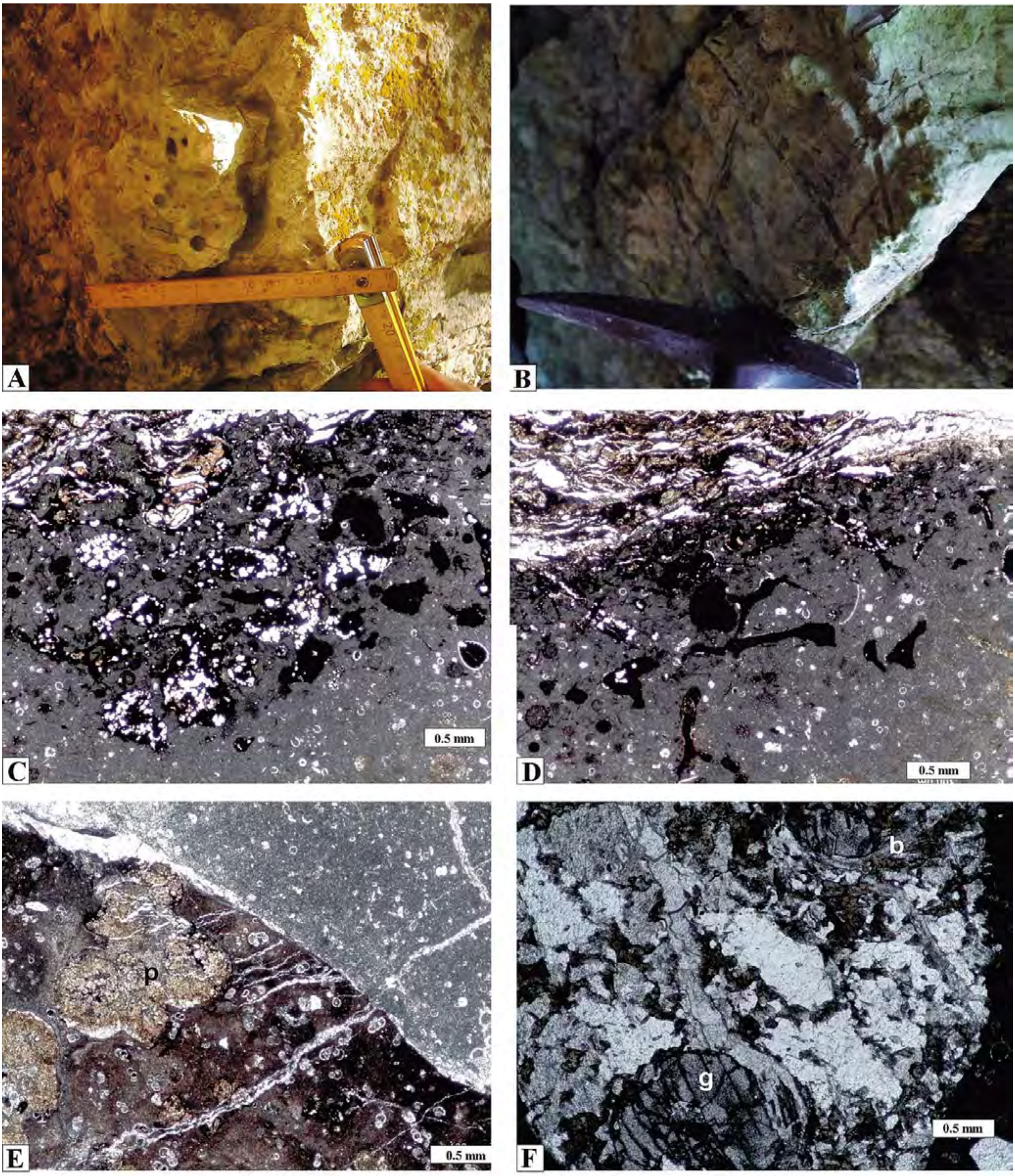

Fig. 10. A – Paleokarst surface at the base of the klippe bored by bivalves (trace fossil *Gastrochenolites*). **B** – Pre-Albian calcite veinlets (appear as straight grooves on the photo) bored by bivalves. **C, D** – Bored limestone of the Sobótka Limestone Member below the base of the Chmielowa Formation. The borings are filled with opaque Fe-Mn minerals. Thin-section, plain polarized light. **E** – Clast of the underlying calpionellid wackestone (the Sobótka Limestone Member, upper right part of the thin-section) in the red marly limestone of the Chmielowa Formation (lower left part). The latter also contains clusters of phosphates (p). Plain polarized light. **F** – Small pebble of garnet gneiss in the Chmielowa Formation. The rock consists of quartz (white to pale-grey), garnet (g) and biotite (b). Thin-section, plain polarized light.

NW of the Ilava town. This locality consists of two tectonic blocks that belong to the Czorsztyn Unit: the Vršatec Castle Klippe (Fig. 13) and the Javornik Klippe. They are formed by a succession of the Middle Jurassic-Lower Cretaceous carbonates that are capped by the Upper Cretaceous marls. Importantly, this locality exposes relatively thick, coral-dominated biohermal deposits, which are missing or very rare in other Jurassic successions of the Pieniny Klippen Belt. Mišík (1979b) described in detail sedimentological features of the two blocks in an E-W oriented transect based on seven stratigraphic sections. He suggested that the blocks consist of two tectonic slices with different stratigraphic successions. According to this hypothesis, the first slice contains the Upper Jurassic biohermal limestones (Vršatec Lst.) that are overlying the Middle Jurassic crinoidal limestones (Smolegowa and Krupianka Lst. Fm.). In the second slice, the Middle Jurassic crinoidal limestones are overlain by the Czorsztyn Lst. Fm. The contact between the two slices should lie within the crinoidal limestones of Middle Jurassic age. However, this hypothesis is contradicted by new litho- and biostratigraphic data (Schlögl *et al.*, 2006) that indicate that only one succession is present in the blocks, probably with high horizontal and lateral variations in facies composition. Firstly, based on geopetal infillings within brachiopod shells, the crinoidal limestones are *overlying* the biohermal limestones. Secondly, biostratigraphic data indicate that the biohermal limestone is older than thought before, probably of Middle Jurassic age.

Fig. 11. Paleokarst depression revealed by bauxite mining. Mojtín.

Fig. 12. Among other constituents, the bauxite ore contains spherical pisoids.

Stratigraphy of the overturned sequence of the Vršatec Klippen.

The Vršatec Lst. (Fig. 14) is formed by white to pinkish biohermal limestones with corals and calcareous sponges, and locally with bivalves and brachiopods. The biohermal limestones are laterally replaced or overlain by pink and grey peribiohermal limestones and reef breccia. The core of the reef is probably preserved near the top of the hill of the Javorník block. Voids and small caverns in the biohermal limestone contain internal sediment, scarce stromatolites of the LLH type (lateral linked hemispheroidal stromatolite) and algae *Verticillodesmis clavaeformis* Dragastan & Mišík. The peribiohermal limestones contain scarce corals, brachiopods, bivalves, sessile foraminifers, crinoidal ossicles, bryozoans, juvenile gastropods, calcified silicisponges and ostracods. The voids range up to dm in size and are filled with laminated muddy limestone with cross-bedding that results from replacement of inflow openings. Bioclasts in the voids and small caverns are mostly represented by ostracods. These crustaceans together with unknown pellet-producers might represent original inhabitants of the caverns.

Based on bivalves (Kochanová, 1978), the biohermal limestones were assigned to the Oxfordian by Mišík (1979b). However, the bivalves described by Kochanová (1978) are stratigraphically inconclusive (Golej, pers. communication). One neptunian dyke cutting the peribiohermal limestones contains the ammonites *Nannolytoceras tripartitum* Raspail of the Latest Bajocian or Early Bathonian age. Moreover, most of the dykes show filamentous microfacies (*Bositra* Limestone), which in the Czorsztyn Unit is restricted mainly to the Bathonian-Callovian. The Oxfordian deposits are already characterized by *Protoglobigerina* microfacies. Thus, based on the infillings of the neptunian dykes, cutting the limestones, the age of the biohermal and peribiohermal limestones is probably Lower Bajocian. The exposed part of the limestones is at least 15 metres thick.

The Smolegowa and Krupianka limestone formations are formed by grey to reddish crinoidal grainstones that are overlying the biohermal Vršatec Lst. The top of the biohermal facies is marked by thin Fe/Mn-crusts and impregnations. In contrast, the boundary between the peribiohermal facies and crinoidal limestones seems to be gradual in most sections. Only some brachiopods were collected from the base of the formation, including long-ranged taxa such as *Acanthothiris spinosa* (Linnaeus), *Striirhynchia subechinata* (Oppel), *Apringia* aff. *polymorpha* (Oppel) with possible stratigraphic range Bajocian-Callovian. Because of the lack of a stratigraphically more valuable fauna, the age of crinoidal limestones is based on the dating of the equal crinoidal deposits in the area as Bajocian. The thickness is around 35 metres.

The Czorsztyn Lst. Fm. consists of red micritic, locally nodular limestones. Based on ten detailed stratigraphic sections along both blocks, the thickness of this formation can vary between 20 cm and more than 15 metres. There is invariably a 0.5-2 cm-thick Mn-crust at the base of the formation, marking the hiatus between the crinoidal and red micritic limestones. Based on ammonites and on data from other sections, the age of the whole formation is Bathonian to Early Tithonian. The thickness of the Bathonian-?Callovian deposits, which are separated from the overlying red micritic limestones by another Mn/Fe-hardground, attains few cm up to 3.5 metres. The deposits contain mainly filaments (filamentous packstones), juvenile gastropods, benthic foraminifers and crinoidal ossicles. The overlying massive limestones show the *Protoglobigerina* microfacies, suggesting their Oxfordian age. The massive limestones pass gradually into massive red micritic limestones with the *Saccocoma* microfacies. Ammonite fauna including *Orthaspidoceras uhlandi* (Oppel) and *Hybonoticeras hybonotum* (Oppel) indicates a Kimmeridgian and Early Tithonian age.

The Dursztyn Lst. Fm. consists of massive, red, pinkish or yellowish micritic limestones. Locally, they can be rich in crinoidal ossicles (forming lenses of crinoidal packstones) and fine shelly debris. The *Saccocoma* microfacies passes gradually into the *Crassicolaria* and *Calpionella* microfacies. The Middle Tithonian to Early Berriasian age of the formation is based on calcareous dinoflagellates and calpionellids.

Fig. 13. View on the Vršatec Castle Klippe. Red micritic filling of the neptunian dykes contrasts with white crinoidal limestones.

The Cretaceous deposits are represented by red marls and marlstones. A tectonic contact of the Upper Tithonian to Berriasian white to pinkish *Calpionella* limestones with the red marls and marlstones is exposed in the road cuts in the saddle above the village Vršatské Podhradie. The sequence of limestones and marls is in reverse position. A normal sedimentological contact between the Dursztyn Lst. Fm. and the red marls is visible at the foot of the Vršatec Castle Klippe, where signs of karstification of the Lower Cretaceous limestones can be observed. The marls are of Late Cenomanian to Campanian age.

Fig. 14. Corals in the Bajocian Vršatec Limestone at the entrance to the Vršatec Castle.

Importance of the locality in the light of paleomagnetic reconstruction of the original klippen orientation

As the sections in the Pieniny Klippen Belt represent isolated blocks and tectonic lenses which were rotated along several axes, paleomagnetic analyses are necessary for the reconstruction of their original palaeogeographic position. Aubrecht and Túnyi (2001) analysed neptunian dyke orientations in four sections in the Pieniny Klippen Belt. They include the Vršatec Castle Klippe, Babiná quarry, Mestečska skala and Bolešovská dolina. In majority, the neptunian dykes are cut into the Bajocian-Bathonian crinoidal limestones (Smolegowa and Krupianka limestone formations) and consist of red micrites or biomicrites. They contain mainly juvenile bivalves or rarely the *Globuligerina* microfacies. These microfacies indicate that the dykes range from the Bathonian to Oxfordian. Exceptionally, neptunian dykes of Tithonian and Albian age were found at the Vršatec locality. However, they represent rejuvenation of older dykes (Mišík, 1979b).

The neptunian dykes (but also crevices in the breccias and even cavities in the stromatactis mud-mounds – see the Babiná and Slavnické Podhorie localities) show presence of cave-dwelling ostracods *Pokornyopsis feifeli* (Triebel) (Fig. 15-16) which are ancestors of the recent genus *Danielopolina* (Fig. 17) which is a common cave dweller in the recent times (mostly in the so-called anchialine caves). This is an evidence that this originally deep-marine fauna started to inhabit submarine cave environment already in Jurassic (Aubrecht and Kozur 1995). Except of pressure and temperature, the cave environment possess all the properties identical to the deep-marine habitats, such as tranquil, steady environment, with lack of light, less competitive organisms and less predators.

The measurements of the neptunian dykes and their evaluation, with utilizing of paleomagnetic correction, enable estimating the paleogeographic orientation of the Czorsztyn Ridge. The mean orientation of the neptunian dykes is NE-SW (with N-S to ENE-WSW variations), thus indicating the most probable orientation of the Czorsztyn Ridge during the Middle Jurassic (Fig. 18). This direction points to the NW-SE oriented Jurassic extension in that area. The paleomagnetic inclination ranging between 21° and 46°, with mean point of about 33°, indicates that the Czorsztyn Ridge was located approximately at 10-30° paleolatitudes in the Middle Jurassic.

Valanginian-Aptian emersion, karstification and Albian drowning of the Czorsztyn Swell – the Vršatec examples.

The Czorsztyn Unit is the shallowest Pienidic unit of the West Carpathian Pieniny Klippen Belt. After the Hauterivian, a hiatus encompassing almost the whole Barremian and Aptian occurred in this unit. Tithonian-Lower Cretaceous limestones are overlain by pelagic Albian marlstones and marly limestones. A nature of this hiatus was many times discussed in the literature. Most authors favoured a submarine non-deposition

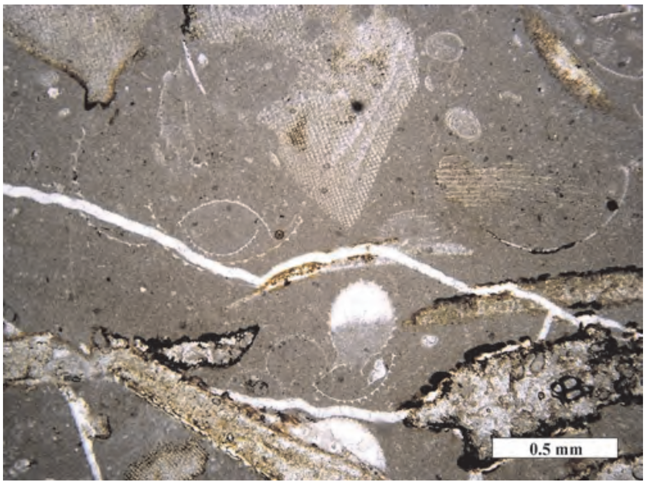

Fig. 15. Cross-sections of cave-dwelling ostracods *Pokornyopsis feifeli* (Triebel) in neptunian dyke filling from Vršatec.

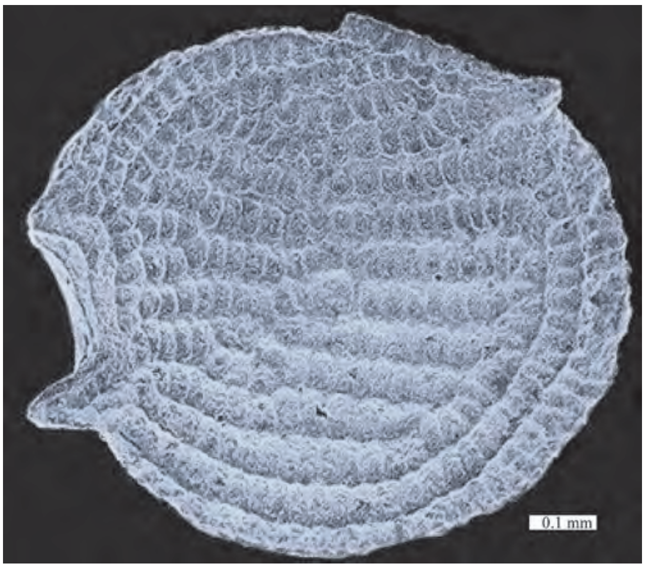

Fig. 16. Holotype of *Pokornyopsis feifeli* (Triebel) from Germany. After Kornicker & Sohn (1976).

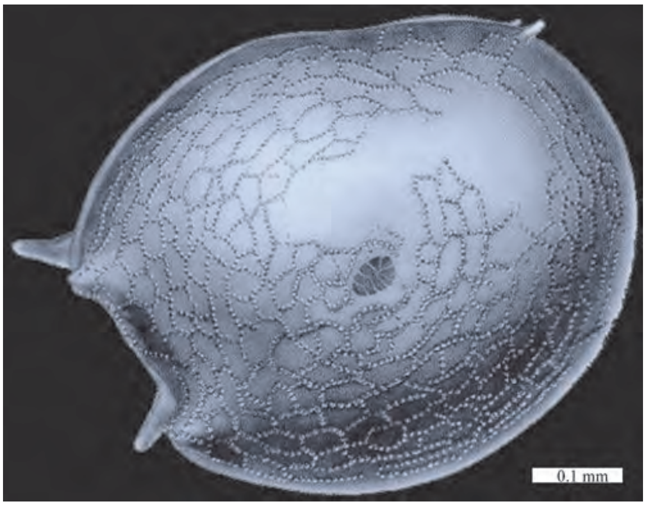

Fig. 17. One of the recent descendants of the Jurassic cave-dwelling ostracod fauna – *Danielopolina orghidani* (Danielopol). After Kornicker & Sohn (1976).

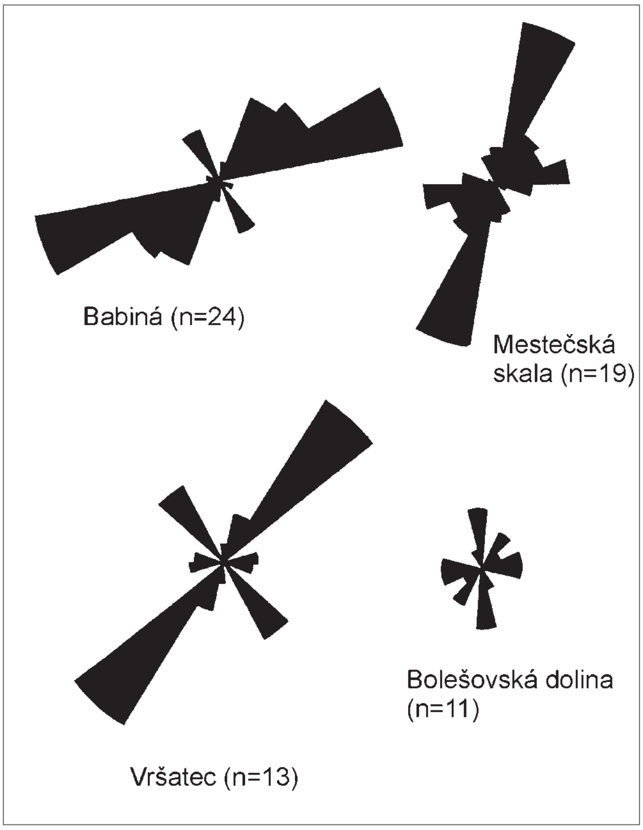

Fig. 18. Evaluation of original orientation (corrected according to paleomagnetic data) of neptunian dykes at four selected localities of the Czorsztyn Succession.

and erosion (Birkenmajer, 1958, 1975), whereas others proposed an emersion of the ridge (Mišík, 1994).

In the last years, most of the formerly known sites were reexamined and some new sites were found with the preserved contact between the Albian and the underlying formations of the Czorsztyn Unit. At two sites, the Albian marlstones and limestones are in contact with rocks older than Tithonian or Neocomian. In Jarabiná, the Barremian-Aptian erosion reached the level of Kimmeridgian red micritic limestones but clasts of limestones with "filamentous" microfacies indicate that Bathonian-Callovian limestones had to be uncovered too. At Horné Srnie, where the deepest erosion level was found, the Albian deposits overlie Bajocian-Bathonian crinoidal limestones. Except of deep erosion, unequivocal signs of subaerial exposure and karstification (karren landform with vertical drainage grooves, small cavities in the bottom rock filled with later sediment, bizarre fractures and veinlets filled with calcite, were revealed, mainly in the Horné Sŕnie and Lednica sites. This was followed by pelagic deposition, documented by Albian marlstones and limestones with pelagic fauna. At this time, the paleokarst was bored by boring bivalves and overgrown by deep-water Fe-Mn to phosphatic stromatolites. This suggests a very rapid relative sea-level rise, most likely due to a marine ingression. A tectonic platform collapse and drawning-can not be excluded. Very similar case of Cretaceous paleokarst was reported from Betic Cordillera, Spain (Martin-Algarra & Vera, 1996).

Several relics of the Albian marlstones overlying the Neocomian limestones, together with some Albian neptunian dykes cutting the underlying rocks, were found in the Vršatec klippen. Most of them are summarized by Mišík (1979b); two localities were revealed not long ago. The basement below the Albian sediments is commonly irregular (Fig. 19), which was most probably caused by karstification and boring animals. Small caverns in the Lower Cretaceous limestones filled by Albian sediments are common too. The Albian deposits are pelagic marlstones to limestones, with fauna of belemnites (for example *Neohibolites minimus* Lister), bivalves *Aucellina* sp. and numerous planktonic foraminifers *Ticinella roberti* (Gandolfi), *Thalmanninella ticinensis* (Gandolfi), *Hedbergella infracretacea* (Glaessner), *Thalmanninella apenninica* (Renz), *Planomalina buxtorfi* (Gandolfi) and many agglutinated foraminifers. The foraminifer assemblage indicates an Albian to Cenomanian age of the overlying beds. Deep-water bacterial Fe-Mn-P stromatolites, oncoids and frutexites are common in the basal parts, sometimes directly overgrowing the underlying limestones. Higher up, some radiolarian cherts were found in the Cenomanian-Turonian marlstones at the southernmost Vršatec klippe (Sýkora *et al.* 1997) which testifies the rapid sea-level rise after drowning of the swell.

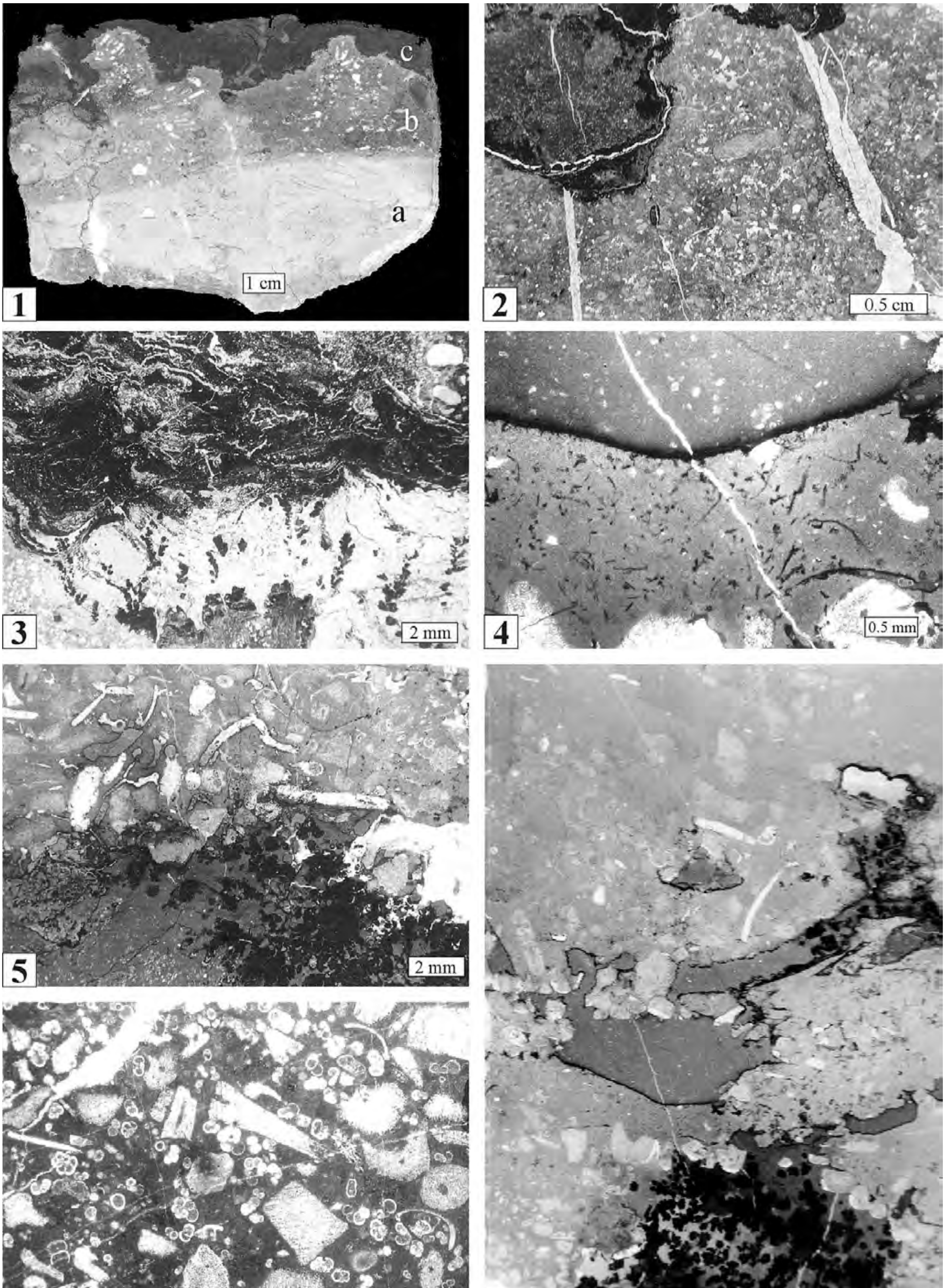

Fig. 19. Slabs and microphotos from the localities at Vršatec. **A** – Slab showing Neocomian limestone (a), covered by Late Albian organodetrital limestone (b) and by P-Fe stromatolite (c) which is the base of pelagic Albian deposit. Note the uneven surface between the Upper

In the Albian sediments of 6 localities (2 from Vršatec), a detrital admixture containing chrome spinels was found (Jablonský *et al*., 2001; Aubrecht *et al*., 2009a). Such minerals, derived from an unknown ophiolitic source area are common in the Albian deposits of the Klape Unit, the Tatric and Fatric units, but they were not found so far in the Czorsztyn Unit. The presence of ophiolitic detritus in the Albian of the Czorsztyn Unit is very surprising and contradicts the classical paleogeographic schemes where the Czorsztyn Swell still in Albian formed an isolated ridge, surrounded by deep troughs.

B4.4 Babiná

(49°01′55″ N, 18°10′47″ E)

The locality is an abandoned quarry located at the foot of Babiná Hill, on the road between Bohunice and Krivoklát villages in the Middle Váh Valley in western Slovakia (Fig. 20). It was described in details by Mišík *et al.* (1994a). An overturned Czorsztyn sequence from the Middle Jurassic to the Neocomian crops out in the quarry (Fig. 21). White and pink Bajocian crinoidal limestones (Smolegowa and Krupianka formations) are exposed in the main SE part of the quarry. The crinoidal limestones are cut by numerous neptunian dykes filled with red mudstones of "filamentous" microfacies (Mišík et al., 1994a; Aubrecht and Túnyi, 2001). The rest of the quarry shows red to pink micritic limestones (mudstones) of the Bohunice Limestone Formation (Bathonian-Kimmeridgian) which gradually pass upwards into Tithonian-Lower Cretaceous limestones (Dursztyn Formation).

The detailed description of the individual lithological units is as follows:

1. White and pink crinoidal limestones (Bajocian) form the dominant (left) part of the quarry. The crinoidal limestones are biosparites with sandy admixture of clastic quartz grains and small yellowish dolomite lithoclasts. A thin intercalation of the fine-grained conglomerate with a pebble of maximum size 6 cm (spongolite) was found. The most numerous are pebbles of vein-quartz (white, pink, honey-yellow), silicates (spongolites or without organic remnants), dolomites (some of them with traces of boring bivalvians), dedolomites, single pyroclastic rock of acid volcanites – tuffite and greywacke with kaolinized feldspars. In the highest part, on the edge of the quarry, the following association of brachiopods was found: *Monsardithyris ventricosa* (Ziet.), *Cymatorhynchia* ex gr. *quadriplicata* (Ziet.), „*Terebratula*" aff. *decipiens* Eud.- Desl., *Linguithyris curviconcha* (Oppel), *Antiptychina* aff. *bivalvata* (Eud.- Desl.), *Caucasella trigona* (Quenst.) and *Sphenorhynchia latereplanata* Seifert (Mišík *et al*., 1994a).

Within the crinoidal limestones, bodies of syndepositional breccias, which originated due the synsedimentary extensional tectonics occur locally (so-called Krasín Breccia). The breccia occurs mostly within the crinoidal limestones in the higher part of the quarry, where it occurs directly within the crinoidal limestone as probable larger cleft filling, as well as at the left part of the quarry, where it is related to networks of neptunian dykes. Both types contain various fillings of interstitial voids but more complex are fillings in the central part of the quarry (Fig. 22A). The breccia has angular to subangular clasts, more or less developed radiaxial fibrous calcite (RFC) crusts (mainly in the breccias from the central part of the quarry), stromatolites (pre- or postdating the RFC, mainly in the left part of the quarry)

Albian limestone and the covering stromatolite. The surface was most likely shaped by karstic dissolution. It provides an evidence of repeated emersion of the sedimentary area still after the first phase of flooding in the Late Aptian. **B** – Two veinlets filled with blocky calcite, cutting the Neocomian organodetritic limestone but not continuing to the Albian stromatolitic hardground above. Their age is then pre-Albian and their filling may be of fresh-water origin. **C** – Albian stromatolite (with ptygmatitically folded calcite veinlets – upper part of the photo) and bush-like *Frutexites*-type stromatolites growing in the Albian sediment towards the stromatolite. The latter means that the sediment represents filling of a larger cavity and the stromatolite above grew on the roof of the cavity. This context could not be recognized in the field. **D** – Network of Mn-oxides filled traces in the Neocomian limestone created by boring organisms, most likely fungi (the traces are locally branching) below the base of the Albian sediments. **E** – Geopetal filling of the leached bivalves in the Neocomian limestone (above) contradicts to the location of the Albian sediment (below). It indicates that the Albian sediment deposited in a cavity (most likely karstic). **F** – Bizarre cavities in the Neocomian limestone filled with Albian micrite. Their geopetal filling enables to orient the photo properly, in spite of the position of the Albian stromatolite and sediment (below). They most probably represent filling of a larger karstic cavity. **G** – Crinoidal-foraminiferal wackestone to packstone of the Late Aptian-Early Albian age, representing sediment of the first phase of flooding after the hiatus.

Fig. 20. Panoramic view on the Babiná quarry.

and the latest, predominantly micritic filling (red in the left part of the quarry and yellowish in the central part) and blocky calcite filling the veinlets and occluding the remaining porosity. Some clasts and cement filling bear signs of leaching, which is indicated by irregular, bizarre surface (Fig. 22C-D). This indicates a likely fresh-water influx into the breccia complex.

Some breccia blocks were found with clasts of crinoidal limestones with simple matrix formed also by crinoidal limestone, free of any additional cement crusts. Moreover, most of such breccias possess the clasts of red crinoidal limestones, whereas the matrix is of white crinoidal limestone (Fig. 22B), i.e. just opposite to the division of Birkenmajer (1977) where the red crinoidal limestone (Krupianka Lst.) should be younger than the white crinoidal limestone (Smolegowa Lst.). This contradiction was mentioned already by Mišík *et al.* (1994a) and Aubrecht *et al.* (1997).

2. Neptunian dykes. Crinoidal limestones are densely penetrated by neptunian dykes with maximum width of 35 cm. Their directions are strongly scattered; the prevailing extension, after dip and paleomagnetic correction was NE-SW (Aubrecht and Túnyi, 2001 – see Fig.16). The filling is red, partly cream-coloured, often with irregular lamination, sometimes oblique or lenticular. Biomicrite (wackestones and packstones) laminae alternate with those of micrite and pelmicrite; frequent intraclasts were derived from the fracture walls. The remaining empty spaces were filled by radiaxial calcite cement. Among organic remnants "filaments" predominate (juvenile bivalves of the Bositra-type, rarely also with thicker shells strongly bored by algae; their tiny canals are impregnated by Fe-hydroxides); the

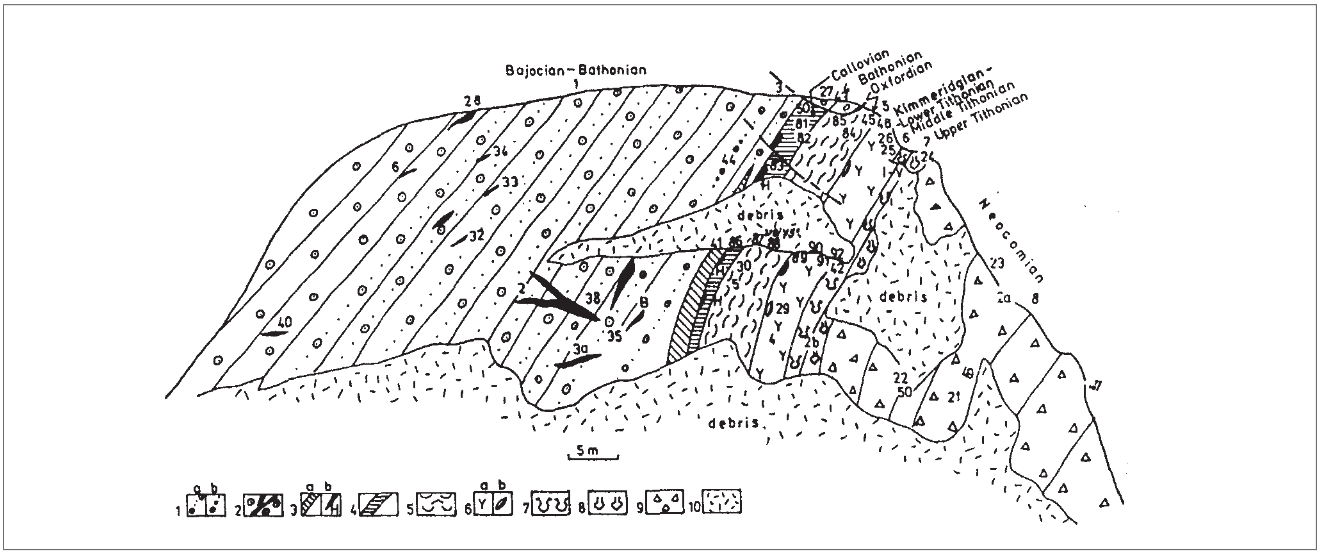

Fig. 21. Lithological sketch of the Babiná quarry. 1a – White and pink crinoidal limestones – Bajocian – Bathonian. 1b – Conglomerate intercalation. 2 – Neptunian dykes – Upper Bathonian – Lower Callovian. 3a – pink biomicrite with "filaments" and stromatactis – Callovian. 3b – Hardground. 4–7 – Bohunice Limestone Formation: 4 – red limestones with "protoglobigerina" – Callovian, 5 – creamy and pink biomicrites with bivalves and *Cadosina parvula* – Oxfordian, 6a – pink biomicrite with Saccocoma and higher with *Parastomiosphaera malmica*, 6b – brachiopods with polarity structures, 7 – pink biomicrite with black coated bivalves – Kimmeridgian – Lower Tithonian. 8–9 – Sobótka Limestone: 8 – white and creamy biomicrite with *Chitinoidella* – Middle Tithonian, 9 – pink biomicrite with black–coated bivalves and Crassicollaria. 10 – Walentowa Breccia – pink and grey limestone breccia with crinoidal matrix – Neocomian. After Mišík et al. (1994a).

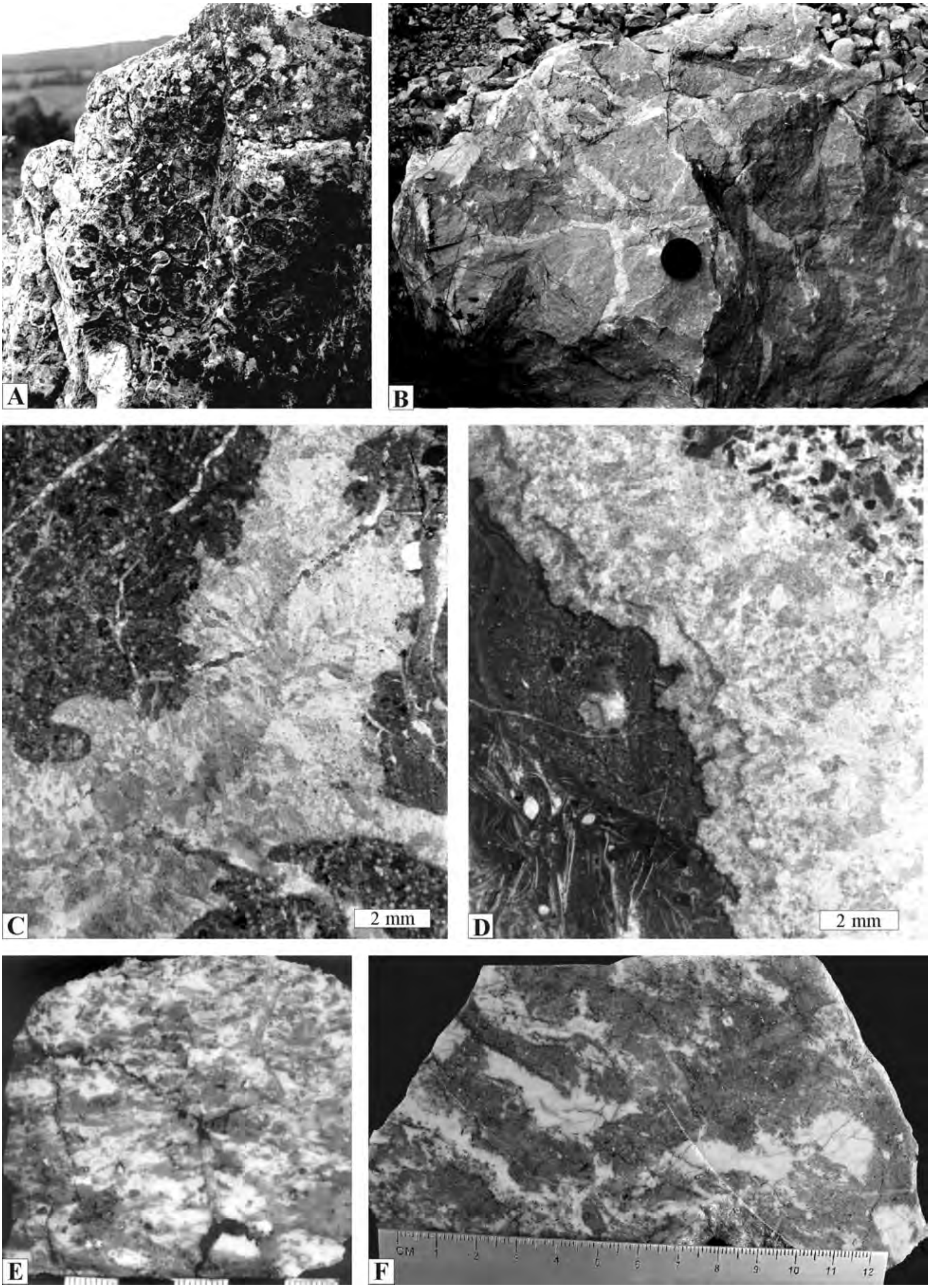

Fig. 22. A – Block of Krasín Breccia with radiaxial fibrous calcite coatings, representing a remnant after Babiná quarry exploitation. Block came most likely from the middle of the quarry. Scale: lens cap is 5.8 cm across. **B** – Block of breccia with clasts of red and matrix of white crinoidal limestone (inverse colouration of the limestones as in the classic scheme of Birkenmajer, 1977). Middle to left part of the quarry. Scale: lens cap is 5.8 cm across. **C** – Irregular surface of the crinoidal limestone clasts, formed probably by etching, healed by RFC. Breccia from the left part of the quarry. **D** – Irregular margin of the RFC crust, related most likely to partial leaching. **E** – Polished slab with anastomosing tiny stromatactis from the layer overlying the crinoidal limestones. **F** – Slab with larger, several cm–size stromatactis.

Fig. 23. View on the abandoned quarry near Slavnické Podhorie.

"umbrella effect" (sparite formed under the concave side protected against the micrite deposition) was frequently observed. Current constituents are echinoderm plates and foraminifers: *Ophthalmidium* cf. *carinatum* Leischner, *Ophthalmidium* sp., *Lenticulina* sp., *Marsonella* sp., *Nodosaria* sp., microforaminifera (Fe-Mn coatings of the juvenile foraminiferal chambers); rare ostracods, globochaete cells, uniserial bryozoans and fucoids are also present. Clastic quartz (to 0.25 mm) and fragments of hardgrounds are very rare. Tiny sterile microdikes penetrate transversally the described neptunian dykes.

There are no direct age indicators concerning the filling of the dykes. It is probably not much younger than the surrounding crinoidal limestones. With regard to the dominant „filament" microfacies and the fact that the dykes do not penetrate into the younger strata, we assume that they are of Upper Bathonian – Lower Callovian age. The „filament" microfacies filling is noteworthy, as such limestones are almost entirely absent in the overlying succession. The fracturation of the white crinoidal limestones and the filling of these fractures took place before the deposition of the next member – creamy and pinkish biomicrites with „protoglobigerina" microfacies.

3. Pink limestone with stromatactis structures (probably Bathonian-Callovian)**.** It is only 80 cm thick and occurs in the middle part of the quarry at the contact of the crinoidal limestones and the hardground. The structure can be characterized as dismicrite with small, atypical stromatactis – irregular anastomosed voids elongated along the plane of stratification (Fig. 22 E-F). The voids are usually limited by thin-shelled bivalves - „filaments" (shelter porosity).

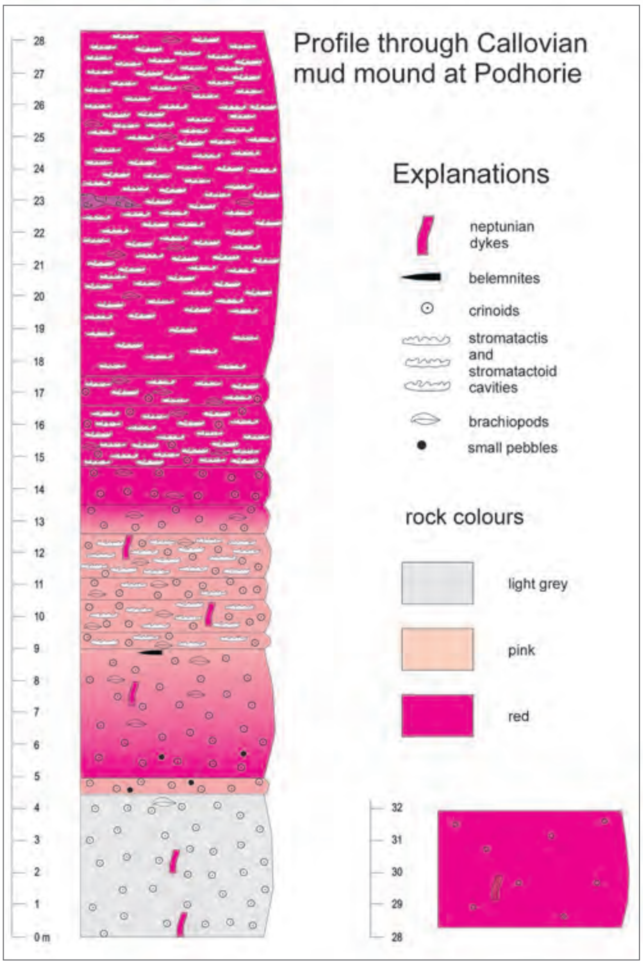

Fig. 24. Section through the core of stromatactis mud-mound at Slavnické Podhorie.

They are filled by radiaxial calcite cement with fluid inclusions and a younger clear blocky cement in their central parts. Sparitic areas are probably enlarged by recrystallization, as can be deduced from the radial aggregates of calcite around the relics of pellets. Besides small bivalves, unusually frequent microforaminifers (basal membranes impregnated by Fe-oxides), echinoderm plates, spicules of siliceous sponges filled by calcite, nubecularids, ophthalmids, single small gastropods and worm tubes occur. Quartz grains are very rare but their size is up to 3 mm. The stromatactis horizon passes in the upper part of the quarry into pink biomicrite with typical „filamentous“ microfacies.

This bed is dominated by "filamentous" microfacies which indicates latest Bajocian to Callovian age (cf. Wierzbowski *et al.*, 1999). The same microfacies also represents the infillings of the neptunian dykes cutting the underlying crinoidal limestones. At the top of the mudstone bed a black manganese crust representing a non-deposition surface occurs.

4. Pink and red limestone layers impregnated by Mn-Fe oxides, with black hardground crust (2 cm) on their base – Oxfordian.

The limestone starts as biointramicrite with „protoglobigerina“ microfacies. It contains frequent planktonic foraminifers *Globuligerina* sp., less numerous benthic forms, such as *Ophthalmidium* sp., *Marssonella* sp. *Spirillina* sp., *Lenticulina* sp., abundant voids after the radiolarians filled by drusy calcite or dark micrite (these radiolarian „ghosts“ resemble round coprolites), originally aragonitic bivalves with red coatings (dissolved and filled by micrite, often with collapsed micritic rims), globochaete cells, ostracods, *Cadosina parvula* Nagy, single juvenile ammonite, rhyncholite, phosphatized fish scale, uniserial bryozoan and echinoid spine. Several intraclasts with the red coatings and traces of dissolution and the fragments of Fe-Mn hardgrounds are further signs of condensed sedimentation. The hardground crust contains 14.3% Mn (= 18.46% MnO), 15.34% Fe_2O_3, 1.92% SiO_2 and 0.54% TiO_2. The presence of *Cadosina parvula* signalized Oxfordian age.

5. Creamy and pink micritic limestones with bivalves – Oxfordian.

Their composition is similar to that of the previous member: abundant radiolarians (frequently only their phantoms reminding coprolites), variable amount of „protoglobigerina“ (*Globuligerina* sp.), *Cadosina parvula* Nagy, single *Colomisphaera* sp. etc. Clastic quartz was absent, except one thin-section with a grain 3 mm in size; cubes of epigenetic pyrite occur. A slight nodularity was observed. The thickness is about 5 m.

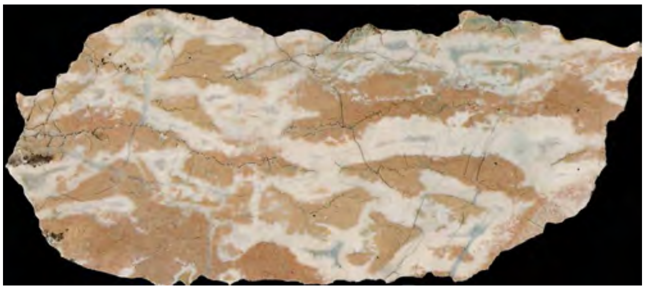

Fig. 25. Slab of the stromatactis-bearing mudstone.

6. Pink micritic limestones – Kimmeridgian – Lower Tithonian.

Generalized characteristic from 5 thin sections: biomicrite, mostly packstone with Saccocoma-Globochaete microfacies, further with numerous juvenile ammonites, foraminifers (genera *Marssonella*, *Involutina*, *Lenticulina*, *Nodophthalmidium* etc.), fragments of brachiopods and bivalves, rare echinoid spines, ostracods and aptychi.

The voids in the microfossils and macrofossils (mainly in brachiopods) contain internal sediment with polarity structures confirming inverted sedimentary succession. Clastic quartz (terrigenous admixture) is absent; rare cubes of epigenetic pyrite up to 0.4 mm occur. Brachiopods *Nucleata bouei* (Zejsz.) and *Lacunosella* aff. *spoliata* (Suess) from point 46 indicate Kimmeridgian. The thickness is about 4.5 m. In this part of the section, stromatactis-like cavities reappear.

7. Pink micritic limestone with small black-coated bivalves – Lower Tithonian.

They can be differentiated only by means of microscope, based on the presence of *Parastomiosphaera malmica* (Borza) and the absence of *Chitinoidella* (Borza, 1984). They are biomicrites with *Saccocoma* microfacies, abundant globochaete cells, bivalves (originally aragonitic ones with the mentioned black coating, red in the thin-sections), rare large crinoidal columnalia (also corroded and with red coatings), *Lenticulina* sp., *Frondicularia* sp., *Bullopora* sp., agglutinated foraminifers, several *Parastomiosphaera malmica* (Borza), *Cadosina parvula* Nagy, *Colomisphaera* sp., tiny filaments genetically connected probably with globochets, single juvenile ammonites, gastropods, calcified radiolarians, aptychi, ostracods, single fish tooth and serpulid worm *Durandella* sp. Rare voids with polarity structures occur. The thickness is 1 m.

The pink and red micritic, massive, not nodular limestones, which locally replace the classical nodular Ammonitico Rosso facies (Czorsztyn Limestone Formation) above the crinoidal limestones was named as the Bohunice Limestone Formation (Mišík et al., 1994a), with stratigraphic span from the latest Bajocian to the Lower Tithonian.

8. White and creamy micritic limestones – Middle Tithonian.

They belong to the *Chitinoidella* zone indicating the Middle Tithonian (Borza, 1984). The generalized description was carried out from nine thin-sections: biomicrites-packstones with *Globochaete-Saccocoma* microfacies containing *Chitinoidella boneti* Doben, voids after dissolved radiolarians filled by calcite, foraminifers (*Involutina* sp., *Marssonella* sp., *Lenticulina* sp.), juvenile ammonites,

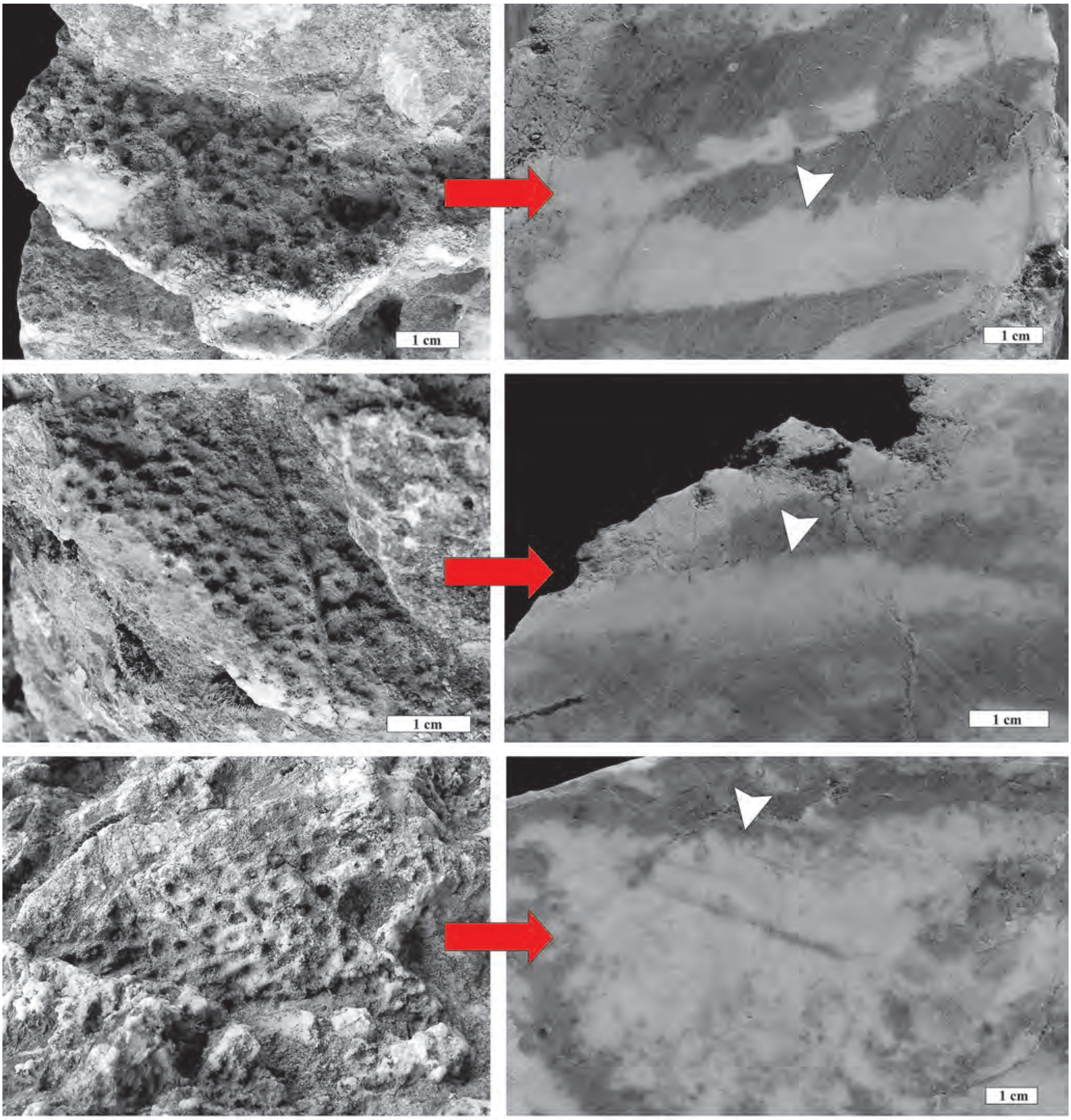

Fig. 26. Relationship between the weathered casts of siliceous sponges (left) and the corresponding cross-sections in slabs (right). The corresponding weathered surfaces are marked with arrows in the slabs. The cross-sections display actual stromatactis shape and composition (relatively flat bottoms and digitate upper parts, initial fillings of radiaxial fibrous calcite and eventual blocky calcite later filling).

tiny filaments with special sculpture, probably connected with globochets, ostracods, *Colomisphaera* sp., aptychi and basket-like sections, probably of a calcareous sponge. The total lack of clastic quartz should be stressed once more. A juvenile specimen of *Pygope* sp. proceeded from these limestones.

9. Pink micritic limestones containing bivalves with black coatings – Upper Tithonian.

They correspond to the Korowa Limestone Member of Birkenmajer (1977). They can be characterized as biomicrites-wackestones, frequently bioturbated with *Crassicollaria* microfacies, mostly with *Crassicollaria intermedia* Durand-Delga, single *Calpionella alpina* Lorenz and *Chitinoidella* sp., abundant globochaete cells and voids after radiolarians filled by calcite, fragments of bivalves, originally aragonitic, with red margins in transmitted light, rarely bordered with black Mn-dendrite; they were dissolved and filled by micritic sediment or by sparitic cement; their micritic rims sometimes collapsed. Single bivalves with prismatic layer in calcitic shell, several juvenile ammonites, ostracods, aptychi, brachiopod fragments, *Spirillina* sp., *Marssonella* sp., *Patellina* sp., *Involutina* sp. and *Cadosina fusca fusca* Wanner have been observed. Corroded and bored intraclasts with thin Fe-crusts occur, as well as voids with polarity structures.

The peculiar very fine-grained pyroclastic admixture (about 20 grains under 0.15 mm in a thin-section) of basic volcanic rocks containing tiny mostly calcified feldspars was identified. The total lack of clastic quartz points to a distant aerial transport from remote volcanic centers probably at the territory of actual Carpathian Ukraine. Another case was identified from the Kyjov-Pusté Pole klippe, Eastern Slovakia, concerning the same stratigraphical horizon and identical unit (Mišík, 1992). Basic volcanites (picrobasalts and basanites) of the same age occur also in the High-Tatric Unit but those submarine effusions hardly could introduce volcanic ash into the atmosphere.

10. Pink and grey fine-grained limestone breccias – Neocomian.

They correspond to the Walentowa Breccia of Birkenmajer (1977) with the exception that *Calpionellites* was not found in the matrix. The predominating size of clasts is 1-2 cm, up to 15 cm. The matrix with echinoderm plates is yellowish or red, the clasts are white, creamy and red. The microscopical description was derived from thin-section study of 13 samples.

Fig. 27. Krasín megabreccia consists of clasts formed by grey crinoidal limestone with matrix of red crinoidal limestone. Krasín Quarry.

The most abundant are lithobiosparrudites. Their matrix is dominated by echinoderm plates including typical brachialia of planctonic crinoids (*Roveacrinidae* ?) with syntaxial rims, frequently limited by the crystal faces. Echinoderm plates are often corroded by Fe-hydroxides along fissility surfaces. Aptychi with cellular structure and bivalves are rare, phosphatic fish teeth exceptional. Some *Hedbergella* sp. found in the matrix allow to suppose the Hauterivian age. The peculiar phosphate intraclasts and intraplasts containing arborescent calcite grains have been already found in the Neocomian limestones in the Krasín klippe (Mišík et al., 1994b). Their syngenetic origin is confirmed by the fact that the phosphate occurs also as the interstitial mass amidst the echinoderm plates in the matrix. The most frequent lithoclasts are biomicrites with the association *Saccocoma* + *Globochaete* + calcified radiolarians (fragments of Kimmeridgian - Lower Tithonian limestones), rarely with *Chitinoidella* (Middle Tithonian); the lithoclasts with *Crassicollaria* (Upper Tithonian) are rarer and smaller. The breccia lacks the quartz. It contains alike cubes and skeletal crystals of epigenetic pyrite as those mentioned in the preceding members, which confirms that the pyrite originated in the whole Callovian - Neocomian successions in the same time, in one of the post-Lower Cretaceous periods.

Sometimes an association of biomicritic lithoclasts with *Saccocoma*, surrounded by the matrix with the structure of ?*Saccocoma* (*Roveacrinidae*) biosparite, has been observed. It can be explained by the existence of the intraformational breccias already in the Kimmeridgian

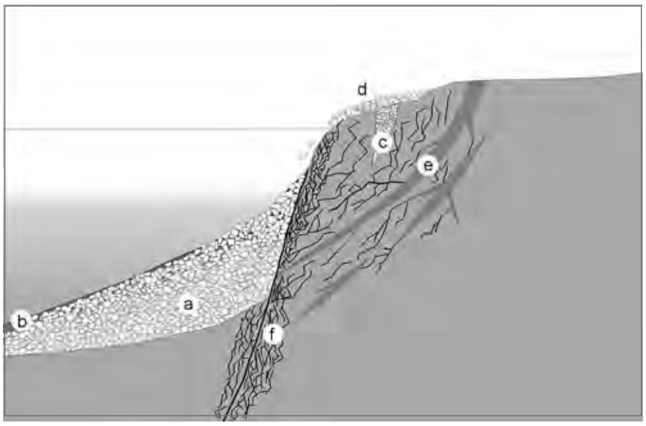

Fig. 28. Model of deposition and cementation of the Krasín Breccia. **a** – inner part of breccia talus in which cements and stromatolite coatings prevail over the internal sediment, **b** - outer part of the talus with predominant sedimentary filling of the interstices, **c** – breccia bodies originated in clefts and caverns, **d** – rubble originated on the emerged land and initially coated with fresh-water stromatolites, **e** – clefts (neptunian dykes) that served as conduits of the fresh water, **f** – in-situ brecciated wall rock (crackle breccia) near the main fault (after Aubrecht & Szulc, 2006).

– Lower Tithonian limestones. The different size of the brachialia in clasts and in the matrix might indicate that they belong to two different genera of planktonic crinoids or it was caused only by hydrodynamic sorting. The existence of big blocks of Kimmeridgian – Lower Tithonian in the Neocomian breccia cannot be excluded (e.g. the lowermost rockwall on the left flank of the quarry).

11. Fine-grained limestone breccia with yellow or red matrix and white micritic limestone lithoclasts – Coniacian.

The matrix of this lithosparrudite is formed by densely packed detritus of double-keeled globotruncanas with some hedbergellas, echinoderm plates with syntaxial rims, fragments of inoceramid bivalves (including isolated prisms) and rare phosphatic fish scales. Among foraminifers the following species were determined: *Falsomarginotruncana angusticarinata* (Gandolfi), *F. pseudolinneiana* (Pessagno), *F. coldreriensis* (Gandolfi), *F. desioi* (Gandolfi), *Marginotruncana schneegansi* (Sigal) and *Clavulinoides* sp. This fauna indicates Coniacian age; no younger forams have been found.

The lithoclasts belong mostly to the biomicrites with *Saccocoma* (Kimmeridgian – Lower Tithonian), rarely with *Crassicollaria* (Upper Tithonian). Neocomian lithoclasts contain small fragments of biomicrites with *Crassicollaria*, without tintinids in the matrix and with phosphatic intraclasts. A lithoclast of red biomicrite with Middle Cretaceous planktonic foraminifers has been found too.

The rock is macroscopically very similar to the Neocomian fine-grained limestone breccia. Such a rock type of Senonian age was unknown from the West Carpathians up till now. We have found it already in 1981 in the outbursted exploitation material in the quarry. The breccia should have filled a pocket within the transgression plane on the emerged Upper Jurassic and Neocomian limestones.

B4.5 Slavnické Podhorie

(49°01′ N, 18°09′31″)

The site lies in the middle part of the Váh River valley, at the village of Slavnické Podhorie, at the foothills of the Biele Karpaty Mts. It represents a tectonically overturned klippe exposed in an abandoned quarry (Fig. 23) revealing a stromatactis mud-mound core. A 32 m-long section was sampled (Fig. 24) in the southern part of the quarry (Aubrecht et al., 2002).

Major part of the quarry cuts the Middle Jurassic crinoidal limestones (Smolegowa Formation) that is stratigraphically older than the mud-mound. In the crinoidal limestone at the base of the profile, a fragment of the ammonite *Parkinsonia* sp. was found indicating the Bajocian/Bathonian boundary. The following Bajocian-Bathonian brachiopod fauna have been collected from the crinoidal limestones by Pevný (1969) and Aubrecht et al. (2002): *Morrisithyris* aff. *phillipsi* (Morris), *Monsardithyris buckmani* (Davidson), *Monsardithyris ventricosa* (Zieten), *Linguithyris bifida* (Rothpletz), *Zeilleria waltoni* (Davidson), *Zeilleria emarginata* (Sowerby), *Zeilleria* aff. *subbucculenta* Chapuis-Dewalque, *Lobothyris ventricosa* (Hartmann), *Loboidothyris perovalis* (Sowerby), *“Terebratula” retrocarinata* Rothpletz, *“Terebratula” varicans* Rothpletz, *Antiptychina puchoviensis* Pevný, *“Sphenorhynchia” rubrisaxensis rectifrons* (Rothpletz), *Acantotharis* sp., *Gnathorhynchia trigona* (Quenstedt), *Sphenorhynchia* aff. *plicatella* (Sowerby), *Sphenorhynchia rubrisaxensis rectifrons* (Rothpletz), *Rhactorhynchia subtetrahedra* (Davidson), *“Rhynchonella”* aff. *obsoleta* (Sowerby), *Cymatorhynchia quadriplicata* (Sowerby), ?*Weberithyris* sp., ?*Caucasella trigonella* (Rothpletz), *Parvirhynchia* sp. The basis of the mudstones is therefore of ?Bajocian-Bathonian age. Some forms as *Caucasella* and *Weberithyris* indicate rather younger, Bathonian-Callovian age. This is also supported by a *Pygope* aff. *janitor* Pictet in the debris near the entrance of the quarry, but this species has not been found in the profile.

The mudstones that overlie the crinoidal deposits are dominated by a microfacies with *Bositra* sp. shells which extends to the end of the Callovian. As only very rare foraminifers *Globuligerina* sp. have been found in the mudstones, mass occurrence of which is indicative for the Oxfordian in this basin, the section does not reach the Oxfordian age.

Section description

The stratigraphical basis of the examined profile is formed by colour crinoidal limestones (0-13 m), passing gradually into pink and red micritic limestone (13-32 m). Stromatactis cavities appear as low as the crinoidal limestone (9-13 m) but they reach their maximum in the micritic limestones (15-28 m – Fig. 25). At the 28 m level, the stromatactis cavities disappear. Since the stromatactis cavities are approximately parallel to stratification, the examined section may probably represent the core part of the mound. As the klippe is just a large tectonic block, no transition to the offmound facies has been observed.

Crinoidal limestones represent skeletal packstones to grainstones with micritic to sparitic matrix. Sparite occurs in the parts where micrite was winnowed. It is clear blocky calcite, locally with margins rich in inclusions. Where the stromatactis cavities occur, the matrix is locally pelmicritic to sparitic. However, in contrast to the clear blocky calcite mentioned above, the spar is mostly represented by short-bladed fibrous calcite. It is obviously related to the radiaxial fibrous calcite filling of the stromatactis cavities. The sediment was relatively poorly sorted. Besides crinoidal ossicles, sand-sized detrital quartz grains are abundant. Bryozoan fragments, echinoid spines, ostracod shells, foraminifers (*Lenticulina* sp.), agglutinated foraminifers (*Ophthalmidium* sp.) and fragments of pelecypods and brachiopods are ubiquitous. Upsection, bivalves and brachiopods gradually prevail and thin-shelled bivalves appear, passing to the overlying mudstones. Many allochems are affected by heavy micritization and microborings.

The pink, red to yellowish mudstones form the main host rock of the stromatactis cavities and are predominantly wackestone to packstone (biomicrite, biopelmicrite) and even to grainstone (biopelsparite). In the limestone, thin-shelled bivalves (mainly *Bositra* sp.), thin-shelled ostracods and foraminifers (*Ophthalmidium* sp., *Lenticulina* sp., *Patellina* sp., *Spirillina* sp., *Dorothia* sp., sessile nubeculariid foraminifers, nodosariid foraminifers and "microforaminifers") occur. Detritus from thicker-walled bivalves (commonly dissolved and replaced by micrite) and brachiopods, rare gastropods, juvenile ammonites, echinoid spines and serpulid worm tubes are quite common. Calcareous sponges, silicisponge spicules, fragments of corals and bryozoans are rarely preserved. Crinoidal ossicles, which are common in the lower, transitional parts, are less frequent in the mudstone. Rare quartz grains occur, too. The relatively monotonous "filamentous" microfacies (packstone) with its micritic matrix, free of peloids, also represents the main part of the micritic limestones at the top of the profile (28-32 m), where stromatactis cavities are absent. Unlike in the lower levels, signs of bioturbation are ubiquitous. The same material fills the neptunian dikes found at 10, 12.5, 22.89 (dike with breccious filling) and 29.5 meter levels. In the topmost part of the profile, *Globuligerina* sp. sparcely appears.

The typical stromatactis cavities with flat bottom and undulated top are present in the examined site, but irregular ones are also present. The first and the main filling of the stromatactis cavities is represented by radiaxial fibrous calcite. The radiaxial fibrous calcite is followed by internal micritic filling and by blocky calcite cement.

Stromatactis was first described in the 19th century and it is still an enigmatic phenomenon. There is still no agreement in opinions concerning its origin. The suggested origins for stromatactis included internal erosion and reworking of small cavities, dewatering or escape of fluids, neomorphism or recrystallization of calcareous mud, dynamic metamorphism, slumps and fresh-water karstification. The most recent ideas involve cavities remained after decomposed clathrates in calcareous mud or the cavities are interpreted as a result of sedimentation of stirred poly-disperse sediment. Biogenic origins for stromatactis have also been suggested. The most widely invoked origin for stromatactis is that they are cavities which remained after decomposition of an unknown soft-bodied organism or by neomorphism of carbonate-secreting organism. The suggested organisms include stromatoporoids, bryozoans, algae, stromatolites, microbial colonies, and burrowing activity of crustaceans.

The organisms which are most frequently mentioned in the stromatactis literature are sponges. At Slavnické Podhorie, the sparry masses that fill stromatactis cavities are weathered out and show casts of sponges (Aubrecht *et al.*, 2009b). A parallel study of the weathered casts and their cross-sections in slabs (Fig. 26) showed that they bear all the signs of stromatactis (relatively flat bottoms and digitate upper parts, radiaxial fibrous calcite initial fillings and eventual blocky calcite later filling). Almost no original sponge structures were preserved. This strongly supports the possible sponge-related origin for the stromatactis cavities.

B4.6 Dolná Súča – Krasín

(48°57′47″ N, 18°01′24″ E)

Locality called Krasín Klippe is situated in an abandoned quarry W of the Dolná Súča village and belongs to the shallow-water Czorsztyn Unit. However, it differs from the classical Czorsztyn Succession by some peculiarities:
1. presence of the submarine breccias of the Middle Jurassic age,
2. Upper Jurassic limestones removed by erosion (except the Oxfordian bioherm limestone filling a cleft),
3. Lower Cretaceous sediments overlying the Middle Jurassic limestones in the large clefts.

The Krasín Breccia is an example of Jurassic syntectonic sedimentary breccia (Fig. 27), witness of extensional tectonic movements tied to Jurassic rifting (Mišík et al., 1994a; Aubrecht and Szulc, 2006). It is unique and differs from other similar facies, which are exclusively composed of clasts and matrix in its complex post-depositional filling and cementation history that infers a special depositional and post-depositional environment (Fig. 28).

Following members may be discerned there (Mišík et al. 1994b):

Smolegowa Lst Fm.: White bedded to massive crinoidal limestones with ammonite *Teloceras blagdeni* Sowerby, with small fragments of dolomites, rare red neptunian dykes and void fillings. Clastic admixture is more or less abundant, mainly represented by quartz grains and dolomites. The limestones form also the whole crest of the Krasín klippe. Stratigraphic age is Bajocian.

Krupianka Lst Fm.: Greyish fine-grained crinoidal limestones with brown chert nodules and red crinoidal limestones with loafy weathering forms. They are limited only to the northern confines of the klippe; the best outcrops could be found in the old quarry, now entirely covered by vegetation. Supposed age is Bajocian.

Krasín Breccia: Grey, pinkish and red brecciated crinoidal limestones (submarine scarp-breccia), massive with small dolomite fragments and frequent void fillings, penetrated by neptunian dykes of red micritic limestone, roughly of the same age. Supposed stratigraphic age is Bajocian-Bathonian. This rubble breccia usually has very complex filling. The clasts are coated by at least one generation of stromatolite (mostly cryptic stromatolites) and subsequently cemented by radiaxial fibrous calcite. The remaining void filling starts with the crinoidal detritus, which indicates that the breccia was formed due to synsedimentary tectonics occurring during the deposition of crinoidal limestones. Next infilling step is represented by micritic limestone with filamentous microfacies (Bathonian-Callovian) and by almost sterile micrite with cavity-dwelling ostracods. The breccia bears evidence of numerous instances of disturbance, resedimentation and recementation. Moreover the isotope composition of some early generations of stromatolites and early cements indicate possible fresh-water diagenesis.

?Vršatec Lst.: Light grey and pinkish bioherm breccia with dolomite lithoclasts. It fills only a pocket in the left upper part of the quarry. The stratigraphic position of the limestone is unclear, although the Bajocian age of the lithoclasts of biohermal facies can be supposed.

Walentowa Breccia. The breccia is formed by clasts of the red crinoidal limestones and small fragments of white *Crassicollaria*-bearing limestones. They filled some clefts with variable thickness, penetrating the Middle Jurassic limestones. Supposed age is Valanginian-(?)Hauterivian.

In one of the clefts, red marls with intercalations of the fine-grained limestones with *Hedbergella* were found. Their supposed age is Albian.

B4.7 Pustá Ves

(48°37′39″ N, 17°39′05″ E)

The oldest sediments of the Late Cretaceous sedimentary megacycle are represented by fresh-water oncolitic limestones (Pustá Ves Formation). They are known from two areas in the Central Western Carpathians: at the NE termination of the Malé Karpaty Mts. (Brezovské and Čachtické Karpaty Mts.) and in the Spiš-Gemer Ore Mts. (mainly the Stratená Mts.). They occur in the two largest areas with remnants of the Senonian marine sequences in the Central Western Carpathians. The distribution of these rocks is not congruent with the configuration of the succeeding Gosau basins.

Three outcrops are known in the Brezovské- and Čachtické Karpaty Mts. area. The first one, Hrdlákova Skala, W from Čachtice has been erroneously attributed to the Triassic by Hanáček (1954). Brown oncolitic limestones overlie the Anisian Gutenstein Limestone here. The second outcrop is known near the Černík gamekeeper‘s cottage N from Chtelnica, the third one is situated on the Mladé Háje Hill SE from Pustá Ves, N from Kačín (the two last mentioned localities were described by Mello in Salaj et al., 1987). Pebbles of these limestones were found in the Coniacian Valchov Conglomerate on the stratotype locality (Borza 1962) and in the Karpatian Jablonica Conglomerates (Mišík 1986). The limestones contain characeans, but no representatives of *Munieria*.

The typical rock of the Pustá Ves Formation is represented by brown biomicritic limestones with ostracods, gastropods, algae (*Munieria* and other characeans as well as until now undescribed new taxa of fresh-water algae). Cracks and desiccation pores occur frequently. Almost complete lack of terrigenous admixture indicates sedimentation in shallow lakes on a pediplained surface. Such conditions have arisen after Middle Cretaceous Austrian nappe transport and extensive erosion.

Fresh-water origin of the Pustá Ves Limestone was indicated also by isotopic analyses by Kantor and Mišík (1992) which yielded the following values: $\delta^{13}C$ = -9.49 ‰, $\delta^{18}O$ = -7.87 ‰.

B4.8 Brezová pod Bradlom – Valchovský mlyn

(48° 39′06″ N, 17°30′35″ E)

The escarpment by the road between Jablonica and Brezová pod Bradlom exposes the contact of the Coniacian Valchov Conglomerate with the underlying Upper Triassic Hauptdolomit of the Nedzov Nappe. Dolomite layers are of cyclic character with fine clastic base, indistinct bands of detritus with occasional pseudomorphs after evaporites in the middle part and terminate with loferitic algal-mat lamination.

The Valchov Conglomerate starts with unsorted dolomite breccia alternating with yellow clayey intercalations. The main part of the conglomerate body consists of well rounded clasts of local material with red matrix. The conglomerate represents the basal unit of the Brezová Group which is an equivalent to the Gosau Group of the Eastern Alps and represents the first post-tectonic cover of the Central Western Carpathians, after the nappe thrusting in the Turonian. The conglomerate deposition was preceded by local deposition of fresh-water oncoidal limestones (Pustá Ves Limestone) of presumably Late Turonian age. These limestones, together with the Triassic limestones and dolomites from the basement, form pebbles in the Valchov Conglomerate. Along with these rocks, clasts of the Liassic Adnet Limestone (with Pliensbachian fauna), crinoidal cherty limestones (Early/ Middle Jurassic), shallow-water Malm limestones with dasycladal algae *Clypeina* sp., demosponges *Cladocoropsis* sp. and with foraminifers *Protopeneroplis striata*, sandy limestones with hedbergelids (Barremian to Albian) were found, too.

B4.9 Sološnica

(48°27′17″ N, 17°14′19″ E)

The locality Sološnica represents an abandoned quarry located on the left side of the Sološnica Valley, at the foot of the Veľká Vápenná Mt. Anisian dark grey Annaberg Limestone belonging to the Veterlin Nappe. Upper Paleocene/Lower Eocene thick-bedded sandy limestones were quarried here.

The Triassic limestones are covered by a breccia with red matrix, called the Kržľa Breccia (Fig.33). It forms irregular nest-like bodies filling small cavities and fissures in the Triassic limestone. Red colour of its matrix is interpreted as a result of karstic weathering of the underlying limestone basement. Larger cavities filled with laminated, graded, red silty marls with ripplemarks on the bedding planes were observed on the top of the nearby Veľká Vápenná Mt. (Michalík, 1984). Seventy five percent of the clasts (0.02-0.6 m^3 in size) consist of the Annaberg Limestone; the rest are composed of the Raming Limestone, Reifling Limestone, and dolomites.

Fig. 29. Senonian-Paleocene Kržľa Breccia – paleokarst breccia with clasts of Annaberg Limestone and terra rossa matrix. Sološnica Quarry.

The matrix forms more important part of the rock (2-5 %) if compared with the Bartalová Breccia. In the Omlaď borehole, located about 800 m to SW, foraminifers and nannoplankton of Paleocene age have been found in the red breccias below the base of the Borové Formation.

The Kržľa Breccia is covered by the base of the Borové Formation (Fig. 29–30) consisting of thick-bedded sandy limestones and calcareous sandstones, rich in organic detritus, including nummulite tests. The fauna comprises Lower Eocene forms, such as *Nummulites* cf. *inkermanensis* Schaub, *N. burdigaliensis* De la Harpe, *Assilina placentula* (Deshayes), *Alveolina* sp. and *Discocyclina* sp. (Buday et al., 1967). Several beds bear marks of submarine slumping.

Fig. 30. Kržľa Breccia (red) is overlain by Borové Formation (yellowish), representing Upper Paleocene-Eocene *Discocyclina* limestone.

B4.10 Devín Castle

(48°10′27″N, 16°58′38″ E)

Devín Castle was built on a cliff at the confluence of the Danube and Morava rivers. From E to W, the Devín castle hill is built of phyllites of the Tatric crystalline complexes of the Malé Karpaty Mts., covered by Upper Permian terrestrial clastics and Lower Triassic quartzites. Then the succession continues with carbonates, e.g., Middle Triassic dolomites and Jurassic limestones and breccias. The western cliff wall (Fig. 31) is formed of Middle Liassic biodetritic (crinoids, belemnites, brachiopods) breccia limestones with angular clasts of the underlying dolomites and limestones (Fig. 32). The limestones intrude deeply into the Triassic basement in fissure fillings and neptunian dykes, pointing to extensive erosion and faulting before the Lower Jurassic transgression. The breccias originated due to Juras-

Fig. 31. The western cliff wall on which Devín Castle was built

Fig. 32. Middle Jurassic breccia formed by clasts of older, Middle Triassic dolomitic limestones and dolomites. The breccia originated due to Penninic Rifting.

sic rifting related to the opening of the Penninic Ocean (Michalík & Vlčko, 2011).

About four small paleokarst caves and several fractures filled with Neogene sediments were recognized in the carbonates and breccia forming the westernmost parts of the castle hill (Kahan et al. 1973). In some of them, old sinters were preserved (Fig. 33), with subsequent filling of marine Upper Badenian sands. Locally, traces after bivalve borings are preserved.

B4.11 Devínska Nova Ves – Sandberg

(48°12′03″ N, 16° 58′26″ E)

The locality is situated on the W slope of the Devínska Kobyla Hill and it represents a facies stratotype of the Upper Badenian (Kosovian, Bulimina-Bolivina Zone) (Švagrovský in Papp et al. 1978). The Upper Badenian Sandberg Formation (Baráth et al. 1994, see Fig. 6) contains more than 300 species of fossil organisms. The sequence is characterized by clastic sediments lying transgressively and discordantly on Jurassic and Lower Cretaceous limestones which formed a cliff in the Late Badenian. An evidence of this are frequent occurrences of traces after boring bivalves *Lithophaga*, worms *Polydora* and sponges *Cliona*, similarly as sessile bivalves *Ostrea digitalina* Dub.

Another evidence of the marine transgression are sea caves formed by abrasion. Below Sandberg, there is a small abrasion cave (48°12′07″ N, E 16°58′16″ E) preserved from this time (Fig. 34). It occurs in the wall of a former quarry, about 20 m above the road connecting Devínska Nová Ves and Devín. It was formed in Tithonian marly limestones and shales. Mišík (1979a)

Fig. 34. Abrasion sea cave below the Sandberg Hill originated due to Upper Badenian transgression.

described it as a sea cave. The cave is about 8 m long, 3 m wide and up to 4 m high. Its bottom slightly rises and the cave narrows inward. The cave is mostly filled with sands (locally cross-bedded), less by gravels and clasts of limestones, which are partly lithified by secondary calcite. At the cave entrance there are cylindrical borings with diamater up to 2–3 cm, after the bivalves *Lithodomus lithophagus* (Fig. 35).

Another abrasion sea cave is preserved in a nearby two-floor high abandoned quarry (Weit's Quarry: 48°11′40″ N, 16°58′50″ E), where it cuts into grey limestones, dolomites and carbonate breccias of Liassic age (Fig. 36). In the left and upper walls of the quarry, as well as on the second floor of the quarry, the Liassic limestones are unconformably overlain by Upper Badenian breccias cemented by sandy matrix, then subhorizontally layered sandstones, sands (locally cross-bedded – Fig. 37) and gravels. Some larger openings (abrasion sea caves) are filled with Upper Badenian partly lithified sands and to a

Fig. 33. Miocene sinter in the Middle Jurassic breccias.

Fig. 35. Upper Jurassic platy limestones drilled by boring bivalves.

lesser extent by gravels. Remnants of fossil seals *Devinophoca claytoni* (originally described as *Pristophoca vetusta*) from the cavern filling were described from this sea cave. Clasts and blocks of sinters can be found at this locality, too (including sole blocks with stalagmites). Unlike at other similar localities in the Malé Karpaty Mts., sinter-cemented breccias are rare in this quarry.

Fig. 36. Sediment-filled abrasion sea-cave in Weit's Quarry. The cave was formed in grey limestones, dolomites and carbonate breccias of Liassic age.

Fig. 37. Cross-bedding in the sandy filling of the sea cave in Weit's Quarry.

Fig. 38. Coralgal limestones are typical for the upper part of the former quarry.

The succession of open marine sediments on Sandberg Hill is the following: Polymict breccias and conglomerates with sandy calcareous cement, containing gravel lenses lie at the base of the open-marine sequence. Their clastic material is composed mainly of rocks from the near surroundings: granites, pegmatites, amphibolites, limestones, phyllites and quartzites (Mišík, 1979a). Predominant heavy minerals are zircon, apatite, rutile, anatase, sphene, ilmenite, garnet and biotite, indicating sources predominantly from granites and biotite paragneisses of the Bratislava Nappe. Frequent phenomena are cross-bedding and bioturbation with crab tunnels (*Ophiomorpha*); teeth of sharks and fish bones can be found as well.

The sequence continues with light yellowish-grey mica-rich coarse-grained sands with cross-bedding and beds and lenses of massive calcareous sandstones with gravel intercalations. They contain abundant mollusc fauna, mostly bivalves *Pecten aduncus* (Eichwald), *Flabellipecten solarium* (Lamarck), *Cardita* (*Megacardita*) *jouanetti* Basterot, *Panopea menardi* Deshayes, *Spondylus crassicosta* Lamarck etc.; less frequent are gastropods – *Turitella tricina* Borson, *Conus* sp., frequent are also foraminifers (*Amphistegina*, *Heterostegina*), bryozoans and worm tubes (*Ditrupa cornea* Linné).

Higher up, yellowish grey fine-grained mica-rich sands are exposed, with cross-bedding and lenses of fine-grained gravel. They contain remnants of marine vertebrates, including fish, and of land vertebrates.

Above these beds lie light-coloured yellowish grey fine-grained sands with beds of more massive calcareous sandstones containing abundant fauna of foraminifers, bryozoans and molluscs. They contain fillings of crab tunnels, corals, echinoids and brachiopods. The sandstones include numerous continuous clusters of coralline algae (Figs. 38–39), which form lenses of calcareous lithothamnium sandstones to sandy limestones. These are more widespread on the NE and S slopes of the Devínska Kobyla Hill.

The uppermost part of the sequence is formed by clayey sandstones to sandy claystones with increasing content of gastropod fauna – *Calliostoma trigonum* (Eichwald), *Bolma meynardi* (Mitschi), *Turritella subangulata polonica* Friedberg, etc., indicating gradual decrease of salinity.

Fig. 39. Detail of the coralgal limestone (Leithakalk) from the upper part of the Sandberg quarry.

Fig. 40. Abandoned quarry of the former Stockerau lime factory.

Clastic sediments of Sandberg Hill pass towards the Vienna Basin into marine claystones of the Studienka Fm., cropping out 3 km N of Sandberg in a brickyard pit. The claystones contain abundant Upper Badenian microfauna of foraminifers and calcareous nannoplankton; frequent are remnants of the marine fish *Clupea*.

As far as foraminifers are concerned, rich communities with a prevalence of bolivinas, buliminas and uvigerinas have been found. The determination of the Upper Badenian – Kosovian sediments has been done on the basis of *Bolivina dilatata maxima* Cicha & Zapletalova and *Uvigerina liesingensis* Toula. The communities contain taxa tolerant to oxygen decrease. Layers of only planktonic foraminifers are an evidence of sporadic oscillation of the oxic/anoxic boundary around the sediment/water column interface. Planktonic foraminifers form 20-100% of foraminiferal communities. The communities are diversified, predominant is *Globigerina bulloides* D'Orbigny. Further there are *Globigerionides trilobus* (Reuss), *Globorotalia siakensis* Le Roy, *Globigerina diplostoma* Reuss, *Globigerina druryi* Akers.

The high content of planktonic foraminifers has been caused most likely by decreased oxygen content and it is not a result of the character of the sedimentation basin, since we do not assume the described sediments to have deposited in depths greater than neritic.

Nannoplankton communities are rich, dominated by *Cyclococcolithus rotula* (Kamptner), frequent are *Micrantholithus* sp., *Ponthosphaera multipora* (Kamptner) Roth, *Discoaster variabilis* Martini & Bram, i.e. a community which has been presented as a typical one for the Upper Badenian of the Western Carpathians.

In the wash-out of some beds, some fish remnants can be found (teeth, bones, scales); sponge spicules and echinoid needles are frequent in the whole profile.

B4.12 Devínska Nova Ves – former Quarry of Stockerau Lime Factory

(48°12′13″ N, 17°00′11″ E)

The abandoned quarry (Fig. 40) which belonged to Stockerau Lime Factory is situated on the northern slope of Devínska Kobyla Hill, by the railroad from Bratislava to Devínska Nova Ves. The quarry was cut in Middle Triassic to Liassic limestones. The limestones are tectonically disrupted. The tectonic fractures developed to clefts, which are locally 3.5 m wide, and to various karstic forms. In the Middle Miocene, between Upper Karpatian and Middle Badenian (17–15 Ma), this area was emerged (Mišík, 1979a). This is the only place in Slovakia with a preserved wall covered with paleokarst sinter older than 15 Ma (Mišík, 1980), forming stalactites and draperies (Fig. 41).

The clefts acted as natural traps for smaller but also for bigger animals (mostly vertebrates). Accumulations of vertebrate bones and teeth were mixed with yellowish soil (terra fusca).

The Late Badenian marine transgression disintegrated some of the caves and the rocky shore often covered with sinters was bored by marine bivalves *Lithophaga* (the borings are visible at several places – Fig. 42). The transgressive surface is covered with yellowish sands with marine fauna.

From the paleokarst cavities, two important places are preserved in the quarry. The first one are so-called Zapfe's clefts (German: Spalten) which were named after

Fig. 41. Miocene (pre-Badenian) sinter preserved on the wall of an ancient cave.

Fig. 42. Sinter bored by bivalves during the Middle/Upper Badenian transgression.

the Austrian professor Helmuth Zapfe from Vienna University who described the mammal fauna trapped in the clefts. The clefts were discovered by mining during the 2nd World War when there was a labour camp in the quarry. The technical manager of the quarry was Ing. Bruno Zapfe, a brother of Helmuth Zapfe. During mining they discovered a ca. 1.8 m wide cleft containing many vertebrate bones. This material was transported to the Vienna Museum, where most of the material is deposited. The most important findings described by Zapfe were apes *Pliopithecus* (*Epipliopithecus*) *vindobonensis* (Zapfe & Hürzeller) and ungulates *Chalicotherium grande* (Lartet).

Further excavations were performed here in the years 2003-2004. The new material is still under investigation. The investigations confirmed the Middle Badenian age of the terrestric part of the cleft fillings (lower part of the MN 6 biozone; > 13.5 Ma)

Another important locality named Bonanza was found in 1982 by an amateur paleontologist Štefan Mesároš. This is a cleft about 3.5 m wide situated directly above the railway track, on the other side of the cliff with the aforementioned sinter wall (Fig. 43). Along with remnants of terrestric fauna, this cleft also contained marine fauna, e.g. shark teeth, fish and seal bones (Sabol, 2005a, b; Sabol and Kováč, 2006). On the basis of this fauna, the age of the filling was determined as Upper Badenian (upper part of the MN 6 biozone; < 13.5 Ma). The most important fossil vertebrates found at this locality were an early toad *Bufo priscus* Spinar, Klembara & Mesaros, a seal *Devinophoca claytoni* Koretsky & Holec and antelopes *Lagomerix parvulus* (Roger).

Besides these localities, several smaller clefts with possible faunal occurrences are known. They are, however, poorly accessible and investigation of their fillings would be risky.

B4.13 Záhorská Bystrica

(48°13′41″ N, 17°03′09″ E)

A Miocene cliff-boulder mass near Bratislava in Southern Slovakia is exposed in a quarry situated on a hill 1.5 km SE of Záhorská Bystrica (Fig. 44). The locality was described in detail by Radwański (1968). The boulder mass is a product of Badenian transgression and represents a thick series of conglomerates which rest on

Fig. 43. Bonanza locality – the latest discovered paleokarst cleft with rich terrestric and marine Neogene fauna.

Fig. 44. Abandoned quarry at Záhorská Bystrica revealing transgressive, coarse-psephitic sediments overlying dark Triassic and Jurassic limestones.

an uneven surface of black limestone breccias, assigned to the Gutenstein Formation (Anisian) and breccias assigned to the Pleš Formation (Jurassic) of the Tatric Mesozoic cover unit of the Malé Karpaty Mts.

Just like at previous localities, the carbonate basement below the Miocene transgressive sediments was fractured and karstified. The fractures were first filled with isopachous sinters and then the remaining spaces were filled with Miocene sands (Fig. 45).

The boulder mass can be examined at three successive exploitation levels of the quarry, where it may be clearly seen that the uneven bottom surface of the boulder mass rises gradually upwards, more or less parallel with the present surface of the hill. The result is that, although at the individual exploitation levels the boulder mass shows only thicknesses of several meters each, the total thickness exceeds 11 meters.

The cliff-boulder mass at Záhorská Bystrica consists of a set of deposits mostly coarse-psephitic in character and individual elements reach diameters up to two meters; the largest block observed was 3.4 x 2.5 x 1.1 m in size. The coarse-psephitic elements of some half meter to one or two meters in size have the appearance of rounded boulders; those of smaller dimensions rather look like cobbles or pebbles, or they are irregularly shaped. The material was mostly derived from black limestones of the Triassic and Liassic limestones and also from phyllites and other rocks of the crystalline basement. The fine-psephitic and psammitic fraction filling the remaining space consists mostly of quartz material of more allochthonous character.

The bedding of the cliff-boulder mass is very distinct, It is developed as alternating layers with big pebbles, cobbles and boulders on the one hand, and layers of fine-gravelly and psammitic material on the other. Most of the individual layers grow rapidly thinner and laterally peter out streak-like, or they are locally developed in unequal-size depressions and in rough parts of the substratum. The slight westward dip of the layers, of some 10–15°, seems to be mostly of sedimentary origin, as if the deposits had been laid down on the hill slope.

A characteristic feature of the majority of the calcareous blocks are numerous borings of various lithophags (Fig. 54-49); most numerous are gigant borings made by the pelecypods *Lithophaga* sp. and, owing to their size, they are well visible from a distance. Single blocks show borings either on one side only, or all over. By the frequency at which the individual lithophags occur, the assemblage of lithophag borings, i.e. the lithophagocenosis, may be characterized as follows:

1. Pelecypods *Lithophaga* sp. For the most part their cigar-shape borings attain considerable dimensions, up to 12-14 cm in length. The openings of the gigantic forms are almost always abraded while minor forms, distributed over the uneven surfaces of larger blocks, remained

Fig. 45. Prior to the transgression, the limestone basement was fractured and the fractures were partially filled with sinters and then by marine sands.

Fig. 46. Various types of borings on boulders.

Fig. 47. Various types of borings on boulders.

sometimes intact. The problem of a specific assignation of these large specimens of *Lithophaga* sp. has not been elucidated so far; all known species, modern and fossil, are much smaller.

2. Pelecypods *Barnea* sp. Their borings are pear-shaped, mostly slightly wider in one direction where arc-like grooves are visible, made by the pelecypods while they mechanically increased their borings with the valve rims. These borings are also relatively large, up to 8 cm long and 3-3.5 cm in their widest part, and here, also, the outlets are mostly abraded.

3. Various species of sponges of the genus *Cliona* Grant; most common among them are the species *Cliona vastifica* Hancock and likewise *Cliona celata* Grant. Much less frequent is *Cliona viridis* (Schmidt). These species can only be identified when the system of their borings is well preserved. Where abrasion has been more intensive, any identification becomes difficult and is open to doubt. It seems certain that some fragments of borings may originate from other species of these sponges.

4. Polychaetes *Potamilla reniformis* (Müller). These borings are round in cross-section and up to 15 cm long; they are mostly twisted or almost meandering. Many borings run directly under the rock surface and are these are often damaged by abrasion.

5. Minor borings made by pelecypods, belonging to the genus *Gastrochaena* Spengler, usually with abraded openings.

6. Locally occurring U-shaped borings (Fig. 3 D) made by polychaetes *Polydora ciliata* (Johnston); usually their openings are also very much abraded.

7. Additionally, there are small borings made by indeterminable polychaetes.

The above list shows that within the discussed assemblage of boring animals, pelecypods and sponges predominated. The structural and textural features of the deposits at Záhorská Bystrica as well as the state of preservation of the borings indicate an eulittoral cliff environment in which the blocks and pebbles have developed, and a similar environment for their deposition: all this rock material has probably been laid down in local depressions of a rocky seashore.

It should be noted that in the boulder material at Záhorská Bystrica, mostly the biggest blocks and boulders were invaded by lithophags. It is likely that only these larger rock elements rested motionless long enough at the sea bottom to become the habitat of the lithophags. Only

Fig. 48. Various types of borings on boulders.

Fig. 49. Various types of borings on boulders.

such large objects were not subject to surface abrasion, and this favored the development of boring animals up to the time when violent storms moved and transported all rock material resting on the sea bottom. On the other hand, finer material like cobbles and pebbles were probably in constant motion and continuously broken up or abraded between the larger boulders and blocks which for long periods had been motionless and firmly anchored to the sea bottom. This would explain why only sporadically the smaller rock elements became the habitat of lithophags.

As the result of diagenetic processes within the boulder-mass material, indistinct pit spots appear at points of contact between individual rock elements, pebbles or boulders. They originated from weakly advanced pitting processes; the full effect of these processes which finally would have produced distinct pits in the surfaces, has been inhibited by the presence of great quantities of matrix occupying most part of the space between adjacent pebbles and boulders.

Acknowledgements. The author acknowledges financial support from grants APVV 0212-12 and VEGA 1/0095/14.

References

Aubrecht, R. & Kozur, H., 1995. *Pokornyopsis* (Ostracoda) from submarine fissure fillings and cavities in the Late Jurassic of Czorsztyn Unit and the possible origin of the Recent anchialine faunas. *Neues Jahrbuch für Geologie und Paläontologie, Abhandlungen*, 196: 1–17.

Aubrecht, R., Krobicki, M., Sýkora, M., Mišík, M., Boorová, D., Schlögl, J., Šamajová, E. & Golonka, J., 2006. Early Cretaceous hiatus in the Czorsztyn Succession (Pieniny Klippen Belt, Western Carpathians): Submarine erosion or emersion? *Annales Societatis Geologorum Poloniae*, 76: 161–196.

Aubrecht, R., Méres, S., Sýkora, M. & Mikuš, T., 2009a. Provenance of the detrital garnets and spinels from the Albian sediments of the Czorstyn Unit (Pieniny Klippen Belt, Western Carpathians, Slovakia). *Geologica Carpathica*, 60: 463-483.

Aubrecht, R., Mišík, M. & Sýkora, M., 1997. Jurassic synrift sedimentation on the Czorsztyn Swell of the Pieniny Klippen Belt in Western Slovakia. – In: Plašienka, D., Hók, J., Voáar, J. & Elečko, M. (eds.): *Alpine evolution of the Western Carpathians and related areas. International conference., Sept. 1997, Introductory articles to the excursion*, Geological Survey of Slovak Republic, D. Stur Publ., Bratislava, 53-64.

Aubrecht, R., Schlögl, J., Krobicki, M., Wierzbowski, H., Matyja, B. A. & Wierzbowski, A., 2009b. Middle Jurassic stromatactis mud-mounds in the Pieniny Klippen Belt (Carpathians) – A possible clue to the origin of stromatactis. *Sedimentary Geology*, 213: 97–112.

Aubrecht, R. & Szulc, J., 2006. Deciphering of the complex depositional and diagenetic history of a scarp limestone breccia (Middle Jurassic Krasín Breccia, Pieniny Klippen Belt, Western Carpathians). *Sedimentary Geology*, 186: 265–281.

Aubrecht, R., Szulc, J., Michalík, J., Schlögl, J. & Wagreich, M., 2002. Middle Jurassic stromatactis mud-mound in the Pieniny Klippen Belt (Western Carpahtians). *Facies*, 47: 113–126.

Aubrecht, R. & Túnyi, I., 2001. Original orientation of neptunian dykes in the Pieniny Klippen Belt (Western Carpahtians): the first results. *Contributions to Geophysics and Geodesy*, 31: 557-578.

Baráth, I., Nagy, A. & Kováč, M., 1994. Sandberg Formation - Upper Badenian marginal sediments of the eastern margin of the Vienna Basin. *Geologické práce, Správy*, 99: 59-66 [in Slovak, English abstract.]

Birkenmajer, K., 1958. Submarine Erosional Breaks and Late Jurassic Synorogenic Movements in the Pieniny Klippen-belt Geosyncline. *Bulletin de l'Academie Polonaise des Sciences, Serie des Sciences chimique, geologique et geographique*, 6: 551–558.

Birkenmajer, K., 1975. Tectonic control of sedimentation at the Jurassic-Cretaceous boundary in the Pieniny Klippen Belt, Carpathians. *Memoires du Bureau de recherches geologiques et minieres*, 86: 294-299.

Birkenmajer, K., 1977. Jurassic and Cretaceous lithostratigraphic units of the Pieniny Klippen Belt, Carpathians, Poland. *Studia Geologica Polonica*, 45: 1-158.

Borza, K., 1962. Petrographic investigation of pebbles of sedimentary rocks of Cretaceous and Paleogene conglomerates in the Brezovské pohorie Mts. and Myjavská Pahorkatina Highland. *Geologický zborník*, 13: 241-256 [in Slovak with English summary.]

Borza, K,. 1984. The Upper Jurassic – Lower Cretaceous parabiostratigraphic scale on the basis of Tintinninae, Cadosinidae, Stomiosphaeridae, Calcisphaerulidae and other microfossils from the West Carpathians. *Geologica Carpathica*, 35: 539–550.

Buday, T., Kodym, O., Maheľ, M., Máška, M., Matějka, A., Svoboda, J. & Zoubek, V., 1967. *Regional geology of CSSR II. Western Carpathians*, (UUG) Praha 2: 651 pp.

Čičel, B., 1958. Príspevok k mineralógii bauxitov z okolia Mojtína. *Geologické práce, Zprávy*, 14: 40–55 [in Slovak.]

Hanáček, J., 1954. Die Geologie des Nedzov-Gebirges. *Geologický Zborník SAV*, 5: 59–83 [in Slovak with German summary.]

Jablonský, J., Sýkora, M. & Aubrecht, R., 2001. Detritic Cr-spinels in Mesozoic sedimentary rocks of the Western Carpathians (overview of the latest knowledge). *Mineralia Slovaca*, 33: 487–498 [in Slovak with English summary.]

Jamrichová, M., Józsa, Š., Aubrecht, R. & Schlögl, J., 2012. Lower Cretaceous paleokarst in a klippe of the Czorsztyn Succession north of Zázrivá (Pieniny Klippen Belt, Orava sector, northern Slovakia). *Acta Geologica Slovaca*, 4: 75-90.

Kahan, S., Šajgalík, J. & Mock, R., 1973. Die geologischen Verhältnisse des Areals der Burg Devín von dem Gesichspunkt seiner Sanierung. *Acta Geologica et Geographica Universitatis Comenianae, Geologia*, 26: 243-266.

Kantor, J. & Mišík, M., 1992. Isotopic composition of oxygen and carbon in selected Mesozoic and Tertiary limestones and dolomites in Slovakia. *Západné Karpaty, sér.MPGM*, 15: 7–27.

Kochanová, M., 1978. Die bivalven des Juras der Vršatec-Klippe. *Západné Karpaty, séria paleontológia*, 4: 7–35.

Kornicker, L. S. & Sohn, I. G., 1976. Phylogeny, ontogeny, and morphology of living and fossil Thaumatocypridacea (Myodocopa: Ostracoda). *Smithsonian Contributions to Zoology*, 219: 1–124.

Kováč, M., Baráth, I., Harzhauser,M., Hlavatý, I. & Hudáčková, N., 2004. Miocene depositional systems and sequence stratigraphy of the Vienna Basin. *Courier Forschungsinstitut Senckenberg*, 246: 187–212.

Martin-Algarra, A. & Vera, J. A., 1996. Paleokarren landforms on a Mesozoic pelagic plateau (Penibetic, Betic Cordillera, Southern Spain). In: Fornos, J. -J. & Gines, A. (eds.), *Karren landforms. Universitat deles Illes Baleares*. Palma de Mallorca: 297-321.

Michalík, J., 1984. Some remarks on developmental and structural interpretation of the northwestern part of the Male Karpaty Mts. (West Carpathians). *Geologicky zbornik - Geologica Carpathica*, 35/4, 489–504.

Michalík, J. & Vlčko, J., 2011. Genesis of the Middle Jurassic breccias in the Devín Unit of the Male Karpaty Mts. – Mineralia Slovaca, 43: 129–136 [in Slovak with English summary.]

Mišík, M. 1979a. *Geological excursions around Slovakia.* (SPN) Bratislava, 359 pp. [in Slovak.]

Mišík, M., 1979b. Sedimentological and microfacial study in the Jurassic of the Vršatec (castle) klippe – neptunic dykes, Oxfordian bioherm facies. *Západné Karpaty, séria geologia* 5: 7–56 [in Slovak with English summary.

]Mišík, M., 1980. Miocene sinter crusts (speleothems) and calcrete deposits from neptunian dykes, Male Karpaty Mts. *Geologický zborník – Geologica Carphatica*, 31: 495–512.

Mišík, M., 1986. Petrographic-microfacial analysis of pebbles and interpretation of sources areas of the Jablonica Conglomerates (Lower Miocene of the NW margin of the Malé Karpaty Mts.). *Geologický zborník – Geologica Carpathica*, 37: 405–448.

Mišík, M., 1992. Pieniny Klippen Belt in relationship with Mesozoic and Tertiary volcanism. *Západné Karpaty, Sér. geológia*, 16: 47–64.

Mišík, M., 1994. The Czorsztyn submarine ridge (Jurassic-Lower Cretaceous, Pieniny Klippen Belt): an example of a pelagic swell. *Mitteillungen der Österreichischen Geologischen Gesselschaft*, 86: 133-140.

Mišík M., Siblík, M., Sýkora, M. & Aubrecht, R., 1994a. Jurassic brachiopods and sedimentological study of the Babiná klippe near Bohunice (Czorsztyn Unit, Pieniny Klippen belt). *Mineralia Slovaca*, 26: 255–266.

Mišík M., Sýkora, M. & Aubrecht, R., 1994b. Middle Jurassic scarp breccias with clefts filled by Oxfordian and Valanginian-Hauterivian sediments, Krasín near Dolná Súča (Pieniny Klippen Belt). *Geologica Carpathica*, 45: 343–356.

Papp, A., Cicha, I., Seneš, J. & Steininger, F. (eds.): *M4 - Badenien (Moravien, Wielicien, Kosovien). – Chronostratigraphie und Neostratotypen. Miozän der Zentralen Paratethys*, vol. 6. Slowakische Akademie des Wissenschaften, Bratislava, 594 pp.

Pevný, J., 1969. Middle Jurassic brachiopods in the Klippen Belt of the central Váh Valley. *Geologické práce, Správy*, 50: 133–160 [in Slovak with English summary].

Radwański, A., 1968. Tortonian cliff deposits at Záhorská Bystrica near Bratislava. *Bulletin de l'Academie Polonaise des Sciences, Serie des sciences geologique et geographique*, 16/2: 97–102.

Sabol, M., 2005a. Middle Miocene assemblage of Rodents from Bonanza site near Devínska Nová Ves (Slovakia). *Mineralia Slovaca*, 11: 269–282.

Sabol, M., 2005b. Middle Miocene assemblage of Insectivores from Bonanza site near Devínska Nová Ves (Slovakia). *Geologica Carpathica*, 56: 433–445.

Sabol, M. & Kováč, M., 2006. Badenian Palaeoenvironment, Faunal Succession and Biostratigraphy: A Case Study from Northern Vienna Basin, Devínska Nová Ves-Bonanza site (Western Carpathians, Slovakia). *Beiträge zur Paläontologie*, 30: 415–425.

Salaj, J. (ed.), Began, A., Hanáček, J., Mello, J., Kullman, E., Čechová, A. & Šucha, P., 1987. *Explanations to the geological map of the Myjava Highland and Čachtické Karpaty Mts. 1:50 000.* –Publ GÚDŠ, 1-181, Bratislava [in Slovak with English summary.]

Schlögl, J., Tomašových, A. & Aubrecht, R., 2006. Stop B3.5 – Vršatec Klippen (Fig. B3.1D) – Czorsztyn Succession (Bajocian to Berriasian); Middle Jurassic biohermal limestones; palaeomagnetic interpretations. – In: Wierzbowski, A., Aubrecht, R., Golonka, J., Gutowski, J., Krobicki, M., Matyja, B.A., Pieńkowski, G. & Uchman, A. (eds.), 2006. *Jurassic of Poland and adjacent Slovakian Carpathians. Field trip guidebook of 7th International Congress of the Jurassic System, Poland, Krakow, September 6–18, 2006*. Polish Geological Institute, Warszawa, pp. 89–92.

Sýkora M., Ožvoldová L. & Boorová D., 1997. Turonian silicified sediments in the Czorsztyn Succession of the Pieniny Klippen Belt (Western Carpathians, Slovakia). *Geologica Carpathica*, 48: 243-261.

Wierzbowski, A., Jaworska, M. & Krobicki, M., 1999. Jurassic (Upper Bajocian-lowest Oxfordian) ammonitico rosso facies in the Pieniny Klippen Belt, Carpathians, Poland: its fauna, age, microfacies and sedimentary environment. *Studia Geologica Polonica*, 115: 7–74.

The Mid-Triassic Muschelkalk in southern Poland: shallow-marine carbonate sedimentation in a tectonically active basin

Joachim Szulc[1], Michał Matysik[2], Hans Hagdorn[3]

[1]Institute of Geological Sciences, Jagiellonian University, Kraków, Poland (joachim.szulc@uj.edu.pl)

[2]Natural History Museum of Denmark, University of Copenhagen, Denmark (ma4tys@interia.pl)

[3]Muschelkalk Musem, Ingelfingen, Germany (encrinus@hagdorn-ingelfingen)

Route (Fig. 1): From Kraków we take motorway A4 west to Chrzanów; we leave it for road 781 to **Płaza** (Kans-Pol quarry, **stop B5.1**). From Płaza we return to A4, continue west to Mysłowice and leave for road A1 to **Siewierz** (GZD **quarry**, **stop B5.2**). From Siewierz we drive A1 south to Podskale cross where we leave for S1 westbound to Pyrzowice and then by road 78 to Niezdara. Then we take road 912 northward to Żyglin (**Żyglin quarry**, **stop B5.3**). From Żyglin we drive by road 908 to Tarnowskie Góry then to NW by road 11 to Tworog. From Tworog west by road 907 to Toszek and then west by road 94 to Strzelce Opolskie. From Strzelce Opolskie we take road 409 to Kalinów and then turn south onto a local road to **Góra Sw. Anny** (**accomodation**). From Góra św. Anny we drive north by a local road and then west by road 409 to Gogolin (**Gogolin** quarry**,**

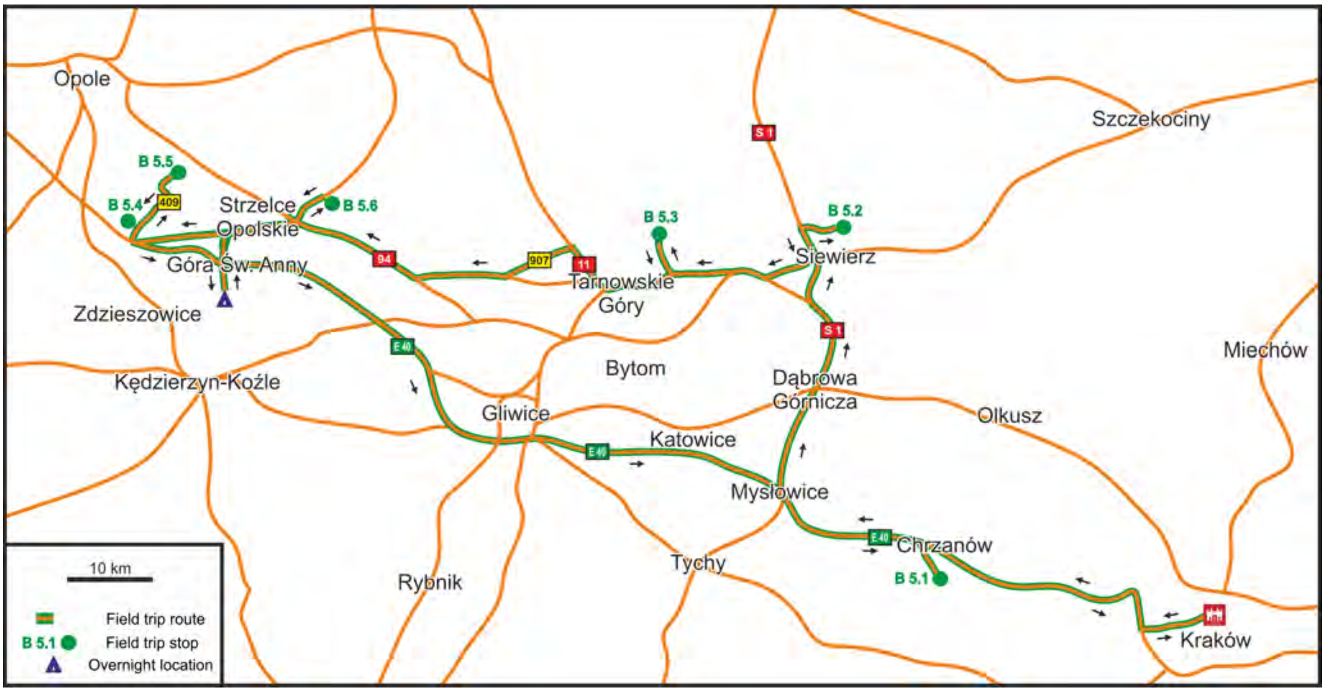

Fig. 1. Route map of field trip B5.

Szulc, J., Matysik, M. & Hagdorn, H., 2015. The Mid-Triassic Muschelkalk in southern Poland: shallow-marine carbonate sedimentation in a tectonically active basin. In: Haczewski, G. (ed.), *Guidebook for field trips accompanying IAS 31st Meeting of Sedimentology held in Kraków on 22nd–25th of June 2015*. Polish Geological Society, Kraków, pp. 195–216.
Guidebook is available online at www.ing.uj.edu.pl/ims2015
Polskie Towarzystwo Geologiczne 2015, ISBN 978-83-942304-0-1

stop B5.4). From Gogolin we travel north by local roads to **Tarnów Opolski** (Opolwap-Lhoist quarry, **stop B5.5**) and then east by road 94 to **Strzelce Opolskie** (Heidelberg Cement quarry**, stop B5.6**). From Strzelce Opolskie we get to motorway A4 and return to Kraków.

Introduction to the trip

Tectonic setting of the eastern Peri-Tethys Basin in Triassic times

Joachim Szulc

During Triassic times Silesia was a SE part of the Germanic Basin which pertained to the northern periphery of the Western Tethys Ocean. The eastern part of the Germanic Basin was strongly influenced by reactivated Variscan structures which controlled the basin differentiation, subsidence pattern and Tethys-Peritethys palaeocirculation pattern in Triassic times (Fig. 2). The Silesian part of the Germanic Basin was controlled by the Silesian-Moravian Fault and the Kraków–Odra-Hamburg Fault (Fig. 2).

Synsedimentary tectonics, resulting in structural differentiation of the Germanic Basin, was active practically throughout the entire Triassic. In early Triassic several phases of block tectonics resulted in basinwide Buntsandstein discordances (Volpriehausen, Detfurth and Hardegsen unconformities). Migration of the Muschelkalk depocentre in Mid Triassic times from Central Poland to Central Germany is another example illustrating well the crustal mobility (Szulc, 2000). Differentiated crustal movements continued also in late Triassic producing several prominent tectonically induced unconformities (Beutler, 2005).

Apart from above mentioned, large-scale indicators of the basin tectonics, there are common direct evidences of syndepositional crustal mobility: small synsedimentary faults and dilatation cracks that developed within the Triassic deposits and reached the basement rocks, or seismically-induced liquefaction and fluidization phenomena visible already in Buntsandstein clastics (Schüler *et al.*, 1989). Seismically induced synsedimentary deformations are particularly common in the marine Muschelkalk

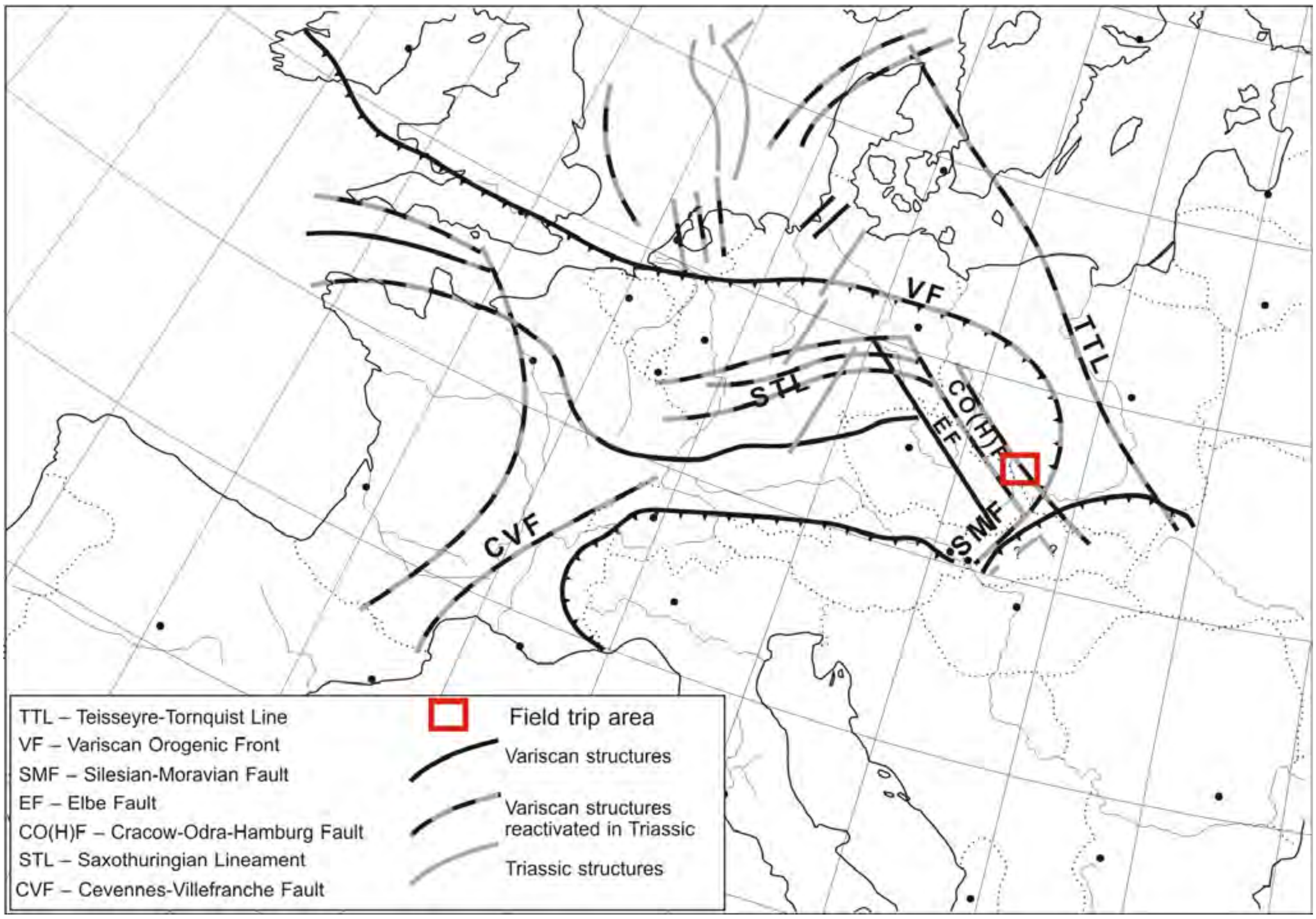

Fig. 2. Principal tectonic elements controlling the eastern part of the Germanic Basin in Triassic times.
TTL – Teiseyere-Tornquist Line, VF – Variscan orogenic front, SMF – Silesian-Moravian Fault; COH – Cracow-Hamburg Fault line; EF – Elbe Fault; STL – Saxothuringian Lineament. Trip area in red.

carbonates (Szulc, 1993; Voigt and Linnemann, 1996; Rüffer, 1996) and in Upper Triassic sediments (Szulc, 2005; Szulc *et al.,* 2006).

In spite of the intense tectonic activity the main eustatic pulses in the Triassic are generally well marked in the Peri-Tethys basins, in particular for the late Olenekian – early Carnian interval. Significant progress of sequence stratigraphy and magnetostratigraphy has improved the potential and reliability of dating and correlation of the most pronounced transgressive-regressive pulses recognized in the area. The sequence stratigraphic frameworks from the Alpine and Germanic basins display good correlation at the level of 3rd order sedimentary sequences (see discussion in Szulc, 2000). As became clear from very careful studies by Matysik (2014; 2015) the higher frequency cycles (4th and 5th order) are much more susceptible to local factors (storms, tectonics) hence an attempt of ascribing them to overregional controls (for instance to Milankovitch orbital rhythms) is a risky, speculative and unreliable procedure.

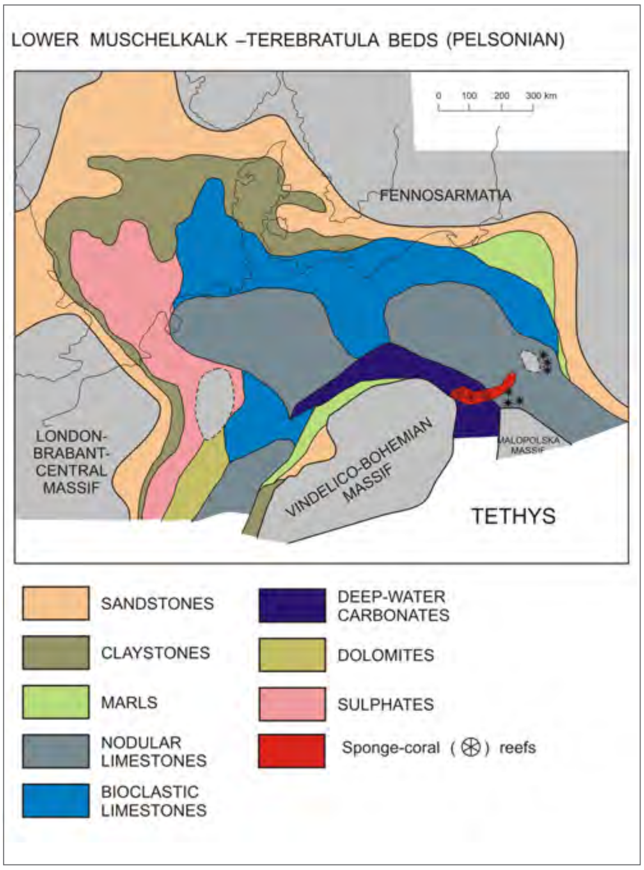

Fig. 3. Palaeofacies map of the Peri-Tethys domain for the Pelsonian interval (after Szulc, 2000).

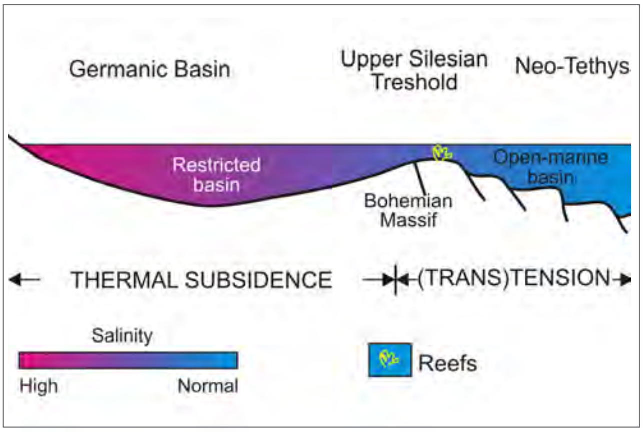

Fig. 4. Schematic model of basin dynamics and circulation regime in the Northern Peri-Tethys domain.

General setting of the Silesian Röt and Muschelkalk

Joachim Szulc

In late Olenekian time, a free communication between the Tethys and Germanic basins was established and the southernmost part of the Polish basin became an integral part of the Tethys Ocean. It concerns, first of all, the Upper Silesian area that formed tectonically mobile threshold block dividing the open ocean domain from a vast inner back-ramp "lagoonal" basin (i.e. Germanic Basin *s.s.*) (Fig. 4). Such configuration resulted in palaeocirculation pattern typical of semi-closed marine basins. Normal marine conditions dominated in the Upper Silesia, whereas northward and westward from the Silesian and East Carpathians domains the environments became more and more restricted. Marine incursions entered from the Tethys Ocean *via* the Silesian-Moravian Gate (SMG), while the other sides of the basin were closed. Normal marine water flowing from the SE accumulated in the depocentre and underwent evaporation, leading to halite/gypsum precipitation (Fig. 3).

Palaeoceanographic circulation pattern established in late Olenekian continued also in Anisian time. The main communication pathways between the Tethys and Germanic basins led through the SMG and East Carpathian Gate (ECG). Since Pelsonian time also the western, Allemanic Gate or (former Burgundy Gate), became active.

The basin reorganization commenced at the beginning of the Ladinian when intense crustal uplift in the eastern province resulted in an increase of clastic supply in uppermost Muschelkalk-Lower Keuper times and led finally to emersion and a stratigraphic hiatus encompassing the late Ladinian (Fassanian) interval.

Stratigraphy of the Silesian Röt-Muschelkalk and its correlation with the alpine Triassic

Joachim Szulc

Owing to free communication of the Silesian area with the open Tethys Ocean and common occurrence of the alpine index fossils (conodonts, ammonoids), the marine Röt – Muschelkalk succession in southern Poland acquires quite detailed biostratigraphy enabling its correlation with the Tethyan realm (Kozur, 1974; Trammer, 1975; Zawidzka, 1975; Brack *et al.*, 1999; Narkiewicz and Szulc, 2004).

Muschelkalk biostratigraphy has been improved by investigations on crinoids and echinoids, which appeared to be very useful tools for correlation with the Tethyan realm (Hagdorn and Głuchowski, 1993). Also palynofacies analysis has been used as a tool for basin-wide correlation and high-resolution sequence stratigraphic interpretation in the Middle Triassic of the Germanic realm (Götz *et al.*, 2005) as well as for correlation of depositional sequences of the northwestern Tethys shelf area with the northern Peri-Tethyan Basin (Götz *et al.,* 2005).

The Middle Muschelkak, devoid of conodonts and other index fossils, has been divided by Kotański (1994) into 6 dasycladacean zones. According to Kotański, the Pelsonian/Illyrian boundary lies in the lower part of the Diplopora Beds and is defined by first occurrence of several species of diplopores e.g., *D. annulatisima*, *D. silesiaca* and *D. multiserialis*.

The chronostratigraphical framework of the Röt – Muschelkalk (late Olenekian – early Ladinian) in southern Poland (Fig. 5) has been supported and refined by magnetostratigraphical and sequence stratigraphical studies (Nawrocki and Szulc, 2000; Szulc, 2000)

Evolution of the Silesian Basin in late Olenekian – early Ladinian times

Joachim Szulc

The Silesian basin experienced several transgression-regression events well illustrated by 3rd order depositional sequences setting (Fig. 5).

The Röt deposits encompass two 3rd order depositional sequences (Szulc, 2000). The first one is very well developed in Upper Silesia where it commences with

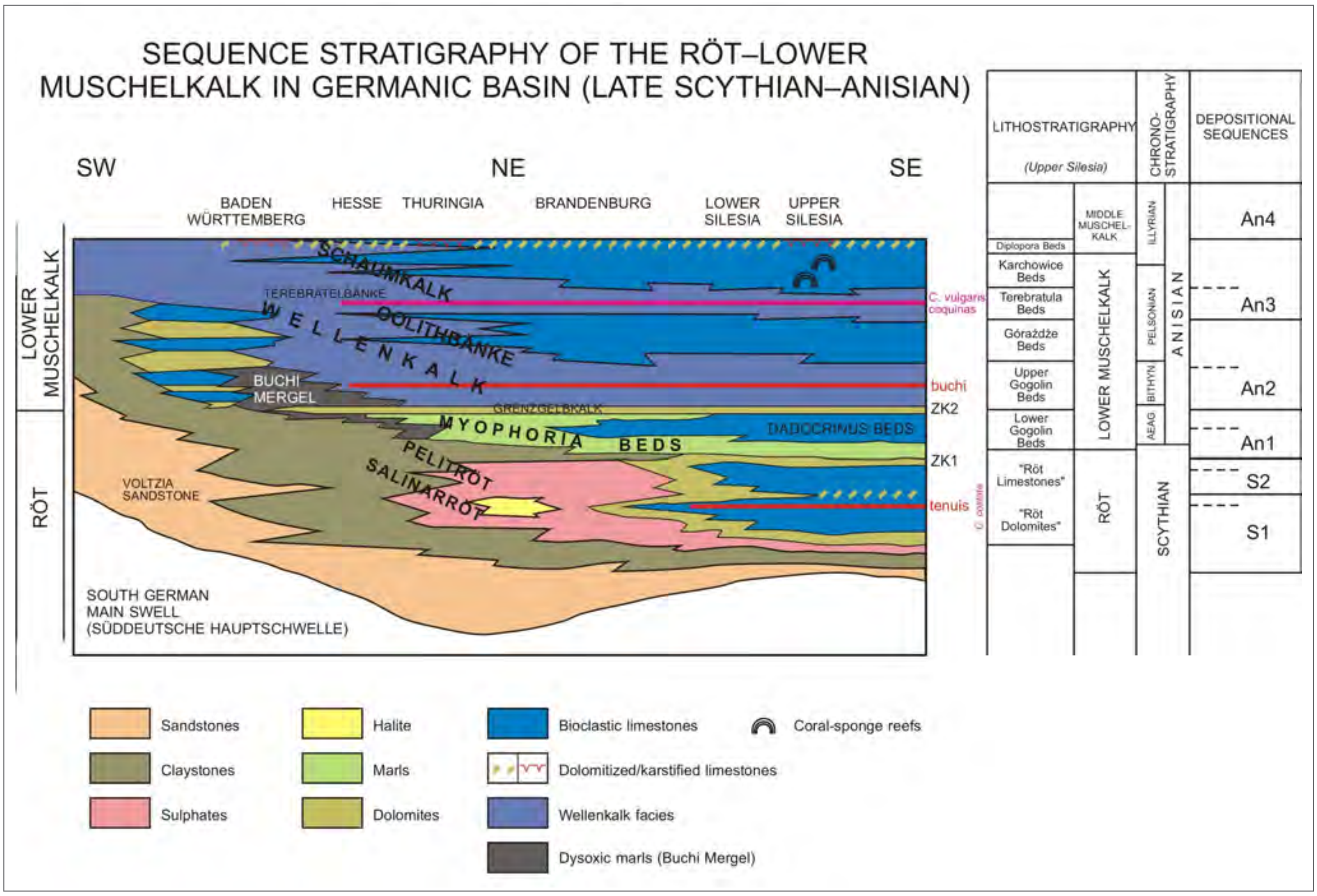

Fig. 5. Sequence-stratigraphic framework of the Lower Muschelkalk of the Germanic Basin (from Szulc, 2000).

fine-grained clastics followed by dolomites, sulphates and bioclastic and oolitic limestones. The carbonates contain relatively rich assemblages of gastropods and bivalves; *Costatoria costata* coquinas are dominant. Limestone beds in the upper part of the succession contain numerous cephalopods (*Beneckeia tenuis*) and crinoids that record the first maximum flooding stage (Fig. 5).

The second transgression in the Germanic Basin generally encompassed the same area as the first one. The lithofacies pattern shows a similar distribution; carbonate sedimentation was again dominant in the areas of the Silesian-Moravian and East Carpathian gates, while basinward both, dolomites and sulphates were deposited.

The Lower-Middle Muschelkalk is composed of four 3rd order depositional sequences.

Their boundaries are well defined by emersion horizons displaying features of meteoric diagenesis (dissolution, dolomitisation, karstification, palaeosoil and ferricrete formation).

The prograding global Anisian transgression is marked by some important events defining the maximum flooding zones of the subsequent depositional sequences i.e. An2 and An3. First appearance of index conodonts (e.g. *Neogondolella bulgarica, Neogondolella regale*, *Nicoraella kockeli*,) and Tethyan ammonoids (*Balatonites ottonis*, *Acrochordiceras*) is the most important bioevent defining the maximum flooding surface (MFS) of the An2 seuquence. These fossils date the of the An 2 sequence as coincidental with the beginning of the Pelsonian stage and have enabled a reliable correlation of the Muschelkalk deposits with the Tethyan successions.

The MFS of the 3rd Anisian sequence is characterized by explosive appearance of *Coenothyris vulgaris* brachiopods building the so-called Terebratula Beds (Fig. 5). According to sedimentological citeria (Szulc, 1993) and palynofacies data (Götz *et al*., 2005) the transgressive Terebratula Beds represent the Anisian maximum flooding surface recognized over the whole Germanic basin (Aigner and Bachmann, 1992; Szulc, 1995). Exceptionally great number of Tethyan faunal elements: brachiopods, pelecypods, echinoderms, conodonts, corals and dasycladales occurring in Silesia (Assmann, 1944; Hagdorn, 1991, Szulc, 2000) unequivocally indicates that during this interval, the communication between the Germanic Sea and Tethys Ocean reached its optimum.

In Upper Silesia the HST of the An3 sequence climaxed with sponge-coral-echinoderm buildups (Fig. 9). The Anisian (late Pelsonian-early Illyrian) buildups belong to the oldest *in situ* found, well dated scleractinans reefs. The hitherto gathered coral collection comprises specimens representing about 20 species (see Morycowa, 1988). The most frequent genera and bioherm constructors are: *Pamiroseris*, *Volzeia*, *Koilocoenia, Eckastraea* and solitary corals described as "*Montlivaltia*".

From the palaeobiogeographical point of view, the Silesian reef belt formed a Tethys marginal "reefal" rim dividing the offshore, Tethyan open marine zone from the backreef area (Fig. 4). Thus, it represents a fragment of the circum-Tethyan "reef" belt, that fortuitously avoided later subduction.

Final stages of the HST in Silesia are represented by *Girvanella* oncoliths, dasycladacean debrites and finally by oolitic bars which begin the basin-wide regression stage of the Middle Muschelkalk.

The Middle Muschelkalk in Silesia is represented by dolomites, sulphates and fossil-poor limestones diplaying common features of subaerial exposure.

The Upper Muschelkalk, poorly exposed in Silesia is built by dolomitic limestones followed by coquina deposits and condensed limestones.

The biostratigraphical data indicate that in the eastern parts of the Germanic basin, normal marine conditions have been replaced by brackish environments three conodont zones earlier than in southwestern Germany (Fassanian in Silesia *vs*. Longobardian in SW Germany) (Kozur, 1974; Trammer, 1975; Zawidzka, 1975; Narkiewicz and Szulc, 2004). The end of normal marine sedimentation in the Polish basin was coincidental with the *cycloides*-Bank *i.e.* with the maximum flooding phase of the Upper Muschelkalk in Germany.

Middle Triassic macrofauna in Silesia and its connection with the Tethys (Figs 6–9)

Hans Hagdorn

The Silesian Röt and Muschelkalk is widely known with its very rich fossil assemblage. It is noteworthy that the earliest descriptions of Triassic fossils from Upper Silesia, those by Meyer (1849), Dunker (1851) and Eck (1865), emphasized the close similarity of the Silesian

Muschelkalk with the alpine Triassic. In reviews of the Upper Silesian Muschelkalk faunas, Ahlburg (1906) and Assmann (1913, 1915, 1924, 1925, 1927, 1937, 1944) demonstrated that the percentage of Tethyan macrofaunal elements reached its peak in the Karchowice Beds and in the Diplopora Dolomite i.e. in the formations representing the maximum transgression stage in Anisian (Pelsonian). These data were supported also by later microfauna studies of condonts (Kozur, 1974; Zawidzka, 1975; Narkiewicz and Szulc, 2004).

The earliest marine ingression in Triassic times reached southeastern Poland during the late Olenekian when the Röt Dolomite was deposited. Its fauna is dominated by the myophoriid bivalve *Costatoria costata* and by the modiolids (*Modiolus* (?) *triquetrus).* Additional common fossils are the bakevelliids (*Hoernesia socialis* and *Bakevellia costata)*, the pectinoid *Leptochondria albertii*, *Pseudomyoconcha gastrochana*, the gastropod *Wortheniella* and the hedenstroemiid ammonoid *Beneckeia tenuis).* It is worth to note that some crinoid remains have been found in the Röt of southern Silesia (Alexandrowicz and Siedlecki, 1960). By means of *Costatoria costata*, the Röt Dolomite has already been correlated by Eck (1865) with the Werfen Formation of the Tethyan Triassic, though *Beneckeia* has not been found there.

Due to normal salinity and a greater variety of substrates, the Muschelkalk faunas are much more diverse than the Röt ones. The diversity depends on the progressive opening of the marine gates that connected the Central European Basin with the Tethys. Generally, in late Anisian (Pelsonian and early Illyrian) times, Silesia rather belonged to the Tethyan faunal domain than to the epicontinental Germanic province.

The lowermost Muschelkalk (Gogolin Beds), displays massive occurrence of stenohaline crinoids (*Dadocrinus* sp., *Holocrinus acutangulus,* evidencing normal marine environments. The crinoids were accompanied by ophiuroids (*Aspiduriella*, *Arenorbis*), mudsticking bivalves like *Bakevellia mytiloides*, *Hoernesia socialis*, *Pseudomyoconcha*, the myophoriids *Myophoria vulgaris*, *Neoschizodus laevigatus*, *Elegantinia elegans*, *Pseudocorbula*, *Pleuromya cf. fassaensis*, the gastropod *Omphaloptycha gregaria* and the nautiloids *Germanonautilus dolomiticus* and *G. salinarius* and, more rarely, the ammonoids, *Beneckeia buchi*, *Noetlingites strombecki*, *Balatonites ottonis*, *Acrochordiceras* that allow correlation with the Anisian Angolo Limestone of the Southern Alps.

During the Pelsonian communication between the Tethys and Silesia reached its climax as suggests common occurrence of the typical Tethyan cephalopods *Pleuronautilus planki*, *Balatonites*, *Bulogites* and *Paraceratites*, articulate brachiopods *Tetractinella trigonella*, *Mentzelia mentzeli*, and *Decurtella decurtata* as well as the dasycladacean green alga *Gyroporella minutula.* This is especially true for the corals (more than 20 species, including *Volzeia szulci* (Fig. 9c), *Pamiroseris silesiaca* (Fig. 9b), *Eckastraea prisca,* "*Montlivaltia*") and hexactinellid sponges (*Tremadictyon*, *Calycomorpha*, and *Silesiaspongia* and *Hexactinoderma*) that built the first, dated Mesozoic reefs after the P/T reefbuilders extinction.

The wealth of echinoderms also clearly indicates the Tethyan realm. Additionally to the encrinids *Encrinus robustus*, *E.* cf. *aculeatus*, *Carnallicrinus carnalli*, *Chelocrinus* sp. indet., and *Holocrinus dubius* that were dispersed over the entire Muschelkalk Basin, typical *Encrinus aculeatus*, *E. spinosus*, *Holocrinus meyeri*, *Eckicrinus radiates*, and the poorly known *Silesiacrinus silesiacus* are Tethyan crinoids that are also found in the Alps (Recoaro Fm.) and in Hungary (Hagdorn and Gluchowski 1993).

According to Assmann (1944), the bivalve fauna comprises 44 species, among which 15 are endemic in Upper Silesia, 12 are exclusively Germanic Muschelkalk, 4 are Alpine, and 13 occur in both the Alpine and the Germanic provinces. Among the 33 gastropod species, the Tethyan influence is even more evident. However, two thirds of the gastropod taxa, many of which have been found in a single specimen only, are endemic to Upper Silesia, 5 species are Alpine and 2 are Germanic. The most remarkable elements are large, ornamented archaeogastropods that inhabited the reefs.

In contrast to the Lower Muschelkalk the Middle and Upper Muschelkalk of Silesia is much poorer in number and species of invertebrate fossils and is dominated by germanotype faunal elements.

Syndepositional record of seismic activity in the Muschelkalk basin

Joachim Szulc

Earthquake events are commonly recognized as a trigger mechanism of mass movements in both, conti-

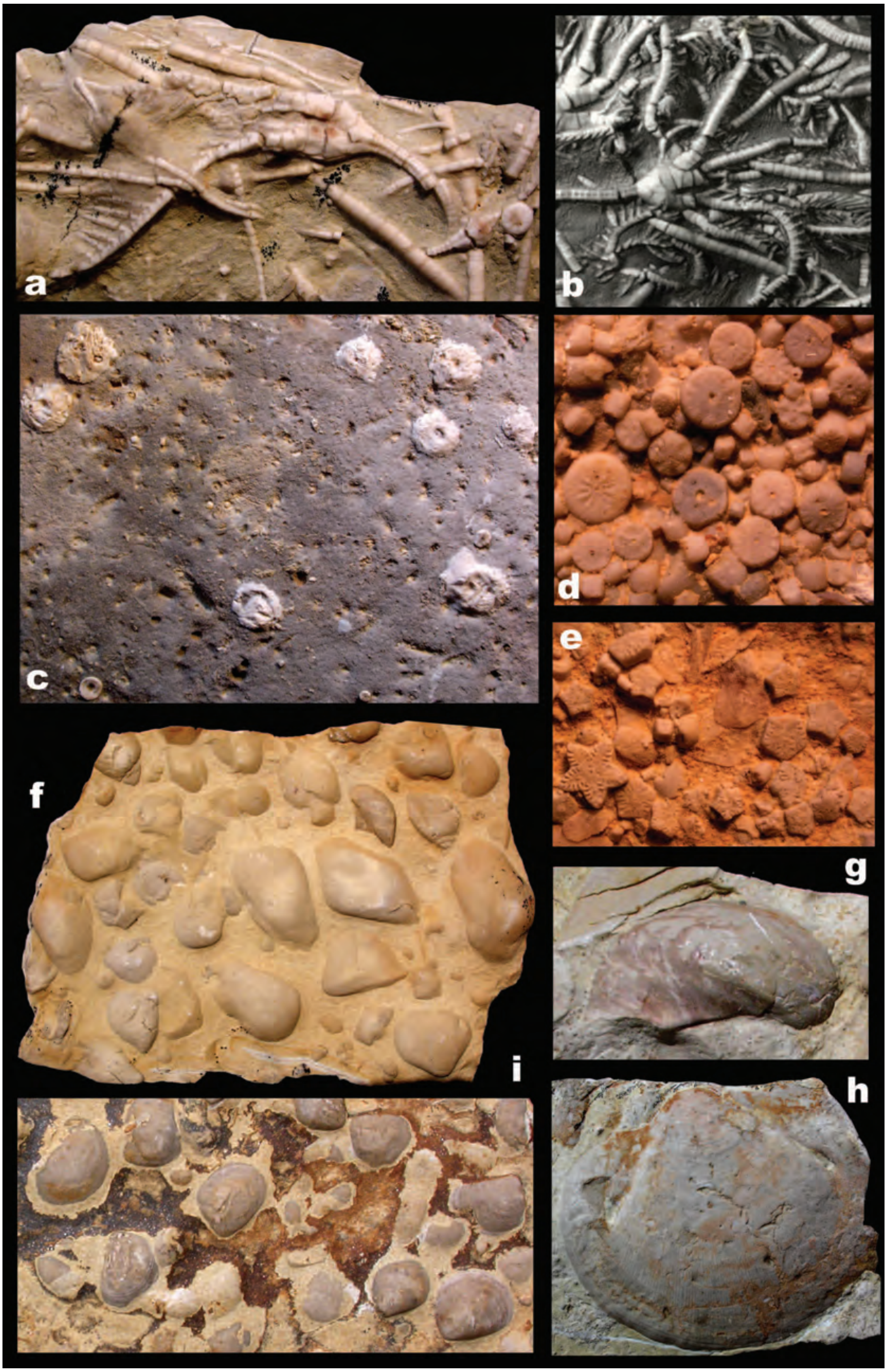

Fig. 6. Fauna of the Gogolin Formation. **a.** *Dadocrinus* sp., crown and stem fragments of a small, still undescribed dadocrinid from the Lower Gogolin Fm. of Milowice (x 2,5). **b.** *Dadocrinus kunischi*, the largest dadocrinid. Lower Gogolin Fm., Gogolin (x 0,8). **c.** Holdfasts of dadocrinids on top of a large intraclast; note the openings of *Trypanites* borings. Lower Gogolin Fm., Ząbkowice Bedzinskie (x 1). **d.** Dadocrinid columnals, Lower Gogolin Fm., Zyglin (x 2,5). **e.** *Holocrinus acutangulus*, columnals. Upper Gogolin Fm., Wojkowice Komorne (x 2,5). **f.** Soft bottom palaeocommunity of *Arcomya* cf. *fassaensis*, *Myophoria vulgaris*, *Bakevellia costata*, *Omphaloptycha gregaria*. Lower Gogolin Fm., Żyglin (x 0,8). **g.** *Hoernesia socialis*. Lower Gogolin Fm., Gogolin (x 1). **h.** *Entolium* cf. *E. discites*. Lower Gogolin Fm., Wojkowice Komorne (x 0,6). **i.** *Plagiostoma beyrichi*. Upper Gogolin Fm., Plaza (x 1). All specimens Muschelkalkmuseum Ingelfingen.

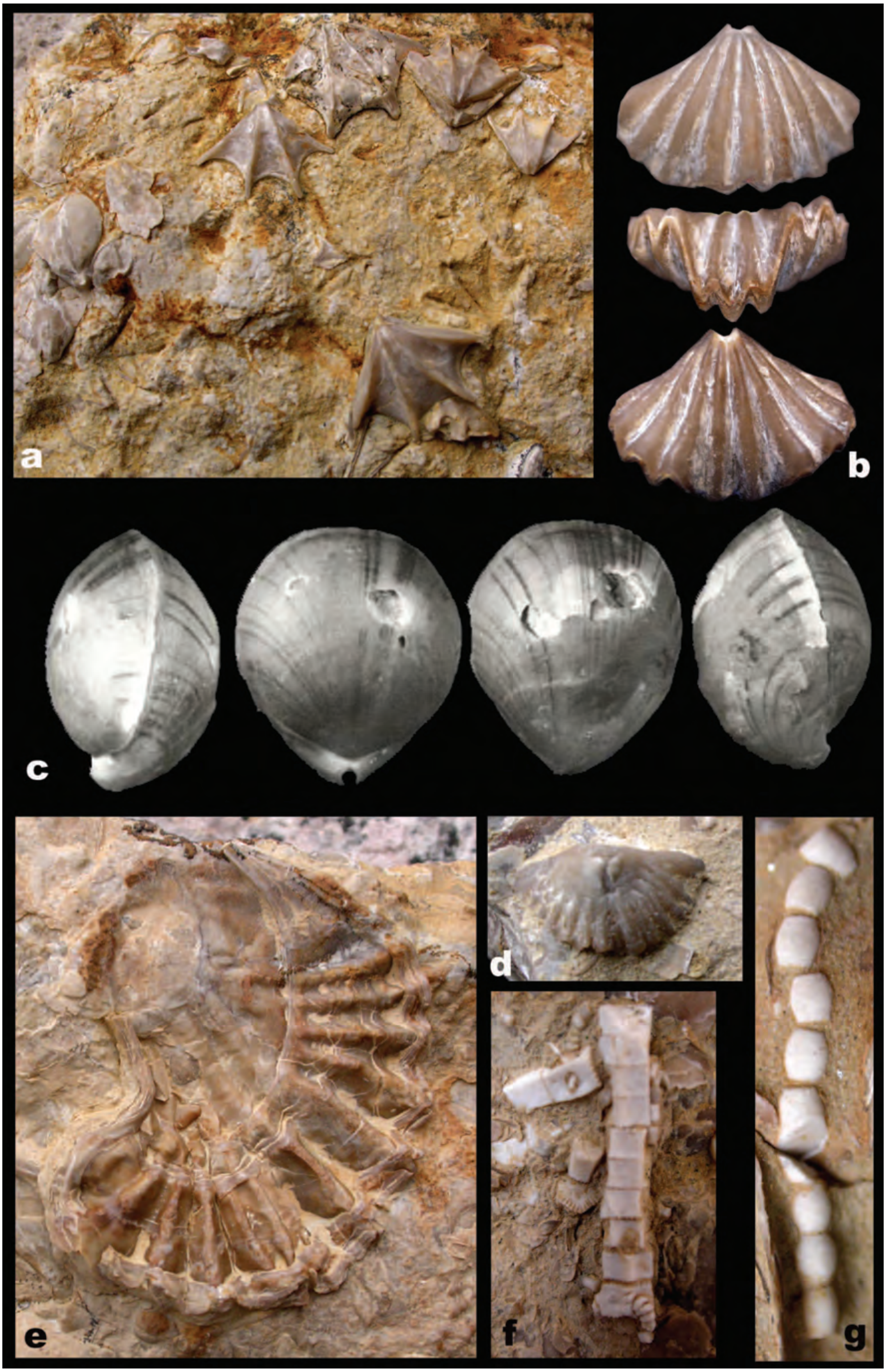

Fig. 7. Fauna of Terebratula Beds (Dziewkowice Formation). **a.** *Tetractinella trigonella, Silesiathyris angusta*. Strzelce Opolskie (x 2). **b.** .*Decurtella decurtata*. Strzelce Opolskie (x 3,8). **c.** *Coenothyris vulgaris*, with color bands. Strzelce Opolskie (x 1,7). **d.** *Hirsutella hirsuta*. Gorazdze (x 3). **e.** *Umbrostrea difformis*. Strzelce Opolskie (x 2). **f.** *Holocrinus dubius*, noditaxis of 10 columnals, with a cirrinodal at its lower end indicating an intermediate stage of disarticulation. Strzelce Opolskie (x 3,4). **g.** Indeterminate encrinid or dadocrinid with barrel-shaped columnals. Strzelce Opolskie (x 5). All specimens Muschelkalkmuseum Ingelfingen.

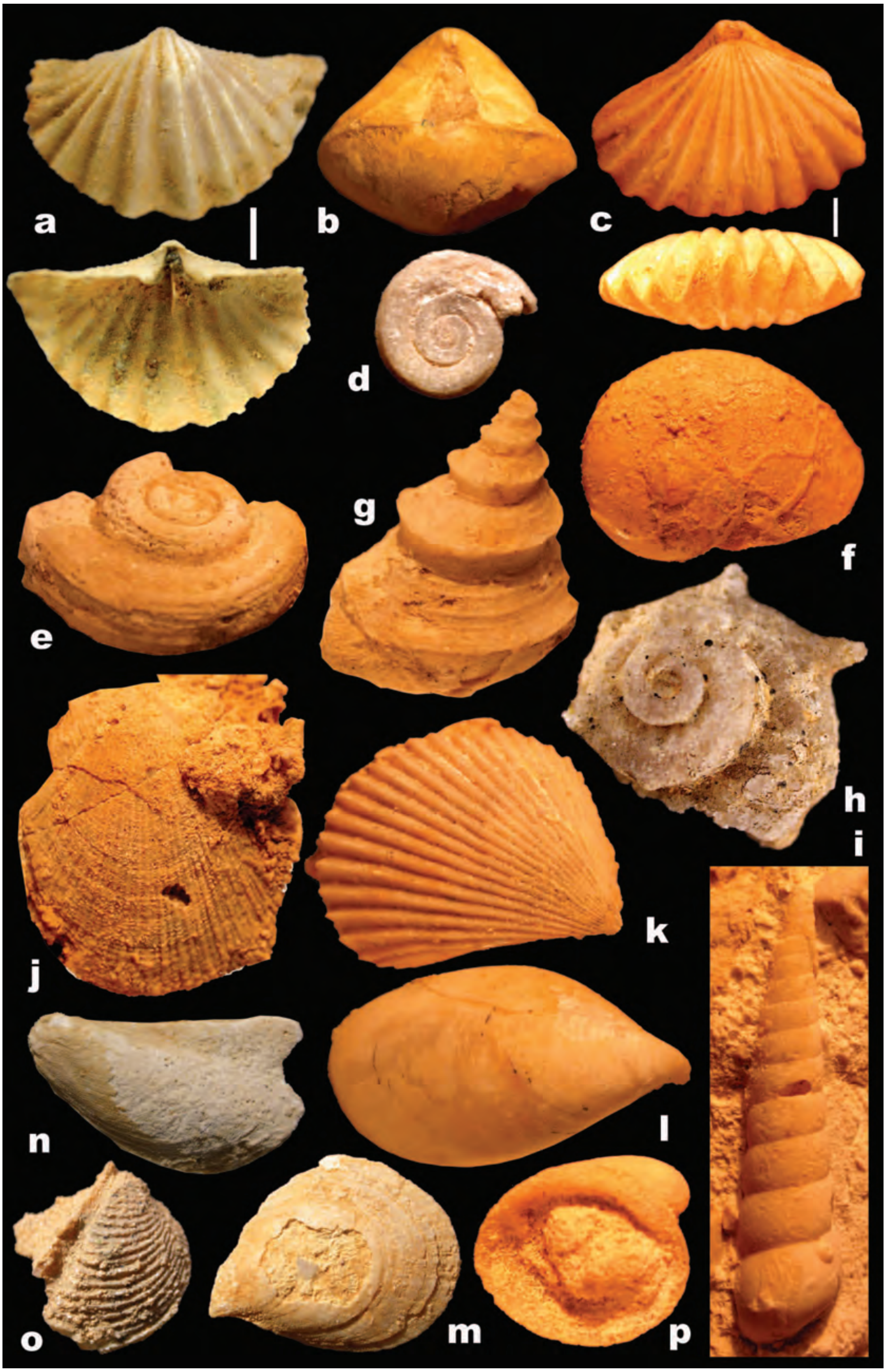

Fig. 8. Brachiopods, gastropods, and bivalves of the Karchowice Formation. **a.** *Punctospirella fragilis*, pedicle valve. Strzelce Opolskie (x 2,5). **b.** *Mentzelia mentzeli*. Tarnów Opolski (x 3,5). **c.** *Costirhynchopsis mentzeli*. Tarnów Opolski (x 3). **d.** *Discohelix (Amphitomaria) arietina*. Tarnów Opolski. (x 6) **e.** *Euomphalus semiplanus*. Tarnów Opolski (x 3,3). **f.** *Neritaria* cf. *N. comensis*, with encrusting serpulid (?). Tarnów Opolski (x 2,5). **g.** *Wortheniella* sp. Tarnów Opolski (x 2). **h.** *Coelocentrus silesiacus*. Tarnów Opolski (x 3,8). **i.** *Trypanostylus* sp. Tarnów Opolski (x 4). **j.** *Praechlamys schroeteri*. Strzelce Opolskie (x 2,5). **k.** *Lima acutecostata*. Strzelce Opolskie (x 2,5). **l.** *Promysidiella praecursor*. Tarnów Opolski (x 2). **m.** *Mysidioptera fassaensis*. Tarnów Opolski (x 2,5). **n.** *Bakevellia* cf. *B. costata*. Tarnów Opolski (x 2). **o.** *Elegantinia elegans*. Tarnów Opolski (x 2,5). **p.** *Schafhaeutlia* sp. Tarnów Opolski (x 5). All specimens Muschelkalkmuseum Ingelfingen.

Fig. 9. Sponges and corals of the Karchowice Formation.
a. *Silesiaspongia rimosa*. Strzelce Opolskie (x 2,2). **b.** *Pamiroseris silesiaca*. Tarnów Opolski (x 2,5). **c.** *Volzeia szulci*. Tarnów Opolski (x 2,8). **d.** *Coelocoenia exporrecta*. Strzelce Opolskie. (x 2). **e.** *Pinacophyllum* (?). Tarnów Opolski (x 2). **f.** *Montlivaltia* (?). Tarnów Opolski (x 2,5). All specimens Muschelkalkmuseum Ingelfingen.

nental and submarine environments. However, the resulted gravity mass-transported deposits: rockfalls, debris flows, slumps and turbidites are sedimentary fabrics that may originate also without seismic stimulus, but may be caused by other factors e.g. slope failure by overload or by impact of storm waves. In order to avoid misinterpretation of sedimentary structures postulated as seismically-induced fabrics, they should be always referred to their sedimentary context. Such circumstantial criteria as geodynamic position of the basin (tectonically active *vs.* passive), very abrupt lateral and vertical facies succession, basin geometry (gentle slopes) and first of all, some indicative deformational structures are arguments in favour of unequivocal palaeoseismic interpretations.

The Muschelkalk basin was situated in the northern periphery of the rifted Tethys Ocean and gentle sloped ramp geometries dominated over the basin. Sedimentary sequences of the Muschelkalk are mostly composed of fine-grained carbonates (*Wellenkalk* facies) with subordinate contribution of coarse bioclastic and biolithic limestones and evaporites. As discussed above, the basin was influenced by syndepositional tectonism related to activity of several master faults that transmitted the crustal motion produced in the Tethys intra-rift belt into its peripheries (Szulc, 1993, 2000).

Synsedimentary seismic activity in the Muschelkalk basin has long been postulated on the grounds of common plastic deformations of limestones (Schwarz, 1970). Comprehensive list of structures unequivocally evidencing seismic controls of the Muschelkalk basin has first been presented by Szulc (1993).

The most undoubted evidence of syndepositionary seismicity are phenomenona of sediment liquefaction and fluidization. In contrats to loosely packed siliciclastic deposits, early cementation of carbonates promotes their plasticity, hence the affected young lime sediments (fine-grained carbonates in particular) behave in a soft or ductile way. This in turn, favours development of plastic, cohesive deformations such as creeping, glides or slumping of material that has not undergone liquefaction and did not lose completely its original sedimentary attributes such as bedding or lamination. The ductile reaction makes the carbonates a natural sensitive seismograph, capable of precise recording of seismic tremors.

Faults, joints, breccias, neptunian and injection dykes

The synsedimentary faults in the Muschelkalk carbonates range in scale from a few centimeters to several meters (Figs 10A, 11A–C). Small scale brittle defomations are represented by slicken-sided faulting and sigmoidal fracturing (Fig. 10D–F). The brittle faults affected completely lithified carbonates but they are commonly accompanied by contemporaneous breccias and by flowage of the unconsolidated sediments (Fig. 11G–I). A particularly interesting example comes from eastern Silesia where an archipelago of fault-bounded islands linking a transpression zone developed in Middle Triassic times (Szulc, 1991). The uplifted Paleozoic basement rocks over there, display cracking veinlets (Fig. 10C–D) originated by hydraulic fracturing typical of earthquake relaxation (Masson, 1972).

Non-displacive deformations

This type of deformation is conspicuous by lack of any vertical and lateral translation of the deformed sediments. These deformations occur either as isolated crumples or as nodular, crumpled clusters and they range from several centimeters to 1 meter in size. (Fig. 12A–C). The crumpled fabrics adjoin directly the undeformed, stratified sediments. On the other hand, the deformations match generally the joint pattern of the encompassing rocks. This may be interpreted as an effect of incongruent progress of carbonate cementation. The unlithified carbonates became deformed plastically and/or homogenized in isolated centers while the completely lithified sediment underwent brittle jointing (Fig. 12A–B).

Load deformations

At first glance, the load structures look similar to the non-displacive deformations. However unlike the latter, the load deformations display obvious vertical translation, depending essentially on sinking of coarser-grained deposits (mostly calcarenites and calcisiltites) into lime muds (Fig. 12D–F).

Fault-graded beds

Seilacher (1969) was the first who ascribed this complex deformation to seismic trigger and named it. The deformations reflect consolidation gradient in quake-affected sediments. As a rule, the older, consolidated part undergoes brittle fracturing while the younger, semiconsolidated and/or unconsolidated tiers respond by ductile flowage or complete homogenization. The fault-graded beds are well developed in fine-grained, thin-stratified limestones of the Silesian Muschelkalk (Fig. 11G–H). Like the stationary deformations, this type of deformations is a very convincing diagnostic feature of palaeo-earthquake shocks. The presented tiering of disintegration is characteristic for lime sediments displaying progressive lithification.

Quake- induced sedimentary structures

For the following considerations, it is worth of notion that the basin floor had very gentle (<0.5°) or even flat floor with low hummocks (up to 2-3 m high) produced by storm waves and currents or built by colonial organisms (e.g. brachiopods or oysters). Such geometry predestinated slow, cohesive mass displacements rather than incoherent, gravity grain-flow transport. Indeed, in the Muschelkalk sedimentary sequences the elastic and plastic translations predominated, whilst the cohesionless redeposition was less frequent and is represented exclusively by high-density debris flow deposits.

The mass movements were initiated mostly by synsedimentary faulting which involved deplacement of nearby sediments. The faults exhibit both normal (mostly listric) and reversed sense of dislocation (Fig. 14). Depending on the consolidation stage and mechanical properties (competent *vs.* incompetent) of the affected sediments, various deformations originated along the drag plane. The unconsolidated deposits behave plastically (creeping) while the semiconsolidated (competent) limestones responded by gliding (Fig. 11J–L).

The slumps show rotational sliding of thick (up to 4m) packages of ductile lime mud. During sliding the mud underwent multiple overfolding giving very complex internal features of the slumping horizons (Fig. 11M) which could be correlated over the distance of several tens of km. Depth range of the faults rarely exceeds 2 m and they fade shortly.

The debris flows have been observed in the intervals of notably intense tectonic activity in the basin, which correspond to the beginning and the maximum stages of the Lower Muschelkalk transgression. Both sequences consist of intercalated limestone and marl beds. During a quake the lithified limestones ruptured, while unconsolidated marls underwent liquefaction and served as an easy-slip medium. If the distance of redeposition was relatively short, the failed horizon became a completely jumbled mass of broken fragments carried in more movable material (Fig. 13A–G). By a longer translation, the debris was fractionated by flotation of the lighter components and the basal angular slabs were shingled downslope (Fig. 13C). The largest slabs may reach 5 m in size. Lower boundaries of the debris-flows are sharp and rugged since the subjacent beds were distorted by drag and bulldozing as the moving mass was emplaced.

Tsunami deposits and the S-T dyads

Fossil tsunami deposits as gravity flow deposits are difficult to recognize without their reference to the sedimentary context and the associated deformational structures. In general, the most conceivable tsunamites are the graded beds following directly quake-induced deformations (Fig. 13). In the Silesian Muschelkalk basin such coupled occurrence of earthquake-induced deformations and associated tsunami deposits has first been recognized in the Silesian basin and called *Seismite-Tsunamite Dyad* or *S-T dyad* (Szulc, 1993; Fig. 13E–G). Composition of the S-T dyads changes upsection and reflects the transgressive trend in the basin. In the lower part, corresponding to the initial phase of transgression, the quake-induced slumps and debris-flow packages are covered with current transported, onshore and land-derived material. The last-named consists of rewashed red kaolinite clays evidencing its continental provenance (Figs 13E–F). In the basinal facies representing the maximum flooding event, the slumped, fossils-poor lime muds, are eroded and covered by graded, bioclastic debris (Fig. 13G).

Bipartite coquina beds are another example of seismically induced sedimentary structures (Fig. 13H). The beds represent a coupled sequence consisting of lower horizon of convex-down authochthonous shells entombed in lime mud (seismite) and the superjacent part composed of current-transported allochthonous skeletal debris, with shells settled in convex-up position (tsunamite).

Stop descriptions

Please note that almost all stops (beside stop B 5.4.) are situated in active quarries where permission for access is required

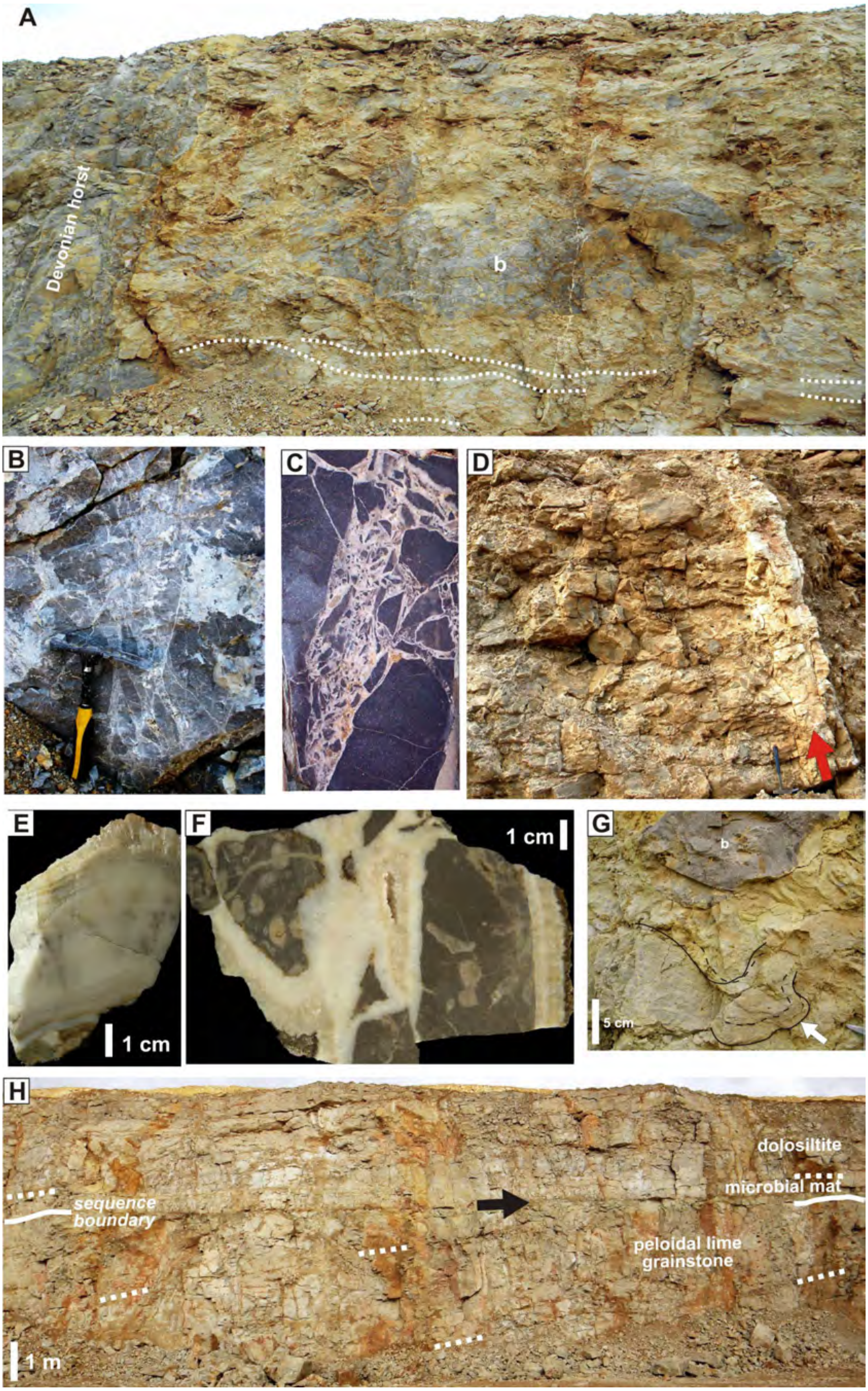

Fig. 10. Manifestation of synsedimentary tectonics in the GZD quarry, Nowa Wioska. Fault scarp and 7-m block of Devonian rocks (b) fallen to unlithified Triassic sediments. Note plastic deformation of the substrate. **A** – Hydraulic breccia developed in lagoonal dolomites, **B** – Details from Fig. 10 A, **C** – Outcrop view of a 40 cm-thick calcite vein (red arrow) piercing the Givetian black dolomites, **D** – Close up of the vein, **E** – Dissolution vugs filled with hydrothermal dolomite fill, **F** – 50 cm-large boulder of Devonian dolostone (b) deforming the underlying laminated Triassic calcarenites, **G** – Angular disconformity between 2nd and 3rd Anisian sequences (Olkusz Beds/Diplopora Beds).

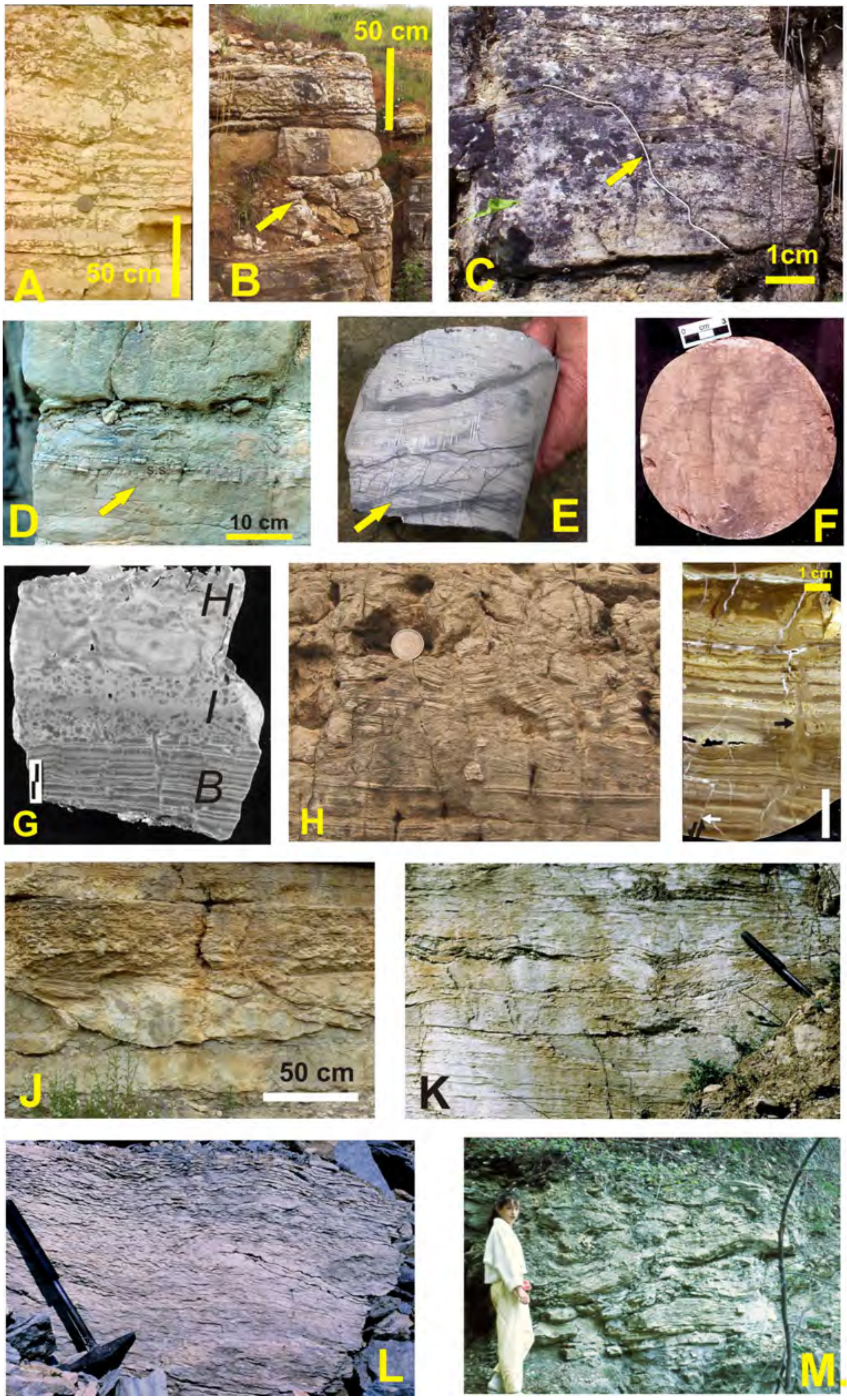

Fig. 11. Brittle and plastic quake-related deformations affecting the Muschelkalk limestones. **A** – Synsedimentary fault in Lower Gogolin Beds. Gogolin quarry, **B** – Synsedimentary fault in Gorażdże Beds, Naplatki quarry, **C** – Synsedimentary fault (arrow) in Lower Gogolin Beds, Libiąż, **D** – Slicken-sided faults (arrow) from Diplopora Beds. Libiąż quarry, **E** – Sigmoidal joints in Lower Muschelkalk. Gorzów Wielkopolski borehole, **F** – Plane view of joints from Fig. 11E, **G** – Fault-graded bed. Gogolin Beds, Płaza quarry. *B*- brittle fracturing, *H*- homogenisation, *I* – intermediate deformations, **H** – Quake-realted small synsedimentary faults, Górażdże Beds, Szymiszów quarry, **I** – Liquefaction injection dyke cutting microbial mats (black arrow). GZD quarry, Nowa Wioska, **J** – Synsedimentary intraformational slide slabs within the Górażdże Beds, Dąbrówka quarry, **K** – Gliding deformations from Terebratula Beds. Strzelce Opolskie quarry, **L** – Gliding and creeping deformations from Terebratula Beds. Strzelce Opolskie quarry, **M** – Overfolded and distorted limestones, Terebratula Beds. Góra św. Anny.

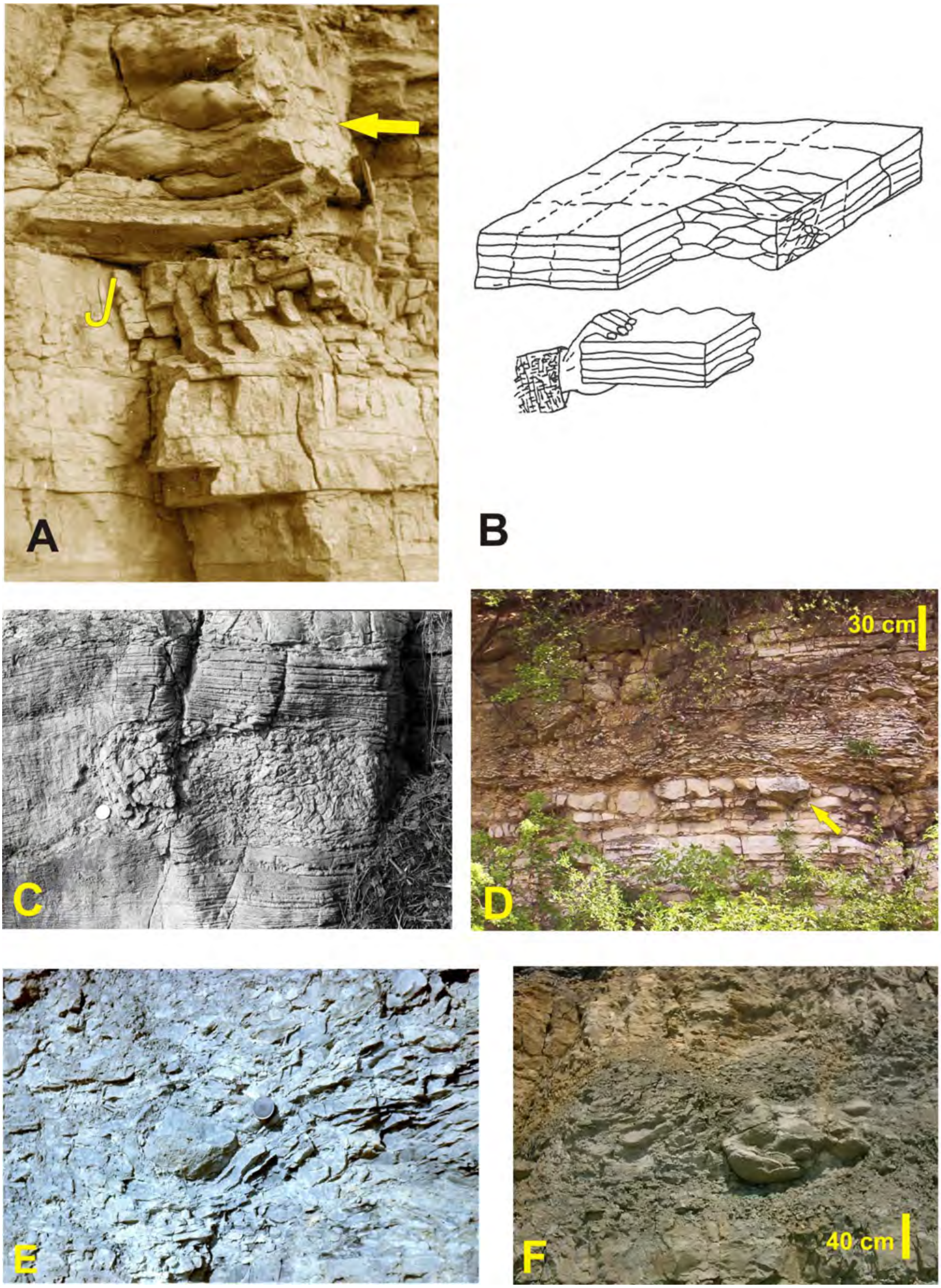

Fig. 12. Sedimentary and deformations related to Triassic synsedimentary tectonic activity in southern Poland. **A-B**. Photograph and drawing of non-displacive crumpled seismic deformations and joints, Lower Gogolin Beds. Gogolin, **C** – In-place crumpled seismic deformations. Gorażdże Beds, Raciborowice quarry, Lower Silesia, **D** – Load deformations from Gogolin Beds in Libiąż quarry, **E** – Isolated ball of calcarenites entombed in soft lime muds. Strzelce Opolskie quarry, **F** – Brachiopods colony sunken in lime muds. Strzelce Opolskie quarry.

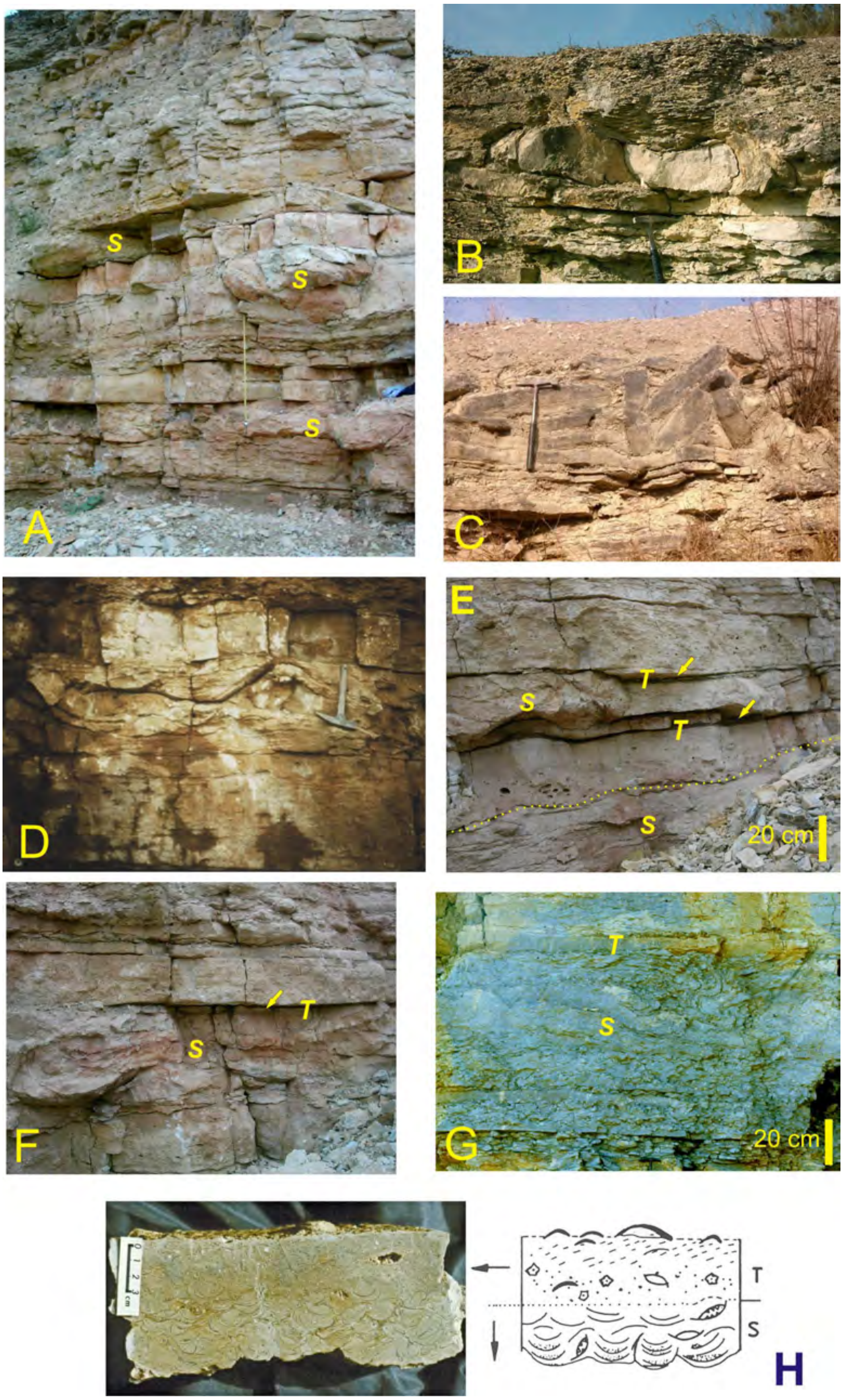

Fig. 13. Sedimentary deformations related to Triassic synsedimentary tectonic activity in southern Poland. **A** – Three, quake-triggered, debris flows (s) in Lower Gogolin Beds. Żyglin, **B-C** – Quake-triggered debris flows in Lower Gogolin Beds. Gogolin, **D** – Quake-triggered deformations in Lower Gogolin Beds. Płaza, **E-F** – Seismite-tsunamite dyads in Lower Gogolin Beds, from Żyglin. S – seismically disturbed sediments (seismite), T – tsunami backflow deposits (tsunamite) composed of offshore-derived intraclastic sediment and land-derived red clayey drape (arrows), **G** – Seismite-tsunamite dyad from Terebratula Beds. Strzelce Opolskie quarry. S – quake-induced slump of lime muds, T – tsunami backflow coquinas bed, **H** – Photograph and drawing of quake-generated bipartite coquina bed from Terebratula Beds. S – convex-down disposed *Coenothyris vulgaris* shells (seismite), unidirectionaly transported skeletal debris (tsunamite). Arrows indicate sense of deplacement.

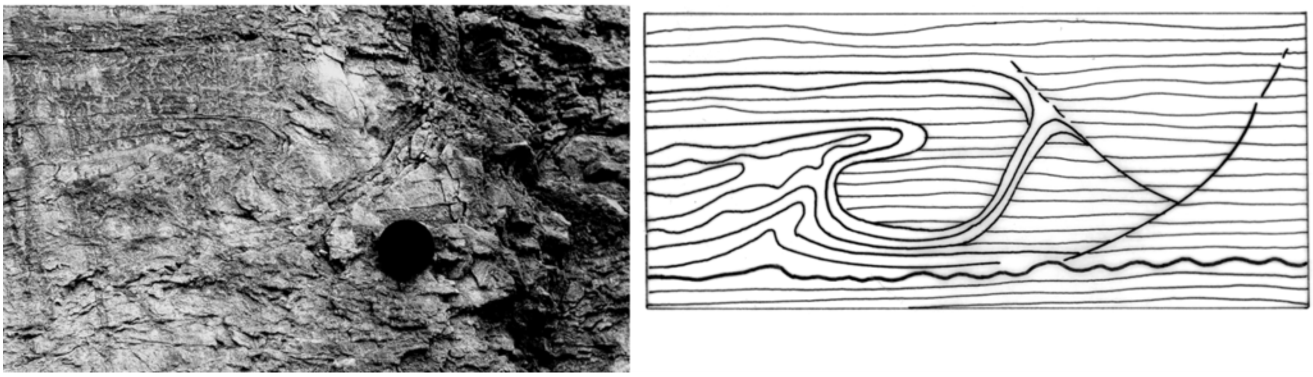

Fig. 14. Photograph and drawing of complex fault-and-fold deformations developed in lime muds affected by seismic shock. Terebratula Beds. Strzelce Opolskie quarry.

B5.1 Płaza. Active quarry of "Kans-Pol" Płaza

The quarry is situated by the railway station "Płaza", some 2 km NW from the village centre. (50°10′55″ N; 19°43′95″ E)

Leaders: Michał Matysik, Joachim Szulc

The ca. 40 meters thick profile begins with the Upper Röt carbonates, which encompass dolomitic rocks displaying many indicators of extremely shallow environment (coastal sabkha) such as stromatolites, tepee structures, desiccation cracks and postevaporitic silicification. The fauna is limited to linguloids and vertebrate bones and fish scales.

The sabkha sediments are passing upwards into hummocky cross-stratified limestones containing more open-marine fauna i.e. *Myophoria vulgaris* and gastropods. Higher up, the first dadocrinids appear indicating stenohaline, normal marine conditions. This part of the section comprises 3 slumped horizons (Fig. 13D), which could be used as excellent stratigraphic correlation tool with the equivalent sections at Gogolin (stop B5.4) and Żyglin (stop B5.3). The *Placunopsis*-encrusted hardground occurring in this complex, marks the MFS of the An1 depositional sequence. The sequence finishes with vuggy dolomites marking a significant sea-level drop. The subsequent conglomeratic and wavy limestones alternated with tempestites (Upper Gogolin Beds) represent the TST deposits.

The relatively deep-water facies grade into calcarenites and calcisiltites of the Górażdze Beds. These sediments representing the HST deposits terminate the presented profile.

B5.2 Siewierz. "GZD" active quarry

(50°49′83″ N; 19°21′35″ E)

Leaders: Michał Matysik, Joachim Szulc

The site is situated close to the ancestral Kraków-Lubliniec-Hamburg master fault zone (Fig, 2) active also in Middle Triassic. The basement rocks cropping out in the quarry are built of black Devonian (Givetian) dolostones that underwent subaerial weathering and karstification before the Muschelkalk transgression. In the middle of the outcrop, the Devonian basement rocks form a cliff-edged elongate horst. During the Muschelkalk transgression the horst was a fault-bounded island, some 200 m wide and 30–50 meters high, overlapped gradually by Triassic deposits. The island is one of the tectonically controlled horsts, forming a palaeoarchipelago in the Muschelkalk sea (Szulc, 1991). The outcrop abounds in records indicative of tectonic and, in particular, palaeoseismic activity in Triassic time.

The Devonian basement rocks over there, display cracking veinlets (Fig. 10) originated by hydraulic fracturing of rocks (Masson, 1972). Since the cracks were filled with unlithified Muschelkalk material they date the seismic events as Anisian in age.

The frontal, marine/land setting of the fault-bounded island has a profound bearing on seismic activity in the region. Water provided lubricant medium that enhanced fault breaking on the one hand and acted as blasting material (hydraulic fracturing) by its injection into the seismically opened cracks on the other hand.

The Devonian rocks, and sporadically the Muschelkalk limestones, are cut by subvertical calcitic veins. The veins are 1 to 50 cm wide and are filled with several generations of calcite lining (Figs 10D–F). The veins strike generally NNW–SSE and apparently follow the dominant direction of the master fault. According to stable isotope data, the calcite precipitated from hydrothermal solutions that were most likely discharged by quake-pumping mechanism (Sibson, 1987)

Of particular interest are breccias composed of Devonian clasts fallen to the Triassic unlithified sediments. The falling blocks (up to 10 m across in size) deformed the underlying Muschelkalk sediments (Fig. 10A, 10G). As indicates the rockfall debris deposited as fault-scarp screes, several major quakes wreaked havoc with the island coasts.

An intrafomational disconformity separating two Muschelkalk sequences is another evidence of synsedimentary tilting in the region (Fig. 10H). It is very probable that also very rapid vertical changes between subtidal and supratidal facies, common in the Diplopora Beds, resulted from spasmodic vertical displacements (*yo-yo tectonics*), typical for tectonically active regions (see e.g. Plafker, 1972)

Another indicator of synsedimentary seismic activity are small-scale deformations affecting the fine-grained Muschelkalk deposits and particularly well preserved in microbial mats. There are both small brittle deformations like joints, faults and slicked-sided cracks. They are commonly accompanied by soft-sediment deformation structures: small-scale intraformational folding and liquefaction (Fig. 11I) what indicates their seismic origin.

B5.3 Żyglin – small active quarry

Three small quarries are situated on the left side of a local road heading eastward from the village centre, (nearby church) to the forest (about 1.5 km). (50°48′08″N; 18°96′61″ E)

Leader: Joachim Szulc

The outcrop exposes the Lower Gogolin Beds and enables their comparison with their counterparts in the other presented sections, in Gogolin (ca. 50 km to W) and in Plaza (ca. 40 km to SE). In spite of some subordinate differences, all the sections display close similarity in general lithofacies and biota successions. Also the quake-triggered deformational horizons are recognizable in the mentioned section, thus enhancing the reliability of their correlation (Fig. 13A, E–F).

The presented section comprises two lithofacies assemblages which reflect the progressing earliest Anisian transgression. The lower assemblage encompasses the bioclastic, calcarenitic limestones (Myophoria- and Pecten and Dadorinus Beds) displaying features of proximal tempestites. Upsection, the bioclastic, calcareous sands are replaced by calcilutites with finer-grained tempestitic layers, typical for advanced TST.

These limestones are, in turn, followed by dolomitic marls terminating with cellular limestones. The cellular limestones mark an emersion event identifiable over the entire Silesian subbasin.

However, the most important correlation tool are three contorted horizons which affect the lower part of the presented section. These up to 1 m thick deformed beds may be easily correlated with their counterparts in the Gogolin and Plaza sections. These horizons are of particular interest because their internal composition informs about the sequel phenomena of the seismic tremors. As a rule, a deformed horizon commences with plastically deformed set covered with erosionally overlying gravity-flow sediments (Fig. 13E–F). The last mentioned are mostly twofold: the lower part comprises skeletal debris of offshore fauna whereas the upper one is formed by reddish, kaolinitic clays. Such a sequence may be unequivocally related to seismic-tsunami succession, where the deformed lower part represents the seismite *s.s.* while the overlying offshore-derived sediments have been transported by surge, tsunami back flow.

B5.4 Gogolin – abandoned quarry

The outcrop is situated at the eastern end of the communal waste depot in Gogolin, some 1.5 km from the village centre. (50°50′29″ N; 18°03′09″ E)

Leader: Joachim Szulc

The section presents transgressive succession from evaporitic Röt sediments to normal marine limestones of the Lower Muchelkalk.

The Röt is represented by reddish and ochre-coloured limestones and dolomites, comprising molds after gypsum and halite evaporites. Hopper halite crystals, displacive and reworked gypsum crystals and lack of fauna (but rare bones) as well as chertified stromatolites

(Bodzioch and Kwiatkowski, 1992) indicate very shallow, coastal sabkha environments. Meteoric water influxes and emersion events are evidenced by a quartzose conglomerate horizon and solution breccias which mark the boundary of the 1st Anisian sequence.

The sabkha evaporites are succeeded by more and more open marine carbonates as evidenced by increasing faunal quantity and diversity. The transgression climaxed with bioclastic thick-bedded, cross-stratified limestones with stenohaline dadocrinids (so called Beds with Pecten and Dadocrinus).

The following HST is formed by tempestitic shelly limestones and marls which grade uspection to evaporitic dolomites.

The section affords excellent structures related to synsedimentary seismic activity; faults, joints, liquefaction and three debris flows with deplaced slabs reaching 4 meters in size (Fig. 13B–C). The latter are equivalents of those presented at Płaza and Żyglin.

B5.5 Tarnów Opolski. Active quarry of Opolwap – Lhoist

Entrance to the vast quarry (some 10 km^2) is situated 400 m east from the railway station Tarnów Opolski. (50°55′29″ N; 18°08′51″ E)

Leaders: Hans Hagdorn, Michał Matysik, Joachim Szulc

The quarry exposes the uppermost part of the Terebratula Beds and the complete section of the Karchowice Beds.

The deeper-water, fine-grained limestones and marls of the Terebratula Beds evolve gradually into massive, bioclastic Karchowice Beds by 4 meters-thick set of firmgrounds alternated with tempestitic encrinites. The bioclastic sands form locally several meters high dunes, composed of amalgamated cross-stratified sandbodies.

Biolithic complex which developed upwards is dominated by sponge constructions; biostromes, and higher up, by bioherms. The latter reach up to 7 m in height and several tens of meter in width. The other contributors of the bioherms are encrusting worms and forams, crinoids, brachiopods, gastropods and scleractinian corals (Figs. 6–9). The corals are represented by some 20 species which makes this assemblage the oldest (and richest) known scleractinian coral colonies at all (Morycowa, 1988).

The biohermal complex of the Karchowice Beds is bipartite. In the lower part, between the hexactinellid sponges, the colonies of denroid-phaceoloid *Volzeia szulci* occur (Fig. 9c). Delicate branching coral habits, suggest a relatively quiet environment. The corals and sponges form knobs clustered together. This complex is capped by a crust of lamellar colonies of *Pamiroseris silesiaca* (Fig. 9b). Encrusting form of the coral colonies is typical for turbulent environment and indicates that the reef structures reached its shallowest growth phase. The crests of the lower biohermal complex were partly emerged and underwent meteoric diagenesis (dolomitisation, karstfication), while the in local depressions the *Girvanella* oncoliths formed. The bioherms are composed mainly of relatively homogenous, massive or nodular micritic fabrics, which represent aggregates of automicritic carbonate originated by microbially mediated decay of the sponge bodies.

During the next transgressive pulse, the second biohermal complex formed. Its structural framework is similar like in the lower one, but the branching corals are absent.

Total thickness of the biohermal complexes in the reef-core area reaches up to 25 meters.

Vertical succession in the buildup composition reflects ecological evolution related to a highstand shallowing trend, typical of the “catch-up reef” *sensu* James & Mcintyre (1985). As a rule, the succession begins with biostromes built by prostrate colonies of sponges (stabilization-colonisation stage) The biostromes are replaced, first by low-relief, and then by high-relief biohermal buildups, encompassing also branching corals and clusters of other organisms (diversification stage). The reef cap formed by encrusting corals is typical for the final, domination stage of the reef evolution.

The eventual shallowing resulted in decline of the sponge-coral association which has been replaced by oncolithic and oolitic limestones of the Diplopora Beds.

It is worthy to note that the Karchowice Beds display intense lateral variation both on a bed level and within the entire unit. Such a variation challenges the merit of the cyclostratigraphical interpretations for the higher frequency, 4th and 5th orders, depositional sequences.

B5.6 Strzelce Opolskie. Active quarry of Heidelberg Cement GmbH

The huge quarry is situated 1 km east from the local road Strzelce Opolskie- Rozmierka. (50°53′20″ N; 18°30′93″E)

Leaders: Michał Matysik, Joachim Szulc

The section exposes the most complete Lower Muschelkalk outcrop encompassing sediments of two Anisian depositional sequences; A2 and A3 (Fig. 5).

The exposed section commences with marls and distal calcareous tempestites representing maximum flooding zone of the sequence A2, which is concurrent with beginning of the Pelsonian stage. First appearance of the index conodonts, ammonoids and crinoids is the most important bioevent recorded in this interval, indicating open communication with the Tethys.

The subsequent thick-bedded and coarse-grained bioclastic, oncoidal and oolitic limestones build a 15 m thick shoalbar set of the Górazdże Beds. The Gorażdże Beds, which represent HST of the A2 sequence, are built by alternated calcarenites and finer-grained limestones. The calcarenites are cross-stratified, amalgamated oscillatory ripples, transported and deposited under storm wave and current action. The interbedded, fine-grained limestones are fair-weather sediments are intensively bioturbated, which resulted in their nodular character. It is worthy to note, that the oncoids are built mostly by foraminiferal aggregates. The other bioclasts comprise debris of gastropods, pelecypods, crinoids, corals and sponge spicules.

Oomoldic porosity and ferricrete crust featuring the topmost part of the Gorażdze Beds indicate meteoric influences as the shoalbar became emerged (Szulc, 1999). Therefore, one may accept the top of the Gorażdze Beds as a boundary of the next depositional sequence.

This sequence boundary is covered sharply by dark, finely laminated limestones, typical for TST, beginning the Terebratula Beds. These calcilutites are impoverished in body- and ichnofossils, which indicates very fast advancement of the transgression and poorly ventilated, starving basin conditions. This horizon (ca. 1.5–2 m thick) is slumped and totally contorted (Fig. 11M), which suggests a quake-triggered mechanism of the deplacement on the one hand, and tectonically forced deepening on the other hand (Szulc, 1993).

The slumped set is replaced by a 1.5 thick, amalgamated encrinitic bank (so called *Hauptcrinoidenbank* of Assmann, 1944) indicating some shallowing trend. The *Hauptcrinoidenbank* is covered by a 12 meters thick set of slightly dysoxic, grey marls intercalated with dm-thick coquinas, dominated by *Coenothyris vulgaris* shell debris. The Terebratula Beds represent the Anisian maximum flooding interval, recognized over the whole Germanic Basin (Szulc, 1990; Aigner and Bachmann, 1992). Total thickness of the Terebratula Beds reaches ca. 20 meters in the quarry.

The Terebratula Beds are followed by bioclastic (mostly crinoidal) calcarenites alternated with firmground horizons and then by spongean structures forming the Karchowice Beds.

Acknowledgements: This field-trip guidebook is partly based on guidebooks prepared on the occasion of some former conferences, particularly, 6th Annual Conference of SEPM-CES Field Guide (Szulc *et al.*, 2009) and Fieldtrip Guide of 4th Meeting on Pan-European Correlation of the Epicontinental Triassic (Szulc *et al.*, 2007).

References

Ahlburg, J., 1906. Die Trias im südlichen Oberschlesien. *Abhandlungen der königlich-preußischen geologischen Landesanstalt N. F.*, 50: 1–163.

Aigner, T. & Bachmann, G., 1992 . Sequence-stratigraphic framework of the German Triassic. *Sedimentary Geology,* 80: 115–135.

Alexandrowicz, S. & Siedlecki, S., 1960. Bunter deposits in the vicinity of Rybnik, Upper Silesia. *Rocznik Polskiego Towarzystwa Geologicznego*, 30: 167–199. [in Polish, English summary.]

Assmann, P., 1913. Beitrag zur Kenntnis der Stratigraphie des oberschlesischen Muschelkalks. *Jahrbuch der königlich preußischen geologischen Landesanstalt*, 34: 268–340.

Assmann, P., 1915. Die Brachiopoden und Lamellibranchiaten der oberschlesischen Trias. *Jahrbuch der königlich preußischen geologischen Landesanstalt,* 36: 586-683.

Assmann, P., 1924. Die Gastropoden der oberschlesischen

Trias. *Jahrbuch der preußischen geologischen Landesanstalt,* 44: 1–50.

Assmann, P., 1925. Die Fauna der Wirbellosen und die Diploporen der oberschlesischen Trias mit Ausnahme der Brachiopoden, Lamellibranchiaten, Gastropoden und Korallen. *Jahrbuch der preußischen geologischen Landesanstalt,* 46: 504–577

Assmann, P., 1927. Die Decapodenkrebse des deustchen Muschelkalks. *Jahrbuch der preußischen geologischen Landesanstalt,* 48: 332–356.

Assmann, P., 1937. Revision der Fauna de Wirbellosen der oberschlesischen Trias. *Abhandlungen. der preußischen geologischen Landesanstalt N. F.*, 170: 1–134.

Assmann, P., 1944. Die Stratigraphie der oberschlesischen Trias. Teil 2: Der Muschelkalk. *Abhandlungen. des Reichsamts für Bodenforschung*, 2: 1–124.

Beutler G., 2005. Diskordanzen im Keuper. In: *Stratigpraphie von Deutschland IV – Keuper*, *Courier Forschungsinstitut Senckenberg*, 253: 85–93.

Bodzioch, A. & Kwiatkowski, S., 1992. Sedimentation and early diagenesis of Cavernous Limestone (Roet) of Gogolin, Silesian-Kraków Upland. *Annales Societatis Geologorum Poloniae,* 62: 223–254.

Brack, P., Rieber, H. & Ulrichs, M., 1999. Pelagic successions in the Southern Alps and their correlation with the Germanic Middle Triassic. *Zentralblatt für Geologie und Paläontologie* Teil I, 1998 (7–8): 813–852.

Dunker, W., 1851. Ueber die im Muschelkalk von Oberschlesien bis jetzt gefundenen Mollusken. *Palaeontographica,* 1: 283–310.

Eck, H., 1865. *Ueber die Formationen des bunten Sandsteins und des Muschelkalks in Oberschlesien und ihre Versteinerungen*. Berlin, Friedländer u. Sohn, 149 pp.

Götz, E. E., Szulc, J. & Feist-Burkhardt, S., 2005. Distribution of sedimentary organic matter in Anisian carbonate series of S Poland: evidence of third-order sea-level fluctuations. *International Journal of Earth Sciences*, 94: 267–274.

Hagdorn, H., 1991. The Muschelkalk in Germany – An Introduction. In: Hagdorn, H., Simon, T. & Szulc, J. (eds), *Muschelkalk. A Field Guide*. Goldschneck-Verlag. Stuttgart, 80 pp.

Hagdorn, H. & Głuchowski, E., 1993. Paleobiogeography and Stratigraphy of Muschelkalk Echinoderms (Crinoidea, Echinoidea) in Upper Silesia. In: Hagdorn, H. & Seilacher, A. (eds), *Muschelkalk*. Goldschneck V. Stuttgart: 165–176.

James, N. P. & Mcintyre J. G., 1985. Carbonate depositional environments, modern and ancient. *Quaterly Journal of the Colorado School of Mines*, 80: 1–70.

Kotański, Z., 1994. Middle Triassic Dasycladacea of the Upper Silesian-Cracow region and their stratigraphical and palaeoecological significance. In: *3rd International Meeting of Peri-Tethyan Epicratonic Basins*, *Cracow, 29 August–3 September 1994. Excursion Guidebook*. PIG Warsaw, pp. 59–66.

Kozur, H., 1974. Probleme der Triasgliederung und Parallerisierung der germanischen und tethyalen Trias. Teil I: Abgrenzung und Gliederung der Trias. *Freiberger Forschungshefte*, C 298: 139–198.

Masson, H., 1972. Sur lorigine de la cornieule par fracturation hydraulique. *Eclogae Geologicae Helvetiae*, 65: 27-41.

Matysik, M., 2014. Sedimentology of the „ore-bearing dolomite" of the Kraków-Silesia region (Middle Triassic, southern Poland). *Annales Societatis Geologorum Poloniae*, 84: 81–112.

Matysik, M., 2015 (in press). Facies types and depositional environments of a morphologically diverse carbonate platform: a case study from the Muschelkalk (Middle Triassic) of Upper Silesia, southern Poland. *Annales Societatis Geologorum Poloniae*.

Meyer, H. von, 1849. Fische, Crustaceen, Echinodermen und andere Versteinerungen aus dem Muschelkalk Oberschlesiens. *Palaeontographica*, 1 (5): 216–242, (6): 243–279

Morycowa, E., 1988. Middle Triassic Scleractinia from the Cracow-Silesia region, Poland. *Acta Paleontologica Polonica*, 33: 91–121.

Narkiewicz, K. & Szulc, J. 2004. Controls of migration of conodont fauna in peripheral oceanic areas. An example from the Middle Triassic of the Northern Peri-Tethys. *Géobios*, 37: 425–436.

Nawrocki, J. & Szulc, J., 2000. The Middle Triassic magnetostratigraphy from the Peri-Tethys basin in Poland. *Earth and Planetary Science Letters,* 182: 77–92.

Plafker, G., 1972. Alaskan earthquake of 1964 and Chilean earthquake of 1960: implications for arc tectonics. *Journal of Geophysical Research*, 77: 901–924.

Rüffer, T., 1996. Seismite im Unteren Muschelkalk westlich von Halle. *Hallesches Jahrbuch fuer Geowissenschaften,* 18: 119–130.

Seilacher, A., 1969. Fault-graded beds interpreted as seismites. *Sedimentology*, 17: 155–159.

Sibson, R. H., 1987. Earthquake rupturing as a mineralizing agent in hydrothermal systems, *Geology*, 15: 701–704.

Schüller, F., Beutler, G & Frantzke, H. J., 1989. Über synsedimentäre Bruchtektonik an der Grenze Unterer/Mittlerer Buntsandstein auf der Hermundurischen Scholle. *Hallesches Jahrbuch für Geowissenschaften*, 14: 49–54.

Schwarz, H.-U., 1970. *Zur Sedimentologie und Fazies des Unteren Muschelkalkes in Südwestdeutschland und angrenzenden Gebieten*. PhD Diss. of the Tübingen University: 297 pp.

Szulc, J., 1990. Diagenesis. IAS International Workshop – Field Seminar. In: *The Muschelkalk – Sedimentary Environments, Facies and Diagenesis. Cracow – Opole. Excursion Guidebook and Abstracts*: pp. 26–28.

Szulc, J., 1991. The Upper Silesian Muschelkalk – a general setting. In: Hagdorn, H., Simon, T. & Szulc, J. (eds), *Muschelkalk. A Field Guide*. Goldschneck V., Stuttgart, pp. 61–63.

Szulc, J., 1993. Early Alpine Tectonics and Lithofacies Succession in the Silesian Part of the Muschelkalk Basin. A Synopsis. In: Hagdorn, H. and Seilacher A., (eds), *Muschelkalk*. Goldschneck V. Stuttgart : 19-28.

Szulc, J., 1995. Schemat stratygrafii sekwencyjnej epikontynentalnego triasu; rola tektoniki i eustatyki. In: *IV Krajowe Spotkanie Sedymentologów P.T.G.*, Kraków, pp. 112–113 [in Polish.]

Szulc, J., 1999. Anisian-Carnian evolution of the Germanic basin and its eustatic, tectonic and climatic controls. *In*: Bachmann, G. H. & Lerche, I. (eds), Epicontinental Triassic. *Zentralblatt für Geologie und Paläontologie, Teil I*, 1998, 7-8: 813–852

Szulc, J., 2000., Middle Triassic evolution of the nortnern Peri-Tethys as influenced by early opening of the Tethys Ocean. *Annales Societatis Geologorum Poloniae*, 70: 1–48.

Szulc, J., 2005. Sedimentary environments of the vertebrate-bearing Norian deposits from Krasiejow, Upper Silesia (Poland). *Hallesches Jahrbuch für Geowissenschaften, Reihe B*, 19: 161-170.

Szulc , J., Gradzinski, M., Lewandowska, A. & Heunisch, C. 2006. The Upper Triassic crenogenic limestones in Upper Silesia (southern Poland) and their paleoenvironmental context. In: Alonso-Zarza, A. & Tanner, L. H. (eds), *Paleoenvironmental Record and Applications of Calcretes and Palustrine Carbonates*. Geological Society of America Special Paper, 416: 133-151.

Trammer, J., 1975. Stratigraphy and facies development of the Muschelkalk in the south-western Holy Cross Mts. *Acta Geologica Polonica,* 25: 179–216.

Voigt, T. & Linnemann, U., 1996. Resedimentation im Unteren Muschelkalk- das Profil am Jenzig bei Jena. *Beitraege zur Geologie Thüringen*, *N.F.*, 3: 153–167.

Zawidzka, K., 1975. Conodont stratigraphy and sedimentary environment of the Muschelkalk in Upper Silesia. *Acta Geologica Polonica,* 25: 217–257.

Cenozoic freshwater carbonates of the Central Carpathians (Slovakia): facies, environments, hydrological control and depositional history

Michał Gradziński[1], Wojciech Wróblewski[1], Pavel Bella[2, 3]

[1]Institute of Geological Sciences, Jagiellonian University, Kraków, Poland (michal.gradzinski@uj.edu.pl) (wojciech, wroblewski@uj.edu.pl)

[2]Slovak Caves Administration, Liptovský Mikuláš, Slovakia (pavel.bella@ssj.sk)

[3]Catholic University in Ružomberok, Slovakia

Route (Fig. 1): From Kraków we follow E77 (S7) south to Rabka, then 47 to Nowy Targ and in town we turn left onto 49. On leaving the town road 49 turns south and crosses the boundary with Slovakia between Jurgów and Podspády. In Slovakia we follow road 67 to **Ždiar Pass (stop B7.1)** with a car park on the right. We follow to Spišská Belá and turn left onto road 77. At Nižné Ružbachy we turn left onto a local road to **Vyšné Ružbachy (stop B7.2)**. From Vyšné Ružbachy we return to Spišská Belá and take road 77 to Kežmarok. There we turn left onto local road 536 to Jánovce and turn east onto road 18. Leaving on the left the mediaeval town of Levoča (with Spišská Kapitula and Spišský hrad parts of the UNESCO World Heritage) we drive 10 km east, leaving aside the entrance on the motorway, to **Sivá brada (stop B7.3)** on the right, at a junction with a side road lined with tall trees. From Sivá brada we drive the side road eastward and then south through the medieval town Spišská Kapitula and descend to Spišské Podhradie. We turn right, continue south, with a travertine ridge on the left, and reach the headquarters of the Euro Kameň company. From the headquarters we follow along the slope of the north-south trending travertine ridge, pass by a small active quarry to reach inactive **Žehra quarry (stop B7.4)**, at the southern end of the travertine ridge. We depart Žehra quarry and the headquarters of the Euro Kameň company by road 547 south, to Spišské Vlachy. There we turn right to road 536 and continue west to Spišská Nová Ves, where we turn left and proceed south, crossing a forested mountain chain of the Slovak Ore Mountains. We reach road 67 and continue SE towards Rožňava (in Hungarian – Rozsnyó, in German – Rosenau), which is a centre of the historic region called Gemer. The city has an old mining tradition; silver, gold and especially iron ores were exploited there. On the second day, after an overnight stay in Rožňava, the trip departs via the village of Jovice and arrives at the village of Krásnohorská Dlhá Lúka. We reach **Buzgó stream (stop B7.5)** by a 650 m walk along the foot of the Silica Plateau. From the village of Krásnohorská Dlhá Lúka we drive east, along a local road and next turn right onto road 50 and after crossing a pass between Silica Plateau and Horný Vrch Plateau we descend to the Turňa Basin and continue eastward. After 23 km we turn left onto a local

Gradziński, M., Wróblewski, W. & Bella, P., 2015. Cenozoic freshwater carbonates of the Central Carpathians (Slovakia): facies, environments, hydrological control and depositional history. In: Haczewski, G. (ed.), *Guidebook for field trips accompanying 31st IAS Meeting of Sedimentology held in Kraków on 22nd–25th of June 2015*. Polish Geological Society, Kraków, pp. 217–245. Guidebook is available online at www.ing.uj.edu.pl/ims2015

road and pass by the village of Háj (in Hungarian – Áj) to enter a narrow **Háj Valley (stop B7.6)**, with outcrops of inactive Holocene tufa and modern tufa sites. After visiting the Háj Valley we drive back through Rožňava and across the Slovak Ore Mountains to the foot of the Tatras. Then, we enter motorway D1 and continue east to the village of **Bešeňová (stop B7.7)**. After visiting two localities in Bešeňová we drive back to D1 and east to Liptovský Mikuláš, where we turn onto road 584 to reach the outskirts of the village of Demänová, at the foot of the Low Tatras. After an overnight stay in Demänová, we drive south into the Low Tatras 4 km up the Demänová Valley to visit **Demänová Cave System (stop B7.8)**. From there we drive back to Liptovský Mikuláš, then westward by D1 to Bešénová, where we turn onto a local road to the north and through the village of Liptovská Teplá we reach the village of **Lúčky (stop B7.9)**. From Lúčky, we drive to the state boundary at Trstená-Chyżne and back to Kraków along E77 (S7).

Fig. 1. Route map of field trip B7.

Introduction to the trip

Main topics

The field trip is an answer to rapidly growing interest in freshwater carbonates which, on the one hand, reflects their potential as a palaeoenvironmental archive and, on the other hand, is associated with the discovery of oil and gas in such kind of rocks in the South Atlantic. To some extent the trip follows the idea of similar ones organized during the former IAS conferences, that is Kraków in 1986 (Gąsiorowski *et al.*, 1986), Fukuoka in 2006 (Kano *et al.*, 2006), Alghero in 2009 (Capezzuoli *et al.*, 2009) and Zaragoza in 2011 (Vázquez-Urbez *et al.*, 2011), as well as some meetings especially devoted to such topics (Tata – 2004, Pammukale – 2005, Hull – 2008, and Abbadia San Salvatore – 2011). The field trip focuses on various types of freshwater carbonates in the Central and Internal Western Carpathians since this area abounds in travertines, tufas and caves highly decorated with speleothems. Travertines and tufas were, and still are, formed in different environmental and hydrological conditions. Their depositional history reflects geomorphic evolution of the area, tectonic events, climate changes, which in turn influenced palaeohydrological conditions, as well as even activity of prehistoric people. The above phenomena have been recorded also in speleothems since their growth are under influence of similar environmental processes.

An overview of geology

Northern Slovakia represents an area of mountain massifs and intervening intramontane basins (Fig. 2). It occupies a part of the Carpathian chain; this part, from the geological point of view, belongs mostly to the Central Carpathians. The mountain massifs are predominantly built up of sedimentary rocks. They comprise carbonates, mostly Mesozoic, and especially Middle Triassic in age (Maheľ and Buday, 1968). Other Mesozoic rocks occur subordinately. The sedimentary rocks cover older, crystalline basements which constitute the cores of many mountain massifs. All the rocks in question were deformed in the Late Cretaceous time; several nappes were formed and pushed to the north as an effect of a crustal shortening resulting from the convergence between Adria-Africa and Europe (Plašienka, 2008). The Central Carpathians were subjected to erosion and denudation during Palaeogene times, to Early Eocene. Subsequently, tectonic subsidence created Central Carpathian Palaeogene Basins filled with deposits of a marine transgression. A sequence comprising conglomerates, limestones, and a thick package (up to 3 km) of flysch-type rocks was laid dawn. This sequence is called the Central Carpathian Palaeogene. In Miocene, some parts of the region started to be uplifted; they presently form mountain massifs composed of Mesozoic rock and their crystalline basement. The intramontane basins are filled with the Central Carpathian Palaeogene, predominantly with carbonate-free flysch sandstones and mudstones. They cover the same Mesozoic rocks which constitute neighbouring uplifted mountain massifs. During the Middle–Late Miocene time, the Central Carpathians started to be under an extension regime due to a switch from an advancing to a retreating convergent system (Plašienka, 2008). At present, the area experiences an NW–SE compression and an NE–SW extension. Volcanic activity persisted in the Internal and Central Carpathians since Miocene (Eggenburgian) through Pleistocene (Lexa and Konečný, 1998).

The development of modern relief of northern Slovakia started in Miocene and it was associated with tectonic activity of the region. The surface fluvial drainage and underground karst drainage systems were created. The latter were drained by karst resurgences. Simultaneously, springs located along faults started to expel deeply circulating water which migrated up across impermeable and insoluble rocks of the Central Carpathian Palaeogene. The recharge areas were located on the elevated massifs, whereas the springs were located mostly in the intramontane basins.

Fig. 2. General geology of the region (after Vozár and Káčer, 1996, modified) with location of the field-trip stops.

The geological history of the Inner Carpathians was slightly different. This region, including the Slovak Karst, experienced long lasting denudation, which started at the end of the Cretaceous (Maheľ and Buday, 1968). The area was drained towards the south, to the Pannonian Sea. In Late Miocene time (at the turn of Pannonian and Pontian), Slovak Karst was uplifted and tilted southward, which caused vigorous entrenchment of deep valleys and development of vertical caves (Gaál, 2008).

Travertines

Actively growing freshwater carbonates occur widely in northern Slovakia (Kovanda, 1971; Demovič *et al.*, 1972; Gradziński, 2010). They are situated near their pre-Holocene predecessors (Gradziński *et al.*, 2008b). The actively growing travertines are located near springs fed with deeply circulating waters, highly charged with CO_2 of crustal or even mantle origin (Hynie, 1963; Cornides and Kecskés, 1982; Leśniak, 1998; Povinec *et al.*, 2010). They display a very wide range of facies types; from those typical of travertines *sensu stricto* to those common in calcareous tufa. However, they have been genetically connected to deeply circulating water, or its mixture with water of shallow circulation. Therefore, for the sake of simplicity, in this guidebook they are named consistently as travertines, regardless of their texture and facies type (for terminological discussion see Pentecost, 2005; Pedley, 2009; Jones and Renaut, 2010; Capezzuoli *et al.*, 2014). Such an approach allows distinguishing between these deposits and calcareous tufas, which are common in southern Slovakia, but have originated in completely different geological and environmental setting.

Recent travertines compose spectacular morphological forms, as craters (some completely dried, some still filled with water; Ružbachy, stop B7.2) and cascades formed on inclined slopes and covered with microgours and microdams (Sivá brada, stop B7.3 and Bešeňová, stop B7.7). The growth rate of modern travertines reaches a few centimetres per year and definitely exceeds the growth rate of calcareous tufa in the same region (Gradziński, 2010).

The growth of travertines is governed by chemistry of parental solution and the rate of CO_2 degassing, which decide upon effective precipitation of calcium carbonates (Pentecost, 2005; Pedley, 2009; Capezzuoli *et al*., 2014). The physico-chemically stimulated quick crystallization of calcium carbonate affects the organisms in the milieu of travertine growth. Moreover, highly mineralized waters impede growth of many microorganisms and plants. Thus, the (micro)organisms seem to play subordinate, if any, role in the formation of many travertines. However, in some cases microbial and algal contribution is important, or even crucial, especially where deeply circulating and highly mineralized water mixes with water of shallow circulation (Lúčky, stop B7.9; Gradziński, 2010). Such settings are densely populated by cyanobacteria, algae, liverworts, mosses, and also higher plants. Some of them, especially those belonging to cyanobacteria and algae, can physiologically stimulate crystallization of calcium carbonate (see Rogerson *et al*., 2008). Moreover, the organisms exert a substantial control on the texture of growing travertine. Comparison of isotopic composition ($\delta^{13}C$ and $\delta^{18}O$) of modern Slovak travertines and isotopic composition of their parental water ($\delta^{18}O$) and dissolved total inorganic carbon ($\delta^{13}C_{DIC}$) reveals that travertines grow out of isotopic equilibrium, because of kinetic effects (see Kele *et al*., 2008, 2011). This limits their usefulness for palaeoclimatic reconstruction.

Fossil, inactive travertines in northern Slovakia form buildups of various shape and dimensions (mounds, ridges, terraces). They reach the height of several dozen metres, whereas their lateral extent exceeds a few kilometres. They were formed, similarly to their modern counterparts, near springs fed with highly mineralized water of deep circulation. Their shape is controlled by the relief of basement surface, location of a potentiometric surface, CO_2 pressure, amount of feeding water and its distribution in travertine growth area, chemistry and temperature of this water, as well as the growth rate of travertine, which strongly depends on the above mentioned factors.

Travertine buildups display a variety of lithotypes, the same as those distinguished in Tuscany travertines by Guo and Riding (1998). The most common are crystalline crusts which developed on inclined slopes of the travertine buildups. At present, this lithotype is formed in cascades at Sivá brada (stop B7.3) and Bešeňová (stop B7.7) which are fed by a thin film of flowing water. Calcite raft lithotype is associated with water ponded in small pools. Various types of rafts are being formed at Sivá brada. Fossil examples of crystalline crusts, calcite rafts as well as lithoclast travertine and coated bubble travertine compose an extensive, inactive travertine ridge, called Dreveník (stop B7.4; Gradziński *et al*., 2014). This ridge was affected also by postdepositional deformation, which resulted in fracturing and brecciation.

Although phytoclastic lithotypes and stromatolites are atypical of travertines, they commonly occur in mixing-water settings. The Lúčky site (stop B7.9) provides both, modern and ancient examples (Gradziński *et al*., 2008b; Gradziński, 2010).

Pre-Holocene travertines in Slovakia are commonly regarded as originated during warm climate phases of Neogene and Pleistocene (interglacials). This notion is based on palaeobotanical, malacologial and geomorphological data (Němejc, 1928, 1931, 1944; Petrbok, 1937; Ložek, 1957, 1961, 1964; Ložek and Prošek, 1957; Vaškovský and Ložek, 1972). However, it is intriguing that, in spite of favourable climatic conditions, the recent growth of travertines seems to be limited in comparison with the wide-spread occurrence and great lateral extent of the pre-Holocene travertine buildups.

Calcareous tufa

Conversely to northern Slovakia, fossil tufa outcrops and sites of modern tufa deposition are common in the Slovak Karst area, in southern part of the country. Kovanda (1971) and Kilík (2008) listed several tufa localities there. The Slovak Karst is a typical karst area with several plateaus built of Mesozoic carbonates. The plateaus are dissected by valleys with bottoms located approximately at elevation of 200–300 m, whereas the plateaus reach 400–800 m. Numerous crags and cliffs built of carbonate rocks occur on the plateau slopes. The plateau tops and north-facing slopes are forested with deciduous trees and their south-facing slopes are covered mainly by xerothermic grasslands and bushes. The plateaus are drained by extensive karst systems leading water to karst springs with average discharge up to 120 L/s (Jakál and Bella, 2008). The water is chiefly of the $Ca–HCO_3$ type and its mineralization exceeds 500 mg/L. The springs are located at the foot of the plateaus.

Active tufas precipitate near almost each spring in the Slovak Karst area (stops B7.5 – Buzgó and B7.6 – Háj). They form tufa barrages and pools, cascades with tufa curtains, and oncoids (Kilík, 2008). The tufa depositional milieu is densely vegetated by cyanobacteria, algae, liverworts and mosses. These organisms are supposed to play an important role in tufa growth in this area (Gradziński, 2010).

Inactive tufas of Holocene age occur adjacent to active springs. The tufas in question are exposed by erosion and downcutting, in some places reaching to the Mesozoic bedrock. In a narrow valley setting tufas form a longitudinal fluvial depositional system with abundant barrages and inter-barrage areas. The former were built of moss, stromatolitic and phytoclastic tufa. The latter are filled with oncoidal and detrital tufas, including intarclastic ones. This tufa depositional system is governed by a limited ability of lateral stream migration. Conversely, tufas representing perched springline depositional system were formed below springs situated on the plateau slopes. Such a setting enabled omitting obstacles, impeded the formation of barrages and, hence, also dammed areas. Thus, cascades built of moss, stromatolites and phytoclastic tufa originated (Gradziński *et al.*, 2013).

In the Slovak Karst, the tufas grew especially vigorously in the Mid-Holocene, namely in the Atlantic and Sub-Boreal times (Gradziński *et al.,* 2013). Subsequently, they experienced substantial erosion and the streams incised down. This could be stimulated by deforestation by prehistoric humans or by late Holocene climate changes. The factors causing decline of the tufa growth ceased to operate, which is proved by the widespread formation of modern tufa in the Slovak Kast area.

Speleothems

Slovakia abounds in caves; more than 7,000 caves are registered (P. Holúbek, personal information, 2015). Some of them are accessible for tourists. Many caves are richly decorated with various types of speleothems. They represent inactive and actively growing ones, which was confirmed by analyses of feeding water.

The speleothems are a robust carrier of palaeoenvironmental information about palaeoclimate, tectonic/seismic activity, and geomorphic evolution of a karst region. Speloethems from Slovak caves have been recently extensively studied for these purposes. The analysis of speleothem growth frequency proved that they crystallized mainly in the warm periods of Pleistocene (Hercman, 2000). However, some far-reaching suggestions on local climate anomalies were also put forward (Hercman *et al.*, 1997, 2008). Dating of speleothems shed some new light on the age of the extensive Demänová Cave System (in Slovak – Demänovský jaskynný systém; stop B7.8) and demonstrated that the lowest 'levels' of this cave are definitely older than it was postulated.

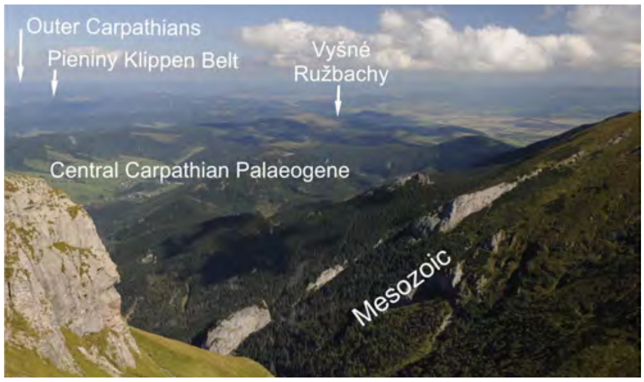

Fig. 3. Geological panoramic view of the area north of the Tatras. Mesozoic carbonates building the northern slopes of the Tatras (in the foreground) deep steeply to the north and plunge below the Central Carpathian Palaeogene. Pieniny Klippen Belt and the Outer Carpathians are visible in the background.

Stop descriptions

B7.1 Ždiar, viewpoint – outline of geology

(49°16′24″ N, 20°13′44″ E)

Leader: Michał Gradziński

This stop located on the edge of the Tatras enables us to familiarize with the general geological structure of the Central Carpathians (Fig. 3). The trip departed from Kraków, located on the boundary between the Kraków Upland (Carpathian foreland), a narrow segment of the Carpathian foredeep, and the Carpathians. Travelling to the south, we crossed several nappes of the Outer Carpathians, thrusted to the north on the foreland basin filled with Miocene deposits. The nappes are composed of uppermost Jurassic to Early Miocene rocks, predominantly of flysch type. Next, we crossed the Pieniny Klippen Belt. It is a narrow zone stretching from Vienna (Austria) to Maramureş (Romania), regarded as a boundary between the Outer and Central Carpathians.

Between the Pieniny Klippen Belt and the Tatras, there is a hilly area clearly visible in the foreground (to the north). Its western part is called Podhale whereas the eastern one – Spisz (in Polish) or Spiš (in Slovak). It is built of Central Carpathian Palaeogene rocks (mainly of siliciclastic flysch) attaining 3 km in thickness and forming an asymmetric syncline.

To the south, in the close vicinity, we can see steep, rocky slopes of the Tatras, in particular their easternmost part, called the Belianske Tatras with their highest summits Havran (2154 m) and Ždiarska Vidla (2148 m). The Tatras are the highest mountain massif of the Carpathians. They culminate in Gerlach (2655 m). They display morphological and geological asymmetry. Their northern slopes are built of several nappes, composed of Mesozoic rocks, predominantly carbonates, whereas their main ridge and, especially, its southern slopes are composed chiefly of various crystalline rocks. In Miocene the Tatras were uplifted along a prominent boundary fault on the south and south-east. Beside the Tatras, a small horst built of Mesozoic rocks is uplifted along this fault. The horst is engulfed by Palaeogene rocks, and due to this, it is called 'an island'. The second stop of this trip is located there.

Palaeogene rocks, which originally covered the Tatras, have been completely eroded since Miocene times. The uplift and glacial erosion led to the formation of high-mountain, alpine-type relief of the Tatras. They underwent repeated glaciations during the Pleistocene. Several cave systems exist in the limestone parts of the Tatras. They discharge waters from the karst massifs in resurgences located at the foot of the mountains, but a substantial portion of water feeds confined aquifer (an artesian basin) located to the north of the Tatras, where Central Carpathian Palaeogene rocks act as confining beds. Such water naturally outflows in the area of the Ružbachy 'island' (Hanzel, 1987).

B7.2 Vyšné Ružbachy spa – Holocene and modern carbonates in the discharge zone of deep-circulation water

Leaders: Michał Gradziński, Michał Gąsiorowski[1], Helena Hercman[1], Jacek Motyka[2], Jacek Pawlak[1], Piotr Smosna[3]

[1]Institute of Geological Sciences, Polish Academy of Sciences, Warsaw, Poland

[2]Faculty of Geology, Geophysics and Environmental Protection, AGH University of Science and Technology, Kraków, Poland

[3]Institute of Geological Sciences, Jagiellonian University, Kraków, Poland

Mineral springs in the village of Vyšné Ružbachy (in Polish – Wyżnie Drużbaki, in German – Oberrauschenbach, in Hungarian – Felsőzúgó) in the Spiš region have been mentioned in literature since 1549. The village has acted as a spa since the end of the 16th century (Potočná, 2007). It is worth mentioning that the first study on medical properties of water from Ružbachy was undertaken in 1635 and funded by Stanisław Lubomirski, the owner of Ružbachy and a prefect of the Spiš district which belonged to Poland at that time. The study was conducted by Jan Innocenty Petrycy, a professor of the Akademia Krakowska (now Jagiellonian University).

There exist nearly 20 natural and artificial (from drilled wells up to a few dozen metres deep) outflows of mineral water in the area of Vyšné Ružbachy. Distribution of the outflows is controlled by the geological structure of the area. Vyšné Ružbachy is located on the outskirts of the so-called 'island'. It is an area where Mesozoic

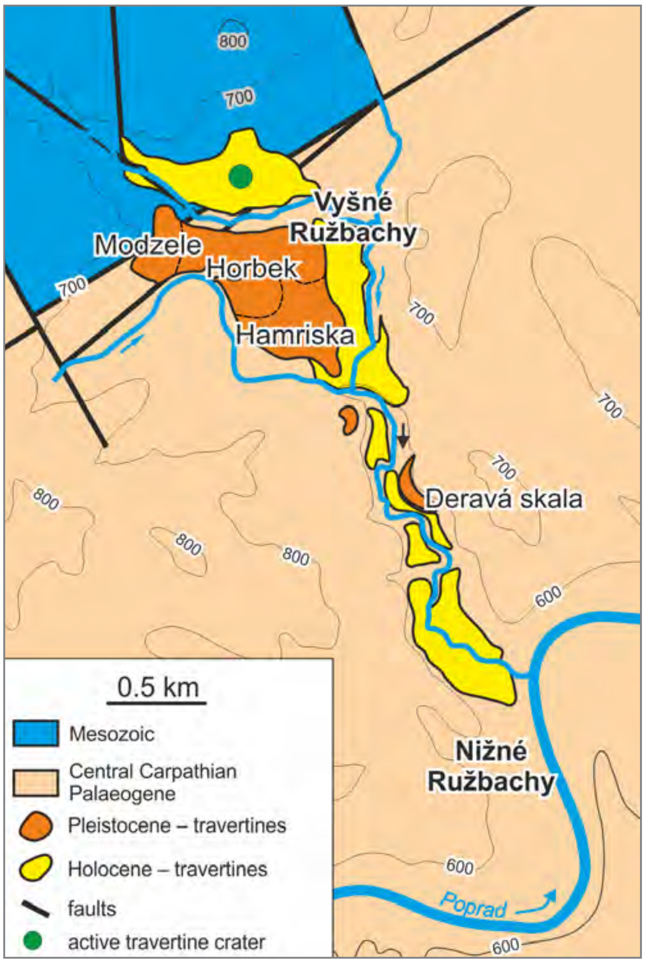

Fig. 4. Simplified geological map of the Ružbachy area (stop 2), after Ložek (1964) and Janočko *et al.* (2000).

rocks crop out from beneath the Central Carpathian Palaeogene siliciclastic rocks (Fig. 4). Mesozoic rocks belong to the Krížna Nappe) and represent the same rock series as in the Tatras, including the Belanské Tatras, which we observed from our first stop. Mesozoic rocks are bordered from the southeast by a fault with a throw of ca. 1.5 km. In the area of Vyšné Ružbachy it runs in the SW–NE direction, and it is the prolongation of the southern boundary fault of the Tatras, called the Sub-Tatric fault. Therefore, the Mesozoic 'island' of Ružbachy resembles to some extent the Tatras in Neogene time, when the Palaeogene cover only started to be eroded and Mesozoic rocks of the Tatras cropped out only locally. The Mesozoic rocks composing the north-eastern part of the Tatras and crystalline rocks of the Tatras core, which are hydraulically connected with them, act as the recharge area for outflows in Vyšné Ružbachy. The Middle Triassic carbonates, and Cretaceous and Eocene limestones constitute a confined aquifer, whereas Central Carpathian Palaeogene impermeable siliciclastics act as confining beds (Fendeková, 2002). The water ascends from beneath the confining beds partly along the Sub-Tatric fault and along smaller faults associated with it, and partly by the 'island' of Ružbachy which acts as a hydrogeological window.

Outflowing water has temperature between 17 °C and 24 °C. Total mineralization is within the range from 1.9–3.6 g/L. The water represents the HCO_3–SO_4–Ca–Mg type. Ca content ranges from 320 mg/L to more than 600 mg/L, HCO_3 from 1135 mg/L to more than 2000 mg/L. Carbonate equilibrium is controlled by the high CO_2 content, which varies between 360 and 1700 mg/L (Fendeková, 2002). H_2S is also present in small amounts (0.1–4.65 mg/L). High carbonate alkalinity of the water implies that carbonate rocks are being actively dissolved in the aquifer. This process takes place in elevated temperature. Therefore, one can presume that hypogenic caves are being formed by ascending water in deep substratum below impermeable Central Carpathian Palaeogene rocks. Such inactive caves have been recognized in northern slopes of the Tatras. One of them is Belianska Cave located in the E margin of the Tatras in the vicinity of the Sub-Tatric fault.

Spontaneous outgassing of CO_2 near the outflow zones enables quick and efficient calcium carbonate precipitation and formation of travertines. Nemejc (1931) found several travertine localities near Vyšné Ružbachy. Subsequently, Ložek (1964) distinguished three generations of travertines (Fig. 4). The first one crops out in the hill called Modzele located west of the spa; it is visible in an abandoned quarry. It represents crystalline crust and coated bubble lithotypes; they are probably early Pleistocene in age (Gradziński *et al.*, 2008b; Rajnoga, 2009). Three localities – Horbek, Hamriska i Deravá skala – located to the S and SW of the spa represent the second generation. The abandoned quarry at Horbek is the largest locality, now hosting an open air gallery of modern sculpture. At Horbek, the travertines are composed of stromatolites, oncoids, phytoclastic and intraclastic lithotypes (Rajnoga, 2009). They most probably originated ca. 200 ka (Gradziński *et al.*, 2008b). The youngest travertine generation is Holocene in age, including recently growing travertines. This generation occurs within the spa and downstream over a distance of 2.5 km to the village of Nižné Ružbachy.

B7.2.1 Inactive travertine craters

(49°18′24″ N, 20°33′27″ E)

Inactive, sub-recent travertine craters are present ca. 250 m NW of the spa centre, at the edge of the forest. They are completely dewatered; grass, bushes and trees grow on their bottoms. The largest is 52 m x 32 m across, and 4.5 m deep. Exhalation of CO_2 is periodically active in one of them, hence it is called 'the death hole' (in Slovak – Jama smrti; Potočná, 2007). Dead animals from small creatures to birds and even foxes were found there. Weathered Upper Triassic rocks are visible to the north of the craters in a forest road.

B 7.2.2 Active travertine crater

(49°18′20″ N, 20°33′37″ E)

A crater spring (*kráter*) is the most widely known travertine site in Vyšné Ružbachy. The rim of the water-filled crater is circular in shape, 19 m across. The crater is up to 3.5 m deep. Water temperature is about 23 °C (Hynie, 1963). Mineralization of the water reaches 2364 mg/L and is dominated by HCO_3 (1384 mg/L), SO_4 (372 mg/L), Ca (393 mg/L), Mg (109 mg/L) and Na (42 mg/L) according to Fendeková (2002). The rim was formed by aggradation of travertine around an artesian spring. Its vertical growth caused ponding of water, which in turn allowed further aggradation. Theoretically, this feedback mechanism can operate till the rim would reach a piezometric surface. The rim does not continue growing; water does not flow over it but is drained by an artificial culvert located in its southwest side and forms a stream.

B 7.2.3 Active travertine cascade

(49°18′16″ N, 20°33′35″ E)

A stream issuing from the crater runs SW and next SE and finally joins the Zálažný Stream which drains the Spišská Magura massif built of Central Carpathian Palaeogene rocks. Just near the crater, a part of water is captured for the spa purposes. Travertine is being precipitated almost along the whole course of the stream. This process is especially vigorous on two cascades, 5 m and 2.5 m high. Both cascades started to develop in 1998 when the stream course was artificially changed to its present position (ing. Maximilian Zavartkay – personal information, 2008). The amount of travertine precipitated on the cascades illustrates the rate and efficiency of its growth. Twice a year fresh travertine is removed to clean the streambed between the cascades in order to concentrate flow and prevent a lawn from flooding (ing. Maximilian Zavartkay – personal information, 2008).

Measurements on the upper cascade between November 2008 and June 2010 have shown that the growth rate of travertine reaches 1.73 mm per day in some places. This enormous growth rate of travertine was fully confirmed by a hydrochemical study. The water feeding the cascade was strongly mineralized (TDS between 1713 and 2286 mg/L) with the Ca content ranging from 239 to 407 mg/L. The content of Ca in water dropped abruptly from the top to the base of the cascade. The maximal drop equalled 99 mg/L. Bearing in mind the discharge of the feeding stream and chemistry of water, one may calculate the amount of calcium carbonate precipitated on the upper cascade per day; it ranges from 5.12 kg to the enormous value of 61.7 kg.

The isotopic composition of travetine at the cascade was studied between April 2008 and September 2009. The values of $\delta^{13}C$ and $\delta^{18}O$ of travertine vary from 4.6 ‰ to 7.5 ‰ and from −10.9 ‰ to −9.8 ‰ vs V-PDB, respectively. Isotopic composition of water at the cascade ranges from 0 ‰ to 10 ‰ (DIC), from −10.4 ‰ to −9.8 ‰ ($\delta^{18}O$) and from −72 ‰ to −77 ‰ (δD). No correlation has been detected between isotopic composition of travertines and air temperature during the year. Uranium and polonium activities vary from 0.001 Bq/g and 0.006 Bq/g and 0.003 Bq/g and 0.020 Bq/g, respectively.

B7.3 Sivá brada – Active travertine cascade, modern calcite rafts

(49°0′22″ N, 20°43′22″ E)

Leaders: Michał Gradziński, Marek Duliński[1], Jacek Motyka, Janusz Baryła[2], Joanna Czerwik-Marcinkowska[3], Mariusz Czop[4], Teresa Mrozińska[3]

[1]Faculty of Physics and Applied Computer Science, AGH University of Science and Technology, Kraków, Poland

[2]Caving Section, High Mountain Club of Kraków, Poland

[3]Institute of Biology, Jan Kochanowski University, Kielce, Poland

[4]Faculty of Geology, Geophysics and Environmental Protection, AGH University of Science and Technology, Kraków, Poland

The hill known under a meaningful name Sivá brada (Grey Beard) is located in the Hornád Intramontane Basin, between two historic towns, Levoča to the west and Spišská Kapitula to the east (Fig. 5). The whole area belongs to the historic region called Spiš (in Polish – Spisz, in German – Zips, in Hungarian – Szepes). This area, or its parts, belonged to Hungary, Poland, Austrian Empire, Austro-Hungarian Monarchy and Slovakia

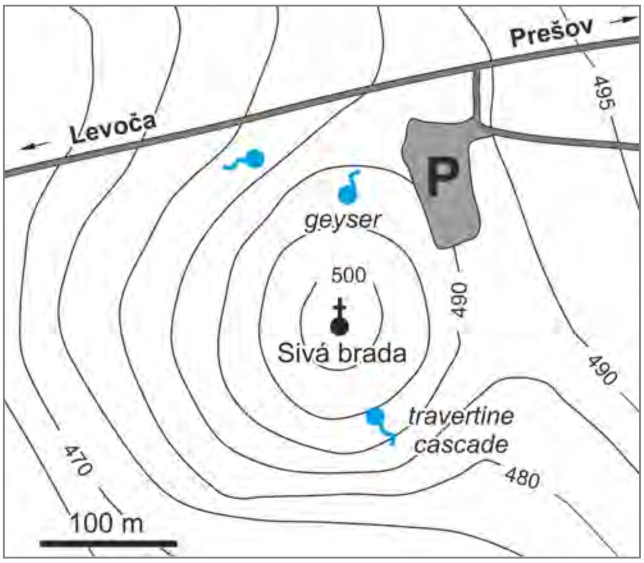

Fig. 5. Location of Sivá brada travertine mound (stop 3).

during its rich history. The hill is well visible from the road 18 Poprad – Prešov, and from the newly constructed motorway. A small chapel stands on the hill's summit (506 m). Springs with travertine precipitation are present on the hill slopes. A CO_2 exhalation is present in a small hollow by the summit chapel. The hill is protected as a nature monument.

Sivá brada is built of travertines and is a travertine mound, similarly as the nearby hills: Pažica, Hradný vrch, Ostrá hora, Dreveník, Sobotisko. The age of Sivá brada is unknown; Maglay and Halouzka (1999) postulate a Pleistocene, whereas Kovanda (1971) suggests a Holocene age. Clastic rocks of the Central Carpathian Palaeogene, up to ca. 1000 m thick, overlie the travertines. The travertines are underlain by Mesozoic carbonate rocks (Gross *et al*., 1999). Sivá brada is located at the intersection of faults which provide suitable migration paths for ascending water from the carbonate bedrock to the surface. Recharge area for waters outflowing in Sivá brada and its vicinity is most probably located to the south, in the elevated area of the Slovak Ore Mountains (in Slovak – Slovenské rudohorie) – a mountain chain built of the same rocks as those underlying the Hornád Intramontane Basin.

The summit of Sivá brada provides an excellent view over the Hornád Intramontane Basin and its vicinity. To the east, several travertine mounds are visible. The closest one, with a small chapel perched on the top, is called Pažica. In the background, the travertine ridge stretches north–south. It comprises three hills, Hradný vrch (hidden behind Pažica), Ostrá hora, Dreveník (with the our next stop). An extensive massif of Branisko is located on the horizon. It is composed of Palaeozoic crystalline rocks and their Mesozoic sedimentary cover, thus it has similar geology to the Tatras. To the south, a hilly area is visible in the foreground. This is the Hornád Intramontane Basin carved in clastic rocks of the Central Carpathian Palaeogene. Farther to the south, lies the forested area of the Slovak Ore Mountains.

A few dozen metres south from the top of Sivá brada and 8 m below it, there is a small travertine cascade. It is fed by ascending water in the two pools located one over another. The lower pool is 5 m x 3.5 m in size and its depth reaches 20 cm. It was artificially created as a small puddle for spa purposes (Hynie, 1963). The discharge of the springs changes with time, one or the other being more active. Water flows down the lower pool, spills over and forms a thin film feeding a travertine cascade. The cascade with microdams and micropools is inclined at an angle of 10°. A similar cascade lies between the pools.

The water is of the Ca–Mg–Na–HCO_3–SO_4 type with TDS reaching 6.9 g/L. Tests have shown absence of tritium, which means that the water as a whole recharged before 1952, that is before the beginning of thermonuclear tests in the atmosphere. It is charged with CO_2 of deep origin, whose content reaches 2343 mg/L. Partial pressure of CO_2 being in contact with water feeding the pool, calculated for the saturation point with respect to $CaCO_3$, equals approximately 6 atm. Mean Ca content is 829 mg/L whereas HCO_3 content is 3804 mg/L. Considering the pH and temperature of water, the calculated saturation index with respect to calcite is ca. 0.71–1.03 and ca. 0.87–1.42 in the lower pool and at the lower cascade, respectively. Such chemical composition of water results in fast and efficient precipitation of calcium carbonate in the pools, especially in the lower one, and on the surface of the cascades.

Two different sedimentary sub-environments of travertine growth are present here. The first are the pools with nearly stagnant water, whereas the cascades with microdams and micropools fed with a thin film of flowing water are the second one. The water feeding the cascades is distributed by 'self built canals', bordered by natural levees. Some clumps of vascular plants occur within a lover travertine cascade, especially in its inactive parts. The plant community comprises *Plantago maritima*, *Triglochin maritima* and *Centaurium littorale* which are classified as halophytes typical of a sea shore (e.g., Košťál, 2011).

Precipitation of calcium carbonate is reflected in the chemical evolution of water along its flow path below the lower pool. CO_2 and Ca contents decrease, whereas pH and saturation index with respect to calcite increases downward.

Calcite rafts are the most common type of carbonate precipitates which are formed in the lower pool. Two types of rafts have been recognized: paper-thin rafts and composite rafts. Both are composed entirely by calcite, although the water is supersaturated also with respect to aragonite. The first group is represented by rafts with up to several micrometers thick. They consist of flat, ultra-thin film of calcite which does not display visible crystals. The lower side of such a film is overgrown by crystal aggregates. They exhibit hemispheric, barrel or dumbbell morphology and are composed of radially oriented needle-shaped subcrystals. This suggests that the crystals grow under disequilibrium conditions (cf. Jones and Renaut, 1995). The paper-thin rafts float freely due to surface tension of water and cover the major part of the pool surface.

The composite rafts float partly submerged in the pool water. They are overgrown by calcite on the upper and lower sides. Commonly, the rafts form piles composed of several individual paper-thin rafts, lying one on another. The rafts are partly broken and arranged subparallel. They do not sink completely because they are supported by an extensive organic buoyant mat, composed mainly of cyanobacteria, diatoms and their extracellular polymeric secretions. Sixteen algal taxa forming a mat have been distinguished. The most common are filamentous cyanobacteria of genus *Phormidium* and diatoms *Achnanthes minuttisma* and *Navicula gregaria*. Diatoms are also attached to the rafts. Although some cyanobacterial sheaths, diatom mucilage and frustules are calcified, the majority of algae are not covered with calcium carbonate, which is proved by observation under scanning electron microscope. It shows that the algae do not participate in this process actively, but act only as a substrate for growing crystals. However, the crystals seem to grow more readily on mineral substrate, that is on sunken calcite rafts.

Outgassing of CO_2 is the principal process responsible for effective precipitation of calcite crystals and raft formation. Kinetics of outgassing depends also on seasonal changes of water temperature in the pool. This causes more efficient growth of the rafts in late spring, summer and the beginning of autumn. The influence of evaporation seems to be insignificant for the raft growth, although this process slightly modifies isotopic composition of the water in the pool.

Although the algae do not contribute actively to calcite precipitation, their role is important in the formation of the rafts since they buoyantly keep the rafts near the surface, where the effects of degassing are strong and supersaturation is high enough for calcite precipitation. Since the process occurs below the water surface, the crystals grow on both bottom and top sides of rafts. Calcite rafts are extremely susceptible to destruction. It particularly concerns the paper-thin ones. Even loading by such a small object as a pollen grain causes deformation of their surfaces. Both, the paper-thin and the composite rafts are destructed by rain; however, the latter obviously have highest potential for preservation. They are a dominant component littering the bottom of the pool. Comparison of the present topography of the pools with an archival photography taken in the middle of the last century (Hynie, 1963, fig. 73 – 1) suggests that the lower pool was filled by deposits several dozen centimetres thick.

The cascades are built of white, laminated travertine composed of calcite crystals ranging from a few dozen to a few hundred micrometres. Observations suggest that vertical growth of the lower cascade exceeds 2.5 cm per year in the zones of active water flow.

Small spheres, up to 1 cm in diameter, composed of calcite crystals, form in micropools. They are encrustations on the surfaces of gas bubbles. In summer, microdams are roofed by a calcite film. It is similar to paper-thin rafts, originated over the water filling the micropools. The film has a slightly convex-up shape due to a meniscus head effect. It is very fragile and can be easily destructed. Debris of the calcite film accumulates in the micropools. Piles of fossil calcite film fragments most probably form puff pastry like fabrics (*sensu* Gandin and Cappezzuli, 2014).

The recently growing travertines (both rafts and cascades) show values $\delta^{13}C$ and $\delta^{18}O$ from +10.4 ‰ to +12.7 ‰ and from −10.0 ‰ to −6.8 ‰ vs V-PDB, respectively. Comparison of $\delta^{13}C$ and $\delta^{18}O$ analytical results with analogous values calculated for the isotopic equilibrium conditions indicate that the travertines grow in isotopic disequilibrium. The lack of equilibrium results from strong kinetic effects related to the fast outgassing of CO_2 to the bulk atmosphere.

An active ‘cold geyser’ on the northern slope of Sivá brada is clearly visible from the car park at the north-east foot of the mound. It is fed by a 135 m deep drill-hole (Jetel, 1999) and it spouts water due to CO_2 pressure. It erupts irregularly. Although at present the eruption height is |a few dozen centimetres, it reached more than 10 m (Kovanda, 1971). Water represents the Ca–Mg–Na–HCO_3–SO_4 type (Jetel, 1999). The geyser orifice is enveloped by actively growing travertine. However, it is constantly destructed by trampling since it is a kind of tourist spot.

B7.4 Dreveník ridge, Žehra quarry – Facies and anatomy of an inactive travertine ridge

(48°58′55″ N, 20°46′28″ E)

Leaders: Wojciech Wróblewski, Michał Gradziński, Marek Duliński, Jacek Grabowski[1], Helena Hercman, Marianna Kováčova[2], Katarzyna Sobień[1]

[1]Polish Geological Institute, National Research Institute, Warsaw, Poland

[2]Faculty of Natural Sciences, Comenius University, Bratislava, Slovakia

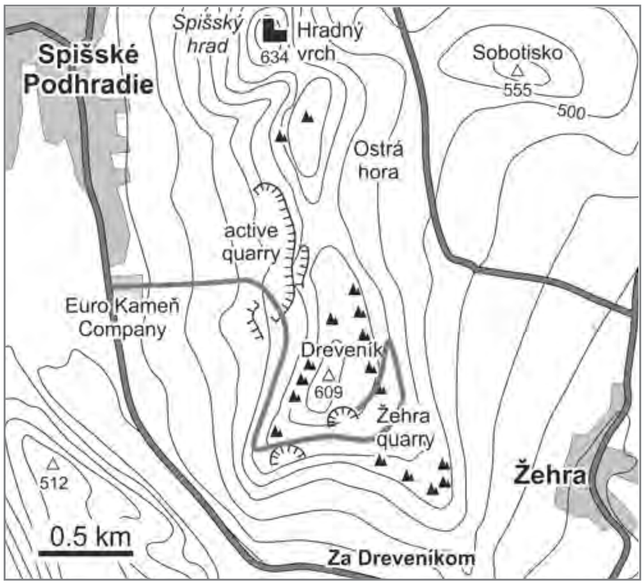

Fig. 6. Location of Žehra quarry (stop 4).

Dreveník is the southernmost part of a meridionally elongated ridge with the ruins of a medieval castle, Spišský hrad, perching on its northernmost part called Hradný vrch (Fig. 6). The castle was erected in 11th and 12th centuries; it covered approximately 4 hectares. The castle was built of local stone, predominantly travertine. Dreveník rises up to altitude of 609 m and is 2.5 km long and 1 km wide (Tulis and Novotný, 2008). It is one of the biggest travertine buildups in Central Europe. Travertine is up to 80 m thick and it overlies flysch deposits of the Central Carpathian Palaeogene, which plays a hydrological role of the confining bed (Fig. 7; Gross *et al*., 1999). The orientation of the Dreveník ridge follows a fault in the basement. The age of travertine is considered to be Pliocene–Pleistocene based on the palaeobotanical (Němejc, 1944) and palaeontological finds (Holec, 1992; Tóth and Krepmaská, 2008) but it has not been defined precisely yet. Travertine is intensively eroded. It has undergone gravitational processes and karstification (Fusggänger, 1985; Tulis and Novotný, 2008). Many post-depositional features are present there, including widened fissures, cracks, karren, caves filled with secondary deposits of different origin (Wróblewski *et al.,* 2010).

Fifteen quarries exist at various points of the Dreveník ridge (Tulis and Novotný, 2008). The largest one, continuously active and used by the Euro Kameň company, is located on the western slope of the ridge. An abandoned quarry on the southern side of the Dreveník ridge, named Žehra quarry, will be visited during the trip. Visiting of the quarry is allowed; however, the road used during the trip is closed and driving needs permission of an owner of the Euro Kameň company. The quarry may be accessed on feet from public roads around the hill and from Spišský hrad. The quarry was exploited from the seventies to the nineties of the last century (Tulis and Novotný, 2008). The quarry has eight levels. Travertine was mined by using saw ropes, hence the quarry walls consist of flat surfaces up to 1.8 m high several meters long. This allows us to observe various travertine lithotypes (*sensu* Guo and Riding, 1998), their spatial relationships and post- and syn-depositional features (Gradziński *et al.,* 2014).

Layered light grey and yellowish crystalline crusts travertine is the dominant lithotype in the quarry (Fig. 8A, B). Individual layers are between 0.5 cm and several centimetres thick. This facies has a very low porosity. The layers are inclined usually between 20° and 30°, rarely up to 70°. Crystalline crust travertine is composed of fan–shaped sparry calcites which grew from a thin water film on the ridge slope.

Lithoclast travertine is the second most common lithotype in the quarry (Fig. 8A). It forms four lobe-shaped bodies of different size, interbedded with crystalline crusts and other lithotypes and 0.2 m to 6 m thick. Lithoclast travertine is composed of subangular and angular clasts of different size (from a few millimetres to several decimetres) composed mainly of crystalline crust travertine, subordinately of vein calcites and micritic

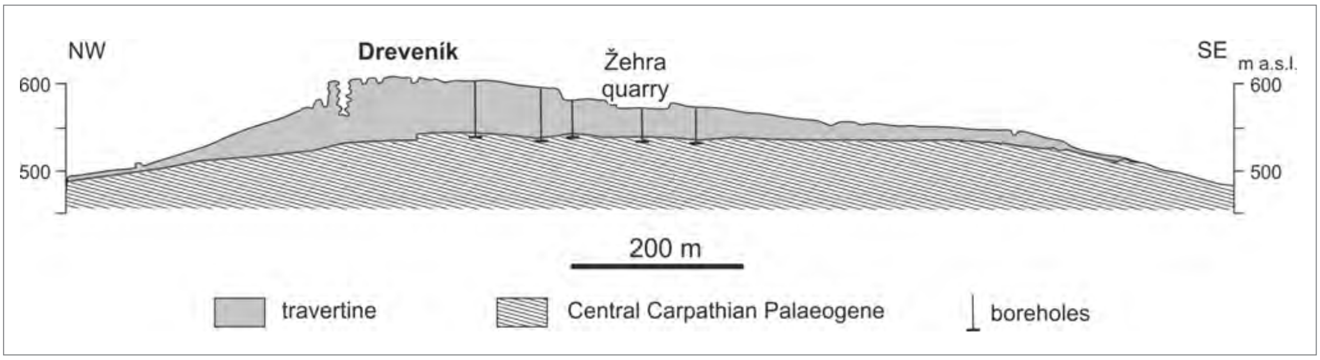

Fig. 7. Cross-section through Dreveník travertine ridge, after Tulis and Novotný (2008), modified.

travertine. The clasts were transported and deposited due to episodic rock falls (Gradziński *et al*., 2014).

Fine-grained lithoclast travertine is another lithotype recognized in the Žehra quarry. It forms two lenticular bodies, up to 0.8 m thick. The lithoclasts are built mainly of crystalline crust travertine. Individual clasts reach up to several centimetres in size. Fine-grained lithoclast travertine is more porous than lithoclast travertine. It originates from erosion on the external parts of the travertine ridge and redeposition of its small fragments downslope in periods of limited spring water supply. It corresponds to hillwash breccia (*sensu* Pedley, 2009).

Coated bubble travertine and paper-thin raft travertine occur subordinately in the Žehra quarry (Fig. 8B, C). They usually form horizontal or sub-horizontal layers within crystalline crust travertine. The individual bubbles are vertically elongated and are up to 3 cm high. They grew on small ponds formed on the ridge slope. Paper-thin raft travertine comprises cemented thin rafts (up to 2 mm of thickness) accumulated in small pools or they fill empty spaces within intraclast breccia (Fig. 8B).

Several features including intraclast breccia, ground and long fissures, karst cavities related to syn- and post-depositional processes have been described in the Žehra quarry (Wróblewski et al., 2010; Gradziński *et al*., 2014).

Intraclast breccia is a product of syn-depositional brittle deformations. It occurs below the bodies of lithoclast travertine. Intraclast breccia consists of crystalline crust travertine clasts (Fig. 8B). The clasts are up to several decimetres in size. Individual clasts display limited displacement and they fit one another like parts of a jigsaw puzzle.

Long fissures constitute sub-vertical and vertical cracks in travertine (Fig. 8C). Their vertical extent exceeds 20 m. They are up to 0.7 m wide and are mainly filled with vein spelean calcites of phreatic origin (Gradziński *et al*., 2014).

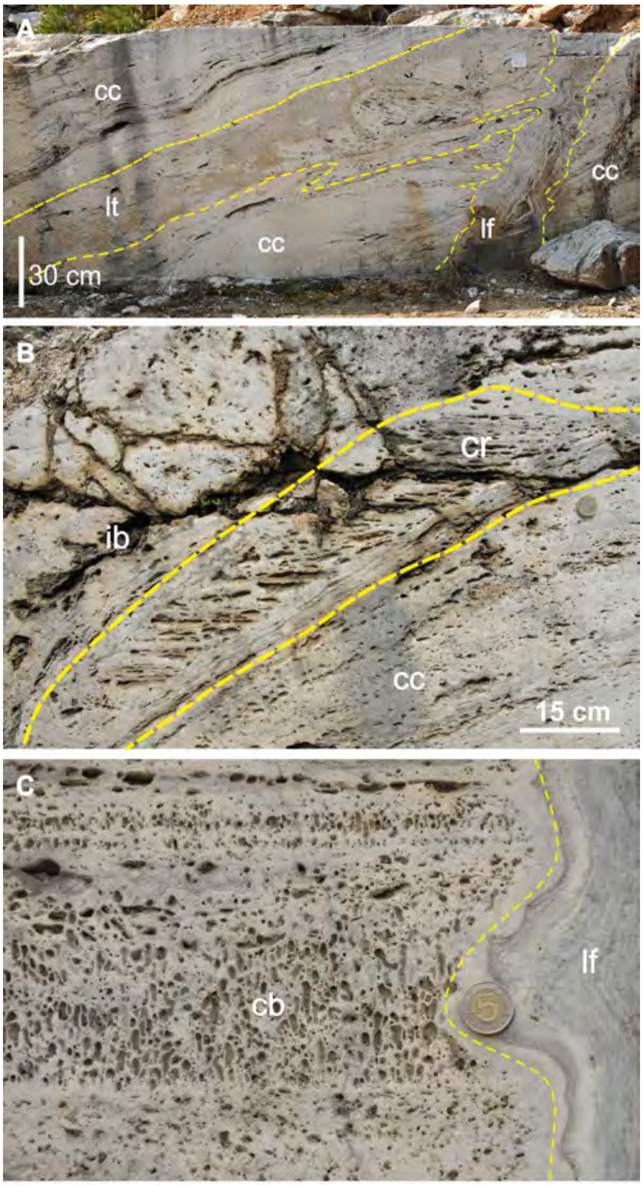

Fig. 8. Selected travertine lithotypes in Žehra quarry (stop 4). **A**) Lithoclast travertine (lt) interfingers between crystalline crust travertine (cc) and, younger long fissure (lf) is filled with vein calcite; **B**) Calcite rafts (cr) filling ground fissure between crystalline crusts (cc) and intraclast breccia (ib); **C**) Coated bubble travertine (cb) cut by long fissure (lf) with vein calcite.

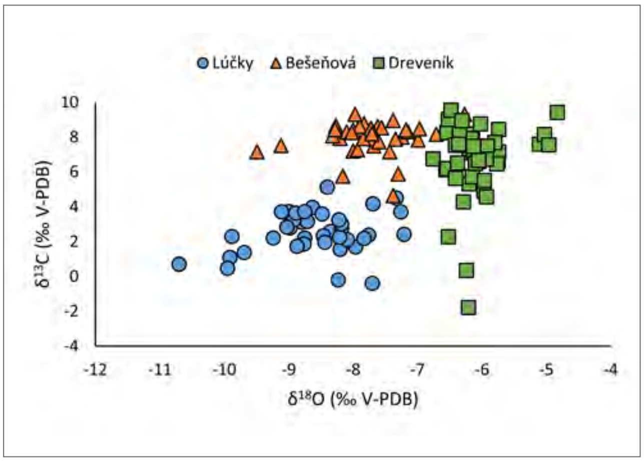

Fig. 9. Carbon and oxygen stable isotope composition of pre-Holocene travertine from Dreveník, Bešeňová and Lúčky, after Gradziński *et al.* (2008b, 2014) and unpublished data.

Ground fissures represent a group of cracks which are filled with several types of travertine, including crystalline crust travertine, lithoclast travertine and calcite rafts. They are shorter and less open than long fissures.

The travertine at Dreveník is of Pliocene age. This age is supported by findings of a pollen assemblage typical of the Central Carpathian Neogene. This assemblage includes pollens of *Carya* sp. and *Tsuga* sp. Palaeomagnetic study proved that it is normally magnetized. These data collectively suggest that the travertine was formed between 3.4 and 2.48 Ma.

The Dreveník travertine represents smooth slope facies (*sensu* Guo and Riding, 1998). Travertine was fed with highly-mineralized waters of deep circulation flowing out along the faults cutting the Central Carpathian Palaeogene rocks. Their $\delta^{13}C$ values are between –2.0 ‰ and +9.6 ‰ V-PDB, indicating that the waters were charged with CO_2 of geogenic origin (Fig. 9; Gradziński *et al.*, 2014). The Dreveník travertine can be regarded as a fossil analogue of the travertine ridges known from Turkey (e.g., Mesci *et al.*, 2007; Piper *et al.*, 2007; De Filippis *et al.*, 2012), Tuscany (Brogi and Capezzuoli, 2009; Pedley, 2009) and USA (De Filippis and Billi, 2012). The deposition of lithoclast travertine, as well as origin of its deformation is interpreted as a result of seismic shocks (Gradziński *et al.*, 2014). The seismic events exerted indirect control over the facies distribution. Local hydrological conditions changed after the shocks, which led to ponding of water and formation of paper-thin raft travertine.

B7.5 Buzgó stream – Deposition of modern fluvial calcareous tufa

(48°37′02″ N, 20°35′04″ E)

Leaders: Wojciech Wróblewski, Michał Gradziński, Jaroslav Stankovič[1], Dorota Podgórska[2], Katarzyna Rycerz[2]

[1]Minotaurus Caving Club, Rožňava, Slovakia
[2]Institute of Geological Sciences, Jagiellonian University, Kraków, Poland

Buzgó is one of the sites of present-day calcareous tufa sedimentation in the Slovak Karst. It is located in southern peripheries of the village Krásnohorská Dlhá Lúka, ca. 5 km SE of Rožňava (Fig. 10). The area is protected as a part of a national park. The site is named after the stream flowing over the fluvial terrace of the Čremošná river (Gaál, 2008). The Buzgó stream debouches in the resurgence of Krásnohorská Cave (in Slovak – Krásnohorská jaskyňa) which originated as the underground drainage of the northern part of the Silica Plateau (Orvan, 1980). The resurgence is located at the altitude of 316 m, at the foot of the plateau, approximately 1 km southeast of the village centre (Bella, 2008; Haviarová *et al.*, 2012). Its discharge ranges from 6 to 1300 L/s (Stankovič *et al.*, 2005).

Freshwater carbonates form in surface and subsurface (cave) section of the Buzgó stream. In the cave section of the stream, freshwater carbonates form subaqueous flowstones which are present on the streambed (Fig. 11A) along the distance of approximately 150 m upstream from the resurgence. Calcareous tufas are being formed in the surface section of the stream (Fig. 11B). Tufas commence to accumulate in the upper

Fig. 10. Location of Buzgó resurgence (stop 5).

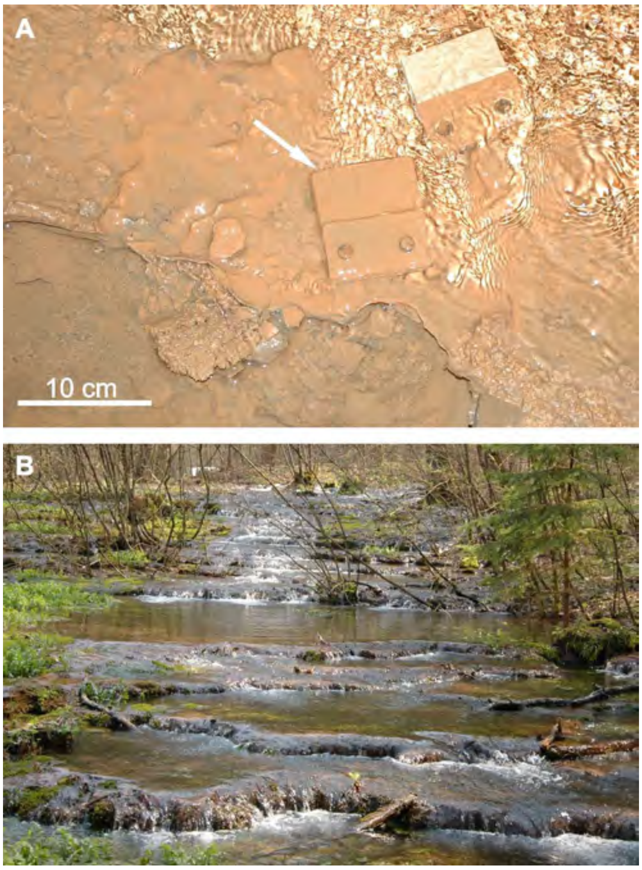

Fig. 11. Buzgó stream. **A**) subaqueous flowstones in subsurface section of the stream, the tablet arrowed was exposed in the stream during 128 days; **B**) multi-stepped tufa barrages in surface section of the stream.

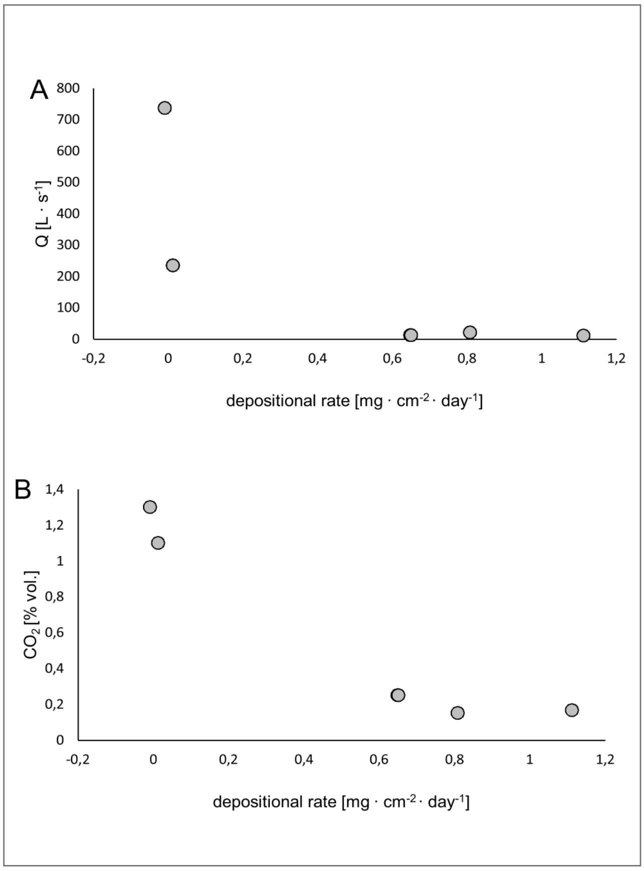

Fig. 12. Depositional rate of calcite measured on plates located 40 m downstream the resurgence depends on spring discharge (**A**) and mean CO_2 concentration in cave atmoshere (**B**).

reaches of the stream, approximately 20 m downstream of the resurgence. They construct multi-stepped barrages (Fig. 11B). Tufa covers an area up to 1 ha (Stankovič *et al*., 2005). The tufas represent perched springline facies association (*sensu* Pedley *et al*., 2003), including such facies as stromatolitic tufa, phytoclastic tufa, moss tufa and oncoidal tufa. Stromatolitic tufas are the dominant ones. They are laminated and mainly composed of calcified cyanobacterial filaments. Stromatolitic tufas form barrages orientated perpendicular to the flow direction. Locally stromatolitic tufas interbed with layers and lenses of phytoclastic and moss tufas. Oncoids occur in small pools formed upstream barrages. Oncoids are sub-angular whereas their shape is cylindrical and spherical. They range from 1 to 15 cm across. Their formation is probably related to biological activity of some microorganisms in mid-energetic conditions.

Water of the Buzgó stream represents the Ca–HCO_3 type. Its TDS ranges from 367 to 836 mg/L (mean value = 565 mg/L). Other parameters are as follows: mean pH – 7.73, mean HCO_3 content – 367 mg/L, whereas mean Ca content – 124 mg/L. Waters are predominantly supersaturated with respect to calcite during the year (mean value SI = 0.68). The temperature is quite constant and oscillates around 9.5 °C.

Seasonal observations (water chemistry, precipitation rate on and CO_2 concentration in cave atmosphere) were conducted between August 2010 and September 2012. They show that precipitation of calcium carbonate is almost continuous all year round. The highest depositional rate was noted in the winter–spring season of 2012 (1.11 mg · cm^{-2} · day^{-1}). Changes in the depositional rate of tufa positively correlate with fluctuation of groundwater levels (Fig. 12A) and CO_2 concentration in the cave atmosphere (Fig. 12B). This suggests that depositional processes are significantly modified by groundwater level fluctuations. Low groundwater levels in the subsurface segment of the Buzgó stream make ventilation of the karst system more effective, which in turn affects precipitation of calcium carbonate. This fully confirms the opinion formulated by Kano *et al*. (2003) and Kawai *et al*. (2006) on the influence of subsurface processes on tufa growth.

B7.6 Háj Valley – Facies and depositional history of Holocene fluvial calcareous tufa

(48°38′23″N, 20°50′57″E)

Leaders: Michał Gradziński,
Joanna Czerwik-Marcinkowska, Helena Hercman,
Martyna Jaśkiewicz[1], Jacek Motyka,
Teresa Mrozińska, Stanisław Szczurek[1, 2]

[1]Institute of Geological Sciences, Jagiellonian University, Kraków, Poland

[2]Faculty of Geology, Geophysics and Environmental Protection, AGH University of Science and Technology, Kraków, Poland

The Háj Valley (in Slovak – Hájska dolina) is narrow and it is incised to a depth ca. 150–200 m into the surrounding carbonate plateau built up of Triassic carbonates of the Silica Nappe. The head segment of the valley is carved into the Bôrka Nappe which is mainly composed of metamorphic rocks (Mello *et al*., 1996). The trip will visit the middle segment of the valley. The coordinates given above point to a small car park on the west side of the road. The whole area is protected as a part of a national park.

Tufa extends over the distance of 900 m up the valley from the village of Háj (Fig. 13; Gradziński *et al*., 2013). The stream flows down the valley from a series of karst springs. It forms four waterfalls, each a few metres high. Recently tufa is being formed in the stream as small barrages and scenic curtains hanging down from the heads of the waterfalls (Gradziński, 2010). The water is of the Ca–HCO_3 type; its TDS varies from 315 to 421 mg/L, whereas SI is between 0.17 and 1.1.

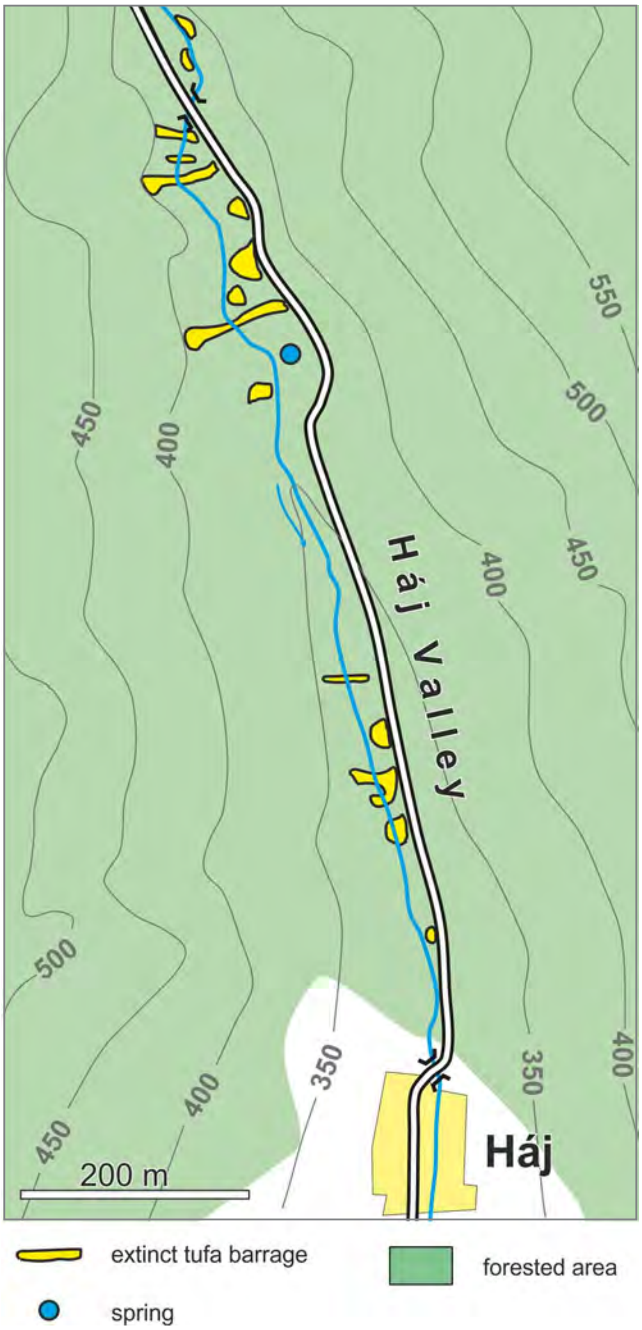

Fig. 13. Location of Holocene tufa barrages in the Háj Valley (stop 6; after Gradziński *et al*., 2013, modified).

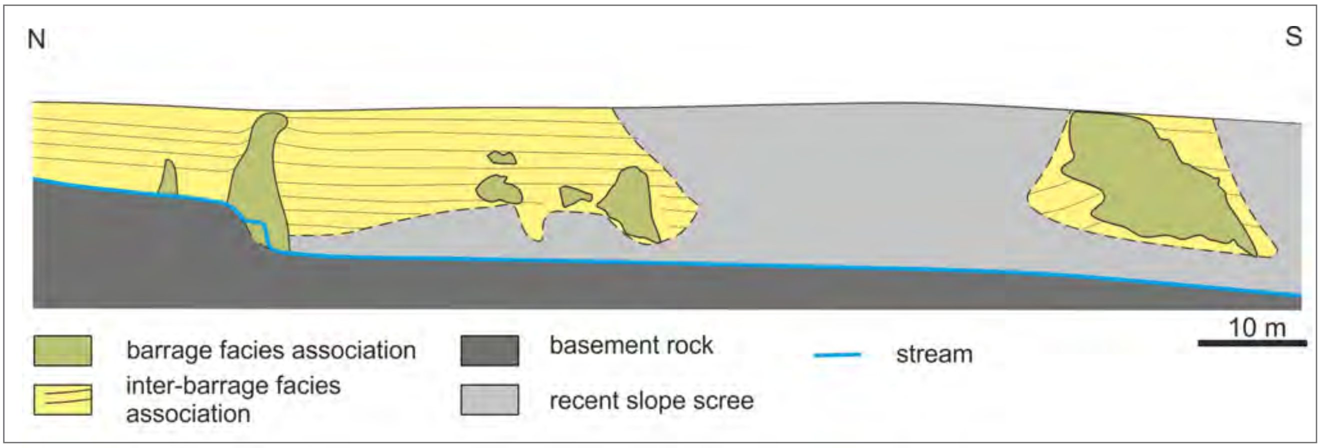

Fig. 14. Spatial distribution of barrage facies association and inter-barrage facies association in the upper segment of the Háj Valley, cross-section, after Gradziński *et al.* (2013), modified.

Inactive tufa partly fills the bottom part of the valley. It is incised, in many places even to its Mesozoic bedrock. Tufa sections crop out on terrace risers. The present relief of the valley clearly reflects the distribution of facies type associations of inactive tufa. The relatively hard and resistant tufa forms jumps and constrictions in the longitudinal profile of the valley, whereas wider valley segments are carved in loosely cemented tufa (Fig. 14; Gradziński *et al.*, 2013).

Tufa in the Háj Valley was noticed by Kormos (1912). Petrbok (1937) and Ložek (1958) carried out detailed malacological studies whereas Němejc (1936, 1944) studied plant fossils.

Tufas in the Háj Valley correspond to a longitudinal fluvial system (Gradziński *et al.*, 2013). It comprises barrage and inter-barrage facies association (Fig. 14). Barrages are composed of moss tufa which comprises three-dimensional, reticulate fabrics built of calcite-encrusted moss stems and leaves. Phytoclastic tufa, formed by calcite encrustation on plant fragments which are preserved as empty moulds, co-occurs with moss tufa. Stromatolitic tufa is the third facies building barrages. Seventeen inactive barrages, up to 12 m high, occur in the Háj Valley (Fig. 13, Gradziński *et al.*, 2013). They are ponding water in the upstream reaches of the valley, where inter-barrage facies association was laid down. It constitutes oncoidal and intraclastic tufa which display grading and cross-bedding. Thus, this facies association originated in flowing water not in stagnant ponds. It corresponds to the 'braided fluviatile model' of Pedley (1990) or 'free flowing water channel-filling sequences' of Vázquez-Urbez *et al.* (2012).

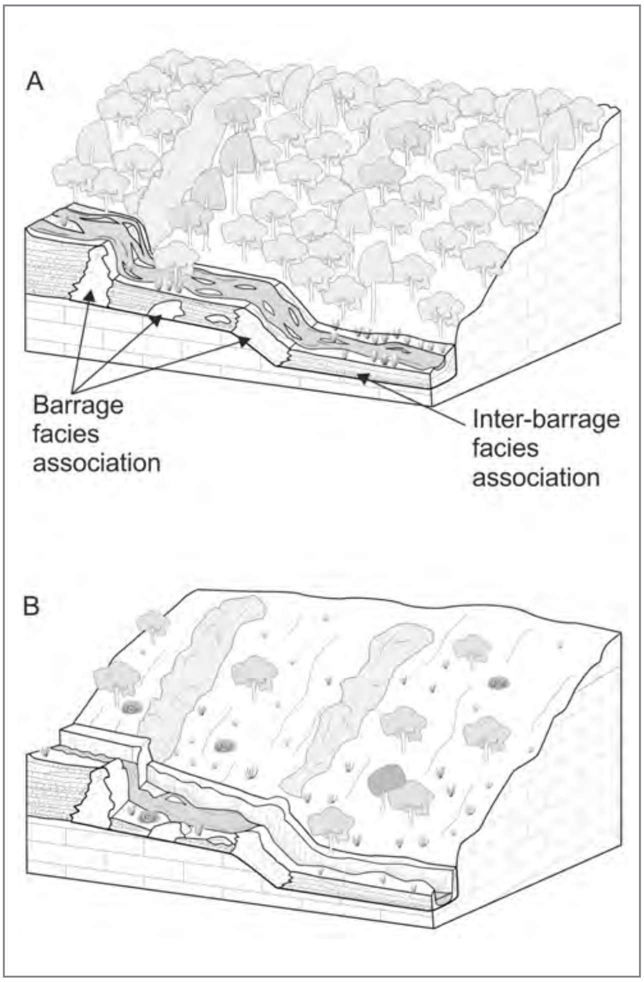

Fig. 15. Deposition (A) and subsequent erosion (B) of tufa in the Háj Valley (after Gradziński *et al.*, 2013).

Tufas are locally covered with colluvial breccias composed of angular, poorly sorted clasts of Triassic carbonates (Gradziński *et al.*, 2013). They are bound by stromatolitic coatings, whereas intraclastic tufa acts as matrix. The clasts derived from upper slopes of the valley and are a rockfall or rockslide deposits introduced into the tufa-depositing system.

Radiocarbon dating proves that tufa grew in Mid Holocene time, that is during the Atlantic and Sub-Boreal intervals (ca. 7.5–3.5 ka BP; Fig. 15A; Gradziński *et al.*, 2013). The growth rate can be estimated at around 2.5 cm per year. Redeposition from the slopes and deposition of coarse-grained colluvium preceded tufa erosion and the stream incision (Fig. 16B). Such a phenomenon is clearly visible in many European tufa complexes. Goudie *et al.* (1993) coined a term 'late Holocene tufa decline' and discussed several factors that may have been responsible for it. In the Slovak Karst case, erosion is hypothesized to have been stimulated by deforestation caused by prehistoric humans (Gradziński *et al.*, 2013); however, other reasons cannot be unequivocally excluded.

The factors responsible for tufa erosion must have ceased to operate; modern tufa grows vigorously in the Háj Valley. The study conducted in 2002 and 2003 documents the tufa growth rate. Tufa, which constructs a curtain constantly flushed with water in the upper segment of the valley, is precipitated at a rate up to 0.3 mg · cm^{-2} · day^{-1} (Gradziński, 2010). The curtain is constructed of encrusted cyanobacteria (*Phormidium favosum*, *Ph. tenue*, *Oscillatoria limosa*), algae (*Cladophora glomerata*, *Vaucheria* sp.) and mosses (*Brachythecium rutabulum* – R. Ochyra, pers. inf., 2003).

Stop B7.7 Bešeňová – Pleistocene and recent travertines

Leaders: Michał Gradziński, Pavel Bella

The village of Bešeňová is located at the boundary of the Liptov Basin (in Slovak–Liptovská kotlina) and the Choč Mountains ca. 12 km west of Liptovský Mikuláš. An aquapark complex with thermal water is located in the centre of the village. An active travertine cascade is being developed ca. 400 m north of the village centre, whereas several outcrops of inactive travertines are located on the slopes above the cascade, mostly in small, inactive quarries (Fig. 16).

The Liptov Basin is one of the intramontane basins in the Central Western Carpathians. It is aligned W–E and located between the Alpine-type mountain chains – the Tatras and the Choč Mts on the north and the Low Tatras on the south (in Slovak – Nízke Tatry). The basin is filled with the Central Carpathian Palaeogene 100 to 2200 m thick (Remšík *et al.*, 2005). These rocks are the regional confining bed whereas underlying carbonates are regarded as an aquifer (Hynie, 1963).

The travertines in the vicinity of Bešeňová are situated on a fault stretching W–E, parallel to the Choč–Tatra Fault which is a main tectonic line bordering the Liptov Basin on the north (Gross *et al.*, 1979; Gross, 1980). Additionally, a W–E stretching fault intersects a meridional fault (Bešeňová Fault – Fendek *et al.*, 2015) bordering from the west the so-called Bešeňová elevation, that is a transverse horst within the Liptov Basin. The faults cut relatively impermeable rocks of the Central Carpathian Palaeogene creating flow path for water ascending from the Mesozoic carbonate aquifer. The aquifer in question is probably a complex hydrological structure whose recharge is supposed to be on the northern slopes of the Low Tatras (Fričovský *et al.*, 2015). The piezometric level of water in the borehole located in the village of Bešeňová is ca. 190 m above the ground surface (Remšík, 2005).

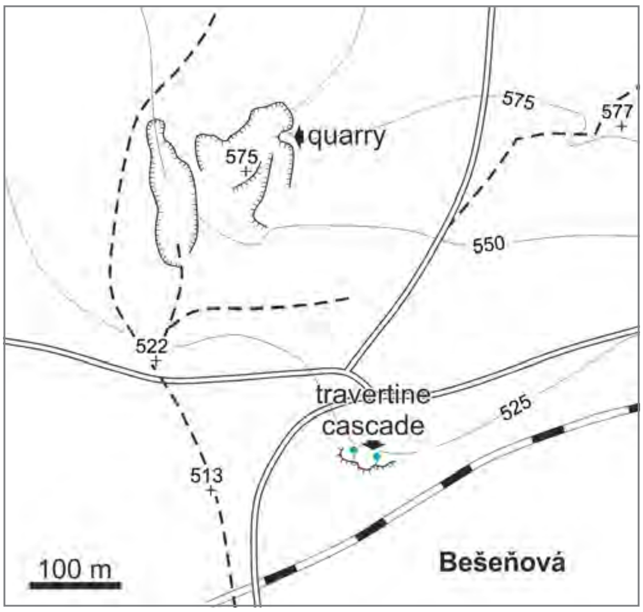

Fig. 16. Location of travertine sites (stops 7.1 and 7.2) presented in Bešeňová.

Stop B7.7.1 Bešeňová – Recent travertine cascade

(49°06′14″N, 19°26′09″E)

Leaders: Michał Gradziński, Pavel Bella, Maria Jolanta Chmiel[1], Joanna Czerwik-Marcinkowska, Marek Duliński, Jacek Motyka, Teresa Mrozińska

[1]Department of Microbiology, University of Agriculture, Kraków, Poland

The almost 10 m high cascade is a well known tourist attraction. It is developed on the lower part of slopes north of the Bešeňová village (Fig. 16). The cascade is protected as a natural monument. It is fed by water issuing in a series of small springs, some of which are artificially widened. The springs are distant from a few to a dozen metres from the cascade crest. The water is of the Ca–Mg–HCO_3–SO_4 type. It has almost constant temperature throughout the year (between 14.2 °C and 15.6 °C). The water is charged with CO_2 whose pressure at the outflow reaches 1.05 atm. Its mineralization is ca. 3.6 g/L. Mean Ca content is 829 mg/L, HCO_3 content is 3804 mg/L, whereas Fe concentration reaches 0.055 mg/L. The above features suggest that the water is of deep circulation, as is confirmed by the lack of tritium.

Water from the springs flows almost horizontally southward by a system of 'self-built canals'; it reaches the crest of the travertine cascade and forms a thin film seeping down the cascade face. The face is steep, in some segments vertical and covered with microdams and micropools. Precipitation of calcium carbonate is reflected in the chemical evolution of water along its flow path below the lower pool. Concentrations of CO_2 and Ca decrease, whereas pH and saturation index with respect to calcite increase downward.

Travertine formed in the head part of the flow path is deep-orange to intense red in colour, whereas that precipitated in the cascade face is whitish-grey. The former one contains a substantial amount of iron oxides (up to 45 wt%). It is composed of calcite, goethite and amorphous iron oxyhydroxides. The iron compounds precipitate within a slimy biofilm built of filamentous cyanobacteria (mostly different species of *Phormidium*) and diatoms (e.g., *Achnanthes lanceolata*, *A. minutissima*, *Cymbella minuta*, *C. laevis*, *Navicula menisculus*). Iron-bacteria have been also detected (*Metallogenium* sp., *Thiobacillus* sp.).

Travertine precipitated on the cascade face is of crystalline crust type. The spatial arrangement of laminae mirrors the surface of the cascade face, that is its microdam and micropool relief. The exploratory study shows chemical evolution of water along its flow path from the spring to the foot of the cascade as related to CO_2 degassing and precipitation of calcite and iron minerals. Isotopic study of water and modern travertine suggests that the travertine grows in conditions out of isotopic equilibrium.

Stop B7.7.2 Bešeňová, inactive quarry – Pleistocene travertine formed in shallow pond

(49°06′25″ N, 19°26′04″ E)

Leaders: Michał Gradziński, Marek Duliński, Jacek Grabowski, Helena Hercman, Peter Holúbek[1], Marianna Kováčova, Katarzyna Sobień

[1]Slovak Museum of Nature Protection and Speleology, Liptovský Mikuláš, Slovakia

A series of small, abandoned quarries extends above the cascade, on the hill slope called Skala (Fig. 16). They are known as Báňa. The quarries were in use until the second half of the last century. The travertine, with characteristic yellow to pale orange colour, was used as polished building stone for elevations and floors. It was exported to several European countries, including Poland, and to the USA (Pivko, 1999). The quarries are now abandoned and densely vegetated. The clearly visible rock crag crowned with a cross is practically the only available outcrop. The crag is located in the north-eastern part of the quarries. It is proctected as a nature monument.

The rock crag is 9 m high. It is built of layered travertine dipping slightly to the west. The crag walls are weathered. Huge travertine blocks partly dismembered and slightly tilted are present in the southern and western parts of the crag. They are separated from the crag by opened and partly karstified fissures.

Laminated micritic travertine is the dominant lithotype in the crag. Calcite rafts and pisoids occur subordinately (Fig. 17). Vertically oriented coated bubbles form individual layers, 1 to 4 cm thick. Such layers are clearly visible, especially in the top part of the crag. Intraclast breccia layers up to 10 cm thick are also present. They are more prone to weathering and they are marked by concave zones in the crag faces. Deformation structures of brittle and ductile type are discernible on the south facing wall of the crag. They are interpreted as a result of a seismic shock in consolidated and unconsolidated travertine, respectively. In spite of its colour, travertine contains only up to 1 wt % of Fe_2O_3.

The travertine lacks faunal remains and plant imprints. Pollen assemblage points at its origin under warm, interglacial climate. U-series dating suggests that it is older than 350 ka but younger than 1.2 ma. Exploratory palaeomagnetic study proves that it is normally magnetized, which implies the age younger than 780 ka.

Facies of the travertine in the rock crag seem to have formed in a shallow pond, or ponds fed with highly mineralized water charged with CO_2 of deep geogenic origin, as evidenced by the $\delta^{13}C$ values of travertine, ranging from +4.6 to +9.3 ‰ vs V-PDB (Fig. 12; see Gradziński *et al.*, 2008b). The water outflowed along the faults from the Mesozoic carbonates underlying the Central Carpathian

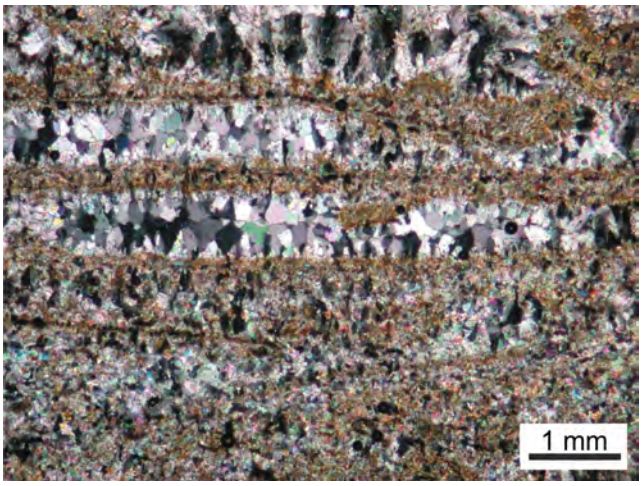

Fig. 17. Calcite rafts cemented with sparry calcite (thin-section), Bešeňová abandoned quarry (stop 7.2).

Palaeogene rocks. Thus, from general genetic point of view, the travertine is an analogue of the modern cascade (Stop B7.7.1). On the other hand, it was laid down in different environmental conditions.

Breccias and crystalline crusts built of phreatic calcite spar are visible on the walls of the rock crag. They filled the fissures which cut the travertine buildup and were exposed during exploitation of travertine. The fissures were also filled with loose deposit, orange, red or pale brown in colour. It comprised rich assemblage of interglacial molluscs (Vaškovský and Ložek, 1972; Vaškovský, 1980) and bones of mammals living in forest and steppe environments (Sabol, 2003). Among others, a skull of a rare bear species (*Ursus taubachensis*) was found. Calcite rafts cemented to a rocky wall are exposed in a small quarry located to the west (Kostecka, 1992). They originated within open fissures during the last glacial.

Stop B7.8 Demänová Cave System – Multi-storey cave system richly decorated with speleothems

(Mramorové rečisko entrance: 49°01′59″ N, 19°34′57″ E)

Leaders: Pavel Bella, Michał Gradziński, Dagmar Haviarová[1], Helena Hercman, Peter Holúbek, Jacek Motyka

[1]Slovak Caves Administration, Liptovský Mikuláš, Slovakia

The Demänová Cave System (DCS; in Slovak – Demänovský jaskynný systém) is situated on the eastern side of the Demänová Valley (in Slovak – Demänovská dolina; Fig. 18; Droppa, 1957). The total length of the DCS exceeds 40 km and its vertical extent equals 202 m (Bella *et al.*, 2014; authors' unpublished data). The system includes ten caves, among which Demänová Cave of Liberty is the longest (in Slovak – Demänovská jaskyňa slobody) and this cave will be visited. The cave lies within a national park, it is protected and its entrances are gated. Some cave parts are accessible for tourists all year round (see http://www.ssj.sk/en/jaskyna/4-demanovska-cave-of-liberty). Three stops, namely B7.8.2–B7.8.4) are located on a tourist trail within the cave.

The cave system is developed within Anisian limestones and dolomites of the Gutenstein type. These limestones belong to the allochthonous Krížna Nappe that makes the northern sedimentary cover of the Low Tatras crystalline core composed of granitoids (Fig. 19; Droppa, 1957; Bella et al., 2014). The upper part of the Demänová Valley was glaciated at least twice during the Middle Pleistocene. The DCS, however, occurs in a narrow canyon located downstream of the glaciated part of the valley and below the preserved till deposits (Droppa, 1972). The DCS originated by corrosion and

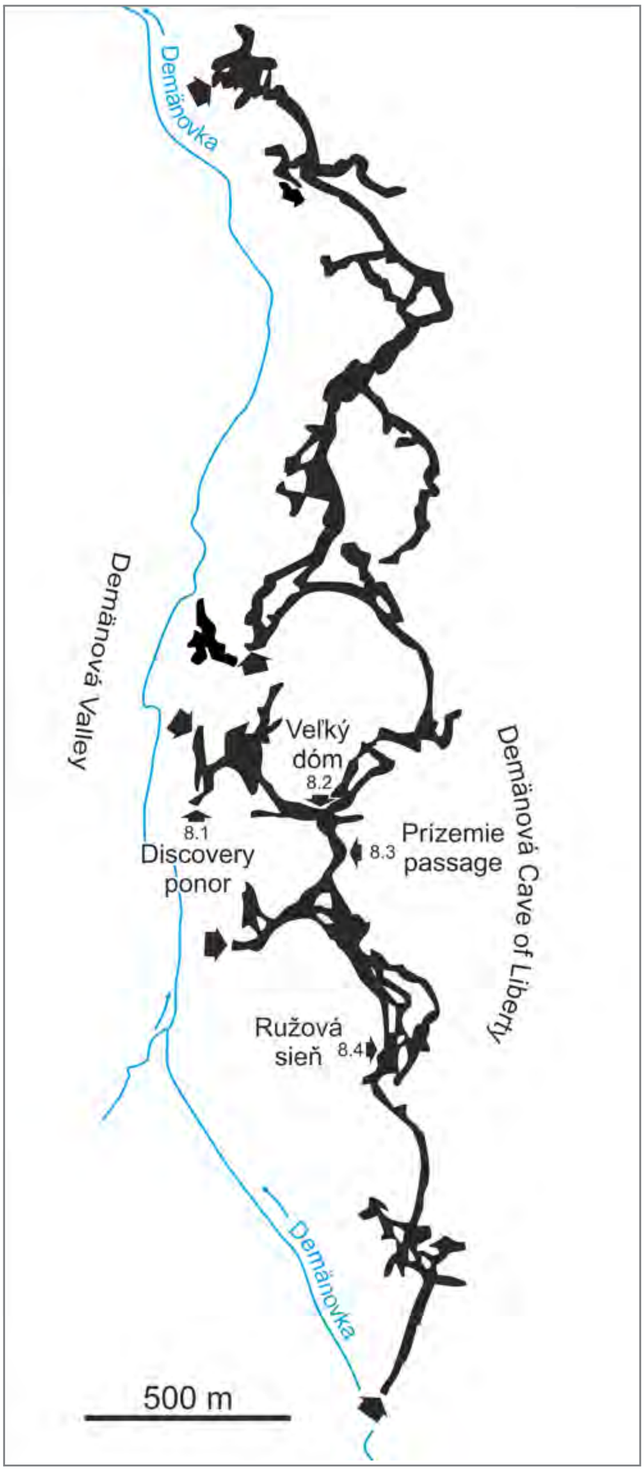

Fig. 18. Map of the Demänová Cave System (after Kučera *et al.*, 1981, simplified), big arrows indicate cave entrances, small arrows indicate stops.

erosion of allochthonous waters. Now the Demänovka stream enters the karst area in Lúčky at the altitude of 950 m, where it sinks underground partly or entirely, depending upon its discharge (Fig. 19).

Droppa (1957) distinguished nine cave levels in the DCS (Fig. 20). In subsequent papers he correlated these levels with the fluvial terraces of the Demänovka stream, and with those of the Váh River and its tributaries (e.g., Droppa, 1966). He assigned individual cave levels to successive glacial stages, using the classical Alpine morphostratigraphic scheme. More recent, detailed studies indicate, however, that the origin of this system was more complicated (e.g., Hochmuth, 1993; Bella et al., 2014). Bella (1993) assigned the individual DCS cave levels distinguished by Droppa (1957) to the ideal watertable caves or to the mixture of phreatic and watertable levelled caves (sensu Ford and Ewers, 1978).

Dating of age boundaries in this system by independent physical methods is of crucial importance for further discussion. Isotopic dating of speleothems is the most appropriate method in this respect. Based of the dating

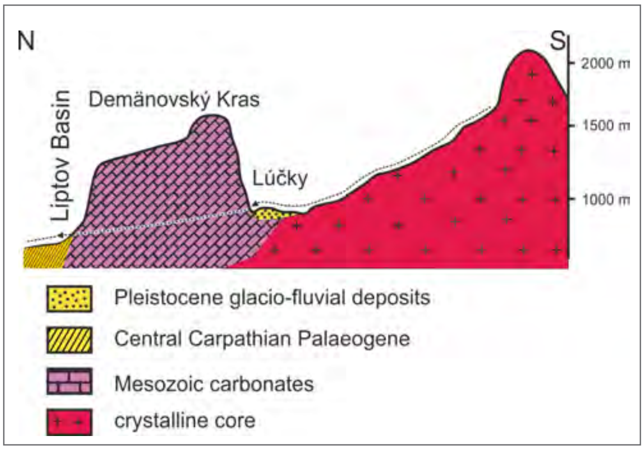

Fig. 19. Simplified geological location of the Demänová Cave System (after Bella, 1994).

results, one can distinguish in the DCS several generations of speleothems which developed chiefly in the warm periods of Pleistocene and in Holocene (Hercman *et al.*, 1997; Hercman, 2000; Hercman and Pawlak, 2012). It is justified to conclude that the age of the oldest speleothems occurring in a particular cave level of the DCS is the minimum age of dewatering of this level (Hercman *et al.*, 1997).

Stop B7.8.1 Discovery Ponor of Demänová Cave of Liberty

(49°0′3″ N, 19°35′ E)

The ponor (swallow hole) is situated on the right (eastern) side of the valley, at the altitude of 805 m, close to a turist trail running along the valley. It is the lowermost ponor of the Demänovka river. Demänová Cave of Liberty (DCL) was discovered by A. Král with the help of A. Mišura and other surveyors through this sinkhole in 1921. The discovery of DCL featured a definite impulse for the development of speleology in Slovakia. A part of the cave from the Mramorové rečisko passage through the Veľký dóm chamber has been opened to the public since 1924 by an old entrance which is situated 8 metres above the Discovery Ponor.

Stop B7.8.2 Demänová Cave of Liberty – Veľký dóm

Veľký dóm is one of the biggest chambers in DCL. Its height reaches 41 m, whereas its lateral extent is 75 m x 45 m (Droppa, 1957). It was formed at the intersection of two fissures striking 300° and 70°. The chamber floor is littered with scree composed of individual blocks up to a few metres across. This material originated from

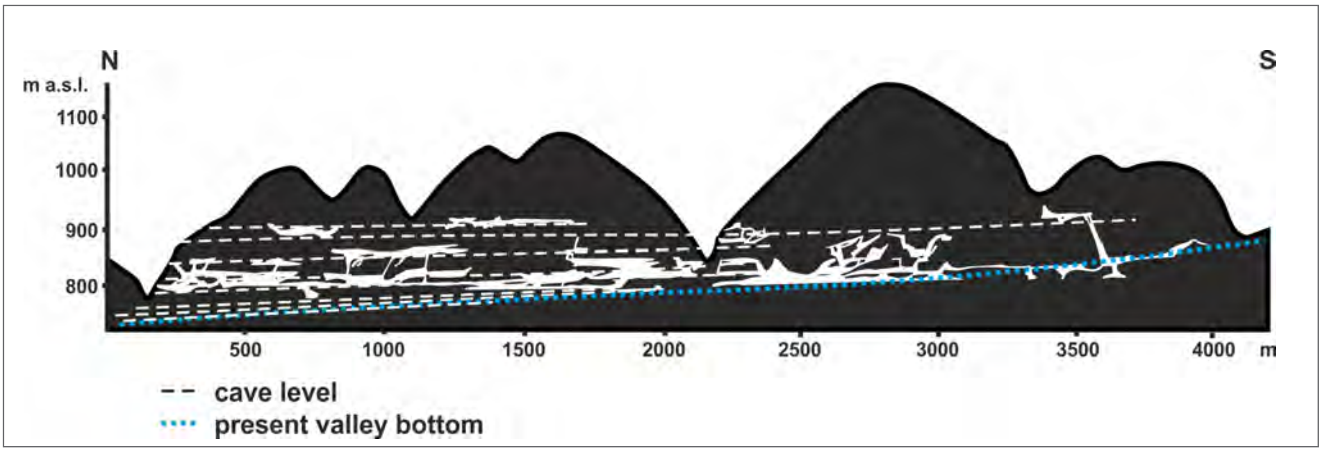

Fig. 20. Longitudinal cross-section of the Demänová Cave System (after Droppa, 1966, simplified).

a collapse or collapses of the chamber ceiling. The underground segment of the Demänovka river flows below the blocks. The scree is overgrown with stalagmites, some of them up to 1 m high (Droppa, 1957). Dating of the stalagmites revealed their Holocene age (authors' unpublished data), which suggests the age of the youngest collapse event in the chamber. North-east wall of the chamber is covered with extensive active moonmilk flowstone.

Stop B7.8.3 Demänová Cave of Liberty – Prízemie passage

The studied sediment section is located at the level of the active underground course of the Demänovka river. The section is more than 4 m thick (Fig. 21). It is composed of clastic deposits divided by several flowstone floors. The oldest visible deposits consist of gravels covered by flowstones and stalagmites, the oldest of which are dated at 236 ± 10 ka. Some parts of this flowstone are in the actual river bed. Higher flowstone floors that occur within clastic deposits have been dated to the last glacial period and Holocene. The ages of these flowstones prove that the lowermost level of DCL (sensu Droppa, 1966) is, at least in this part of the cave, considerably older than the Holocene.

Stop B7.8.4 Demänová Cave of Liberty – Ružová sieň

After walking along several passages and chambers, the trip reaches Ružová sieň, which represents one of the most beautifully decorated parts of DCL. There are several stalagmites and rimestone pools constantly filled with water. The hydrochemical study reveals that the water mineralization (TDS) reaches 300 mg/L, pH varies between 7.8 and 8.5. The water represents the

Fig. 21. General view of the Prízemie passage, the age and location of the oldest flowstone are indicated.

Mg–Ca–HCO_3 type. Elevated concentrations of such ions as Al, Cu, Mo, Ni, Pb and Zn, as compared to other underground pools in DCL (see Motyka *et al.*, 2005), most probably results from coins dropped into the studied rimestone pool. Saturation indices imply that water is in equilibrium or, sometimes, saturated with respect to calcite and aragonite. This suggests that speleothems constantly grow in this part of the cave, which is in line with their fresh appearance.

Stop B7.9 Lúčky – Travertine fed by a mixture of deep- and shallow-circulating waters

Leaders: Michał Gradziński, Pavel Bella

The village of Lúčky is located on the boundary of the Liptov Basin and the Choč Mountains ca. 15 km WWN of Liptovský Mikuláš (Fig. 22). It is situated straight on the major fault bordering the Liptov Basin from the north and separating it from the Choč Mts and the Tatras (Gross, 1980). Additionally, this fault intersects a meridonal one. The Teplianka Valley in the Choč Mts, north of the village, is developed along the latter fault.

The Teplianka stream drains the Choč Mts and flows southward to the Váh river. In its upper course it flows in a narrow, deeply entrenched valley, which is widened near its mouth to the Liptov Basin. The water of the Teplianka stream derives from shallow circulation and its recharge zone is located in the Choč Mts, at altitudes up to 1611 m. It is weakly mineralized (TDS = ca. 320 mg/L) and represents the Ca–Mg–HCO_3 or Ca–HCO_3 types. In the area of the Lúčky spa, this water forms a mixture with artesian water of deep circulation (Franko and Hanzel, 1980). Actively growing travertine is fed by a mixture of both types of water.

Vaškovský and Ložek (1972) recognized three generations of travertines, besides the actively growing ones, near the village of Lúčky. The oldest one crops out in small, abandoned quarries in the south-east outskirts of the village. The second generation provides the most spectacular outcrops. It forms a distinct escarpment and a terrace on the western side of the valley, above the old part of the village and below the spa. The accessible outcrops are artificial – road cuts and abandoned quarries. One of them is presented during the trip (Stop

B7.9.3). The youngest, third generation, is of Holocene age. It crops out in a terrace riser over an artificial lake below the village church. There is a picturesque waterfall, rising up to 15 m over the lake. Modern travertine is being precipitated vigorously on the waterfall (Stop B7.9.2).

Stop B7.9.1 Lúčky spa – Outflow of deep-circulating water

(49°08′05″N, 19°24′14″E)

Leaders: Michał Gradziński, Pavel Bella, Marek Duliński, Jacek Motyka

The Lúčky spa (in Slovak – Lúčky kúpele) lies at the mouth of the Teplianka Valley. The stop is located close to the road, within the spa buildings at the capture of water from borehole Valentína (Fig. 22).

The mineral springs at Lúčky were noticed in a manuscript dated at 1712 and later, in 1736, by Slovak naturalist Matej Bel (Moravčík, 2012). The water has been used for medical purposes since 1761. The natural springs are located at the altitude of 610–620 m. At present, they are captured for the spa which additionally takes water from boreholes. The recharge area may be located in the western part of the Tatras, in the Low Tatras and in the Choč Mts (Hynie, 1963; Franko and Hanzel, 1980; Franko, 2002; Fendek *et al.*, 2015).

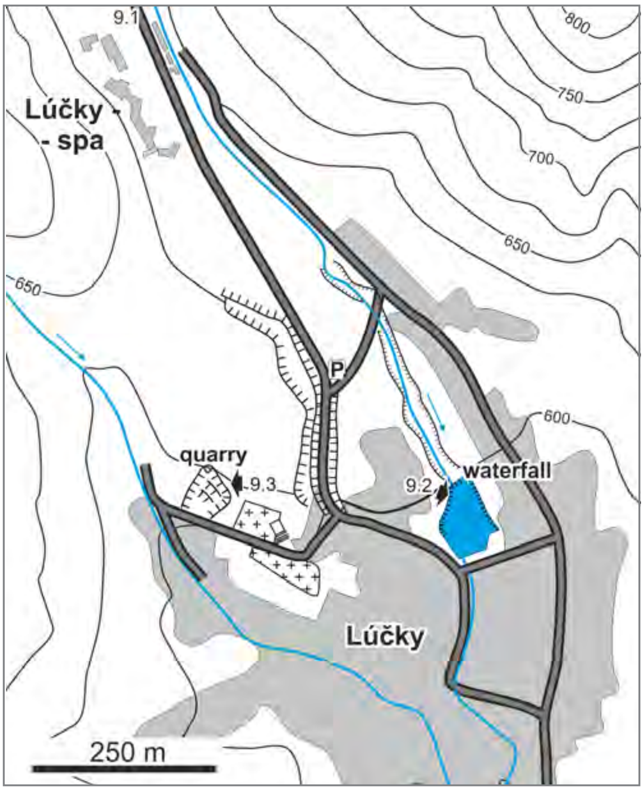

Fig. 22. Location of sites presented in Lúčky (stops 9.1–9.3).

The water from the spa feeds the Teplianka stream.

Mineral water (TDS = ca. 2.6 g/L, temperature at the outflow ca. 30 °C) is exploited from a borehole. It represents the Ca–Mg–HCO_3–SO_4 type under a pressure of ca. 0.5 atm. It represents the Ca–Mg–HCO_3–SO_4 type. Carbon dioxide present in water is probably of mantle origin. Its $\delta^{13}C$ is close to −6.0 ‰ vs V-PDB. The water does not contain tritium. Stable isotope composition $\delta^{18}O$ and $\delta^{2}H$ of this water is close to −10.8 ‰ and −74 ‰, respectively. Thus, it is only slightly lower than that observed for present infiltration waters in this area.

Stop B7.9.2 Lúčky waterfall – Environmental control on deposition of modern travertine

(49°07′47″N, 19°24′12″E)

Leaders: Michał Gradziński, Pavel Bella, Joanna Czerwik-Marcinkowska, Marek Duliński, Peter Holúbek, Jacek Motyka, Teresa Mrozińska

Waterfall is located in the centre of the village, ca. 100 m south-east of the church (Fig. 22). Waterfall and its vicinity are proctected as a nature monument.

Travertine is being precipitated along the riverbed of the Teplianka stream, especially on the waterfall. Upstream of the waterfall the stream flows swiftly down; the water spills over some artificially created dams. The water runs on the terrace tread which is built of detritic deposits of Teplianka and travertines. The thickness of these deposits reaches 30 m, and locally rises to 45 m (Mitter, 1979). The waterfall is located in the northernmost point of a funnel-shaped, 120 m long gully widening to the south. Its steep walls are built of poorly cemented, bedded travertine. Palaeobotanical study by Němejc (1928) indicates its Holocene (Atlantic) age. Exploratory ^{14}C dating gives 7845 ± 45 years BP. However, this date must be treated with caution due to the so-called 'dead carbon effect'.

The waterfall main face is exposed to the south. Its height is 12 m. It is engulfed by two concave formations of vertical drops intervened by small horizontal shelves. Presently, the eastern formation is almost dry after construction of an articial dam above the waterfall, but water distribution on the waterfall changes also naturally. The waterfall face is formed by several overlapping travertine curtains. Three small caves occur behind some curtains. The biggest of them is 10 m long. They represent an uncommon type of caves, created due to progradation of a travertine (or tufa) cascade.

The waterfall is supplied by the stream whose flow is composed of at least two components. One represents the water of deep circulation, which is characterized in the previous stop. This water is mixed above the waterfall with typical shallow water drained by the stream, transporting dissolved biogenic CO_2, derived from decomposition of organic matter or root respiration. As a result of mixing, the water feeding the cascade is dominated by carbon of deep origin (ca. 70 %). This influences the $\delta^{13}C$ of total dissolved inorganic carbon, which varies between –3.2 ‰ and +0.2 ‰ vs V-PDB. The water is oversaturated with respect to calcite. Its saturation index with respect to calcite ranges from 0.67 to 1.27, whereas TDS varies from 507 mg/L to 1023 mg/L (Gradziński, 2010).

Travertine is being precipitated in the streambed over the waterfall, on the waterfall and below it in an artificial channel which leads water through the village. The growing travertine displays great variation of lithotypes (Gradziński, 2010). Porous travertine with encrustation on filamentous cyanobacteria and algae and compact crystalline crust are the most common ones. The former grows in fast-flow settings (see Pedley, 2000; Pedley and Rogerson, 2010). Its formation results from relatively high supersaturation. The vigorous growth of elongated organic filaments seems to be forced by their encrustation with calcium carbonate (Kano *et al.*, 2003; Gradziński, 2010). Algae of genus *Vaucheria* and cyanobacteria of genus *Phormidium* were identified. The former tend to inhabit well irradiated locations and dominate in spring season, whereas the latter are more tolerant to low light intensity. Several taxa of diatoms, other cyanobacteria and algae also occur at the waterfall. Crystalline crust is developed in fast-flow settings under conditions of high supersaturation (see Pedley, 2000). Its formation results from fast abiogenic crystallization of calcite, which impedes colonization and growth of cyanobacteria and algae. In spite of specific character of carbonate system, which is dominated by the carbon of deep origin, the precipitated travertine records markedly even subtle hydrological changes in the catchment. The episodes of fast growth reflect cessation of stream-water supply from the catchment. Conversely, laminae abounding in detritic components record increase in surface runoff (e.g., snow-melt episodes; Gradziński, 2010).

The mean growth rate of travertine at the Lúčky waterfall, studied between 2002 and 2003, was 4.994 $mg \cdot cm^{-2} \cdot day^{-1}$ (Gradziński, 2010). It definitely exceeds the rate of growth of tufa fed with water of shallow-circulation but it is lower than the growth rate of thermal travertine, which can reach 30.9 $mg \cdot cm^{-2} \cdot day^{-1}$ (Pentecost and Coletta, 2007).

The values of $\delta^{13}C$ and $\delta^{18}O$ of the travertine vary from +0.6 ‰ to +3.3 ‰ and from –10.9 ‰ to –8.6 ‰ vs V-PDB, respectively. The comparison of the above values with the isotopic parameters of feeding water implies that oxygen isotopes are not kinetically fractionated during calcite crystallization, whereas carbon isotopes of travertine are affected by kinetic fractionation, probably in CO_2 outgassing process.

Stop B7.9.3 Lúčky, inactive quarry – Facies of Pleistocene travertine fed by mixed water

(49°07′48″ N, 19°23′54″ E)

Leaders: Michał Gradziński, Pavel Bella, Marek Duliński, Helena Hercman, Peter Holúbek, Ewa Stworzewicz[1]

[1]Institute of Systematics and Evolution of Animals, Polish Academy of Sciences, Kraków, Poland

Yellow bedded travertine crops out in an inactive quarry near the village cemetery on the north-west outskirst of the village (Fig. 22). The quarry is protected as a nature monument. The beds dip towards the south-east at an angle of 15° to 65° which reflects the preexisting relief. Travertines are mostly represented by two facies: (i) phytoclastic travertine which abounds in leaf imprints, twig and stem empty moulds, and (ii) cyanobacterial and algal stromatolites. Moss tufa occurs subordinately.

In the western part of the quarry, where the oldest rocks are exposed, phytoclastic travertine predominates. The empty moulds of twigs and stems are horizontally or subhorizontally oriented. Some of them reach diameter of 0.5 m and lengths up to 3.5 m (Gradziński, 2008). Leaf and tree-needle imprints are common, cone imprints occur as well. Grass blades imprints are in life position. They are cemented by sparry calcite, which most probably encrusted algae and cyanobacteria.

Stromatolites crop out in the central and eastern part of the quarry. They were constructed by filamentous cyanobacteria and algae (Fig. 23). In the uppermost beds, a level with gravel of Triassic carbonates, partly covered with stromatolites, has been found.

Snail shells occur within both facies of travertine. They are numerous in some places. They represent land and freshwater snails (Vaškovský and Ložek, 1972).

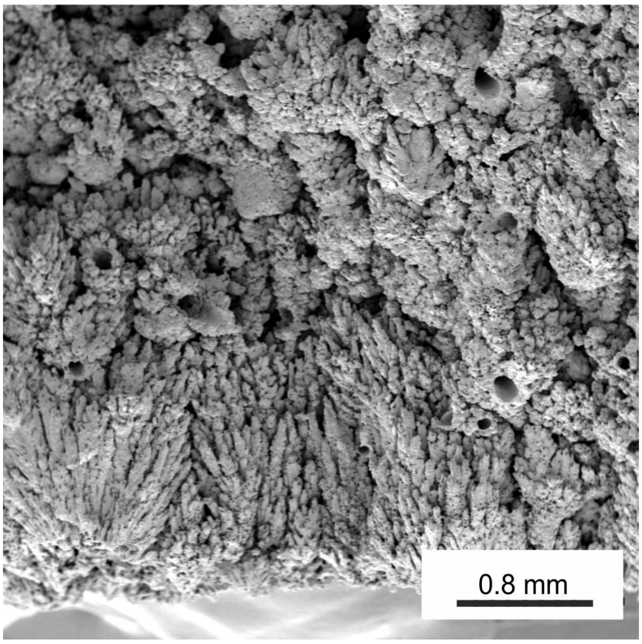

Fig. 23. Stromatolites composed of cyanobacteria (radiating fans in the lower part), which alternate with algae (empty moulds in the upper part), SEM image.

The age of the lower part of the section, determined by U-series method, is equal to ka, whereas the age of upper part is equal to. This is in agreement with the former opinions by Němejc (1928) and Vaškovský and Ložek (1972) based on palaeobotanical and malacological data, respectively.

Facies of the travertine which crops out in the quarry bear a strong resemblance to those of calcareous tufa which is fed with meteoric water of shallow circulation (see Pedley, 2009; Vázquez-Urbez *et al.*, 2012). However, the values of $\delta^{13}C$ of travertine discussed fall between −0.4 ‰ and +4.5 ‰ vs V-PDB (Fig. 12). Such carbon isotopic composition is different form composition typical for calcareous tufa. Conversely, it clearly indicates that the travertine was intimately associated with geogenic CO_2. Thus, one can presume that it can be regarded, to a great extent, as an analogue of recent travertines observed at the Lúčky waterfall.

Acknowledgement

This field-trip guidebook is partly based on guidebooks prepared on the occasion of some earlier conferences, particularly Climate Changes, The Karst Record II (Bella *et al.*, 2000), 1st Polish Geological Congress (Gradziński *et al.*, 2008a) and LXXIX Annual Meeting of the Polish Geological Society (Gradziński *et al.*, 2009). The field-trip is supported by Slovak Caves Administration.

References

Bella, P., 1993. Remarks on the genesis of the Demänová Cave System. *Slovenský Kras*, 31: 43–53. [In Slovak, with English abstract.]

Bella, P., 1994. *Caves and Man. Karst of Demänová Valley*. Slovak Museum of Nature Protection and Speleology, Liptovský Mikulaš, 14 pp.

Bella, P., 2008. The most important caves and abysses of the World Heritage. In: Jakál, J. & Bella, P. (eds), *Caves of the World Heritage in Slovakia*. Slovak Caves Administration, Liptovský Mikuláš, pp. 139–154.

Bella, P., Bosák, P., Głazek, J., Gradziński, M., Hercman, H., Kadlec, J., Kępińska, B., Lalkovič, M., Madeyska, T., Nowicki, T. & Pruner, P., 2000. *Climate Changes – The Karst Record II. Guidebook of Post-Conference Excursion*. Kraków, 32 pp.

Bella, P., Haviarová, D., Kováč, L., Sabol, M., Soják, M., Struhár, V., Višňovská, Z. & Zelinka, J., 2014. *Caves of the Demänová Valley. Speleologia Slovaca*, 4: 1–200. [In Slovak, with English summary.]

Brogi, A. & Capezzuoli, E., 2009. Travertine deposition and faulting: the fault-related travertine fissure-ridge at Terme S. Giovanni, Rapolano Terme (Italy). *International Journal of Earth Sciences*, 98: 931–947.

Capezzuoli, E., Gandin, A. & Pedley, H. M., 2009. Travertine and calcareous tufa in Tuscany (Central Italy). Pre-Conference Trip Ft7. In: Pascucci, V. & Andreucci, S. (eds), *Field Trip Guide Book, 27th IAS Meeting of Sedimentology. September 20–23, 2009, Alghero*. EDES, Sassari, pp. 129–158.

Capezzuoli, E., Gandin, A. & Pedley, M., 2014. Decoding tufa and travertine (fresh water carbonates) in the sedimentary record: The state of the art. *Sedimentology*, 61: 1–21.

Cornides, I. & Kecskés, A., 1982. Deep-seated carbon dioxide in Slovakia: the problem of its origin. *Geologica Carpathica*, 33: 183–190.

De Filippis, L. & Billi, A., 2012. Morphotectonics of fissure ridge travertines from geothermal areas of Mammoth Hot Springs (Wyoming) and Bridgeport (California). *Tectonophysics*, 548–549: 34–48.

De Filippis, L., Faccenna, C., Billi, A., Anzalone, E., Brilli, M., Özkul, M., Soligo, M., Tuccimei, P. & Villa, I., 2012. Growth of fissure ridge travertines from geothermal springs of Denizli basin, western Turkey. *Geological Society of America Bulletin*, 124: 1629–1645.

Demovič, R., Hoefs, J. & Wedephol, K. H., 1972. Geochemische Untersungen an Travertinen der Slovakei. *Contributions to Mineralogy and Petrology*, 37: 15–28.

Droppa, A., 1957. Die Höhlen Demänovské Jaskyne. *Vydavatelstvo Slovenskej Akadémie Vied*, Bratislava, 289 pp. [In Slovak, with German summary.]

Droppa, A., 1966. The correlation of some horizontal caves with river terraces. *Studies in Speleology*, 1: 186–192.

Droppa, A., 1972. Die geomorphologischen Verhältnisse im Demänovská-Tal. *Slovenský Kras*, 10: 9–46. [In Slovak, with German summary.]

Fendek, M., Daniel, S., Grand, T. & Kultan, V., 2015. Delineation of geothermal aquifers by magnetotelluric methods in Besenova – Lucky area, northern Slovakia. In: *Proceedings of the World Geothermal Congress 2015, Melbourne, Australia.* https://pangea.stanford.edu/ERE/db/WGC/papers/WGC/2015/13127.pdf [26.04.2015]

Fendeková, M., 2002. *Zdroje minerálnych vôd v oblasti Vyšných Ružbach a možnosti získania záložného zdroja*. Unpublished report. Hydrofen, Bratislava, 23 pp. [In Slovak.]

Ford, D. C. & Ewers, R. O., 1978. The development of limestone cave systems in the dimensions of lenght and depth. *Canadian Journal of Earth Sciences*, 15: 1783–1798.

Franko, O., 2002. Topical views of the hydrogeological structure of mineral waters in spa Lúčky. *Podzemná Voda*, 8: 123–132. [In Slovak, with English summary,]

Franko, O. & Hanzel, V., 1980. Hydrogeologické pomery Liptovskej kotliny. In: Gross, P. & Köhler, E. (eds), Geológia Liptovskej Kotliny. Geologický Ústav Dionýza Štúra, Bratislava, pp. 126–137. [In Slovak.]

Fričovský, B., Tometz, L., Fendek, M. & Gumáňová, L., 2015. Update ion composite geochemical conceptual model for the Bešeňová Elevation geothermal structure, Liptov Basin, Northern Slovakia. In: *Proceedings of the World Geothermal Congress 2015, Melbourne, Australia.* https://pangea.stanford.edu/ERE/db/WGC/papers/WGC/2015/14092.pdf [26.04.2015].

Fussgänger, E., 1985. Poznatky z terénneho výskumu plazivých svahových pohybov travertínových blokov na Spišskom hrade. *Mineralia Slovaca,* 1: 15–24. [In Slovak.]

Gaál, Ľ., 2008. Soluble rocks – the environment for karst and cave development. In: Jakál, J. & Bella, P. (eds), *Caves of the World Heritage in Slovakia*. Slovak Caves Administration, Liptovský Mikuláš, pp. 17–24.

Gandin, A. & Capezzuoli, E., 2014. Travertine: Distinctive depositional fabrics of carbonates from thermal spring system. *Sedimentology*, 61: 264–290.

Gąsiorowski, S. M., Michalik, M., Paszkowski, M., Piekarska, E. & Szulc, J., 1986. Excursion B-10. Shallow-water and subaerial carbonates of the Czestochowa-Kraków Upland. Case histories from the Lower Carboniferous to Holocene. In: Teisseyre, A. K. (ed.), *7th European Regional Meeting Kraków-Poland Excursion Guidebook*. Ossolineum, Wrocław, pp. 179–201.

Goudie, A. S., Viles, H. A. & Pentecost, A., 1993. The late-Holocene tufa decline in Europe. *Holocene*, 3: 181–186.

Gradziński, M., 2008. Origin of a unique tree-mould type cave in travertine based on examples from the village of Lúčky (Liptov, Slovakia). *Slovenský Kras*, 46: 325–331.

Gradziński, M., 2010. Factors controlling growth of modern tufa: results of a field experiment. In: Pedley, H. M. & Rogerson, M. (eds), *Tufas and Speleothems: Unravelling the Microbial and Physical Controls. Geological Society Special Publications*, 336: 143–191.

Gradziński, M., Bella, P., Czop, M., Duliński, M., Głazek, J., Haviarová, D., Hercman, H., Holúbek, P., Motyka, J., Mrozińska, T., Rajnoga, P., Stworzewicz, E. & Wróblewski, W., 2008a. B5. Trawertyny i kras północnej Słowacji. In: Haczewski, G. (ed.), *Pierwszy Polski Kongres Geologiczny, Kraków 26-28 czerwca 2008, Przewodnik Sesji Terenowych*. Polskie Towarzystwo Geologiczne, Kraków, pp. 101–119. [In Polish.]

Gradziński, M., Czop, M., Duliński, M., Gąsiorowski, M., Grabowski, J., Hercman, H., Holúbek, P., Kováčova, M., Motyka, J., Mrozińska, T., Pawlak, J., Smosna, P., Sobień, K. & Stworzewicz, E., 2009. Sesja terenowa A6.

Trawertyny wokół Tatr. In: Uchman, A. & Chowaniec, J. (eds), *LXXIX Zjazd Polskiego Towarzystwa Geologicznego, Budowa geologiczna Tatr i Podhala ze szczególnym uwzględnieniem zjawisk geotermalnych na Podhalu, Bukowina Tatrzańska, 26-29.09.2009 r. Materiały konferencyjne*. Państwowy Instytut Geologiczny Państwowy Instytut Badawczy, Warszawa, pp. 134–144. [In Polish.]

Gradziński, M., Duliński, M., Hercman, H., Stworzewicz, E., Holúbek, P., Rajnoga, P., Wróblewski, W. & Kováčová, M., 2008b. Facies and age of travertines from Spiš and Liptov regions (Slovakia) – preliminary results. *Slovenský Kras*, 46: 31–40.

Gradziński, M., Hercman, H., Jaśkiewicz, M. & Szczurek, S., 2013. Holocene tufa in the Slovak Karst: facies, sedimentary environments and depositional history. *Geological Quarterly*, 57: 769–788.

Gradziński, M., Wróblewski, W., Duliński, M. & Hercman, H., 2014. Earthquake-affected development of a travertine ridge. *Sedimentology*, 61: 238 – 263.

Gross, P., 1980. Tektonika. In: Gross P. & Köhler E. (eds), *Geológia Liptovskej Kotliny*. Geologický Ústav Dionýza Štúra, Bratislava, pp. 116–121. [In Slovak.]

Gross, P., Buček, S., Ďurkovič, T., Filo, I., Karoli, S., Maglay, J., Nagy, A., Halouzka, R., Spišák, Z., Žec, B., Vozár, J., Borza, V., Lukáčik, E., Mello, J., Polák, M. & Janočko, J., 1999. *Geological Map of Popradská Kotlina Basin, Hornádska Kotlina Basin, Levočské Vrchy Mts., Spišsko-Šarišské Medzihorie Depression, Bachureň Mts. and Šarišská Vrchovina Highland 1: 50 000*. MŽP SR – GSSR, Bratislava.

Gross, P., Vaškovský, I. & Halouzka, R., 1979. *Geologická mapa Liptovskej kotliny* 1: 50 000. GÚDŠ, Bratislava. [In Slovak.]

Guo, L. & Riding, R., 1998. Hot-spring travertine facies and sequences, Late Pleistocene, Rapolano Terme, Italy. *Sedimentology,* 45: 163–180.

Hanzel, V., 1987. Fissure-karst waters of the Belianske Tatry and the High Tatras. Slovenský Kras, 25: 65–82. [In Slovak, with English summary.]

Haviarová, D., Seman, M., Stankovič, J., Fľaková, R. & Ženišová, Z., 2012. Chemical composition and microbiological profile of karst water in the Krásnohorská Cave (Silická plateau, Slovak karst). *Acta Geologica Slovaca*, 4: 31–52. [In Slovak, with English summary.]

Hercman, H., 2000. Reconstruction of palaeoclimatic changes in central Europe between 10 and 200 thousand years BP, based on analysis of growth frequency of speleothems. *Studia Quaternaria*, 17: 35–70.

Hercman, H., Bella, P., Głazek, J., Gradziński, M., Lauritzen, S.-E. & Løvlie, R., 1997. Uranium-series dating of speleothems from Demänova Ice Cave: A step to age estimation of the Demänova Cave System (the Nízke Tatry Mts., Slovakia). *Annales Societatis Geologorum Poloniae*, 67: 439–450.

Hercman, H., Gradziński, M. & Bella, P., 2008. Evolution of Brestovská Cave based on U-series dating of speleothems. *Geochronometria*, 32: 1–12.

Hercman, H. & Pawlak, J., 2012. MOD-AGE: An age-depth model construction algorithm. *Quaternary Geochronology*, 12: 1–10.

Hochmuth, Z., 1993. Results of a detailed mapping and revised geomorphpological survey of the Cave Vyvieranie in the Demänová Valley. *Slovenský Kras*, 31: 29–42. [In Slovak, with English summary.]

Holec, P., 1992. Teeth casts of Mastodont species *Mammut borsoni* (Hays, 1834) from the Dreveník travertine near Spišské Podhradie. *Mineralia Slovaca*, 24: 467–469. [In Slovak, with English summary.]

Hynie, O., 1963. *Hydrogeologie ČSSR, II, Minerálni vody*. Nakladatelství Československé Akademie Véd, Praha, 797 pp. [In Slovak.]

Jakál, J. & Bella, P., 2008. Water – creative agent of karst and caves. In: Jakál, J. & Bella, P. (eds), *Caves of the World Heritage in Slovakia*. Slovak Caves Administration, Liptovský Mikuláš, pp. 25–36.

Janočko, J., Gross, P., Jacko, S. jr., Buček, S., Karoli, S., Žec, B., Polák, M., Rakús, M., Potfaj, M. & Halouzka, R., 2000. *Geological Map of the Spišská Magura Region 1: 50 000*, MŽP SR – ŠGÚDŠ, Bratislava.

Jetel, J., 1999. Hydrogeologické pomery. In: Gross, P. (ed.), *Vysvietlivky ku geologickiej mape Popradskej kotliny, Hornádskej kotliny*, *Levočských* vrchov, *Spišsko-Šarišského medzihoria, Bachurne a Šariškej vrchoviny*. Geologická Služba Slovenskiej Republiky, Bratislava. pp. 166–192. [In Slovak.]

Jones, B. & Renaut, R. W., 1995. Noncrystallographic calcite dendrites from hot-spring deposits at Lake Bogoria, Kenya. *Journal of Sedimentary Research*, 65: 154–169.

Jones, B. & Renaut, R. W., 2010. Calcareous spring deposits in continental settings. *Developments in Sedimentology*, 61: 177–224.

Kano, A., Matsuoka, J., Kojo, T. & Fujii, H., 2003. Origin of annual lamination in tufa deposits, southwest Japan, *Palaegeography, Palaeoclimatology, Palaeoecology*, 191: 243–262.

Kano, A., Takashima, Ch. & Ohtsuka, S., 2006. *FE-A10. Hot-Springs in Eastern Kyushu and Their Related Sedimentation and Microbial Processes. Field Excursion Guidebook 17th International Sedimentological Congress. Fukuoka, Japan*. Sedimentological Society of Japan, pp. 1–10.

Kawai, I., Kano, A., Matsuoka, J. & Ibara, T., 2006. Seasonal variation in water chemistry and depositional processes in tufa–bearing stream in SW–Japan, based on 5 years of monthly observation. *Chemical Geology*, 232: 33–53.

Kele, S., Demény, A., Siklósy, Z., Németh, T., Mária, T. & Kovács, M. B., 2008. Chemical and stable isotope compositions of recent hot-water travertines and associated thermal waters, from Egerszalók, Hungary: depositional facies and non-equilibrium fractionations. *Sedimentary Geology*, 211: 53–72.

Kele, S., Özkul, M., Gögöz, Z., Fórizs, I., Baykara, M. O., Alçiçek, M. C. & Németh, T., 2011. Stable isotope, geochemical and facies study of Pammukale travertines: new evidences of low-temperatures non-equilibrium fractionation. *Sedimentary Geology*, 238: 191–212.

Kilík, J., 2008. Calcareous tufa in Slovak Karst. *Naturae Tutela*, 12: 177–184. [In Slovak, with English summary.]

Kormos, T., 1912. Beitrage zur Kenntnis der pleistozänen Molluskenfauna des Mittelkarpathen-Gebietes. *Jahrbuch der Königlisch ungarischen geologischen Reichsanstalt*, [for 1910]: 326–340.

Kostecka, A., 1992. Calcite veins in travertines at Bešeňová (Liptovska Kotlina basin, Slovakia). *Mineralogia Polonica*, 23: 3–12.

Košťál, J., 2011. Najmenší biotop – Karpatské travertínové slaniská. *Krásy Slovenska*, 88: 28–29. [In Slovak.]

Kovanda, J., 1971. Quaternary limestones of Czechoslovakia. *Sbornik Geologických Vìd, Antropozoikum*, 7A: 7–256. [In Czech, with English summary.]

Kučera, B., Hromas, J. & Skřivánek, F., 1981. *Jeskyně a propasti v Československu*. Academia, Praha, 252 pp. [In Czech.]

Leśniak, P. M., 1998. Origin of carbon dioxide and evolution of CO_2-rich waters in the West Carpathians, Poland. *Acta Geologica Polonica*, 48: 343–368.

Lexa, J. & Konečný, V., 1998. Geodynamic aspects of the Neogene to Quaternary volcanism. In: Rakús, M. (ed.), *Geodynamic Development of the Western Carpathians*. Geologický Ústav Dionýza Štúra, Bratislava, pp. 219–240.

Ložek, V., 1957. Nové interglaciální malakofauny ze Slovenska. *Anthropozoikum*, 7: 37–45. [In Czech.]

Ložek, V., 1958. Stratigraphie und Weichtiere der holozänen Travertine in Háj bei Turňa. *Anthropozoikum*, 7: 27–36. [In Czech, with German summary.]

Ložek, V., 1961. Travertines. *Instytut Geologiczny, Prace*, 34: 81–86.

Ložek, V., 1964. Genéza a vek spišských travertinov. *Sbornik Východoslovenského Múzea*, 5: 7–32. [In Slovak.]

Ložek, V. & Prošek, F., 1957. Krasové zjevy v travertinech a jeich stratigrafický vyznam. *Československý Kras*, 10: 145–158. [In Czech.]

Maglay, J. & Halouzka, R., 1999. Kvartér. In: Gross, P. (ed.), *Vysvetlivky ku geologickej mape Popradskej kotliny, Hornádskej kotliny, Levočských vrvhov, Spišsko--Šarišského medzihoria, Bachurne a Šarišskej vrchoviny*. Geologická Služba Slovenskej Republiky, Bratislava, pp 110–139. [In Slovak.]

Maheľ, M. & Buday, T., 1968. *Regional Geology of Czechoslovakia. Part II. The West Carpathians*. Geological Survey of Czechoslovakia, Academia, Praha, 723 pp.

Mello, J., Elečko, M., Pristaš, J., Reichwalder, P., Snopko, L., Vass, D. & Vozárová, A., 1996. *Geological Map of the Slovenský Kras Mts. 1: 50 000*. MŽP SR – GSSR, Bratislava.

Mesci, L. B., Gürsoy, H. & Tatar, O., 2007. The evolution of travertine masses in the Sivas Area (Central Turkey) and their relationships to active tectonics. *Turkish Journal of Earth Sciences*, 17: 219–240.

Mitter, P., 1979. *Záverečna správa. Relief na travertínoch Slovenska*. Unpublished report. Múzeum Slovenského Krasu, Liptovský Mikulaš, 176 pp. [In Slovak.]

Moravčík, L., 2012. *Pramene zdravia a nádeje. 3000 rokov Kúpeľov Lúčky*. P + M Turany, Turany, 104 pp. [In Slovak.]

Motyka, J., Gradziński, M., Bella, P. & Holúbek, P., 2005. Chemistry of waters from selected caves in Slovakia – a reconnaissance study. *Environmental Geology*, 48: 682–692.

Němejc, F., 1928. Palaeobotanical investigation in the travertine-complex around the village of Lůčky near Růžomberok in Slovakia. *Rozpravy II. Třidy České Akademie*, 37: 1–19.

Němejc, F., 1931. Palaeobotanical researches in the travertine sediments of Vyšní and Nižní Ružbachy at Podolinec (Slovakia) and some additional notes to my studies about the travertines of the Northern Slovakia. *Preslia*, 10: 115–134.

Němejc, F., 1936. The palaeobotanical researches in the travertine deposits of the Slovakian Karst. *Bulletin International de l'Académie des Sciences de Bohême*: 1–48.

Němejc, F., 1944. Výsledky dosavadních výzkumů paleobotanických v kvartéru západního dílu karpatského oblouku. *Rozpravy II. Třidy České Akademie*, 53: 1–47. [In Czech.]

Orvan, J., 1980. Hodnotenie stopovacích (farbiacich) skúšok pri riešení niektorých otázok krasovej hydrológie na území Slovenského krasu. *Slovenský Kras*, 18: 177–181. [In Slovak.]

Pedley, H. M., 1990. Classification and environmental models of cool freshwater tufas. *Sedimentary Geology*, 68: 143–154.

Pedley, M., 2000. Ambient temperature freshwater microbial tufas. In: Riding, R. E. & Awramik, S. M. (eds), *Microbial Sediments*. Springer, Berlin, pp. 179–186.

Pedley, M., 2009. Tufas and travertines of the Mediterranean region: a testing ground for freshwater carbonate concepts and developments. *Sedimentology*, 56: 221–246.

Pedley, M., González Martín, J. A., Ordóñez Delgado, S. & García del Cura, A. G., 2003. Sedimentology of Quaternary perched springline and paludal tufas: criteria for recogfnition, with examples from Guadalajara Province, Spain. *Sedimentology*, 50: 23–44.

Pedley, H. M. & Rogerson, M., 2010. In vitro investigations of the impact of different temperature and flow velocity conditions on tufa microfabric. In: Pedley, H. M. & Rogerson, M. (eds), *Tufas and Speleothems: Unravelling the Microbial and Physical Controls. Geological Society, London, Special Publications*, 336: 193–210.

Pentecost, A., 2005. *Travertine*. Springer, Berlin, 445 pp.

Pentecost, A. & Coletta, P., 2007. The role of photosynthesis and CO_2 evasion in travertine formation: a quantitative investigation at an important travertine-depositing hot spring, Le Zitelle, Lazio, Italy. *Journal of the Geological Society*, 164: 843–853.

Petrbok, J., 1937. Měkkýši travertinů Slovenského krasu, Gánovců s okolím, Spiše a Ružbachů. *Rozpravy II. Třídy České Akademie*, 46: 1–16. [In Czech.]

Piper, J. D. A., Mesci, L. B., Gürsoy, H., Tatar, O. & Davies, C., 2007. Palaeomagnetic and rock magnetic properties of travertine: Its potential as a recorder of geomagnetic palaeosecular variation, environmental change and earthquake activity in the Sicak Çermik geothermal field, Turkey. *Physics of the Earth and Planetary Interiors*, 161: 50–73.

Pivko, D., 1999. Geologická exkurzia po dekoračných kameňoch centra Bratislavy. *Acta Geologica Universitatis Comenianae*, 54: 109–124. [In Slovak.]

Plašienka, D., 2008. The Western Carpathians. In: McCann, T. (ed.), *The Geology of central Europe. Volume 2: Mesozoic and Cenozoic*. The Geological Society, London, pp. 1181–1217.

Potočná, E., 2007. *Vyšné Ružbachy. Kúpelná obec*. Region Poprad s.r.o., Poprad, 184 pp. [In Slovak.]

Povinec, P. P., Franko, O., Šivo, A., Richtárikova, M., Breier, R., Aggarwal, P. K. & Araguás-Araguás, L., 2010. Spatial radiocarbon and stable carbon isotope variability of mineral and thermal waters in Slovakia. *Radiocarbon*, 52: 1056–1067.

Rajnoga, P., 2009. *Facies of pre-Holocene travertines in Ružbachy (Spiš, Slovakia)*. Unpublished MSc. Thesis, Institute of Geological Sciences, Jagiellonian University. [In Polish, with English summary.]

Remšík, A., Fendek, M. & Maďar, D., 2005. Occurrence and distribution of the geothermal water and geothermal energy of the Liptov Basin. *Mineralia Slovaca*, 37: 123–130.

Rogerson, M., Pedley, H. M., Wadhawan, J. D. & Middleton, R., 2008. New insights into biological influence on the geochemistry of freshwater carbonate deposits. *Geochimica et Cosmochimca Acta*, 72: 4976–4987.

Sabol, M., 2003. Bear skull from Bešeňová (northern Slovakia). *Atti del Museo Civico di Storia Naturale – Trieste*, 49: 101–106.

Stankovič, J., Cílek, V., Bruthans, J., Gaál, Ľ., Kovács, Á., Rozložník, M., Schmelzová, R., Zeman, O., Kováč, Ľ., Mock, A., Ľuptáčik, P., Hudec, I., Nováková, A., Košel, V. & Fenďa, P., 2005. *Krásnohorská jaskyňa Buzgó*. Speleoklub MINOTAURUS, Rožňava, 150 pp. [In Slovak.]

Tóth, C. & Krempaská, Z., 2008. Pliocene *Proboscidea* remains from travertine Dreveník site (near Spišské Podhradie, Slovakia). In: Krempaská, Z., (ed.), *6th Meeting of The European Association of Vertebrate Palaeontologists, Spišská Nová Ves 2008, Volume of Abstracts*. p. 116.

Tulis, J. & Novotný, L., 2008. Geological and geomorphological settings of the National Natural Reserve Dreveník. *Slovenský Kras*, 46: 5–30. [In Slovak, with English summary.]

Vaškovský, J., 1980. Geológia kvartérnych sedimentov. In: Gross, P. & Köhler, E. (eds), *Geológia Liptovskej Kotliny*. Geologický Ústav Dionýza Štúra, Bratislava, pp. 96–115. [In Slovak.]

Vaškovský, J. & Ložek, V., 1972. To the Quaternary stratigraphy in the western part of the basin Liptovská kotlina. *Geologické Práce, Správy*, 59: 101–140.

Vázquez-Urbez, M., Arenas, C. & Pardo, G., 2012. A sedimentary facies model for stepped, fluvial tufa system in the Iberian Range (Spain): the Quaternary Piedra and Mesa valleys. *Sedimentology*, 61: 502–526.

Vázquez-Urbez, M., Arenas, C., Sancho, C., Auqué, L.F., Osácar, C. & Pardo, G., 2011. Quaternary and present-day tufa systems of the Rivers Piedra and Añamaza (Iberian Range,Spain). *Geo-Guías*, 8: 241–274.

Vozár, J. & Káčer, Š., eds, 1996. Geologická mapa Slovenskej Republiky 1:500 000. Geologická Služba Slovenskej Republiky, Bratislava. [In Slovak.]

Wróblewski, W., Gradziński, M. & Hercman, H., 2010. Suggestions on the allochthonous origin of terra rossa from Dreveník Hill (Spišs, Slovakia). *Slovenský Kras*, 48: 153–161.

Some current sedimentological controversies in the Polish Carpathian flysch

Stanisław Leszczyński[1], Piotr S. Dziadzio[2], Wojciech Nemec[3]

[1]Jagiellonian University, Poland (stan.leszczynski@uj.edu.pl),
[2]Oil and Gas Institute, Poland (dziadzio@inig.pl)
[3]University of Bergen, Norway (wojtek.nemec@uib.no)

Route (Fig. 1): Early evening transfer from Kraków to Gorlice (**accommodation**), ca. 2.5 hours (133 km), by motorway A4 to the slip road Tarnów Zachód and further south by roads 975, 980 and 977. Excursion route on the first day (26 June) from Gorlice by road 977 to Ciężkowice (stop B8.1), then by roads 977, 979 and 28 to Krosno and further by local road to Odrzykoń (**stop B8.2**) and to Czarnorzeki (**stop B8.3**) – with an evening return to Gorlice by roads 991 and 28. Excursion route on the second day from Gorlice to Ropica Górna (**stop B8.4**) by road 977 and back to the southern suburbs of Gorlice (**stop B8.5**), with an early evening return to Kraków by the same roads as used for arrival.

Introduction to the field trip: The Polish Flysch Carpathians

Stanisław Leszczyński

Carpathians are the European largest (~1500 km long) mountain range formed during the Alpine orogeny, extending as an arc (Fig. 2A) from the Czech Republic (3%) in the northwest through the Slovakia/Poland borderland (27%) to Hungary (4%), eastwards to Ukraine (11%) and further southwards to Romania (53%). As a classic collisional orogen, the Polish Carpathians show the complex tectonic structure and tectonostratigraphy of a fold-and-

Fig. 1. Route map of field trip B8.

Leszczyński, S., Dziadzio, P. S. & Nemec, W., 2015. Some current sedimentological controversies in the Polish Carpathian flysch. In: G. Haczewski (ed.) *Guidebook for field trips accompanying 31st IAS Meeting of Sedimentology held in Kraków on 22nd–25th of June 2015*. Polish Geological Society, Kraków, pp. 247–287.
Guidebook is available online at www.ing.uj.edu.pl/ims2015

thrust belt with a general northern vergence. The whole northern, external part of the orogen extending through southernmost Poland (~300 km long and up to 80 km wide) – known as the Outer Carpathians (Figs 2, 3) – is a Cenozoic accretionary prism composed of flysch deposits (*sensu* Studer, 1827; Dżułyński and Smith, 1964), and hence is referred to also as the Flysch Carpathians. The inner part of the orogen, of which only a small part crops out in Poland (Fig. 2), consists of Palaeozoic crystalline rocks and their post-Carboniferous (mainly Mesozoic to Palaeogene) deformed sedimentary cover. The flysch deposits of the Outer Carpathians are up to 6000 m thick, comprising various turbiditic successions of Tithonian to Miocene age (Fig. 4). They are thought to have accumulated on a thin-stretched continental crust of the European Platform's original passive margin in an array of narrow deep-water basins, which were separated by sediment-supplying subaqueous to subaerial ridges referred to as cordilleras and which continued to accumulate sediment during the subsequent active-margin conditions of subduction to collision in the late Cretaceous–Palaeogene time (Książkiewicz, 1956, 1975). The main flysch sub-basins are now represented by the individual nappes of the Outer Carpathians (Figs 2, 3), in their south to north stacking order: the Magura, Sub-Magura/Dukla, Silesian, Sub-Silesian and Skole nappes. The thin-skinned nappes and intra-nappe imbricate thrust-sheets were tectonically stacked in the late Oligocene to early Miocene by being piled up northwards onto the Miocene foreland basin at the flexural margin of the European Platform (Fig. 3). The development of the flysch basins and cordilleras was probably diachronous, as was also their subsequent tectonic stacking as nappes, whereby the exact palaeogeographic evolution of the Outer Carpathians remains to be disputed.

Extensive geological investigations of the Polish Flysch Carpathians commenced in the second half

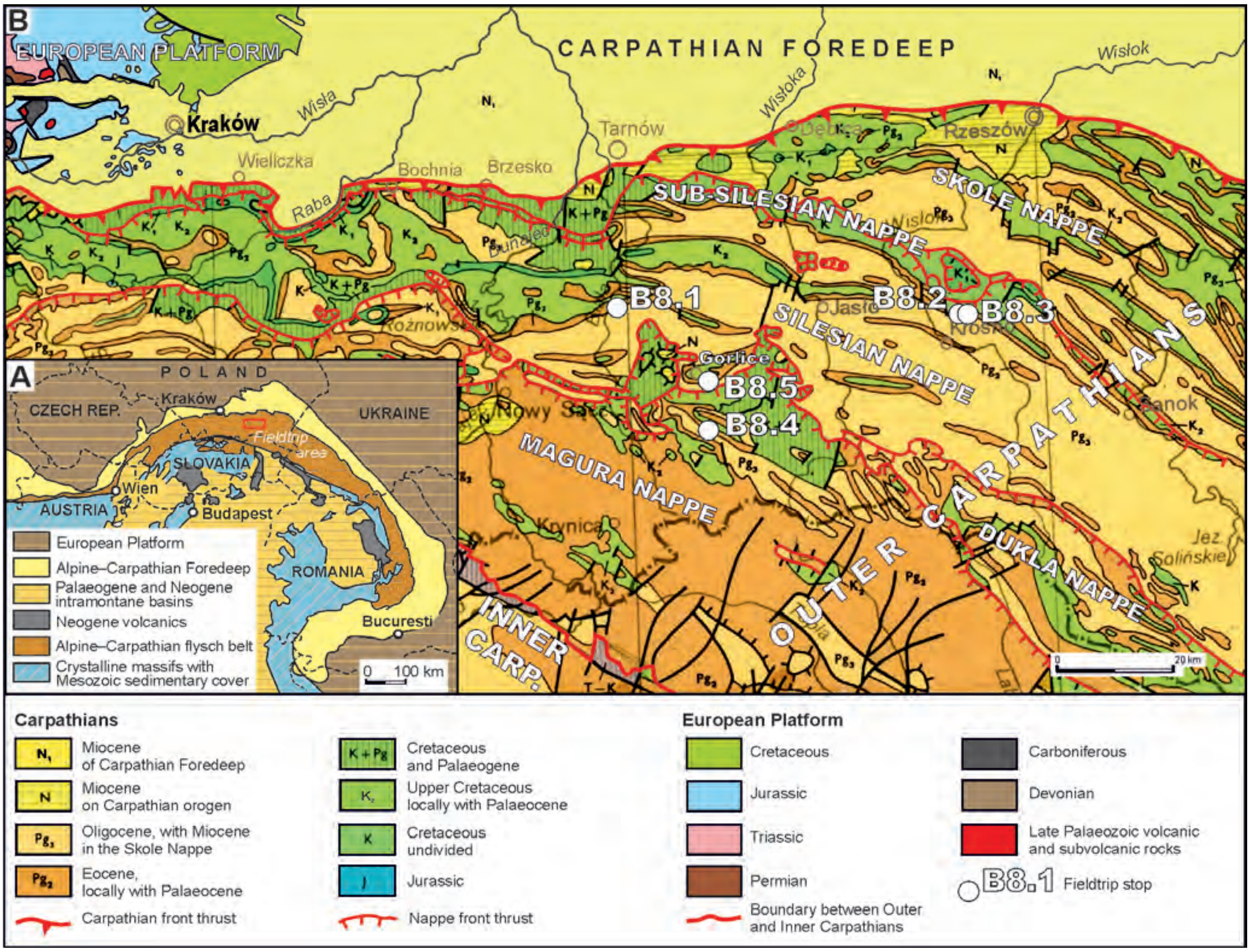

Fig. 2. (**A**) Regional location of the field-trip area within the Outer Carpathian flysch belt and (**B**) the area geological map (based on Geological Map of Poland 1:500 000) with the location of main stops. Note that the stops B8.1–3 and B8.5 are in the Silesian Nappe and stop B8.4 is in the Magura Nappe.

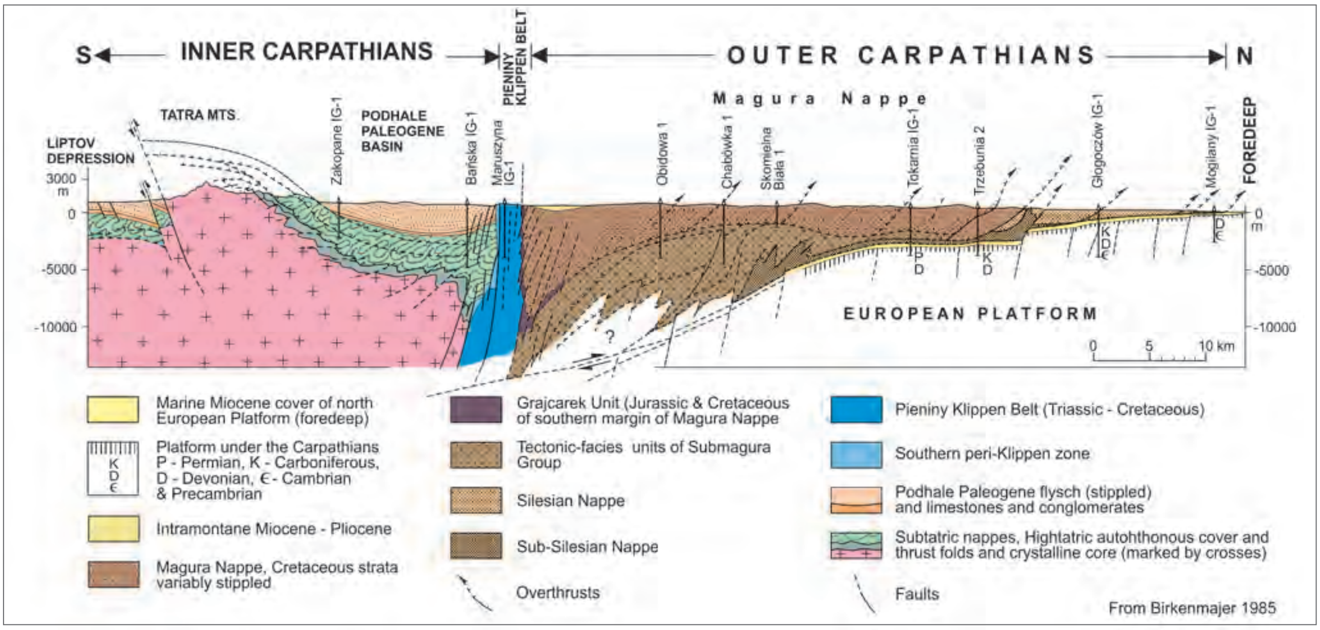

Fig. 3. Geological cross-section through the Polish Carpathians along the S–N traverse Zakopane– Kraków (based on Birkenmajer, 1985).

of the 19th century in connection with the increased demand for hydrocarbons. Detailed sedimentological studies were inspired by the birth of the concept of turbidity current (Kuenen and Migliorini, 1950), as this explanation for the origin of deep-water graded sandstone beds coincided with similar working notions of one of the region's leading investigators – Professor M. Książkiewicz at the Jagiellonian University (e.g., see Książkiewicz, 1948). This is how the so-called 'Kraków School of Flysch Sedimentology' came to life in the 1950s and reached the climax of its prolific activity in the 1960s to 1970s. Inspired by M. Książkiewicz, this informal group of researchers included his most talented disciples: S. Dżułyński, A. Radomski, L. Koszarski, K. Żytko, A. Ślączka, R. Unrug, F. Simpson, J. M. Anketell and many others. Their diligent studies provided new data on the varied sedimentary characteristics of turbidites with suggestions as to their possible origin, including most notably the world's first atlas of flysch lithofacies maps (Książkiewicz, 1962), a comprehensive genetic review and classification of bed solemarks (Dżułyński and Walton, 1965), a pioneering bathymetric interpretation of flysch successions (Książkiewicz, 1975), and a benchmark description of flysch trace fossils and their distribution in sediment successions (Książkiewicz, 1977).

One of the key early discoveries in the Polish Flysch Carpathians was the observation that some of the turbiditic successions consist of sandstone and fine-grained conglomeratic beds whose features cannot be readily explained by Kuenen's original concept of sediment gradual settling from turbulent suspension current. Such abnormal turbidites in the Carpathian flysch were demonstrated to Kuenen by Książkiewicz and Dżułyński during their historical field trip in 1957 and were swiftly mentioned as 'fluxoturbidites' in Kuenen's (1958) next paper, with the term presumably meant to denote fluxes of excessively dense flow within a fully turbulent suspension current. This new term was retained and more elaborately defined by Dżułyński *et al.* (1959). The first day of the present field excursion is focused on such deposits, exemplified by the early Eocene Ciężkowice Sandstone of the Silesian Nappe (Fig. 4), to honour this early pioneering recognition of flows termed later 'high-density' turbidity currents by Lowe (1982) and to compare these deposits with the more recent turbiditic models.

Two other issues are the topic for the second day of the excursion in the Carpathian flysch. One issue pertains to the Glauconitic Magura Beds (late Eocene–early Oligocene, Fig. 4) of the Magura Nappe, where turbidites composed of shelf-derived glauconite-bearing sand tend to be overlain by thick, non-bioturbated dark-grey mudshale capped with a thin, bioturbated greenish-grey mudshale. Can this be evidence of an *en-masse* emplacement of thick, dense co-turbiditic fluidal mud suspension (Baas *et al.*, 2009) or 'linked' mudflow (Haughton *et al.*, 2009), followed by a slow fallout of hemipelagic 'background' mud? The other controversial issue is the origin of the early Oligocene Magdalena Sandstone of the

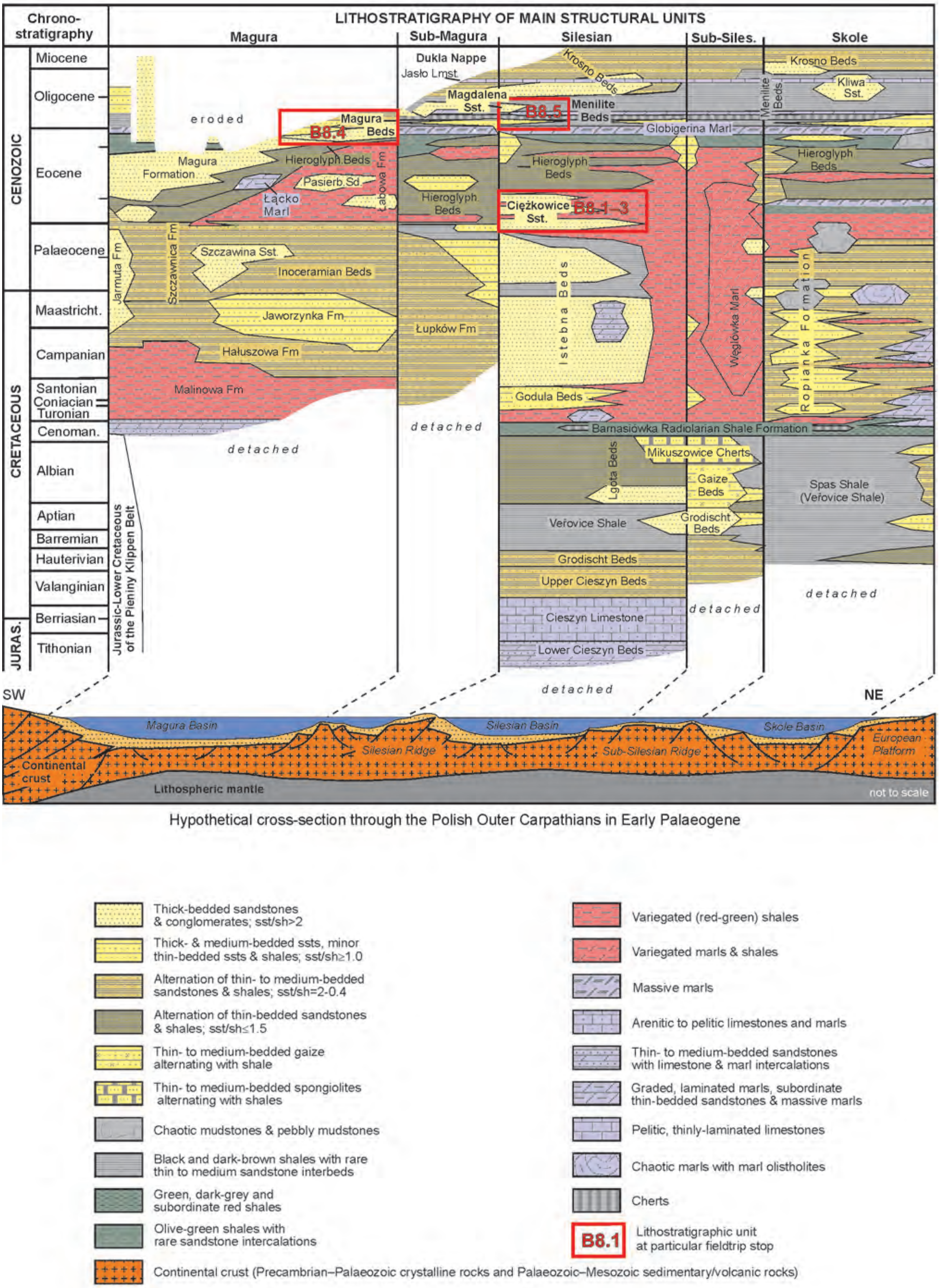

Fig. 4. Lithostratigraphic scheme for the Jurassic–Miocene rock successions of the Polish Outer Carpathians. Modified from Koszarski (1985) and Oszczypko (2004). Note the stratigraphic location of the Ciężkowice Sandstone (field-trip stops B8.1–3), Magura Beds (stop B8.4) and Magdalena Sandstone (stop B8.5).

Silesian Nappe (Fig. 4) near Gorlice: a coarsening-upwards succession (nearly 200 m thick) underlain and overlain by deep-marine flysch, showing heterolithic lenticular and wavy bedding, occasional hummock-like and wave-ripple-like structures and a mouth bar-type bedding architecture towards the top. Can this be an evidence of relatively shallow water and a prograding delta?

Field-trip topic 1: How do the classic 'fluxoturbidites' compare with the latest turbiditic models?

Stanisław Leszczyński, Wojciech Nemec

What are fluxoturbidites?

Until the mid-20th century, sedimentation in deep seas was considered to be almost exclusively pelagic and hemipelagic, with possible sediment mass-transport processes – such as mud slides, slumps and vaguely defined sediment flows – on submarine slopes. Meanwhile, oceanographic data had increasingly indicated deep-water sand dispersal over large areas, and similar evidence of laterally extensive graded sandstone beds came from the successions of ancient deep-marine deposits referred to broadly as flysch (Studer, 1827). This dual evidence, combined with laboratory experiments, had led Kuenen and Migliorini (1950) to the recognition of turbidity currents: sand-laden subaqueous density flows with their sediment load carried in, and gradationally settling from, a fully mixed turbulent suspension. However, the concurrent meticulous studies of the Polish Carpathian flysch had revealed several turbiditic successions – such as the lower Lgota Sandstone (Albian), Istebna Sandstone (Santonian– Palaeocene) and Ciężkowice Sandstone (early Eocene) (Fig. 4) – where deposits were not quite compatible with the original concept of sediment fallout from a fully turbulent density current. For historical reasons, it is worth citing here the original perception of such deposits and notion of their possible origin (Dżułyński *et al.*, 1959, p. 1114):

'A different type of sedimentation is encountered amidst normal turbidites in many places. In this type the grain size is large and the beds tend to be less muddy. The bedding is thick and rather irregular, and the shales between are silty to sandy and thin or even absent. Current sole markings are scarce, load casting is more common, and coarse current bedding of somewhat variable direction is encountered. Indications of slumping are found, and grading is absent, repetitive, irregular, or even inverted, and irregular lenses of coarser grain occur inside the beds. These sandstones may occur as large lenses between normal flysch or shales. In other cases the material or the direction of supply contrast with those of the normal surrounding flysch of the same age. Because characteristics of deposition from turbidity currents appear to be mixed with evidence for sliding, we prefer to call this kind of bed a 'fluxoturbidite'. 'We suggest that the cause for this abnormal type of flysch can be either a deepening of the basin and steepening of the slope, or a quickening of the supply, or a change in position of the supply, for instance the building of a new delta. But whatever the cause, the mode of transportation has changed. Instead of a well-mixed turbulent turbidity current carrying almost the entire load in suspension, one can imagine a turbidity current in which most of the sand and gravel moves in a watery slide along the base. The current is too poor in clay to raise this load in suspension, and the slope is too steep for the load to come to rest until it has spread out in a layer.'

The first detailed documentation of the sedimentary textures and structures of such deposits was given by Unrug (1963) from the Istebna Beds (Fig. 4). His descriptive summary said:

'Fluxoturbidite deposits are characterised by lenticular shapes of beds, coarseness of detrital material, great thickness of beds, low pelite content, prevalence of symmetrical, multiple and discontinuous grading over other types of bedding and occurrence of non-graded beds, traces of strong erosion, lack of sole markings, and poor development of pelitic sediments. Occurrence of armored shale balls arranged in regular layers parallel to the bedding planes within sandstone beds points out to the transition of sand flows into turbidity currents.'

The author referred to the depositional process of fluxoturbidites vaguely as a 'sand flow' and considered it to be a type of mass movement 'intermediate' between a slump and a turbidity current.

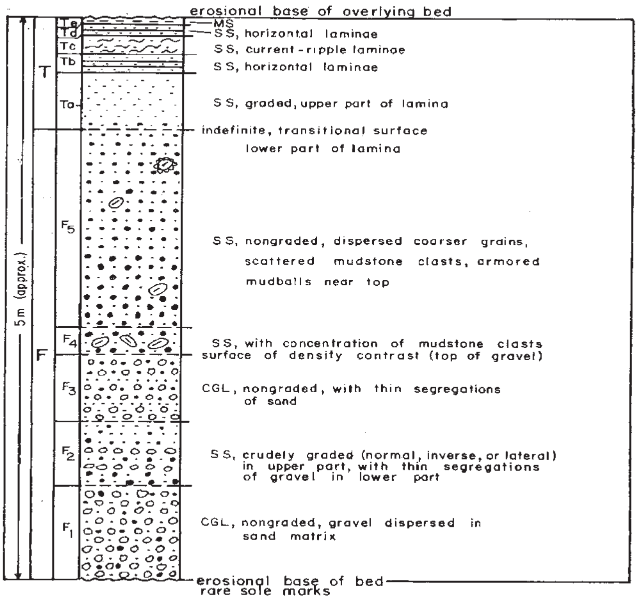

Fig. 5. Model of a complete fluxoturbidite according to Ślączka and Thompson (1981).

Another synthesis of fluxoturbidite characteristics came from Ślączka and Thompson (1981), based on field observations from selected outcrops of the lower Istebna Beds, the Ciężkowice Sandstone and the late Oligocene Krosno Beds (Fig. 4). Their model of a fluxoturbidite deposit (Fig. 5) shows a mainly massive bed of poorly sorted sand and invokes both the possible multitude of grain-support mechanisms in a sedimentgravity flow (Middleton and Hampton, 1973, 1976; Middleton and Southard, 1977) and the Bouma (1962) turbidite divisions as a capping. Fluxoturbidite was suggested to be 'a product of a composite sedimentgravity flow, with a gravity grain flow (or related type) in the lower part and a turbidity flow in the upper part.' Evidence of slumping was said to be unclear. Instead, a liquified flow (*sensu* Lowe, 1979) was implied as a possible initiation mechanism and main component process for the deposition of fluxoturbidites.

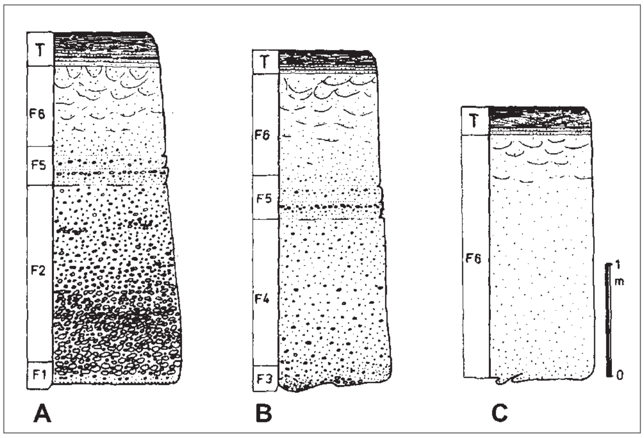

Fig. 6. Models of complete fluxoturbidites according to Leszczyński (1989), showing their (**A**) conglomeratic, (**B**) pebbly-sandstone and (**C**) sandstone bed varieties and their internal divisions.

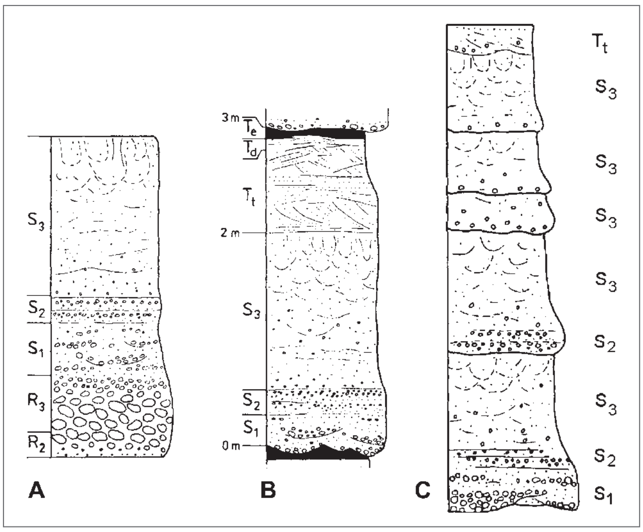

Fig. 7. Models of the deposits of high-density turbidity currents according to Lowe (1982), showing ideal beds of a gravelly (**A**) and a sandy high-density turbidity current (**B**) and a composite bed produced by a multi-surge high-density turbidity current (**C**).

A similar interpretation of fluxoturbidites was given by Leszczyński (1981, 1986, 1989) from a detailed study of the Ciężkowice Sandstone. The deposits showed thick and highly uneven, non-tabular bedding; common erosional amalgamation of beds, with only local separation by relic thin silty or sandy mudshale; poorly developed internal normal grading; massive (non-stratified) internal structure or horizontal to variously inclined parallel stratification, yet with surprisingly thick (2–5 cm) strata; and common diffuse lateral transitions from stratified to massive deposit within a single bed. The models of complete (nontruncated) fluxoturbidite beds (Fig. 6) were attributed to subaqueous high-density bipartite, or two-phase, flows similar to those defined as 'high-density turbidity currents' by Lowe (1982) (Fig. 7), but with a greater emphasis on the role of liquefied flow and cohesionless debris flow as depositional process components. The abundant composite beds were attributed to the amalgamation of successive flow deposits or deposition from multi-surge long-duration flows.

Allaby and Allaby (1999) in their dictionary defined fluxoturbidite vaguely as 'the product of gravity-induced flow in which little turbulent mixing of particles occurs [and which] is transitional between a slump and a turbidity flow.' Such a transitional flow would expectedly be a debris flow (see Middleton and Southard, 1977). Indeed, the deposits of the Istebna Beds originally regarded as fluxoturbidites (Dżułyński *et al.*, 1959; Unrug, 1963; Ślączka and Thompson, 1981) have more recently been interpreted by Strzeboński (2014) as the products of non-cohesive to cohesive sand-gravelly submarine debris flows.

Not surprisingly, the convoluted definition of fluxoturbidites and their somewhat ambiguously inferred mode of deposition have gained little general acceptance. Although many geologists in the Polish Carpathians and elsewhere found it to be a useful label for the flysch facies variety of non-classical turbidites (e.g., Stanley and Unrug, 1972; Schlager and Schlager, 1973) and the term was included in Carter's (1975) early classification of submarine sediment mass-transport processes, several other prominent authors had openly postulated that this term should be abandoned (e.g., Walker, 1967; Hsü, 1989; Shanmugam, 2006) – yet failing to recognize its significance as a genuine precursor of the Lowe (1982) concept

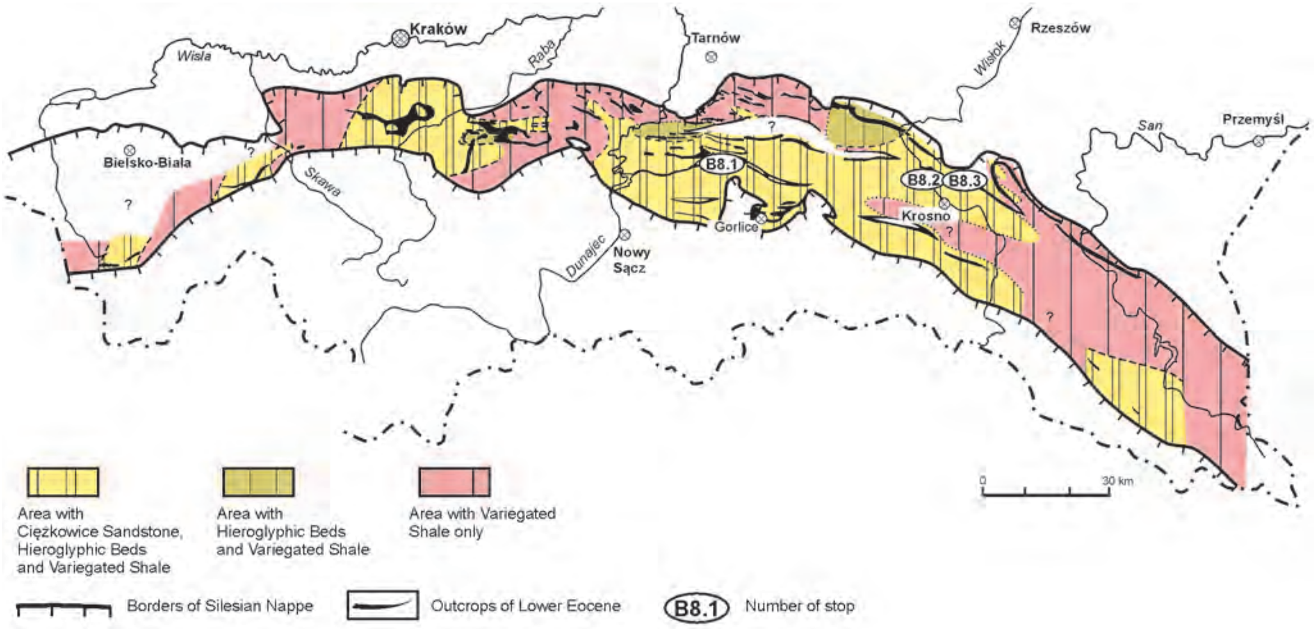

Fig. 8. Interpreted areal distribution of the Ciężkowice Sandstone, Variegated Shales and Hieroglyphic Beds in the latest Paleocene – early Eocene Eocene of the Silesian Basin (modified from Leszczyński, 1986); for lithostratigraphy, see Silesian Nappe in Fig. 4.

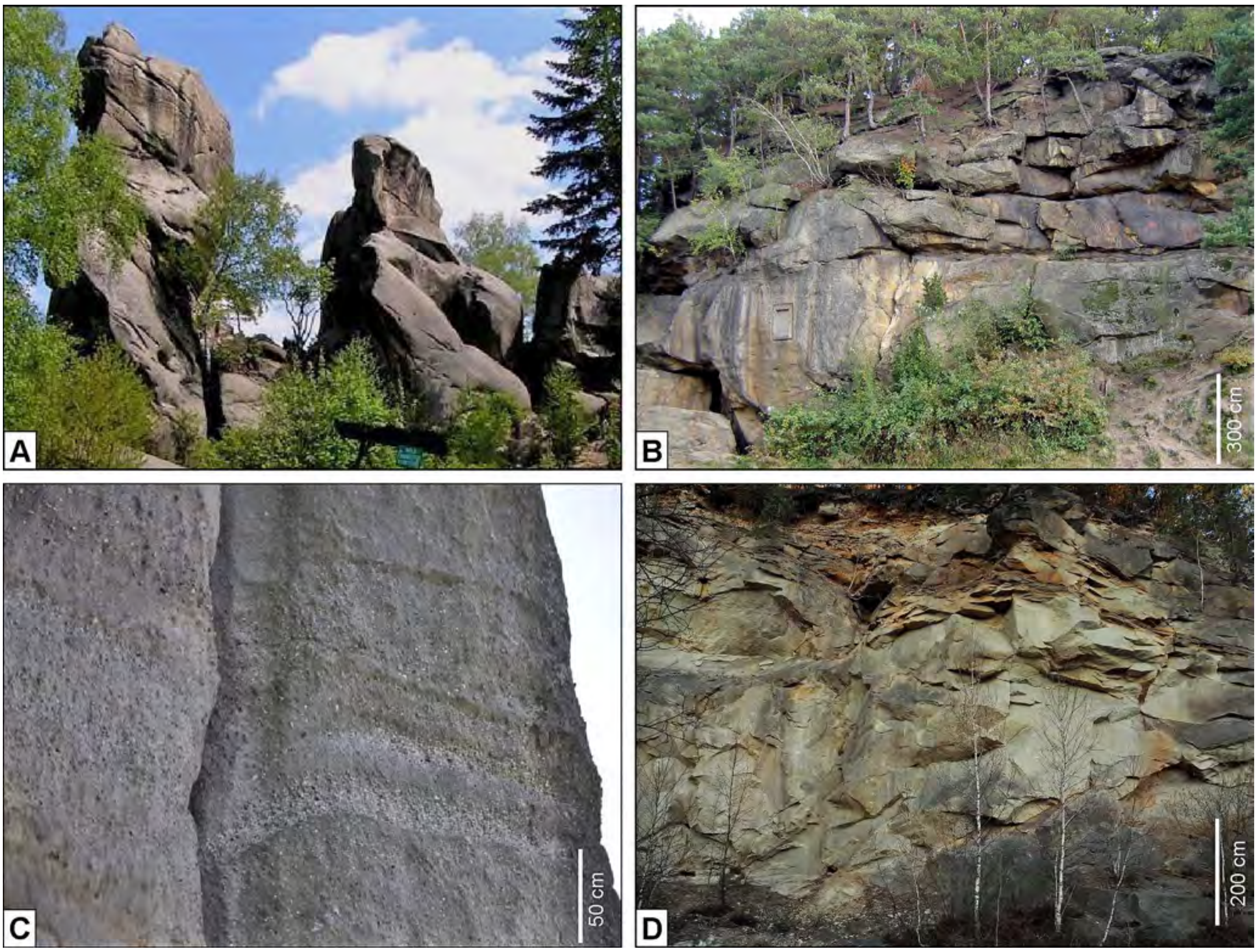

Fig. 9. General characteristics of the Ciężkowice Sandstone. (**A**) Rock tors showing amalgamated thick sandstone beds; nature reserve 'Prządki' (stop B8.3). (**B**) Amalgamated beds of sandstone and granule conglomerate, with the bedding more recognizable to the right; tor 'Grunwald' in the nature reserve 'Skamieniałe Miasto' (stop B8.1). (**C**) Massive and parallel stratified/banded pebbly sandstone and fine-pebble conglomerate, with the conglomerate layers often lenticular and showing inverse to normal grading; rock tor under the northern wall of the Kamieniec Castle (stop B8.2). (**D**) Freshly exposed section of a thick composite unit of amalgamated sandstone beds; quarry in Ostrusza village, SE of Ciężkowice.

of 'high-density turbidity currents'. Some geologists, not only in the Flysch Carpathians, are still using this term nowadays, although not always correctly realizing its original intended meaning (e.g., Huang *et al*., 2012).

Fluxoturbidites of the Ciężkowice Sandstone

The Ciężkowice Sandstone (latest Palaeocene–early Eocene; Fig. 4) is a sand-dominated lithostratigraphic unit, up to 350 m thick, occurring mainly in the southern to middle part of the Silesian Nappe (Fig. 8). It is one of the nappe's main petroleum-producing units. The unit consists of thick-bedded (mainly 1–4 m), coarse-grained sandstones and granule/fine-pebble orthoconglomerates (Fig. 9) with rare thin interbeds of fine-grained sandstones and silty/sandy mudstones. Sandstones are quartzose to subfeldspathic arenites, subordinately low-grade wackes (Leszczyński, 1981). The coarse-grained beds have sharp, erosional and often loaded bases (Fig. 10), are lenticular in flow-transverse sections and occur as isolated or vertically stacked bodies (bed packages up to >50 m thick) within the succession of Variegated Shales (Fig. 4). Beds are mainly non-graded to normal-graded and massive to parallel stratified (Figs 9D, 11), although the strata are often 'stepped', diffuse and unusually thick (Fig. 11). The thickest beds also show inclined stratification mantling massive sand bodies (Fig. 12), trough-shaped scour-and-fill cross-stratification (Fig. 13A, B) and local internal slumps or rotational slides related to substrate re-scouring. Locally present are sets of tensile wing/horestail fractures (Fig. 13C, D), occasionally misinterpreted as

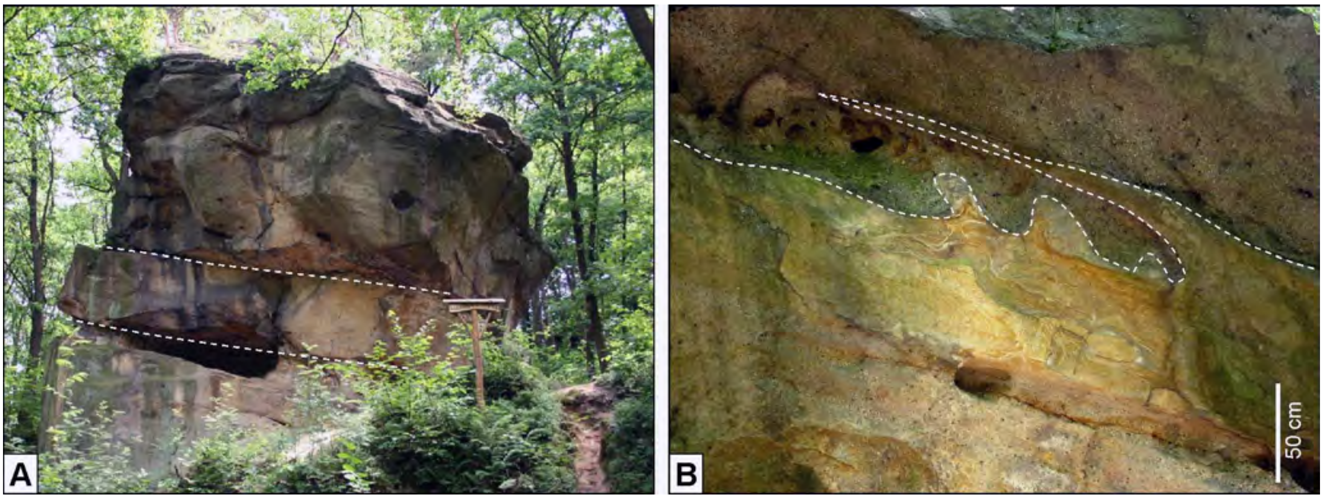

Fig. 10. Variable bed boundaries in the Ciężkowice Sandstone. (**A**) Beds separated by erosional flat surfaces (dashed lines); rock tor 'Warownia Górna' in the nature reserve 'Skamieniałe Miasto' (stop B8.1). (**B**) Highly uneven, loaded erosional contact of fluxoturbidite beds with a large load-flame of sand; detail from rock tor 'Warownia Dolna' in the nature reserve 'Skamieniałe Miasto' (stop B8.1).

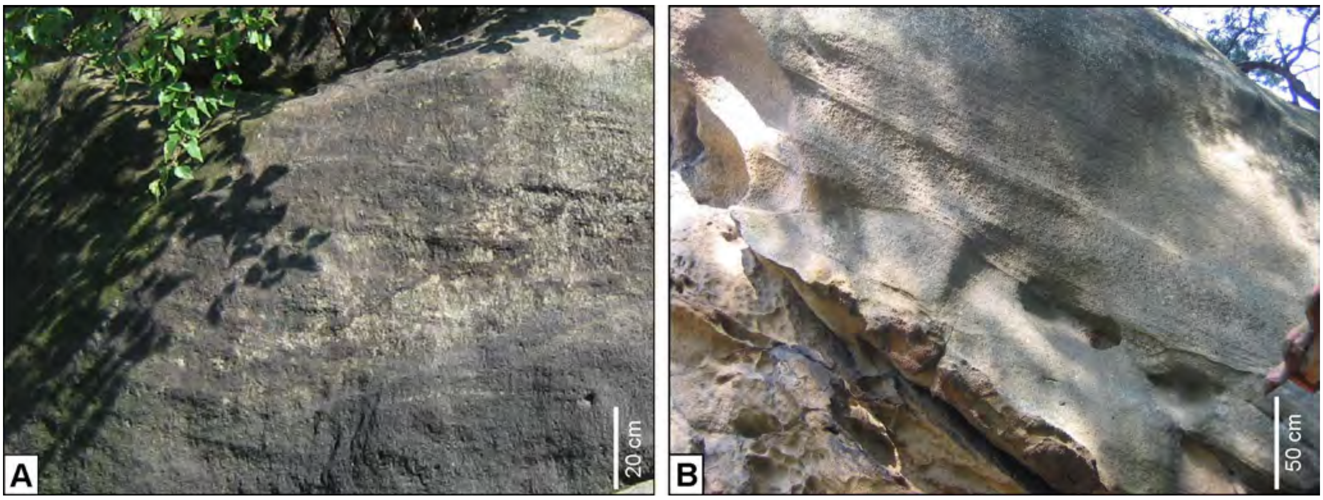

Fig. 11. Variable development of parallel stratification in sandstone beds. (**A**) Diffuse banding and spaced parallel stratification (seen as rock surface ribs), slightly undulating; detail from a rock tor in the nature reserve 'Prządki' (stop B8.3). (**B**) Amalgamated normal-graded sandstone beds, each showing thick banding with spaced parallel stratification and a massive upper part; detail from rock tor at point 3, stop B8.2.

cross-stratification (e.g., Ślączka and Thompson, 1981; Dziadzio *et al*., 2006). Some beds show isolated scour-fill gravel pockets (Fig. 14). Characteristic are short-distance lateral transitions from parallel stratified or shear-band-

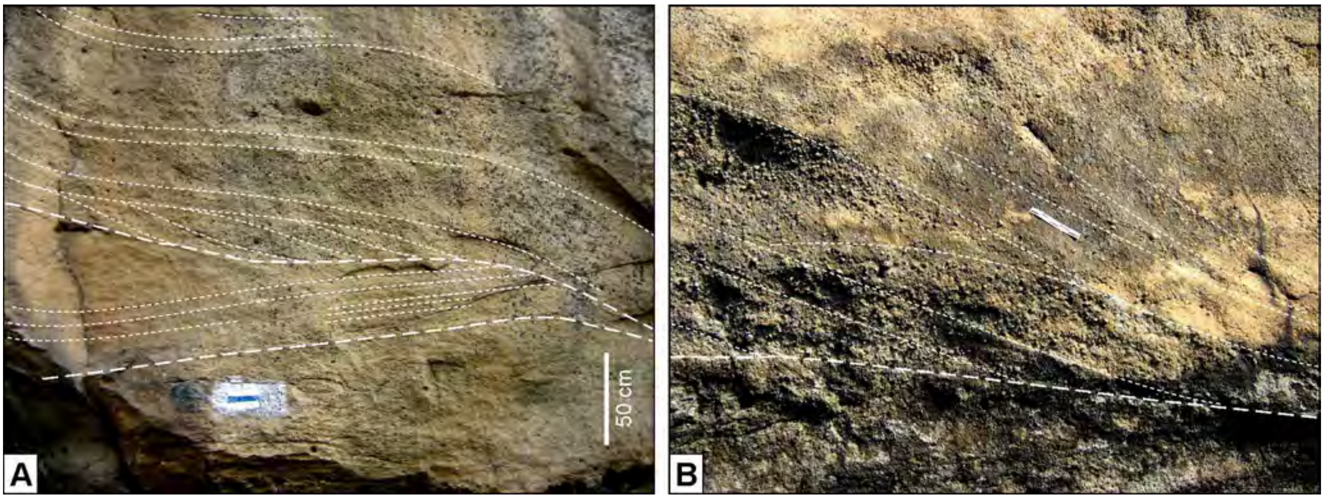

Fig. 12. Cross-stratification in sandstone beds. (**A**) Scour-fill cross-stratification with weak grain-size segregation (see above the upper thick dashed line); detail from rock tor 'Grunwald' in the nature reserve 'Skamieniałe Miasto' (stop B8.1). (**B**) Granule sandstone with planar cross-stratification (above the thick dashed line) scoured to the right and overlain by a massive wedge of granule sandstone mantled with crossstratification; rock tor detail from the nature reserve 'Prządki' (stop 8.3).

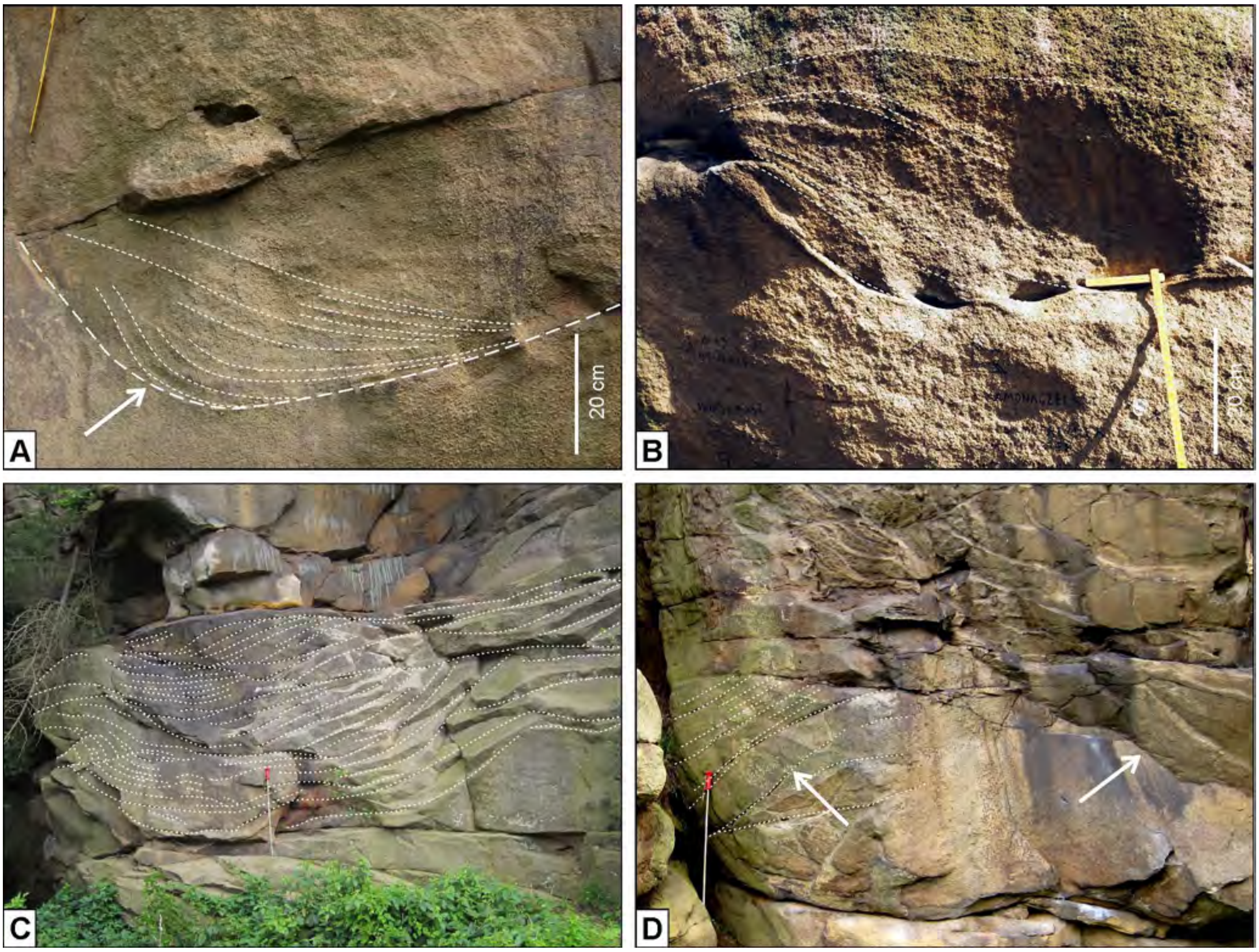

Fig. 13. Pseudo-stratification in sandstone beds. (**A**) Steep shear-banding resembling scour-fill crossstratification; detail from rock tor 'Ratusz' in the nature reserve 'Skamieniałe Miasto' (stop B8.1). (**B**) A similar shear-banding in rock tor "Orzeł" in the same reserve (stop B8.1). (**C**) Sets of wing or horsetail tensile fractures resembling trough cross-stratification; the walking stick (scale) is 1.1 m; from rock tor 'Ratusz' in the same reserve (stop B8.1). (**D**) Similar steep tensile fracturing resembling crossstratification (arrows); the walking stick (scale) is 1.1 m; from rock tor 'Czarownica' in the same reserve (stop B8.1).

ed to massive deposit (Fig. 15). Five main fluxoturbidite facies can be distinguished (Appendix Table 1, Fig. 16). They alternate with one another in amalgamated bed packages, and one facies commonly passes laterally into another within a single bed.

Benthic foraminifers in the 'background' Variegated Shales represent the Recurvoides assemblage of Haig (1979), indicating a bathyal water depth (Olszewska & Malata, 2006). The overlying thin-bedded flysch of the Hieroglyphic Beds, also locally intercalated with the Variegated Shales (Fig. 4), may possibly be almost abyssal (Waśkowska and Cieszkowski, 2014).

The depositional setting of the Ciężkowice Sandstone was interpreted as a submarine fan system with channels and small depositional lobes (Leszczyński, 1981), and

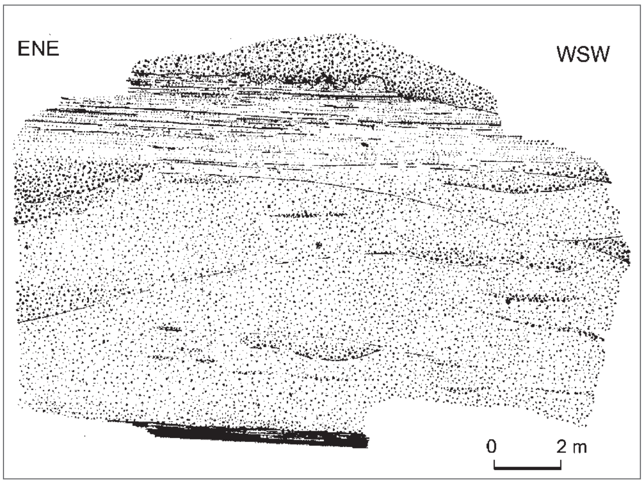

Fig. 14. Graded sandstone with scour-fill gravel pockets, passing upwards into planar parallel- stratified sandstone overlain by a graded pebble conglomerate with load-casted base. Outcrop detail from the old quarry in Kąśna Dolna, 3 km west of Ciężkowice.

was considered to be a basin-floor fan related to a second-order eustatic lowstand (Dziadzio *et al*., 2006). The stratigraphic alternation of sandstone- and shale-dominated deposits was attributed to third-order eustatic cycles (Dziadzio *et al*., 2006). Spatial sand distribution (Fig. 8) indicates main sediment supply from both the south and north, with palaeocurrent directions towards the SE and E and locally to the NE. According to Enfield *et al*. (2001a, b) and Watkinson *et al*. (2001), the bodies of Ciężkowice Sandstone show spatial thickness changes and unconformities suggestive of deposition in half-grabens. A similar interpretation of seismic images was given by Dziadzio *et al*. (2006), suggesting deposition in a series of fault-bounded basin-floor depressions. The sand-prone turbiditic system would thus appear to have extended eastwards along an array of basin-floor troughs, perhaps active blind-thrust synclines evolving into fault-bounded half-grabens, with possible sediment supply from the inter-trough ridges. The lack of lateral-accretion bedding indicates non-meandering, cut-andfill channels of low to negligible sinuosity, apparently non-levéed, which might support the notion of flow confinement by intra-basinal topographic troughs.

Comparison with the latest turbiditic models

As shown by their outcrop review, the Polish Carpathian 'fluxoturbidites' are by no means just a regional curiosity. Such non-classical turbidites are found in flysch

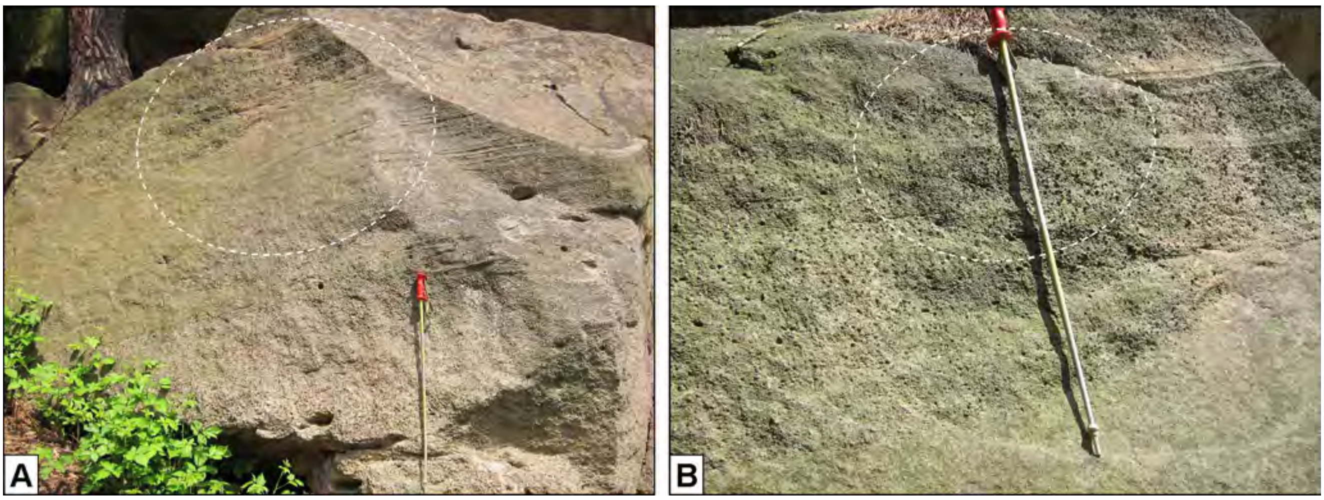

Fig. 15. Short-distance lateral changes in bed structure. (**A**) Granule sandstone bed with planar parallel stratification and traction-carpet banding passing diffusely into massive deposit to the left (encircled). (**B**) Stepped sandy parallel stratification vanishing to the left in a banded granule conglomerate. The walking stick (scale) is 1.1 m. Both details are from detached blocks in the nature reserve 'Skamieniałe Miasto' (stop B8.1).

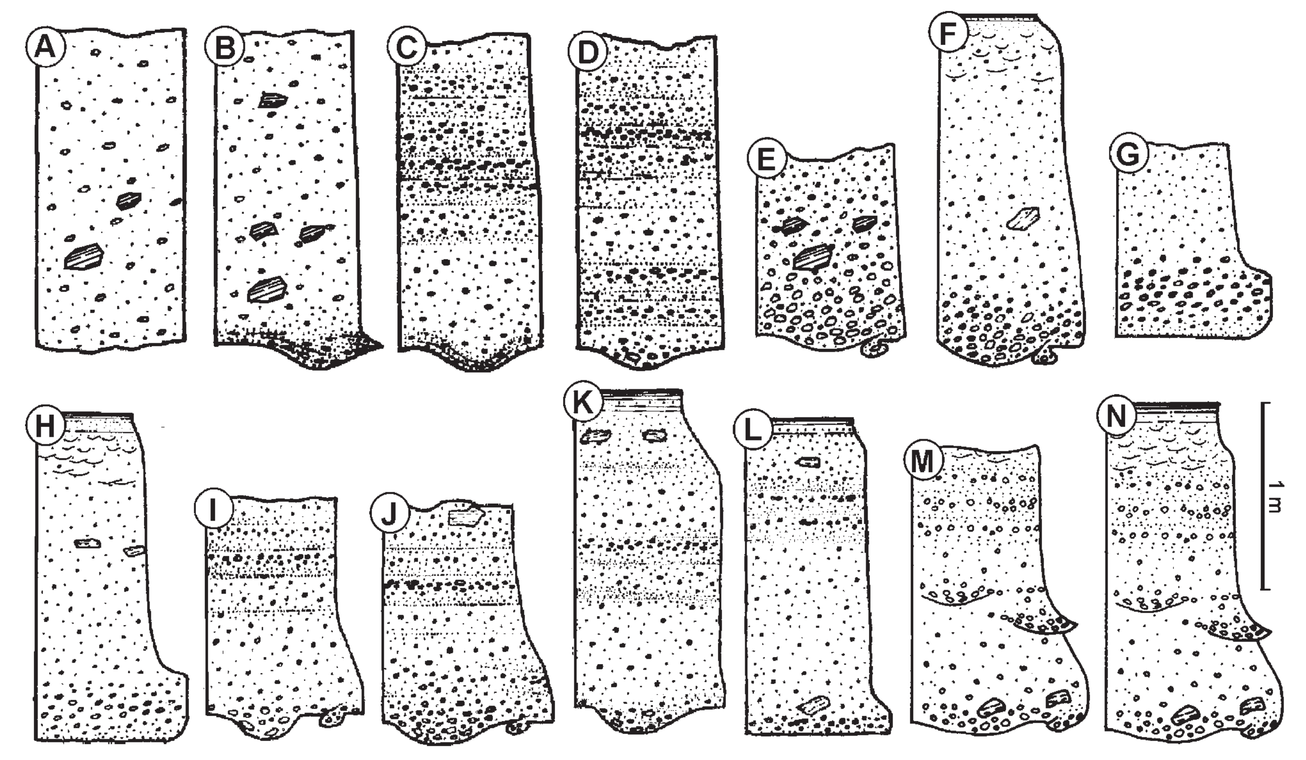

Fig. 16. Summary of the fluxoturbidite facies of Ciężkowice Sandstone (for description, see review in Appendix Table 1). (**A**, **B**) Facies mS: massive, non-graded sandstones with scattered granules/pebbles and local trough-shaped basal scour-fill stratification. (**C**, **D**) Facies tlsS: massive to banded or fully banded beds with local basal scour-and-fill features. (**E**–**H**) Facies gS: graded non-stratified sandstone or conglomerate–sandstone beds. (**I**–**L**) Facies gsS: graded-stratified/banded sandstone and conglomerate-sandstone beds. (**M**, **N**) Facies Scl: graded sandstone beds with lenticular gravel pockets and banded upper part.

basins worldwide. Similar deposits were included in the early turbiditic facies models (see facies A and B of Mutti and Ricchi Lucchi, 1972, 1975; also Walker and Mutti, 1973) and were depicted as channelized-flow facies in the well-known submarine fan model of Walker (1975). The early notion of a high-concentration bipartite (two-phase) turbidity current, highlighted by Dżułyński and Sanders (1962) and Sanders (1965), found its elaborate reflection in Lowe's (1982) benchmark concept of high-density turbidity currents (HDTCs). The depositional mechanisms postulated by Lowe (1982) included: a rapid dumping of graded massive sediment directly from turbulent suspension; in situ or mobile sediment liquefaction; formation of inverse-graded traction carpets, possibly multiple; infilling of syndepositional trough-shaped scours; and a plane- to rippled-bed tractional sediment transport. As pointed out by Leszczyński (1986, 1989), most of the distinctive features of fluxoturbidites could readily be explained by a combination of these various modes of sediment deposition from unsteady or relatively steady HDTCs. The few features not shown in Lowe's (1982) model included bed-scale or localized sediment banding (planar or inclined thick pseudo-stratification, with the sediment layers lacking inverse grading), scour-related local syndepositional sliding, pronounced vertical grain-size fluctuations and the short-distance rapid lateral changes in bed internal characteristics.

However, it is worth noting that Lowe's (1982) depositional model for HDTCs was not faultless. Firstly, he unnecessarily restricted the term 'traction carpet' – originally meant for a laminar-shear dense basal layer of sediment dragged along by turbidity current (Dżułyński and Sanders, 1962) – to denote solely a shearing sediment layer of fallen grains characterized by inverse grading and deposited by frictional freezing when reaching a maximum mobile thickness (see Hiscott, 1994). Secondly, he apparently failed to realize that a certain travel time/distance is required for the inverse grading to develop and that a quickly freezing carpet may thus show little or no such grading, and also that a repetitive pattern of such banded deposition may virtually dominate in a long-duration relatively steady flow. When he later encountered thick banded turbidites composed almost entirely of traction carpets that lacked inverse grading and were attributed to a repetitive combined frictional-cohesive freezing (Lowe and Guy, 2000; Lowe *et al.*, 2003), instead of correcting his initial error – he chose rather to refer to such turbidity currents misleadingly as 'slurry flows'. [The same term was used earlier in Carter's (1975) mass-flow classification to denote cohesive debris flows.]

Various other conceptual models for turbidite deposition have meanwhile proliferated, inspired by the growing evidence from outcrops, well-cores and laboratory experiments. How do the fluxoturbidites relate to these more recent concepts in their historical development? (The following review refers to plates given as appendix illustrations in the digital version of this excursion guide.)

- Postma *et al.* (1988) reported on laboratory experiments where a well-stirred turbulent sediment-water mixture, released from a gate onto a steep (25°) subaqueous slope, had rapidly separated itself into a coarse-grained (pebbly sand) lower non-turbulent phase and a finer-grained (sand), faster-flowing upper turbulent phase (see Plate 1A). The lower phase was flowing chiefly due to its own inertia, while being modestly sheared at the top by the overpassing turbulent flow. The lower inertia flow was subject to laminar shear and came to rest by downward frictional freezing, as a common debris flow. Such a bipartition and combined behaviour of an initially turbulent sediment-gravity flow might explain the thick, non-graded massive lower part of some of the fluxoturbidites (Fig. 16).

- Vrolijk and Southard (1997) reported on laboratory experiments with fast-flowing sandy subaqueous flows, where the sediment dumped from turbulent suspension kept moving as a 'mobile bed' sheared by the overpassing turbulent flow. The mobile bed was freezing upwards as the shear zone was similarly migrating and thinning. The laboratory flows were too thin for recognition of possible shear banding in the deposits, which ranged from non-graded to weakly normal, inverse or inverse-to-normal graded (Plate 1B). Some of the diffusely banded or massive-to-banded and non-graded to weakly graded fluxoturbidites (Fig. 16) might be attributed to this style of deposition.

- Some authors (Mulder and Alexander, 2001; Sohn *et al.*, 2002) suggested a transitional phase of 'hyperconcentrated flow' in the transformation process of a non-turbulent to fully turbulent subaqueous sediment-gravity flow (Plate 2). The fluxoturbidites with their features would fall into this transitional flow category. However, the use of the term hyperconcentrated flow was quite odd, as this term was originally introduced in the literature to denote subaerial flows with 'a behaviour intermediate between that of a common streamflow and that of a mudflow' (Beverage and Culbertson, 1968; see also review and discussion by Nemec, 2009). Notably, neither a fluvial streamflow nor a mudflow is involved in the subaqueous flow transformations envisaged by Mulder and Alexander (2001) and Sohn *et al.* (2002).

- The early concept of a bipartite two-phase flow derived from the Carpathian fluxoturbidites (Sanders, 1965) and the Lowe (1982) concept of HDTCs were both closely followed in the model of a non-turbulent to fully turbulent flow transformation suggested by Mutti (1992) and Mutti *et al.* (2003), where fluxoturbidites would correspond to the turbidite facies F3–F5 and F7– F9 (Plate 3A). It was concurrently argued by Shanmugam (1997, 2000, 2002, 2012) that such high-density flows, with a mainly non-tractional mode of deposition, should rather be regarded as sandy debris flows. (As a paraphrase, it was like saying that a snow scooter is not a scooter because it has sleds instead of wheels. However, it is the sleds that define a snow scooter, just like the non-tractional mode of sediment deposition from turbidity current defines Lowe's HDTC.)

- An opposite way of subaqueous sediment gravity-flow transformation – from a fully turbulent to bipartite laminar-turbulent flow (see earlier Postma *et al.*, 1988) – was suggested by Kane and Pontén (2012), where the fluxoturbidites would again correspond to the 'transitional flow' category (Plate 3B). The notion of a turbidity current with a downflow-increasing sediment concentration came from Haughton *et al.* (2009); see below.

- Haughton *et al.* (2009) distinguished between turbidity currents with a downflow-decreasing and a downflow-increasing sediment concentration (Plate 4A, upper diagram), although this hypothetical notion apparently pertained chiefly to the behaviour of the turbiditic suspension mud cloud – whether diluting and dying out with time/distance or densifying and turning into a 'linked' mudflow. The sandy deposits of the transitional 'hybrid flows' (Plate 4B) seem to share many features with the fluxoturbidites (Fig. 16). Much less clear is Haughton's own classification of subaqueous sediment-gravity flows (Plate 4A, lower diagram), with the category of 'high-density turbidity current' separated from the Lowe and Guy (2000) 'slurry flow' and the enigmatic 'co-genetic flow'. Several questions arise. First, aren't the two latter kinds of flow just specific varieties of HDTC (*sensu* Lowe, 1982)? Second, if a co-genetic flow = hybrid flow = linked mudflow, as the classification implies, then why are so many different terms needed for one and the same thing? And third, how about the co-genetic basal debris flows: a possible relic of parental debris flow that generated the turbidity current (Hampton, 1972), a debris flow spawned by the turbulent current at the outset (Postma *et al.*, 1988) or spawned by the current underway due to its deceleration or turbulence-suppressing bulking of substrate sediment (Kane and Pontén, 2012)?

- In the most recent classification of subaqueous sediment-gravity flows proposed by Talling *et al.* (2012), the fluxoturbidites with their features would be categorized as the deposits of HDTCs (sensu Lowe, 1982), possibly with a 'melted' core of the parental non-cohesive debris flow or liquefied flow (Plate 5A). The authors pointed to a range of modes of sediment deposition that may result in thick banded or massive beds, with or without grain-size grading (Plate 5B). Depending on the relative rates of bottom shear and grain fallout, the banding may range from common tractional plane-bed parallel stratification or 'stepped' stratification to rhythmically freezing graded or non-graded traction carpets and to mobile-bed diffuse shear layers. Although some of the detailed notions in the models (Plate 5) may be disputable, they jointly give a stimulating ground for conceptual considerations.

In summary, the deposits originally labelled as 'fluxoturbidites' represent laterally non-uniform and highly unsteady to fairly steady, cohesionless high-density and mainly long-duration flows (sustained flows *sensu* Kneller and Branney, 1995). Deposits with a similar range of transient modes of sedimentation now feature prominently in all the more recent turbiditic models. The recognition of fluxoturbidites as a distinct facies in the Polish Carpathian flysch was based also on their regional uniqueness in terms of the high mineralogical and textural maturity and their grain-size coarseness. However, it was probably these very sediment characteristics that also determined the relatively 'unusual' mode of sediment transport and deposition. Today, we know that similar coarse-sandy arenitic to gravelly deposits abound in ancient non-meandering turbiditic channel belts worldwide (e.g., Walker, 1975, 1978; Winn and Dott, 1977; Stanley, 1980; Lowe, 1982; Gosh and Lowe, 1993; Hickson and Lowe, 2002; Janbu *et al.*, 2007). In short, there is nothing specifically 'Carpathian' to the classic fluxoturbidites, except for the region of their early first recognition. As a conclusion, it is suggested that the term 'fluxoturbidites' (Dżułyński *et al.*, 1959) – although discarded by the global sedimentological community at the outset and now nearly forgotten – deserves full recognition as an early precursor of the concept of HDTCs (Lowe, 1982). There is also no reason why this term should not be used as a short and informative general facies label in regional studies, as it continues to be used in the Polish Carpathian flysch.

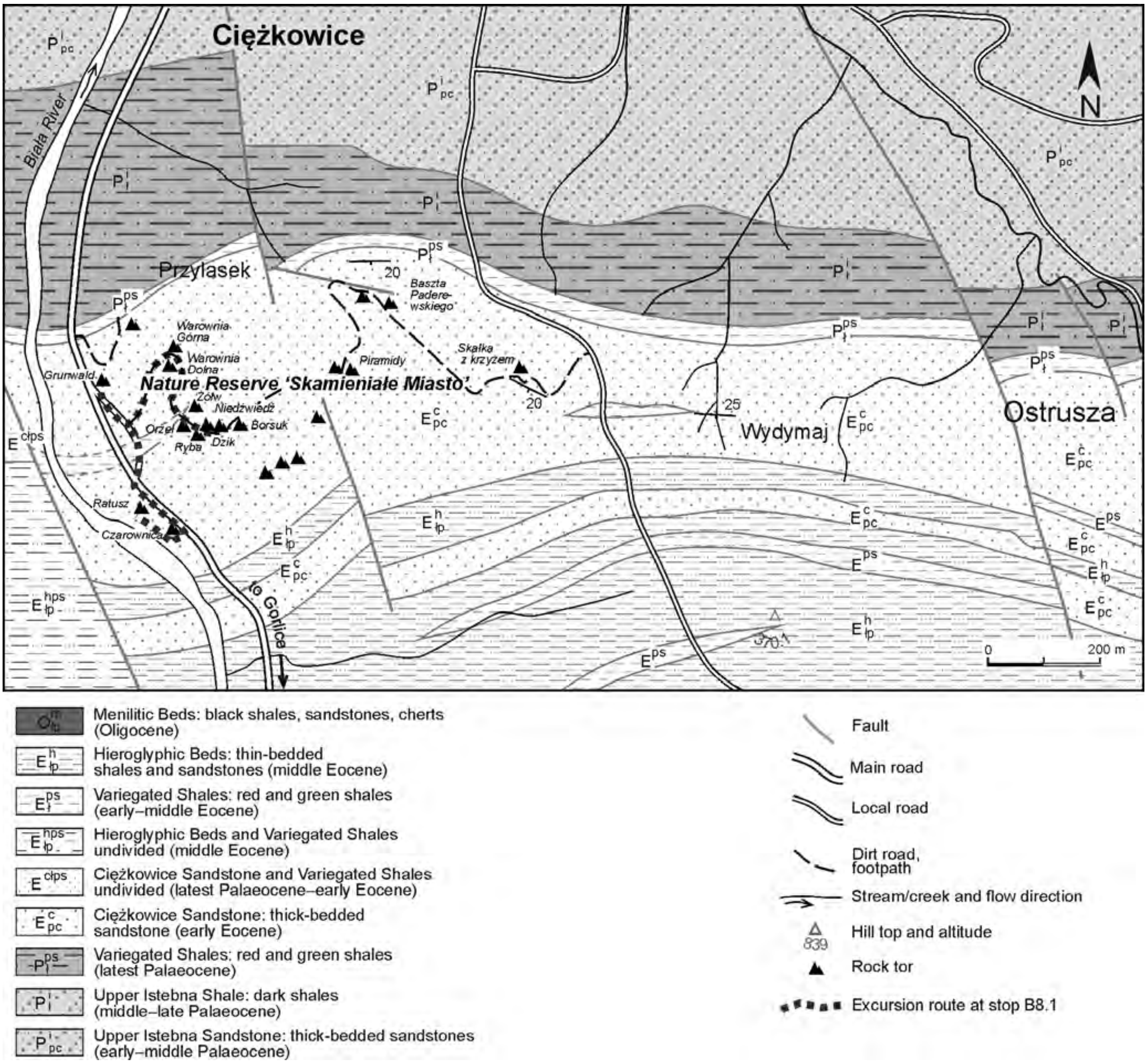

Fig. 17. Geological map of the vicinity of nature reserve 'Skamieniałe Miasto' (modified from Cieszkowski *et al.*, 1991), showing the location of rock tors to be visited at the excursion stop B8.1 (see text).

Stop descriptions for topic 1

Leaders: Stanisław Leszczyński, Wojciech Nemec

The outcrops at stops B8.1–3 are easily accessible by short (5–10 minutes) uphill walks along touristic footpaths. The aim of the field excursion on its first day is to demonstrate and discuss the sedimentary characteristics of classical fluxoturbidites, exemplified by the deposits of the Ciężkowice Sandstone, and to compare these deposits with the more recent turbiditic models published in the sedimentological literature.

B8.1 The nature reserve 'Skamieniałe Miasto'

The nature reserve 'Skamieniałe Miasto (Petrified Town)' is located at the southern outskirts of Ciężkowice (Figs 1, 17). The entrance is free of charge and the reserve has a convenient parking lot with a modest gastronomic facility and with the regulations for visitors displayed. This area in the east-central part of the Silesian Nappe (Figs 2, 8) is considered to be the type locality for the early Eocene Ciężkowice Sandstone (Fig. 4), exposed here as numerous picturesque rock tors scattered in a pine forest. (49°46′36″ N, 20°57′50″ E)

Point 1.1 – The 'Grunwald' tor on the eastern side of the main road, to the left of the main entrance to the reserve (Fig. 17). The outcrop shows thick, amalgamated beds of graded and graded-stratified fine-grained conglomerate to sandstone facies (Fig. 9B). Massive divisions are graded or non-graded. Stratification is mainly planar parallel, thick to thin and marked by grain size segregation, with the fine-grained laminae forming thin ribs on weathered outcrop surfaces (Fig. 12A). Thin parallel stratification (tractional Bouma bdivision) occurs at the top of some beds. Abundant plant detritus occurs on many strata surfaces. The beds are separated by high-relief scour surfaces. Both planar and cross-stratification with inverse grading are visible in the lower part of the outcrop and in the fallen blocks at its foot. Short-distance lateral change from stratified to massive sandstone and granule conglomerate can be seen in a block on the left side of the tor wall (Fig. 15). Holes after armoured mudballs occur in the basal part of the second bed above the tor foot.

Point 1.2 – Tor 'Warownia Dolna (Lower Watchtower)', ca. 100 m to the north-east of the main entrance to

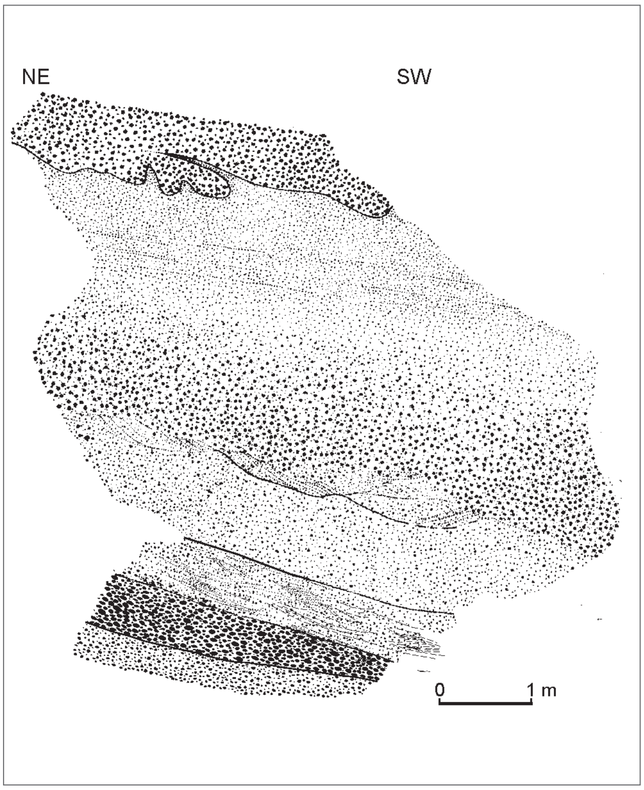

Fig. 18. Outcrop detail from the rock tor 'Warownia Dolna' (stop B8.1, Fig. 17). Note the diffuse parallel banding (traction-carpet layering?), the two levels of trough-shaped multiple scour-fill cross-stratification and the loaded conglomerate base near the top.

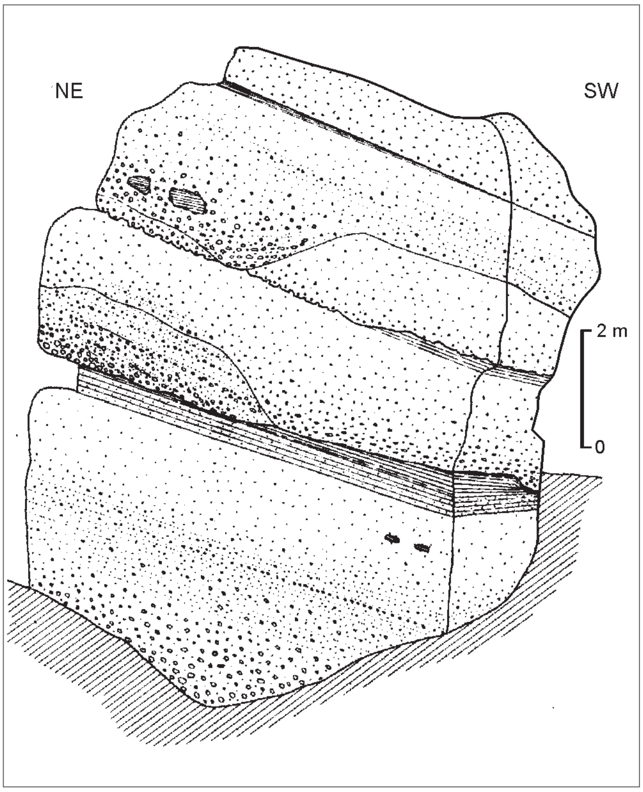

Fig. 19. Amalgamated fluxoturbidites in the north-western wall of 'Warownia Górna' tor (stop B8.1, Fig. 17). Note the evidence of substrate re-scouring by consecutive flows or same-flow surges and the graded-stratified beds with both diffusely banded and well-stratified (Bouma b) divisions.

the reserve (Fig. 17). The outcrop shows thick amalgamated beds of graded and graded-stratified fine-grained conglomerate to sandstone facies (Fig. 18), with common massive, graded or non-graded divisions. Stratification is marked by grain-size segregation and planar parallel, but includes trough cross-strata sets that may represent small 3D dunes or be scour-and-fill features (see in the middle part of the exposed succession on the tor NW and SE walls). The cross-stratification seems to be related to the reworking of substrate sediment by pulse of highly unsteady current. Bed soles are erosional and show load casts, with a large load-flame of fine-grained sand in the tor's upper part (Figs 10B, 18). Visible are also armoured mudballs and holes after their removal by weathering.

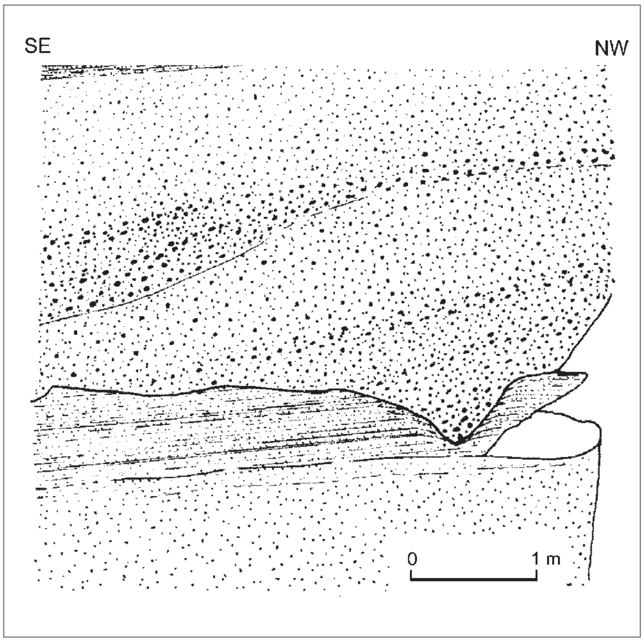

Fig. 20. Graded-stratified sandstone bed overlain erosionally by a granule/pebbly sandstone bed with fluctuating grain size and diffuse banding imitating cross-stratification; detail from the rock tor 'Warownia Górna' (stop B8.1, Fig. 17).

Point 1.3 – Tor 'Warownia Górna (Upper Watchtower)', ca. 20 m to the south-east of point 1.2 (Fig. 17). The outcrop shows amalgamated thick beds of graded and graded-stratified fine-grained conglomerate to sandstone facies (Figs 10A, 19, 20). Bed soles are erosional and show load casts. Graded or non-graded massive divisions irregularly alternate with stratified ones. Planar parallel stratification is marked by segregation of sand and granules, grain composition changes and clast alignment (tractional Bouma b division). However, there is also evidence of shear-banding in the tor's SE wall, indicating an early postdepositional remoulding of sediment by laminar shear. Cross-stratification seems to represent scour-and-fill features, with local syndepositional small-scale rotational sliding. The irregularity of bed divisions indicates highly unsteady currents. Visible are also armoured mudballs and holes after their removal by weathering.

Point 1.4 – Tor 'Orzeł (Eagle)' and the adjacent unnamed tor to the south-east, ca. 100 m to the south of point 1.3 (Fig. 17). Both outcrops show the same beds of graded and graded-stratified sandstone facies. Graded or non-graded massive divisions alternate irregularly with stratified ones. Some of the planar parallel stratification may be laminar shear-banding. Cross-stratification, locally diffuse and unusually steep (Figs 13B, 21), seems to represent scour-and-fill features (slightly deformed by loading) related to the erosive pulses of a highly unsteady current and synsedimentary shearing.

Point 1.5 – Tor 'Czarownica (Witch)' on the western side of the main road, ca. 200 m to the south of the

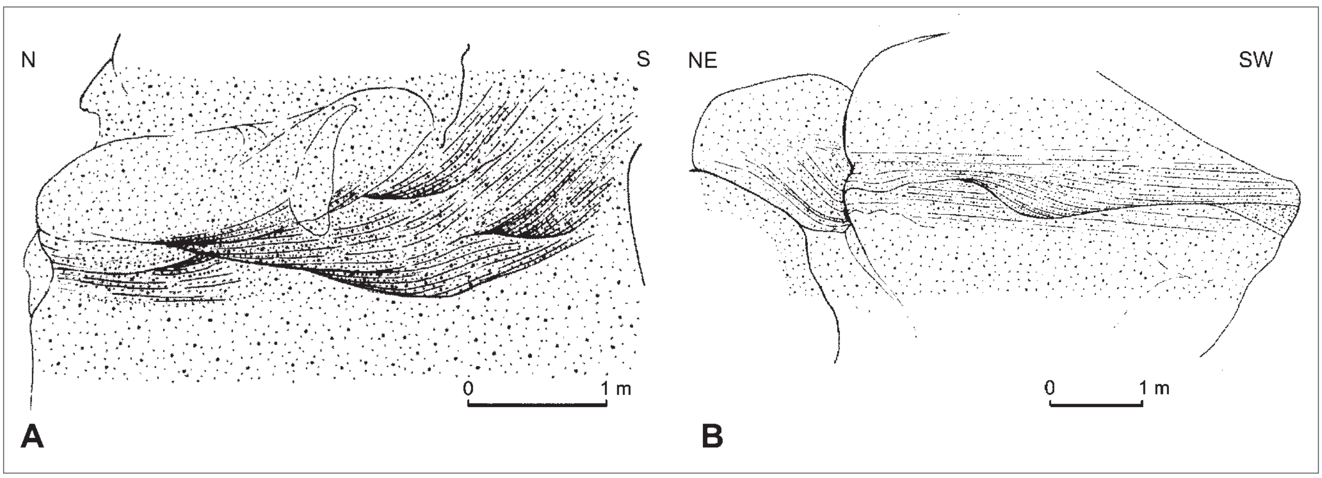

Fig. 21. Diffuse to distinct, multiple scour-and-fill features within thick fluxoturbidites, indicating consecutive flow surges. Both outcrop details (**A**, **B**) are from the 'Orzeł' rock tor (stop B8.1).

main entrance to the reserve (Fig. 17). The outcrop shows another portion of a succession of amalgamated thick beds of graded-stratified and massive coarse-grained sandstones (Figs 13D, 22A). Notable here is the rock frac-

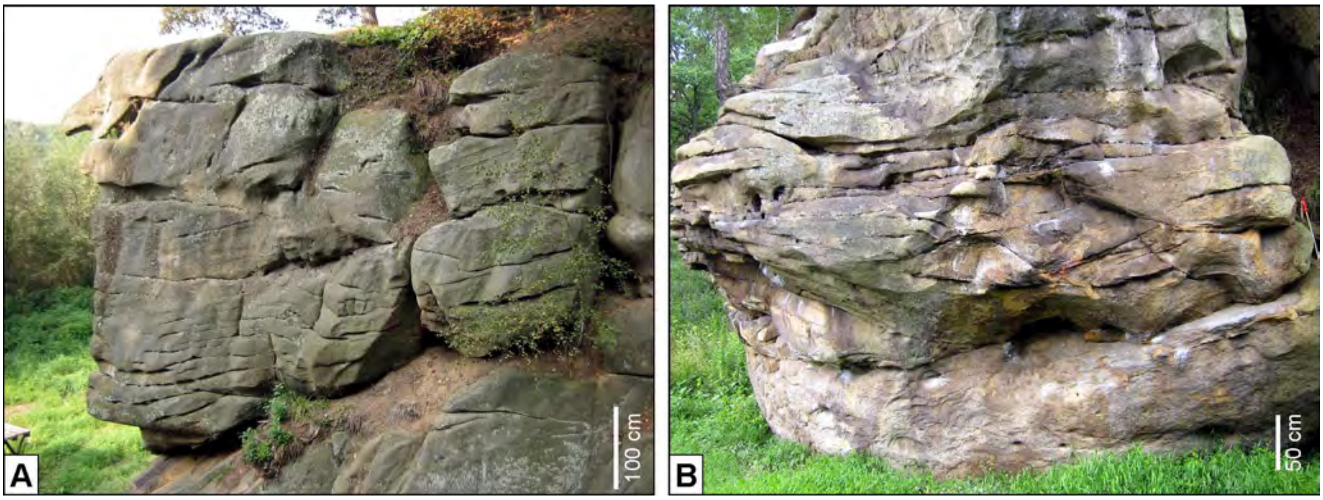

Fig. 22. Sandstone tensile fracturing due to an early post-depositional remobilization by gravitational sliding; rock tor 'Czarownica' at stop B8.1 (Fig. 17). (**A**) The primary leftwards-inclined parallel stratification in the tor southern wall is both accentuated and obliquely cut by sets of concave-upwards fractures imitating trough cross-stratification. (**B**) The tor western wall shows massive sandstone beds cut by sets of similar concave-upwards fractures imitating trough cross-stratification.

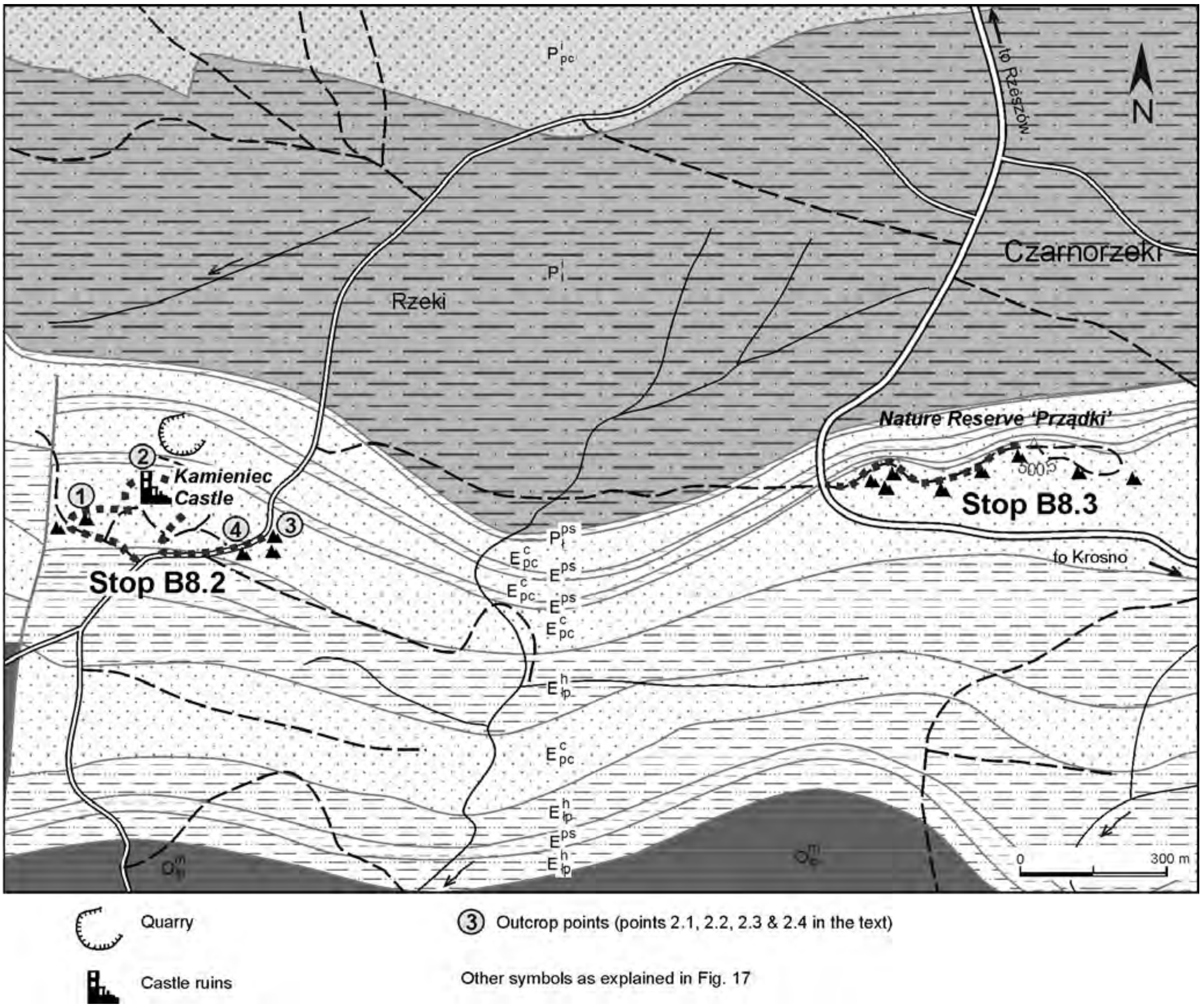

Fig. 23. Geological map of the vicinities of the Kamieniec Castle (stop B8.2, points 1–4) and the nature reserve 'Prządki' (rock tors at stop B8.3). Map modified from Świdziński (1933).

turing that imitates scours and geometrically unusual cross-stratification (Fig. 22B), and which is thought to represent differential synsedimentary shearing with tensile wing cracks at the base of a gravitationally sliding package of deposits.

Point 1.6 – Tor 'Ratusz (Town Hall)' on the western side of main road, half-way between point 5 and the main entrance to the reserve (Fig. 17). The outcrop shows a similar or perhaps the same (if unrecognizably faulted) succession of amalgamated thick beds of graded-stratified and massive coarse-grained sandstones (Figs 13A, C). Also here, a fracturing zone imitates scours and geometrically unusual crossstratification, which is thought to represent early synsedimentary shearing with tensile horsetail or wing cracks at the base of a slowly sliding soft-sediment package of deposits.

B8.2 The hill of Kamieniec Castle in Odrzykoń

(49°44′32″ N, 21°47′04″ E)

The rocky hill hosting the ruins of the 14th-century Kamieniec Castle (Figs 1, 23, left) offers another exposure of the fluxoturbidites of the Ciężkowice Sandstone, with both a broad view and details of syndepositional sediment remobilization and deformation features. Point 2.1 – The tors at the western foots of the castle hill show amalgamated beds of graded and nongraded, massive to faintly planar-stratified fine-pebbly sandstones. The parallel stratification is characterized by thick strata with grain size segregation. Beds on the NE side of the eastern tor show distribution normal grading, low-angle diffuse stratification and syndepositional sediment-remoulding features. The inclined stratification suggests a flow-oblique accretion of sediment mantling a 'frozen' debris flow or liquefied flow. The overlying massive bed of granule conglomerate grades upwards into sandstone and shows basal load casts, with load flames inclined to the south-east. Point 2.2 – Outcrop beneath the NW segment of the castle wall shows pebbly sandstone beds with multiple normal-graded conglomeratic lenses suggesting an unusually thick plane-parallel stratification (Fig. 9C). This crude layering is attributed to highly unsteady, pulsating (multi-surge) long-duration flows. Point 2.3 – Tor on the eastern side of the castle ruins, near the main road (with a roadside shrine), shows a thick graded-stratified bed of granule conglomerate passing upwards into coarse-grained sandstone, with a thick plane-parallel stratification marked by grain size segregation. This sediment layering is thought to represent rapid 'freezing' of the current's successive basal layers of laminar flow. Point 2.4 – Tor on the south-eastern side of castle ruins and near the main road, ca. 60 m to the SW of point 2.3, shows erosionally superimposed graded-stratified thick fine-pebbly sandstone beds. The parallelstratified sandy upper part of beds shows grain size-segregated, yet unusually thick, layering which may represent syndepositional shear-banding.

B8.3 The nature reserve 'Prządki (Spinners)', south of Czarnorzeki

(49° 44′32″ N, 21°47′59″ E)

The rock tors at this locality (Figs 1, 23, right) expose the same stratigraphic level of the Ciężkowice Sandstone as that seen at the previous stop B8.2. The sedimentary succession consists of thick amalgamated beds of massive to faintly parallel-stratified fine-pebbly/granule coarse-grained sandstones (Fig. 9A), with laminar shear-banding and scour-fill or mantling cross-stratification recognizable in the southern wall of the highest tor (Fig. 12B). Visible in one of the tors is also synsedimentary fracturing (cf. outcrop points 1.5 and 1.6), here apparently superimposed on primary cross-stratification.

Field-trip topic 2: Is some thick mud deposited fast and other thin deposited slowly in deep-sea settings?

Stanisław Leszczyński, Ewa Malata[1], Wojciech Nemec, Wojciech Schnabel[1], Sabina Hawryłko[1]

[1]Jagiellonian University, Poland

Introduction

Mud is an immanent component of deep-sea sedimentation, supplied as a hemipelagic to pelagic background suspension and derived from episodic sediment-gravity flows, particularly turbidity currents. The mode and rate of mud supply and its composition and pattern of intrabasinal dispersal may vary greatly, depending up on the basin internal and external conditions (see Stow *et al.*, 1996; Schieber, 1998). Similarly variable may be the mechanism of mud deposition. As pointed out early by Dżułyński *et al.* (1959), the turbiditic mud suspension is seldom an ideal dispersion of clay or clay/silt particles; instead, it commonly involves various particle aggregates: from faecal pellets and clay floccules to mud clots/crumbs and small chips (see also Potter *et al.*, 2005). The traditional deep-sea scenario of a spatially uniform, steady or fluctuating 'rain' of slowly settling mud suspension has recently been challenged in a major progress in our understanding of mud deposition. Evidence from laboratory experiments and microscopic mudrock studies indicates that some mud can be deposited in hydraulically more energetic conditions than previously assumed (Stow *et al.*, 1996; Schieber, 1998; Schieber *et al.*, 2007; Schieber and Southard, 2009) or be emplaced en masse as a gravity-driven, rheologically fluidal to plastic mudflow (Haughton *et al.*, 2003; Baas *et al.*, 2009) generated by the near-bottom densification of a settling mud suspension. The recognition of these various modes of mud deposition, along with the spatial pattern of mud dispersal in a basin, may have important implications for the basin's sedimention conditions and basin-fill stratigraphy.

This sedimentological topic is addressed by the field trip at its stop B8.4 in the context of the Glauconitic Magura Beds (late Eocene–early Oligocene) of the Carpathian Magura Nappe, a regionally extensive succession of turbiditic sandstones commonly capped with mudshales up to a few metres thick. The shale thicknesses correlate negatively with the sandstone bed thicknesses. The key contentious issues are: Are these mudshale beds just regular 'turbidite shales', as originally considered by Radomski (1960), or maybe representing prolonged quiet periods of hemipelagic suspension fall-out? Or perhaps they represent some other modes of mud emplacement, possibly quite rapid? The discussion of field evidence will focus on the thickness, colour variation, grain-size composition, ichnofabric and microfauna content of mudshale beds, as well as on the depositional nature, relative thickness and palaeocurrent directions

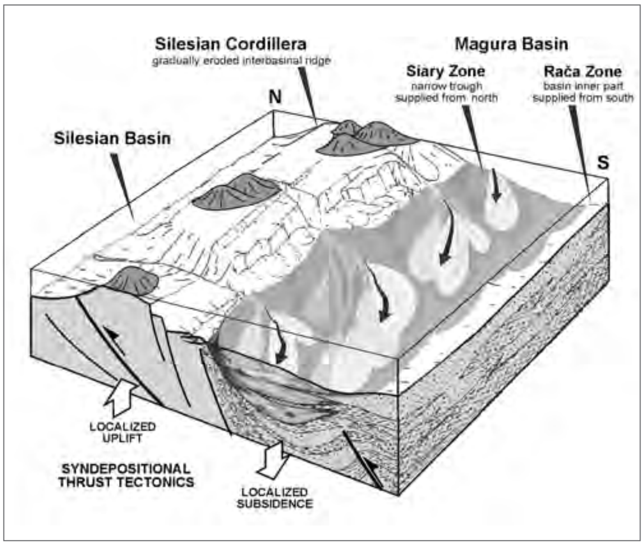

Fig. 24. Depositional model for the Glauconitic Magura Beds (modified from Leszczyński and Malata, 2002).

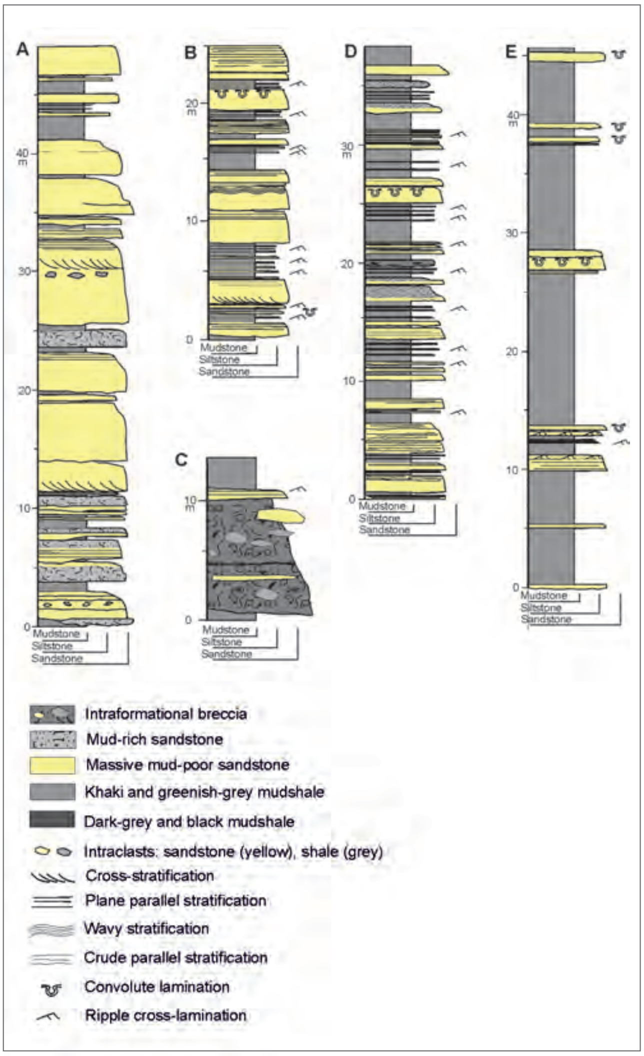

Fig. 25. Facies assemblages of the Glauconitic Magura Beds (modified from Leszczyński *et al.*, 2008). (**A**) Assemblage dominated by very thick sandstone beds (channel/lobe transition deposits); Wątkowa Sandstone near Folusz village, east of Gorlice. (**B**) Assemblage dominated by thin to thick sandstones interbedded with shales (lobe axial deposits); Siary village, NW of Ropica Górna. (**C**) Assemblage with prominent intraformational breccia beds (lobe-flank to interlobe deposits); Ropica Górna. (**D**) Assemblage of thin to medium sandstones and shales (lobe-margin deposits); Siary village. (**E**) Assemblage dominated by very thick shales interspersed with thin/medium sandstones (interlobe deposits); Małastów village, south of Ropica Górna.

of the associated sandstones and their contacts with mudshales.

The Glauconitic Magura Beds

The sedimentary succession known as the Glauconitic Magura Beds (GMB) in the Polish Outer Carpathians forms the uppermost stratigraphic part of the Magura Nappe (Fig. 4) in its frontal northern zone. The Magura Basin was bounded from the north by the Silesian Cordillera, at the foot of which a deep narrow trough formed in the late Eocene–early Oligocene and hosted the GMB base-of-slope depositional system supplied with sediment from the cordillera (Fig. 24). In the regional literature, this narrow northern zone of the Magura Basin is referred to as the Siary Zone. The GMB stratigraphic unit is up to 2000 m thick (Oszczypko-Clowes, 2001) and overlies conformably the Łabowa Formation (Fig. 4) dominated by variegated shales. The GMB unit consists of quartzose to subfeldspathic sandstone beds, thin to thick (Fig. 25), generally glauconite-bearing and commonly mud-rich (wackes); subordinate are beds of granule conglomerate and intraformational sedimentary breccia. The associated mudshale beds (Fig. 25) range from clayey to silty and from calcareous to non-calcareous. Isolated outcrops indicate that the sandstone net/gross (N/G) varies both vertically on a scale of several tens of metres and laterally, along the depositional strike, on a scale of several kilometres. As a broad regional stratigraphic trend, the low N/G lower member of the succession (referred to as the Zembrzyce Beds) passes upwards and also sideways into the high N/G middle member (the Wątkowa Sandstone), which is overlain by the lowest N/G upper member (the Budzów Beds).

The coarse-grained deposits in the GMB range from non-graded to normal-graded and from massive to stratified. The thin sandstone beds are mainly Bouma-type turbidites Ta-c with siltstone to mudstone Tde caps. The mud-poor thick sandstone and granule conglomerate beds are typically normal-graded, massive to banded/stratified (Fig. 25A, B), similar to the fluxoturbidites of Dżułyński *et al.* (1959), and are attributed to deposition by high-density turbidity currents (*sensu* Lowe, 1982). The mud-rich sandstones and intraformational breccia beds are generally massive and poorly graded, occasionally with a graded-stratified upper part (Fig. 25A, C, D), and are considered to be deposits of cohesive debris flows (Lowe, 1982; Nemec and Steel, 1984) and hybrid sedi-

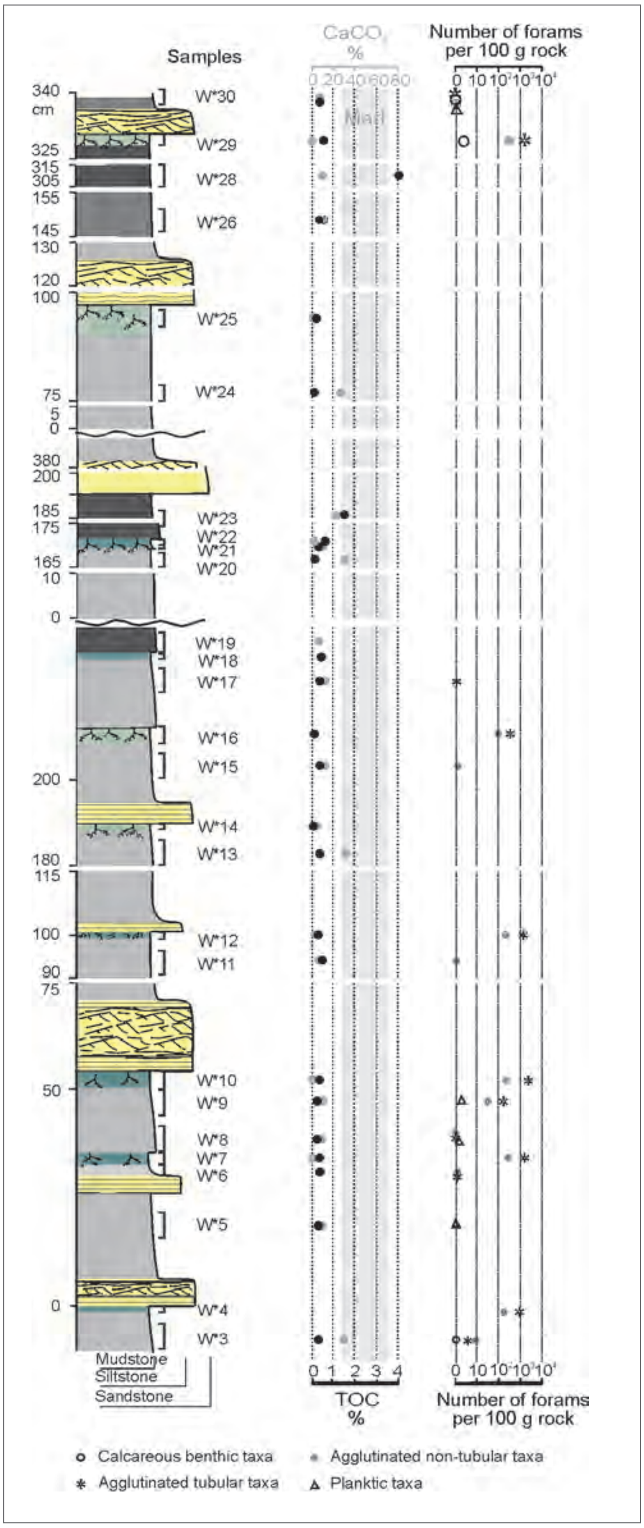

Fig. 26. Vertical variation in the content of $CaCO_3$ and TOC and the frequency and variety of foraminifers in the mudshales of Glauconitic Magura Beds; outcrop section in Węglówka village, ca. 50 km south of Kraków. In the profile, note the tectonic unconformities (wavy lines) and the thickness gaps due to removal of thick sandstone beds; note also the association of burrowing with the green shales. From Leszczyński and Malata (2002).

ment-gravity flows (*sensu* Haughton *et al*., 2009; Kane and Pontén, 2012).

The mudshale beds have a much greater thickness range and are thickest (occasionally up to 20 m) in the stratigraphic intervals with the lowest N/G (e.g., Fig. 25E), such as the upper Budzów Beds. Calcareous mudshales predominate and the rock colour varies from brownish yellow-green (khaki), greyish-green and greenish-grey to dark-grey and black. The dominant grey and black calcareous shales are commonly overlain or separated by a thin (mainly <1 cm) layer of non-calcareous green shale (Fig. 26). The total organic carbon (TOC) content is generally low (<1%) and the black shales are only slightly richer in organic carbon than the grey or green shales (Fig. 26).

The dark shales show a gradational contact with the underlying siltstone or silty sandstone of turbidite bed top. The shale basal part commonly shows normal grading and faint plane-parallel lamination in the basal part. An admixture of very fine sand-sized grains (mainly quartz) occurs in the basal and topmost parts of shale beds, but also as diffuse horizons within the beds (Fig. 27;

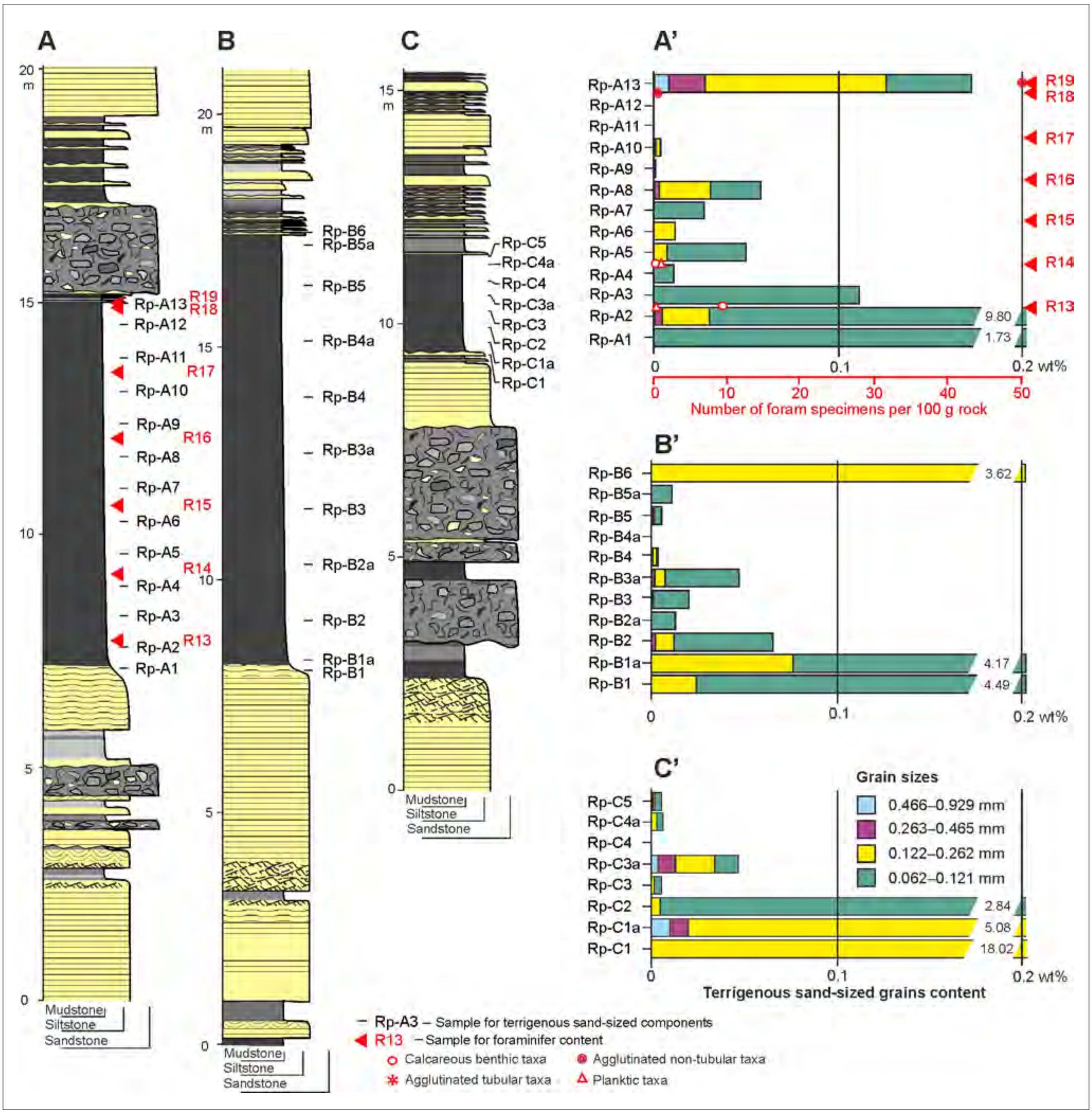

Fig. 27. Vertical changes in sand content and the frequency and type of foraminifers within a thick mudshale unit in the Glauconitic Magura Beds in Ropica Górna (stop B8.4, see outcrop points along the Sękówka river in Fig. 28). (**A**) Outcrop section at point 4.2. (**B**) Outcrop section at point 4.3. (C) Outcrop section ca. 500 m upstream from point 4.3.

Hawryłko, 2009; Schnabel, 2011). Shale beds thicker than 20 cm typically show burrows only in their uppermost part, less than 10 cm thick, with the bioturbation degree and foraminifer content increasing upwards and reaching maxima at the shale top and in its greenish capping.

The non-calcareous green shales contain benthic foraminifers, almost exclusively agglutinated taxa, including: *Nothia excelsa, Rhabdammina cylindrica, Psammosphaera sp., Glomospira glomerata, Haplophragmoides parvulus, Haplophragmoides sp., Paratrochamminoides spp., Ammsphaeroidina pseudopauciloculata and Recurvoides contortus*. The assemblages indicate bathyal water depths, below the present-day calcite lysocline (Leszczyński and Malata, 2002). The calcareous dark shales bear only sporadic planktic and benthic taxa, both calcareous and agglutinated, and chiefly in the basal and topmost part of a bed (Figs 26, 27; Leszczyński and Malata, 2002; Hawryłko, 2009; Schnabel, 2011).

Interpretation of mud deposition

Their intimate association and gradational contact with turbiditic sandstones indicates that the volumetrically dominant grey/black calcareous mudshales are of turbiditic origin, whereas the non-calcareous, foraminifer-rich and heavily bioturbated green mudshales apparently represent hemipelagic 'background' sedimentation. The rate of dark mud deposition must have been very high, preventing bioturbation, whereas the deposition rate of the thin green mud layers was incomparably lower. The glauconite-bearing turbiditic sand suggests resedimentation from a shelf zone (Starzec, 2009), probably narrow and subject to erosion (Fig. 24), with the deposition taking place in a base-of-slope ramp system (*sensu* Reading and Richards, 1994). The resedimentation was vigorous, leaving relatively little time for the background mud fallout. (The following text refers also to plates given as appendix illustrations in the digital version of this excursion guide.)

The large volumes of dark mud are thought to have been entrained by turbidity currents as a turbulent suspension, as indicated by basal normal grading, and were derived probably from the outermost shelf zone or basin-margin slope (Leszczyński and Malata, 1982) by the bypassing erosive currents – remobilizing and sucking-in mud in their wake (Fig. 24). The turbulent mud suspension often followed the parental current in

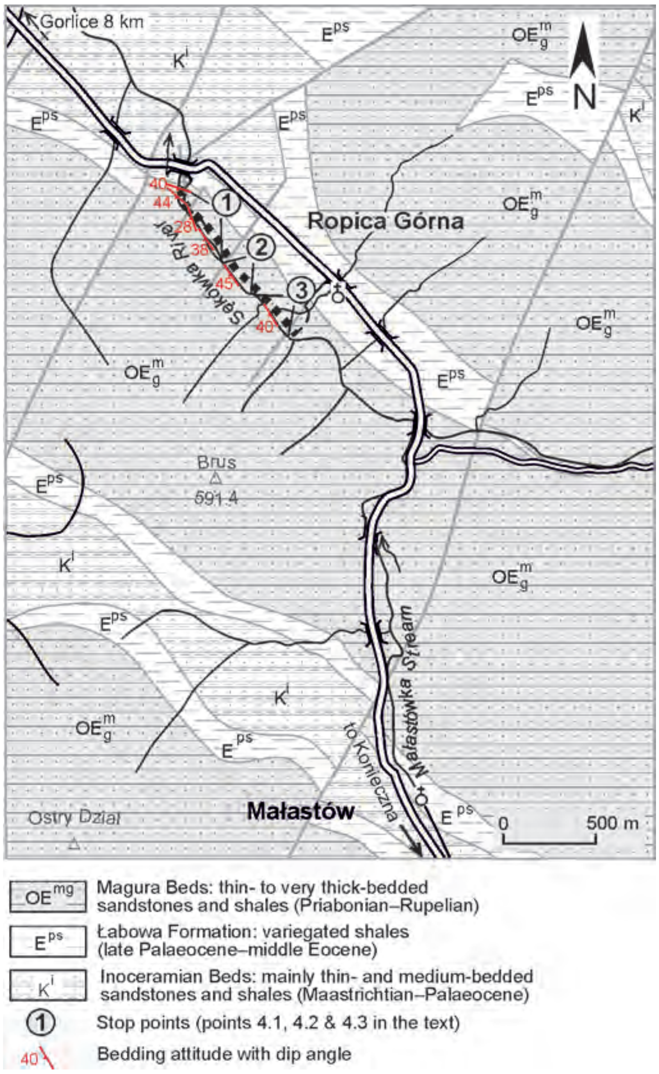

Fig. 28. Geological map of the vicinities of Ropica Górna (stop B8.4); modified from Kopciowski (1996). Note the location of outcrop points (river segments) 4.1–4.3 in the excursion route up the Sękówka river.

two or more successive surges, as indicated by the sand-content fluctuations in mudshale beds. The diffusely parallel-laminated initial stage of mud deposition resembles that of the Bouma turbiditic d-division. The settling of the current-entrained turbulent mud suspension was probably causing its near-bottom densification, turning it into an increasingly laminar flow (see Plate 6A; Baas *et al.*, 2009). The shear pattern and mode of fluid mud emplacement would vary with its volumetric concentration and flow rate (Plate 6; see Baas *et al.*, 2009). Turbulent shear would allow settling of the coarsest grains and development of normal grading. When reaching quickly the non-shearing 'plug flow' phase (*sensu* Baas *et al.*, 2009), the mud might continue to move slowly as a 'linked' mudflow (*sensu* Haughton *et al.*, 2003), possibly carrying scattered sand grains and/or floating mud chips (Plate 6B; see also Torfs *et al.*, 1996; Amy *et al.*, 2006; Talling *et al.*, 2012). Mud chips in a rock are visually difficult to distinguish from a mud matrix of similar composition, but the routine laboratory disintegration of shale samples with Glauber's salt in the present case had indicated some relatively hard mudrock bits which could well be chips/crumbs of a compacted primary mud.

The trailing and densifying thick mud suspension would tend to be driven by gravity independently of the parental fast turbidity current, thereby commonly outrunning the spatial distribution of turbiditic sand (as evidenced by the dark shale beds separated with thin green shale horizons, Fig. 26) and also being drifted sideways into the inter-lobe topographic depressions of the depositional ramp system (Figs 24, 25E). This latter notion is supported by the 'compensational' spatial thickness distribution of shales relative to sandstones and by the observed variability of palaeocurrent directions.

If this hypothetical interpretation is correct, the emplacement of the thick beds of dark mud in the GMB succession might have been nearly as rapid as the deposition of the turbiditic sand and granule gravel beds. The regional stratigraphic significance of the low N/G local successions in the Glauconitic Magura Beds would then need to be reconsidered in terms of the depositional system's morphodynamics and its specific mode of sediment supply.

Stop description for topic 2

Stanisław Leszczyński, Wojciech Nemec

The outcrops at stop B8.4 are in the river bedrock banks and floor, and hence wellingtons (high rubber boots) are needed. The excursion aim at this first stop on the second day is to demonstrate and discuss the sedimentary characteristics of the GMB succession with a special focus on its variety of mudshale beds. The area is in the northern frontal zone of the Magura Nappe (Fig. 2), known as the Siary Zone (Fig. 24), and the GMB succession here is 1000-1400 m thick (Leszczyński *et al.*, 2008). The outcrops in Ropica Górna show a mud-rich inter-lobe part of the

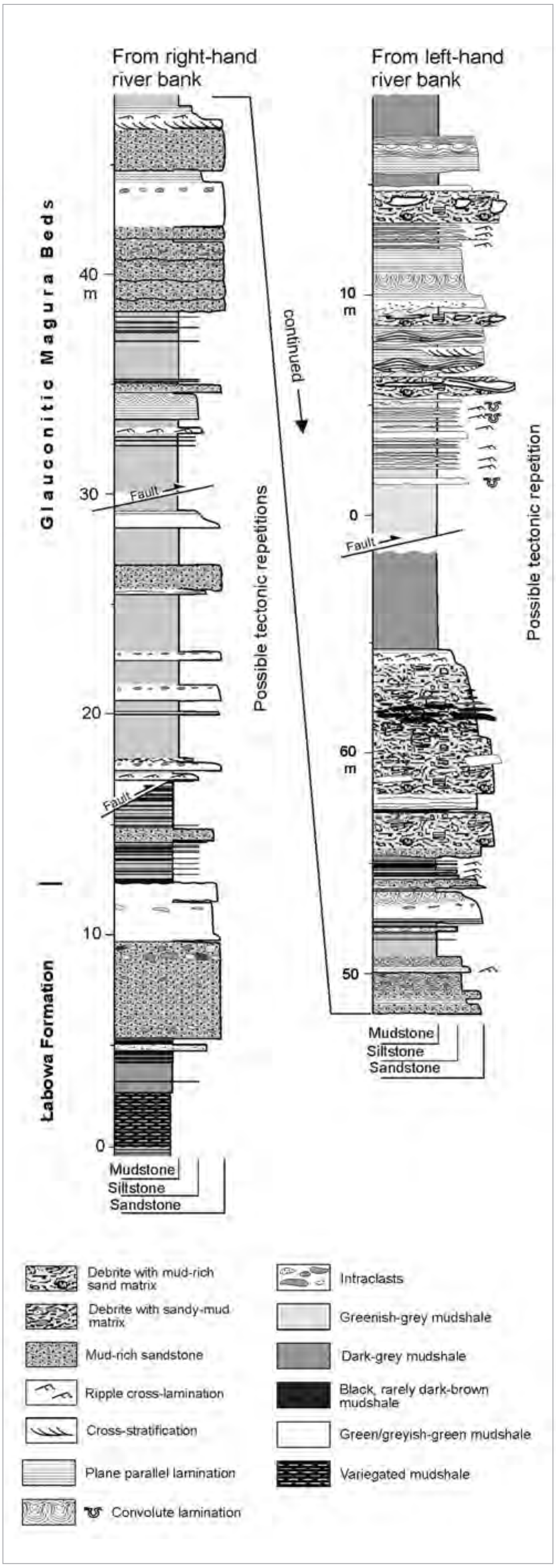

Fig. 29. Sedimentological log of the lower part of Glauconitic Magura Beds and the underlying Łabowa Formation in Ropica Górna (see stop B8.4 in Fig. 28, outcrop point 4.1).

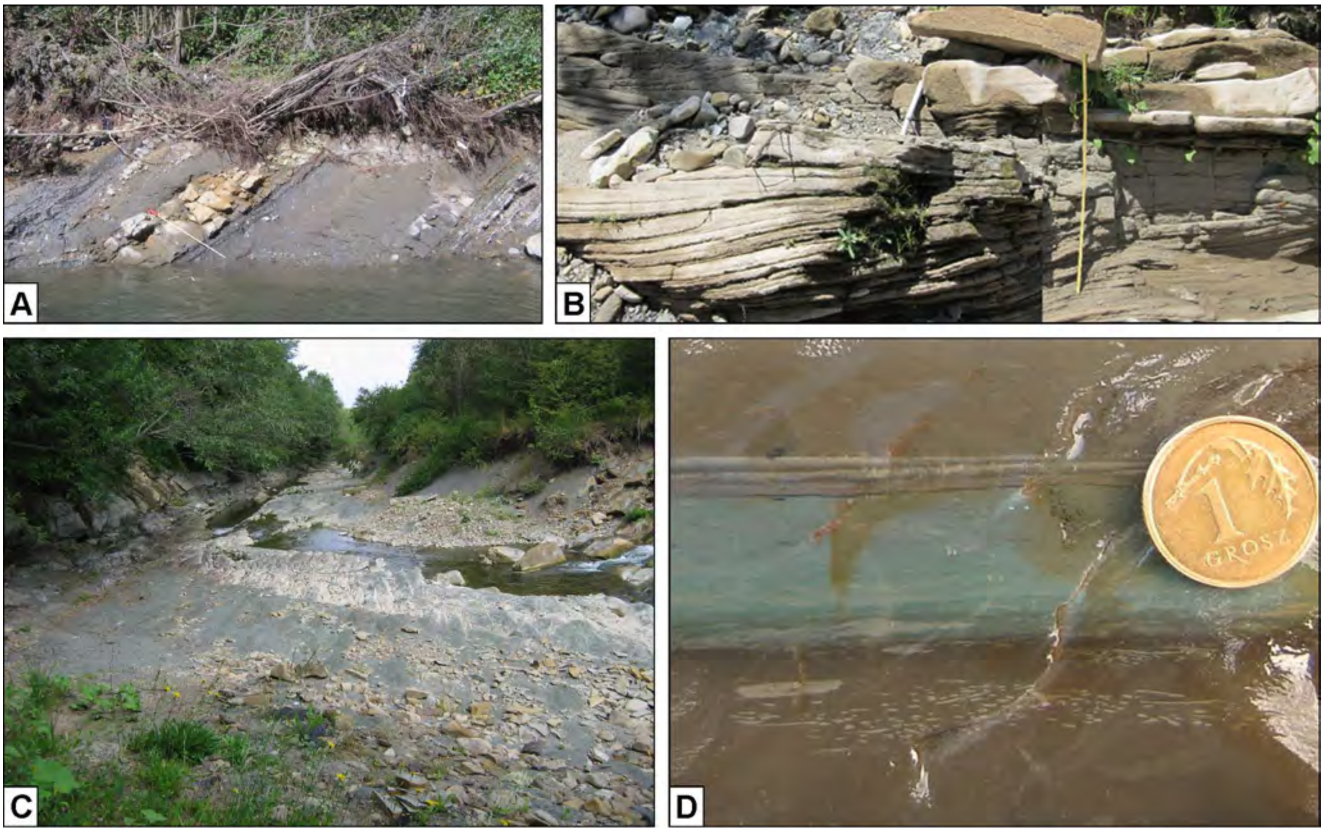

Fig. 30. Outcrop details of the Glauconitic Magura Beds in Ropica Górna (stop B8.4, Fig. 28). (**A**) Succession dominated by mud-rich sandstone and intraformational breccia beds at point 4.1; the walking stick (scale) is 1.1 m. (**B**) Apparent hummocky stratification in a sandstone bed at the upstream end of point 4.1; the measuring stick is 0.9 m. (**C**) The Sękówka river floor exposing an 8-m thick mudshale unit overlain by a 4-m package of beds dominated by intraformational breccias; the upstream end of outcrop point 4.2. (**D**) Close-up detail from the upstream part of outcrop point 4.3, showing calcareous greyish brown mudshales separated by a thin layer of non-calcareous green mudshale; the coin size is 1.5 cm. The brown shales show light-colour silt streaks and the lower one shows clusters of *Chondrites intricatus* burrows. The green shale has a transitional lower boundary and sharp top, and is strongly bioturbated. Analyses of 100-g rock samples show that the brown shales contain only 17–179 foraminifer specimens (calcareous and benthic species), whereas the green shale contains nearly 11 000 specimens of exclusively agglutinated foraminifers.

Siary turbiditic ramp system, passing laterally along the depositional strike into an adjacent sand-rich lobe part within a distance of less than 10 km to the east (see Leszczyński *et al*., 2008).

B8.4.1-4 Ropica Górna

Outcrops at the banks and floor of river Sękówka.
(49°36′02″ N, 21°13′27″ E to 49°35′34″ N, 21°13′58″ E)

The bedrock banks and floor of the north-flowing Sękówka river in Ropica Górna (Fig. 28) afford a nearly continuous outcrop section of the lower part of the GMB succession (Fig. 29), ca. 100 m thick, dated to the latest Eocene (Oszczypko-Clowes, 2001). The GMB succession has a tectonized lower boundary and is cut by a few *en echelon* faults, but contains a marker megabed of sedimentary breccia, 5 m thick, which allows the succession stratigraphy to be followed and its local offset by faults to be estimated at ca. 10–20 m. The consecutive points of the excursion route are in the upstream direction (see Fig. 28).

Point 4.1 – The river floor above the bridge of the main road Gorlice–Konieczna in the northern part of the village (Fig. 28). The basal contact of the GMB with the underlying variegated shales of the Łabowa Formation (Fig. 29, lower left) is disturbed by tectonic thrusting. The lowest part of the GMB (4.6 m thick, Fig. 29) is dominated by dark brownish-grey and greyish-green calcareous shales interbedded with thin glauconitic sandstones, considered by Oszczypko-Clowes (2001) to represent the Zembrzyce Beds. This basal part is separated by a fault from the overlying part (ca. 30 m thick, Fig. 29, left), exposed in the river right-hand bank and composed of dark calcareous and subordinate greenish non-calcareous mudshales intercalated with thin to thick beds of massive arenites and wackes; it is cut by a minor fault in the middle and its proportion of sandstones increases upwards.

The higher part of the succession, ca. 30 m thick (Fig. 29, right), crops out in the river left-hand bank (Fig. 30A). This part of the succession seems to have been repeated by a thrust (Fig. 29, upper right) and can be followed upstream along the strike over a distance of ca. 250 m (Fig. 28), although its exposure is fragmentary and limited mainly to the river floor, The thick mudshale beds here lack bioturbation, whereas the associated sandstone beds show trace fossils on their soles. The succession includes a 10-m package of thick sandstone beds showing trough or scour-and-fill cross-stratification as well as enigmatic hummocky stratification (Fig. 30B). A several metres thick package of interbedded sandstones and dark-grey/black and brown/green mudshales forms the top part of the succession. Common are muddy sandstone beds rich in mudclasts, and also the marker breccia megabed is reached at the upstream end of the strike section, offset by another fault.

Sandstone beds indicate deposition by turbidity currents, cohesive debris flows and intermediate 'hybrid' flows (see Haughton *et al*., 2003; Amy *et al*., 2006; Kane and Pontén, 2012; Talling *et al*., 2012). Short-distane lateral changes in bed thicknesses indicate an uneven depositional topography. The thick non-bioturbated mudshale beds imply rapid emplacement, with an immediate post-depositional colonization by fauna indicated by trace fossils on the overlying sandstone soles. Unclear is the origin of apparent hummocky stratification (first recognized here by Piotr S. Dziadzio).

Point 4.2 – The next upstream segment of the river (Fig. 28), ca. 200 m long, is a strike section of deposits about 10 m above the marker breccia megabed. Prominent here is a very thick (ca. 8 m) unit of massive, dark-grey mudshale (Figs 27A, 30C). The underlying sandstone-rich package and the overlying shale-rich package of turbidites contain isolated subordinate beds of intraformational breccia (Fig. 27A).

A systematic sampling of the thick mudshale unit's vertical profile indicates irregular changes in both its sand content and the abundance and variety of foraminifers (see Fig. 27A and plot A'). This hidden heterogeneity suggests that the shale unit is probably composite, emplaced in at least four successive surges of fluidal mud ranging from weakly turbulent and crudely graded to increasingly non-turbulent, with a sand-bearing rigid plug (see Baas *et al*., 2009).

Point 4.3 – The last upstream segment of river Sękówka, ca. 300 m long, is a strike section of the marker breccia megabed, 5 m thick, exposing it from the top to base. The sedimentary breccia has a muddy sand matrix and contains large rafted fragments of sandy and heterolithic turbidites as well as mudshale blocks as large as 1.7 x 5 m. It is underlain by a 2-m mudshale unit whose top part consists of greyish brown calcareous shale layers (4–4.5 cm thick), with sporadic *Chondrites* and *Phycosiphon* burrows and infrequent foraminifers (solely benthic species, both calcareous and agglutinated), intercalated with strongly bioturbated layers (1–1.5 cm) of green non-calcareous shale (Fig. 30D) rich in exclusively agglutinated foraminifers. The breccia megabed is covered by a sandstone turbidite T(a)bc, 20 cm thick, and further by a calcareous, dark-grey massive mudshale with an exposed thickness of 2.5 m.

At the upstream end of this river segment, across two closely-spaced faults, the thick dark-grey mudshale unit of point 4.2 (Fig. 27A) is exposed in the river left-hand bank, here reaching a thickness of 9.4 m (Fig. 27B). It is underlain by thick sandstone beds and covered with thinly-bedded heterolithic turbidites. The mudshale unit in its vertical profile shows similar fluctuations of sand content (Fig. 27, diagram B') as in its outcrop at point 4.2 (cf. diagram A'). Analogous fluctuations are observed in an outcrop ca. 500 m farther upstream, where the mudshale unit decreases in thickness to 2.6 m (Fig. 27C, diagram C').

Field-trip topic 3: The Lower Oligocene – still deep-water turbidites or rather shallow-marine deposits?

Piotr S. Dziadzio

Introduction

Palaeobathymetry has been a central and controversial issue in the analysis of the flysch basins of the Polish Outer Carpathians, now represented by the individual nappes. Until 1937, the Carpathian flysch was thought to have been deposited in shallow-water conditions, because of the abundance of sandstones and conglomerates. Sujkowski (1938) was probably the first who suggested that the Carpathian flysch was deposited at water depths 'greater than those of the North Sea'. This view soon gained strong support from Książkiewicz (1948), who found the origin of shale-capped graded sandstone beds difficult to reconcile with shallow-water conditions. After the publication of turbidity current hypothesis by Kuenen and Migliorini (1950), the notion of sediment gravity flows and deep-water conditions was swiftly adopted by the Carpathian leading flysch researchers (Vašiček, 1953; Książkiewicz, 1954). On the basis of foraminifer studies, Książkiewicz (1958) suggested that the water depth in the Carpathian flysch basins was mainly bathyal (200–3500 m), but probably varied in space and time, with some deposits possibly neritic. A deepwater origin of the Carpathian flysch was postulated further by Dżułyński *et al.* (1959), Dżułyński and Walton (1965) and several other authors. Koszarski and Żytko (1965) suggested that the flysch basins were relatively shallow during the Early Cretaceous, but attained abyssal depths in the Late Cretaceous and Palaeocene–Eocene before becoming gradually shallower again in the Oligocene. The early bathymetric reconstructions of the Polish Outer Carpathian flysch, based on foraminifers and trace fossils, were given in the benchmark publications by Książkiewicz (1975, 1977).

However, the notion of a deep-water origin of the Carpathian flysch was also concurrently questioned by several researchers in the region (e.g., Hanzlikova and Roth, 1963; Watycha, 1963; Draghinda, 1963; Bieda, 1969). According to Bieda (1969), the flysch formations containing solely agglutinated foraminifers were deposited in lacustrine environments, enclosed shallow-water bays and river-mouth areas, whereas formations with mixed assemblages of agglutinated and calcareous foraminifers were deposited in littoral to neritic environments. This hypothesis was discarded by Książkiewicz (1975) on the basis of the modern distribution of foraminifers. He reinforced the opinion that the Polish Outer Carpathian flysch was deposited at bathyal water depths, perhaps mainly in the upper bathyal zone of 200–600 m.

The latter view was later enhanced by Ślączka and Kaminski (1998), who suggested that all the Jurassic to Miocene deposits in the Polish Outer Carpathians were of deep-water origin. A bathyal to abyssal water depth was postulated by several authors for the Early Cretaceous to

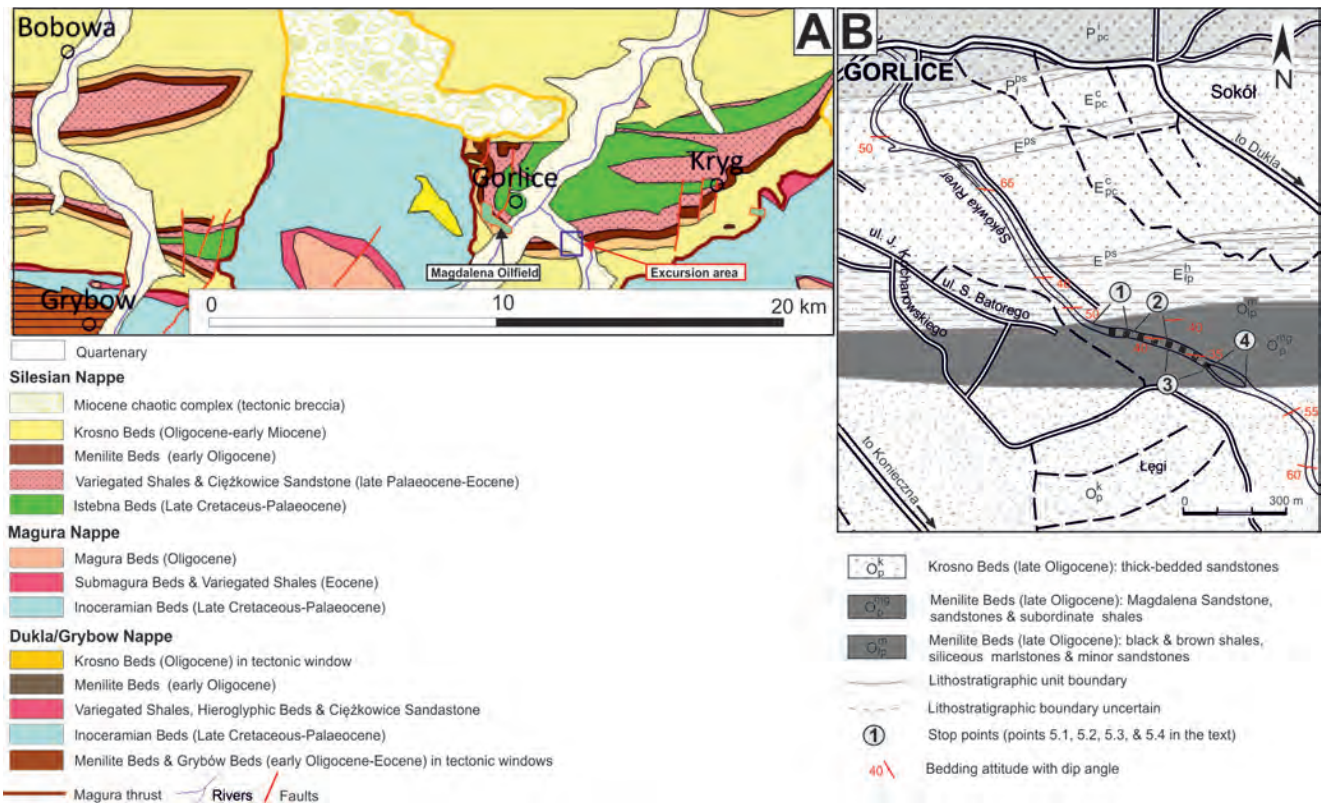

Fig. 31. (**A**) Geological map of the Gorlice area (see also excursion stop 8.5 in Figs 1, 2, 4), showing the location of the excursion area in Menilite Beds and the Magdalena oilfield; map modified from Świdziński (1954). (**B**) Detailed geological map of the excursion area with the location of stops 5.1–5.4; map modified from Szymakowska (1977); for complete legend, see Fig. 17.

Eeocene flysch deposits (Uchman at al., 2006; Słomka *et al*., 2006; Olszewska and Malata, 2006; Waśkowska and Cieszkowski, 2014). Słomka *et al.* (2006) suggested a marked shallowing of the bathyal basins (ca. 1000 m depth) in the late Eocene to late Oligocene. A possible occurrence of shelf environments was inferred by Olszewska and Malata (2006) on the basis of foraminifers for the early Oligocene Menilite Beds.

The regional studies as a whole leave little doubt that the vast majority of the Polish Outer Carpathian flysch was deposited in deep-water settings, bathyal and perhaps locally even abyssal. However, for an evolving array of tectonically active wedge-top basins (*sensu* DeCelles and Giles, 1996) it is also quite likely that many transient zones of shallow-water sedimentation would form and that their deposits, if not cannibalized by erosion, might occasionally be preserved within the ultimate nappe stack. This hypothesis is suggested here to be the case with the Magdalena Sandstone member at the top of the early Oligocene Menilite Beds formation in the Silesian Nappe, at its boundary with the overlying Sub-Magura/Dukla Nappe (Figs 2, 4). The deposits in question, nearly 200 m thick, are both underlain and overlain by deep-water turbiditic successions. The contentious issue is: Can these deposits, in the middle of a very thick deep-marine flysch succession, be of shallow-marine origin?

The Menilite Beds and their uncertain palaeobathymetry

The early Oligocene shale-rich Menilite Beds form a regional lithostratigraphic unit present in all the Polish Outer Carpathian nappes (Fig. 4), which may suggest a palaeogeographic stage of a very broad deep-water basin. The origin of the organic carbon-rich black Menilite shales has long attracted research interest in regional studies (e.g., Kuźniar, 1952; Badak and Grudzień, 1961; Gabinet and Jurczakiewicz, 1962; Köster *et al*., 1998a, b; Koltun, 1992; Koltun *et al*., 1995, 1998; Matyasik and Dziadzio, 2006; Kotarba *et al*., 2013, 2014), with much less focus on the associated sandstones complexes (e.g., Żgiet, 1963; Dżułyński and Smith, 1964; Koszarski, 1965; Ślączka and Unrug, 1966; Kotlarczyk, 1976; Jankowski *et al*., 2012). A possible non-turbiditic origin of sandstone complexes in the Menilite Beds has been suggested briefly by Dżułyński and Kotlarczyk (1962), Dżułyński and Smith (1964) and Jankowski *et al.* (2012).

The Menilite Beds in all nappes, except for the Magura Nappe (Fig. 4), overlie synchronously the regionally-extensive unit of Globigerina Marls (lowest Rupelian) and commence with dark-brown bituminous shales interlayered with cherts and siliceous marls (Gucwa and Ślączka, 1972; Olszewska 1985; Ślączka and Kaminski, 1998). The shaly succession contains three main sandstone complexes: the Cergowa Sandstone in the Dukla Nappe, the Magdalena Sandstone in the Silesian Nappe near Gorlice, and the Kliwa Sandstone in the Skole nappe (Ślączka and Kaminski, 1998). The upper boundary of the Menilite Beds is diachronous, older to the south (Dukla Nappe) and younger, Chattian/Aquitanian to the north (Skole Nappe) (Koszarski and Żytko, 1961; Gucwa and Ślączka, 1980; Olszewska, 1985; Ślączka and Kaminski, 1998; Kotlarczyk *et al*., 2006).

Planktic and benthic foraminifers in the Menilite Beds indicate deposition at sublittoral to upper bathyal water depths (Olszewska, 1985; see also Olszewska and Malata, 2006). Abundant ichtiofauna indicates fish assemblages dwelling in water depths of 200 to 2000 m, but also includes some shallow-water species (Jerzmańska, 1968, Jerzmańska and Kotlarczyk, 1988; Kotlarczyk *et al*., 2006).

More recent sedimentological studies of the Menilite Beds in the Gorlice area (Enfield *et al*., 1998; Dziadzio *et al*., 1998; Watkinson *et al*., 2001; Dziadzio *et al*., 2006) have postulated a shallow-marine origin of this succession including the Magdalena Sandstone with a long-producing hydrocarbon reservoir (eventually abandoned in 2012). The occurrence of features interpreted as hummocky cross-stratification implies deposition above the storm wave base, which means a water depth no greater than 100 m and perhaps less than 50 m on the account of the landlocked nature of the Carpathian Paratethys seaway (Rögl, 1998). As pointed out by Jankowski *et al.* (2012), it could only be the lack of detailed sedimentological studies that allowed these and possibly also some other deposits in the Outer Carpathian flysch to be lumped with the vertically-adjacent deposits as deep-water turbidites. The Menilite Beds with the controversial Magdalena Sandstone are the topic of the excursion stop B8.5 in the Gorlice area (Fig. 31).

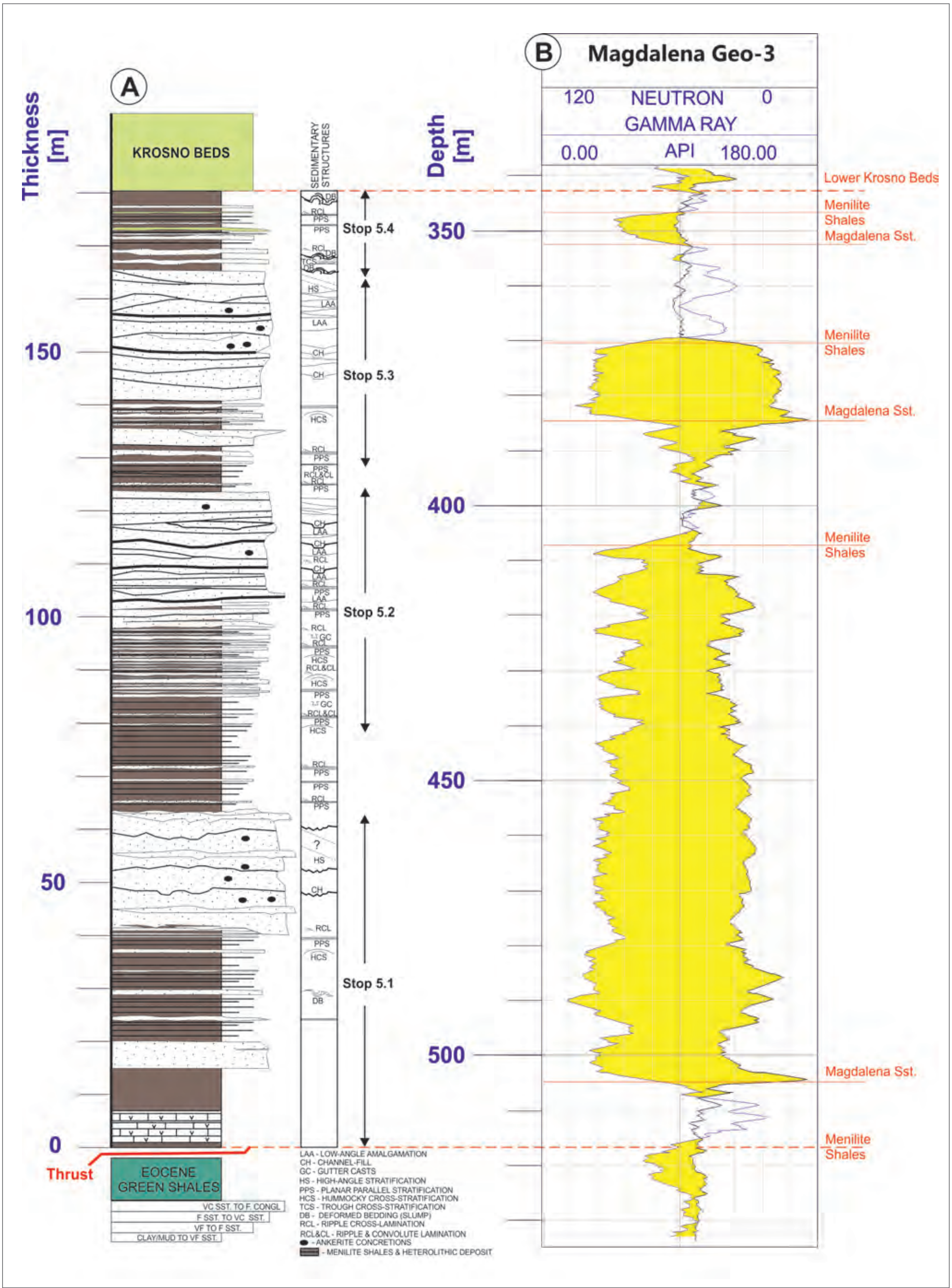

Fig. 32. (**A**) Sedimentological log of the Menilite Beds from the outcrop section in Sękówka river (excursion stop B8.5, Fig. 31B) (**B**) An example geophysical well-log from the nearby Magdalena oilfield (see location in Fig. 31A). The low values of neutron and gamma-ray signals indicate sandstones, whereas the high gamma-ray values indicate shales. The sandstone net thickness in the well is ca. 120 m and the shale net thickness is ca. 60 m (Dziadzio *et al.*, 2006).

The Menilite Beds in Gorlice area

The Menilite Beds succession in the Gorlice area was described stratigraphically by Szymakowska (1979), Karnkowski (1999) and Dziadzio *et al*. (2006). A tectonic thrust separates this unit from the underlying Eocene green shales (Fig. 32), and the unit here differs from its typical other appearances in the Silesian Nappe and in the Skole Nappe (Szymakowska 1979). Siliceous marls, instead of cherts, occur in its lowest part; typical cherty 'menilitic' shales are rare; and the succession is dominated by the quartzose arenites of the Magdalena Sandstone (Fig. 32). The Magdalena Sandstone, named after an estate and oilfield in Gorlice, consists of thick-bedded, coarse- to very coarse-grained and subordinate fine-grained quartz-glauconite sandstones and quartz-rich conglomerates. Cement is calcite with iron compounds. Sandstone beds range from nearly massive to well-stratified. Shale-dominated parts of the succession (Fig. 32) consist of the thin (10–20 cm) to thick (occasionally >1 m) beds of greyish brown, dark-grey and black, organic-rich noncalcareous shales, mainly laminated, with common heterolithic intervals of shale thinly interlayered with greyish white fine-grained sandstones and showing classical lenticular, wavy and flaser bedding. The top part of the succession, at its transition to the turbidites of the Krosno Beds (Fig. 32), shows slump features and consists of shales and heterolithic deposits alternating with thin beds of both the Magdalena-type quartz-glauconite sandstones and the Krosno-type quartz-muscovite calcareous sandstones.

The shales are a good-quality source rock for hydrocarbons. They have a fairly low degree of thermal maturation (T_{max} = 414°C), are rich in organic matter (TOC = 10.12%), and their hydrocarbon yield potential is ca. 45 mg HC per 1 g of the rock. Oil-prone kerogen of type II dominates, with the hydrocarbons rich in aliphatic and naphtenic compounds. However, the content of sulphur is high, which reduces the shale's HC-generation potential. Biomarkers indicate sediment deposition in anoxic conditions. The content of C_{29} hopanes is much higher than that of C_{30} hopanes, which may suggest deposition in a shallow shelf environment (Matyasik and Dziadzio, 2006).

The thickness of the Menilite Beds in the Magdalena oilfield south-west of Gorlice (Fig. 31A) is in the range of 150–180 m. The thickness in the excursion area along the Sękówka river (Fig. 31B) is 180 m (Fig. 32A), but decreases along the strike both westwards (Fig. 31B) and eastwards (Szymakowska, 1979). The unit is only 75 m thick near the village Kryg, 7 km to the east of Gorlice (Fig.

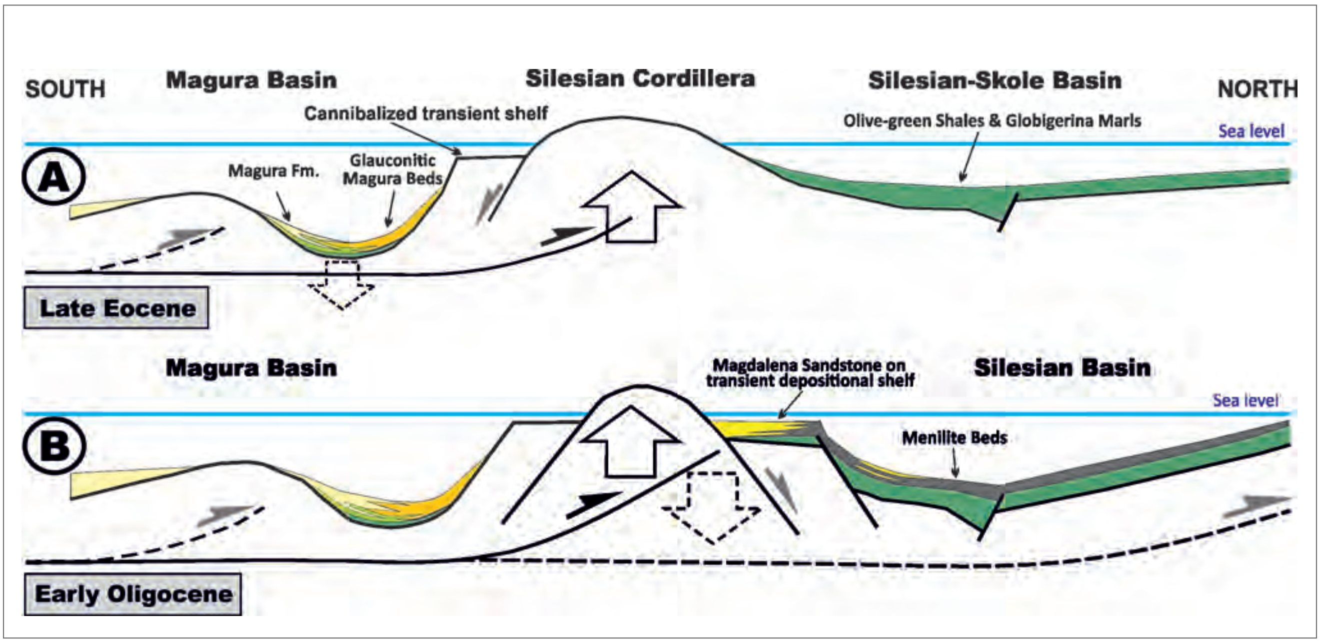

Fig. 33. Schematic hypothetical model (not to scale) for the late Eocene to early Oligocene sedimentation on the flanks of the emerging Silesian Cordillera between the Magura Basin and Silesian Basin. (**A**) Narrow synclinal trough forms at the southern foot of the cordillera, where the late Eocene base-of-slope Glauconitic Magura Beds succession is deposited with sediment derivation from a cannibalized narrow transient shelf (see Fig. 24). (**B**) A narrow transient depositional shelf forms on the northern flank of the cordillera, where the early Oligocene Magdalena Sandstone succession is deposited and becomes preserved by burial when the shelf eventually founders and the Silesian Basin is separated by another blind-thrust anticlinal cordillera from the Skole Basin.

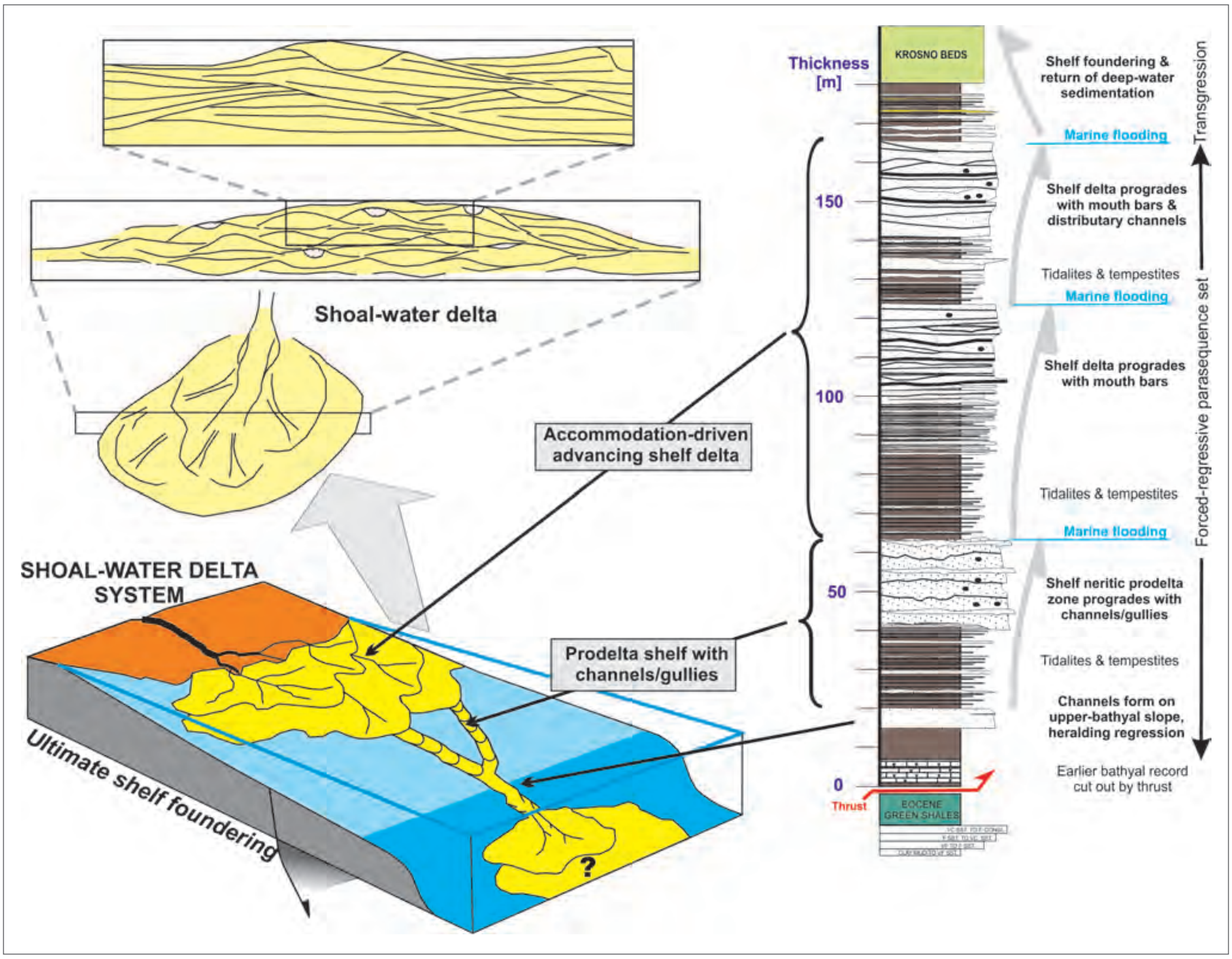

Fig. 34. Stratigraphic interpretation of the Menilite Beds succession in the excursion area in terms of a depositional model of a tide- and storm-influenced narrow shelf onto which a shoal-water delta progrades (see also Fig. 33B); for further interpretive details, see text.

31A), where its profile also shows only two 20-m sandstone packages (Kozikowski, 1966). The thickness of the Menilite Beds decreases to ca. 60 m over a distance 15 km to the north and north-west (Birecki, 1964; Karnkowski, 1959) and to the west (Świdziński, 1950, 1953), where the compositionally different Kliwa Sandstone deposits (Koszarski, 1965) begin to appear laterally. The Magdalena Sandstone occurs in only some wells to the south and virtually pinches out northwards, which jointly indicates a lenticular sandstone complex with an estimated strike-parallel (W–E) width of at least 35 km and a basinward dip-parallel (S–N) extent of ca. 20 km.

Interpretation of the Magdalena Sandstone

The cordilleras separating Carpathian flysch basins, when diachronously uplifted by thrusting, are thought to have developed narrow transient shelf zones hosting neritic to littoral sedimentation (Fig. 33). Most of these fringing shelves were cannibalized by excessive uplift and erosion, as in the case of the Glauconitic Magura Beds (stop B8.4, Fig. 33A), but some others might escape destruction and preserve their shallow-marine deposits when subsiding. This is thought to have been the case with the Magdalena Sandstone – deposited on an uplifted bathyal fringe of the Silesian Basin and then buried when the shelf tectonically foundered (Fig. 33B) and deep-water sedimentation resumed.

The Menilite Beds succession in the present case (Fig. 34, profile) has upper-bathyal but quite atypical 'menilitic' shales at the base, which can be attributed to deposition in the basin's shallowing fringe zone (Fig. 33A). The occurrence of first sand-filled channels (Fig. 34, profile) is a signal of an impending forced regression driven by tectonic uplift, and the subsequent appearance of heterolithic deposits with tidalites and tempestites marks the onset of shelf conditions. The first coarsening-upwards package of deposits (Fig. 34, profile) is a regressive parasequence recording shelf shallowing and formation of shelf-crossing channels.

As discussed by Lewis (1982) in his review of modern and ancient cases, such shelf-crossing channels/gullies – possibly extending down beyond the shelf edge (see Plate 7) – tend to form in the forefront of highly-constructive (i.e., strongly prograding) deltas. They can be formed by: (1) strong rip currents generated by storms on a low-relief coast; (2) down-dip progression of sediment mass failures on a tectonically steepened shelf; (3) retrogressive slumping initiated at the shelf edge or on the slope; or (4) a combination of these processes.

The second coarsening-upwards regressive parasequence (Fig. 34, profile), deposited after an episode of abrupt marine flooding, culminated in a sandy package of offset-stacked distal deltaic mouth-bar lobes – heralding encroachment of a wave-worked shoal-water delta (*sensu* Leeder *et al*., 1988; Postma, 1990) or mouth bar-type delta (*sensu* Dunne and Hempton, 1984; Wood and Ethridge, 1988). The delta advance was interrupted by another episode of abrupt marine flooding, attributed – same as the previous one – to a rapid tectonic subsidence of the shelf (see Fig. 33B).

The third and last regressive parasequence (Fig. 34, profile) culminated in a sandy package of offsetstacked deltaic mouth-bar lobes with distributary channels (see top-left inset diagram in Fig. 34), which indicates an even greater advance of the shoal-water delta. The shelf subsequently foundered and deep-water sedimentation resumed (Fig. 34, profile top) due to progressive thrusting, when also the Silesian Basin was separated from the Skole Basin (Fig. 33B).

As a whole, the Menilite Beds succession in the excursion area is considered to be a parasequence set recording

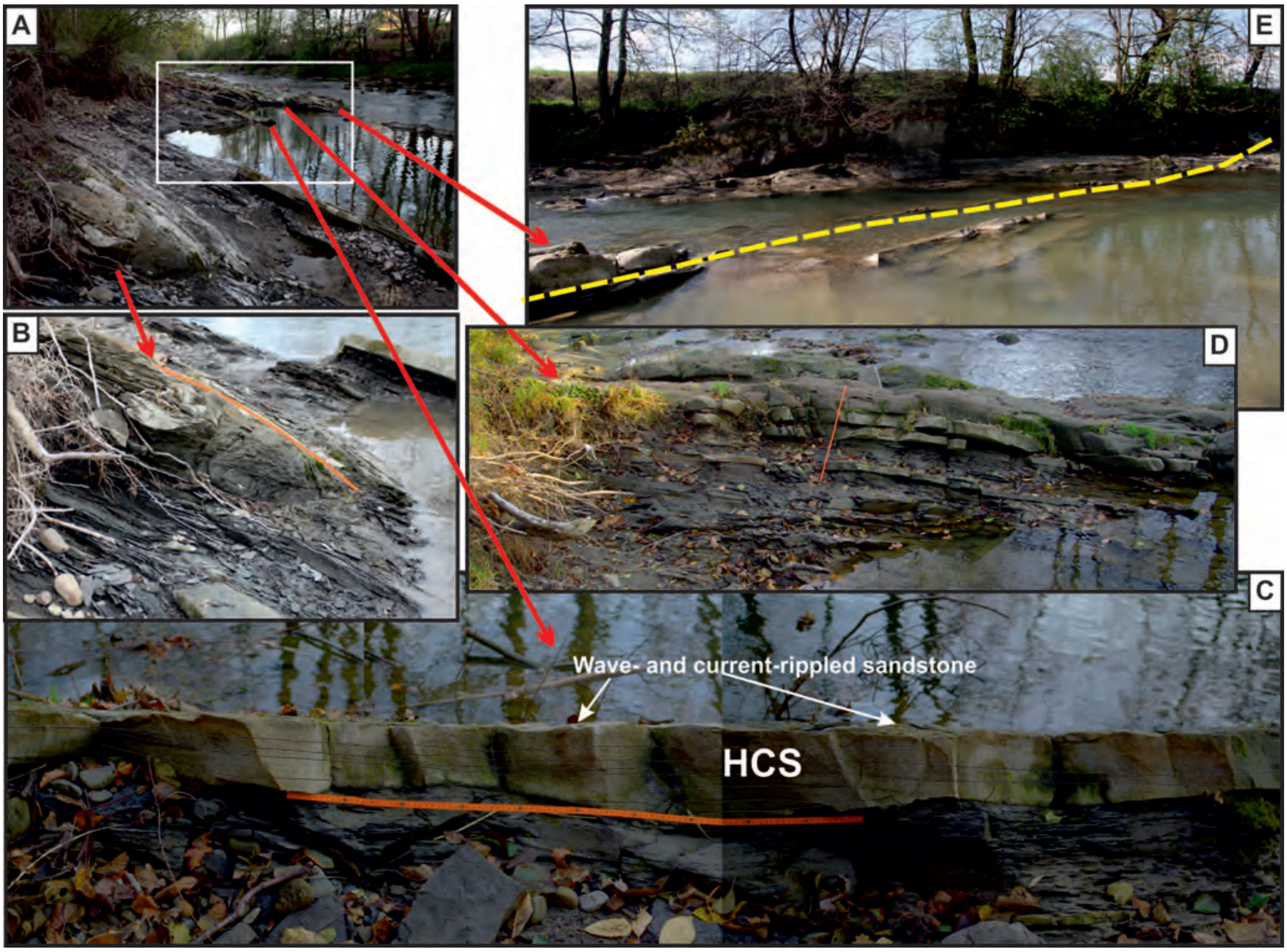

Fig. 35. Outcrop details from the excursion point 5.1 (Figs 31B, 32). (**A**) A typical outcrop of the Menilite Beds in the banks and floor of the Sękówka river. (**B**) Hydroplastically deformed sandstone bed in a heterolithic package, ca. 30 m above the succession base (see log in Fig. 32); the yellow measuring stick is 1 m. (**C**) Sandstone bed with apparent hummocky stratification (HCS), draped with wave- and current-ripple cross-lamination; the yellow measuring stick is 1 m. (**D**) A small-scale coarsening-upwards package of heterolithic deposits capped with hummocky-stratified sandstone beds; the yellow measuring stick is 1 m. (**E**) The sharp erosional base of the sandstone at the top of the heterolithic succession at point 5.1 (see log height of ca. 42 m in Fig. 32).

a tectonically-forced regression punctuated by marine flooding events due to episodic shelf subsidence (incipient structural foundering). The deltaic system is thought to have been 'accommodation-driven' (*sensu* Porębski and Steel, 2003) and hence readily reaching the margin of a narrow shelf. As a shelfedge delta, the Magdalena system and its forefront channels may have supplied considerable volumes of turbiditic sand to the adjacent part of the Silesian Basin where the Menilite Beds were deposited (Fig. 33B; see Porębski and Steel, 2003; Sanchez *et al*., 2012).

Stop description for topic 3

B8.5 Gorlice

Leader: Piotr S. Dziadzio

The outcrops at stop B8.4 also are in the river bedrock banks and floor, and hence wellingtons (high rubber boots) are needed. The excursion aim at this last stop (Fig. 31B) is to show and discuss the key evidence for a shallow-marine origin of the Magdalena Sandstone: the sandstone bodies interpreted as shelf-to-slope palaeochannels; the thinly-bedded heterolithic deposits interpreted as outer-shelf tidalites and distal tempestites; the thicker sandstone beds with apparent HCS and wave-ripple cross-lamination, interpreted as mid-shelf prodelta tempestites; and the offset-stacked parallel-stratified sandstone bodies interpreted as distal to proximal deltaic mouth-bar complexes.

B.5.1–4 (Fig. 31B)

Outcrops in the banks and floor of river Sękówka in its 600-m segment from Gorlice Sokół (49°38′51″ N, 21°10′43″ E) to Gorlice Łęgi (49°38′43" N, 21°11′10″ E)

Point 5.1 – The Sękówka river here (Fig. 31B) exposes the lower boundary and basal part of the Menilite Beds. The Menilite Beds succession commences with a package of grey to brownish-grey siliceous marls that overlie sharply the late Eocene green shales (Fig. 32). Their contact is a tectonic thrust, but perhaps only a few metres of deposits are missing, because the dark brownish-grey shales characteristic of the Menilite Beds occur already as thin interlayers in the underlying package of green shales. Missing here is the regional stratigraphic marker unit known as the Globigerina Marls (Leszczyński, 1997), but the basal part of Menilite Beds, a few metres

Fig. 36. A small-scale coarsening-upwards succession of heterolithic deposits in the middle part of the Menilite Beds profile at the excursion point 5.2 (see Fig. 31B and log in Fig. 32); the measuring stick is 1 m.

Fig. 37. A small-scale coarsening-upwards succession of heterolithic deposits with wave-ripple cross-lamination, overlain by a hummocky-stratified sandstone bed; outcrop detail from the excursion point 5.2 (see Fig. 31B and log in Fig. 32). The measuring stick in the upper photograph is 50 cm.

Fig. 38. Packages of broadly convex-upwards sandstone beds stacked in an offset 'compensational' manner, interpreted to be shingled distal mouth bars of an advancing shoal-water delta (see Fig. 34, upper left). Outcrop detail from the excursion stop 5.3 (see Fig. 31B and log in Fig. 32).

thick, consists of grey and greyish-brown marls above which the typical shales of Menilite Beds appear. These are black and dark-brown, thinly laminated clayshales, with a variable amount of organic matter, interlayered with mudshales and thin siltstones. The shales are sharply, erosively overlain by a thick (5 m) body of poorly sorted, massive sandstone – interpreted as a shelf-margin palaeochannel plugged with sandy deposits of debris flows (*sensu* Lowe, 1982).

The overlying package of heterolithic deposits (22 m thick), with lenticular, wavy and flaser bedding, is intercalated with sheet-like beds of very fine- to fine-grained and occasionally coarse-grained glauconitic sandstones, 10 to 30 cm thick, sporadically up to 60 cm. The sandstone beds occur at random or form, with the underlying heterolithic deposits, small (0.5 to 4 m thick) coarsening-upwards successions (Fig. 35A, D). Some sandstone beds are graded-massive, whereas others show planar parallel stratification, current- and wave-ripple cross-lamination, and occasional hummocky-like stratification (Fig. 35C). Bed tops often show convolutions and some beds are hydroplastically deformed throughout by slump-style folding (Fig. 35B). The sandstone beds are thought to be tempestites (*sensu* Dott and Bourgeois, 1982; Duke *et al*., 1991) and storm-generated turbidites (*sensu* Walker, 1969, 1984) emplaced in a tidally-influenced outer shelf zone. The overlying thick (up to 20 m) body of fine- to very coarse-grained glauconitic sandstones (Fig. 32A) with a sharp erosional base (Fig. 35E), mudclasts and crude upward fining is interpreted to be a shelf-crossing palaeochannel filled through multiple cut-and-fill stages.

Point 5.2 – The river floor here (Fig. 31B) exposes the overlying, coarsening-upwards package of heterolithic deposits (ca. 35 m thick, Fig. 32A) interspersed with sheet-like sandstone beds. The heterolithic deposits often form small-scale coarsening-upwards successions (Fig. 36). The origin of this apparent cyclicity is unclear, but the small parasequences may possibly reflect the impact of the Milankovitch astronomical cycles on the tide and wave climate of the shelf (see De Boer and Smith, 1994; Westerhold *et al*., 2005). The tabular sandstone beds, interpreted as tempestites and storm-derived turbidites, tend here to be thicker than earlier in the succession. Some of the thickest beds show hummocky stratification (Fig. 37). Local gutter casts (Fig. 36) with a SE trend indicate storm-generated geostrophic currents flowing parallel to the shelf strike, as is generally expected for an outer shelf zone (Walker, 1984). The coarsening-upwards heterolithic succession culminates in a 25-m thick sandstone unit (Fig. 32A) composed of broadly lenticular, gently convex-upwards, offset-stacked packages of thin sandstone beds with planar parallel stratification and minor wave-ripple cross-lamination. The lenticular bed packages are interpreted to be shingled, waveworked distal mouth bars of an encroaching shoal-water delta (Fig. 34).

Point 5.3 – The river floor in this segment (Fig. 31B) exposes the next package of coarsening-upwards heterolithic deposits interspersed with sheet-like sandstone beds and culminating in another sandstone unit ca. 25 m thick (Fig. 32A). The heterolithic package again shows small-scale coarsening-upwards cyclothems, some capped with hummocky-stratified sandstone beds. The overlying sandstone unit, much like the previous one (stop 5.2, Fig. 32A), consists of broadly lenticular, gently convex-upwards packages of sandstone beds (Fig. 38) with planar parallel stratification and occasional current- or wave-ripple crosslamination. Many of these offset-stacked packages here are cross-cut by shallow palaeochannels filled with very coarse-grained to pebbly sand. The general palaeotransport direction is to the NE (Szymakowska, 1979), with the palaeochannels trending towards the NE or NNE. This sandstone complex is thought to represent shingled proximal mouth bars of a re-advancing shoal-water delta (Fig. 34).

Point 5.4 – The river floor here (Fig. 31B) exposes the uppermost part of the Menilite Beds succession and its transition to the overlying Krosno Beds (Fig. 32A) whose thick-bedded, quartz-muscovite calcareous sandstones are widely considered to be deep-water turbidites. The top part of the Menilite Beds is heterolithic, with at least two thick (ca. 1 m) erosive beds of massive to trough cross-stratified and ripple-laminated quartz-glauconite sandstone underlain by deformed heterolithic deposits. The Magdalena-type non-calcareous sandstones and Krosno-type calcareous sandstones occur alternatingly in the heterolithic transitional part of the succession. Large slump features occur at the very top of the Menilite Beds succession and are attributed to the shelf instability due its ultimate tectonic foundering (Figs 33, 34).

References

Allaby, A. & Allaby, M., 1999. *A Dictionary of Earth Sciences*. Oxford University Press, 619 pp.

Amy, L. A., Talling, P. J., Edmonds, V. O., Sumner, E. J. & Lesueur, A., 2006. An experimental investigation of sand-mud suspension settling behaviour: implications for bimodal mud contents of submarine flow deposits. *Sedimentology*, 53: 1411–1434.

Baas, J. H., Best, J. L., Peakall, J. & Wang, M., 2009. A phase diagram for turbulent, transitional, and laminar clay suspension flows. *Journal of Sedimentary Research*, 79: 162–183.

Badak, J. & Grudzień J., 1961. Wyniki badań łupków bitumicznych w utworach serii menilitowej obszaru Bezmiechowa–Monasterzec. *Biuletyn Instytutu Geologicznego*, 154: 125–196. [In Polish.]

Beverage, J. P. & Culbertson, J. H., 1964. Hyperconcentrations of suspended sediment. *Proceedings of the American Society of Civil Engineers, Journal of Hydraulic Division*, 90: 117–128.

Bieda F., 1969. Flysch formation of the Tertiary of the Polish Carpathians. *Rocznik Polskiego Towarzystwa Geologicznego,* 39: 488–514. [In Polish, English summary.]

Birecki, T., 1964. Budowa geologiczna synkliny Bobowej. *Prace Geologiczne,* Polska Akademia Nauk-Oddział w Krakowie Komisja Nauk Geologicznych, 21: 1–57. [In Polish.]

Birkenmajer, K., 1985. Fourth Day. In: Birkenmajer, K. (ed.), *Main Geotraverse of the Polish Carpathians (Cracow–Zakopane), Guide to Excursion 2, 12th Congress of the Carpatho-Balkan Geological Association (Kraków).* Wydawnictwa Geologiczne, Warszawa, pp. 90–136.

Bouma, A. H. 1962. *Sedimentology of Some Flysch Deposits.* Elsevier, Amsterdam, 168 pp.

Carter, R. M., 1975. A discussion and classification of subaqueous mass-transport with particular application to grain-flow, slurry-flow, and fluxoturbidites. *Earth-Science Reviews*, 11: 145–177.

Cieszkowski, M., Koszarski, A., Leszczyński, S., Michalik, M., Radomski, A. & Szulc, J., 1991. *Szczegółowa Mapa Geologiczna Polski 1:50 000, Arkusz Ciężkowice.* Państwowy Instytut Geologiczny, Warszawa. [In Polish.]

De Boer, P. L. & Smith, D. G., 1994. Orbital forcing and cyclic sequences. In: De Boer, P. L. & Smith, D. G. (eds), *Orbital Forcing and Cyclic Sequences. International Association of Sedimentologists, Special Publications,* 19: 1–14.

DeCelles, G. P. & Giles, A. K., 1996. Foreland basin systems. *Basin Research*, 8: 105–123.

Dott, R. H., Jr. & Bourgeois, J., 1982. Hummocky stratification: significance of its variable bedding sequences. *Geological Society of America Bulletin,* 93: 663–680.

Draghinda, J., 1963. Contribution a la connaissance de la genèse des formations de flysch. *6th Congress of Carpatho-Balkan Geological Association (Warszawa).* Wydawnictwa Geologiczne, Warszawa, pp. 54–55.

Duke, W. L., Arnott, R.W. & Cheel, R. J. 1991. Shelf sandstones and hummocky cross stratification; new insights on a stormy debate. *Geology*, 19: 625–628.

Dunne, L. A. & Hempton, M. R., 1984. Deltaic sedimentation in the Lake Hazar pull-apart basin, south-eastern Turkey. *Sedimentology*, 31: 401–412.

Dziadzio, P. S., Enfield, M. A. & Watkinson, M., 1998. *A Structural and Sequence Stratigraphic Workshop: Polish Carpathians Field Trip Guide*. Polskie Górnictwo Naftowe i Gazownictwo, Gorlice, 44 pp.

Dziadzio, P. S., Borys, Z., Kuk, S., Masłowski, E., Probulski, J., Pietrusiak, M., Górka, A., Moryc, J., Baszkiewicz, A., Karnkowski, P., Karnkowski, P. H. & Pietrusiak, M., 2006. Hydrocarbon resources of the Polish Outer Carpathians – Reservoir parameters, trap types, and selected hydrocarbon fields: A stratigraphic review. In: Golonka, J. & Picha, F. J. (eds), *The Carpathians and Their Foreland: Geology and Hydrocarbon Resources. American Association of Petroleum Geologists, Memoirs,* 84: 259–291.

Dżułyński, S. & Kotlarczyk, J., 1962. On load-casted ripples. *Rocznik Polskiego Towarzystwa Geologicznego*, 32: 147–160.

Dżułyński, S., Książkiewicz, M. & Kuenen, Ph. H., 1959. Turbidites in flysch of the Polish Carpathian Mountains. *Geological Society of America Bulletin,* 70: 1089–1118.

Dżułyński, S. & Sanders, J. E., 1962. Bottom marks on firm mud bottom. *Transactions of the Connecticut Academy of Arts and Science*, 42: 57–96.

Dżułyński, S. & Smith, A. J., 1964. Flysch facies. *Rocznik Polskiego Towarzystwa Geologicznego*, 34: 245–266.

Dżułyński, S. & Ślączka, A., 1959. Directional structures and sedimentation of the Krosno Beds (Carpathian Flysch). *Rocznik Polskiego Towarzystwa Geologicznego,* 28: 205–260.

Dżułyński, S. & Walton, E. K., 1965. *Sedimentary Features of Flysch and Greywackes*. Elsevier, Amsterdam, 274 pp.

Enfield, M. A., Watkinson, M. P., Blunt, E. P., Philps, B., Vangelov, D., Nemčok, M., Jankowski, L., Dimov, D., Dilov, S., Gurbuz, T. & Seymour, M. 1998. *A Structural and Stratigraphic Re-evaluation of the Western Polish Carpathians: Implications for Hydrocarbon Exploration. Scientific Technical Conference, Wysowa (27–30 May 1998).* Wydawnictwo Stowarzyszenia Inżynierów i Techników Przemysłu Naftowego i Gazowniczego, 76 pp.

Enfield, M. A., Watkinson, M. P. & Seymour, M. D., 2001a. How has new seismic helped us to understand the Polish Carpathians and explore for new hydrocarbon prospects? An integrated approach to exploration. In: Dziadzio, P. (ed.), C*arpathian Petroleum Conference — Application* *of modern exploration methods in a complex petroleum system*, Wysowa, Wydawnictwo Stowarzyszenia Inżynierow i Technikow Przemyslu Naftowego i Gazowniczego, Gorlice, pp. 4–6.

Enfield, M. A., Watkinson, M. P. & Seymour, M. D., 2001b. New high resolution seismic data—Examples of interpretations useful for understanding small-scale structural and stratigraphic relationship in Medusa's Carpathian concession. In: Dziadzio, P. (ed.), *Carpathian Petroleum Conference — Application of modern exploration methods in a complex petroleum system*, Wysowa, Wydawnictwo Stowarzyszenia Inżynierow i Technikow Przemyslu Naftoweg i Gazowniczego, Kraków, pp. 48 –49.

Gabinet, M. P. & Jurczakiewicz, J. M., 1962. Charakterystyka mineralogiczno-geochemiczna warunków facjalnych tworzenia się skał serii menilitowej Wschodnich Karpat. *Rocznik Polskiego Towarzystwa Geologicznego*, 32: 5–29.

Gosh, B. & Lowe, D. R., 1993. The architecture of deep-water channel complexes, Cretaceous Venado Sandstone Member, Sacramento Valley, California. In: Graham, S. A. & Lowe, D. R. (eds), *Advances in the Sedimentary Geology of the Great Valley Group, Sacramentio Valley, California*. Society of Economic Paleontologists and Mineralogists, Pacific Section, Guidebook 73, pp. 51–65.

Gucwa, I. & Ślączka, A., 1972. Changes in geochemical conditions within the Silesian Basin (Polish Flysch Carpathians) and Eocene–Oligocene boundary. *Sedimentary Geology*, 8: 199–223.

Gucwa, I. & Ślączka A., 1980. Trace elements and the growth of phytoplankton in geosynclinal deposits of the Polish Flysch Carpathians. In: *Proceedings 11th Congress of Carpatho-Balkan Geological Association (Kiev), Lithology* . Kiev, pp. 76–81.

Haig, D. W., 1979. Global distribution patterns of mid-Cretaceous foraminiferids. *Journal of Foraminiferal Research*, 9: 29–40.

Hampton, M. A., 1972. The role of subaqueous debris flow in generating turbidity currents. *Journal of Sedimentary Petrology,* 42: 775–793.

Hanzlikova, E. & Roth Z., 1963. Lithofacies, biofacies and sedimentary conditions in the Cretaceous beds of the flysch zone in the Czechoslovakian Carpathians. *Geologicky Sbornik*, 14: 83–100.

Haughton, P. D. W., Barker, S.P. & McCaffrey, W., 2003. 'Linked' debrites in sand-rich turbidite systems – origin and significance. *Sedimentology*, 50: 459–482.

Haughton, P., Davis, C., McCaffrey, W. & Baker, S., 2009. Hybrid sediment gravity flow deposits – Classification, origin and significance. *Marine and Petroleum Geology*, 26: 1900–1918.

Hawryłko, S., 2009. *Rozmieszczenie otwornic w drobnoziarnistych osadach sekwencji turbidyt-interturbidyt na przykładach z warstw magurskich w Ropicy Górnej*. Unpublished M.Sc. Thesis, Jagiellonian University, Kraków, 63 pp. [In Polish.]

Hickson, T. A. & Lowe, D. R., 2002. Facies architecture of a submarine fan channel-levee complex: the Juniper Ridge Conglomerate, Coalinga, California. *Sedimentology*, 49: 335–362.

Hiscott, R. N., 1994. Traction-carpet stratification – fact or fiction? *Journal of Sedimentary Research*, 64A: 204–208.

Hsü, K.J., 1989. *Physical Principles of Sedimentology*. Springer-Verlag, Berlin, 233 pp.

Janbu, N.E., Nemec, W., Kırman, E. & Özaksoy, V., 2007. Facies anatomy of a channelized sand-rich turbiditic system: the Eocene Kusuri Formation in the Sinop Basin, north-central Turkey. In: Nichols, G., Paola, C. & Williams, E.A. (eds), *Sedimentary Environments, Processes and Basins. International Assocociation of Sedimentologists, Special Publications*, 38: 457–517.

Jankowski, L., Kopciowski, R. & Ryłko, W., 2012. The state of knowlage of geological structures of the Other Carpathians between Biała and Rusca Rivers - Discussion. *Biuletyn Państwowego Instytutu Geologicznego*, 449: 203–216. [In Polish.]

Jerzmańska, A., 1968. Ichtyofaune des couches á ménilite (flysch des Karpathes). *Acta Palaentologica Polonica*, 13: 379–488.

Jerzmańska, A. & Kotlarczyk, J., 1988. Punkt A-13. Krępak-serpentyny Proponowany profil stratotypowy warstw menilitowych w polskich Karpatach 1. Podstawy podziału stratygraficznego serii menilitowo-krośnieńskiej Karpat za pomocą ichtiofauny. In: Kotlarczyk, J., Pękala, K. & Gucik, S. (eds), *Przewodnik LIX Zjazdu Polskiego Towarzystwa Geologicznego Karpaty Przemyskie 16-18 września 1988,* Wydawnictwo AGH, Kraków, pp. 102–107. [In Polish.]

Kane, I. A. & Pontén, A. S. M., 2012. Submarine transitional flow deposits in the Paleogene Gulf of Mexico. *Geology*, 40: 1119–1122.

Karnkowski, P., 1959. Budowa geologiczna antykliny Jankowej. *Rocznik Polskiego Towarzystwa Geologicznego*, 29: 281–296.

Karnkowski, P., 1999. *Oil and Gas Deposits in Poland*. The Geosynoptics Society GEOS, University of Mining and Metalurgy, Kraków, 380 pp.

Keferstein, H., 1830. Briefwechsel, Mittheilungen an den Geheimen Rath v. Leonhard gerichtet. *Jahrbuch für Mineralogie Geognosie, Geologie und Petrefaktenkunde*, 1: 299–304**.**

Kneller, B. C. & Branney, M. J., 1995. Sustained high-density turbidity currents and the deposition of thick massive sands. *Sedimentology*, 42: 607–616.

Koltun, Y., 1992. Organic matter in Oligocene Menilite formation rocks of the Ukrainian Carpathians: paleoenviroment and geochemical evolution. *Organic Geochemisty*, 18: 423–430.

Koltun, Y., Espitalie, J., Kotarba, M., Roure, F., Ellouz, N. & Kosakowski, P., 1998. Petroleum generation in the Ukrainian External Carpathians and adjacent foreland. *Journal of Petroleum Geology*, 21: 265–268.

Koltun, Y., Kotarba, M., Kosakowski, P. & Espitalie, J., 1995. Hydrocarbon potential of the Menilite and Spas Beds in the Polish and Ukrainian parts of the Flysch Carpathians. In: *Extended Abstracts Book, Conference and Exhibition Modern Exploration and Improved Oil and Gas Recovery Methods*. Wydawnictwo AGH, Kraków, pp. 147–150.

Kopciowski, R., 1996. Budowa geologiczna strefy Siar między Ropą a Banicą (płaszczowina magurska). *Biuletyn Państwowego Instytutu Geologicznego*, 374: 21–39. [In Polish.]

Koszarski, L., 1956. Observations on the sedimentation of the Ciężkowice Sandstone near Ciężkowice (Carpathian Flysch). *Bulletin de l'Académie Polonaise des Sciences, Classe* 3, 4: 393–398.

Koszarski, L., 1962. Badania nad sedymentacją piaskowców ciężkowickich okolic Iwonicza i Rymanowa. *Sprawozdania z Posiedzeń Komisji PAN, Oddział w Krakowie*, 1–6: 258–260.

Koszarski, L., 1963a. O sedymentacji piaskowców ciężkowickich. *Kwartalnik Geologiczny*, 7: 717–718.

Koszarski, L., 1963b. Zawada–Ciężkowice–Zborowice. In: Wdowiarz, S. & Nowak, W. (eds), *Karpates Externes. Guide des Excursions, 6me Congrés Association Géologique Karpato-Balkanique*. Polska Akademia Nauk, Kraków, pp. 65–78.

Koszarski, L., 1965. Rozwój piaskowców magdaleńskich w Karpatach. *Sprawozdania z Posiedzeń Komisji Nauk PAN, Oddział w Krakowie*, pp. 235–237. [In Polish.]

Koszarski, L., 1985. General outline of geology of central part of Carpathian Foredeep and some essential data on the nappes of Polish Carpathians. In: Koszarski, L. (ed.), *Geology of the Middle Carpathians and the Carpathian Foredeep. Guide to Excursion 3, 13th Congress of Carpatho-Balkan Geological Association (Kraków).* Geological Institute, Warszawa, pp. 11–39.

Koszarski, L., & Żytko, K., 1961. Łupki jasielskie w serii menilitowo-krośnieńskiej w Karpatach Środkowych. *Biuletyn Instytutu Geologicznego*, 166: 87–219. [In Polish.]

Koszarski, L. & Żytko, K., 1965. Le probleme de la profondeur de la mer du geosynclinals karpatique de flysch. In: *Proceedings 7th Congress of Carpatho-Balkan Geological Association (Sofia).* Part II, Vol. 2, pp. 81–86. Bulgarian Academy of Sciences, Sofia.

Kotarba, M. J., Więcław, D., Dziadzio, P., Kowalski, A., Bilkiewicz, E. & Kosakowski, P., 2013. Organic geochemical study of source rocks and natural gas and their genetic correlation in the central part of the Polish Outer Carpathians. *Marine and Petroleum Geology*, 45: 106–120.

Kotarba, M. J., Więcław, D., Dziadzio, P., Kowalski, A., Kosakowski, P. & Bilkiewicz, E., 2014. Organic geochemical study of source rocks and natural gas and their genetic correlation in the eastern part of the Polish Outer Carpathians and Palaeozoic–Mesozoic basement. *Marine and Petroleum Geology*, 56: 97–122.

Kotlarczyk, J., 1976. Przyczynki do wyjaśnienia genezy piaskowców kliwskich w Karpatach polskich. *Sprawozdania z Posiedzeń Komisji Naukowych, Oddział PAN w Krakowie*, 19: 185–187. [In Polish.]

Kotlarczyk, J., Jerzmańska, A., Świdnicka, E. & Wiszniowska, T., 2006. A framework of ichthyofaunal ecostratigraphy of the Oligocene-Early Miocene strata of the Polish Outer Carpathian basin. *Annales Societatis Geologorum Poloniae*, 76: 1–111

Kozikowski, H., 1966. Zarys geologii obszaru Krygu-Lipinek koło Gorlic. *Kwartalnik Geologiczny*, 10: 407–428. [In Polish.]

Köster, J., Kotarba, M., Lafargue, E. & Kosakowski, P., 1998a. Source rock habitat and hydrocarbon potential of Oligocene Menilite Formation (Flysch Carpathians, SE Poland): an organic geochemical and isotope approach. Organic Geochemistry, 29: 543–558.

Köster, J., Rospondek, M., Schouten, S., Kotarba, M., Zubrzycki, A. & Damste, J. S., 1998b. Biomarker geochemistry of a foredeep basin: the Oligocene Menilite Formation in SE Poland. Organic Geochemistry, 29: 649–669.

Książkiewicz, M. 1948. Current bedding in Carpathian flysch. *Rocznik Polskiego Towarzystwa Geologicznego*, 7: 137–152.

Książkiewicz, M., 1954. Graded and laminated bedding in the Carpathian flysch. *Rocznik Polskiego Towarzystwa Geologicznego*, 22: 399–449.

Książkiewicz, M., 1958. Sedimentation in the Carpathian flysch sea. *Geologische Rundschau*, 47: 418–425.

Książkiewicz, M., 1961. Life conditions in flysch basins. *Annales Societatis Geologorum Poloniae*, 31: 3–21.

Książkiewicz, M. (ed.), 1962. Cretaceous and Early Tertiary in the Polish External Carpathians. In: *Geological Atlas of Poland, Stratigraphic and Facial Problems, Fasc. 13*. Instytut Geologiczny, Warszawa.

Książkiewicz, M., 1963. Evolution structurale des Carpathes polonaises. *Société Géologique de France, Fallot Memorial*, 2: 529–562.

Książkiewicz, M. (ed.), 1968. Geology of the Polish Flysch Carpathians. *Guide to Excursion C44, 23rd International Geological Congress (Prague)*. Wydawnictwa Geologiczne, Warszawa.

Książkiewicz, M., 1975. Bathymetry of Carpathian flysch basin. *Acta Geologica Polonica, 25: 309–367.*

Książkiewicz, M., 1977. Trace fossils in the flysch of the Polish Carpathians. *Palaeontologia Polonica*, 36: 1–208.

Kuenen, P. H., 1957. Review of marine sand-transporting mechanisms. *Journal of the Alberta Society of Petroleum Geologists*, 5/4: 59–62.

Kuenen, P. H., 1958. Problems concerning source and transportation of flysch sediments. *Geologie en Mijnbouw*, 20: 329–339.

Kuenen, P. H. & Migliorini, C. I., 1950. Turbidity currents as a cause of graded bedding. *Journal of Geology*, 58: 91–127.

Kuźniar, C., 1952. W sprawie genezy łupków menilitowych. *Rocznik Polskiego Towarzystwa Geologicznego*, 22: 495–496.

Leeder, M. R., Ord, D. M. & Collier, R., 1988. Development of alluvial fans and fan deltas in neotectonic extensional settings: implications for the interpretation of basin-fills. In: Nemec, W. & Steel, R.J. (eds), *Fan Deltas – Sedimentology and Tectonic Settings*. Blackie, London, pp. 173–185.

Leszczyński, S., 1981. Piaskowce ciężkowickie jednostki śląskiej w Karpatach: studium sedymentacji głębokowodnej osadów gruboklastycznych. *Annales Societatis Geologorum Poloniae*, 51: 435–502. [In Polish, with English abstract.]

Leszczyński, S., 1986. Depositional processes of fluxoturbidites on example of the Ciężkowice Sandstone, Polish Carpathians. In: *7th European Regional Meeting Excursion Guidebook*. Ossolineum, Wrocław, pp. 113–121 & 131–135.

Leszczyński, S., 1989. Characteristics and origin of fluxoturbidites from the Carpathian flysch (Cretaceous–Palaeogene), south Poland. *Annales Societatis Geologorum Poloniae,* 59: 351–382.

Leszczyński, S., 1997. Origin of the Submenilite Globigerina Marl (Eocene–Oligocene transition) in the Polish Outer Carpathians. *Annales Societatis Geologorum Poloniae*, 67: 367–427.

Leszczyński, S. & Malata, E., 2002. Sedimentary conditions in the Siary Zone of the Magura Basin (Carpathians) in the late Eocene–early Oligocene. *Annales Societatis Geologorum Poloniae,* 72: 201–239.

Leszczyński, S., Warchoł, M. & Starzec, K., 2008. Zapis ewolucji Karpat polskich w osadach eocenu górnego-oligocenu dolnego. In: Haczewski, G. (ed.), *Pierwszy Polski Kongres Geologiczny Kraków 26-28 czerwca 2008 Przewodnik Sesji Terenowych*. Polskie Towarzystwo Geologiczne, Kraków, pp. 47–77. [In Polish.]

Lewis, D. W., 1982. Channels across continental shelves: Corequisites of canyon-fan systems and potential petroleum conduits, *New Zealand Journal of Geology and Geophysics*, 25: 209–225.

Lowe, D. R., 1979. Subaqueous liquefied and fluidized sediment flows and their deposits. *Sedimentology*, 23: 285–308.

Lowe, D. R., 1982. Sediment gravity flows, 2. Depositional models with special reference to high density turbidity currents. *Journal of Sedimentary Petrology*, 52: 279–298.

Lowe, D. R., 1988. Suspended-load fallout rate as an independent variable in the analysis of current structures. *Sedimentology*, 35: 765–776.

Lowe, D. R. & Guy, M., 2000. Slurry-flow deposits in the Britannia Formation (Lower Cretaceous), North Sea: a new perspective on the turbidity current and debris flow problem. *Sedimentology*, 47: 31–70.

Lowe, D. R., Guy, M. & Palfrey, A., 2003, Facies of slurry-flow deposits, Britannia Formation (Lower Cretaceous), North Sea: implications for flow evolution and deposit geometry. *Sedimentology*, 50: 45–80.

Matyasik, I. & Dziadzio, P. S., 2006. Reconstruction of petroleum system based on integrated geochemical and geological investigation: Selected examples from Middle, Outer Carpathians in Poland, In: Golonka J. & Picha, F. J. (eds), *The Carpathians and Their Foreland: Geology and Hydrocarbon Resources. American Association of Petroleum Geologists, Memoirs,* 84: 479–518.

Middleton, G. V. & Hampton, M. A., 1973. Sediment gravity flows: mechanics of flow and deposition. In: Middleton, G. V. & Bouma, A. H. (eds), *Turbidites and Deep-water Sedimentation.* Short Course No. 1 Lecture Notes, Society of Economic Paleontologists and Mineralogists, Tulsa, pp. 1–38.

Middleton, G. V. & Hampton, M. A., 1976. Subaqueous sediment transport and deposition by sediment gravity waves. In: Stanley, D. J. & Swift, D. J. P. (eds), *Marine Sediment Transport and Environmental Managemen*t. Wiley, New York, pp. 197–218.

Middleton, G. V. & Southard, J. B., 1977. *Mechanics of Sediment Movement.* Short Course No. 3 Lecture Notes, Society of Economic Paleontologists and Mineralogists, Tulsa, 156 pp.

Mulder, T. & Alexander, J., 2001. The physical character of subaqueous sedimentary density currents and their deposits. *Sedimentology*, 48: 269–299.

Mutti, E., 1979. Turbidites et cones sous-marins profonds. In: Homewood, P. (ed.), *Sedimentation detritique (fluvial, littoral et marine).* Institut de Géologie, Université de Fribourg, Suisse, pp. 353–419.

Mutti, E., 1992. *Turbidite Sandstones.* Istituto di Geologia Università di Parma & AGIP, San Donato Milanese, 275 pp.

Mutti, E. & Ricci Lucchi, F., 1972. Le torbiditi dell' Appennino Settentrionale: introduzione all'analisi di facies. *Memorie della Societá Geologica Italiana*, 11: 161–199.

Mutti, E. & Ricci Lucchi, F., 1975. Turbidite facies and facies associations. In: *Examples of Turbidite Facies and Facies Associations from Selected Formations of the Northern Apennines.* Field Trip Guide A-11, 9th International Congress of Sedimentology (Nice), pp. 21–36.

Mutti, E., Tinterri, R., Benevelli, G., di Base, D. & Cavanna, G., 2003. Deltaic, mixed and turbidite sedimentation of ancient foreland basins. *Marine and Petroleum Geology*, 20: 733–755.

Mutti, E., Tinterri, R., Remacha, E., Mavilla, N., Agnella, S. & Fava, L., 1999. An introduction to the analysis of ancient turbidite basins from an outcrop perspective. *American Association of Petroleum Geologists, Continuing Education Course Note Series*, 39, 61 pp.

Nemec, W. (2009) What is a hyperconcentrated flow? In: *Lecture Abstracts, Annual Meeting of the International Association of Sedimentologists (Alghero)*, 2 pp.

Nemec, W. & Steel, R. J., 1984. Alluvial and coastal conglomerates: their significant features and some comments on gravelly mass-flow deposits. In: Koster, E. H. & Steel, R. J. (eds) *Sedimentology of Gravels and Conglomerates. Canadian Society of Petroleum Geologists, Memoirs*, 10: 1–31.

Olszewska, B., 1985. Foraminifera of the Menilite Beds (Polish External Carpathians). *Annales Societatis Geologorum Poloniae*, 55: 201–250.

Olszewska, B. & Malata, E., 2006. Paleonevironmental and paleobathymetric analysis of microfossil assemblages of the Polish Outer Carpathians (in Polish, with English abstract). In: Oszczypko, N., Uchman, A. & Malata, E. (eds), *Palaeotectonic Evolution of the Outer Polish Carpathian and Pieniny Klippen Belt Basins.* Instytut Nauk Geologicznych, Uniwersytet Jagielloński, Kraków, pp. 61–84.

Oszczypko, N., 2004. Geodynamika Karpat i przedgórza w świetle najnowszych badań geologicznych. In: *Materiały Konferencyjne, 75 Zjazd Naukowy Polskiego Towarzystwa Geologicznego (Iwonicz Zdrój).* Polish Geological Society, Kraków, pp. 30–43. [In Polish.]

Oszczypko-Clowes, M., 2001. The nannofossil biostratigraphy of the youngest deposits of the Magura Nappe (east of the Skawa river, Polish Flysch Carpathians) and their palaeoenvironmental conditions. *Annales Societatis Geologorum Poloniae,* 71: 139–188.

Porębski, S. J. & Steel, R. J., 2003. Shelf-margin deltas; their stratigraphic significance and relation to deepwater sands. *Earth-Science Reviews*, 62: 283–326.

Postma, G., 1990. Depositional architecture and facies of river and fan deltas: a synthesis. In: Colella, A. & Prior, D. B. (eds), *Coarse-grained Deltas. International Association of Sedimenologists, Special Publications,* 10: 13–27.

Postma, G., Nemec, W. & Kleinspehn, K. L., 1988. Large floating clasts in turbidites: a mechanism for their emplacement. *Sedimentary Geology*, 58: 47–61.

Potter, P. E., Maynard, J. B. & Depetris, P. J., 2005. *Mud and Mudstones*. Springer-Verlag, Berlin, 295 pp.

Radomski, A., 1960. Remarks on sedimentation of shales in flysch deposits. *Bulletin l'Academiæ Polonaise des Sciences, Serie des Sciences Geologiques et Geographiques*, 8: 123–129.

Reading, H. G. & Richards, M., 1994. Turbidite systems in deep-water basin margins classified by grain size and feeder system. *American Association of Petroleum Geologists Bulletin*, 78: 792–822.

Rögl, F., 1998. Palaeogeographic Considerations for Mediterranean and Paratethys Seaways (Oligocene to Miocene). *Annalen des Naturhistorisches Museum Wien*, 99A: 279–310.

Sanchez, C. M., Fulthorpe, C. S. & Steel, R. J., 2012. Miocene shelf-edge deltas and their impact on deepwater slope progradation and morphology, northwest shelf of Australia. *Basin Research*, 24: 683–698.

Sanders, J. B., 1965. Primary sedimentary structures formed by turbidity currents and related resedimentation mechanisms. In: Middleton G. V. (ed.), *Primary Sedimentary Structures and their Hydrodynamic Interpretation. Society of Economic Paleontologists and Mineralogists, Special Publications*, 12: 192–219.

Schieber, J., 1998. Deposition of mudstones and shales: Overview, problems, and challenges. In: Schieber, J., *et al*. (eds), *Shales and Mudstones, Volume 1: Basin Studies, Sedimentology and Paleontology*. Schweizerbart'sche Verlagsbuchhandlung, Stuttgart, pp. 131–146.

Schieber, J. & Southard, J. B., 2009. Bedload transport of mud by floccule ripples – Direct observations of ripple migration processes and their implications. *Geology*, 37: 483–486.

Schieber, J., Southard, J. B. & Thaisen, K., 2007. Accretion of mudstone beds from migrating floccule ripples. *Science*, 318: 1760–1763.

Schlager, W. & Schlager, M., 1973. Clastic sediments associated with radiolarites (Tauglboden-Schichten, Upper Jurassic, Eastern Alps). *Sedimentology*, 20: 65–89.

Schnabel, W., 2011. *Cechy i geneza gruboławicowych utworów drobnoziarnistych priabonu–rupelu strefy Siar płaszczowiny magurskiej w rejonie Ropicy Górnej*. Unpublished M.Sc. Thesis, Jagiellonian University, 54 pp. [In Polish.]

Shanmugam, G., 1997. The Bouma sequence and the turbidite mind set. *Earth-Science Reviews*, 42: 201–229.

Shanmugam, G., 2000. 50 years of the turbidite paradigm (1950s–1990s): deep-water processes and facies models. *Marine and Petroleum Geology*, 17: 285–342.

Shanmugam, G., 2002. Ten turbidite myths. *Earth-Science Reviews*, 58: 311–341.

Shanmugam, G., 2006. The tsunamite problem. *Journal of Sedimentary Research*, 76: 718–730.

Shanmugam, G., 2012. New perspectives on deep-water sandstones: Origin, recognition, initiation and reservoir quality. *Handbook of Petroleum Exploration and Production*, 9: 1–488. Elsevier, Amsterdam.

Słomka, T., Malata, T., Olszewska, B., Leśniak, T., Oszczypko, N. & Poprawa, P., 2006. Evolution of the Silesian and Subsilesian Basins. In: Oszczypko, N, Uchman, A. & Malata, E., (eds), *Paleotectonic Evolution of the Outer Carpathians and Pieniny Klipen Basins*. Instytut Nauk Geologicznych, Uniwersytet Jagielloński, Kraków, pp. 111–126.

Sohn, Y. K., Choe, M. Y. & Jo, H. R., 2002. Transformation from debris flow to hyperconcentrated flow in a submarine channel (the Cretaceous Cerro Toto Formation, southern Chile). *Terra Nova*, 14: 405–415.

Stanley, D. J., 1980. The Saint-Antonin Conglomerate in the Maritime Alps: a model for coarse sedimentation on a submarine slope. *Smithsonian Contributions to the Marine Sciences*, 5: 1-25.

Stanley, D. J. & Unrug, R., 1972. Submarine channel deposits, fluxoturbidites and other indicators of slope and base-of-slope environments in modern and ancient marine basins. In: Rigby, J. K. & Hamblin, W. K. (eds), *Recognition of Ancient Sedimentary Environments. Society of Economic Paleontologists and Mineralogists, Special Publications*, 16: 287–340.

Starzec, K. 2009. *Glaukonit jako wskaźnik sedymentogenezy piaskowców z warstw magurskich strefy Siar płaszczowiny magurskiej (Karpaty)*. Unpublished Ph.D. Thesis, Jagiellonian University, 262 pp. [In Polish.]

Stow, D. A. V., Reading, H. G. & Collinson, J. D., 1996. Deep seas. In: Reading, H. G. (ed.), *Sedimentary Environments: Processes, Facies and Stratigraphy*. Blackwell, Oxford, pp. 395–453.

Studer, B., 1827. Remarques géognostiques sur quelques parties de la chaîne septentrionale des Alpes. *Annales des Sciences naturelles (Paris)*, 11: 1–47.

Sujkowski, Z., 1938. Les series de Szipot dans les Karpates polonaises orientales. Etude geologique et petrographique d'un complexe de Flysch. *Prace Państwowego Instytutu Geologicznego*, 3: 5–105. [In Polish, with French abstract.]

Ślączka, A., & Kaminski, M. A., 1998. *A Guidebook to Excursions in the Polish Flysch Carpathians. Field Trips for Geoscientists, Grzybowski Foundation Special Publi-*

cations, 6: 1–173. Kraków.

Ślączka, A. & Thompson, S., III, 1981. A revision of the fluxoturbidite concept based on type examples in the Polish Carpathian Flysch. *Annales Societatis Geologorum Poloniae*, 51: 3–44.

Ślączka, A. & Unrug, R., 1966. Sedimentary structures and petrology of some sandstone members of the Menilite Beds, Carpathians. *Rocznik Polskiego Towarzystwa Geologicznego*, 36: 155–180. [In Polish, with English abstract.]

Świdziński, H., 1933. „Prządki" – skałki piaskowca ciężkowickiego pod Krosnem. *Zabytki Przyrody Nieożywionej RP*, 2: 94–120. [In Polish.]

Świdziński, H., 1950. Łuska Stróż koło Grybowa. *Biuletyn Państwowego Instytutu Geologicznego*, 59: 5–70. [In Polish.]

Świdziński H., 1953. Karpaty fliszowe między Dunajcem a Sanem. In: *Regionalna Geologia Polski, Vol. 1. Karpaty. Tektonika*. Panstwowe Wydawnictwa Geologiczne, Warszawa, pp. 362–422. [In Polish.]

Szymakowska F., 1979. Budowa geologiczna południowego skrzydła fałdu Gorlic między Gorlicami a Krygiem (Karpaty Środkowe). *Rocznik Polskiego Towarzystwa Geologicznego,* 49: 85–103.

Talling, P. J., Masson, D. G., Sumner, E. J. & Malgesini, G., 2012. Subaqueous sediment density flows: depositional processes and deposit types. *Sedimentology*, 59: 1937–2003.

Talling, P. J., Malgesini, G. & Felletti, F., 2013. Can liquefied debris flows deposit clean sand over large areas of sea floor? Field evidence from the Marnoso Arenacea Formation, Italian Apennines. *Sedimentology*, 60: 720–762.

Torfs, H., Mitchener, H., Huysentruyt, H. & Toorman, E., 1996. Settling and consolidation of mud/sand mixtures. *Coastal Engineering*, 29: 27–45.

Uchman, A., Malata E., Olszewska, B. & Oszczypko N., 2006. Paleobatymetry of the Outer Carpathian Basins. In: Oszczypko, N., Uchman, A. & Malata, E. (eds), *Paleotectonic Evolution of the Outer Carpathians and Pieniny Klipen Basins*. Instytut Nauk Geologicznych, Uniwersytet Jagielloński, Kraków, pp. 85–102.

Unrug, R., 1963. Istebna Beds – a fluxoturbiditic formation in the Carpathian Flysch. *Rocznik Polskiego Towarzystwa Geologicznego,* 33: 49–92.

Unrug, R., 1965. Le facies de Flysch a fluxoturbidites dans les Carpathes polonaises. In: *Abstracts, 7me Congrés Association Géologique Karpato-Balkaniques (Sofia), Classe 2*, 1: 301–303.

Vašiček, M., 1953. Conditions of the origin of Tegel, Schlier and Flysch and the problem of their stratigraphy. *Sborník Ústředního ústavu geologického (Praha)*, *Geologia*, 20: 69–100.

Vrolijk, P. J. & Southard, J. B., 1997. Experiments on rapid deposition of sand from high-velocity flows. *Geoscience Canada*, 24, 45–54.

Walker, R. G., 1967. Turbidite sedimentary structures and their relationship to proximal and distal depositional environments. *Journal of Sedimentary Petrology*, 37: 25–43.

Walker, R. G., 1969. The juxtaposition of turbidites and shallow-water sediments: study of a regressive sequence in the Pennsylvanian of North Devon, England. *Journal of Geology,* 77: 125–142.

Walker, R. G., 1970. Review of the geometry and facies organization of turbidites and turbidite-bearing beds. In: Lajoie, K. R. (ed.), *Flysch Sedimentology in North America*. *Geological Association of Canada, Special Papers,* 7: 219–251.

Walker, R. G., 1975. Conglomerate: sedimentary structures and facies models. In: Harms, J. C., Walker R. G. & Spearing D. (eds.), *Depositional Environments as interpreted from Primary Sedimentary Structures and Stratification Sequences. Short Course No. 12 Lecture Notes, SEPM,* Tulsa, pp. 133–161.

Walker, R. G., 1978. Deep-water sandstone facies and ancient submarine fans – models for exploration and for stratigraphic traps. *American Association of Petroleum Geologists Bulletin*, 62: 932–966.

Walker, R. G., 1984. Shelf and shallow marine sands. In: Walker, R. G. (ed.), *Facies Models*. 2nd Edn, *Geoscience Canada Reprint Series*, 1: 141–170.

Walker, R. G. & Mutti, E., 1973. Turbidite facies and facies associations. In: Middleton, G. V. & Bouma, A. H. (eds), *Turbidites and Deep-water Sedimentation*. Short Course Lecture Notes, Pacific Section, Society of Economic Paleontologists and Mineralogists, Anaheim, pp. 119–157.

Waśkowska, A. & Cieszkowski, M., 2014. Biostratigraphy and depositional anatomy of a large olistostrome in the Eocene Hieroglyphic Formation of the Silesian Nappe, Polish Outer Carpathians. *Annales Societatis Geologorum Poloniae*, 84: 51–70.

Watkinson, M. P., Enfield, M. A. & Seymour, M. D., 2001. Predicting turbidite reservoir presence and quality in the Polish Carpathians – application of sequence stratigraphy in exploration. In: Dziadzio P., (ed.), *Carpathian Petroleum Conference – Application of Modern Exploration Methods in a Complex Petroleum System (Wysowa)*. Wydawnictwo Stowarzyszenia Inżynierów i Techników Przemysłu Naftowego i Gazowniczego, Kraków, pp. 8–10.

Watycha, L. 1963. Some remarks on the South China Sea shore and on the flysch sedimentation. *Przegląd Geologiczny*, 6: 219–282. [In Polish.]

Westerhold, T., Bickert, T. & Röhl, U., 2005. Middle to late Miocene oxygen isotope stratigraphy of ODP site 1085 (SE Atlantic): new constraints on Miocene climate variability and sea-level fluctuations. *Palaeogeography Palaeoclimatology Palaeoecology*, 217: 205–222.

Winn, R. D. & Dott, R. H., Jr., 1977. Large-scale traction produced structures in deep-water fan-channel conglomerates in southern Chile. *Geology*, 5: 41–44.

Wood, M. L. & Ethridge, F. G., 1988. Sedimentology and architecture of Gilbert-type and mouth bar-type fan deltas, Paradox Basin, Colorado. In: Nemec, W. & Steel, R. J. (eds), *Fan Deltas – Sedimentology and Tectonic Settings*. Blackie, London, pp. 251–264.

Żgiet, J., 1963. Wstępna charakterystyka sedymentologiczna piaskowców kliwskich. *Kwartalnik Geologiczny*, 7: 715–716. [In Polish.]

Appendix Table 1. Fluxoturbidite facies of the Ciężkowice Sandstone.

Facies (bed varieties)	**Descriptive characteristics**
Facies mS massive non-graded sandstone	Beds of massive (non-stratified) and non-graded coarse sandstone, usually rich in granules, with erosional bases (Fig. 16A, B). Beds are up to a few metres thick and often amalgamated into thicker packages. The deposit is a mixture of sand, granules/small pebbles and some silt. Bedding-parallel alignment of clasts indicates laminar shear, but internal textural discontinuities, inclined local shear banding and relics of scour-fill cross-strata suggest incremental deposition and transient flow turbulence. Some beds show dewatering structures. Rip-up mudstone clasts occur, up to several decimetres in size and usually armoured. These deposits shows locally lateral transition into normal-graded sandstone or conglomerate–sandstone, or planar-stratified sandstone.
Facies tlsS thickly stratified (layered or banded) sandstone	Beds of massive coarse sandstone and granule/fine-pebble conglomerate up to a few metres thick, often erosionally amalgamated, showing thick faint to distinct parallel stratification or banding (Fig. 16C, D). The strata, marked by grain size segregation, are planar or inclined and several millimetres to decimetre in thickness. They form thin laminae sets of fine to medium sand separated by massive coarser-sand layers, or form thicker bands of finer and coarser sand. The inversely- graded layers of fine/medium to coarse sand or granule gravel resemble both the S_2 division of Lowe (1982) and the 'spaced/stepped-laminated' division T_{B-3} of Talling et al. (2012). The faint stratification is usually slightly undulating, made visible on rock surfaces as alternating delicate, concave/convex bands or spaced ribs by differential weathering. Otherwise, the beds show no overall grading. Some beds have thick massive lower division. An inclined banding or diffuse scour-fill cross-stratification are sporadically observed at the bed bases.
Facies gS graded massive sandstone or fine conglomerate to sandstone	Beds of graded massive coarse sandstone (often with scattered pebbles) or fine-grained conglomerate passing upwards into coarse sandstone (Fig. 16E–H), up to a few metres thick, isolated or amalgamated into thicker packages. Bed bases are erosional and occasionally show load casts. This is the most common facies of the Ciężkowice Sandstone. The gravelly division is inversely graded in its basal part in some cases. Mudstone rip-up clasts, up to a few decimetres in size and usually armoured, occur in the lower or upper part of some beds, particularly at the transition from coarse- to finer-grained sandstone. The massive sandstone shows locally dewatering structures in the upper part. The flat bed tops are occasionally capped with a thin Bouma-type turbidite Tbcd or Tde.
Facies gsS graded-stratified sandstone or fine conglomerate to sandstone	Beds of graded-stratified coarse sandstone or fine-grained conglomerate passing upwards into sandstone, up to a few metres thick (Fig. 16I–L). The lower parts of beds are usually massive and normally graded, but the conglomeratic ones occasionally show inverse grading at the base. Mudstone rip-up clasts, up to several decimetres in size and usually armoured, occur in the massive part of some beds. Stratification resembles that in facies tlsS and is most visible at the conglomerate/sandstone transition, including planar, inclined and trough-shaped scour-fill varieties. Pebbles tend to show flow-aligned imbricate fabric. Beds with flat, non-truncated top are usually capped with a Bouma-type fine-grained turbidite Tbcd or Tde. Beds with a massive upper part tend to show dewatering structures.
Facies Scl sandstone with conglomerate lenses	Beds of graded-stratified coarse sandstone or fine-grained conglomerate passing upward to sandstone, up to a few metres thick (Fig. 16M, N). Stratification is accentuated by flat lenses of granule and/or fine-pebble conglomerate, isolated or multiple, occurring in bed lower parts. The upper parts of beds show planar parallel stratification as in the Bouma turbidite b-division.

THE ORGANIZING COMMITTEE WOULD LIKE TO ACKNOWLEDGE THE GENEROUS SUPPORT OF OUR SPONSORS, PATRONS, PARTNERS AND EXHIBITORS

Ministry of Science and Higher Education
Republic of Poland

SILVER PARTNER

PGNiG
Polish Oil & Gas Company

USB FLASH-DRIVE SPONSOR

WILEY

PATRON SPONSOR

BETA
Radiocarbon Dating
Consistent Accuracy Delivered On-Time
Beta Analytic Ltd.

CoCARDE

European Science Foundation

ZGH BOLESŁAW

Muszynianka

PLATINUM SPONSOR

ORLEN Upstream

SILVER SPONSOR

Springer

PATRON

WIELICZKA SALT MINE

WRITING-PAD & WRITING-PEN SPONSOR

SHALETECH ENERGY

LANYARD SPONSOR

ZEISS

EXHIBITORS

geokrak

SYL & ANT Instruments

INTROLIGATORNIA
Wiesław Nowotarski

2015

KRAKÓW